

RI/RD 91-118 p387

HEAVY HYDROCARBON MAIN INJECTOR TECHNOLOGY PROGRAM FINAL REPORT

by
H.A. Arbit, L.M. Tuegel, F.E. Dodd

ROCKWELL INTERNATIONAL
ROCKETDYNE DIVISION

prepared for
NATIONAL AERONAUTICS AND SPACE ADMINISTRATION
HUNTSVILLE, ALABAMA 35812

APRIL 1991

MARSHALL SPACE FLIGHT CENTER
CONTRACT NAS8-36369

2184/61
(NASA-CR-~~388682~~) HEAVY HYDROCARBON MAIN
INJECTOR TECHNOLOGY PROGRAM Final Report,
Apr. 1987 - Jan. 1991 (Rockwell
International Corp.) 387 p

CSCL 21H

N91-21235

Unclass
G3/20 0007592

**HEAVY HYDROCARBON MAIN INJECTOR TECHNOLOGY PROGRAM
FINAL REPORT**

CONTRACT NAS8-36369

APRIL 1991

**ORIGINAL CONTAINS
COLOR ILLUSTRATIONS**

Prepared for:
NATIONAL AERONAUTICS AND SPACE ADMINISTRATION
MARSHALL SPACE FLIGHT CENTER
HUNTSVILLE, ALABAMA 35812

Prepared by:
H. A. Arbit, L. M. Tuegel, F. E. Dodd

Approved by:



for
J. C. Volkmann
Project Manager



H. C. Dodson
Program Manager

ROCKETDYNE DIVISION OF ROCKWELL INTERNATIONAL CORPORATION
6633 Canoga Avenue, Canoga Park, CA 91303

FORWARD

The Heavy Hydrocarbon Main Injector Technology Program was carried out by the Rocketdyne Division of Rockwell International Corporation for NASA-Marshall Space Flight Center, under Contract NAS8-36369. C. R. Bailey, J. Hutt and M. Rocker were the NASA-MSFC Project Managers. H. C. Dodson was the Rocketdyne Program Manager. This Final Report covers Phases A and B of the two-phase overall program; it was conducted by the following Rocketdyne personnel:

S. C. Fisher	Project Manager
H. A. Arbit	Project Engineer
L. M. Tuegel	Project Engineer
F. E. Dodd	Stability & Performance Analysis
V. W. Jaqua	Injector Concepts and Design
J. C. Craddock	Hardware Design
T. D. Chwiedor	Hardware Design
E. G. Schipper	Hardware Design
R. J. DeMinico	Hardware Design
R. G. Grant	Hardware Design
R. J. Jensen	Stability Analysis
B. M. Trueblood	Stability Analysis
W. R. Wagner	Thermal Analysis
H. Pongracz	Structural Analysis
T. R. Tarn	Test Engineer

The Phase A effort was begun in April 1987 and completed in August 1989. Phase B was started in September 1989 and completed in January 1991.

ABSTRACT

The Heavy Hydrocarbon Main Injector Technology Program, sponsored by NASA-MSFC, was an analytical, design and test program to demonstrate an injection concept applicable to an Isolated Combustion Compartment (ICC) of a full scale, high-pressure, LOX/RP-1 engine.

In Phase A of the two-phase program, several injector patterns were tested in a 3.5-inch combustor. Based on these test results, features of the most promising injector design were incorporated into a 5.7-inch injector which was then hot-fire tested. In turn, a preliminary design of a 5-compartment 2-D combustor was based on this pattern.

The analytical and design efforts were preceded by a review of the technology of LOX/RP-1 main injectors, which indicated, in essence, that existing technology was not adequate for design of a high-pressure LOX/RP-1 injector with high performance, stable combustion, and manageable heat flux.

The 3.5-inch diameter injectors (3 like-doublet patterns, 1 O-F-O Triplet, 1 LOX Showerhead) were tested with LOX/RP-1 at 2000 psia chamber pressure and 2.8 mixture ratio. Initial screening test results showed that the like-doublets had the highest performance (c^* efficiency = 95-96%), heat flux levels were high (~60 Btu/sec/in² at the throat), and the like-doublet patterns were spontaneously stable with acoustic cavities while the unlike triplet was not (longitudinal mode). A 5.7-inch diameter like-doublet injector with small orifices ($D_o = .058$ in., $D_f = .037$ in.) and spray fans canted into each other was designed and tested in a limited number of firings. It was found that the c^* efficiency (97%) of this injector was higher than that of the 3.5-inch diameter like-doublet injectors and the throat heat flux (50 Btu/sec/in²) was slightly lower. With a single-mode (1T) acoustic cavity, combustion was spontaneously stable. However, a bomb-initiated dynamic instability was observed. Analysis indicated the instability could be eliminated by modification of the acoustic cavity to a bimodal configuration.

During Phase B, it was felt that additional subscale work was required and technology could be advanced by substituting additional subscale testing for the original program plan to design and fabricate a 2-D combustor to be tested by MSFC. The additional subscale injector testing and analysis was performed with an emphasis on improving analytical techniques and

acoustic cavity design methodology. Several of the existing 3.5-inch diameter injectors were hot-fire tested with and without acoustic cavities for spontaneous and dynamic stability characteristics.

SUMMARY AND CONCLUSIONS

This final report covers both phases of a two-phase analytical, design, and test program to develop and demonstrate an injection concept applicable to a large (750,000-lb-thrust), high-pressure (>2000 psia), LOX/RP-1 engine. Functional goals of the injector were stable, high performance (minimum 96-percent c^* efficiency), and manageable heat flux. The full-scale engine would employ the Isolated Combustion Compartment (ICC) concept, in which a number of identical small injectors are combined to form a larger unit. The approach taken in this program involved, in Phase A, a review of current high-pressure LOX/RP-1 injector technology and outline of a technical plan for filling the voids in existing technology; design, fabrication, and test of several injection patterns in a 3.5-inch combustor; selection of the most promising pattern as the basis for a 5.7-inch, ICC-type injector; design, fabrication, and test of this injector in a calorimeter combustor to determine its performance, stability, and heat flux characteristics; and preliminary design of a 2-D combustor which incorporates five ICC injectors. In Phase B of the program, additional testing and analysis of the 3.5-inch injectors was performed to increase the generic technology base of the LOX/RP-1 propellant combination at high chamber pressures, improve existing stability and performance design and analysis techniques, and improve acoustic cavity design methodology.

The technology review indicated that very limited experimental work had been done with LOX/RP-1 injectors at high chamber pressure (2000 psia and over). The existing data base with LOX/RP-1 propellants confirmed the difficulty of achieving high performance in combination with stable combustion and manageable heat flux. Injection element parameters which give good mixing and atomization and therefore high performance (such as unlike impingement, very small orifice diameters, high element density, and efficient intra- and inter-element mixing) may have to be compromised because of their adverse effects on stability and heat flux. With the existing data base, there was little likelihood that a high-performance LOX/RP-1 injector would be dynamically stable without stability aids such as baffles and/or acoustic cavities or liners.

A technical plan to advance LOX/RP-1 injector technology was developed. It involved, primarily, selection of a cooling method, which may basically affect the injector type and design, because stability aids can probably damp any combustion pressure oscillations and the design requirements for high performance are fairly well defined. The cooling choices to

be made are the use of RP-1, LOX or perhaps LH₂ (in a tripropellant engine) as coolant, which also involves selection of the engine cycle.

Following stability, performance and thermal analyses and cold-flow mixing experiments of several model injector patterns, five injectors were designed and tested at 2000 psia chamber pressure in a 3.5-inch calorimeter combustor. One of these was a derivative of the classic, like-impinging, H-1 design which was designed, fabricated and tested under a Rocketdyne IR&D task and served as a "baseline" for contract injectors. Other injectors included a LOX showerhead pattern, (an attempt to maximize stability at the expense of performance), an unlike-impinging triplet (for high performance, based on work done at Aerojet and NASA-LeRC) and two like-impinging patterns, a circumferential fan and a "box" arrangement. The three like-doublet injectors gave the highest performance (95 to 96 percent c^* efficiency), had fairly high heat flux levels (50-64 Btu/sec/in² at the throat), and had the lowest amplitude pressure oscillations (\pm 5-percent of chamber pressure) with acoustic cavities at the chamber inlet. It was concluded that the conservative approach to a comparatively stable, high performing, high pressure, LOX/RP-1 injector is a like-doublet pattern, with orifices small enough to give good atomization and in an arrangement that maximizes mixing efficiency and coolant wall compatibility.

With this background and additional analytical effort, a canted-fan like-doublet injection pattern was selected for the 5.7-inch ICC prototype. The 5.7 inch injector was based on the 3.5 inch circumferential fan injector, but the orifice pattern was changed to a ring pattern to facilitate manifolding requirements and a cant was added to increase performance. A data base had previously been collected with this type of an injector with a LOX/JP-4 injector; at 440 psia. The JP-4 injector showed high performance (99-percent c^* efficiency), low heat flux (with carbon deposition on the chamber walls) and stable combustion (\pm 3-percent oscillations, with trimodal acoustic cavity slots). The 5.7-inch injector was designed and fabricated, and subsequently tested in a calorimeter chamber. The results indicated that c^* efficiency (97-percent) was higher than that of the 3.5-inch like-doublet injectors and heat flux at the throat (50 Btu/sec/in²) was slightly lower. With a single-mode (1T) acoustic cavity, combustion was spontaneously stable. However, during the final test with the injector, a dynamic instability with single mode cavities was initiated with the use of a stability rating bomb which resulted in irreparable damage to the injector. Dynamic stability with the 5.7-inch injector was not pursued, however, it is believed that dynamic instabilities could probably have been eliminated by modification of the acoustic cavity to a bimodal configuration.

As the last task under Phase A, the preliminary design of a 5-compartment, 2-D combustor was prepared, based on the following requirements: use of the ICC concept; 150,000-200,000 lb thrust level; structural and thermal characteristics suitable for ten; two-second, dynamic stability tests at 2000 psia chamber pressure; and use of the like-doublet, canted-fan, injection pattern. The design parameters were selected to duplicate those of a 750,000-lb-thrust, full-scale, 3-D combustor and to emphasize fabrication and operational simplicity. Layout drawings of the 2-D combustor, which consists of an injector assembly and chamber assembly bolted together, were prepared. An uncooled design (copper walls and ablative throat section in a steel shell) was employed, with five individual injector/acoustic cavity units combined in the overall injector assembly.

Phase B of the program was modified to expand the 3.5 inch LOX/RP-1 data base. This change of direction in program logic was based on the 5.7 inch injector test results. During Phase B, the Heavy Hydrocarbon Main Injector Technology Program had two primary objectives, both of which were achieved. The first objective was to develop an injector element configuration, applicable to large booster engines, to be incorporated within a baffle compartment or Isolated Combustion Compartment (ICC) with appropriate damping. The second objective was to increase the generic technology base of the LOX/RP-1 propellant combination at high chamber pressures and, with additional test data, improve existing stability and performance design and analysis techniques, as well as improve acoustic cavity design methodology.

The first objective (ICC concept) was met when the H-1 Derivative injector tests were completed. The H-1 Derivative injector displayed performance values from 96 to 98 percent c-star efficiency, and was also dynamically stable when bomb tested without acoustic cavities. The last criteria (dynamically stable without acoustic cavities) was not an ICC criteria, but might suggest that a larger compartment size may be feasible with an H-1 Derivative injector pattern. Furthermore, the H-1 Derivative injector was tested at various operating conditions. These included operation at chamber pressures greater than 2300 psia and with a 30% reduction in chamber length with no decrease in performance or stability margin at either operating condition.

The second objective during Phase B of this program, which included increasing the LOX/RP-1 propellant generic data base, improving existing stability design and analysis techniques, and improving the acoustic cavity design methodology, was achieved with the analysis and testing. The LOX/RP-1 propellant time lag data base was increased by 150%.

Data was collected with respect to the thermal environments which exist in acoustic cavities during operation, and classical analyses, such as the Standardized Distributed Energy Release (SDER) computer code were incorporated to show injection patterns which influence both performance and near injector chamber compatibility.

In summary, this program realized important positive results with the LOX/RP-1 propellants:

- 1) High performance is achievable with LOX/RP-1 propellants at high chamber pressures (96 - 98%).
- 2) The heat flux which results from high performance and high chamber pressure is manageable (<50 Btu/sec/in²).
- 3) The LOX/RP-1 propellant data base has been significantly increased at higher chamber pressures.
- 4) A high performing, dynamically stable injector pattern has been demonstrated which meets the ICC concept requirements.

During November of 1990, a plan for an add-on/new start program was presented to NASA-MSFC personnel which included cold flow and hot-fire tests to determine the key stability differences between the dynamically unstable Box-Doublet and the dynamically stable H-1 Derivative injectors.

Based on the results of the Heavy Hydrocarbon Main Injector Technology Program, improved analytical approaches, more research and more technology work are still required before large engine programs can proceed with a high level of confidence that expensive stability development programs will not be required. This will require further technology and stability code anchoring activities.

TABLE OF CONTENTS

	<u>Page No.</u>
1.0 INTRODUCTION	1 - 1
1.1 Background and Objective	1 - 1
1.2 Technical Approach and Program Logic	1 - 1
2.0 PHASE A (Tasks I and II)	2 - 1
3.0 INJECTOR TECHNOLOGY REVIEW AND PROGRAM PLAN	3 - 1
3.1 Introduction	3 - 1
3.2 Injector Technology	3 - 1
3.3 Technology Plan	3 - 3
4.0 MODEL INJECTOR COLD-FLOW TESTS	4 - 1
4.1 Introduction	4 - 1
4.2 Test Injectors	4 - 1
4.3 Experimental	4 - 4
4.4 Injector Pattern Selection	4 - 13
5.0 ANALYSIS, DESIGN AND TEST OF 3.5-INCH INJECTORS	5 - 1
5.1 Introduction	5 - 1
5.2 Acoustic Analyses	5 - 1
5.3 Injector Patterns for Hot-Fire Testing	5 - 17
5.4 Combustor Components	5 - 25
5.5 Test Facility, Instrumentation and Procedures	5 - 32
5.6 Test Results and Discussion	5 - 45
6.0 ANALYSIS, DESIGN AND TEST OF 5.7-INCH INJECTOR	6 - 1
6.1 Introduction	6 - 1
6.2 Injector Selection and Design	6 - 1
6.3 Combustor Components	6 - 6
6.4 Test Facility, Instrumentation and Procedures	6 - 14
6.5 Test Results and Discussion	6 - 20

	<u>Page No.</u>
7.0 TWO-DIMENSIONAL COMBUSTOR PRELIMINARY DESIGN	7 - 1
7.1 Introduction	7 - 1
7.2 Requirements of the 2-D Combustor	7 - 1
7.3 Design Methodology	7 - 2
7.4 Combustor Design and Assembly	7 - 3
 <u>8.0 PHASE B</u> (Task III)	 8 - 1
 9.0 INTRODUCTION	 9 - 1
 10.0 PRETEST ANALYSIS	 10 - 1
10.1 Introduction	10 - 1
10.2 Performance Analysis Results	10 - 1
10.3 Stability Analysis Results	10 - 22
 11.0 TASK II TEST SUMMARY	 11 - 1
11.1 Introduction	11 - 1
11.2 Data Summary	11 - 1
 12.0 HOT-FIRE TEST PLANS	 12 - 1
12.1 Test Hardware and Facility	12 - 1
12.2 Test Logic	12 - 1
 13.0 3.5-INCH INJECTOR SCREENING TEST SERIES	 13 - 1
13.1 Introduction	13 - 1
13.2 H-1 Derivative Injector	13 - 1
13.3 Circumferential-Fan Injector	13 - 5
13.4 Box-Doublet Injector	13 - 21
13.5 O-F-O Triplet Injector	13 - 26
13.6 Bomb Redesign	13 - 32
 14.0 INJECTOR DOWN-SELECTION	 14 - 1
14.1 Injector Selection	14 - 1
14.2 Test Results	14 - 6

	<u>Page No.</u>
REFERENCES	15 - 1
APPENDICES	
A. INJECTOR TECHNOLOGY REVIEW AND TECHNICAL PROGRAM PLAN	A - 1
B. INJECTOR DETAIL DRAWINGS	B - 1
C. DATA REDUCTION METHODS	C - 1
D. TABULAR SUMMARY OF SUBSCALE LOX/RP-1 TESTING	D - 1

LIST OF FIGURES

<u>Figure No.</u>		<u>Page No.</u>
1.	ICC Injector Development Logic	1 - 2
2.	Phase A Program Flow Diagram	1 - 4
3.	Phase B Program Flow Diagram	1 - 6
4.	Selection of Engine Cycle, Cooling Method, and Injection Mode	3 - 5
5.	Injector Model No. 1	4 - 3
6.	Injector Model No. 2	4 - 3
7.	Injector Model No. 3	4 - 5
8.	Injector Model No. 4	4 - 5
9.	Injector Model No. 5	4 - 6
10.	Cold-Flow Mixing Test Facility	4 - 6
11.	Injector No. 6, Like-Impinging Elements, Ring Configuration	5 - 3
12.	Dimensions of Acoustic Cavities	5 - 5
13.	Sensitive Time Lag Correlation, Non-Coaxial Injectors, Non-Hypergolic Propellants	5 - 7
14.	Pressure Interaction Index Correlation, Non-Coaxial Injectors, Non-Hypergolic Propellants	5 - 7
15.	Response Curves of LOX Showerhead Injectors, No. 1 & 4	5 - 8
16.	Response Curves of LOX Quadlet Injectors, No. 2 & 3	5 - 10
17.	Response Curves of Box-Type, Like-Doublet Injector, No. 5	5 - 11
18.	Response Curves of Ring-Type, Like-Impinging Injector, No. 6	5 - 12
19.	Response Curves of Candidate O-F-O Triplet Injector, No. 7	5 - 13
20.	Response Curves of Aerojet O-F-O Triplet Injector	5 - 14
21.	Webber Stability Parameters for Indicated Injectors and Combustors	5 - 16
22.	H-1 Derivative Injector (Photo)	5 - 21

<u>Figure No.</u>		<u>Page No.</u>
23.	LOX Showerhead Injector (Photo)	5 - 22
24.	O-F-O Triplet Injector (Photo)	5 - 22
25.	Circumferential Fan, Like-Douplet Injector (Photo)	5 - 24
26.	Box Pattern, Like-Douplet Injector (Photo)	5 - 24
27.	3.5-inch Combustor Assembly Schematic	5 - 27
28.	3.5-inch Combustor Assembly Mounted on Test Stand (Photo)	5 - 27
29.	LOX Dome Joined to Fuel Manifold, 3.5-inch Combustor (Photo)	5 - 27
30.	Acoustic Cavity Ring, 3.5-inch Combustor (Photo)	5 - 29
31.	Instrumentation Ring, 3.5-inch Combustor (Photo)	5 - 29
32.	Chamber Spool, 3.5-inch Combustor	5 - 31
33.	Throat Section, 3.5-inch Combustor	5 - 31
34.	LOX System Schematic, Mike Stand	5 - 34
35.	RP-1 System Schematic, Mike Stand	5 - 34
36.	TEA/TEB System Schematic, Mike Stand	5 - 35
37.	Coolant Water Schematic, Mike Stand	5 - 36
38.	Mike Stand Test Sequence	5 - 43
39.	Static Chamber Pressure (Inj. End), Test 015-013, H-1 Derivative Injector	5 - 46
40.	Axial Heat Flux Profile, Test 015-013, H-1 Derivative Injector	5 - 47
41.	Static Chamber Pressure (Inj. End), Test 015-023, LOX Showerhead Injector	5 - 50
42.	Static Chamber Pressure (Inj. End), Test 015-024, LOX Showerhead Injector	5 - 50
43.	Axial Heat Flux Profile, Test 015-023, LOX Showerhead Injector	5 - 51
44.	Axial Heat Flux Profile, Test 015-024, LOX Showerhead Injector	5 - 51
45.	Static Chamber Pressure (Inj. End), Test 015-028, O-F-O Triplet Injector	5 - 52

<u>Figure No.</u>		<u>Page No.</u>
46.	Axial Heat Flux Profile, Test 015-028, O-F-O Triplet Injector	5 - 52
47.	Static Chamber Pressure (Inj. End), Test 015-031, Circumferential-Fan Injector	5 - 54
48.	Axial Heat Flux Profile, Test 015-031, Circumferential-Fan Injector	5 - 54
49.	Static Chamber Pressure (Inj. End), Test 015-033, Box-Doublet Injector	5 - 55
50.	Axial Heat Flux Profile, Test 015-033, Box-Doublet Injector	5 - 55
51.	Test 015-031 High Frequency Data	5 - 58
52.	LOX/JP-4 Injector for 30 MW MHD Combustor (Photo)	6 - 3
53.	Canted-Fan Like-Doublet Injection Element	6 - 3
54.	Canted-Fan Like-Doublet Pattern, 5.7-inch Injector	6 - 5
55.	5.7-Inch Canted-Fan, Like-Doublet Injector Face (Photo)	6 - 7
56.	5.7-Inch Canted-Fan, Like Doublet Injector Body (Photo)	6 - 8
57.	Assembly Schematic of 5.7-inch Combustor	6 - 8
58.	LOX Dome, 5.7-inch Combustor (Photo)	6 - 10
59.	Fuel Manifold, 5.7-inch Combustor (Photo)	6 - 10
60.	Acoustic Cavity Ring, 5.7-inch Combustor (Photo)	6 - 12
61.	Instrumentation Ring, 5.7-inch Combustor (Photo)	6 - 12
62.	Chamber Spool, 8-inch Length, 5.7-inch Combustor (Photo)	6 - 13
63.	Chamber Spool, 4-inch Length, 5.7-inch Combustor (Photo)	6 - 13
64.	Throat Section, 5.7-inch Combustor (Photo)	6 - 15
65.	5.7-Inch Combustor Assembly Mounted on Test Stand (Photo)	6 - 15
66.	Static Chamber Pressure (Inj. End), Test 015-006, Canted-Fan Injector	6 - 21
67.	Fuel Injection and Purge Pressures, Test 015-006, Canted-Fan Injector	6 - 21

<u>Figure No.</u>		<u>Page No.</u>
68.	Axial Heat Flux Profile, Test No. 6, 5.7-inch Injector	6 - 23
69.	Static Chamber Pressure (Inj. End), Test 015-007, Canted-Fan Injector	6 - 25
70.	Static Chamber Pressure (Inj. End), Test 015-008, Canted-Fan Injector	6 - 25
71.	Injector Face, Showing Eight Oxidizer Orifices Plugged Prior to Test 015-008 and Three Missing Plugs Post-Test	6 - 27
72.	Static Chamber Pressure (Inj. End), Test 015-009, Canted-Fan Injector	6 - 27
73.	LOX Manifold Priming Oscillation, 400 Hz (Test No. 3)	6 - 30
74.	LOX Manifold Oscillation, Transition to Mainstage, 1125 Hz (Test No. 7)	6 - 30
75.	LOX Manifold Shutdown Chug, 825 Hz (Test No. 7)	6 - 30
76.	Test No. 7 High-Frequency Data	6 - 31
77.	Test No. 9 High-Frequency Data	6 - 32
78.	Neutral Stability Map of 5.7-inch Combustor, with and without Bimodal Acoustic Cavities	6 - 34
79.	Neutral Stability Map of 5.7-inch Combustor, Unimodal Acoustic Cavities	6 - 34
80.	Neutral Stability Map of 5.7-inch Combustor, Showing Tangential Modes with Expanded Injector Combustion Response	6 - 35
81.	ICC Configurations in Full-Size 3-D Combustor	7 - 6
82.	Relationships of Subscale, 2-D and Full-Size 3-D Combustors	7 - 7
83.	Full-size, 3-D, Compartmental Injection Concept	7 - 8
84.	Chamber Assembly Layout, 2-D Combustor	7 - 12
85.	Nodal Network for Thermal Model of 2-D Combustor Wall	7 - 13
86.	Temperature of Copper Wall at Junction with Ablative Throat Insert	7 - 13
87.	Estimated Temperature (°F) of Coated Copper Liner of 2-D Combustor at End of 2-sec. Firing at 2000 psia Pc	7 - 14

<u>Figure No.</u>		<u>Page No.</u>
88.	Injector Assembly Layout, 2-D Combustor	7 - 16
89.	Quadrant of 2-D ICC Canted-Fan Like-Doublet Injection Pattern	7 - 18
90.	Comparison of Canted-Fan Like-Doublet Elements in 5.7-inch and 2-D ICC Injectors	7 - 18
91.	Acoustic Cavity Configuration, 2-D ICC	7 - 21
92.	Vaporization Efficiency of RP-1 Like-Doublet Elements	7 - 21
93.	Phase B Program Flow Diagram	9 - 3
94.	Normalized Fuel Fraction Contours of the H-1 Derivative Injector	10 - 2
95.	Normalized Fuel Fraction Plot of the H-1 Derivative Injector	10 - 3
96.	Mass Flux Contour of the H-1 Derivative Injector	10 - 5
97.	Normalized Fuel Fraction Contours of the O-F-O Triplet Injector	10 - 6
98.	Normalized Fuel Fraction Plot of the O-F-O Triplet Injector	10 - 7
99.	Mass Flux Contour of the O-F-O Triplet Injector	10 - 8
100.	Normalized Fuel Fraction Contours of the Original Circumferential-Fan Injector	10 - 10
101.	Normalized Fuel Fraction Contours of the Modified Circumferential-Fan Injector	10 - 11
102.	Normalized Fuel Fraction Plot of the Original Circumferential-Fan Injector	10 - 12
103.	Normalized Fuel Fraction Plot of the Modified Circumferential-Fan Injector	10 - 13
104.	Mass Flux Contour of the Modified Circumferential-Fan Injector	10 - 14
105.	Normalized Fuel Fraction Contours of the Box-Doublet Injector	10 - 16
106.	Normalized Fuel Fraction Plot of the Box-Doublet Injector	10 - 17
107.	Mass Flux Contour of the Box-Doublet Injector	10 - 18
108.	Normalized Fuel Fraction Contours of the LOX Showerhead Injector	10 - 19
109.	Normalized Fuel Fraction Plot of the LOX Showerhead Injector	10 - 20

<u>Figure No.</u>		<u>Page No.</u>
110.	Mass Flux Contour of the LOX Showerhead Injector	10-21
111.	Propellant Reaction Profiles	10-24
112.	H-1 Derivative Injector Neutral Stability Map	10-24
113.	Sensitive Time Lag Correlation, Non-Coaxial Injectors, Non-Hypergolic Propellants	10-26
114.	Pressure Interaction Index Correlation, Non-Coaxial Injectors, Non-Hypergolic Propellants	10-26
115.	O-F-O Triplet Injector Neutral Stability Map	10-27
116.	Circumferential-Fan Injector Neutral Stability Map	10-27
117.	Box-Doublet Injector Neutral Stability Map	10-28
118.	LOX Showerhead Injector Neutral Stability Map	10-28
119.	O-F-O Triplet Injector Test High Frequency Data	10-30
120.	O-F-O Triplet Injector Longitudinal Stability Investigation Data	10-30
121.	H-1 Derivative Injector Pattern and Cross-Section	11-4
122.	Box-Doublet Injector Pattern and Cross-Section	11-4
123.	Circumferential-Fan Injector Pattern and Cross-Section	11-5
124.	O-F-O Triplet Injector Pattern and Cross-Section	11-5
125.	LOX Showerhead Injector Pattern and Cross-Section	11-6
126.	Task III Test Logic	12-2
127.	H-1 Derivative Injector Bomb Test Data	13-3
128.	Static Chamber Pressure (Inj. End), Test 015-010, H-1 Derivative Injector	13-4
129.	Static Chamber Pressure (Inj. End), Test 015-011, H-1 Derivative Injector	13-4
130.	Test 015-011 High Frequency Data	13-6
131.	Static Chamber Pressure (Inj. End), Test 015-012, Circumferential-Fan Injector	13-6

<u>Figure No.</u>		<u>Page No.</u>
132.	Test 015-012 High Frequency Data	13 - 7
133.	Static Chamber Pressure (Inj. End), Test 015-013, Circumferential-Fan Injector	13 - 9
134.	Test 015-013 High Frequency Data - Initial Wave Motion	13 - 10
135.	Test 015-013 High Frequency Data - Sustained Wave Motion	13 - 11
136.	Test 015-013 High Frequency Data - Large Amplitude Pressure Disturbance	13 - 12
137.	Test 015-016 High Frequency Data - Early Perturbation	13 - 13
138.	Static Chamber Pressure (Inj. End), Test 015-016, Circumferential-Fan Injector	13 - 15
139.	Static Chamber Pressure (Inj. End), Test 015-017, Circumferential-Fan Injector	13 - 15
140.	Test 015-017 High Frequency Data - Initial Wave Motion	13 - 16
141.	Test 015-017 High Frequency Data - PCB Malfunction	13 - 17
142.	Test 015-017 High Frequency Data - Initial Wave Motion	13 - 18
143.	Test 015-017 High Frequency Data - Sustained Wave Motion	13 - 19
144.	Test 015-017 High Frequency Data - PCB Structural Failure	13 - 20
145.	Static Chamber Pressure (Inj. End), Test 015-014, Box-Doublet Injector	13 - 22
146.	Test 015-014 High Frequency Data at Cut-Off	13 - 23
147.	Static Chamber Pressure (Inj. End), Test 015-015, Box-Doublet Injector	13 - 24
148.	Test 015-015 High Frequency Data - Bomb Detonation & Instability	13 - 25
149.	Static Chamber Pressure (Inj. End), Test 015-018, O-F-O Triplet Injector	13 - 27
150.	O-F-O Triplet Injector High Frequency Test Data (Chamber Length = 13.4-in.)	13 - 28
151.	Static Chamber Pressure (Inj. End), Test 015-019, O-F-O Triplet Injector	13 - 30

<u>Figure No.</u>		<u>Page No.</u>
152.	O-F-O Triplet Injector High Frequency Test Data (Chamber Length = 13.4-in.)	13 - 31
153.	Stability Rating Bomb Redesign	13 - 34
154.	Task III Revised Test Matrix	14 - 5
155.	Static Chamber Pressure (Inj. End), Test 015-032, Box-Doublet Injector	14 - 7
156.	Test 015-032 High Frequency Data	14 - 8
157.	Static Chamber Pressure (Inj. End), Test 015-033, Box-Doublet Injector	14 - 10
158.	Static Chamber Pressure (Inj. End), Test 015-034, Box-Doublet Injector	14 - 10
159.	Test 015-034 High Frequency Data	14 - 11
160.	Test 015-034 High Frequency Data	14 - 12
161.	PCB Adapter Design	14 - 14
162.	Static Chamber Pressure (Inj. End), Test 015-035, Box-Doublet Injector	14 - 14
163.	Test 015-035 High Frequency Data	14 - 15
164.	Test 015-035 High Frequency Data	14 - 16
165.	Test 015-035 PCB #4 Isoplot	14 - 17
166.	Test 015-035 PCB #5 Isoplot	14 - 17
167.	Predicted Cavity for Test 015-035	14 - 19
168.	Test 015-035 Acoustic Cavity Temperature	14 - 19
169.	Modified Task III Test Matrix	14 - 20
170.	Static Chamber Pressure (Inj. End), Test 015-036, Box-Doublet Injector	14 - 22
171.	Test 015-036 High Frequency Data	14 - 23
172.	Test 015-036 High Frequency Data	14 - 24
173.	Test 015-036 PCB #4 Isoplot	14 - 25

<u>Figure No.</u>		<u>Page No.</u>
174.	Test 015-036 PCB #5 Isoplot	14 - 25
175.	Static Chamber Pressure (Inj. End), Test 015-038, H-1 Derivative Injector	14 - 27
176.	Static Chamber Pressure (Inj. End), Test 015-039, H-1 Derivative Injector	14 - 27
177.	Static Chamber Pressure (Inj. End), Test 015-041, H-1 Derivative Injector	14 - 28
178.	Injector Droplet Size Comparison	14 - 30
179.	Injector Velocity Comparison	14 - 30
180.	Static Chamber Pressure (Inj. End), Test 015-042, Box-Doublet Injector	14 - 32
181.	Test 015-042 High Frequency Data	14 - 33
182.	Test 015-042 PCB #5 Isoplot	14 - 34
183.	Static Chamber Pressure (Inj. End), Test 015-043, Box-Doublet Injector	14 - 34
184.	Test 015-043 High Frequency Data	14 - 36
185.	Test 015-043 PCB #5 Isoplot	14 - 37
186.	Test 015-046 PCB #4 Isoplot	14 - 37
187.	Like Element LOX/RP-1 Time Lag Data	14 - 39
A-1.	Schematic of Pre-atomized Triplet Injector Element	A - 9
A-2.	Selection of Engine Cycle, Cooling Method and Injection Mode	A - 29
A-3.	Selection and Demonstration of Injection Concept	A - 34
A-4.	Technology Development Schedule	A - 35
B-1-A.	H-1 Derivative Injector, 3.5-inch Diameter, Sheet 1	B - 2
B-1-B.	H-1 Derivative Injector, 3.5-inch Diameter, Sheet 2	B - 3
B-2-A.	LOX Showerhead Injector, 3.5-inch Diameter, Sheet 1	B - 4
B-2-B.	LOX Showerhead Injector, 3.5-inch Diameter, Sheet 2	B - 5

<u>Figure No.</u>	<u>Page No.</u>
B-3-A. O-F-O Triplet Injector, 3.5-inch Diameter, Sheet 1	B - 6
B-3-B. O-F-O Triplet Injector, 3.5-inch Diameter, Sheet 2	B - 7
B-4-A. Like-Douplet, Circumferential-Fan Injector, 3.5-inch Diameter Sheet 1	B - 8
B-4-B. Like-Douplet, Circumferential-Fan Injector, 3.5-inch Diameter Sheet 2	B - 9
B-5-A. Like-Douplet, Box Pattern Injector, 3.5-inch Diameter, Sheet 1	B - 10
B-5-B. Like-Douplet, Box Pattern Injector, 3.5-inch Diameter, Sheet 2	B - 11
B-6-A. Like-Douplet, Canted-Fan Injector, 3.5-inch Diameter, Sheet 1	B - 12
B-6-B. Like-Douplet, Canted-Fan Injector, 3.5-inch Diameter, Sheet 2	B - 13
C-1. LOX/RP-1 Theoretical c^* with Heat Loss to Fuel	C-7
C-2. LOX/RP-1 Theoretical c^* with Heat Loss to Fuel	C-8

LIST OF TABLES

<u>Table No.</u>		<u>Page No.</u>
1.	Data Summary, Cold-Flow Mixing Tests	4 - 1
2.	Orifice Parameters of 3.5-inch, H-1 Derivative Injector	5 - 2 1
3.	Instrumentation List, 3.5-inch Injector Tests	5 - 3 8
4.	Digital Event Recorder Parameters	5 - 4 2
5.	Redline Parameters	5 - 4 4
6.	Performance Data Summary	5 - 4 6
7.	Heat Flux Data Summary	5 - 4 7
8.	Stability Data Summary	5 - 4 9
9.	Orifices in 5.7-inch Injector	6 - 7
10.	Instrumentation List, 5.7-inch Injector Tests	6 - 1 7
11.	High-Frequency Test Data	6 - 2 9
12.	Combustor Parameters	7 - 4
13.	Acoustic Cavity Slots for 2-D ICC	7 - 2 0
14.	Ignition, Instrumentation, and Bomb Locations	7 - 2 4
15.	Stability Analysis Results	10 - 2 3
16.	Summary of Task II 3.5-Inch Injector Tests	11 - 3
17.	Injector Configurations	11 - 3
18.	Stability Bomb Test Specimen Summary	13 - 3 3
A-1.	Production Engine LOX/RP-1 Injectors	A - 3
A-2.	LOX/RP-1 Test Data (Pavli, NASA Lewis, 1979)	A - 6
D-1	Hot-Fire Test Summary Table	D - 1

1.0 INTRODUCTION

1.1 BACKGROUND AND OBJECTIVE

Recent systems studies have indicated that high-pressure LOX/Hydrocarbon engines will be viable candidates for several foreseeable applications, such as boosters for new expendable earth-to-orbit vehicles. In particular, the LOX/RP-1 propellant combination would warrant consideration because of its high propellant bulk density and relatively high specific impulse*. Extensive experience with "classic" LOX/RP-1 engines, however, has shown that stable combustion may be very difficult to achieve simultaneously with high performance and acceptable levels of heat flux. Furthermore, existing LOX/RP-1 injector technology is not adequate to serve as the basis for development of a full-scale high-pressure engine injector. The objective of the present program, therefore, is to advance this technology to a level which can support development of a 750,000-lb-thrust engine, with the following functional goals: chamber pressure of 2000 to 2500 psia at 2.8 mixture ratio, minimum characteristic velocity efficiency of 97 percent, stable combustion (chamber pressure oscillations no greater than ± 5 percent of mean chamber pressure) and manageable heat flux.

1.2 TECHNICAL APPROACH AND PROGRAM LOGIC

The approach adopted in this program was based on the recognition that injector face baffles which, in effect, divide the combustion zone into a number of relatively small compartments, are essential for stable LOX/RP-1 combustion in large chambers and that such compartmentalization should be incorporated into the engine design from the outset. This can be accomplished by application of the Isolated Combustion Compartment (ICC) concept, in which the injector/combustion zone of a large engine consists of an assemblage of small compartments, or "cans". A typical compartment can be developed and demonstrated to exhibit the required stability, performance, and heat flux prior to assembly of multiple compartments into a full-scale combustor. The ICC concept development process is sketched in Figure 1.

* It was determined at the start of this study that there would be no advantage in considering heavy hydrocarbons other than RP-1 (such as JP-4 or gasoline) as fuels.

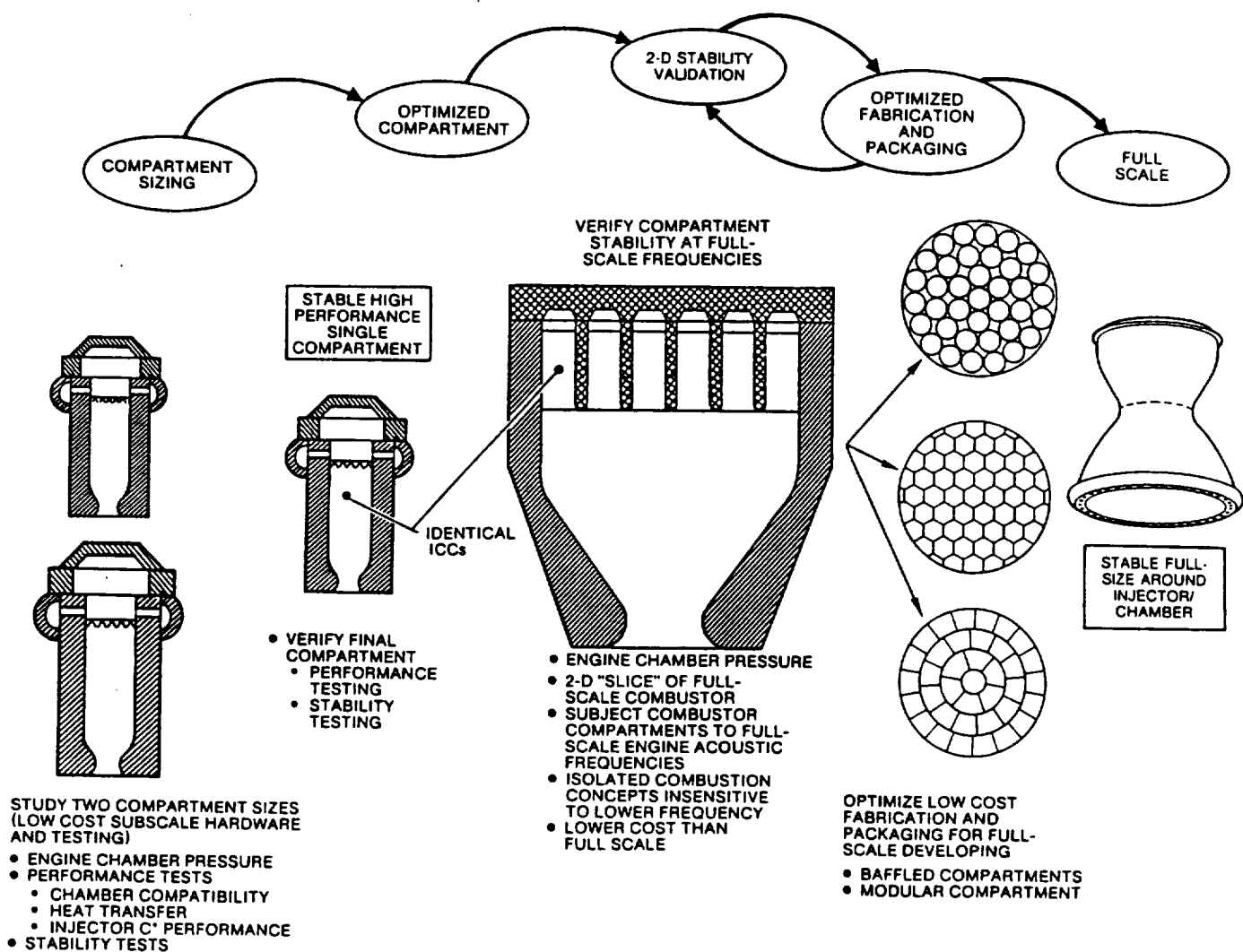


Figure 1. ICC Injector Development Logic

The overall program was organized into two phases. The first, Phase A, which included Task I and Task II, followed the logic plan illustrated in Figure 2:

1. LOX/RP-1 Injector Technology Review and Plan. Existing LOX/RP-1 main injector technology was reviewed, with emphasis on the effects of injector design on stability, performance, and heat flux. Technology deficiencies which would impede the development of a full-scale injector to meet the goals of an advanced engine were identified. A plan to generate the requisite technology advances was recommended.
2. Advanced Injection Concepts. Three applicable LOX/RP-1 injectors were available for test in this program from concurrent IR&D and contractual studies. Two other advanced injector designs were generated on the basis of stability, performance, and thermal analyses, cold-flow mixing tests of candidate patterns, and existing hot-fire test data and experience. The five injectors were tested at nominal conditions in a 3.5-inch-diameter calorimeter chamber to characterize their stability, performance, and heat flux.
3. ICC Injector. On the basis of the 3.5-inch injector test results, additional analyses, and produceability considerations, a pattern for a typical ICC-size injector (5.7-inch diameter) was selected; following design and fabrication of the injector and a calorimeter chamber, a series of tests was carried out to characterize the injector.
4. 2-D Combustor Design. The injection pattern of the 5.7-inch injector was adapted to a 2-D combustor incorporating five ICC units; a preliminary design for the 2-D combustor was generated.

The program continued in Phase B. The plan for Phase B had originally included the detail design and fabrication of the aforementioned 2-D combustor which was based on the 5.7-inch injector design. However, based on the 5.7-inch injector test results, it was determined that a greater benefit to LOX/RP-1 technology could be derived by conducting additional 3.5-inch subscale tests. Thus, with NASA's concurrence, Phase B was restructured to include in-depth stability analysis and hot-fire testing of subscale injectors with two major objectives:

TASK I - REVIEW AND PLANNING

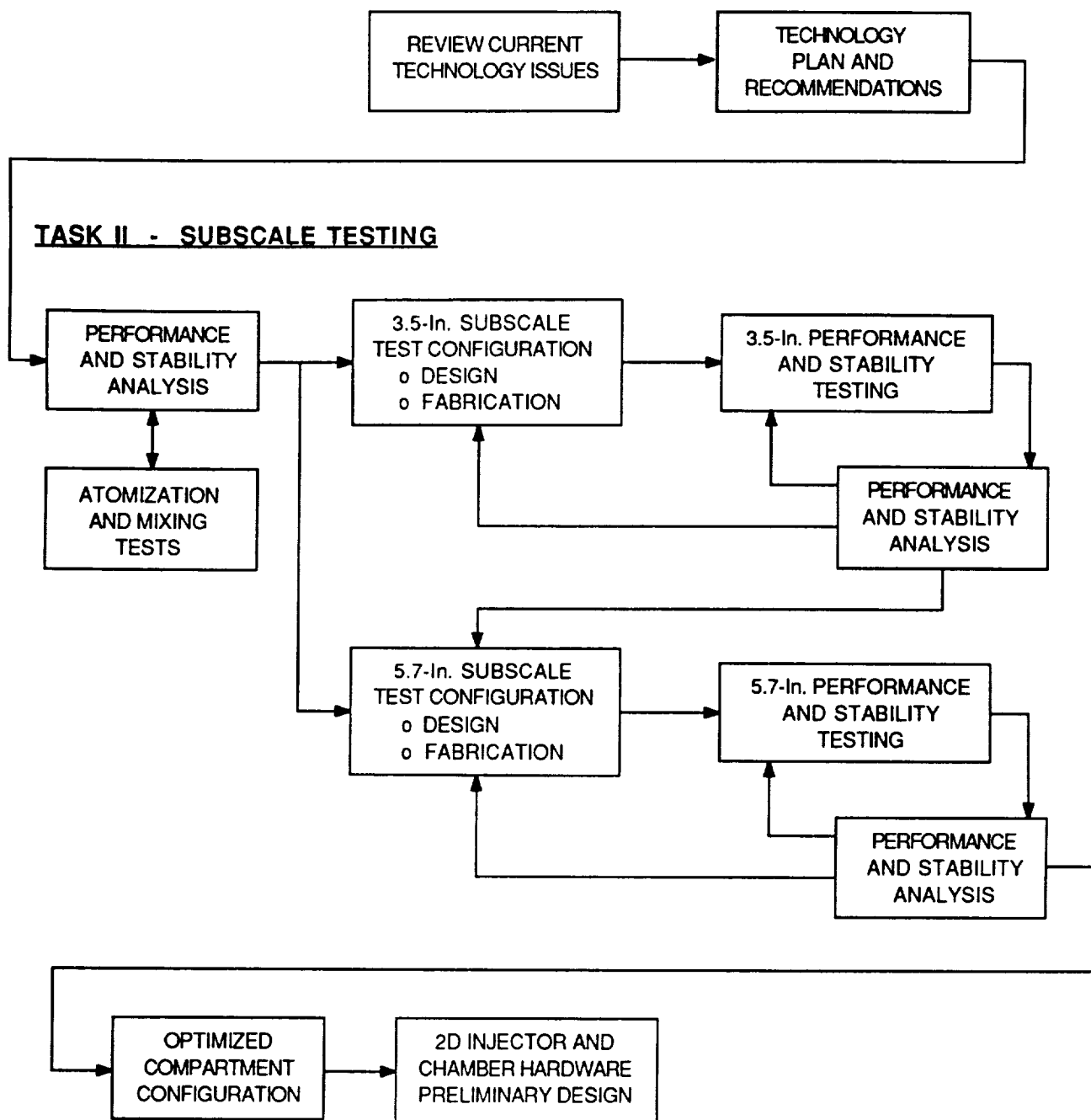
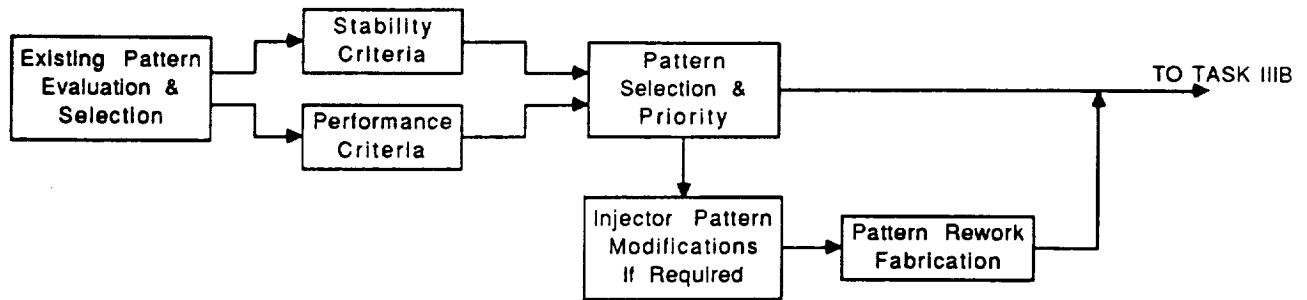


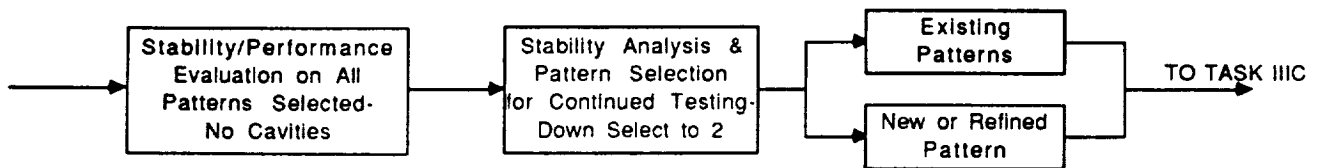
Figure 2. Phase A Program Flow Diagram

1. Characterize and develop a main injector element configuration, applicable to large booster engines, to be incorporated within a baffle compartment or Isolated Combustion Compartment (ICC) with appropriate acoustic damping.
2. Increase the generic technology base of the LOX/RP-1 propellant combination at high chamber pressures and, with the additional test data, improve existing stability and performance design and analysis techniques, as well as improve acoustic cavity design methodology.

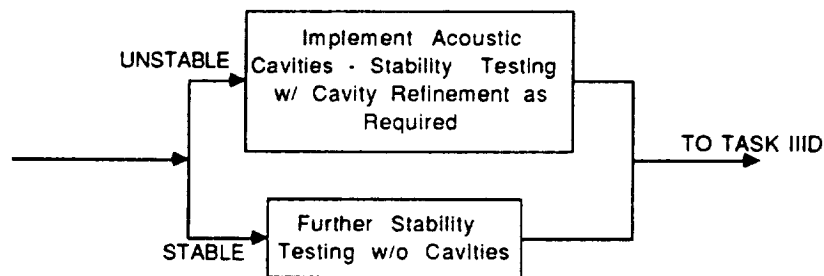
The logic diagram for the replanned Phase B, which was comprised only of Task III, is shown in Figure 3. The approach to the Phase B was to review the existing subscale test data with regards to stability and performance characteristics and, based on the results of this review, several injector configurations were selected for continued testing. Extensive analysis and testing was conducted on these injectors, including comprehensive acoustic cavity development. This effort was accompanied by the use of stability and performance analytical tools.



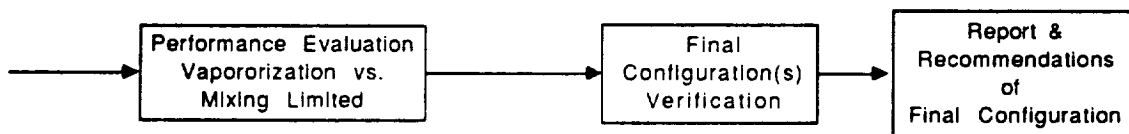
TASK IIIA - REVIEW & PLANNING



TASK IIIB - SCREENING TESTS



TASK IIIC - STABILITY EVALUATION



TASK IIID - PERFORMANCE EVALUATION

TASK IIIE - FINAL DOWN SELECT

Figure 3. Phase B Program Flow Diagram

2.0 PHASE A

Task I - Review and Planning

Task II - Subscale Testing

TASK I

3.0 INJECTOR TECHNOLOGY REVIEW AND PROGRAM PLAN

3.1 INTRODUCTION

This portion of the program effort consisted of two parts. In the first, the status of LOX/RP-1 injector technology was reviewed, primarily to identify technology deficiencies which would impede the development of an injector for a large (750,000-lb-thrust), high-pressure (2000-3000 psia), LOX/RP-1 engine. In the second part, a program plan to remedy these deficiencies was outlined, including any which may not be addressed in the present program, and possible time phasing of the various tasks was indicated.

Details of the technology review and program plan are given in Appendix A. A brief summary is presented below.

3.2 INJECTOR TECHNOLOGY REVIEW

The review discusses LOX/RP-1 injector technology in terms of the three basic combustor characteristics which are largely determined by injector design: performance, stability and heat flux.

3.2.1 PERFORMANCE

Results of the limited experimental work that had been carried out with LOX/RP-1 injectors at high chamber pressure (≥ 2000 psia) confirm the inherent difficulty of achieving high performance ($\eta_{c^*} \geq 97\%$) in combination with stable combustion and manageable heat flux levels. With like-impinging injection elements, reported c^* efficiencies (at $P_c = 2000$ psia and $M.R. = 2.8$) were in the 91-96 percent range; with unlike impinging elements, c^* efficiencies up to 100 percent had been reported, but the data were not unequivocal.

3.2.2 STABILITY

Available analytical methods could not reliably and consistently predict the damping capability of stability aids, particularly in regimes for which there were no anchoring test data. Neither could the tendency toward instability initiation of a given injection element be reliably predicted at untested operating conditions. Consequently, the likelihood that any injector type would initiate and sustain combustion instability must be predicted as well as possible from both test experience and analysis, and stability aids must be designed on the same basis. The combined effects of injector type and stability aids must be verified by hot-fire testing at the expected operating conditions.

The review showed that spontaneous and dynamic stability had been demonstrated with both like- and unlike-impinging LOX/RP-1 injection elements when used with suitable acoustic aids (baffles or cavities) at high chamber pressures.

3.2.3 HEAT FLUX

Chamber heat flux considerations can affect the design of a high pressure LOX/RP-1 injector in several ways. Analyses and background experience indicated that, at the start of this program, only a regeneratively cooled, high-strength copper alloy combustion chamber would be appropriate for this type of engine. Given that requirement, there were several factors and options that further influence the heat transfer aspects of injector design:

1. Use of RP-1 as regenerative coolant, without enhancement, limited chamber pressure to the 2000-psi range. Such enhancement techniques were not considered part of injector development technology.
2. Special considerations in the use of RP-1 as coolant related to coking, erosion and material compatibility. Again, these are important problems but were not considered as part of injector technology.
3. If RP-1 were used as a coolant, it would enter the injector manifold at elevated temperatures, which would be further raised as the RP-1 flows through the injector

face. This could affect injector design because hot RP-1 increases the possibility of progressive coking and blocking of orifices, particularly if the orifices are small.

4. Cooling with LOX is an alternative to cooling with RP-1. Limited experimental data indicated that such cooling is feasible. LOX cooling could also raise the maximum feasible chamber pressure compared to that with RP-1 cooling, although conflicting estimates had been reported in this regard. The important effect on injector design of using LOX as coolant would be the conversion to gas/liquid injection from liquid/liquid injection.
5. Hydrogen could also be used as chamber coolant. This would require a tri-propellant engine system and would permit chamber pressures possibly as high as 4000 psia. The effect on the main injector design of using hydrogen cooling depends on the particular engine system configuration.

3.3 TECHNOLOGY PLAN

The review of high pressure LOX/RP-1 injector technology showed that substantial technology advances would be required to meet the goals of high performance, stable combustion, and manageable heat flux.

Because of the potential difficulties associated with the use of RP-1 as a regenerative coolant in a high pressure combustion chamber, alternate cooling methods could be used. The injection process would then involve fluids other than LOX and liquid RP-1, even though the engine remains a LOX/RP-1 system. Depending on the choice of engine cycle and coolant, the main injector may alternatively be a gas/liquid type (GOX/RP-1) or a tri-propellant type (LOX/RP-1/GH₂), each depending on a technology base substantially different from that of a liquid/liquid injector. The first task of this injector technology plan was to choose an appropriate cooling technique for the selected LOX/RP-1 engine.

The injection type selection process is indicated in Figure 4. The choice of cycle for the LOX/RP-1 engine, the chamber pressure to be used and the injection mode was based on four factors:

- Mission requirements
- Engine cycle analyses
- LOX/RP-1 engine experience
- Available cooling methods.

Once the injector type was selected, the process of developing an injection configuration which optimizes performance, stability and heat flux would follow the course used in the present program. After study of the available analytical and experimental data, several candidate concepts were generated, designed into hardware and tested. This process, systematically applied, produced the configuration(s) which offer the best trade-offs of the targeted goals. A rough schedule for technology development is included in Appendix A.

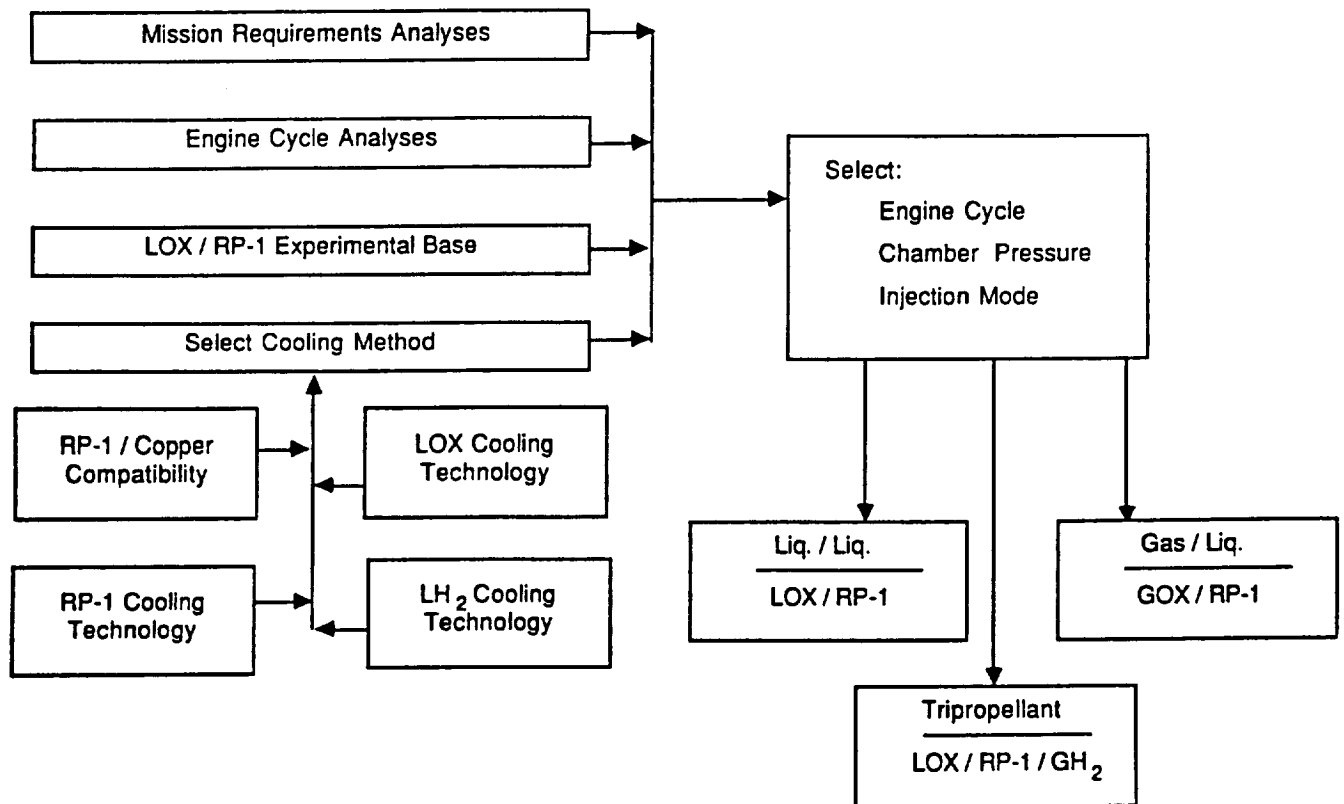


Figure 4. Selection of Engine Cycle, Cooling Method and Injection Mode

TASK II

4.0 MODEL INJECTOR COLD-FLOW TESTS

4.1 INTRODUCTION

A series of cold-flow mixing tests was performed with simulated propellants on five model injectors to determine their comparative mixing characteristics and mixing-limited c^* efficiencies. The models represented element configurations which were possible candidates for use in high-pressure, high-performance, LOX/RP-1 injectors. The mixing data were used to aid in the selection of patterns for the hot-fire injectors.

Descriptions of the cold-flow model injectors, test facility, and experimental procedures and a discussion of the experimental results and conclusions are presented in this section.

4.2 TEST INJECTORS

The five cold-flow injector models represented two basic injection concepts. The first concept, with two patterns, consisted of fuel spray fans impinging on showerhead oxidizer streams. The second concept, with three patterns, used like-impingement propellant spray formation, with subsequent interaction of the sprays.

The rationale underlying the oxidizer showerhead/fuel spray fan concept was improvement of combustion stability by extension of the reaction zone beyond the vicinity of the injector face. Delaying the atomization and vaporization of the oxidizer and encompassing the oxidizer stream with fuel simulates the generally successful gas/liquid coaxial injection concept.

The three like-impinging patterns are variations of a "box" type configuration of interacting oxidizer and fuel sprays. This concept has demonstrated very high c^* efficiency in storable propellant injectors. Basically, the first injection concept emphasizes improvement of stability while the second emphasizes improvement of performance.

4.2.1 INJECTOR MODELS

The injector models for the cold-flow tests were fabricated from transparent acrylic plastic, to give low-cost lightweight units which permitted visual inspection of the orifices and manifolds. The models were sized at twice the hot-fire scale; i.e., each model was a 2X photographic enlargement of a pattern which would be applicable to a 3.5-inch diameter, 2500-psia, LOX/RP-1 combustor. This gave a 0.75-inch model unit cell, or pattern repeat logic, for adequate resolution of the flow fields with the available collection grid. The hot-fire injectors have 0.375-inch unit cells and orifice diameters one-half those of their cold-flow counterparts.

The five cold-flow injector models are described as follows:

4.2.1.1 Injector No. 1 (Dwg. No. 7R035271)

This pattern (Figure 5) has showerhead oxidizer orifices, each associated with four, shared pairs of fuel doublets. The edges of the fuel spray fans impinge on the central oxidizer stream. The unit cell, indicated by the dashed-line, has a nominal orifice count of four fuel to one oxidizer.

4.2.1.2 Injector No. 2 (Dwg. No. 7R035274)

This pattern (Figure 6) is a box configuration with a like-impinging, central, oxidizer quadlet, which forms a star-shaped, four-armed spray. The flat sides of four, shared fuel spray fans formed by pairs of like-impinging doublets impinge on the cusps of the oxidizer spray star. This is the only test injector pattern of the five tested in which the unit cell boundary does not pass through any of the orifices.

4.2.1.3 Injector No. 3 (Dwg. No. 7R035273)

This is the second LOX quadlet configuration (Figure 7). It has the same 4-orifice, like-impinging oxidizer pattern at the center surrounded by four, shared pairs of like-impinging fuel doublets as Injector No. 2, except that the fuel fans now impinge edgewise between the cusps of the oxidizer spray. Although edge-impingement of the fuel fans on the cusps of the

LOX Showerhead (Box Pattern)

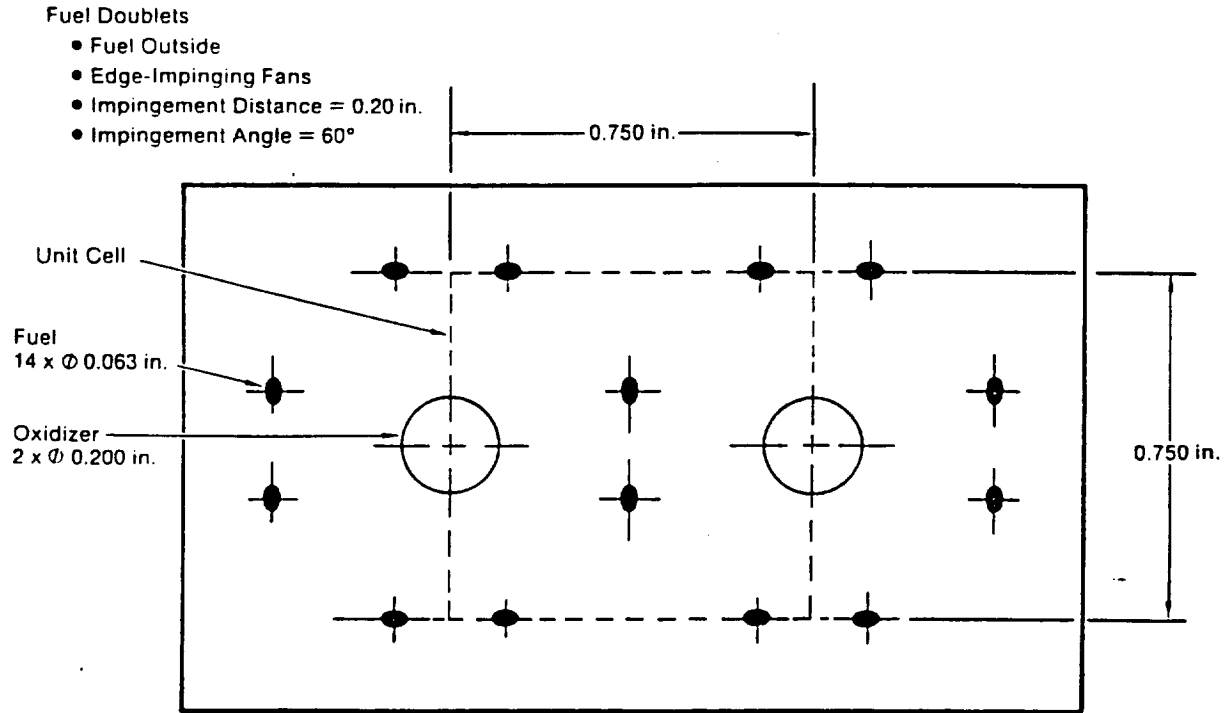


Figure 5. Injector Model No. 1

LOX Quadlet (Flat Fans)

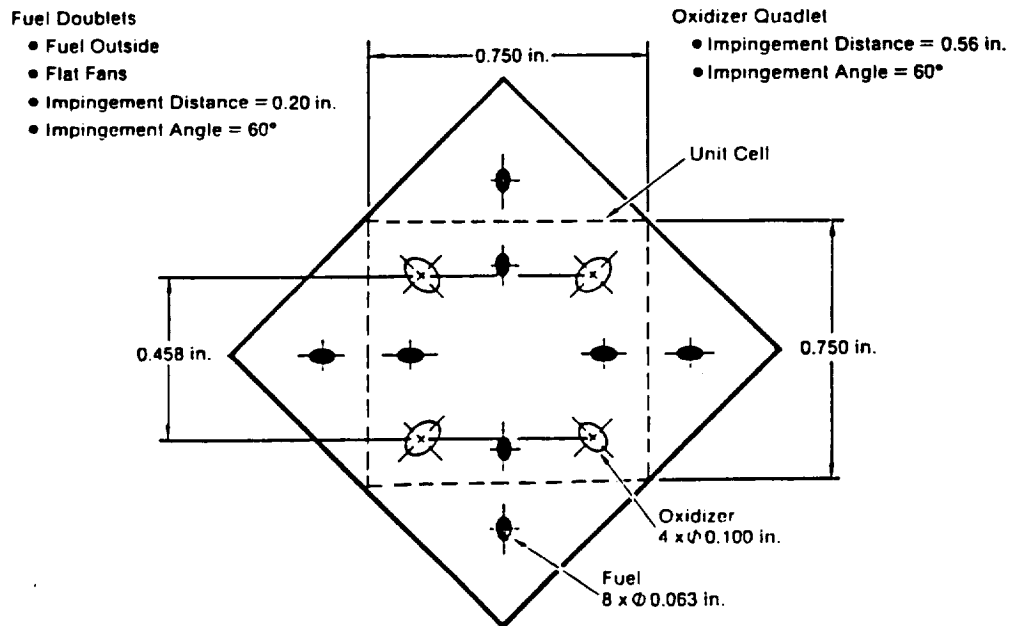


Figure 6. Injector Model No. 2

oxidizer star spray would probably be preferable, such a configuration would be difficult to manifold.

4.2.1.4 Injector No. 4 (Dwg. No. 7R035272)

This is the second LOX showerhead pattern (Figure 8). It differs from the first (Figure 5) in having six (shared) fuel doublets associated with each oxidizer orifice, in a hexagonal array. Again, the fuel spray fans impinge edgewise on the oxidizer stream. Use of six fuel fans per oxidizer stream instead of four should improve mixing efficiency.

4.2.1.5 Injector No. 5 (Dwg. No. 7R035275)

This is the "box doublet" configuration (Figure 9), with four (shared) like-impinging fuel doublets associated with each oxidizer doublet. The oxidizer doublets have alternating orientations in adjacent unit cells and the fuel fans are alternately edge-impinging and flat impinging on each oxidizer fan. This pattern has two fuel orifices for each oxidizer orifice.

4.3 EXPERIMENTAL

4.3.1 TEST FACILITY

The cold-flow mixing tests were carried out at the Rocketdyne Engineering Development Laboratory. A schematic of the flow facility is sketched in Figure 10. The propellant simulants (red-dyed 1,1,1-trichloroethane for LOX, water for RP-1) were supplied to the test injector from pressurized tanks through calibrated cavitating venturis, which functioned as flow-controllers and meters. Pressure measurements were made at the indicated locations.

The collection grid was a 13 by 20 array of square tubes, each with exterior dimensions of 0.125-in by 0.125-in and 0.005-in wall thickness. Each inlet tube was joined to a 50-ml graduated glass cylinder by Tygon tubing. A shutter over the cluster of tube inlets deflected the flowing liquids before and after the steady-state collection period.

LOX Quadlet (Edge Impinging)

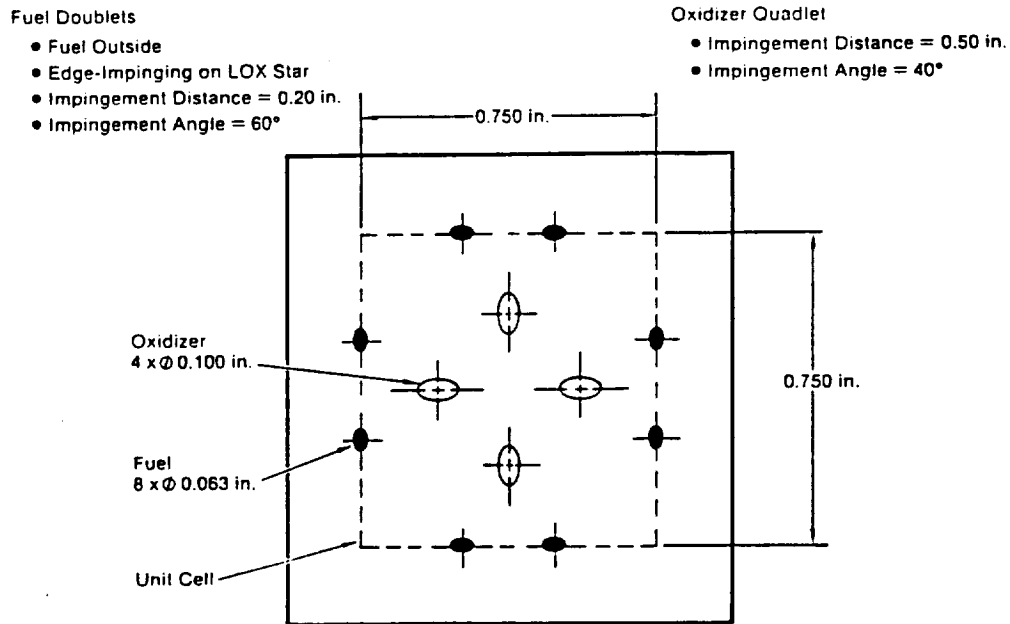


Figure 7. Injector Model No. 3

LOX Showerhead (Hex Pattern)

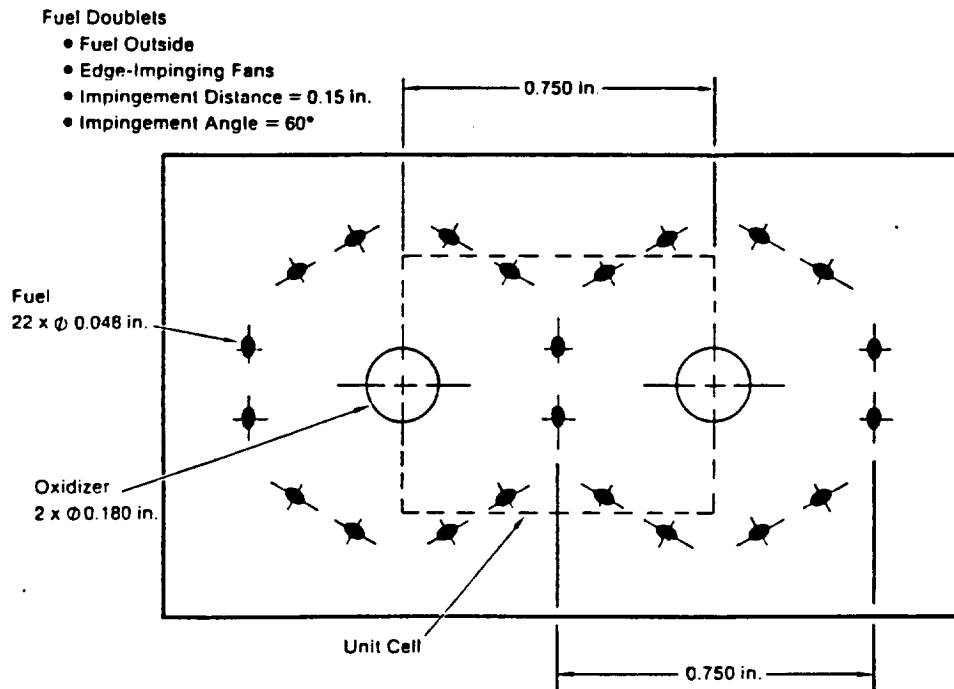


Figure 8. Injector Model No. 4

Box Pattern

Oxidizer and Fuel Doublets

- Alternating Edge-Impinging LOX Fans
- Impingement Distance = 0.325 in.
- Impingement Angle = 60°

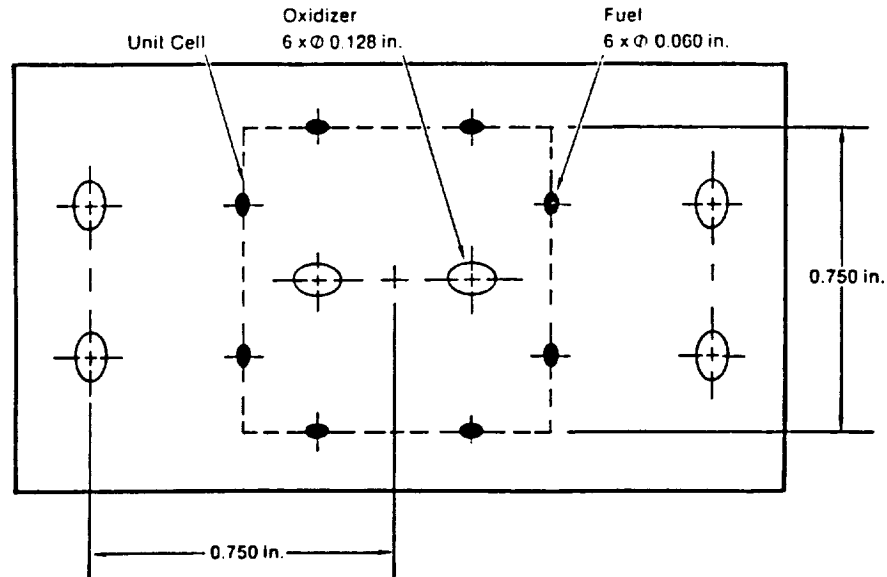


Figure 9. Injector Model No. 5

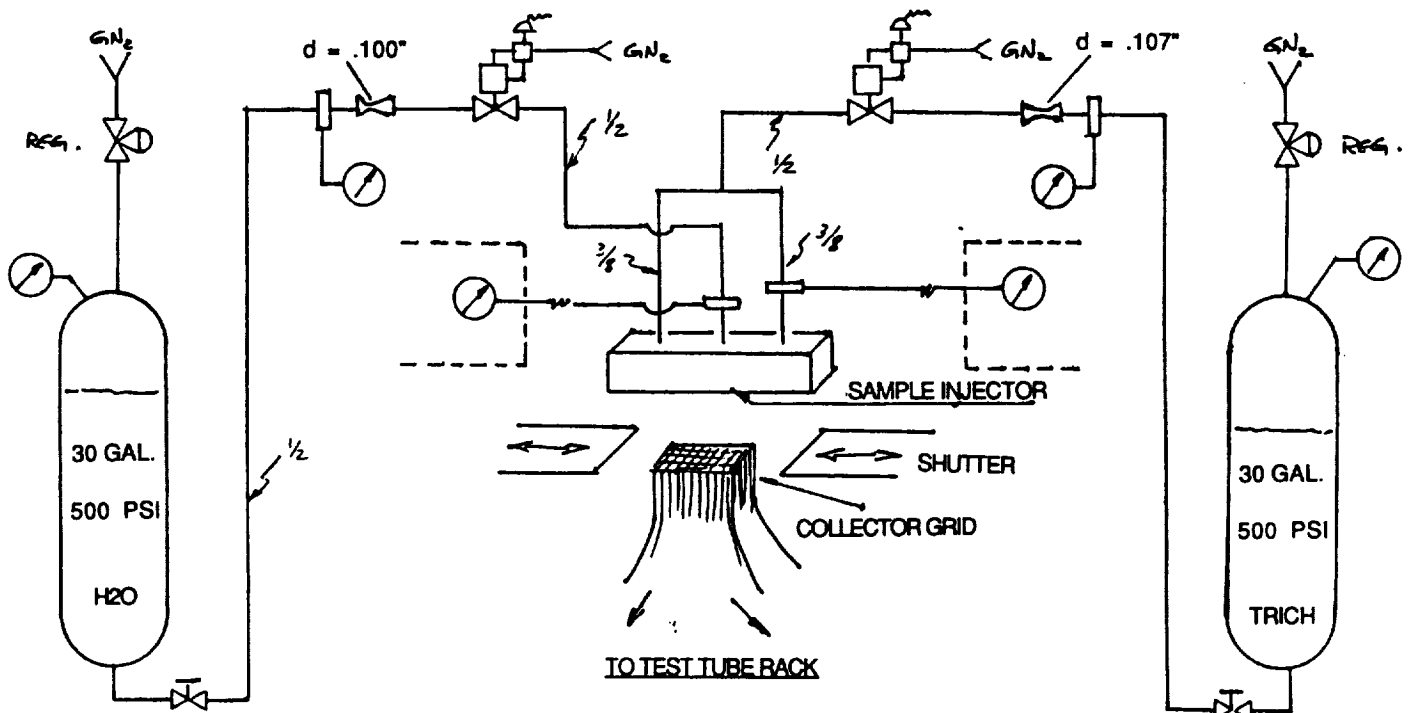


Figure 10. Cold-Flow Mixing Test Facility

4.3.2 TEST PROCEDURE AND DATA REDUCTION METHODS

4.3.2.1 Test Procedure

The injector being tested was mounted directly above the collection grid in an orientation which placed the 0.75-inch-square unit cell over a 6x6 array of tube inlets. To carry out a test, the main valves in each liquid line were opened simultaneously. After about six seconds of flow to establish steady state, the shutter over the tube inlets was opened very rapidly by pneumatic actuation. Sample collection time was about five seconds, after which the shutters were closed and the main valves shut. The volumes of trichloroethane and water in each of the 260 collection cylinders were read and recorded, together with liquid pressures and flowrates during the collection period.

The sampling distance (injector face to collection tube inlets) was 1.5 and 2.0 inches for each injector, to determine the effect of this parameter on mixing efficiency.

4.3.2.2 Simulant Liquid Flowrates

The mass flux of propellants through the injection orifices of an advanced, high-pressure, LOX/RP-1 combustor is too high for duplication in cold-flow mixing tests. To permit physical sampling of the simulant liquids and to avoid cavitation in injection orifices flowing to atmosphere, the simulant flowrates must be much lower than the corresponding propellant flowrates. Nevertheless, valid comparative data can be obtained in cold-flow mixing tests if the hot-fire propellant momentum and velocity ratios are duplicated by the simulants.

The density ratios of LOX/RP-1 and trichloroethane/water (1.33 and 1.32, respectively) are nearly identical. Consequently, the critical mixing parameters (mixture ratio, velocity ratio and momentum ratio) are the same in the unit cells of the cold-flow and hot-fire injection elements and they would therefore have the same mixing characteristics. However, the target mixture ratio (2.8) in the unit cells of the cold-flow injector models differs from the overall model injector mixture ratios because the latter must include the flows through orifices outside the unit cells.

4.3.2.3 Data Reduction

The 36 collection tubes directly under the 0.75-inch-square unit cells of the model injectors received the bulk of the liquid flows. It was found, however, that limiting the data reduction to this 6x6 unit cell grid was not satisfactory because the sprays diverged after formation and a larger grid was required to collect all the liquids from the unit cells. Effective sampling areas were therefore delineated on the basis of the observed mass flux in the collection tubes and correlation of the measured unit cell mass flux with the actual fluid flowrates. This resulted in coherent and reproducible reduced data.

4.3.3 TEST RESULTS

4.3.3.1 Mixing Efficiency Parameters

The mixing efficiencies of the model injectors are presented in two ways. The first uses the Rupe mixing efficiency index, E_m , which is a mass-weighted summation of the variations of local mixture ratios* from the overall average mixture ratio (Ref. 1). For computation, the index is given by the following expression:

$$E_m = 1 - \sum_i^N MF_i \frac{R-r_i}{R} - \sum_i^{\bar{N}} MF_i \frac{R-r_i}{R-1} \quad (1)$$

where

- MF_i = mass fraction in i^{th} tube, $\frac{\text{total mass in tube}}{\text{total mass collected}}$
- R = overall mixture ratio
- r_i = mixture ratio in i^{th} tube
- N = number of tubes in which $r_i < R$
- \bar{N} = number of tubes in which $r_i > R$

* In connection with E_m calculations, the term "mixture ratio" is the mass fraction of oxidizer (W_o/W_T) rather than the usual W_o/W_F .

For tubes in which $r_i = R$, each of the summation terms in Eq. 1 is identically zero. But where $r_i \neq R$, one of the summation terms is employed (depending on whether $r_i >$ or $< R$), subtracting an appropriate quantity from unity. The quantity subtracted depends on both the difference between the sample mixture ratio and the overall mixture ratio and the mass fraction of the sample. Thus, E_m is a measure of the fraction of the total spray which achieved the injected overall mixture ratio. This index has no direct relationship to the hot-fire characteristics of specific propellants; it is merely a measure of the degree of mixing uniformity of the simulant liquids. When E_m is unity, all the collected samples have the same mixture ratio; when E_m is zero, all the samples contain only one of the unmixed liquids.

The second method of expressing mixing efficiency uses the "mixing limited c^* " parameter, which refers to a specific propellant combination. It is computed as a mass-weighted, single stream tube, performance model and sums the products of collected sample mass and the theoretical c^* value at the collected mixture ratio:

$$\text{Mixing-limited } c^* = \sum_i \frac{M_i c^*_i}{M_T} \quad (2)$$

where

M_i = mass of simulant liquids in i^{th} tube

c^*_i = theoretical c^* at mixture ratio in i^{th} tube

(based on combustion performance calculations)

M_T = total collected mass of simulant liquids

The mixing-limited c^* efficiency is the ratio of this value to the theoretical c^* at the overall mixture ratio:

$$\text{Mixing-limited } c^* \text{ efficiency} = \frac{\text{Mixing-limited } c^*}{\text{Theoretical } c^*} \quad (3)$$

This efficiency is usually significantly higher than E_m . It is impacted by the shape of the c^* -mixture ratio curve and the overall mixture ratio and is a good indication of the effect of mixing deficiencies on hot-fire performance.

4.3.3.2 Test Data

Mixing test data for the injector models are summarized in Table 1. "Total Simulant Flow" is the flow through the entire model; the unit cell characteristics were obtained from the listed grid matrices. In all tests, the targeted unit cell mixture ratio was 2.8.

Injector No. 1 (LOX showerhead, four fuel spray fans). This configuration is a good example of the concept of delaying oxidizer atomization and vaporization while surrounding it with atomized fuel. The edge impingement of the fuel sprays on the oxidizer stream promotes the oxidizer atomization and the LOX/fuel mixing processes. The fine spray resulting from the small fuel orifices improves fuel vaporization, so that, overall, the oxidizer and fuel vaporize at more nearly comparable rates than in impinging-oxidizer-stream injector patterns, which give oxidizer-rich, extremely reactive zones close to the injector face.

The cold-flow data support the anticipated low mixing efficiency of this configuration, demonstrating that the fuel simulant does indeed surround the oxidizer stream, with an adverse effect on mixing. Increasing the sample collection distance from 1.5 to 2.0 inches showed a significant increase in mixing efficiency. Since the models are twice scale, the 2-inch distance corresponds to 1-inch in a hot-fire injector. The extent of diffusion mixing (as against momentum-related mixing) is relatively limited, so this element configuration would require fairly close spacing to give high combustion efficiency in moderate length chambers. The 0.375-inch pitch in a hot-fire injector would be reasonable for satisfactory performance in an 18- to 24-inch chamber.

Injector No. 2 (LOX quadlet, flat-impinging fuel fans). Injectors No. 2 and 3 are variations of a configuration of fuel spray fans outside a central, star-shaped, oxidizer spray produced by four streams impinging at a single point. The four points, or cusps, of the oxidizer "star" are located between adjacent impinging streams. In Injector No. 2, the fuel fans are oriented to produce flat impingement on the oxidizer cusps. This pattern was designed to provide better oxidizer atomization than in the LOX showerhead configuration as well as better mixing. The test data indicate, however, that the mixing efficiency of the LOX quadlet pattern is lower than those of the LOX showerhead designs. In addition, Injector No.

TABLE 1. DATA SUMMARY, COLD-FLOW MIXING TESTS

INJECTOR MODEL	TEST NO.	COLLEC. DIST., IN	TOTAL SIMULANT FLOW			UNIT CELL CHARACTERISTICS				
			OXID., LB/SEC	FUEL, LB/SEC	O/F	GRID MATRIX	O/F	E_m	C* MIX EFF.	
									MEAS.	AVG.
<u>INJECTOR NO.1</u> LOX SHOWERHEAD WITH FOUR EDGE-IMPINGING FUEL FANS ("BOX" PATTERN)	1 - 2	1.5	0.88	0.55	1.60	6 x 7 14 x 8	2.65 3.12	0.49 0.48	0.69 0.70	0.69
	1 - 3	2.0	0.88	0.55	1.60	6 x 7 14 x 7	3.12 3.22	0.59 0.58	0.78 0.77	0.78
<u>INJECTOR NO.2</u> LOX LIKE-QUADLET WITH FLAT-IMPINGING FUEL FANS	2 - 1	1.5	0.44	0.32	1.38	8 x 8 9 x 9	4.11 3.39	0.42 0.38	0.68 0.63	0.65
	2 - 2	2.0	0.44	0.32	1.38	8 x 8 9 x 9	3.76 3.07	0.32 0.30	0.60 0.54	0.57
<u>INJECTOR NO.3</u> LOX LIKE-QUADLET WITH EDGE-IMPINGING FUEL FANS	3 - 1B	1.5	0.44	0.32	1.38	7 x 7 8 x 8	3.12 2.58	0.49 0.46	0.70 0.68	0.69
	3 - 2	2.0	0.44	0.32	1.38	7 x 6 7 x 7	2.82 2.57	0.61 0.59	0.78 0.77	0.78
<u>INJECTOR NO.4</u> LOX SHOWERHEAD WITH SIX EDGE-IMPINGING FUEL FANS ("HEX" PATTERN)	4 - 1	1.5	0.88	0.58	1.52	7 x 7 14 x 8 7 x 8	2.93 2.68 2.77	0.66 0.64 0.66	0.82 0.81 0.82	0.82
	4 - 2	2.0	0.88	0.58	1.52	7 x 7 14 x 8	3.03 2.79	0.54 0.51	0.74 0.71	0.72
<u>INJECTOR NO.5</u> CENTRAL LOX LIKE-DOUBLET WITH EDGE-IMPINGING FUEL FANS ("BOX" PATTERN)	5 - 1B	1.5	0.88	0.21	4.19	7 x 7 8 x 8	3.02 2.89	0.68 0.69	0.84 0.85	0.84
	5 - 2	2.0	0.88	0.21	4.19	7 x 7 8 x 8	3.30 3.00	0.80 0.81	0.93 0.93	0.93

2 showed lower mixing efficiency at the 2.0-inch distance than at the 1.5-inch distance, but this anomaly was not investigated because this pattern was not considered for hot-fire evaluation.

Injector No. 3 (LOX quadlet, edge-impinging fuel fans). This is the same concept as Injector No. 2 except that the fuel fans now impinge edgewise between the cusps of the oxidizer spray. Although the mixing efficiency of Injector No. 3 was higher than that of No. 2, it was at about the same level as the LOX showerhead pattern (No. 1), in spite of considerably greater complexity. This concept was also eliminated as a candidate for hot-fire evaluation.

Injector No. 4 (LOX showerhead, six fuel spray fans). This pattern is similar to Injector No. 1, but has two more fuel fans per oxidizer stream, with the same edgewise impingement. The mixing efficiency of Injector No. 4 was significantly higher than that of No. 1 at the 1.5-inch distance, but decreased at the 2.0-inch distance. If real, the better mixing at the closer distance may indicate that the higher number of fuel fans, even with lower flowrates per fuel orifice, improves mixing because of more intersections with the oxidizer stream. As in Injector No. 2, the lower mixing efficiency at the greater sampling distance appears anomalous, but since the LOX showerhead concept would be evaluated in hot-fire tests by Injector No. 1 (because of the difficulty of manifolding No. 4), this behavior was not investigated further.

Injector No. 5 ("Box" doublet). This configuration has a single oxidizer doublet in each box, with a fuel doublet on each of the four sides of the box. The mixing efficiency of this pattern was the highest of the five tested, with correspondingly high mixing-limited c^* efficiency. With two fuel orifices for each oxidizer orifice, the latter are large enough to delay oxidizer vaporization significantly. Use of like-impingement oxidizer doublets allows variations of the oxidizer stream impingement angle and distance to be made to tailor the oxidizer atomization and vaporization characteristics for high performance. It may be noted that a reverse configuration of this box pattern (fuel inner doublet surrounded by oxidizer doublets on the sides of the box) has demonstrated very high performance levels as well as dynamically stable combustion with storeable propellants (NTO/MMH) on Rocketdyne's XLR-132 program.

4.4 INJECTOR PATTERN SELECTION

The cold-flow mixing study of five injector models aided in the selection of patterns for the hot-fire LOX/RP-1 testing. The LOX showerhead/fuel spray fan concept had the attributes for which the design was intended and exhibited higher levels of mixing efficiency than might have been expected. The configurations with central LOX quadlet elements had poorer mixing characteristics than anticipated, and were no better than the LOX showerhead patterns at equal sampling distances. The box like-doublet pattern data verified the high level of mixing predicted for it. The cold-flow mixing test results indicated, therefore, that the simple LOX showerhead and the box doublet configurations should be included in the patterns chosen for hot-fire evaluation.

TASK II

5.0 ANALYSIS, DESIGN AND TEST OF 3.5-INCH INJECTORS

5.1 INTRODUCTION

At the time that this task was started, the existing data base for high-pressure LOX/RP-1 injectors was limited (see Appendix A). To augment this base prior to selection of an injection concept for an ICC injector, a series of hot-fire tests was performed to evaluate five injector patterns in a 3.5-inch combustor. Following acoustic analyses of various types of injectors, the concepts to be tested were chosen on the basis of their perceived potentials of satisfying the performance, heat flux, and stability goals previously discussed. A test combustor to provide the requisite experimental data was designed and fabricated as part of the test effort.

This section of the report discusses the acoustic analyses, selection of the injector concepts to be tested, design of the 3.5-inch combustor components, and the test facility and procedures. The test results are then presented and discussed in terms of their application to the selection of an injection concept for the 5.7-inch combustor, which was the prototype of the ICC for the 2-D conceptual design.

5.2 ACOUSTIC ANALYSES

Acoustic stability analyses by the "sensitive time lag" technique were carried out for several candidate injectors in a 3.5-inch-diameter chamber, with and without acoustic cavities. For comparison, analyses were also conducted for an Aerojet injector used in LOX/RP-1 tests in a 7.68-inch-diameter chamber. In addition, the stability potentials of the injectors were rated by the Webber stability correlation. The injectors and acoustic cavities used in these analyses and the analytical methodologies and results are discussed in this section.

5.2.1 INJECTORS AND ACOUSTIC CAVITIES

Analyses were performed on the following eight injection patterns, five of which were tested in the cold-flow mixing tests previously discussed.

5.2.1.1 Injector Pattern No. 1 (Figure 5)

In this pattern, showerhead oxidizer orifices interact with four, shared edge-impinging fuel fans.

5.2.1.2 Injector Pattern No. 2 (Figure 6)

This pattern consists of an oxidizer quadlet, which forms a star-shaped spray, with the flat side of a (shared) fuel fan impinging on each cusp of the oxidizer spray.

5.2.1.3 Injector Pattern No. 3 (Figure 7)

This pattern has an oxidizer quadlet similar to that in Injector No. 2 with four, shared fuel fans edge-impinging between the cusps of the oxidizer spray star.

5.2.1.4 Injector Pattern No. 4 (Figure 8)

This is a showerhead oxidizer element, as in Injector No. 1, with six, shared fuel fans edge-impinging on each oxidizer stream instead of four.

5.2.1.5 Injector Pattern No. 5 (Figure 9)

This is a "box" pattern of like-impinging doublets, in which four, shared fuel spray fans impinge on each oxidizer fan, with alternating edge and flat impingement.

5.2.1.6 Injector Pattern No. 6 (Figure 11)

This injector, derived from the H-1 pattern, has alternating rings of like-impinging doublets and triplets, typical of the early LOX/RP-1 production-type injectors.

5.2.1.7 Injector No. 7

This is a hypothetical 3.5-inch-diameter, 24-element, O-F-O triplet pattern, with a characteristically short combustion zone and 0.10-inch oxidizer and fuel orifice diameters.

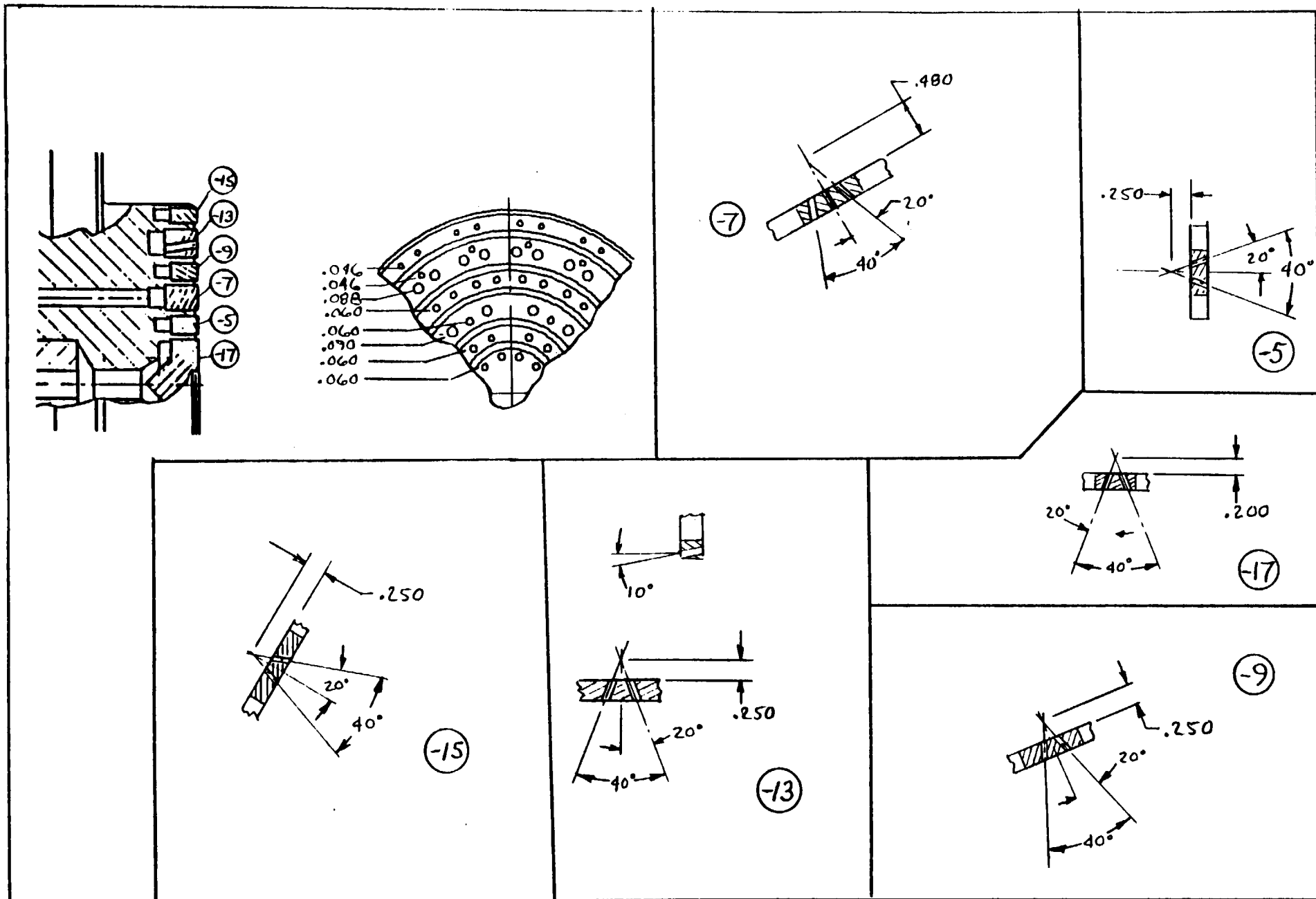


Figure 11. Injector No. 6, Like-Impinging Elements, Ring Configuration

5.2.1.8 Injector No. 8

This 7.68-inch-diameter injector has 39 O-F-O triplet elements, with 0.125-inch diameter oxidizer and fuel orifices. It was designed and tested by Aerojet TechSystems Company in a LOX/RP-1 combustor (Ref. 2).

Two axially-oriented acoustic cavity configurations, which had only very minor differences, were used in the analyses. They were designated "IR&D" and "Contract A", and are described in Figure 12.

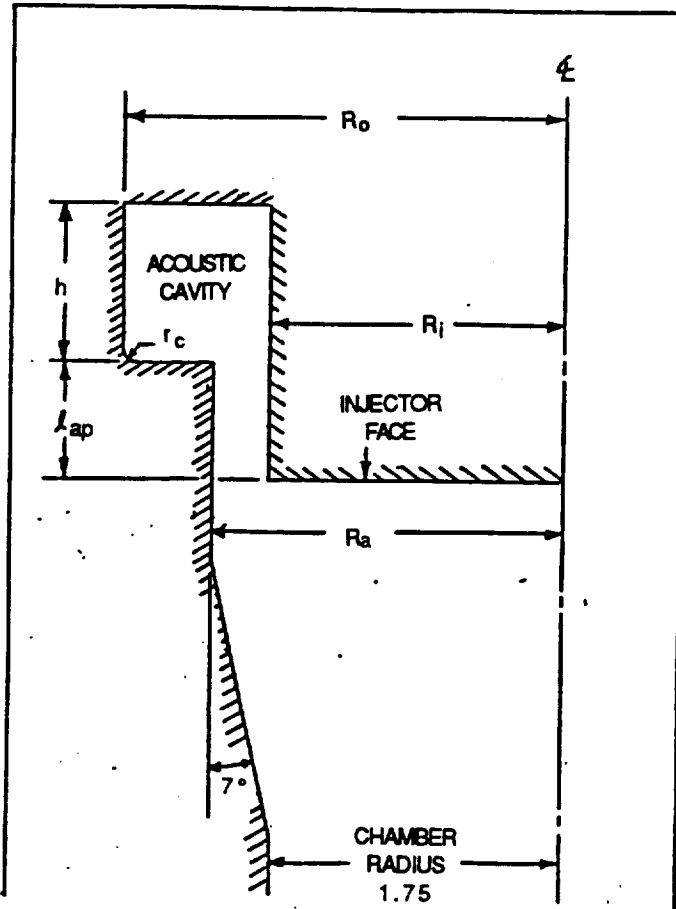
5.2.2 SENSITIVE TIME LAG ANALYSES

5.2.2.1 Methodology

The acoustic analyses were based on the sensitive time lag or "n-tau" theory (Ref. 3), for which a well-developed computer code is available (Ref. 4). Program input values included: chamber pressure of 2000 psia, acoustic cavity gas temperature equivalent to 60-percent of chamber temperature, and combustion zone lengths varying from 0.2 to 12 inches, depending on the injection pattern. Combustion zone length is defined as the distance between the injector face and the plane at which combustion ends, with linear release of combustion products up to that plane. The code computes the neutrally stable, or borderline, combustion response for the given injector/chamber combination, in the form of a pressure interaction index, n , as a function of the sensitive time lag (τ). During early studies of combustion instability, Crocco (Ref. 5) speculated that even though unstable combustion was a function of several combustion chamber variables, the general understanding could be correlated to unsteady pressure. The relationship between the combustion response, n and τ , and unsteady pressure and mass flow is given in the following equation:

$$N = \frac{\dot{w}' \bar{P}_c}{\bar{w} P_c'} = n (1 - e^{-i\omega\tau})$$

(where N is the chamber response, w is flowrate, P_c is chamber pressure, variables denoted with a prime are unsteady components of the variable, and variables denoted with a bar are steady state values)



Acoustic Cavity	IR&D	Contract A
Part Number	7R034085-11	7R034085-21
Open Area (Based on Injector Face Area), %	26	22
R_o , in	2.095	2.04
R_i , in	1.554	1.598
R_a , in	1.81	1.81
h , in	0.475	0.32
l_{ap} , in	0.300	0.305
Number of Dams	7	7
Dam Width, in	0.17	0.17
Dam Fillet Radius, in	0.09	0.09
Corner Radius, r_c , in	0.09	0.09

Figure 12. Dimensions of Acoustic Cavities

From a feedback loop perspective, n would be the response amplitude and τ can be interpreted as the response phasing.

Injector response was estimated from standardized empirical correlations of experimental data, shown in Figures 13 and 14 (from Ref. 6), in which:

d_i = Orifice diameter of rate-controlling propellant (RP-1, in the LOX/RP-1 combination).

M_c = Chamber Mach number at start of convergence

τ = Sensitive time lag

β_p = Pressure dependence factor; $\beta_p = 1.0$ when reduced chamber pressure (P_c/P_{crit}) of rate-controlling propellant is greater than unity (P_{crit} of RP-1 is 310 psia)

The injector response was plotted (as small rectangles, to include estimated error bands) on the same figure as the combustor response. On the n - τ plane, injector responses which lie above the parabola-shaped neutral stability curve (the "chamber transfer function") indicate linear growth of the oscillations, or instability; conversely, injector responses below the chamber transfer function indicate oscillatory decay, or stability.

5.2.2.2 Analytical Results

Responses of the LOX showerhead patterns (Injectors No. 1 and 4) are shown in Figure 15, with and without the "Contract A" acoustic cavities. The ratio of the combustion zone length to chamber radius (Z_c/r_{ch}) was set at 6.86. This is a estimated value, corresponding to the extended combustion length characteristic of these patterns ($Z_c = 12$ in). Both injectors are predicted to be unstable without acoustic cavities. The calculations of combustion responses with the acoustic cavities are incomplete, as shown, because of convergence problems in the code which are associated with longitudinal modes whose combustion responses are close to, or overlap, the first tangential mode. Thus, the two lowest points on the acoustic cavity curve correspond to a combination of the 1T and 1L modes, as indicated. However, extrapolation with a "knee" typical of n - τ curves indicates that the injectors would probably be stable with acoustic cavities.

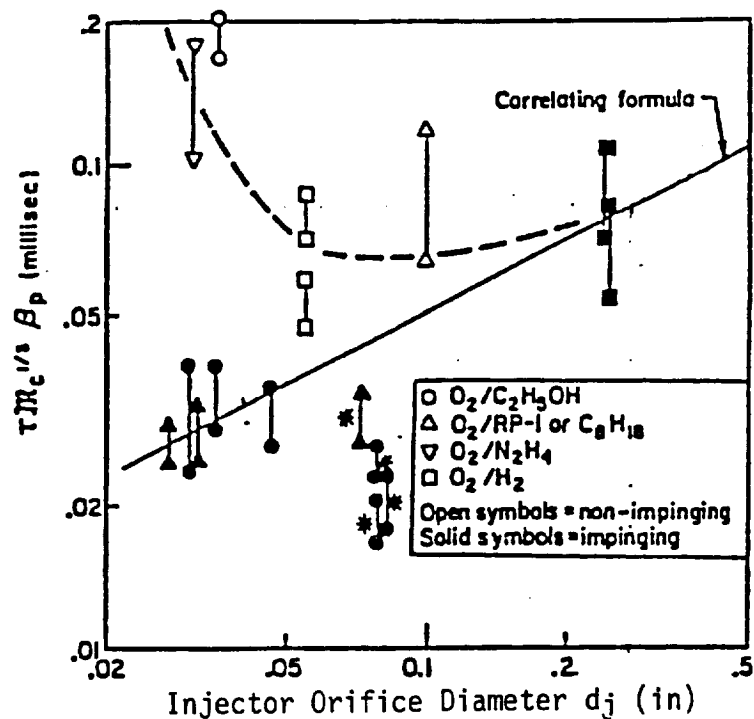


Figure 13. Sensitive Time Lag Correlation, Non-Coaxial Injectors, Non-Hypergolic Propellants (Ref. 6)

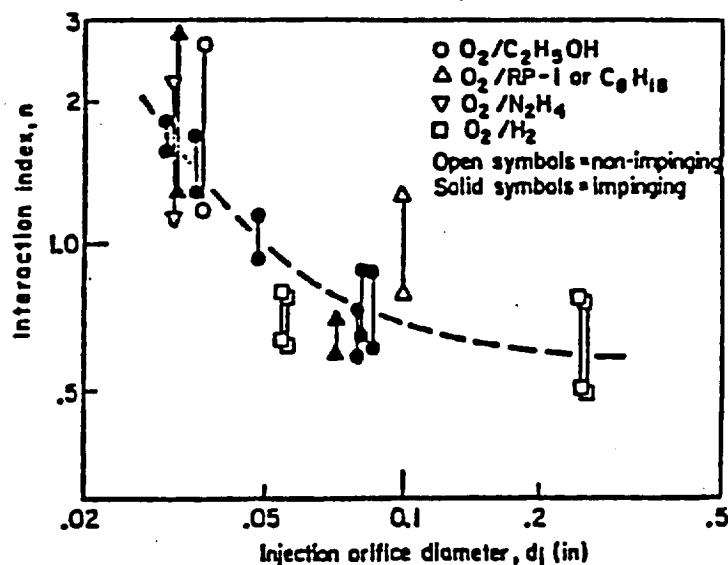


Figure 14. Pressure Interaction Index Correlation, Non-Coaxial Injectors, Non-Hypergolic Propellants (Ref. 6)

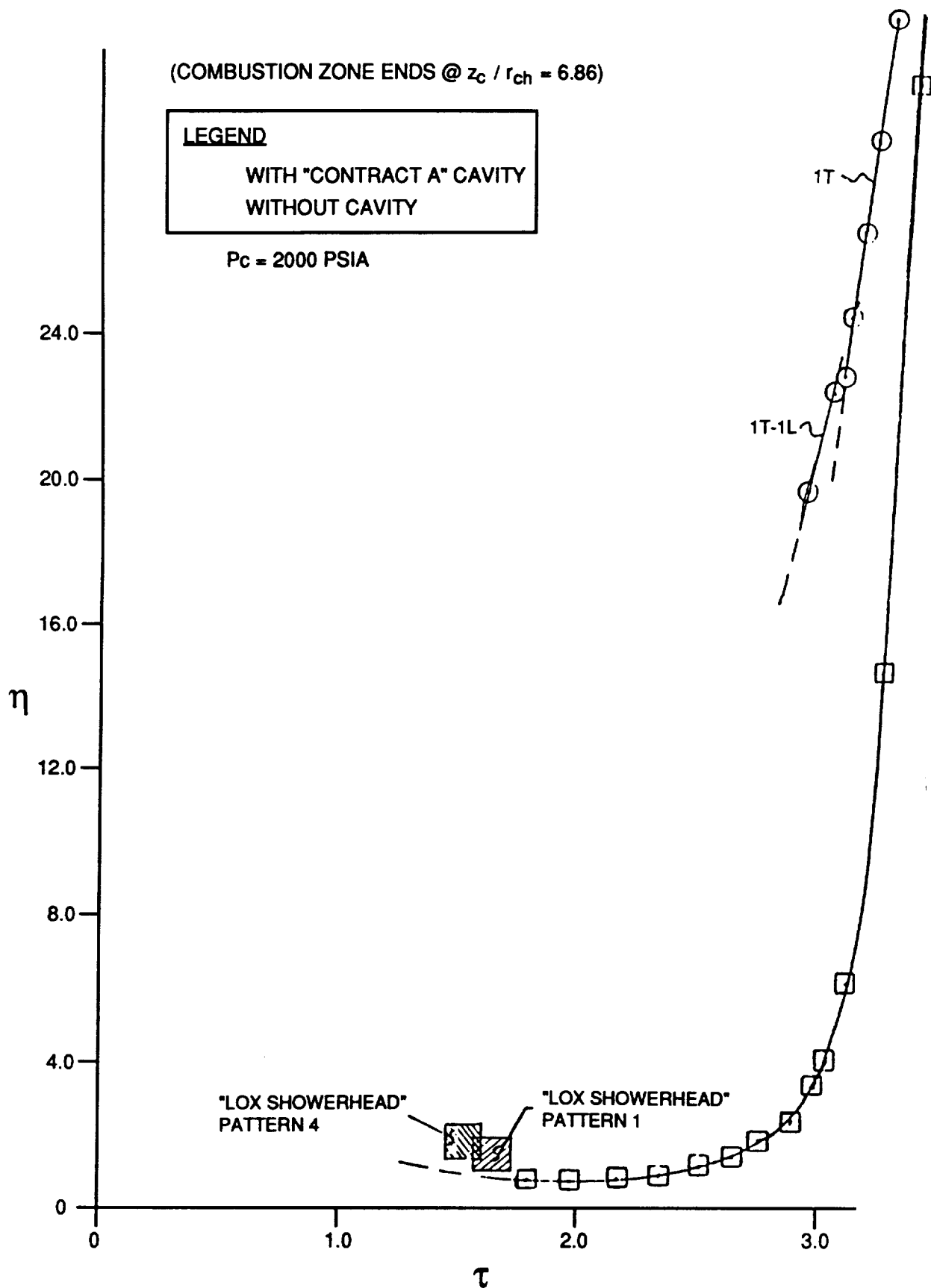


Figure 15. Response Curves of LOX Showerhead Injectors (No. 1 and 4), With and Without "Contract A" Acoustic Cavities

Response curves of the LOX quadlet patterns (Injectors No. 2 and 3) are shown in Figure 16, for a combustion zone length of 1.75 inches. The results indicate that both injectors would be stable with the "Contract A" acoustic cavities and unstable without them.

Results for Injector No. 5, the "box" pattern of impinging like-doublers, are plotted in Figure 17, for a 1.75-inch combustion zone. Again, the calculations indicate that this injector would be stable with "Contract A" acoustic cavities and unstable without them.

Response curves for the like-impinging ring-type injector (No. 6) are shown in Figure 18. This injector is predicted to be marginal without the "IR&D" acoustic cavities and stable with the cavities. As with the LOX showerhead injectors, the cavity computation is incomplete due to convergence problems associated with overlapping longitudinal modes.

The triplet injector (No. 7) responses are shown in Figure 19. Stability is predicted even without "Contract A" acoustic cavities.

Responses of the large-diameter O-F-O triplet injector (No. 8) are plotted in Figure 20 for the 20-inch chamber length, with and without two different 1T-tuned cavities (14- and 25-percent open areas). The Aerojet predictions are also indicated. The system is predicted to be marginal without cavities and stable with cavities.

The general conclusion of the sensitive time lag analyses is that all the patterns examined were predicted to be stable with acoustic cavities and marginally stable or definitely unstable without cavities.

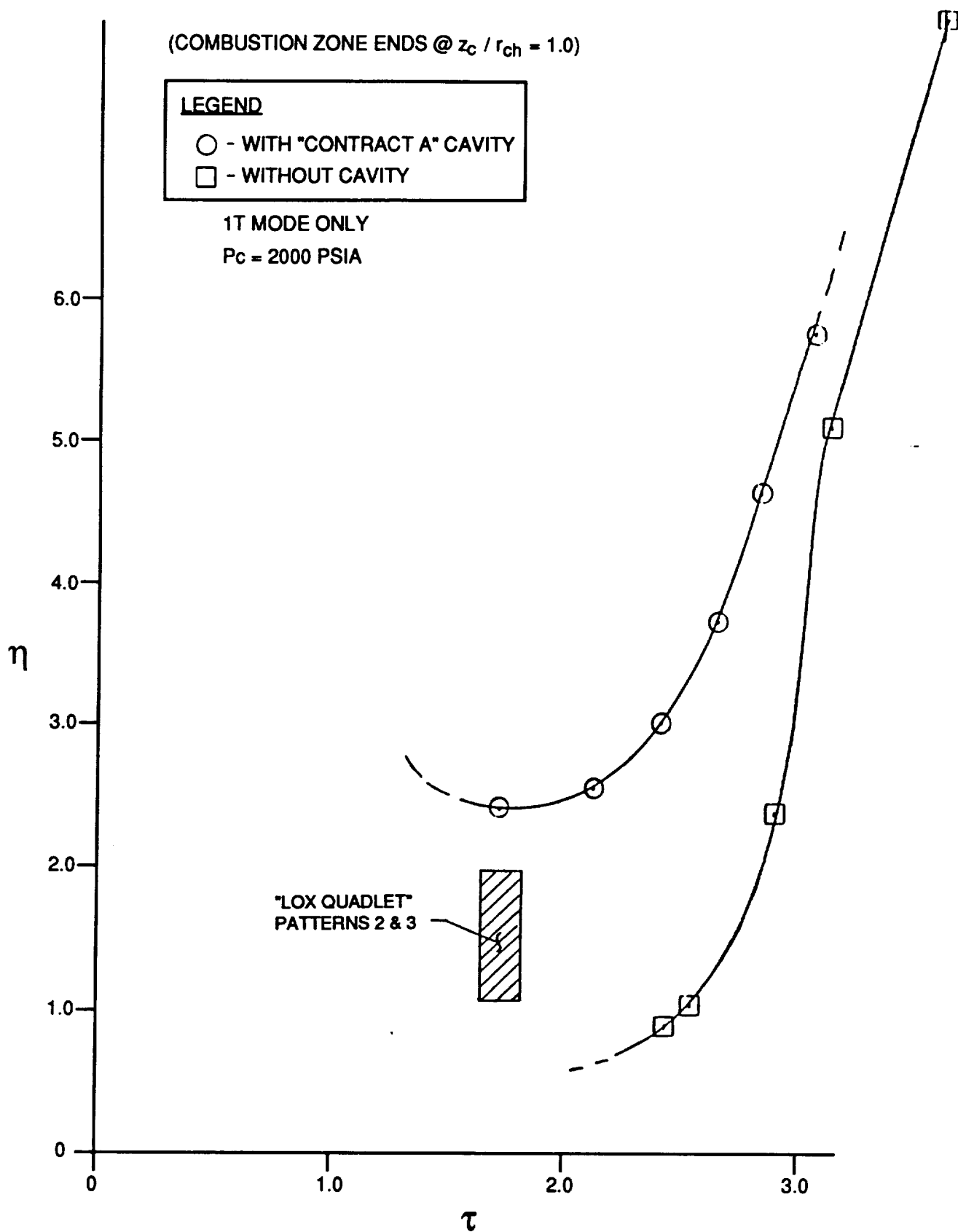


Figure 16. Response Curves of LOX Quadlet Injectors (No. 2 and 3),
With and Without "Contract A" Acoustic Cavities

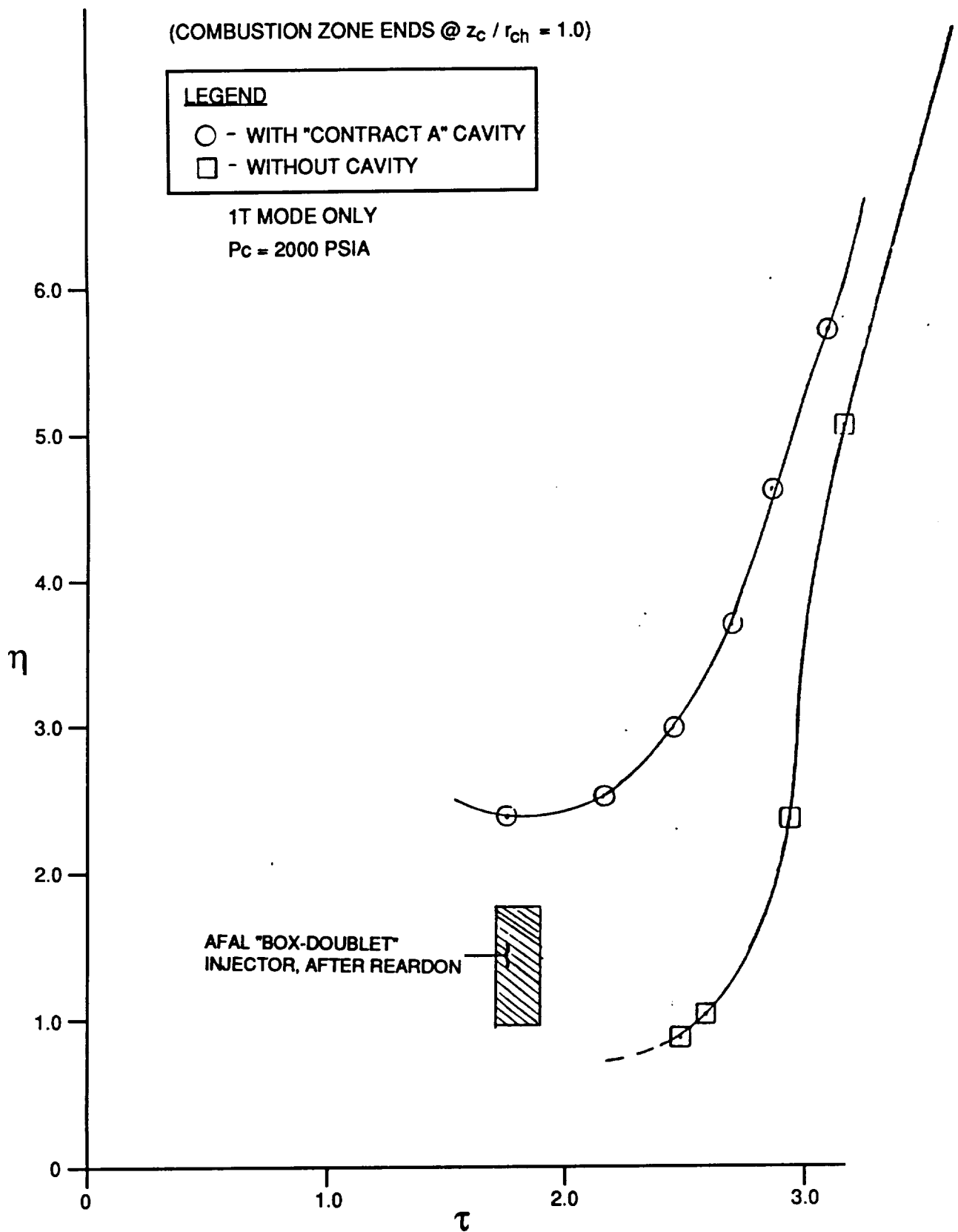


Figure 17. Response Curves of Box-Type, Like-Doublet Injector (No. 5), With and Without "Contract A" Acoustic Cavities

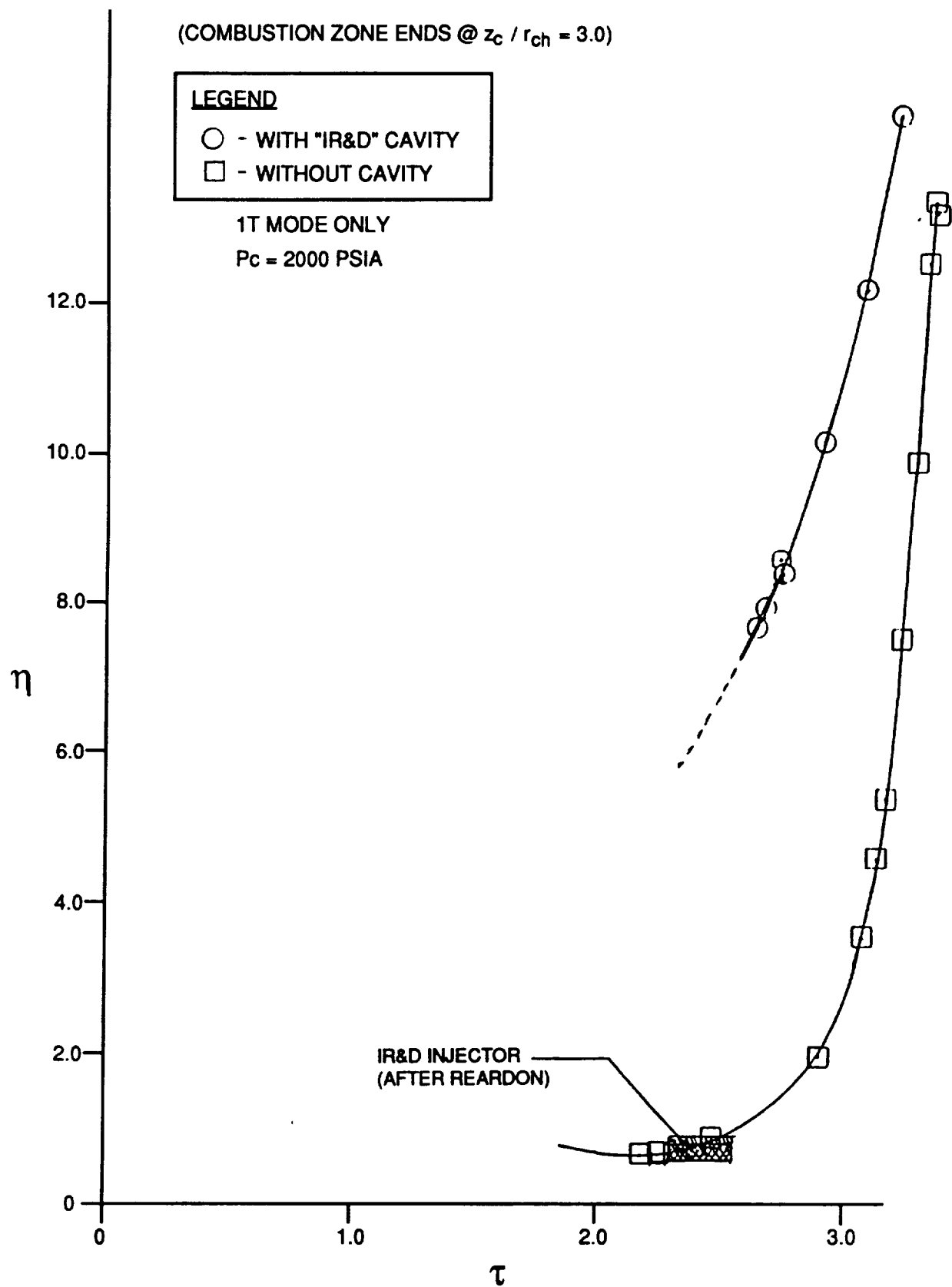


Figure 18. Response Curves of Ring-Type, Like-Impinging Injector (No. 6), With and Without "IR&D" Acoustic Cavities

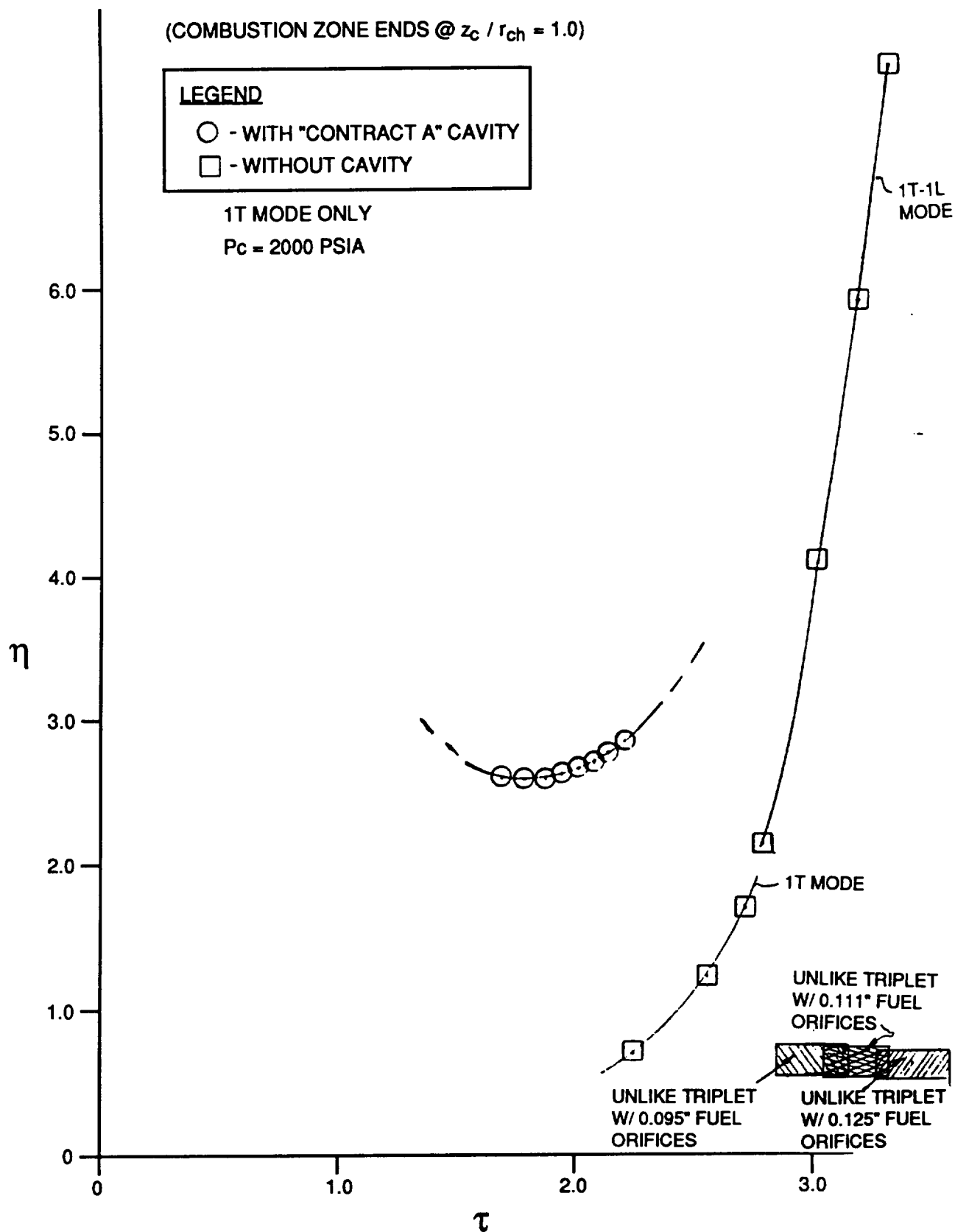


Figure 19. Response Curves of Candidate O-F-O Triplet Injector (No. 7),
With and Without "Contract A" Acoustic Cavities

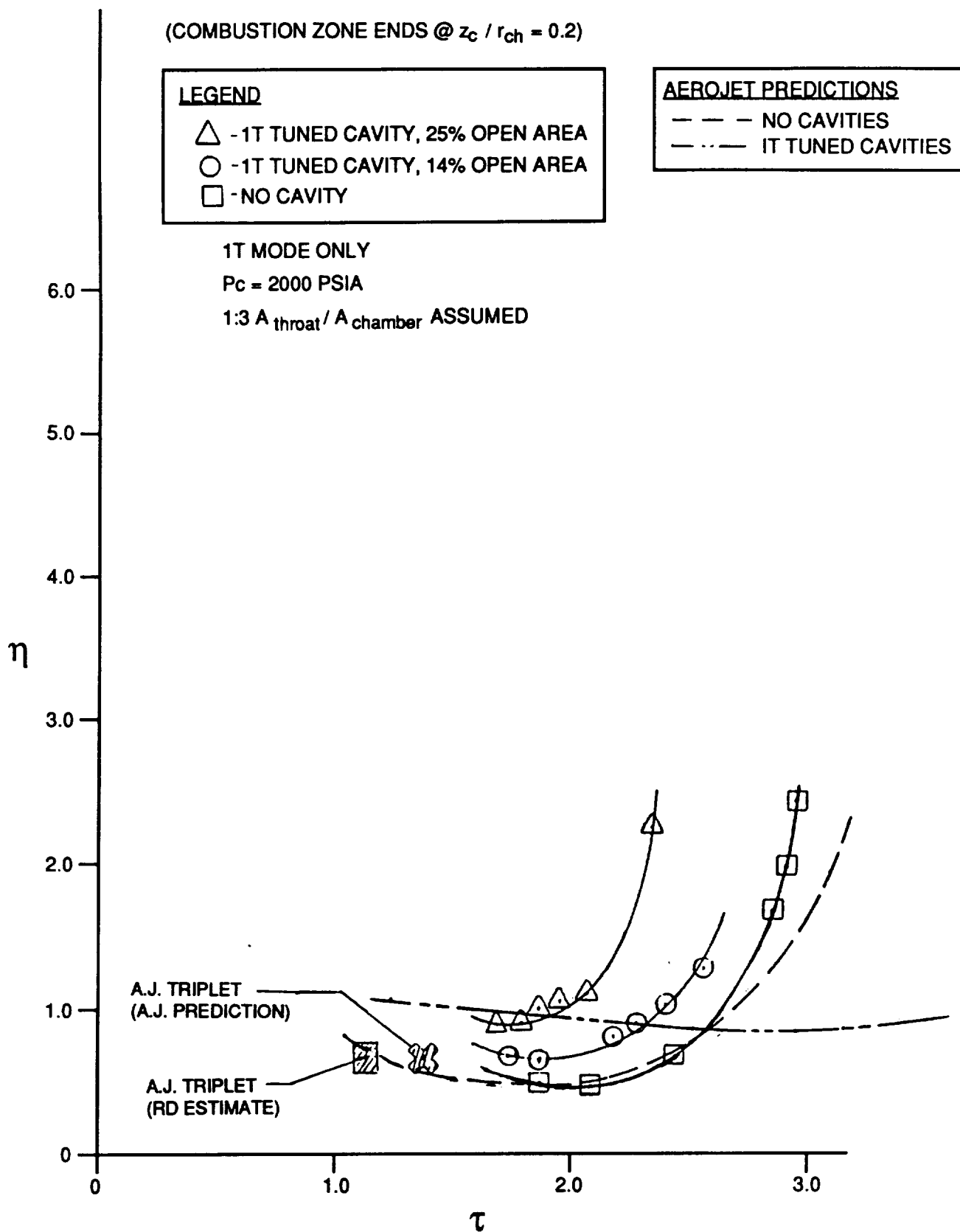


Figure 20. Response Curves of Aerojet O-F-O Triplet Injector, With and Without Tuned Acoustic Cavities, in 20-inch Chamber

5.2.3 WEBBER CORRELATIONS

The Webber correlation (Ref. 7) resulted from a completely empirical examination of the acoustic mode combustion instabilities encountered in a large variety of rocket engines. A dimensional probability factor was defined as follows:

$$I = (D_c/D_j)(P_c^{0.333})$$

where

D_c = Diameter of baffle compartment or chamber, inches

D_j = Average diameter of injection orifices, inches

P_c = Chamber pressure, psia

The probability of combustion instability occurrence is very low if the value of I is less than about 600 in a chamber without acoustic cavities and less than about 1100 in a chamber with acoustic cavities.

Although the parameters included in the rating number, I , are related to stability, no account is taken of other factors that are also important, such as element type, propellant combination, etc. This correlation should therefore be considered only as a very general guide to indicate when the risk of instability may be high.

A plot of the (D_c/D_j) ratio as a function of chamber pressure is shown in Figure 21. The reference lines represent I values of 1100 and 600, as the recommended maxima with and without acoustic cavities, respectively. All of the analyzed LOX/RP-1 injectors for the 3.5-inch-chamber are plotted on the chart, together with the Aerojet O-F-O triplet and, for comparison, the Lunar Module Ascent (LMA), Atlas Sustainer, F-1, and XLR-132 (triplet and like-doublet) injectors. The 3.5-inch injectors are indicated to be stable when used with acoustic cavities. A 24-element, O-F-O triplet injector for the 3.5-inch chamber is predicted to be the most stable, because of its comparatively large orifices ($D \sim 0.10$ in).

Again, these correlations show that all of the candidate LOX/RP-1 injectors would probably be stable with properly tuned acoustic cavities and marginally stable or unstable without cavities.

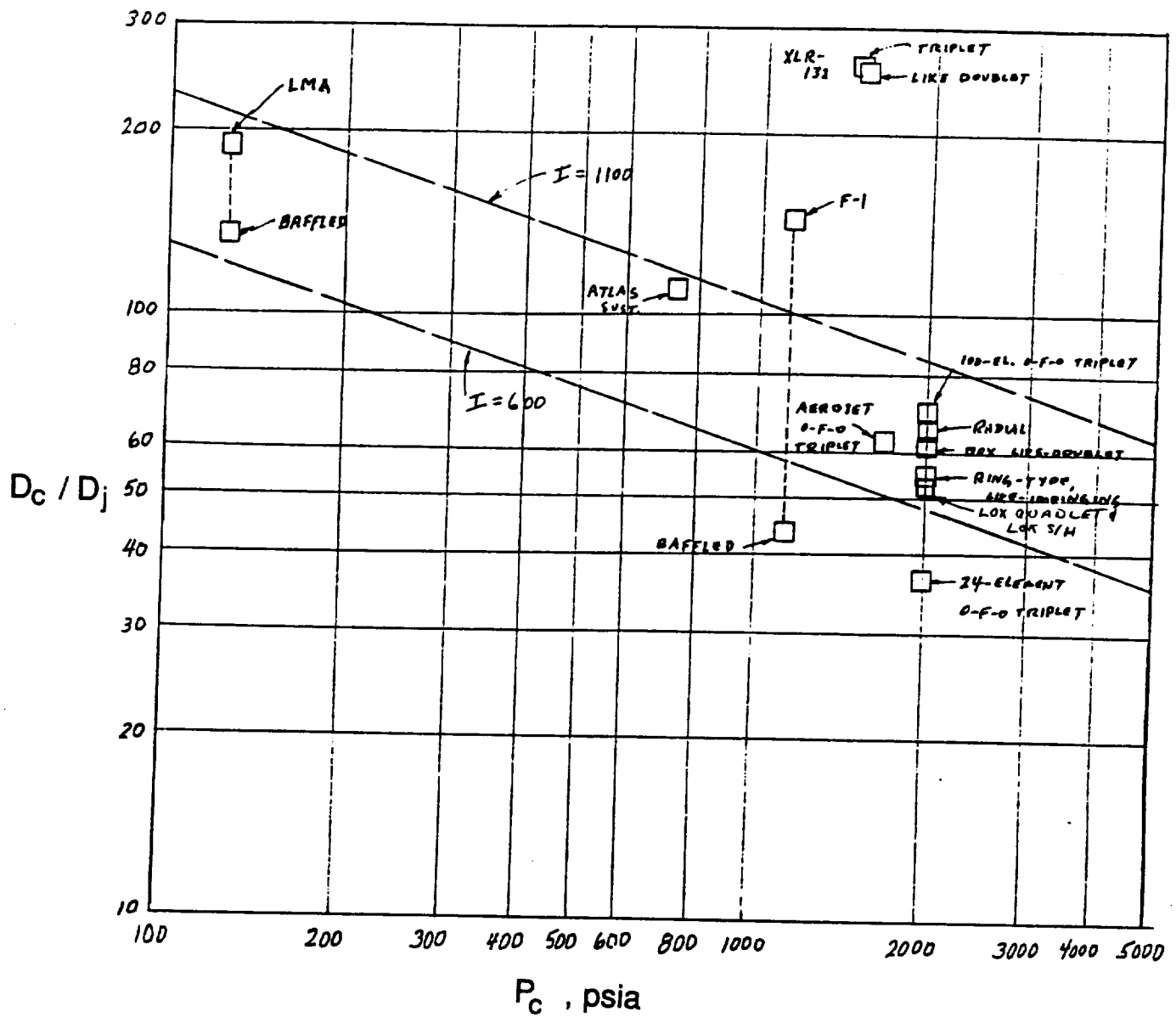


Figure 21. Webber Stability Parameters for Indicated Injectors and Combustors

The O-F-O triplet pattern (Injector No. 7) is predicted to have the largest margin of stability in both the sensitive time lag analysis (Figure 17) and the Webber correlation.

5.3 INJECTOR PATTERNS FOR HOT-FIRE TESTING

Following the cold-flow tests, acoustic analyses, and critical review of existing LOX/RP-1 injector technology, the following five patterns were selected for evaluation in the 3.5-inch combustor:

1. H-1 Derivative*
2. LOX Showerhead
3. O-F-O Triplet
4. Like-Doublet, Circumferential Fans**
5. Like-Doublet, Box Pattern**

Descriptions of these patterns and a discussion of the rationale underlying their selection are presented in this section.

5.3.1 H-1 DERIVATIVE INJECTOR PATTERN (Drawing No. 7R033441)

A pattern derived from that of the H-1 (Type 5588) injector was selected to serve as baseline for the 3.5-inch injector series. This H-1 injector used like-impinging doublet and triplet elements arranged in concentric alternating rings. Operating at a chamber pressure of 705 psia, it had a shifting equilibrium c^* efficiency of 96-percent, based on thrust measurements, and good statistical and dynamic combustion stability, determined in a large number of tests. In terms of performance and stability, the H-1 was the most successful of the classic LOX/RP-1 injectors.

* This injector was designed, fabricated, and tested as part of a Rocketdyne IR&D program (Ref. 6). It is included in the present discussion to present a complete report of the subscale LOX/RP-1 injector evaluation effort.

** These injectors were designed and fabricated under Air Force Contract No. F04611-86-C-0088 ("LOX/Hydrocarbon Thrust Chamber Technology"). They were tested (with AF authorization) in the present program to enlarge the experimental base for LOX/RP-1 subscale injector evaluation.

Application of the design of a large-diameter, low-pressure injector to a small diameter, high pressure unit involves compromises on element size and spacing. For example, the peripheral region is the most critical area of any injector, because the outer row of elements controls wall compatibility and also supplies most of the energy for tangential instability modes. In a large-diameter injector, this zone has a comparatively small proportion of the total mass flow, hence its impact on combustion efficiency is correspondingly low. In the 3.5-inch unit, however, the outer row, with a high proportion of the total mass flow, has a great effect on combustion efficiency. Further, the higher chamber pressure of the small combustor requires higher mass flux density, with a correspondingly finer injection pattern and smaller orifices.

The widths of the H-1 injector manifold rings were reduced for the 3.5-inch injector to maximize the number of element rows. As in the H-1, the outer row of like-impinging fuel doublets was radially oriented in line with the second row of self-impinging oxidizer triplets. The number of elements in this outer zone was established by the maximum number of oxidizer triplets that could be provided in the second row. Since this injector was used with acoustic cavities around its circumference, the distance between the outer row of elements and the chamber wall was significantly greater than in the H-1 injector, which was baffled. With impinging-element injectors, this wall gap usually produces recirculation of the oxidizer-rich gases at the injector face, leading to high heat flux levels at the head-end wall. For this reason, the outer oxidizer row elements were angled slightly outward, to better fill the mass-deficient zone with combustion gases.

As many elements as possible were placed in the inner rows of the 3.5-inch injector, with no regard for clocking adjacent rows of fuel and oxidizer, just as in the H-1 injector. This led to a greater number of fuel elements than oxidizer elements. Although the elements were scaled down, i.e., they were smaller and more closely spaced than in the H-1, the basic layout and the mixing and atomization characteristics reflect the H-1 design approach as faithfully as possible. Nevertheless, even the scaled-down, closer-spaced pattern is still comparatively coarse, and mixing losses might be expected to be relatively high.

The impingement angle of the H-1 doublet and triplet elements was 40-degrees. Although this is significantly lower than the 60-degree angle used in current like-

impinging element designs, it was retained in the 3.5-inch derivative because it permits more elements to be included in each ring. The shallow angle probably lowers atomization and mixing efficiencies but may improve the stability potential.

A photograph of the face of the H-1 Derivative injector is shown in Figure 22. Detail design drawings are reproduced in Fig. B-1 (Appendix B).

Orifice parameters of the 3.5-inch, H-1 Derivative, injector pattern are summarized in Table 2 .

5.3.2 LOX SHOWERHEAD INJECTOR PATTERN (Drawing No. 7R035305)

The injection element in this pattern consists of a central, showerhead, oxidizer orifice within four (shared) like-impinging fuel doublets. Each fuel spray impinges edgewise on two adjacent oxidizer streams.

This pattern was selected to emphasize stability potential over performance potential. The concept of an unatomized central oxidizer stream interacting with a spray of fuel around its perimeter resembles that of a coaxial element which, in many cases, is known to have high performance as well as stable combustion. It was recognized, however, that without atomization of the oxidizer stream its vaporization would be greatly delayed and also that this pattern would have low mixing efficiency, as indicated in the cold-flow tests. Both factors lead to lowered combustion efficiency. However, the hot-fire tests would demonstrate whether movement of the flame front a considerable distance away from the injector face would markedly improve stability.

To provide a slight positive mass flux bias at the injector periphery (which partially compensates for the effect of the acoustic cavities, as discussed above), the outermost oxidizer and fuel orifices were made slightly larger than the inner orifices and eight extra fuel orifices were added at the "open" areas of the periphery. The orifice dimensions in this injector were as follows:

LOX : 32 orifices, D = .096-in.
20 orifices, D = .106-in

RP-1 : 208 orifices, $D = .030\text{-in.}$

16 orifices, $D = .040\text{-in.}$

8 orifices, $D = .025\text{-in.}$

A photograph of the injector is shown in Figure 23; detail design drawings are reproduced in Figure B-2 (Appendix B).

5.3.3 O-F-O TRIPLET INJECTOR PATTERN (Drawing No. 7R035320)

Since the development of the "classic" LOX/RP-1 production engine injectors, unlike-impinging elements have been considered to be too prone to instability for use with this propellant combination. More recent work, however, has indicated that such instability can be controlled with acoustic cavities or baffles (ref. Appendix A), particularly if the injection orifices were comparatively large. Although the resulting decrease in atomization efficiency might lower the performance from the high level inherent in unlike-impinging injectors, the resulting combination of good stability with an acceptable performance level would make this concept a viable candidate for a high-pressure LOX/RP-1 injector. An O-F-O triplet element injector with comparatively large orifice diameters was therefore selected for evaluation in the hot-fire tests.

A photograph of the injector face is shown in Figure 24; the detailed design drawings are reproduced in Figure B-3 (Appendix B).

The diameter of the O-F-O Triplet injector was 3.5-in., which was achieved by orienting the acoustic cavity 20-degrees from the axial direction. In the other four injectors, the face diameter was 3.2-in, which allowed for axial acoustic cavity inlets around the injector circumference.

Two small showerhead fuel orifices were provided at each outboard oxidizer orifice to avoid the possibility of pure oxidizer at the chamber walls. This injector incorporated 16 triplet elements, with 32 LOX orifices ($D_o = 0.125\text{-in.}$) and 16 fuel orifices ($D_f = 0.111\text{-in.}$) plus 24 auxiliary fuel orifices ($D_f = 0.026\text{-in.}$) at the perimeter.

ORIGINAL PAGE
BLACK AND WHITE PHOTOGRAPH

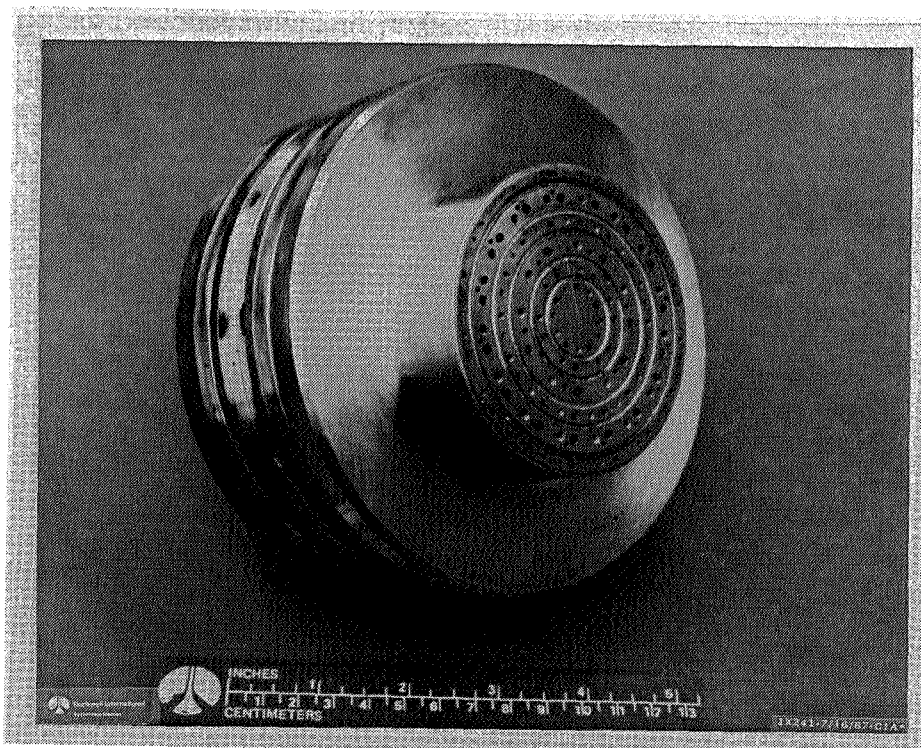


Figure 22. H-1 Derivative Injector

Table 2. Orifice Parameters of 3.5-Inch, H-1 Derivative Injector

Row No.	Propellant	No. of Orifices	Orifice Diam., in.	Impingement Distance, in.
1 (Center Plate)	Oxid.	12 (6 Doublets)	.060	.200
2	Fuel	12 (6 Doublets)	.060	.250
3	Oxid.	6 12 (6 Triplets)	.060 .090	Showerhead .480
4	Fuel	30 (15 Doublets)	.060	.250
5	Oxid.	16 32 (16 Triplets)	.046 .088	Showerhead .250
6 (Outer Row)	Fuel	32 (16 Doublets)	.046	.250

ORIGINAL PAGE
BLACK AND WHITE PHOTOGRAPH

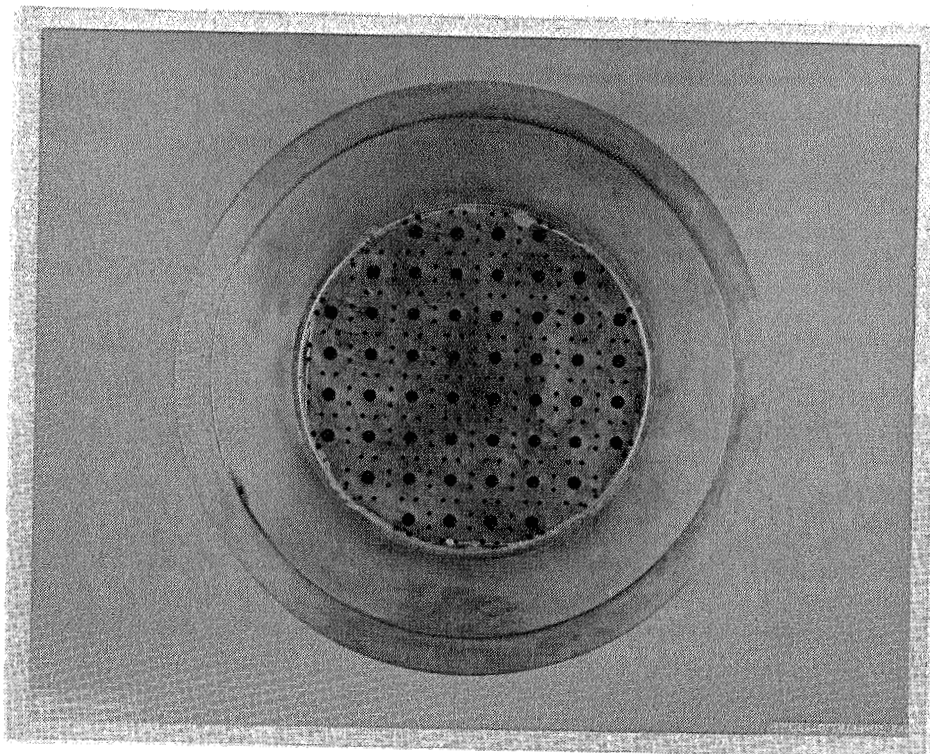


Figure 23. LOX Showerhead Injector

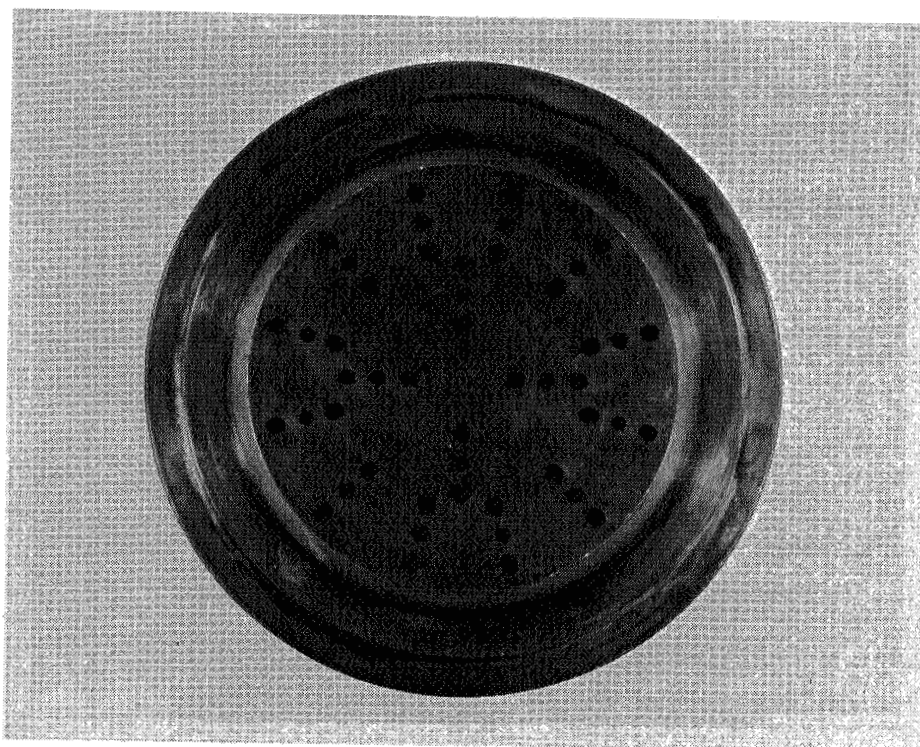


Figure 24. O-F-O Triplet Injector

5.3.4 LIKE-DOUBLET, CIRCUMFERENTIAL-FANS (Dwg. No. 7R033670)

A photograph of this injector face is shown in Figure 25; the detail drawing of the injector is reproduced in Figure B-4 of Appendix B.

This injector has three rings of like-impinging doublet elements, with alternating oxidizer and fuel doublets in each ring. The spray fans are oriented parallel to the wall, hence "circumferential" fans, and impinge edgewise, to give high mixing efficiency. Although this is a like-doublet configuration frequently employed with storable propellants, it was not used in earlier LOX/RP-1 injectors, which had radial orientation of the spray fans. The number of elements was maximized, to permit small orifice diameters and high degrees of atomization. The tangential orientation of the fans avoids their edge impingement on the chamber wall. An operational injector of this type would probably add a row of fuel film cooling orifices around the periphery; the 3.5-inch injector, however, had no film cooling.

The Circumferential-Fan injector has 120 oxidizer orifices ($D_o = 0.064\text{-in.}$) and 120 fuel orifices ($D_f = 0.042\text{-in.}$).

5.3.5 LIKE-DOUBLET, BOX PATTERN INJECTOR (Drawing No. 7R033663)

This injector face is shown in Figure 26; detail design drawings are reproduced in Figure B-5 (Appendix B).

The box pattern concept, departing from conventional circular distribution patterns, uses a repeating grid type configuration. Each self-impinging LOX doublet is encompassed by four (shared) self-impinging fuel doublets. The LOX spray fan impinges edgewise with two of the fuel fans and the edges of the other two fuel fans impinge on the flat sides of the LOX fan. This pattern makes a square box which is repeated across the face, with the orientation of the LOX fans alternating 90-degrees in adjacent squares. It showed the highest mixing efficiency of the five concepts studied in the cold-flow tests (Figure 8).

The pattern is designed to provide good edge-impinging characteristics while encasing the oxidizer fans in fuel sprays. The oxidizer orifices are substantially larger than the

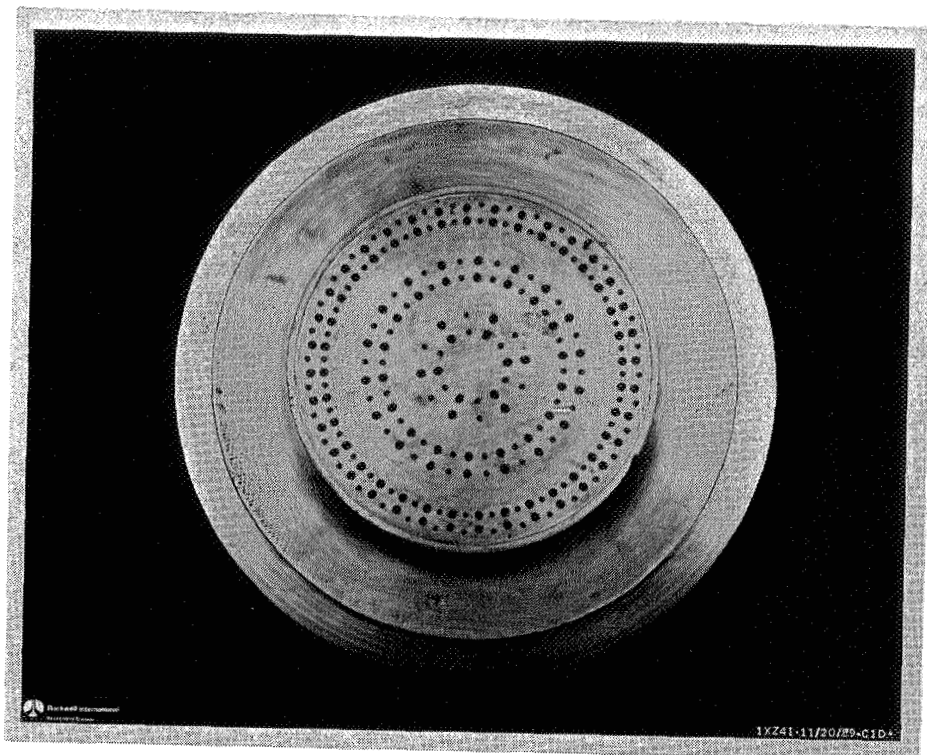


Figure 25. Circumferential-Fan, Like-Doublet Injector

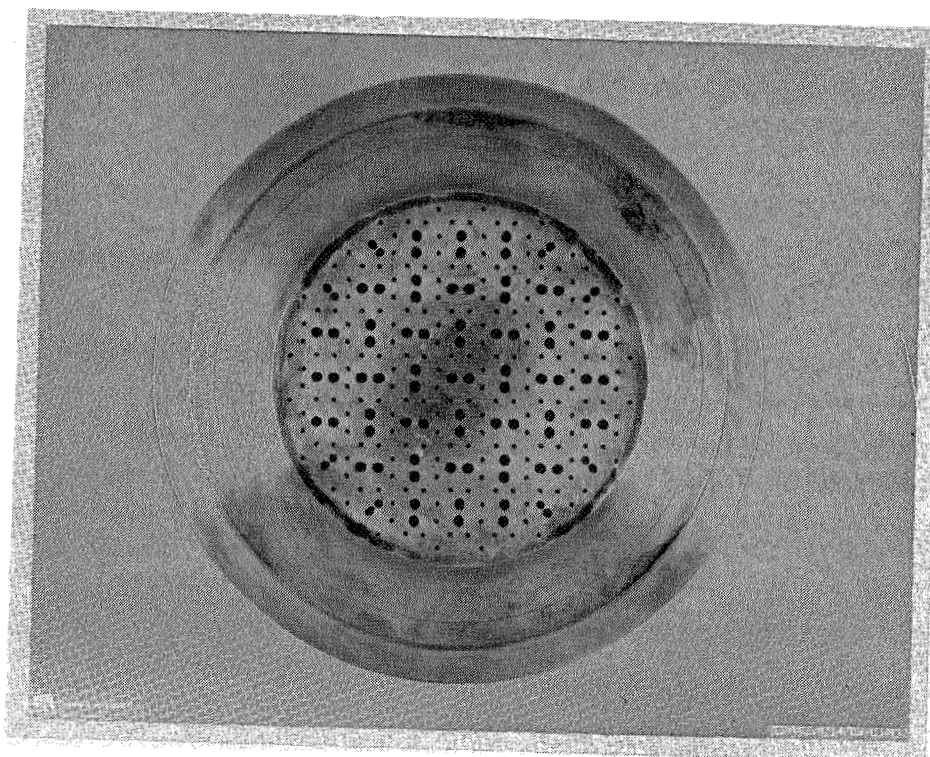


Figure 26. Box-Pattern, Like-Doublet Injector

fuel orifices to facilitate rapid vaporization of the RP-1 while delaying LOX vaporization. Like the LOX Showerhead pattern, this concept also simulates co-axial injection, attempting to provide high performance with stable combustion and good chamber compatibility. Delaying vaporization of the LOX should provide a stabilizing influence without large performance penalties. With its relatively large injection orifices, this pattern was intended to yield reasonably good performance combined with combustion stability. The injector incorporates 90 oxidizer orifices ($D_o = 0.079$ -in.) and 200 fuel orifices ($D_f = 0.033$ -in.), with 16 of the latter functioning as boundary layer coolant orifices around the injector periphery.

5.4 COMBUSTOR COMPONENTS

The 3.5-inch injectors were tested in a water-cooled calorimetric combustor to measure c^* efficiency, stability, and heat flux. The combustor assembly (Drawing No. 7R034104), shown schematically in Figure 27, consisted of the following components:

- LOX Dome
- Fuel Manifold
- Injector
- Acoustic Cavity Ring
- Instrumentation Ring
- Combustion Chamber Spools
- Throat Spool

A photograph of the assembled combustor on the test stand is shown in Figure 28. The combustor components were designed for operation at chamber pressures up to 3000 psia, although all tests in the present series were carried out in the 2000 psia range.

5.4.1 PROPELLANT MANIFOLDS

A bolt-on, 321-CRES, dome-type manifold (Drawing No. 7R034356) was used to supply the oxidizer to the back of the injector. A 304-CRES annular manifold (Drawing No. 7R034357) supplied fuel to the periphery of the cylindrical injector insert which fit into it. Figure 29 is a photograph of the propellant manifolds bolted together.

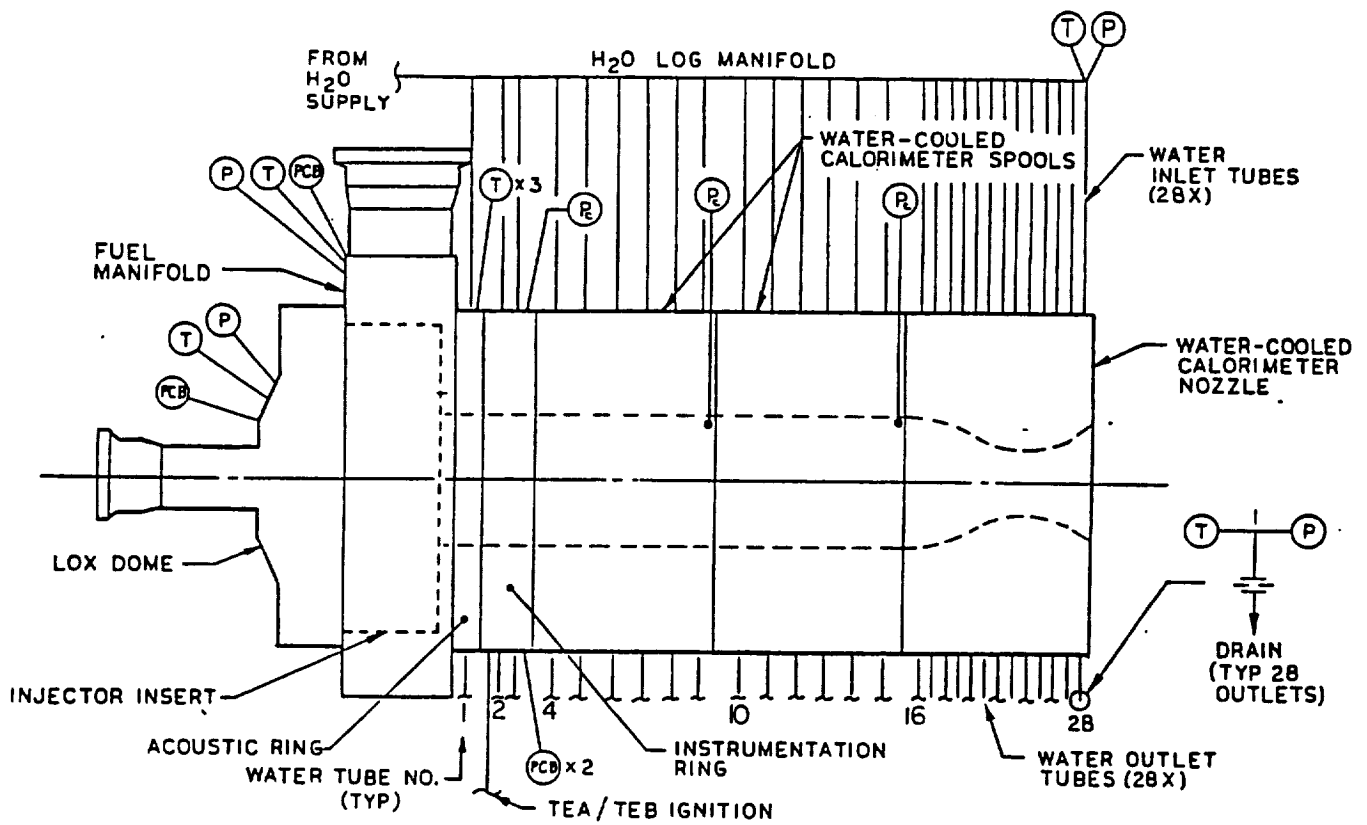


Figure 27. 3.5-Inch Combustor Assembly Schematic

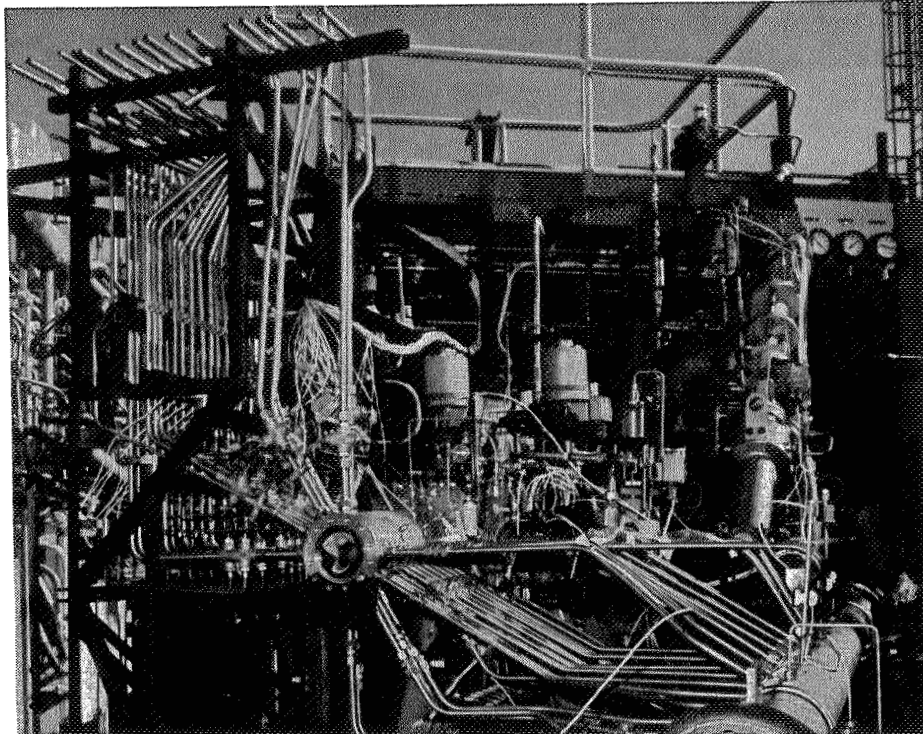


Figure 28. 3.5-Inch Combustor Assembly Mounted on Test Stand

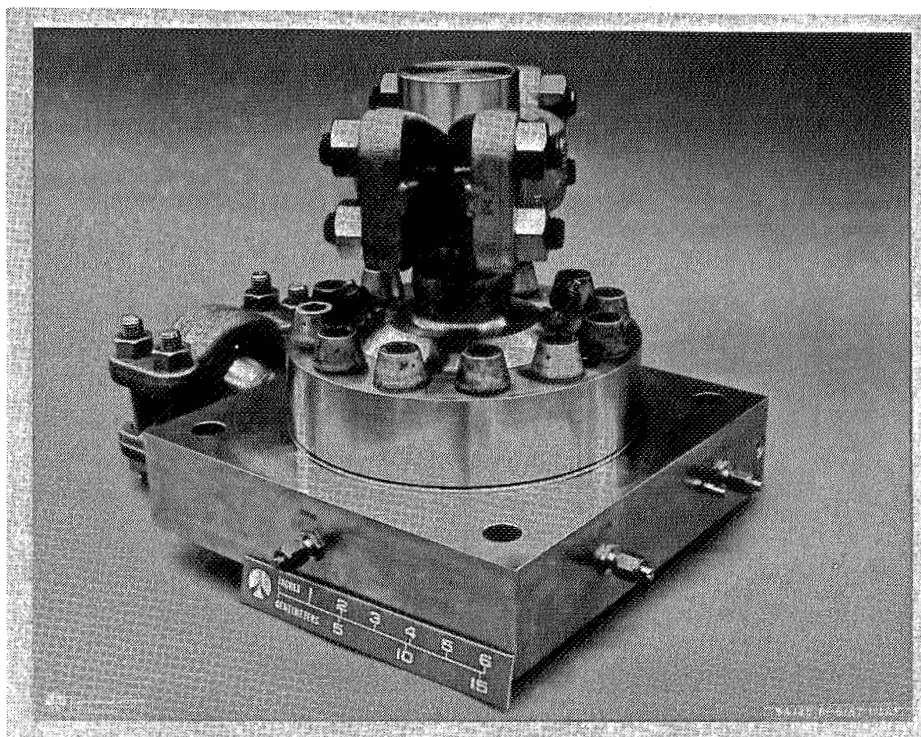


Figure 29. LOX Dome Joined to Fuel Manifold, 3.5-Inch Combustor

5.4.2 INJECTORS

Details of the injector patterns used in this test series were discussed in the preceding section. The center of each 3.5-inch injector, and the entire O-F-O Triplet injector, was fabricated as a "hockey puck" cylinder of OFHC copper, cooled only by the propellants flowing through it. In the combustor assembly, the injectors were inserted into the center of the fuel manifold. They could be replaced simply by removal of the LOX dome, without disturbing the remainder of the the combustor assembly.

5.4.3 ACOUSTIC CAVITY RING

The acoustic cavity ring (Drawing No. 7R034085) is shown in Figure 30. The OFHC copper liner formed seven L-shaped, Helmholtz-type cavities which were tuned for the first tangential mode of oscillation (8.02 kHz), assuming the cavity temperature to be 36-percent of the theoretical chamber temperature at 2.8 mixture ratio. The cavity open area was 25-percent of the chamber cross-sectional area. The orientation of the acoustic cavity inlet passage was axial for all the injectors except the O-F-O Triplet, for which it was 20-degrees off-axial to accommodate the 3.5-in. face diameter.

The acoustic cavity liner was brazed into a 347-CRES shell and was circumferentially channeled for water cooling. Exterior ports were drilled through to five of the cavities (three for thermocouples and two for drainage).

5.4.4 INSTRUMENTATION RING

A two-inch-long instrumentation ring (Drawing No. 7R034095) was located between the acoustic cavity ring and the chamber spool. This ring (Figure 31) had a NARloy-Z core in a 321-CRES housing, with circumferential channels in the core for water cooling. Four ports were provided: one for measurement of static chamber pressure, two (120-degrees apart) for high-frequency pressure measurements (with PCB transducers), and one for introduction of TEA/TEB igniter.

An uncooled, OFHC copper, instrumentation ring (Drawing No. 7R034398) was used in two one-second tests in which a stability rating bomb was detonated to determine the dynamic stability of one of the test injectors. This ring contained the same transducer

ORIGINAL PAGE
BLACK AND WHITE PHOTOGRAPH

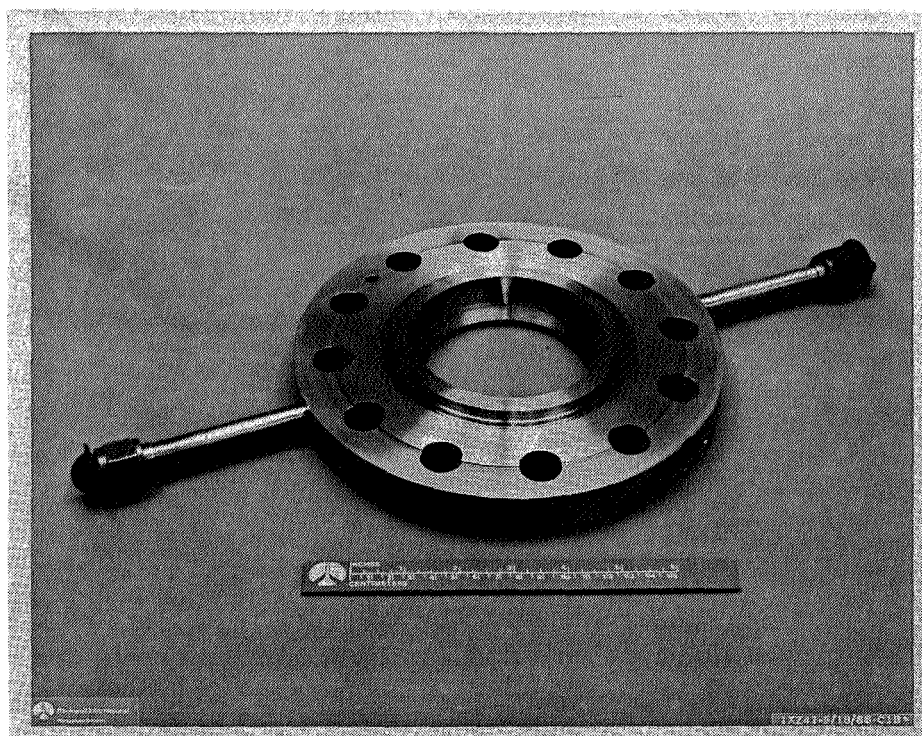


Figure 30. Acoustic Cavity Ring, 3.5-Inch Combustor

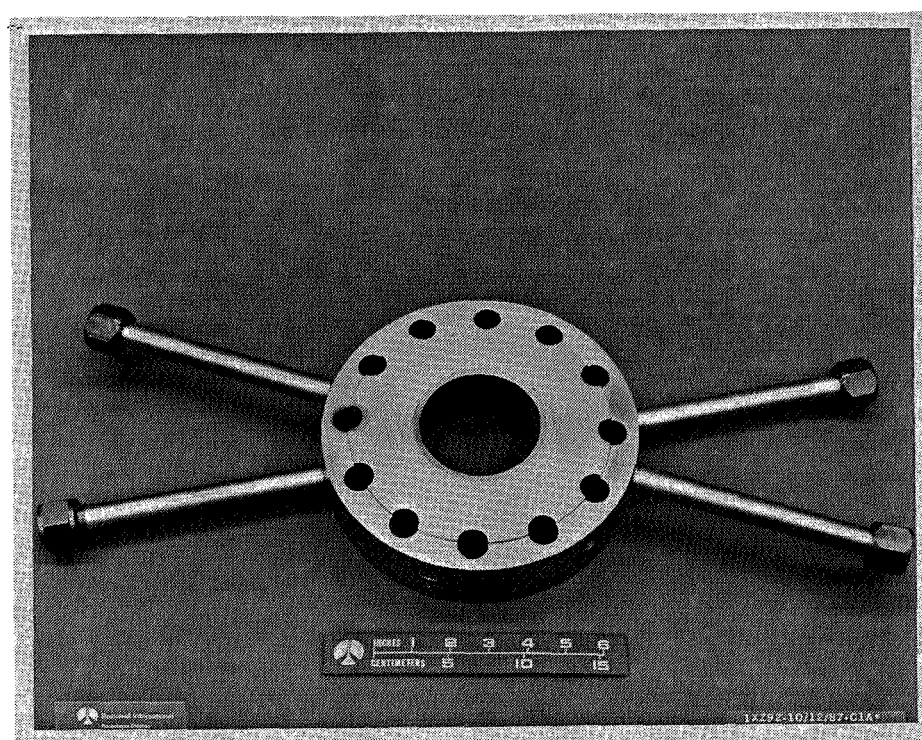


Figure 31. Instrumentation Ring, 3.5-Inch Combustor

ports as the water-cooled instrumentation ring; in addition, a port was provided for the bomb holder.

5.4.5 CHAMBER SPOOL

Two identical, 6-inch-long, calorimetric chamber spools (Drawing No. 7R034358) were used in the 3.5-inch combustor. Each spool (Figure 32) consisted of a NARloy-Z liner within a 304-CRES housing. Circumferential coolant channels were machined along the liner to provide axial heat flux measurement capability.

5.4.6 THROAT SPOOL

The throat spool (Drawing No. 7R034395) also consisted of a circumferentially channeled NARloy-Z liner brazed into a 304-CRES shell, with 13 inlet and 13 outlet coolant water tubes (Figure 33).

5.4.7 COMBUSTOR DIMENSIONS

Pertinent combustor dimensions are as follows:

- Chamber diameter = 3.50 in.
- Throat diameter = 2.20 in.
- Contraction ratio = 2.53
- Expansion ratio = 4.43
- Chamber length (injector face to throat) = 19.0 in.
- Chamber L^* = 44 in.

ORIGINAL PAGE
BLACK AND WHITE PHOTOGRAPH

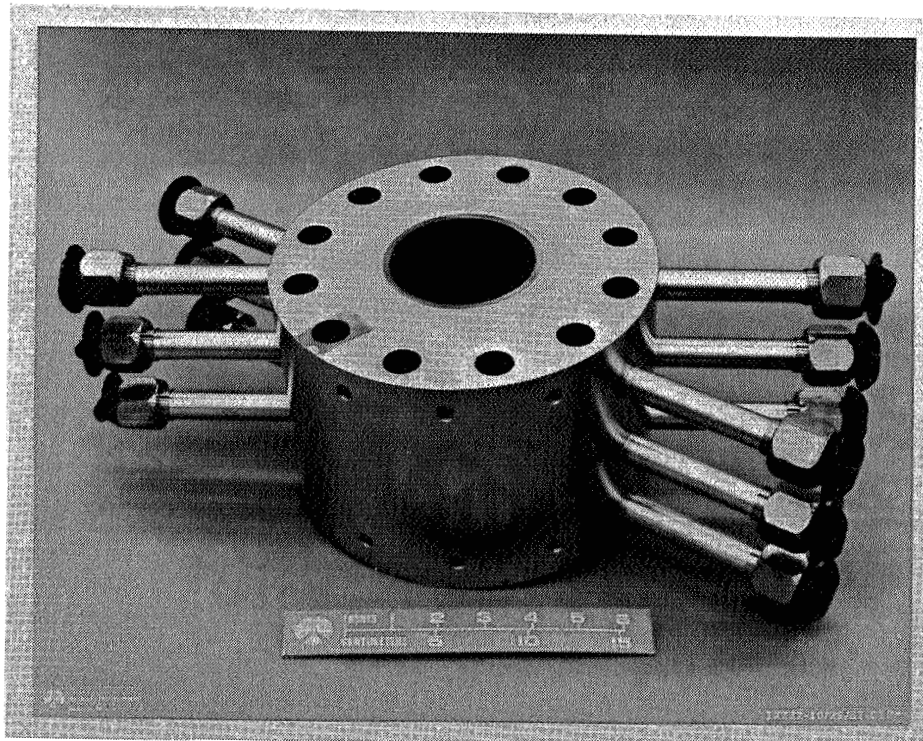


Figure 32. Chamber Spool, 3.5-Inch Combustor

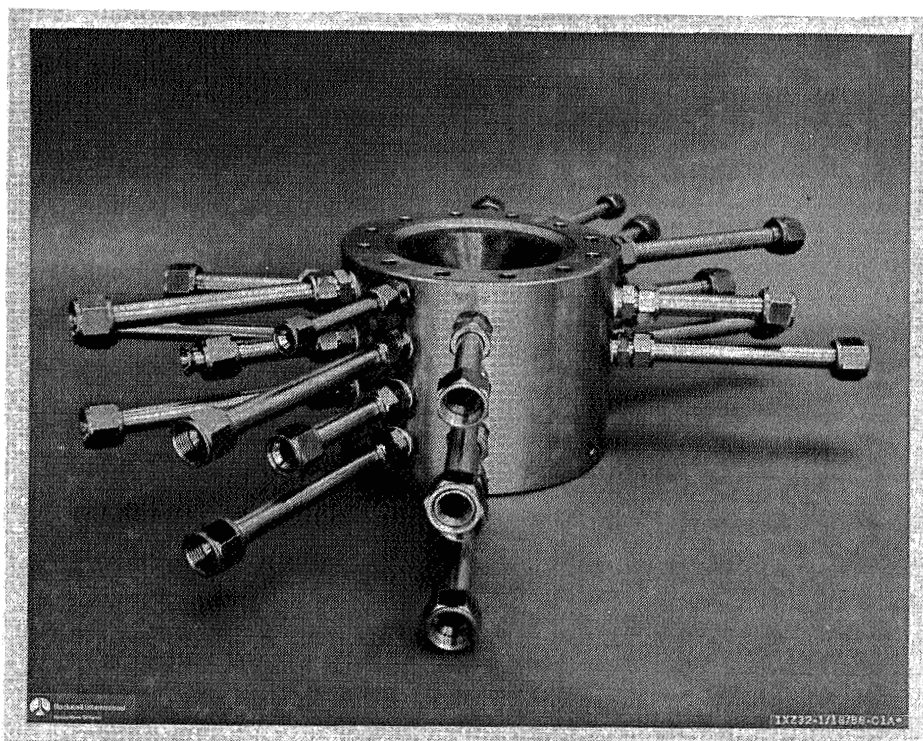


Figure 33. Throat Section, 3.5-Inch Combustor

5.5 TEST FACILITY, INSTRUMENTATION AND PROCEDURES

5.5.1 TEST FACILITY

The hot-fire tests were conducted on Mike Stand, in the Advanced Programs Test Facility at Rocketdyne's Santa Susana Field Laboratory. This is a recently activated test position for water-cooled LOX/RP-1 combustors operating at chamber pressures up to 3000 psi and thrust levels up to 40,000 lb.

The test combustor was bolted to the stand mount through an adapter designed so that the chamber axis was directed four degrees downward from the horizontal to facilitate drainage of any liquid RP-1 which might accumulate. At the nozzle exit, the hardware was joined to a fixed support anchored in the concrete pad, to minimize transient vibrations at ignition. No thrust measurements were made in this test series.

The test stand includes the following fluid systems:

Oxidizer:	LOX	Coolant:	Water
Fuel:	RP-1	Ox. Pressurant & Purge:	GN ₂
Igniter:	TEA/TEB	Fuel Pressurant & Purge:	He

5.5.1.1 LOX System

A sketch of the facility LOX system is shown in Figure 34. The system is rated at 5000 psi; it includes a 180-gallon run tank and a 4-inch supply line to the test hardware. Two main valves are available, one for the LOX flowrate level appropriate to the 3.5-inch-diameter combustor (30-50 lb/sec, 20K nominal thrust) and the other for the flowrate of the 5.7-inch-diameter unit (60-100 lb/sec, 40K nominal thrust). The tank and supply system are insulated, but not jacketed. Flowrates are controlled and measured with a cavitating venturi located upstream of the main valves.

5.5.1.2 RP-1 System

The RP-1 system is shown in Figure 35. The 5000-psi, 180-gallon run tank supplies a 2-inch line to two main valves, one for the flowrate level (10-20 lb/sec) used in the

3.5-inch combustor and the other for the level (20-40 lb/sec) used in the 5.7-inch unit. The supply line includes a 10-micron filter. Flowrates are controlled and measured with a cavitating venturi.

5.5.1.3 TEA/TEB System

A mixture of triethylaluminum (TEA) and triethylborane (TEB) (15/85 weight percent) was used for hypergolic ignition with oxygen. It was supplied from a 13-in³ run cylinder in a 4000-psi rated system (Figure 36). The entire contents of the run tank (about 0.39 lb) can be injected into the combustor in each test. If smaller amounts are used, the remainder is burned post-test.

5.5.1.4 Water Coolant System

The calorimetric test hardware was cooled by filtered (10-micron) water from a 5000-psi, 3500-gallon tank in a blowdown system (Figure 37) in which the tank ullage (GN₂) is the pressurant. Immediately prior to test, the entire cooling circuit was filled with water by bleeding through the test hardware. This provided an incompressible medium downstream of the main valve when it was opened at test start and lessened the impact of the large pressure increase in the water lines. The main valve is servo-controlled to permit a controlled opening time and a regulated pressure. Water flowrate was controlled by system pressure drops and calibrated orifices at the outlets of the test hardware coolant lines.

5.5.1.5 Pressurant and Purge Systems

The LOX tank was pressurized with GN₂. To avoid possible hazards of using a common-source pressurant for oxidizer and fuel systems, the RP-1 and TEA/TEB tanks were pressurized with helium from the area supply tanks.

Nitrogen was used as oxidizer system purge gas. Helium was the fuel systems purge gas for RP-1 and TEA/TEB.

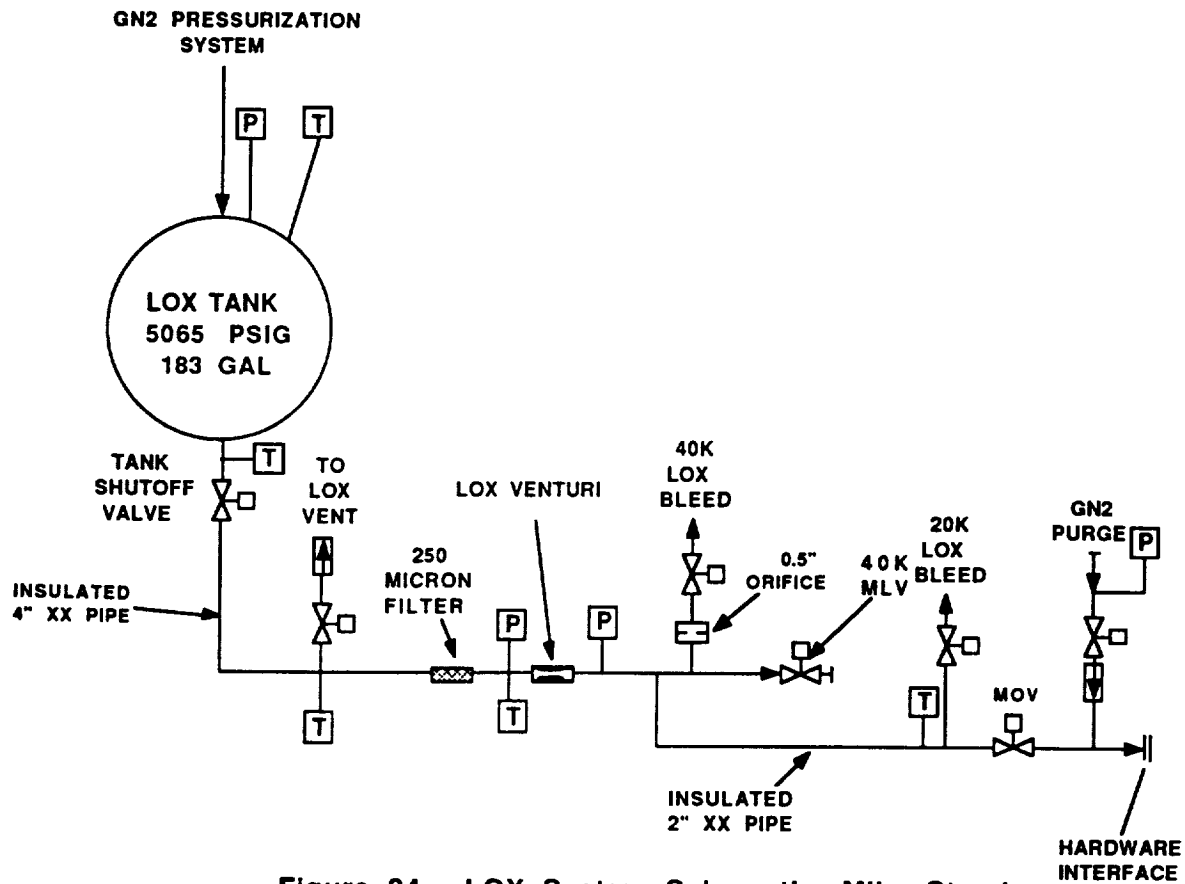


Figure 34. LOX System Schematic, Mike Stand

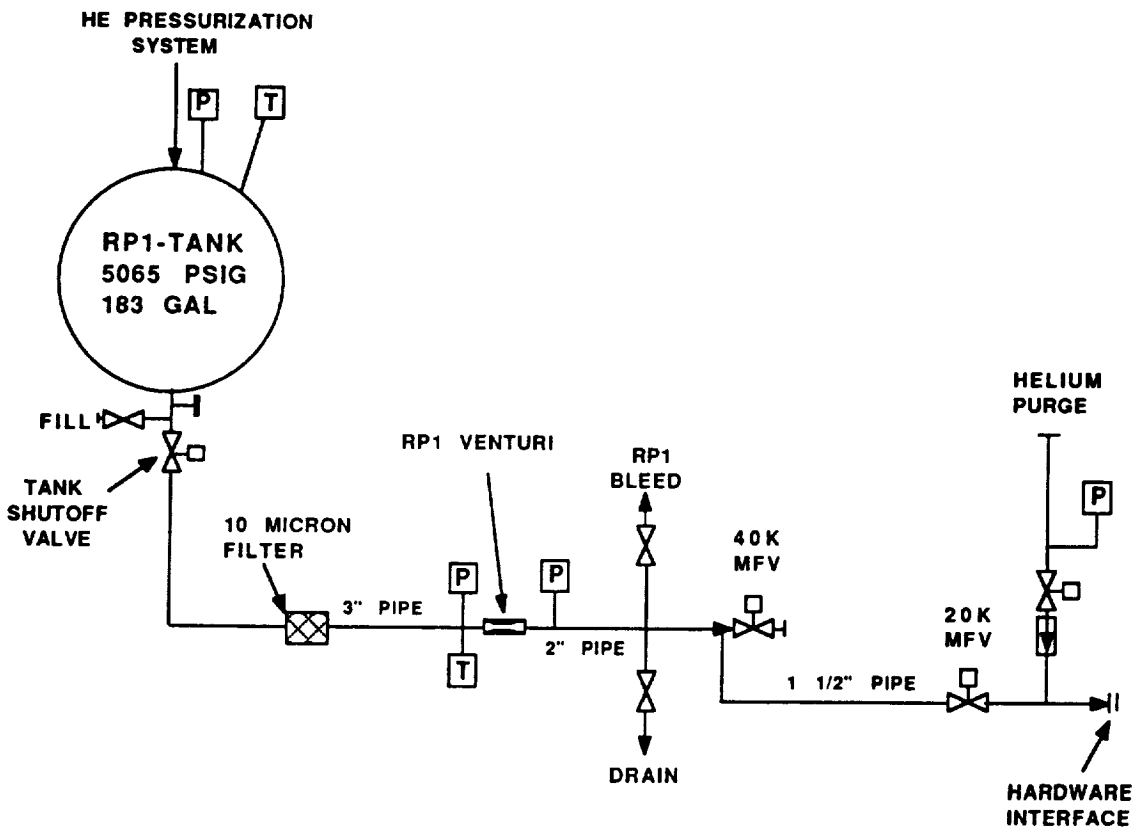


Figure 35. RP-1 System Schematic, Mike Stand

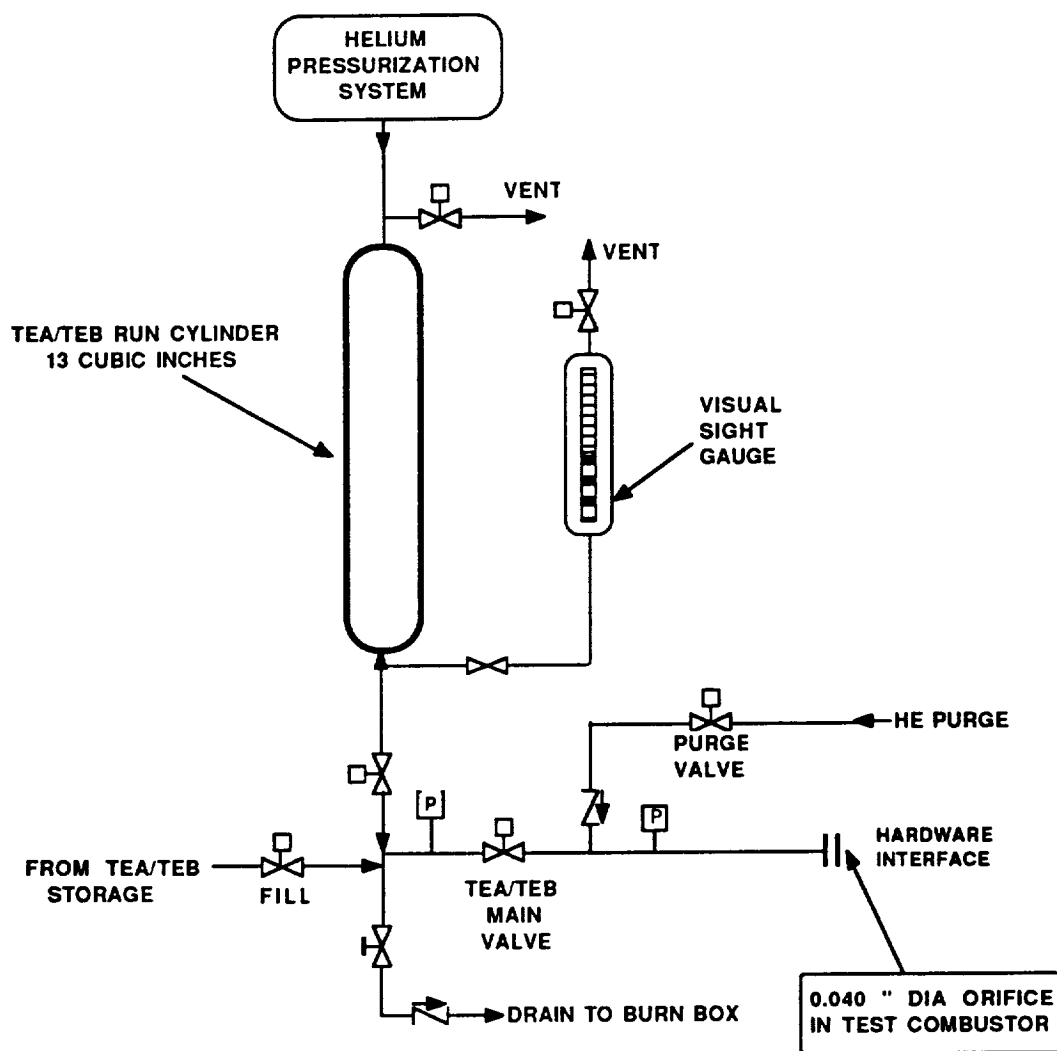


Figure 36. TEA/TEB System Schematic, Mike Stand

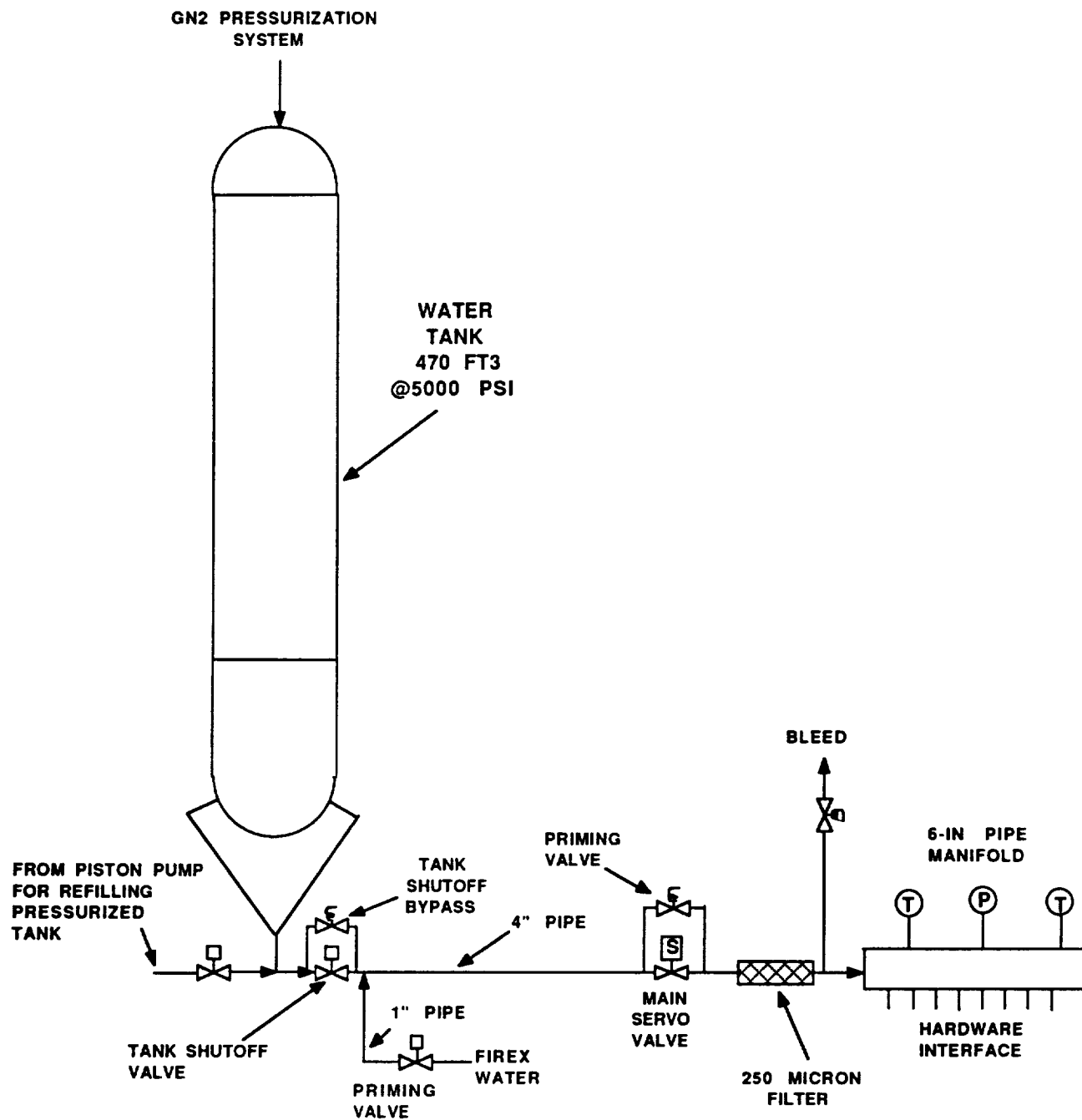


Figure 37. Coolant Water Schematic, Mike Stand

5.5.2 INSTRUMENTATION AND DATA RECORDING

5.5.2.1 Transducers and Sensors

Test parameters were measured by standard types of transducers:

Pressure (low frequency):	Taber strain gage transducers
Pressure (high frequency):	PCB piezoelectric transducers
Temperature:	Chrome/Alumel thermocouples
	Temperature resistance bulbs
Flowrate:	Cavitating venturis
Acceleration:	Endevco accelerometers

Critical valves were fitted with microswitch sensors for timing measurements and for verification of OPEN/CLOSE positions.

5.5.2.2 Test Instrumentation and Data Recording

Table 3 lists the test data parameters and instrumentation. Transducer locations are shown in the fluid system schematics (Figures 33-37) and the combustor assembly schematic (Figure 27). Run data from all transducers (except the high-frequency units) were digitized and tape recorded by the test area computers for immediate post-test retrieval, tabulation, and CRT plotting. In addition, outputs of the high-frequency instrumentation (PCBs and accelerometers) were recorded on FM tape and oscillographs, together with selected events and reference parameters (such as chamber and injection pressures and shut-down signal) for stability-related analyses. Axial and tangential accelerometer outputs were also monitored on TASCOS* vibration cut-off devices, which would terminate a test if pre-specified oscillation amplitude and duration are exceeded.

* Turbine Accelerometer Safety Cutoff System

Table 3. Instrumentation List, 3.5-Inch Injector Tests

MSI NO.	PARAMETER	RANGE	TRANS- DUCER	OSC GRAPH	F/M TAPE
812	LOX TANK PRESS 5000 PSI	TABER			
24	LOX VENTURI U/S PRESS	5000 PSI	TABER		
98	LOX VENTURI U/S TEMP	-300 F	T/C		
25	LOX VENTURI D/S PRESS	5000 PSI	TABER		
26	LOX INJEC. PRESS	5000 PSI	TABER		
-	LOX INJEC. PRESS-HI FREQ		PCB	X	X
132	LOX INJEC. TEMP -300 F	T/C			
29	LOX PURGE PRESS	3000 PSI	TABER		
813	RP-1 TANK PRESS	5000 PSI	TABER		
30	RP-1 VENTURI U/S PRESS	5000 PSI	TABER		
130	RP-1 VENTURI U/S TEMP	150 F	T/C		
32	RP-1 VENUTI D/S PRESS	5000 PSI	TABER		
31	RP-1 INJEC. PRESS	5000 PSI	TABER		
-	RP-1 INJEC. PRESS, HI FREQ-1		PCB	X	X
-	RP-1 INJEC. PRESS, HI FREQ-2		PCB		X
129	RP-1 INJEC. TEMP	150 F	T/C		
33	RP-1 PURGE PRESS	3000 PSI	TABER		
37	TEAB TANK PRESS	5000 PSI	TABER		
38	TEAB INJECT PRESS	5000 PSI	TABER		
864	GN ₂ 5K SUPPLY PRESS.	5000 PSI	TABER		
125	ACOUSTIC CAVITY TEMP -1	2000 F	T/C		
126	ACOUSTIC CAVITY TEMP -2	2000 F	T/C		
127	ACOUSTIC CAVITY TEMP -3	2000 F	T/C		
28	CHAMBER PRESS-1	3000 PSI	TABER	X	
41	CHAMBER PRESS-2	3000 PSI	TABER		
42	CHAMBER PRESS-3	3000 PSI	TABER		
-	CHAMBER PRESS, HI-FREQ -4	PCB		X	
-	CHAMBER PRESS, HI-FREQ -5	PCB		X	
-	ACCELEROMETER-AXIAL	1000 g	ENDEVCO	X	X
-	ACCELEROMETER-RADIAL	1000 g	ENDEVCO	X	X
-	ACCELEROMETER-TANGENTIAL	1000 g	ENDEVCO	X	X

Table 3. Instrumentation List (continued)

MSI NO.	PARAMETER	RANGE	TRANS- DUCER	OSC.- GRAPH	F/M TAPE
507	WATER TANK PRESS	5000 PSI	TABER		
814	WATER INLET MANIF. PRESS	5000 PSI	TABER		
123	WATER INLET MANIF. TEMP-1	150 F	T/C		
124	WATER INLET MANIF. TEMP-2	150 F	T/C		
826	WATER VALVE POSITION	0-100%	LVTD		
	WATER OUTLET PRESS:				
1	(ACOUSTIC CAV.)	1	3500 PSI	TABER	
2		2	3500 PSI	TABER	
3	(INST. RING)	3	3500 PSI	TABER	
4		4	3500 PSI	TABER	
5		5	3500 PSI	TABER	
6		6	3500 PSI	TABER	
7	(CHAM. #1)	7	3500 PSI	TABER	
8		8	3500 PSI	TABER	
9		9	3500 PSI	TABER	
10		10	3500 PSI	TABER	
11		11	3500 PSI	TABER	
12		12	5000 PSI	TABER	
13	(CHAM. #2)	13	3500 PSI	TABER	
14		14	3500 PSI	TABER	
15		15	3500 PSI	TABER	
16		16	3000 PSI	TABER	
17		17	3000 PSI	TABER	
18		18	3000 PSI	TABER	
19		19	3000 PSI	TABER	
20		20	3000 PSI	TABER	
21		21	3000 PSI	TABER	
22	(THROAT)	22	3000 PSI	TABER	
43		23	3000 PSI	TABER	
44		24	3000 PSI	TABER	
45		25	3000 PSI	TABER	
46		26	3000 PSI	TABER	
47		27	5000 PSI	TABER	
48		28	5000 PSI	TABER	

Table 3. Instrumentation List (continued)

MSI NO.	PARAMETER	RANGE	TRANS- DUCER	OSC.- GRAPH	F/M TAPE
WATER OUTLET TEMP.:					
101	(ACOUSTIC CAV.)	1	200 F	T/C	
102	(INST. RING)	2	200 F	T/C	
103		3	200 F	T/C	
104		4	200 F	T/C	
105		5	200 F	T/C	
106		6	200 F	T/C	
107	(CHAM. #1)	7	200 F	T/C	
108		8	200 F	T/C	
109		9	200 F	T/C	
110		10	200 F	T/C	
111		11	200 F	T/C	
112		12	200 F	T/C	
113	(CHAM. #2)	13	200 F	T/C	
114		14	200 F	T/C	
115		15	200 F	T/C	
116		16	200 F	T/C	
117		17	200 F	T/C	
118		18	200 F	T/C	
119		19	200 F	T/C	
120		20	200 F	T/C	
121		21	200 F	T/C	
122	(THROAT)	22	200 F	T/C	
128		23	200 F	T/C	
131		24	200 F	T/C	
133		25	200 F	T/C	
134		26	200 F	T/C	
135		27	200 F	T/C	
136		28	200 F	T/C	

Auxiliary data recording was provided by a real-time digital event recorder (DER) as well as by direct inking graphic recorders (DIGRs), for quick-look data examination. Parameters recorded on the DER are listed in Table 4.

Test documentation included high-speed motion pictures (400 frames/sec), still cameras (3 frames/sec), and video cameras.

5.5.3 TEST PROCEDURES

Pre-test, test, and post-test procedures were conducted in accord with written check lists, following established practices and safety requirements.

5.5.3.1 Test Sequencing

Typical test sequencing, shown in Figure 38, included the following characteristics:

1. Verifications of run tank and purge pressure levels and LOX bleed temperature were required for test start.
2. Coolant water flows were begun and verified about two seconds prior to ignition. (The coolant system was primed before test start.)
3. LOX-TEA/TEB ignition was detected (by chamber pressure rise) before the RP-1 main valve was opened.
4. When RP-1 ignition was detected (by chamber pressure rise) the TEA/TEB main valve was closed.
5. A fuel-rich shutdown was programmed.

The water servovalve was programmed to provide a slow buildup of water pressure in the coolant system. About 0.39 lb. of TEA/TEB was loaded into the run tank to provide up to 1.5 seconds of flow at 0.25 lb/sec.

Redline parameters and settings are listed in Table 5.

Table 4. Digital Event Recorder Parameters

LOX MAIN VALVE SIGNAL, ON AND OFF
LOX MAIN VALVE MICROSWITCH, OPEN AND CLOSE
20K LOX BLEED VALVE SIGNAL, ON AND OFF
20K LOX BLEED VALVE MICROSWITCH, OPEN AND CLOSE
40K LOX BLEED VALVE SIGNAL, ON AND OFF
40K LOX BLEED VALVE MICROSWITCH, OPEN AND CLOSE
RUNLINE LOX BLEED VALVE SIGNAL, ON AND OFF
RUNLINE LOX BLEED VALVE MICROSWITCH, OPEN AND CLOSE
RP-1 MAIN VALVE SIGNAL, ON AND OFF
RP-1 MAIN VALVE MICROSWITCH, OPEN AND CLOSE
TEA/TEB MAIN VALVE SIGNAL, ON AND OFF
WATER MAIN VALVE SIGNAL, ON AND OFF
LOX PURGE VALVE SIGNAL, ON AND OFF
LOX PURGE VALVE MICROSWITCH, OPEN AND CLOSE
RP-1 PURGE VALVE SIGNAL, ON AND OFF
RP-1 PURGE CALVE MICROSWITCH, OPEN AND CLOSE
TEA/TEB PURGE VALVE SIGNAL, ON AND OFF
BOMB FIRE
CUT SIGNALS (DURATION, REDLINE, TASCOS, ETC.)

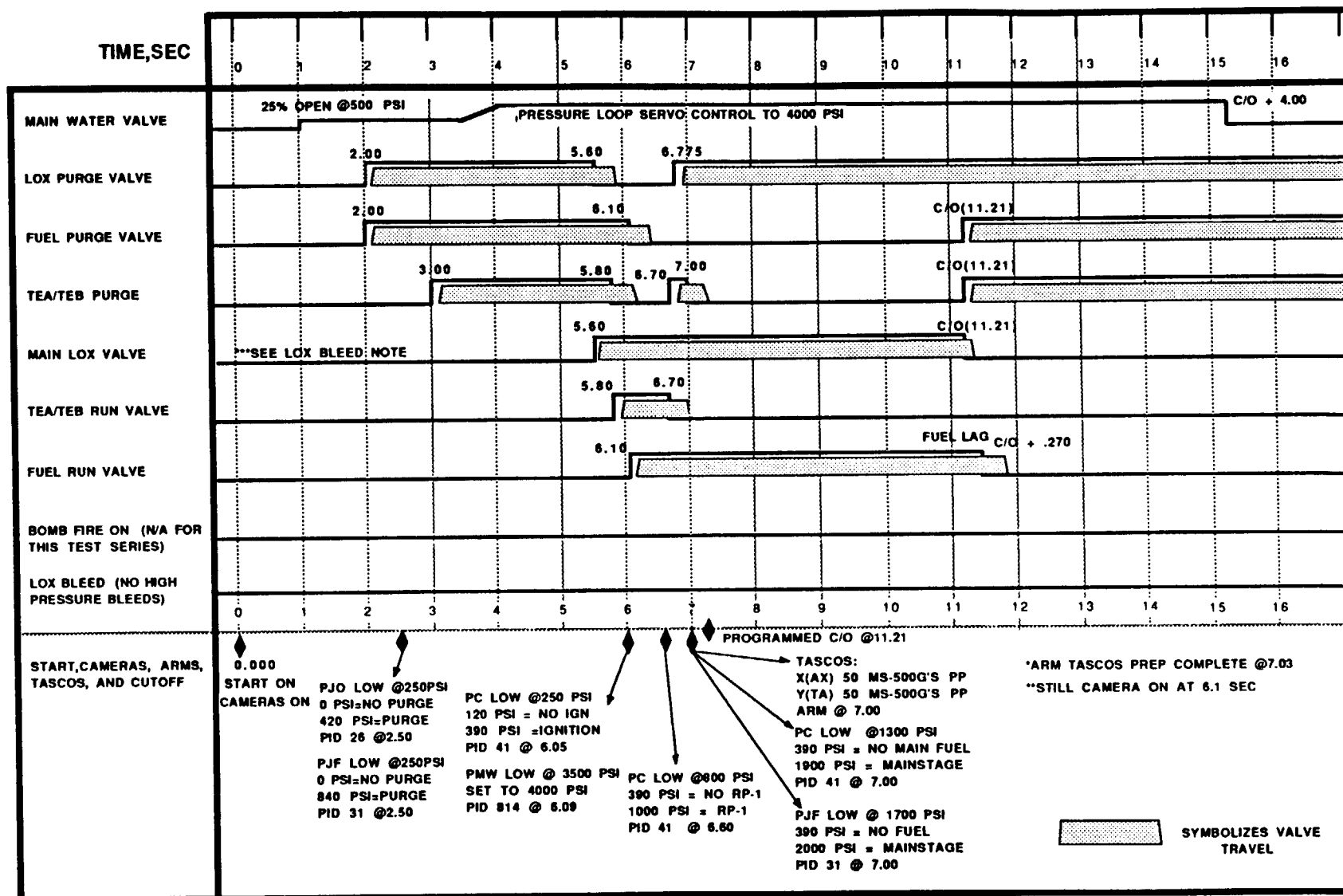


Figure 38. Mike Stand Test Sequence

Table 5. Hardware Redline Parameters

PARAMETER	STATE	TIMING	FUNCTION
LOX Injection Purge Pressure (PJO)	Minimum	0.5 to 1.0 sec after purge valve signal on	Verify purge is operating prior to opening of fuel valves to prevent fuel contamination of LOX system.
Fuel Injection Purge Pressure (PJF)	Minimum	0.5 to 1.0 sec after purge valve signal on	Verify purge is operating prior to opening of LOX valve to prevent inter- propellant mixing in fuel manifold.
H ₂ O Manifold Pressure (PMW)	Minimum	10 msec before RP-1 main valve signal on	Verify sufficient chamber cooling is present before mainstage P _C .
Chamber Pressure, TEA/TEB Ignition (PC)	Minimum	50 msec before RP-1 main valve signal on	Verify TEA/TEB has ignited before opening main fuel valve
Chamber Pressure RP-1 Ignition (PC)	Minimum	10 msec before TEA/ TEB valve signal off	Verify RP-1 has ignited before closing TEA/TEB valve.
Chamber Pressure Mainstage (PC)	Minimum	0.7 to 0.9 sec after RP-1 main valve signal on	Verify system is not operating outside of design P _C conditions.
LOX Injection Pressure (PJO)	Minimum	1 sec before TEA/TEB valve signal off	Verify LOX flow before opening TEA/TEB valve.
RP-1 Injection Pressure (PJF)	Minimum	0.7 to 0.9 sec after RP-1 main valve signal on	Verify system is not operating outside of design mixture ratio conditions.
TASCOS	Maximum	0.7 to 0.9 sec after RP-1 main valve signal on.	Prevents continued operation during unstable conditions.

5.6 TEST RESULTS AND DISCUSSION

Performance, heat flux, and stability data obtained with each of the five, 3.5-inch, subscale injectors are presented in this section, followed by a discussion and comparison of the characteristics of the tested injection patterns. Typically, the performance, heat flux, and spontaneous stability characteristics of each injector were determined in a 5-second test at nominal chamber pressure (2000 psia) and mixture ratio (2.80). These basic data were supplemented by two dynamic stability tests (with the H-1 Derivative injector) and by one test at 2.4 mixture ratio (with the LOX Showerhead injector). The data reduction methods are discussed in Appendix C.

5.6.1 TEST RESULTS

5.6.1.1 H-1 Derivative Injector

Although this injector was tested in an IR&D program (Ref. 9), it is included in the present discussion because the H-1 Derivative pattern provides a baseline with which the other subscale injectors can be compared. This is because of its similarity to the classic LOX/RP-1 injectors.

The CRT plot of chamber pressure at the injector end for a 5-second test (Test No. 015-013) of the H-1 Derivative injector is shown in Figure 39. The three steps in the ignition process prior to mainstage represent, successively, purge flow, oxidizer flow, and oxidizer/TEAB combustion. The abrupt drop in chamber pressure midway through mainstage was due to a leak between the LOX dome and the injector. Performance data were therefore averaged over the time span marked "c". Test parameters and c^* efficiency are listed in Table 6.

A plot of measured heat flux in Test No. 015-013 is shown in Figure 40. In this and subsequent heat flux plots, the distances on the abscissa represent data from the acoustic cavity ring (1 point, at -18.5 in.), instrumentation ring (2 points, at -16 to -17.5 in.), upstream chamber section (6 points, at -16 to -11 in.), downstream chamber section (6 points, at -10 to -4 in.), and throat spool (12 points, at -3 to +2.5 in.). The heat flux results are listed in Table 7.

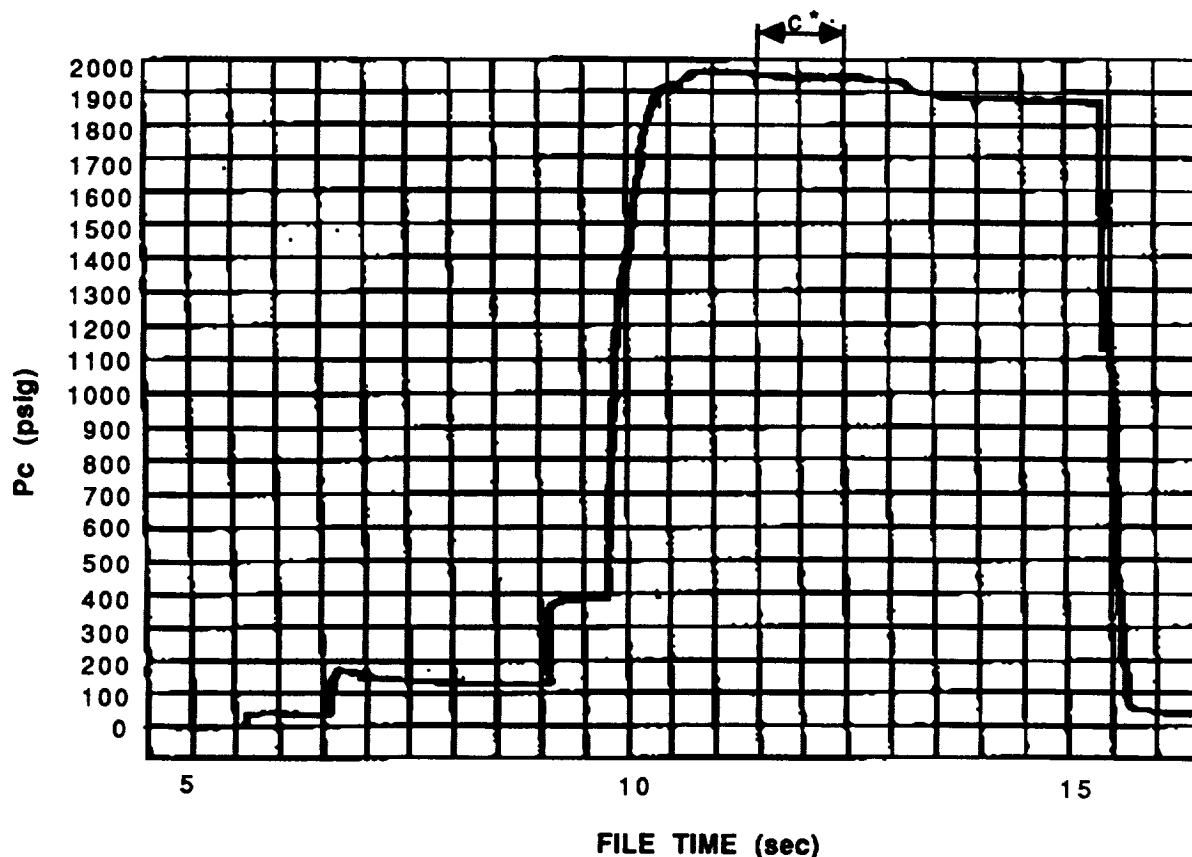


Figure 39. Static Chamber Pressure (Injector End), Test 015-013, H-1 Derivative Injector

Table 6. Performance Data Summary

TEST NO. (1)	INJECTOR PATTERN	Pc, psia (throat stag) (2)	M. R.	\dot{w}_T lb/sec	η_{c^*} (uncorr.), %	η_{c^*} (corr.), % (5)	η_{c^*} (corr.), % (3)
13	H-1 Derivative ⁽⁴⁾	1919	2.75	42.52	93.5	95.3	94.5
23	LOX Showerhead	1957	2.77	45.80	88.6	89.4	88.9
24	LOX Showerhead	1878	2.38	43.30	88.8	89.6	89.2
28	O-F-O Triplet	1900	2.74	43.20	91.1	92.5	91.9
31	Circumferential Fan, Like Doublet	2029	2.78	45.45	92.7	94.9	93.8
33	Box Like Doublet	1982	2.79	45.30	93.1	94.2	93.6

(1) All test durations = 5 seconds

(2) Based on pressure at start of nozzle convergence

(3) Corrected for chamber heat loss, using enthalpy removal from injected RP-1 (Preferred method, cf. Appendix C)

(4) Tested under Rocketdyne IR&D, Ref. 6

(5) Corrected for chamber heat loss, using frozen Cp values for gas temperature decrease

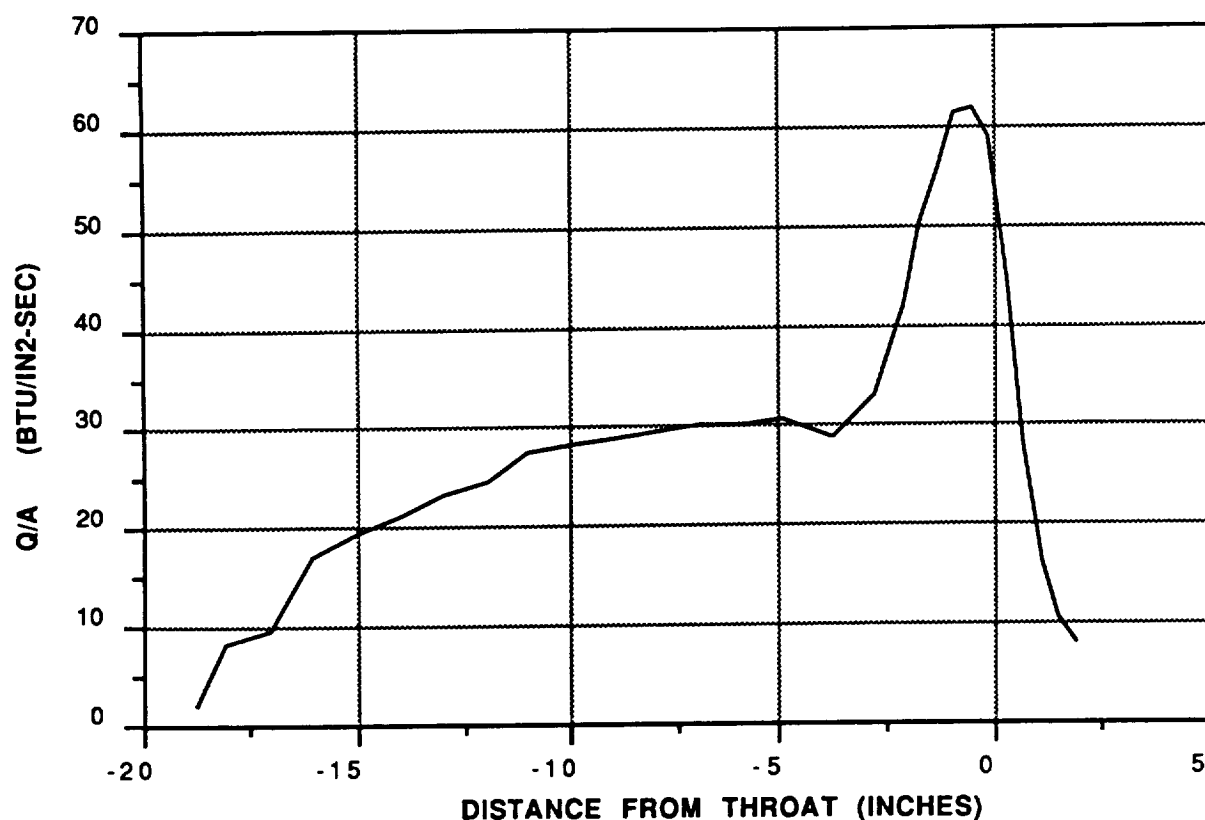


Figure 40. Axial Heat Flux Profile, Test 015-013, H-1 Derivative Injector

Table 7. Heat Flux Summary

TEST NO.	INJECTOR PATTERN	M. R.	FUEL IN PERIPHERY	CHAMBER HEAT FLUX*, Btu/Sec - in ²	PEAK HEAT FLUX*, Btu/sec-in ²	Q _{Total} , Injec → Throat Btu/ sec
13	H-1 Derivative	2.75	Yes**	30	64	5218
23	LOX Showerhead	2.77	Yes	9	37	2215
24	LOX Showerhead	2.38	Yes	8	27	1772
28	O-F-O Triplet	2.74	Yes	27	52	4608
31	Circumferential Fan, Like Doublet	2.78	No	34	62	6350
33	Box Like Doublet	2.79	Yes	15	48	3086

* Normalized to $P_c = 2000$ psia

** Outer fuel ring

Stability data obtained in Test No. 015-013 are summarized in Table 8. In addition to these statistical stability results, two 1.1-second dynamic stability tests were carried out with the H-1 Derivative injector (with acoustic cavities). Bomb detonations were signaled about midway through mainstage. In Test No. 015-019, a 4-grain RDX charge was used, which produced an overpressure of 154-percent; in Test No. 015-020, the bomb charge was reduced to 2 grains, giving an overpressure of 117-percent. Combustion recovery time in both cases was 4 to 5 msec.

5.6.1.2 LOX Showerhead Injector

The LOX Showerhead injector was tested at mixture ratios of 2.8 (Test No. 015-023) and 2.4 (Test No. 015-024). CRT plots of static chamber pressure at the injector end are shown in Figures 41 and 42, respectively, with the indicated time spans of c^* measurement. Performance data are summarized in Table 6.

Axial heat flux curves are shown in Figures 43 and 44 for Tests No. 015-023 and 015-024, respectively. Data are given in Table 7.

Stability measurements obtained in each of the two LOX Showerhead injector tests are summarized in Table 8.

5.6.1.3 O-F-O Triplet Injector

The CRT plot of injector end chamber pressure for the 5-second test (Test No. 015-028) of the O-F-O Triplet injector is shown in Figure 45. Performance data are summarized in Table 6.

Heat flux data from Test No. 015-028 are plotted in Figure 46 and listed in Table 7.

Stability data from Test No. 015-028 are summarized in Table 8.

Table 8. Stability Data Summary

TEST NO.	INJECTOR	Oxidizer Dome			Fuel Manifold			Chamber #1			Chamber #2		
		P-P psi	% Pc	Freq. Hz	P-P psi	% Pc	Freq. Hz	P-P psi	% Pc	Freq. Hz	P-P psi	% Pc	Freq. Hz
13	H-1 Derivative	428	22	3500	108	6	*	153	8	*	200	10	*
23	LOX Showerhead	749	38	3000	519	27	3800	204	10	500	200	10	500
24	LOX Showerhead	514	27	3000	395	21	3000	132	7	500	200	11	500
28	O-F-O Triplet	1400 ^{**}	74	1350 2850	500	26	1350	640	34	1350	920	48	1500
31	Circumferential Fan, Like Doublet	812	40	2000 3000	294	14	*	102	5	*	100	5	*
33	Box Like Doublet	162	8	2000 3000	N.A.	-	-	64	3	1300 2000	100	5	1300 2000

* No organized tuned frequencies below 15k Hz

** Present prior to test start

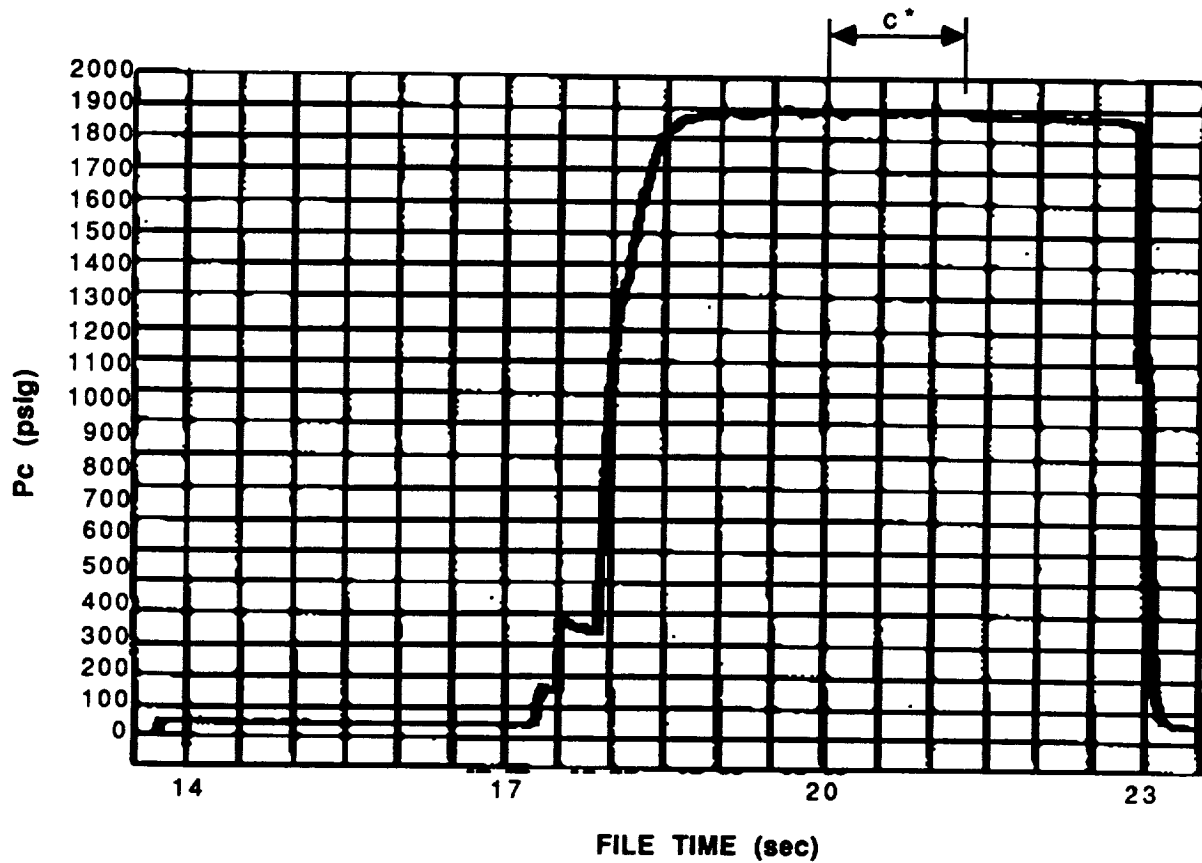


Figure 41. Static Chamber Pressure (Inj. End), Test 015-023, LOX Showerhead Injector

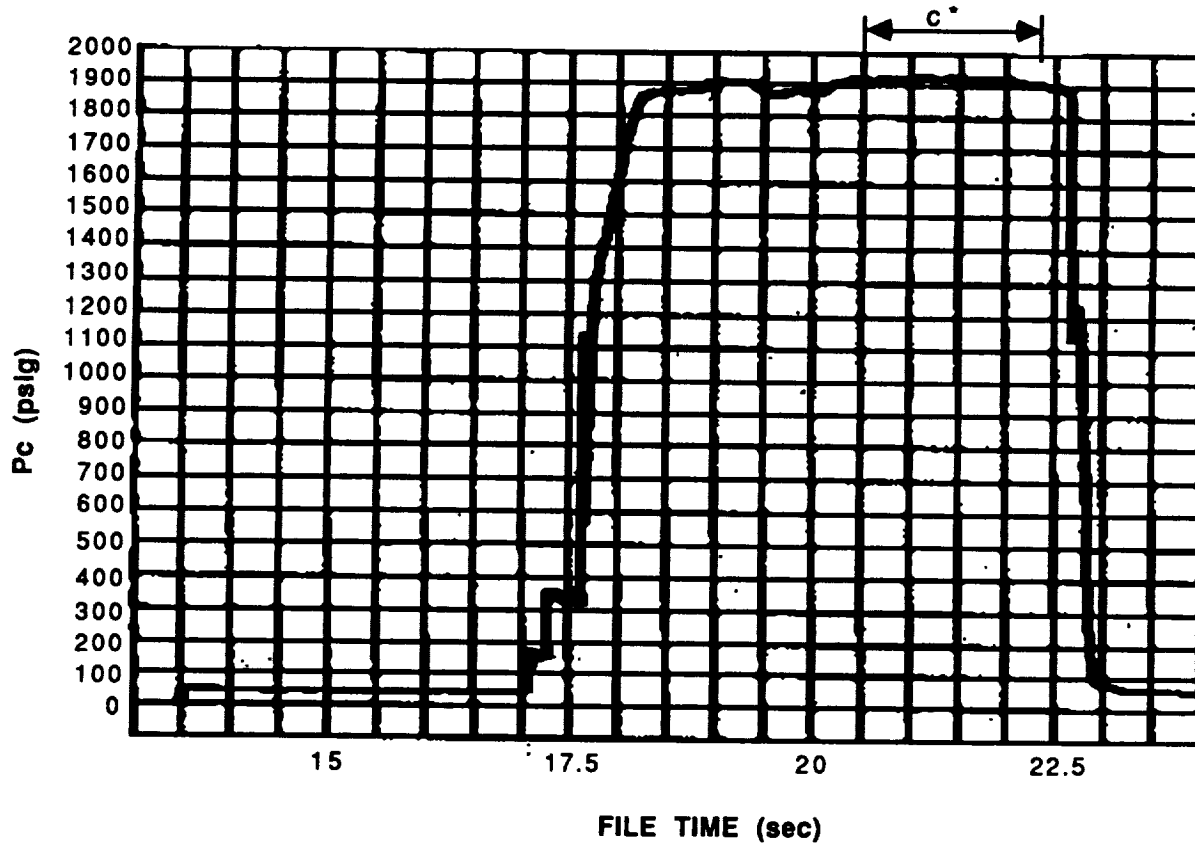


Figure 42. Static Chamber Pressure (Inj. End), Test 015-024, LOX Showerhead Injector

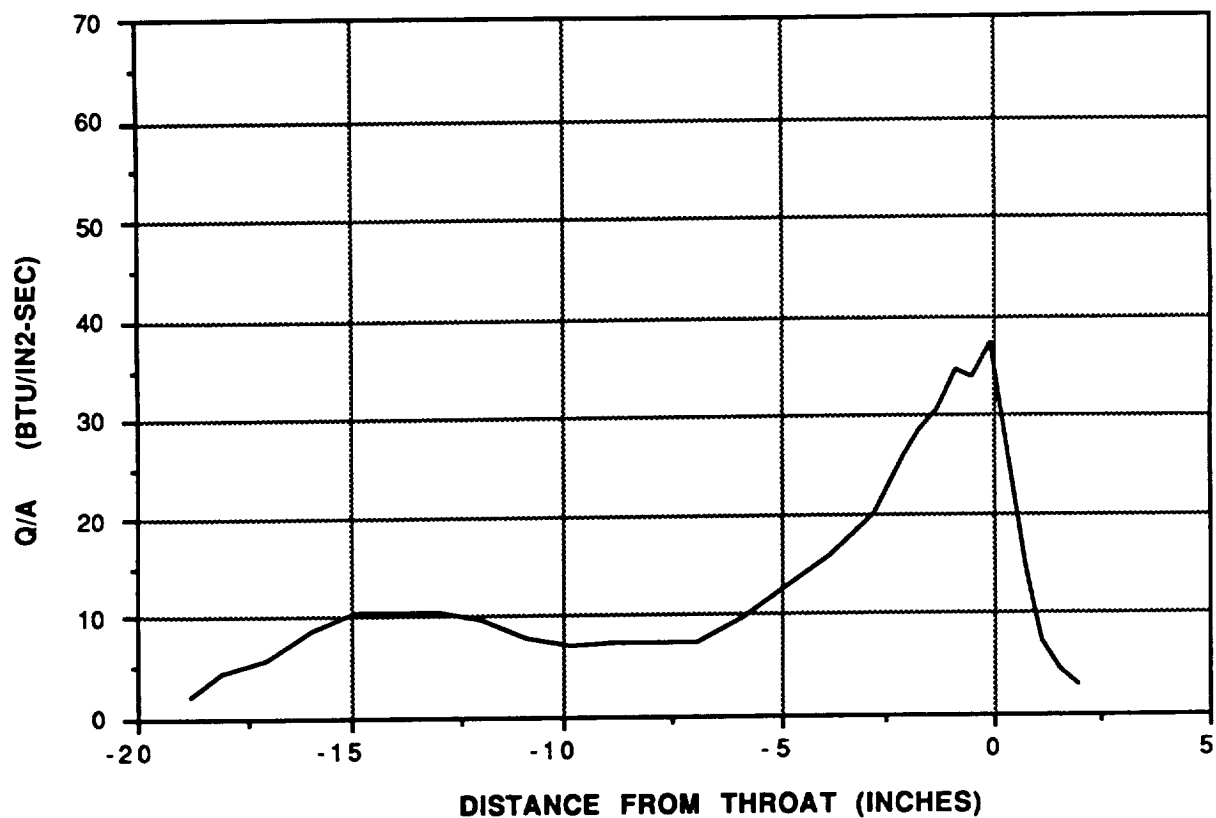


Figure 43. Axial Heat Flux Profile, Test 015-023, LOX Showerhead Injector

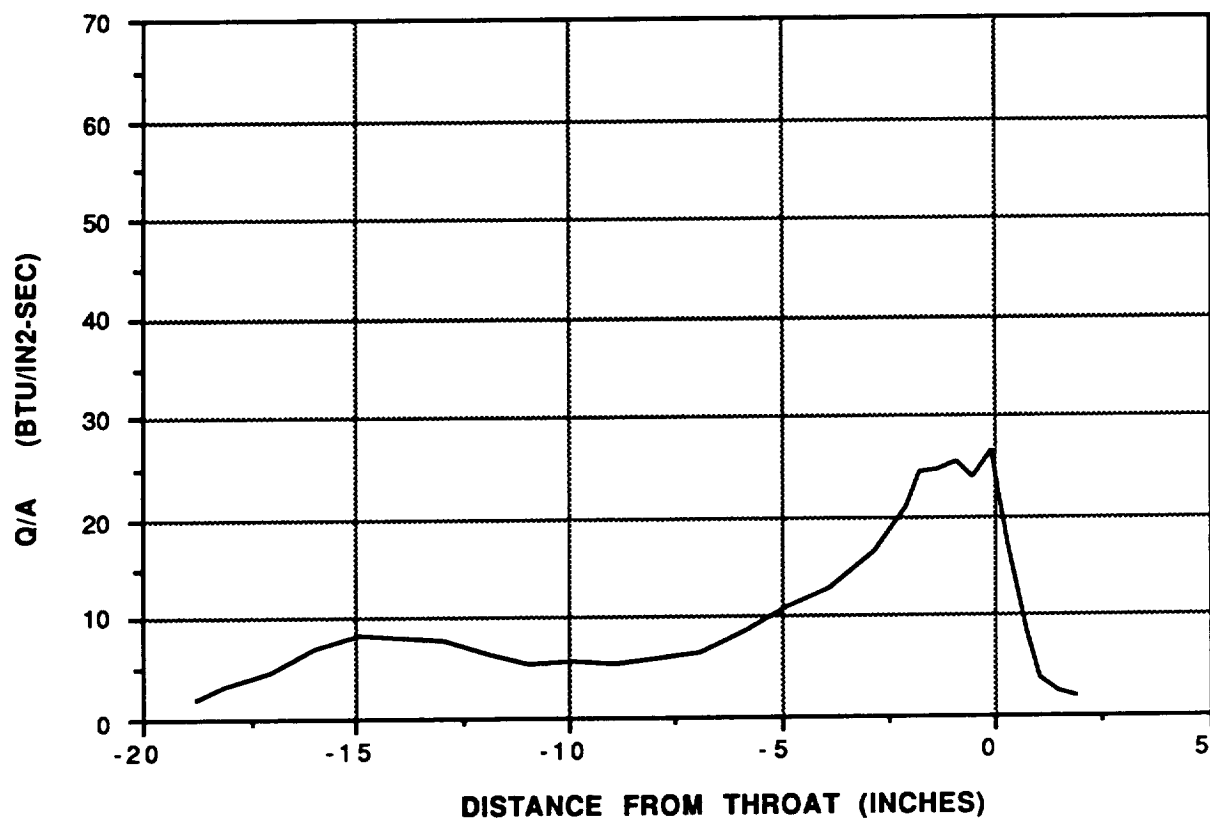


Figure 44. Axial Heat Flux Profile, Test 015-024, LOX Showerhead Injector

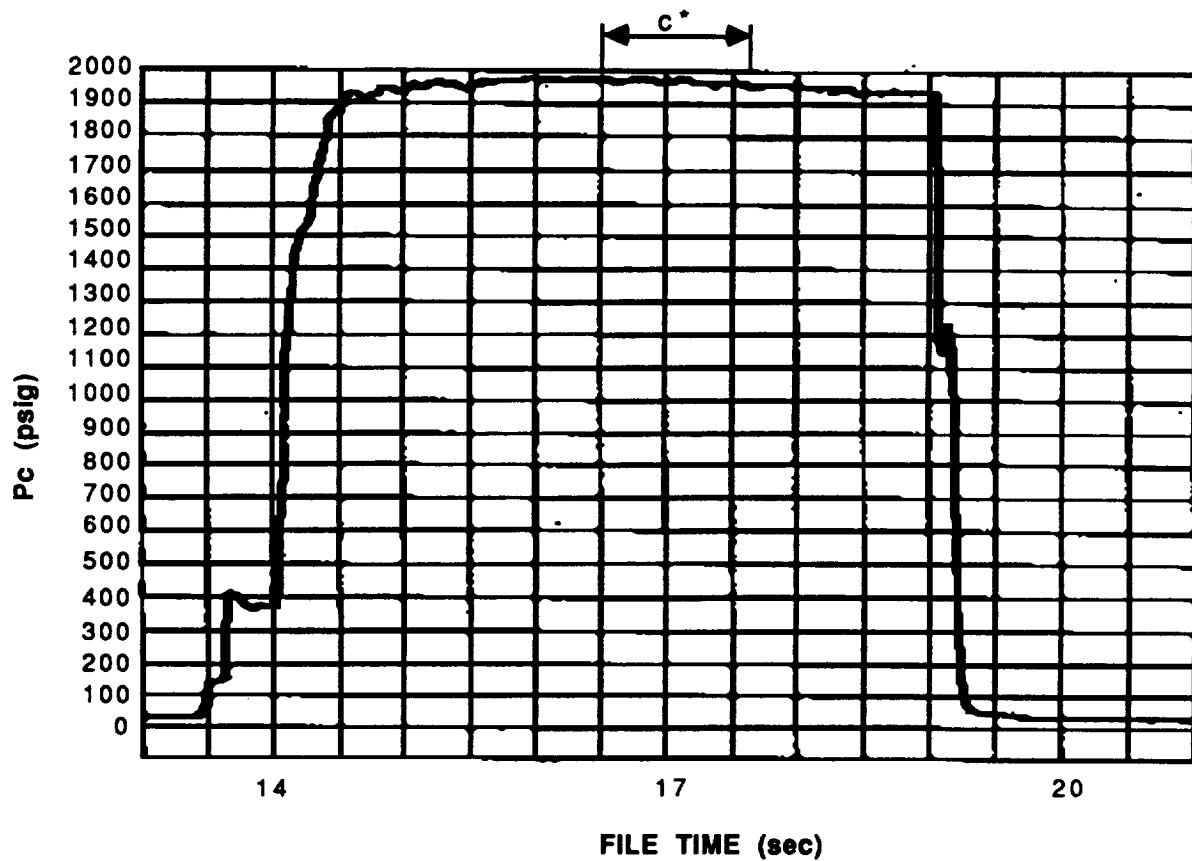


Figure 45. Static Chamber Pressure (Inj. End), Test 015-028, O-F-O Triplet Injector

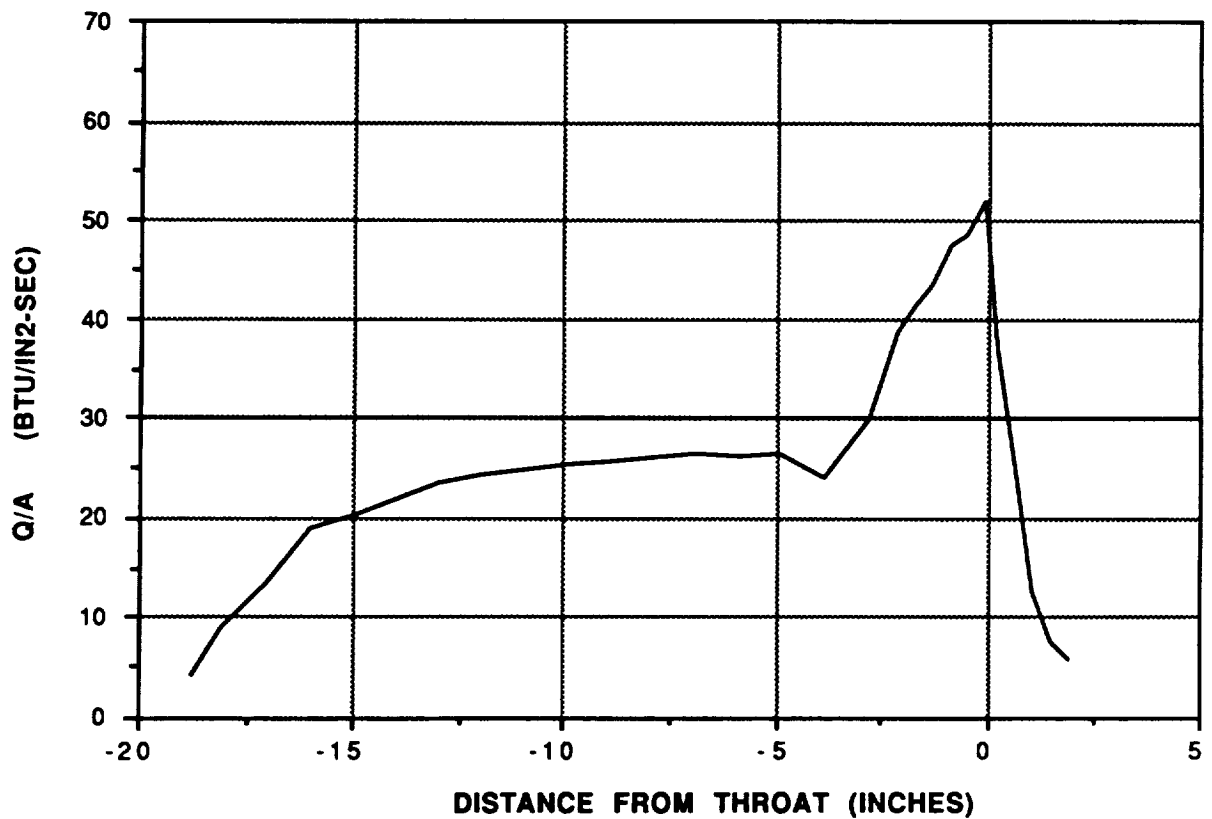


Figure 46. Axial Heat Flux Profile, Test 015-028, O-F-O Triplet Injector

5.6.1.4 Like-Doublet, Circumferential Fan Injector

Test No. 015-031 was the 5-second test of the Circumferential-Fan injector. Injector end static pressure is shown in Figure 47. Performance data are summarized in Table 6.

Heat flux data of Test No. 015-031 are plotted in Figure 48 and summarized in Table 7.

Stability data from Test No. 015-031 are given in Table 8.

5.6.1.5 Like-Doublet, Box Pattern Injector

The static chamber pressure at the injector end for the 5-second test (Test No. 015-033) of the Box-Doublet injector is shown in Figure 49. Data for the c^* measurement were taken during the steady portion of the test about midway through mainstage, as indicated. An unexplained drop in chamber pressure occurred during the last third of the firing. Performance data are summarized in Table 6.

The heat flux plot of Test No. 015-033 is shown in Figure 50; data are given in Table 7.

Stability results obtained in this test are listed in Table 8.

5.6.2 DISCUSSION

5.6.2.1 Performance

The measured c^* efficiencies of the five injector patterns tested are listed in Table 6. Since all the injectors were tested in the same combustor and facility, with the same instrumentation and procedures, and all the tests were carried out over a short period of time, the relative values of the efficiencies have a high degree of validity. The highest performance level was shown by the three self-impinging, high element density patterns (H-1 Derivative, Circumferential Fan Like-Doublet and Box Like-Doublet).

About two percent lower c^* efficiency was measured with the O-F-O Triplet injector, which had large orifices and low element density. Although O-F-O Triplet elements with

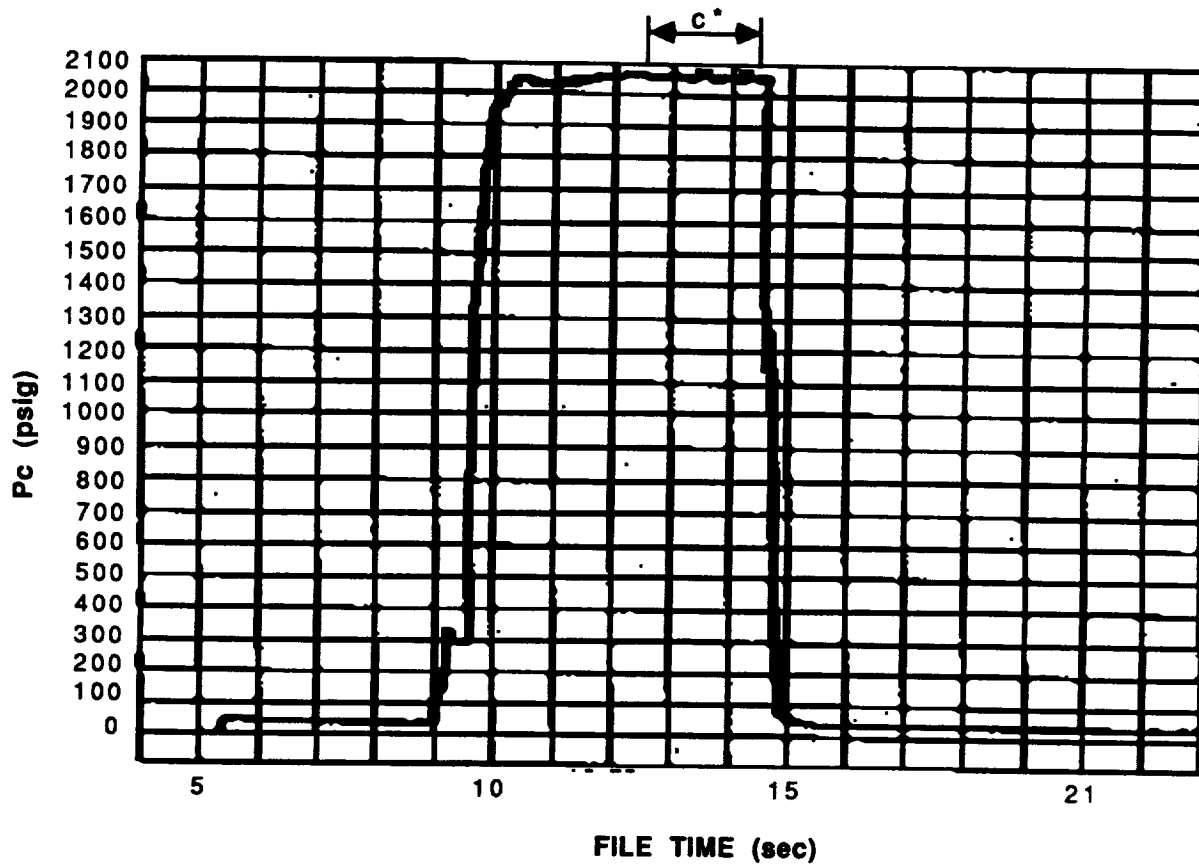


Figure 47. Static Chamber Pressure (Inj. End), Test 015-031, Circumferential-Fan Injector

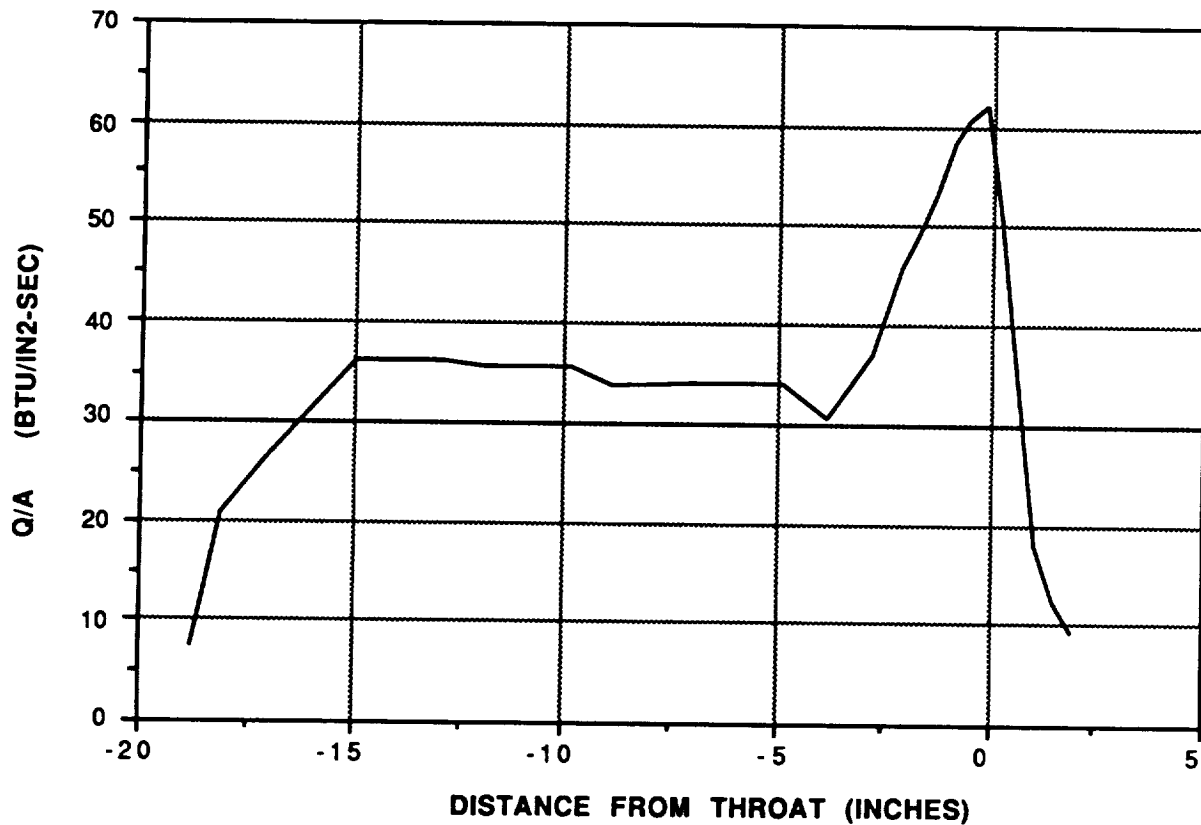


Figure 48. Axial Heat Flux Profile, Test 015-031, Circumferential-Fan Injector

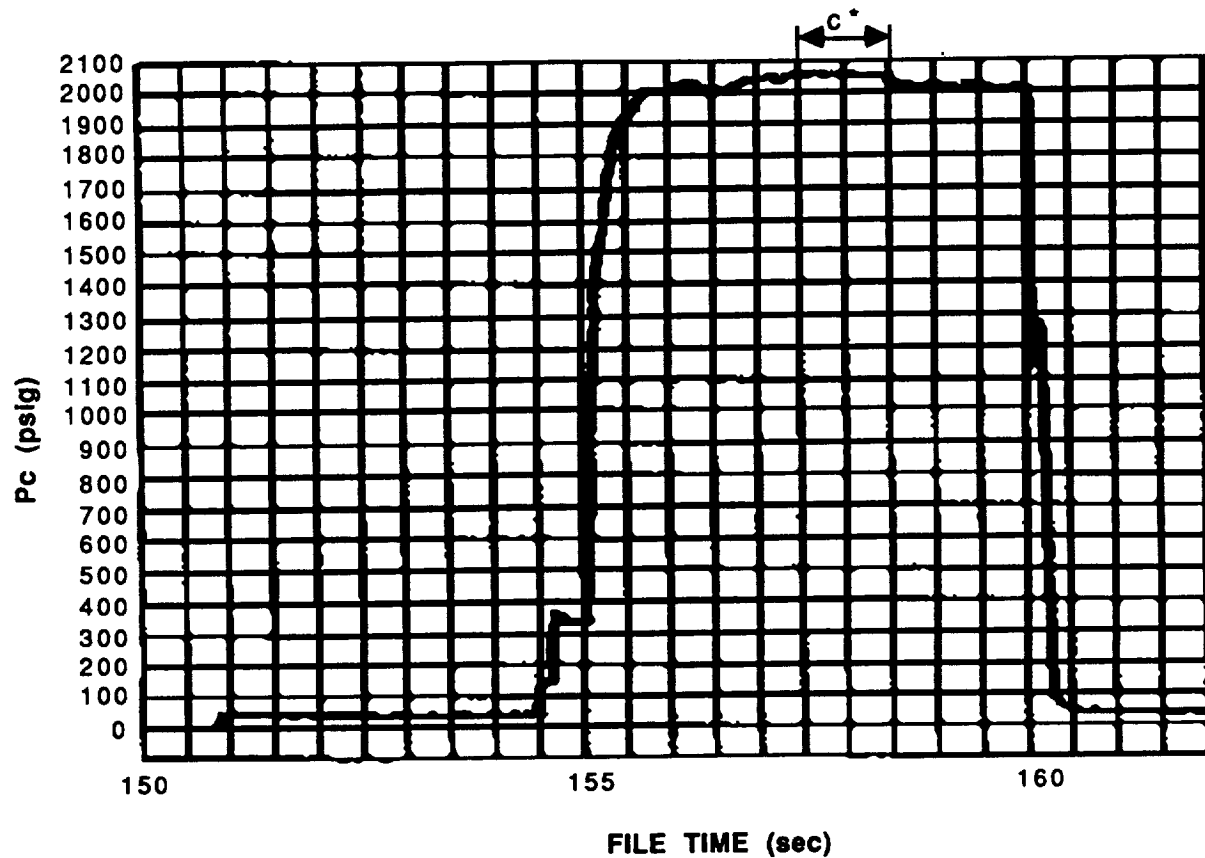


Figure 49. Static Chamber Pressure (Inj. End), Test 015-033, Box-Doublet Injector

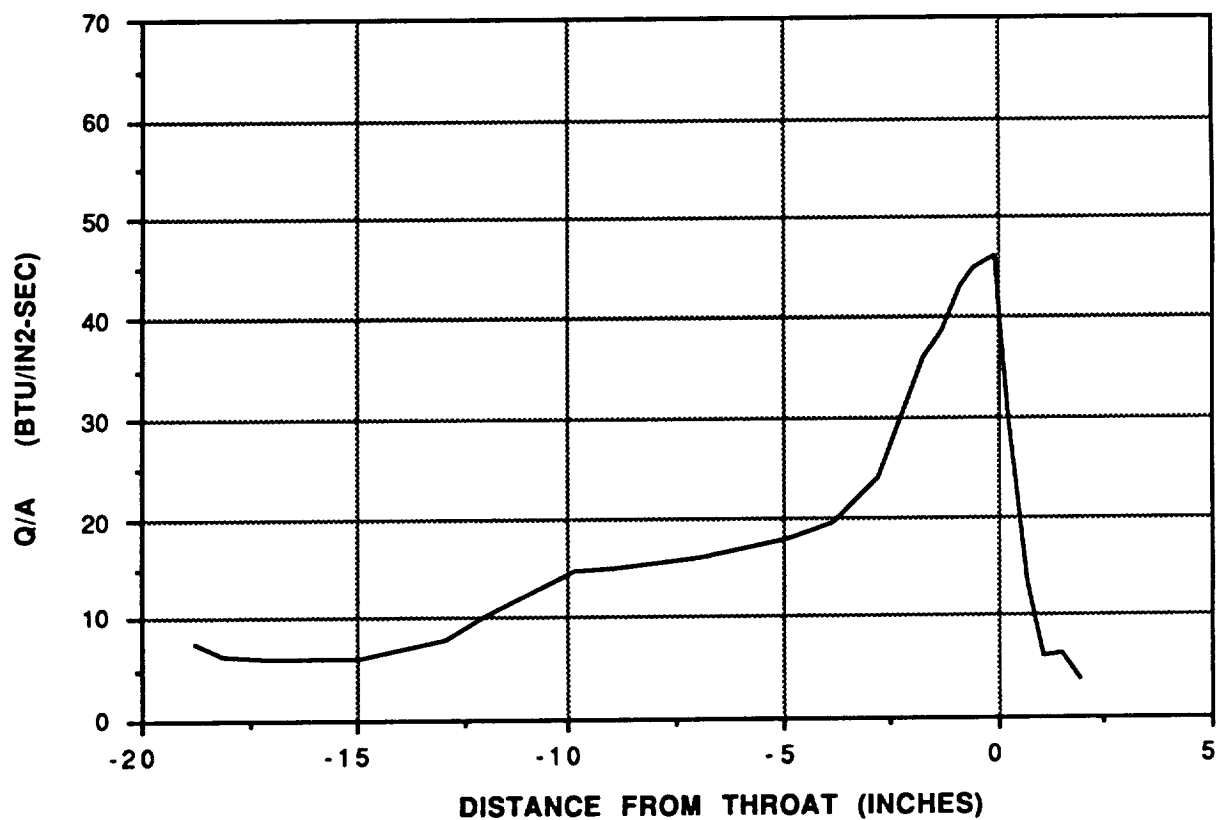


Figure 50. Axial Heat Flux Profile, Test 015-033, Box-Doublet Injector

large orifices have been reported to show high c^* efficiency levels (Ref. 2), those measurements were made with a 7.7-inch-diameter injector under non-steady-state conditions. Other LOX/RP-1 tests, with smaller O-F-O element orifices, in a 5.4-inch chamber, showed high c^* efficiencies (Ref. 10).

As expected, the lowest c^* efficiencies were exhibited by the LOX Showerhead injector, primarily because of its poor mixing characteristics. Performance of this injector would very likely be significantly improved by the comparatively simple expedient of adding swirlers to the LOX orifices.

5.6.2.2 Heat Flux

The heat flux characteristics of the five injectors are summarized in Table 7. The "Fuel in Periphery" column indicates whether or not there was a fuel-rich bias around the injector circumference which would affect the chamber wall heat load. Several factors related to chamber and throat heat flux are indicated by the data:

1. Heat flux levels can be substantially affected by performance levels. The low-performing LOX Showerhead injector had total heat loads less than half those of the higher performance patterns. In addition, decreasing the mixture ratio from 2.8 to 2.4 significantly decreased the heat flux in the chamber and throat.
2. The use of an outer fuel ring in which only enough fuel is injected to react with the adjacent oxidizer ring (as in the H-1 Derivative injector) did not reduce heat flux significantly.
3. With injectors at the same performance level, such as the Circumferential-Fan and Box-Doublet injectors, the presence of boundary layer coolant (BLC) significantly reduced heat flux levels.
4. The Box-Doublet, which has BLC, exhibited about the same c^* efficiency as the Circumferential-Fan injector without BLC.

5.6.2.3 Stability

Data were obtained from seven high-frequency transducers in each of the injector tests: 3 accelerometers (axial, tangential, and radial) and four PCBs (one in each propellant manifold and two in the chamber instrumentation ring, 1.5-in from the injector face and 120-degrees apart). STATOS and isoplot records were generated for each transducer output and examined to determine the timing, frequency, and amplitude of the oscillations. Primary attention was paid to the PCB data, because the accelerometers were installed primarily to trigger the automatic cut-off devices in the event of high-amplitude instability and as back-up to the PCBs.

Data from the PCB transducers obtained during the mainstage portion of a five-second test with each injector are summarized in Table 8. The natural frequencies of the 3.5-inch combustor are 1260 Hz (1L), 8020 Hz (1T) and 13,300 Hz (2T).

The most stable injectors were the Circumferential-Fan and Box-Doublet; the H-1 Derivative and LOX Showerhead injectors were less stable; and the least stable, by a substantial margin, was the O-F-O Triplet, contrary to the analytical predictions.

In all the tests, the highest oscillation amplitudes were observed in the oxidizer dome. With the O-F-O Triplet injector, the high-amplitude oxidizer dome oscillations, at about 1350 Hz, started before the main fuel valve was opened; a secondary oscillation at 2850 Hz also appeared in the isoplot. The chamber high-frequency oscillations, at 1350 and 1500 Hz, were in phase with the dome oscillations. Similar frequency, but lower amplitude, oscillations in the fuel manifold lagged the activity in the dome and chamber. The 1350 Hz oscillations were apparently a dome mode which coupled with the 1L chamber mode.

The stable combustion behavior of the Circumferential-Fan injector is indicated in a section of the expanded STATOS record during mainstage, shown in Figure 51. Oscillatory amplitudes in the chamber are low, with no organized tuned frequencies. The Box-Doublet injector gave similar traces.

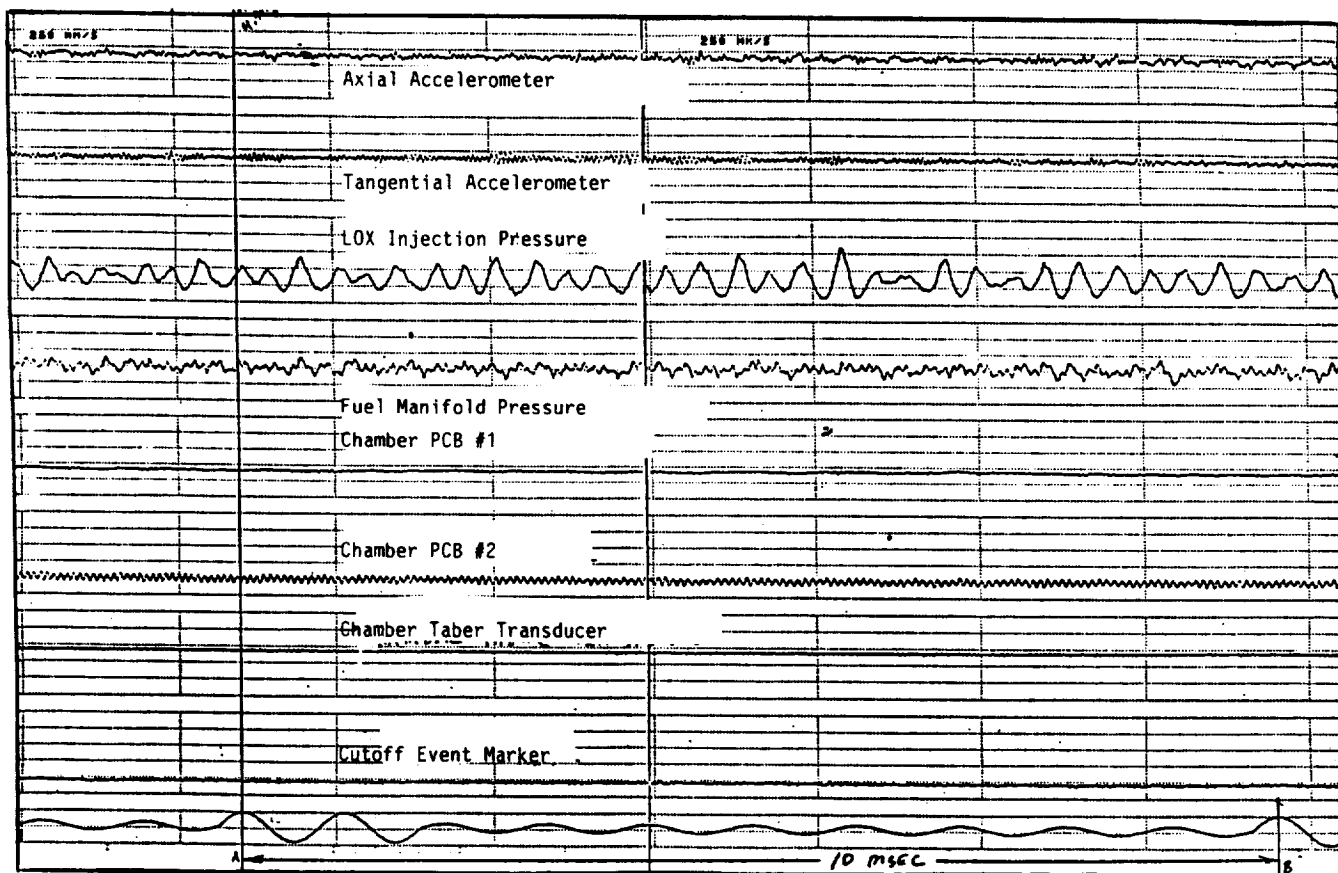


Figure 51. Test 015-031 High Frequency Data

5.6.2.4 Conclusions

Although the targeted goal of 97-percent c^* efficiency was not reached with any of the 3.5-inch injectors, the performance data showed that like-impinging injection patterns remain the preferred conservative approach to moderately high c^* efficiency with LOX/RP-1. Unlike-impinging elements with small orifices would probably give high performance, but they would be more difficult to stabilize. Thus, the indicated approach to a comparatively stable, high performance, LOX/RP-1 injector is a like-doublet pattern, with orifices small enough to give good atomization in an arrangement that maximizes mixing efficiency.

The heat flux levels measured in these tests are substantially higher than would be extrapolated from those of the classic LOX/RP-1 injectors, very probably due to the absence of significant soot deposits at the high chamber pressures and the use of lesser proportions of BLC, if any. Nevertheless, design of high-pressure LOX/RP-1 injectors should primarily target high performance rather than low heat flux, because use of BLC or other techniques can bring chamber and throat region heat loads down to manageable levels.

The stability data indicate that the acoustic cavity configurations used in the 3.5-inch combustor tests maintained chamber stability for four of the injectors. For the fifth, the O-F-O Triplet, oscillation amplitudes in the chamber were unacceptably high. Modification of the cavities or use of a bimodal configuration would very probably dampen the amplitudes considerably. However, only one of the 3.5-inch injectors, the H-1 Derivative injector, was tested for dynamic stability during this phase of the program. It proved to be dynamically stable with acoustic cavities. There are four major considerations with respect to injector design. Other less important concerns exist, but the four major concerns are stability, performance, heat flux and fabricability. All of these criteria must be weighted equally during the injector design process.

TASK II

6.0 ANALYSIS, DESIGN, AND TEST OF 5.7-INCH INJECTOR

6.1 INTRODUCTION

This section discusses first the selection of the 5.7-inch injector pattern, which was also intended for use in the ICC injectors of subsequent 2-D and full scale 3-D LOX/RP-1 combustors. The designs of the injector and the other components of the 5.7-inch calorimetric combustor are then presented, followed by a description of the hot-fire tests and a discussion of the test results.

6.2 INJECTOR SELECTION AND DESIGN

6.2.1 INJECTOR SELECTION

The 5.7-inch injector concept was selected on the basis of available high-pressure LOX/RP-1 test data and judgements as to the potential of various patterns to meet the performance, heat flux, and stability goals. Since the 5.7-inch combustor was intended to be a model of the ICC's of the subsequent 2-D and full-scale 3-D combustors, pertinent requirements of the latter two were also included in the injector selection and design considerations.

A review of the 3.5-inch injector test data discussed in Section 5.0, together with the results of a comprehensive literature survey of high pressure LOX/RP-1 injectors (Appendix A), led to three candidates for the 5.7-inch injector pattern: an O-F-O triplet, a box-type like doublet, and a canted-fan like doublet.

The triplet pattern was eliminated because previous experience with unlike-impinging LOX/RP-1 injectors indicated that achievement of statistically stable combustion would be difficult with orifice sizes small enough to give high performance. Further effort to develop stability aids which would consistently stabilize such patterns may demonstrate the simultaneous achievement of high performance and reliable stability. In the absence of such demonstration, however, it was decided not to use the O-F-O Triplet for this "one shot" design.

The Box-Doublet pattern was a viable candidate. Its performance level in the 3.5-inch combustor was about the same as that of the best classic-type LOX/RP-1 injector (the H-1 Derivative pattern); its heat flux was moderate (with boundary layer cooling); and it exhibited stable combustion. The Circumferential-Fan pattern in the 3.5-inch configuration was demonstrated to have the same c^* efficiency and stability behavior as the Box-Doublet and is included in the discussion below on the canted-fan like-doublet pattern.

The third injector candidate was a canted-fan like-doublet pattern, which had not been used previously in this program. It had been employed in a rectangular LOX/JP-4 injector (Figure 52), similar to the one planned for the 2-D combustor ICC's. In this pattern, the spray fans formed by an adjoining pair of oxidizer and fuel orifices impinge edgewise and are angled into each other to improve mixing of the atomized liquids (Figure 53). This injector was tested in an experimental program which demonstrated its performance, heat flux, and stability characteristics when operated with LOX and JP-4 (containing cesium carbonate "seed") for application in a 30 MW magnetohydrodynamic power system (Ref. 11). The injector was designed for high performance, stable combustion and provision of a highly uniform flow field across the rectangular cross-section. A quarter-wave slot was included around the injector periphery for acoustic damping. Test results at 440 psia chamber pressure were summarized as follows: c^* efficiency (based on chamber pressure measured at the nozzle inlet, corrected to throat stagnation pressure) was 99-percent at the design (stoichiometric) mixture ratio of 3.34 and remained between 98- and 99-percent down to a mixture ratio of 2.8. Static wall pressure measurements along the combustion chamber indicated that combustion was essentially complete at about 12-in. from the injector face. The chamber and throat heat transfer film coefficients were substantially lower than analytical predictions; this was ascribed to carbon deposition. Chamber pressure oscillations were less than 3-percent peak-to-peak with trimodal acoustic cavity slots incorporating an open area of about 15-percent. It was with this pattern in mind that the 3.5-inch Circumferential-Fan injector was developed, in which the fans were side-impinging alternating fuel and oxidizer pairs. It differed in that the fans were circumferentially rather than radially oriented and there was no cant angle.

These experimental data, demonstrating the simultaneous achievement of high performance, moderate heat flux without film cooling, and stable combustion, were the

ORIGINAL PAGE
BLACK AND WHITE PHOTOGRAPH

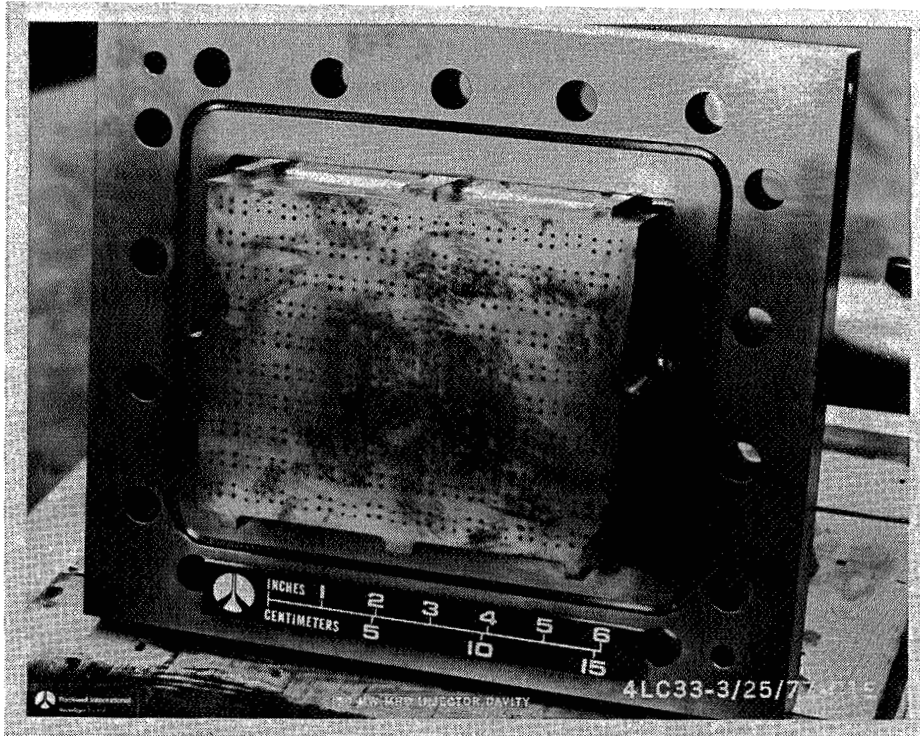


Figure 52. LOX/JP-4 Injector for 30 MW MHD Combustor

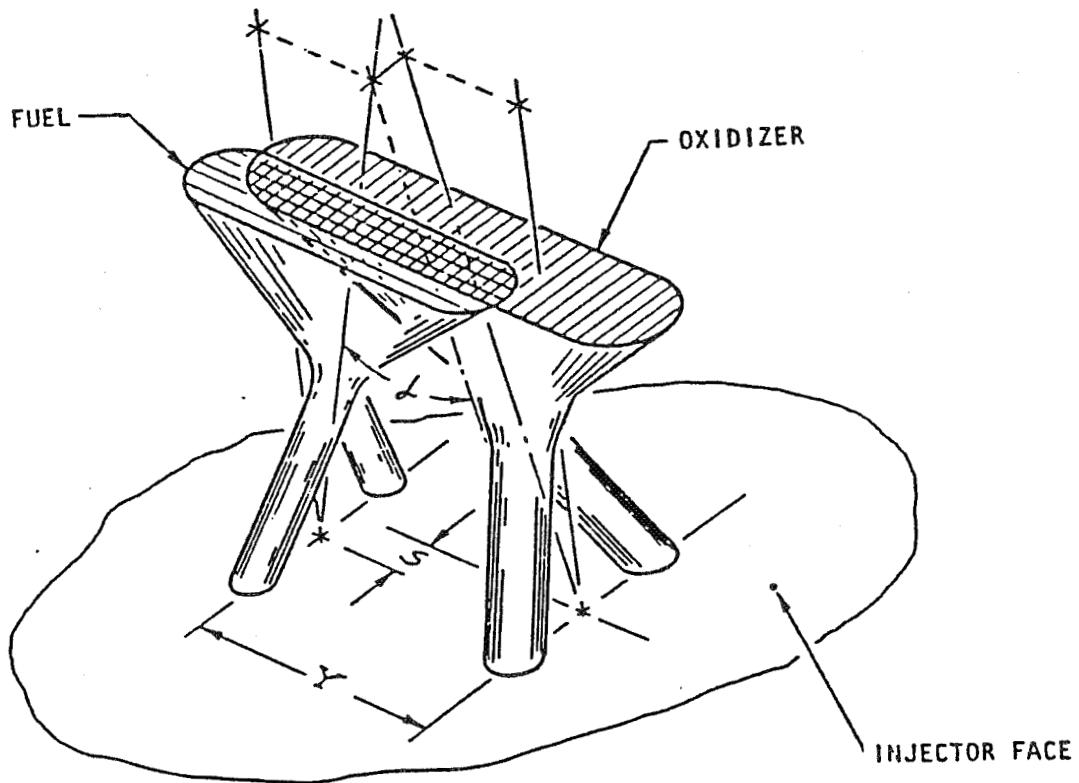


Figure 53. Canted-Fan Like-Douplet Injection Element

deciding factors in the selection of the canted-fan like-doublet pattern for the 5.7-inch and 2-D injectors. The resultant 5.7-inch diameter injector evaluated on this program was an attempt to combine the best features of both injectors. Due to limitations in the fabricability of a circumferential-fan pattern in 2-D and full-scale combustors, the fans were rotated to a radial orientation, still side-impinging, and cant angles were added for improved mixing characteristics.

6.2.2 INJECTOR DESIGN

The design criteria for the 5.7-inch injector were based on the following considerations:

- 1. Performance**

To maintain the high performance of the 30 MW injector, the 5.7-inch design retained the pattern configuration, the orifice size range, and the element separation of the low-pressure design.

- 2. Heat Flux**

To alleviate the high heat flux levels often associated with high performance at elevated chamber pressures, addition of boundary layer cooling obtained from a small fraction of the total fuel flow was incorporated.

- 3. Stability**

Properly designed acoustic cavities have been demonstrated to provide stable combustion even at high chamber pressures and were included in this configuration.

These concepts were implemented by the design sketched in Figure 54. Alternating rings of edge-impinging, radial-fan, oxidizer and fuel doublets, with 60-degree self-impingement angles, are configured to provide a 14-degree cant angle between the fans, as indicated. The 4-degree oxidizer fan cant and 10-degree fuel fan cant balance the radial momentum components to give the resulting mixture an axial flow direction. The injector pattern has 372 oxidizer orifices (184 doublets plus 4 singlets at the center) and 408 fuel orifices (188 doublets plus 32 singlet BLC). The distribution

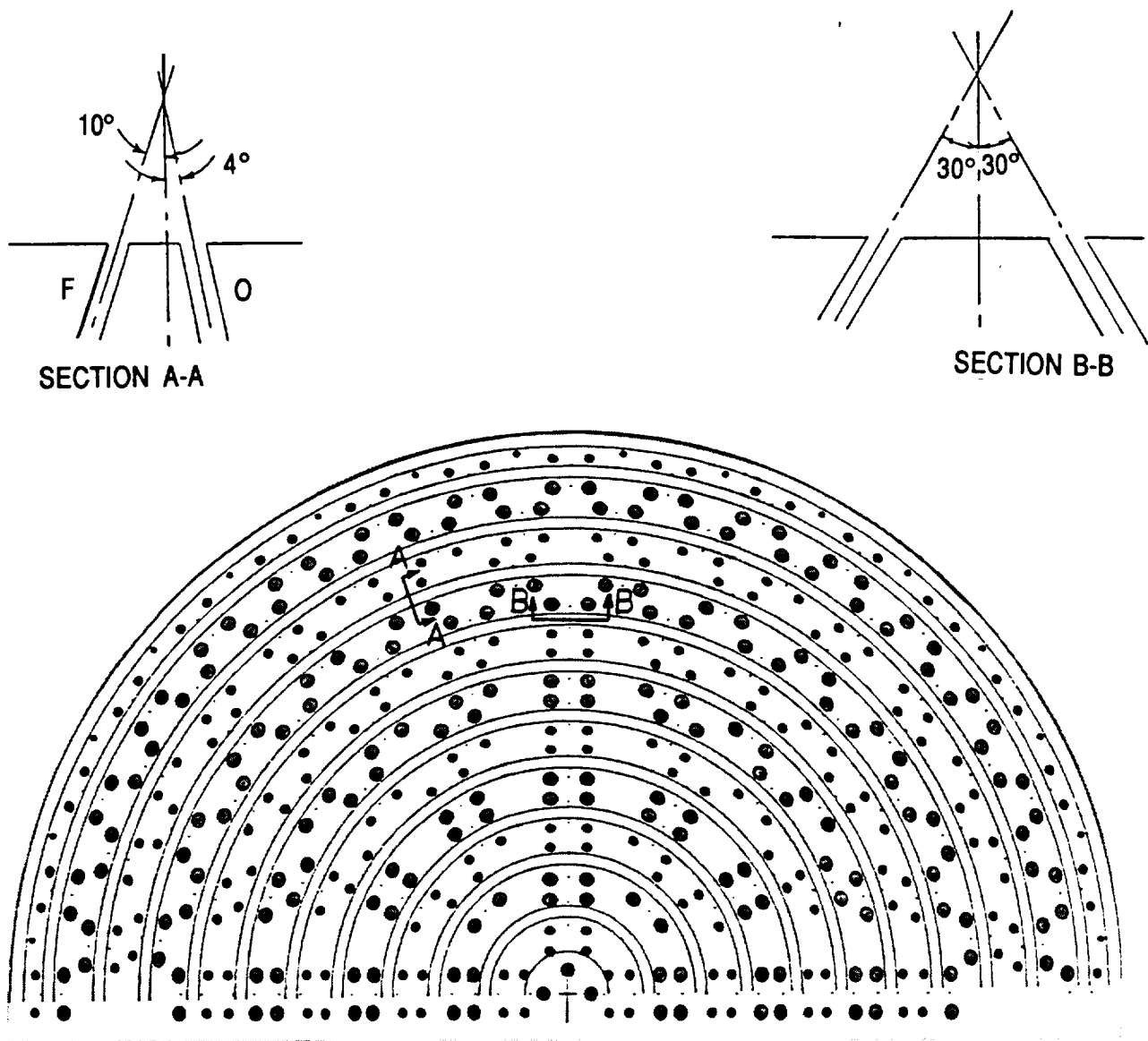


Figure 54. Canted-Fan Like-Doublet Pattern, 5.7-inch Injector

and sizes of the injection orifices are listed in Table 9.

The injector was designed as a cylindrical insert to fit into the center of the fuel manifold. It consists of a 347-CRES body into which the OFHC copper orifice rings were brazed. Following ultrasonic inspection of the copper-CRES braze joints, the orifices were EDM-drilled into the face rings. An efficient process for rapid EDM fabrication of orifices in copper plates was used.

The detailed drawing of the 5.7-inch injector (Drawing No. 7R035427) is reproduced in Figure B-6 of Appendix B. A photograph of the injector face is shown in Figure 55; the entire injector body is shown in Figure 56.

6.3 COMBUSTOR COMPONENTS

Designs of the components of the 5.7-inch combustor followed closely those of the 3.5-inch combustor, to satisfy the same basic requirement: acquisition of LOX/RP-1 performance, heat flux, and stability data at up to 3000 psia chamber pressure.

For design purposes and structural analyses, chamber pressure was stipulated as 3600 psia. The factor-of-safety criteria for structural adequacy, which were satisfied by all the components, were:

(F.S.) ultimate	≥ 1.4	(combined loads)
	≥ 1.5	(pressure loads)
(F.S.) yield	≥ 1.1	
(F.S.) shear, ult.	≥ 2.0	

In all cases, a limit load factor of 1.2 for pressures was used. The analyses were based on worst case operating conditions. For example, the NARloy-Z liners of the cooled components were analyzed on the basis of maximum channel pressures, at maximum operating temperatures, with zero chamber pressure (i.e., at test shutdown). In addition, all braze joints were assumed to have only 50-percent braze coverage.

The calorimetric combustor assembly schematic is shown in Figure 57. Except for the size factor, it differs from the 3.5-inch combustor assembly in only two minor respects:

Table 9. Orifices in 5.7-Inch Injector

Ring No.	Propellant	Pattern	OXID. ORIFICES		FUEL ORIFICES	
			No.	Diam., in.	No.	Diam., in.
1	Fuel	32 S/H			32	.024
		32 Doublets			64	.037
2	Oxid.	32 Doublets	64	.058		
		32 Doublets	64	.058		
3	Fuel	32 Doublets			64	.037
		24 Doublets			48	.037
4	Oxid.	24 Doublets	48	.058		
		24 Doublets	48	.058		
5	Fuel	24 Doublets			48	.037
		20 Doublets			40	.037
6	Oxid.	20 Doublets	40	.058		
		16 Doublets	32	.058		
7	Fuel	16 Doublets			32	.037
		12 Doublets			24	.037
8	Oxid.	12 Doublets	24	.058		
		12 Doublets	24	.058		
9	Fuel	12 Doublets			24	.037
		8 Doublets			16	.037
10	Oxid.	8 Doublets	16	.058		
		4 Doublets	8	.058		
11	Fuel	4 Doublets			8	.037
		4 Doublets			8	.037
12	Oxid.	4 Singlets	4	.058		

ORIGINAL PAGE
BLACK AND WHITE PHOTOGRAPH

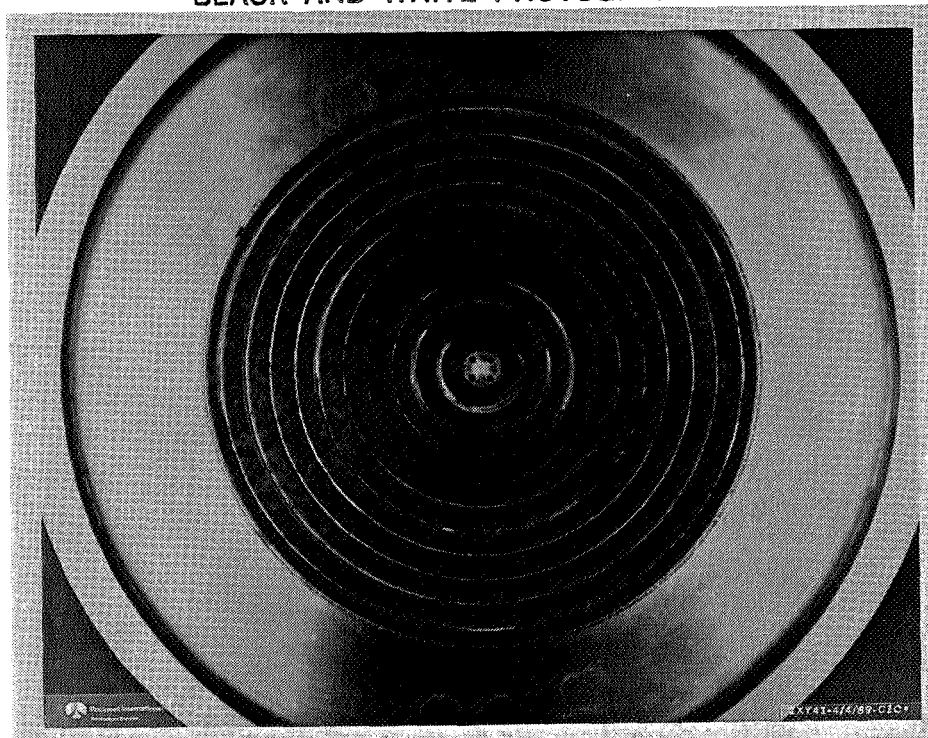


Figure 55. 5.7-Inch Canted-Fan, Like-Doublet Injector Face

ORIGINAL PAGE
BLACK AND WHITE PHOTOGRAPH



Figure 56. 5.7-Inch Canted-Fan, Like-Doublet Injector Body

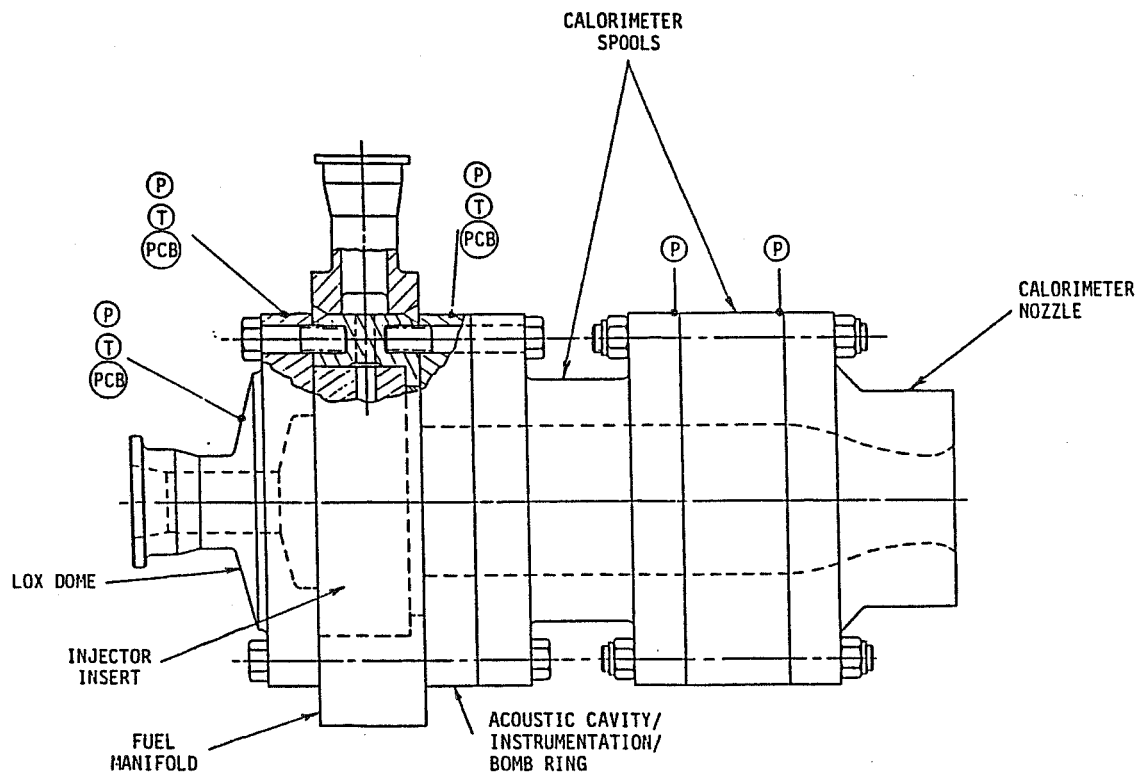


Figure 57. Assembly Schematic of 5.7-Inch Combustor
(Coolant Water Tubes Not Shown)

1. The chamber spool lengths in the 3.5-inch combustor are identical (6-in.) while different lengths (8-in. and 4-in.) are used in the 5.7-inch combustor.
2. None of the components of the 3.5-inch combustor is flanged; in the 5.7-inch combustor, the 8-in. chamber spool and the throat spool are flanged.

6.3.1 LOX DOME (Drawing No. 7R035366)

The LOX dome, which feeds the back of the injector through a single 3-inch Grayloc inlet, is constructed of CRES-304L. One pressure and one temperature port are provided for measurement of oxidizer injection parameters, as well as one port for a high-frequency pressure transducer. A photograph of the oxidizer dome is shown in Figure 58.

6.3.2 FUEL MANIFOLD (Drawing No. 7R034367)

Fuel is supplied to the injector periphery by an annular distribution manifold which encompasses the injector body. The manifold, made of CRES-304L, has a 2-inch inlet and ports for low- and high-frequency pressure transducers and for a thermocouple. A photograph of the fuel manifold is shown in Figure 59.

6.3.3 ACOUSTIC CAVITY RING (Drawing No. 7R035426)

The acoustic cavity ring, 1.33-in. in length, consists of a NARloy-Z liner brazed into a CRES-304L housing. The liner has six circumferential coolant channels fed and drained by single tubes. The ring is designed to provide seven, quarter-wave, axial acoustic cavity slots, four tuned to the 1T chamber frequency and three to the 2T. Instrumentation ports are provided for seven thermocouples (one in each cavity) and two low-frequency pressure transducers (one in a 1T cavity and the other in a 2T cavity). One drainage port is also provided. The total acoustic slot open inlet area is 8.6-percent of the chamber area for the 1T mode and 6.4-percent for the 2T mode, for a total of 15-percent. A photograph of the acoustic cavity, with dams and thermocouples, is shown in Figure 60.

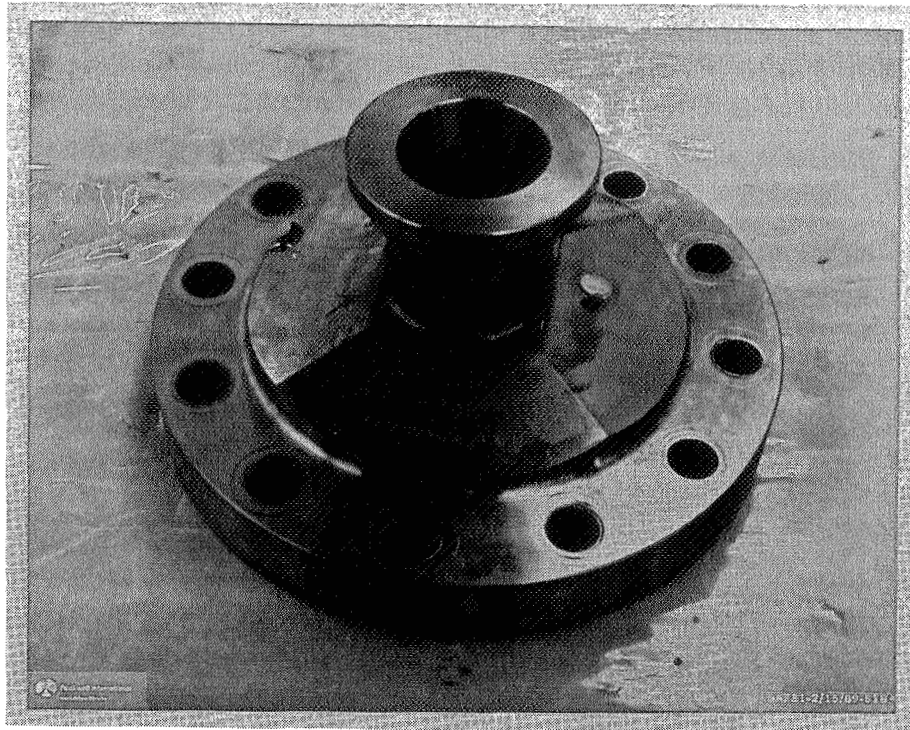


Figure 58. LOX Dome, 5.7-Inch Combustor

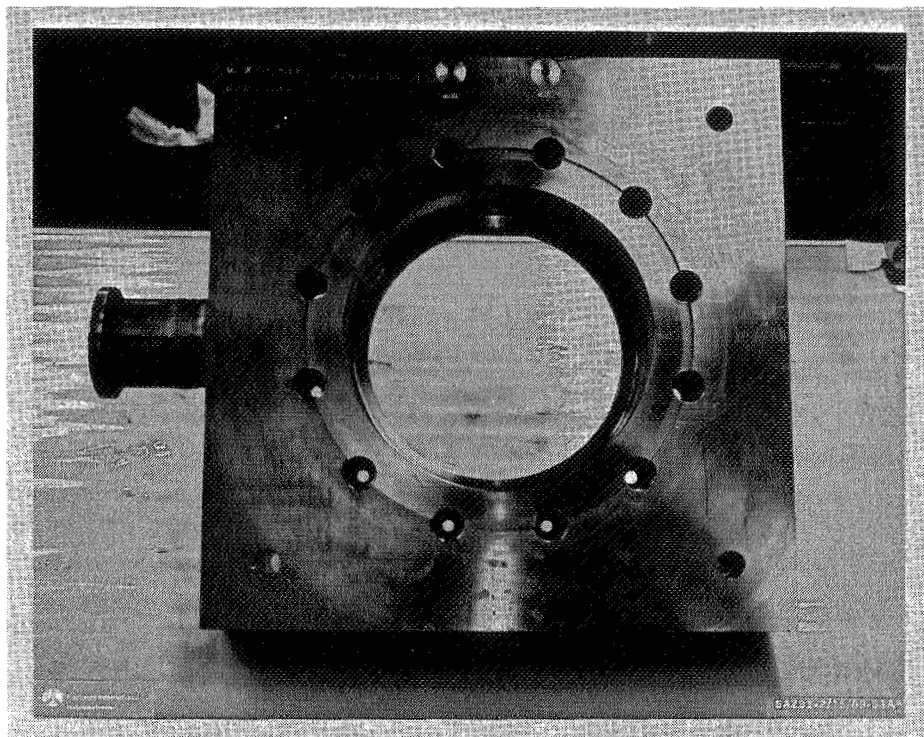


Figure 59. Fuel Manifold, 5.7-Inch Combustor

6.3.4 INSTRUMENTATION RING (Drawing No. 7R034368)

The 2.0-inch-long instrumentation ring also consists of a NARloy-Z liner brazed into a CRES-304L shell. Two each water inlet and outlet tubes are provided for the 14 circumferential coolant channels in the liner. In addition to one inlet for TEA/TAB igniter, ports are provided for two low-frequency pressure transducers and three high-frequency pressure transducers located at 0-, 90- and 210-degrees. A photograph of the instrumentation ring is shown in Figure 61.

6.3.5 BOMB RING (Drawing No. 7R035425)

An uncooled "bomb" ring replaces the water-cooled instrumentation ring in short-duration tests in which a stability rating bomb is detonated to determine the dynamic stability of the injector. The bomb ring consists of a NARloy-Z core in a CRES-304L housing. The same instrumentation ports are provided as in the instrumentation ring plus an additional port for the bomb mounting (considering the bomb port to be located at 0-degrees, the three high-frequency transducers are located at 30-, 120-, and 240-degrees).

6.3.6 CHAMBER SPOOL, 8-INCH (Drawing No. 7R035369)

The flanged, 8-inch, chamber spool consists of a NARloy-Z liner brazed into a CRES-304L housing. The liner has 64 circumferential coolant channels machined around it which are supplied and drained by eight each inlet and outlet water tubes. A static pressure port is provided at the spool exit. A photograph of the chamber spool is shown in Figure 62.

6.3.7 CHAMBER SPOOL, 4-INCH (Drawing No. 7R035370)

The 4-inch chamber spool is not flanged. It has a NARloy-Z liner brazed into a CRES-304L housing. Thirty-two circumferential coolant grooves machined into the liner are fed by four water lines and drained by four lines. A static pressure tap is provided at the chamber exit. A photograph of the component is shown in Figure 63.

ORIGINAL PAGE
BLACK AND WHITE PHOTOGRAPH

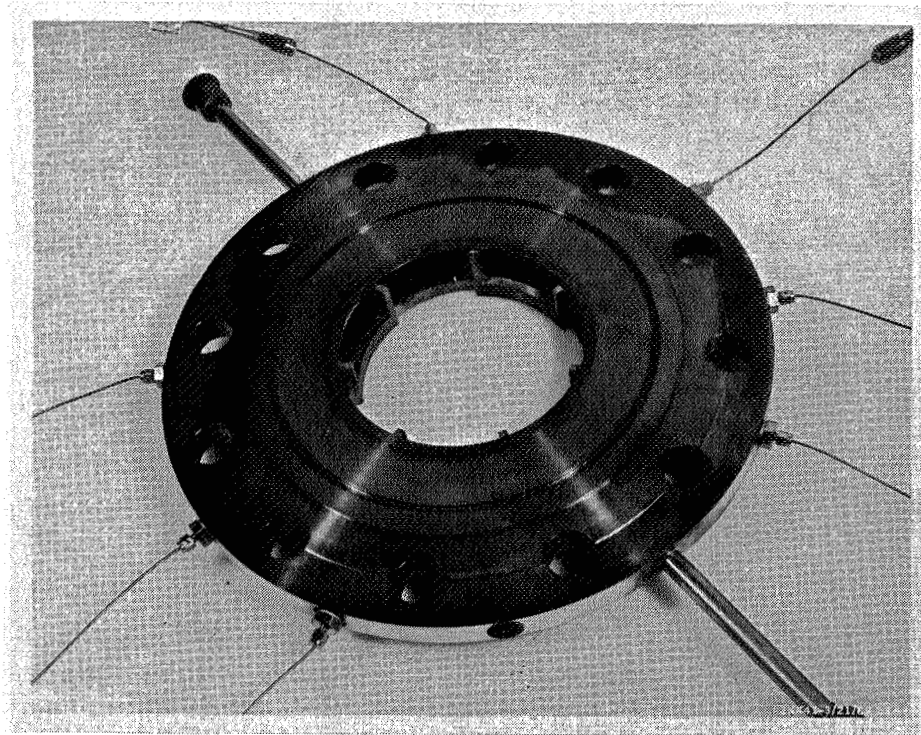


Figure 60. Acoustic Cavity Ring, 5.7-Inch Combustor

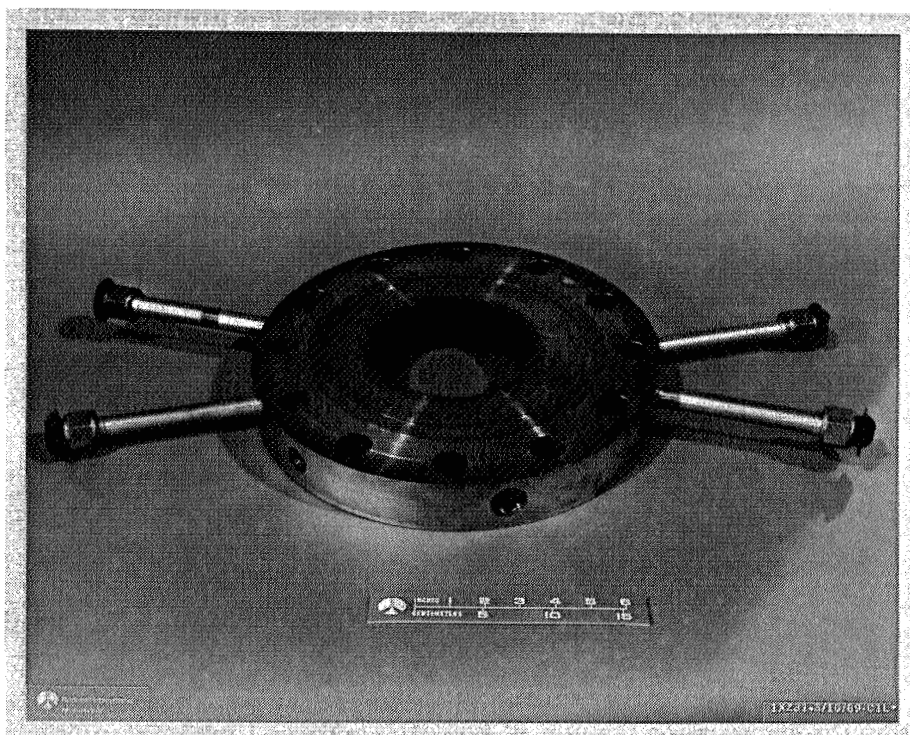


Figure 61. Instrumentation Ring, 5.7-Inch Combustor

ORIGINAL PAGE
BLACK AND WHITE PHOTOGRAPH

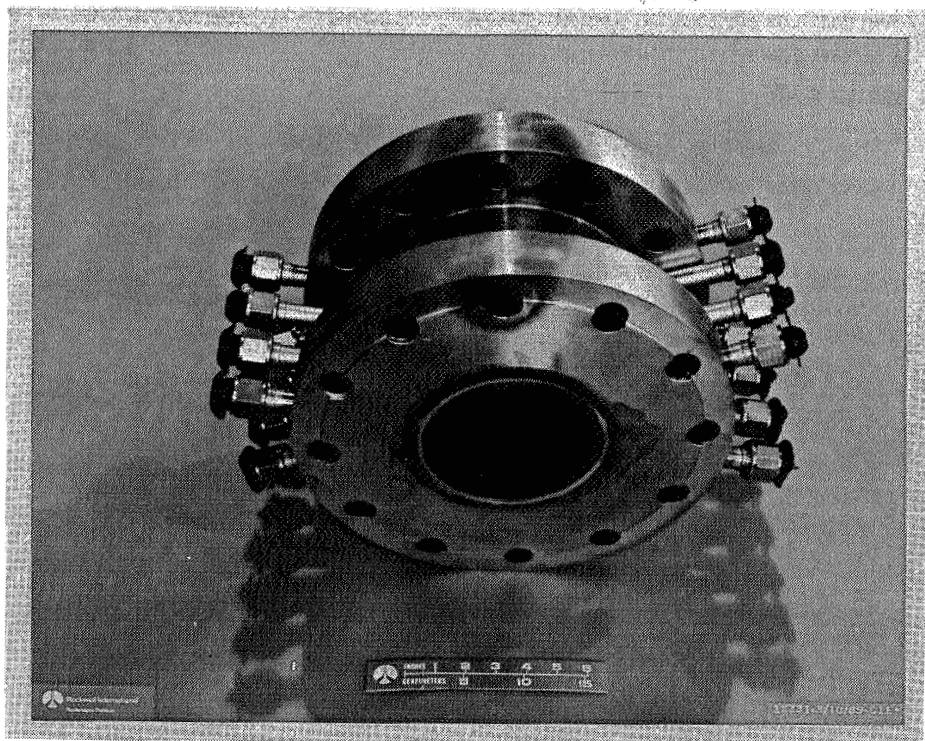


Figure 62. Chamber Spool, 8-Inch Length, 5.7-Inch Combustor

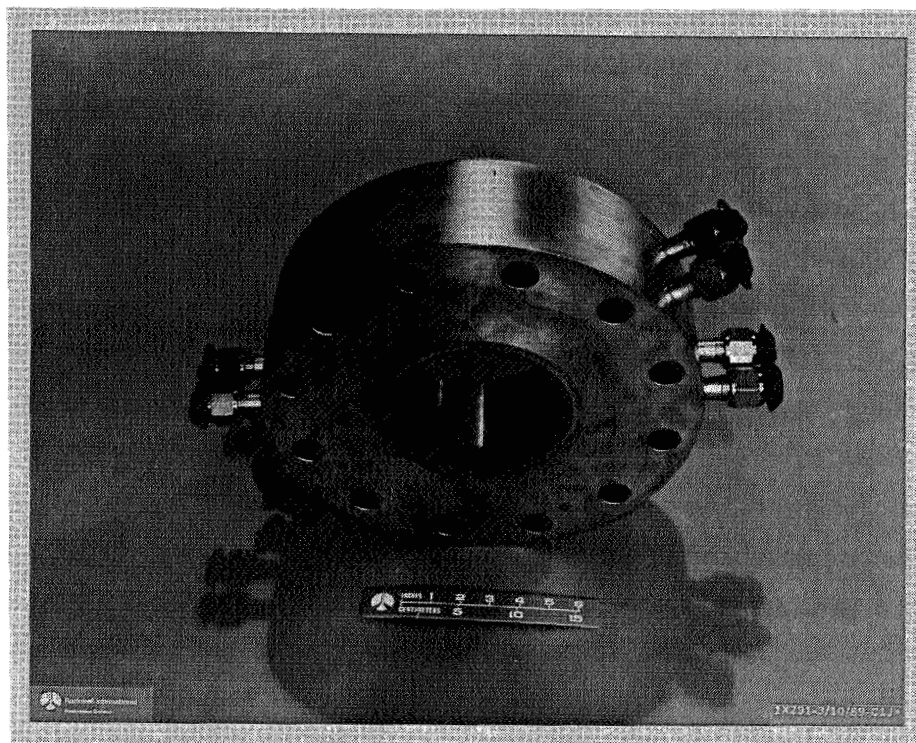


Figure 63. Chamber Spool, 4-Inch Length, 5.7-Inch Combustor

6.3.8 THROAT SPOOL* (Drawing No. 7R034093)

The throat spool, shown in Figure 64, consists of a NARloy-Z core brazed into an Inconel-625 shell. Fourteen inlet water tubes and fourteen outlet tubes service the 62 circumferential coolant channels machined into the liner and closed out with brazed-in OFHC copper wafers. The overall length of the throat spool is 7.0 in.

6.3.9 COMBUSTOR ASSEMBLY (Drawing No. 7R035319)

In the 5.7-inch combustor assembly (Figure 57), the upstream flange of the 8-inch spool is joined to the forward components (LOX dome, fuel manifold, acoustic cavity, and instrumentation or bomb ring) and the downstream flange is joined to the aft components (4-inch chamber spool, which is optional, and the throat spool). Twelve one-inch studs are used as fasteners. A photograph of the assembled combustor on the test stand is shown in Figure 65.

Pertinent dimensions of the combustor are as follows:

Chamber diameter	=	5.66 in.
Throat diameter	=	3.58 in.
Contraction ratio	=	2.50
Expansion ratio	=	1.60
Injector face to throat distance	=	19.75 in.
L *	=	45 in. (with both chamber spools)

6.4 TEST FACILITY, INSTRUMENTATION AND PROCEDURES

6.4.1 FACILITY

Tests of the 5.7-inch combustor were conducted at the same facility as the 3.5-inch combustor tests, described in a preceding section of this report. Only the following modifications were required to accommodate the higher propellant flowrates and thrust level:

* The throat spool was designed and fabricated for a Rocketdyne IR&D task, from which it was borrowed for the present series of tests.

ORIGINAL PAGE
BLACK AND WHITE PHOTOGRAPH

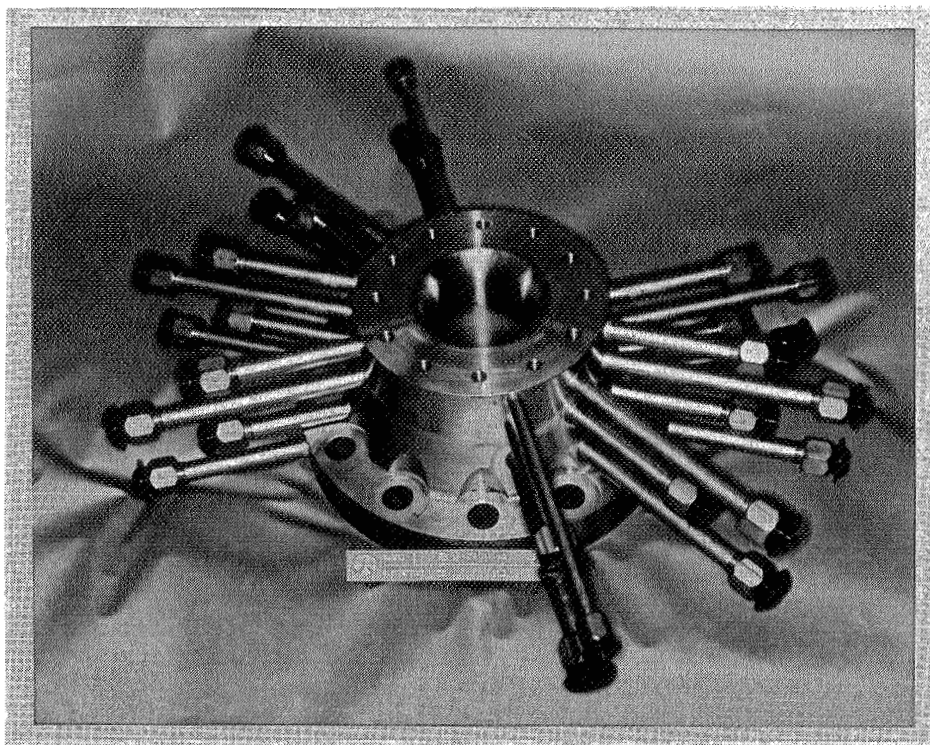


Figure 64. Throat Section, 5.7-Inch Combustor

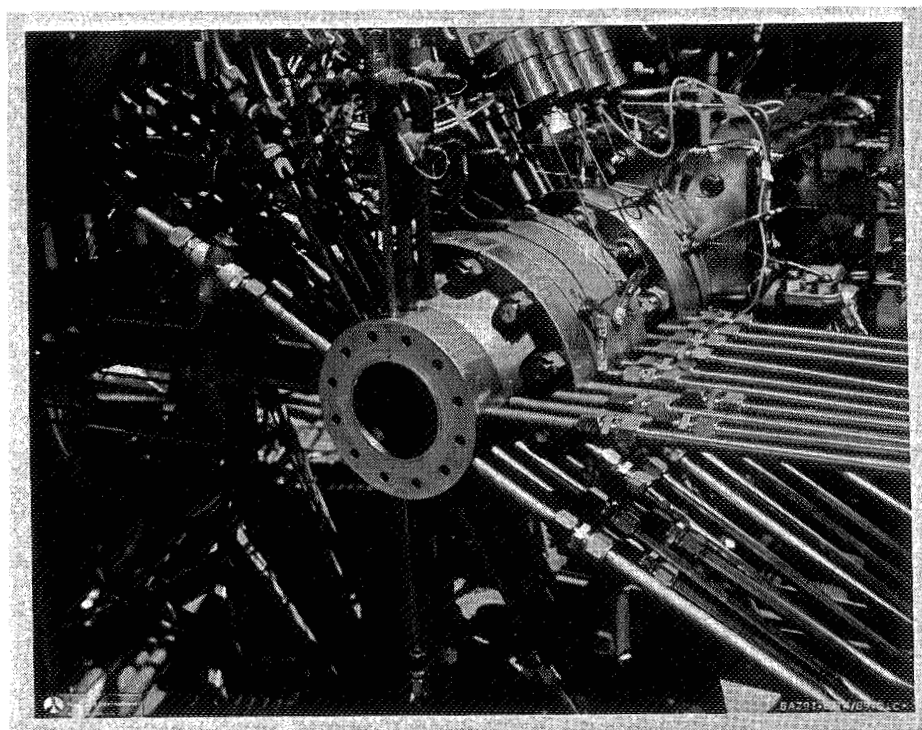


Figure 65. 5.7-Inch Combustor Assembly Mounted on Test Stand

1. An uprated hardware support, referred to as the "milk-stool", was installed. The combustor assembly is bolted to this support which, in turn, is fastened to the test stand thrust mount. The milk stool was designed to slope the chamber axis 3.4-degrees downward from the horizontal.
2. The LOX and RP-1 cavitating venturis were replaced by units appropriate to the higher flowrates:

LOX : $(D_t)_{\text{cav. vent.}} = 0.570 \text{ in.}$

RP-1 : $(D_t)_{\text{cav. vent.}} = 0.378 \text{ in.}$

3. New LOX and RP-1 study lines were installed between the combustor and the 40K main valves. (The 20K main valves had been used for the 3.5-inch combustor tests).

6.4.2 INSTRUMENTATION

Test instrumentation and data recording (Table 10) were the same as with the smaller combustor, except for the addition of four acoustical cavity temperatures to the three previously installed plus additional low-frequency and high-frequency pressure transducers in the instrumentation ring.

6.4.3 PROCEDURES

Test procedures were essentially unchanged from those used in the 3.5-inch combustor tests. Minor alterations were made in valve signal timing to accommodate the characteristics of the larger main and purge valves, to ensure timely displacement of helium from the fuel manifold at test start and rapid displacement of LOX from the oxidizer dome at test cut, consistent with a fuel-rich shutdown.

Table 10. Instrumentation List. 5.7-Inch Injector Tests

MSI NO.	PARAMETER	RANGE	TRANS- DUCER	OBC GRAPH	F/M TAPE
812	LOX TANK PRESS	5000 PSI	TABER		
24	LOX VENTURI U/S PRESS	5000 PSI	TABER		
112	LOX VENTURI U/S TEMP	-300 F	T/C		
25	LOX VENTURI D/S PRESS	5000 PSI	TABER		
26	LOX INJEC. PRESS	5000 PSI	TABER		
-	LOX INJEC. PRESS-HI FREQ		PCB	X	X
132	LOX INJEC. TEMP -300 F	T/C			
27	LOX PURGE PRESS	3000 PSI	TABER		
106	20K LOX BLEED TEMP	-300 F	T/C		
131	LOX RUNLINE TEMP	-300 F	T/C		
99	LOX TANK OUTLET TEMP	-300 F	BULB		
813	RP-1 TANK PRESS	5000 PSI	TABER		
30	RP-1 VENTURI U/S PRESS	5000 PSI	TABER		
130	RP-1 VENTURI U/S TEMP	150 F	T/C		
32	RP-1 VENUTI D/S PRESS	5000 PSI	TABER		
31	RP-1 INJEC. PRESS	5000 PSI	TABER		
-	RP-1 INJEC. PRESS, HI FREQ-1		PCB	X	X
-	RP-1 INJEC. PRESS, HI FREQ-2		PCB		X
33	RP-1 PURGE PRESS	3000 PSI	TABER		
37	TEAB SUPPLY PRESS	5000 PSI	TABER		
38	TEAB INJECT PRESS	5000 PSI	TABER		
864	GN2 5K SUPPLY PRESS.	5000 PSI	TABER		
125	ACOUSTIC CAVITY TEMP -1	2380 F	T/C		
	ACOUSTIC CAVITY TEMP -2	2380 F	T/C		
127	ACOUSTIC CAVITY TEMP -3	2380 F	T/C		
41	CHAMBER PRESS-1	3000 PSI	TABER	X	
42	CHAMBER PRESS-2	3000 PSI	TABER		
	CHAMBER PRESS-3	3000 PSI	TABER		
	CHAMBER PRESS -4	3000 PSI	TABER		
-	CHAMBER PRESS, HI-FREQ -1		PCB	X	X
-	CHAMBER PRESS, HI-FREQ -2	PCB		X	
-	CHAMBER PRESS, HI-FREQ -3	PCB		X	
-	ACCELEROMETER-AXIAL	1000 g	ENDEVCO	X	X
-	ACCELEROMETER-RADIAL	1000 g	ENDEVCO	X	X
-	ACCELEROMETER-TANGENTIAL	1000 g	ENDEVCO	X	X

Table 10. Instrumentation List (continued)

MSI NO.	PARAMETER	RANGE	TRANS- DUCER	OSC.- GRAPH	F/M TAPE
507	WATER TANK PRESS	5000 PSI	TABER		
814	WATER INLET MANIF. PRESS	5000 PSI	TABER		
123	WATER INLET MANIF. TEMP-1	150 F	T/C		
826	WATER VALVE POSITION	0-100%	LVTD		
	WATER OUTLET PRESS:				
1	(ACOUSTIC CAV.)	1	3500 PSI	TABER	
2		2	3500 PSI	TABER	
3	(INST. RING)	3	3500 PSI	TABER	
4		4	3500 PSI	TABER	
5		5	3500 PSI	TABER	
6		6	3500 PSI	TABER	
7	(CHAM. #1)	7	3500 PSI	TABER	
8		8	3500 PSI	TABER	
9		9	3500 PSI	TABER	
10		10	3500 PSI	TABER	
11		11	3500 PSI	TABER	
12		12	5000 PSI	TABER	
13	(CHAM. #2)	13	3500 PSI	TABER	
14		14	3500 PSI	TABER	
15		15	3500 PSI	TABER	
16		16	3000 PSI	TABER	
17		17	3000 PSI	TABER	
18		18	3000 PSI	TABER	
19		19	3000 PSI	TABER	
20		20	3000 PSI	TABER	
21		21	3000 PSI	TABER	
22	(THROAT)	22	3000 PSI	TABER	
43		23	3000 PSI	TABER	
44		24	3000 PSI	TABER	
45		25	3000 PSI	TABER	
46		26	3000 PSI	TABER	
47		27	5000 PSI	TABER	
48		28	5000 PSI	TABER	
		29	5000 PSI	TABER	

Table 10. Instrumentation List (continued)

MSI NO.	PARAMETER	RANGE	TRANS- DUCER	OSC.- GRAPH	F/M TAPE
WATER OUTLET TEMP.:					
101	(ACOUSTIC CAV.)	1	200 F	T/C	
102	(INST. RWG)	2	200 F	T/C	
103		3	200 F	T/C	
104		4	200 F	T/C	
105		5	200 F	T/C	
126		6	200 F	T/C	
107	(CHAM. #1)	7	200 F	T/C	
121		8	200 F	T/C	
109		9	200 F	T/C	
128		10	200 F	T/C	
111		11	200 F	T/C	
110		12	200 F	T/C	
113	(CHAM. #2)	13	200 F	T/C	
124		14	200 F	T/C	
115		15	200 F	T/C	
116		16	200 F	T/C	
117		17	200 F	T/C	
118		18	200 F	T/C	
119		19	200 F	T/C	
120		20	200 F	T/C	
108		21	200 F	T/C	
122	(THROAT)	22	200 F	T/C	
		23	200 F	T/C	
114		24	200 F	T/C	
133		25	200 F	T/C	
134		26	200 F	T/C	
135		27	200 F	T/C	
136		28	200 F	T/C	
		29	200 F	T/C	

6.5 TEST RESULTS AND DISCUSSION

6.5.1 TEST RESULTS

The 5.7-inch injector was characterized in a test matrix consisting of a series of four preliminary blowdown and ignition tests followed by four mainstage tests in which performance, heat flux, and stability were determined.

6.5.1.1 Tests No. 1-4

This experimental series was begun with four preliminary tests to characterize the functioning of the water, propellant, and purge systems, verify the data acquisition and redline systems, establish the timing and set levels of redlines, and check the start and cutoff sequencing, including the LOX/TEA/TEB combustion stage and subsequent transition to mainstage. As a result of these tests, minor modifications and improvements were made in the start sequencing and in the purge systems. For example, an overlap of the fuel purge and fuel flows at test start was decreased to shorten the rise time to mainstage chamber pressure, and the oxidizer purge supply system was enlarged, to provide adequate purge flow at test cutoff, which eliminated shutdown chugging.

All other facility and operational functions were nominal and indicated that the test facility, hardware, and procedures were ready for mainstage firings.

6.5.1.2 Test No 6*

The primary purpose of the first mainstage firing was to evaluate hardware behavior at 1750 psia chamber pressure in a 2-second-duration test, as well as to obtain preliminary measurements of performance and heat flux. These test conditions were achieved (Figure 66). The interruption in the rise of chamber pressure to mainstage level at file time 23.6 seconds was due to the fact that the fuel purge pressure was still higher than the fuel injection pressure at that point (Figure 67). Post-test hardware examination of the injector showed slight erosion in a small area at the edge and general

* Test No. 5 was cut prior to mainstage by an erroneous redline setting on the fuel injection pressure.

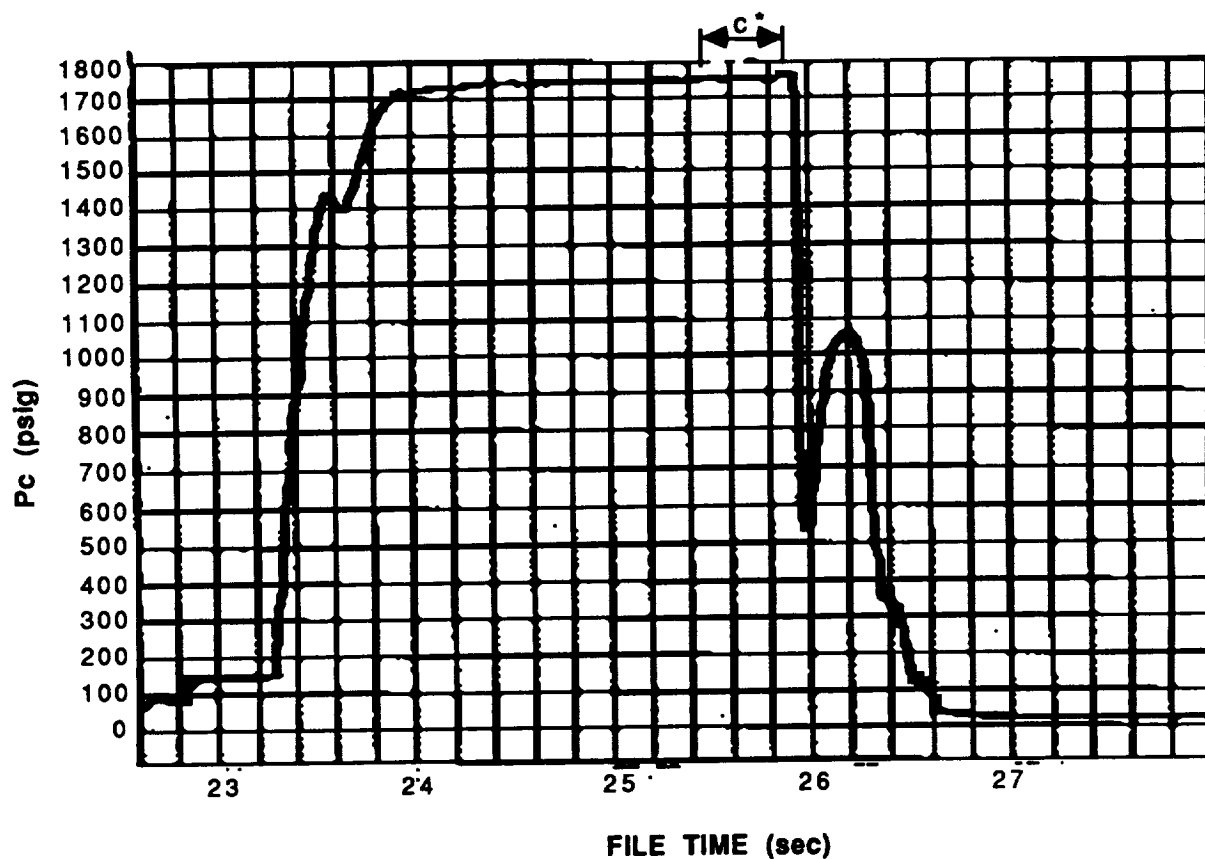


Figure 66. Static Chamber Pressure (Inj. End), Test 015-006, Canted-Fan Injector

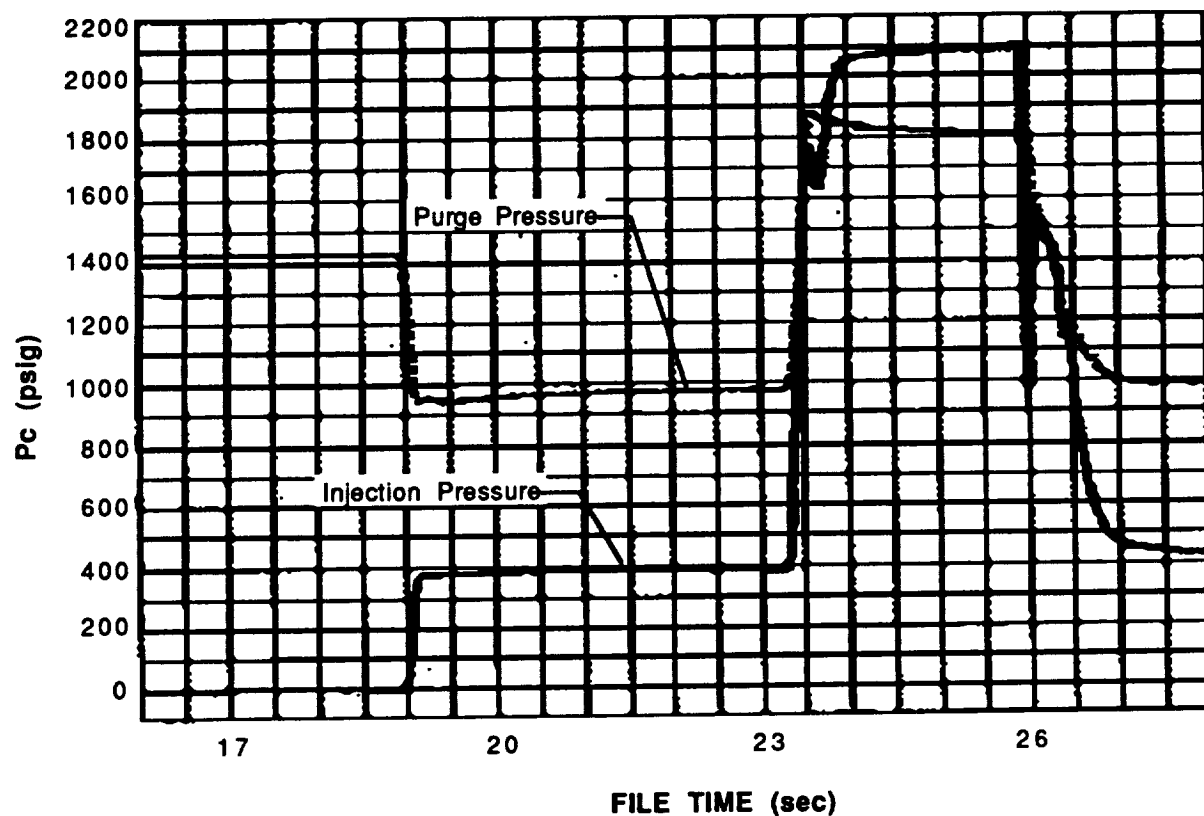


Figure 67. Fuel Injection and Purge Pressures, Test 015-006, Canted-Fan Injector

darkening of the face. Of the seven dams in the acoustic cavity, six had partially melted or burned away and one was bent. Measured temperatures in the acoustic cavities were on the order of 2400° F or higher, and the uncooled dams could not withstand these high temperatures. In addition, some blanching occurred on the convergent section wall surface upstream of the throat.

Performance data are summarized as follows:

P_c	=	1770 psia
w_T	=	100.6 lb/sec.
M.R.	=	2.85
$\eta_{c^*}(\text{uncorr.})$	=	96.6%
$\eta_{c^*}(\text{corr.})$	=	97.0%

Throat stagnation pressure was based on chamber pressure measured at the start of convergence; c^* was corrected only for the measured heat loss to the chamber walls.

Coolant water temperature data were taken just prior to test cutoff, when essentially steady-state conditions had been attained. Chamber heat flux is shown in Figure 68; peak heat flux at the throat was about 50 Btu/sec/in².

Stability characteristics of this test are discussed in Section 6.5.1.6.

6.5.1.3 Test No. 7

The primary objective of this test was to determine the dynamic stability of the canted-fan injector by measuring the recovery time from detonation of a 2-grain RDX bomb in the combustion chamber, at 2000-psi chamber pressure and 2.6 mixture ratio. Prior to this test, the injector sides and the inner wall of the bomb spool (which replaced the instrumentation ring) were coated with zirconium oxide. The injector was coated to minimize the erosive effects of the high-temperature recirculation gases; and the uncooled bomb spool was coated to improve its durability. In addition, the acoustic cavity dams (which are not considered necessary for proper functioning of the acoustic cavities) were removed and minor changes were made in the fuel purge system (reduced supply pressure, longer valve opening time, shorter valve closing time) to minimize or eliminate the delay in the start transient observed in the previous tests.

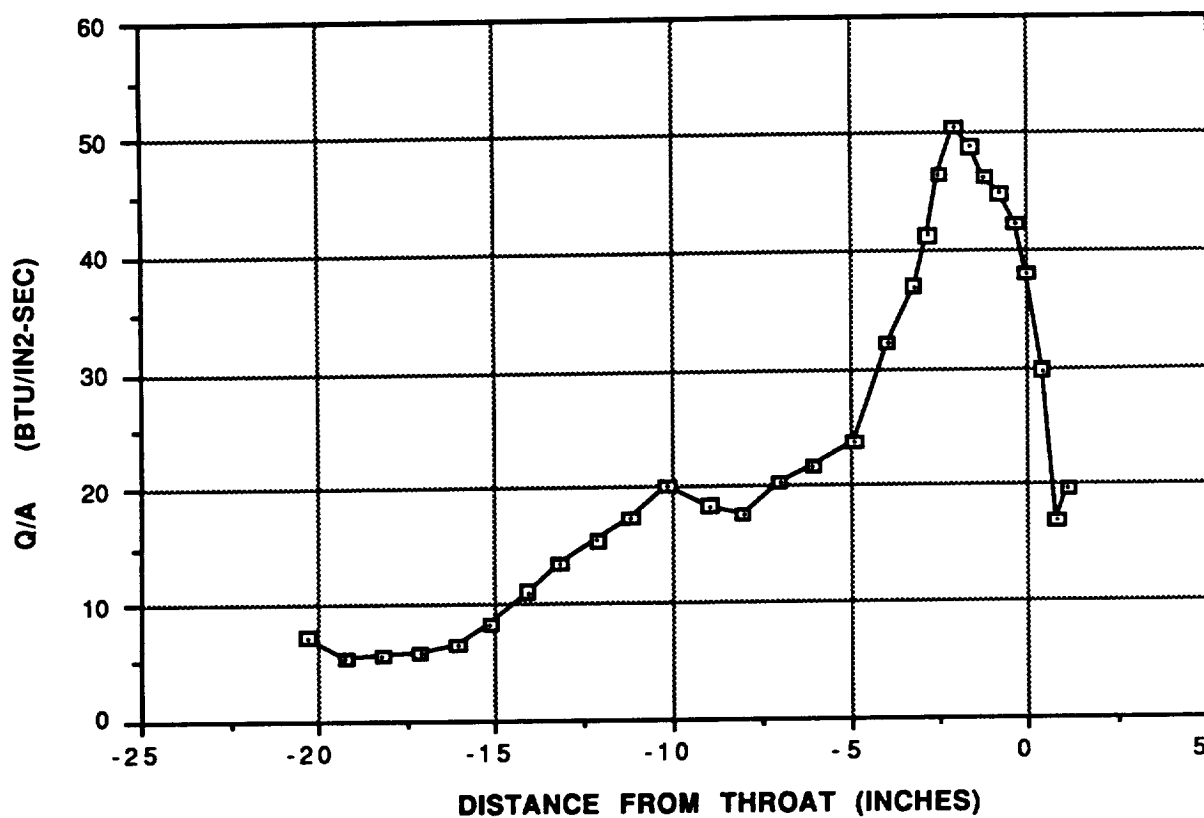


Figure 68. Axial Heat Flux Profile, Test 015-006, 5.7-Inch Canted-Fan Injector

Figure 69 is the trace of injector-end chamber pressure of Test No. 7. The fuel purge system modifications were successful in eliminating the start transient delay. At time 19.15, coincident with the dip in chamber pressure, unstable oscillations started which triggered a test cutoff by the TASCOS detector prior to the bomb fire signal. About 0.6 second of mainstage was achieved. The bomb was not physically present in the chamber after the test. Whether it detonated prematurely during the test or on shutdown or whether it was expelled from the chamber without detonation could not be determined. However, the pressure oscillations did not appear to have been triggered by a detonation.

Post-test hardware examination results were as follows: the injector face and orifices were in good condition, except for some slight erosion of the outer fuel ring in the region behind the bomb; the zirconium oxide coatings on the injector side wall and on the inner wall of the bomb spool showed no signs of erosion or spalling; there was no "mushrooming" enlargement of the bomb port; the region of the converging portion of the throat spool which had been blached in Test No. 6 and was polished smooth before Test No. 7 remained smooth; and all acoustic cavity thermocouples survived the test (in earlier tests, many had been burned away), probably because they had been installed slightly closer to the cavity wall and because the lowered mixture ratio in this test resulted in temperatures of about 2000° F in the cavities.

Although chamber pressure ($P_{stag} = 1934$ psia), propellant flowrates ($w_T = 112.2$ lb/sec), and mixture ratio (M.R. = 2.60) were close to the targeted values, the very short duration of the test and the instability oscillations precluded meaningful determinations of c^* efficiency and heat flux.

The stability aspects of this firing are discussed in Section 6.5.1.6.

6.5.1.4 Test No. 8

This test was conducted without a bomb to evaluate spontaneous stability characteristics with a unimodal (1T) acoustic cavity (which replaced the bimodal configuration used in Tests 1-7) and with plugs in eight outer-row oxidizer orifices in the region of the bomb port (to avoid oxidizer impingement on the bomb holder in subsequent bombed tests). The test was targeted at 2000 psi chamber pressure, 2.80 mixture ratio and 1.4-second duration. Ignition and transition to mainstage were normal (Figure 70). As chamber pressure was leveling out at 2000 psi, the test was cut by a signal from the TASCOS

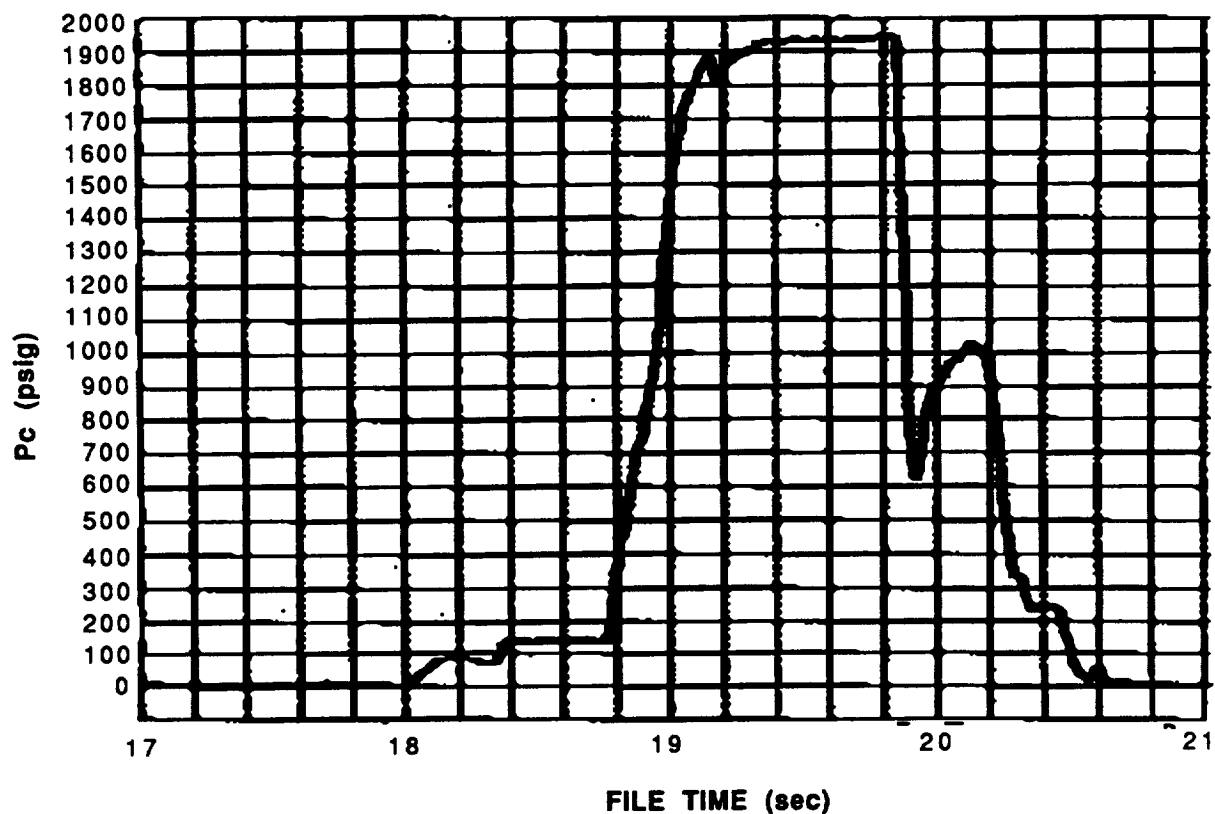


Figure 69. Static Chamber Pressure (Inj. End), Test 015-007, Canted-Fan Injector

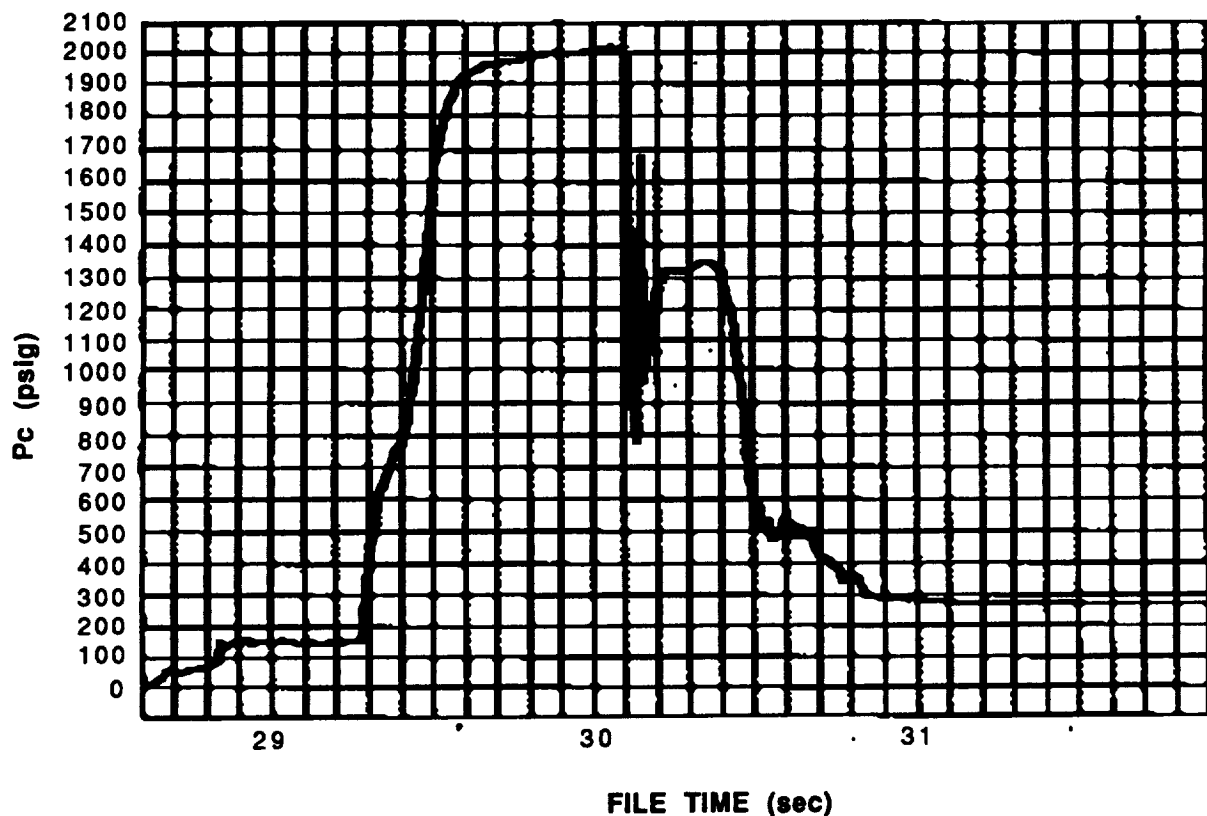


Figure 70. Static Chamber Pressure (Inj. End), Test 015-008, Canted-Fan Injector

detector. The signal was triggered by background noise, for which insufficient allowance had been made, not by instability oscillations. The targeted conditions were achieved, but mainstage duration was too short for reliable c^* and heat flux measurements.

Post-test, three of the pins in the plugged injection orifices were missing (Figure 71); there was very little additional erosion at the center and outer edges of the injector; the NARloy-Z liner at the exit braze joint of the throat spool was partially delaminated from the Inconel housing; and the chamber inner wall was smooth except for very slight roughness near the throat.

The three thermocouples in the acoustic cavity registered temperatures greater than 2400° F, their upper limit.

Combustion was stable in this test, as discussed in Section 6.5.1.6.

6.5.1.5 Test No. 9

Prior to this test, the three missing oxidizer orifice pins were replaced and all eight pins were staked to the surface of the injector face. The throat spool outlet was repaired by brazing a NARloy-Z ring at the exit, eliminating the last coolant channel. To prevent further erosion, the hot gas wall of the throat section was coated with zirconium-oxide.

Test No. 9 was a dynamic stability test, targeted at 2000 psia chamber pressure, 2.80 mixture ratio, and 2.0-second duration, with bomb detonation scheduled 0.5-second into mainstage. The detonation triggered combustion oscillations which caused a TASCOS cutoff (Figure 72). The short duration of this test precluded reliable determinations of steady state performance or heat flux.

Post-test, the injector face, particularly the center plate, was significantly eroded; the chamber and throat wall and the coating were in excellent condition; and the repaired region at the throat spool exit was unchanged.

Because further testing of this injector was not possible without major rework, the test program was terminated after Test No. 9.

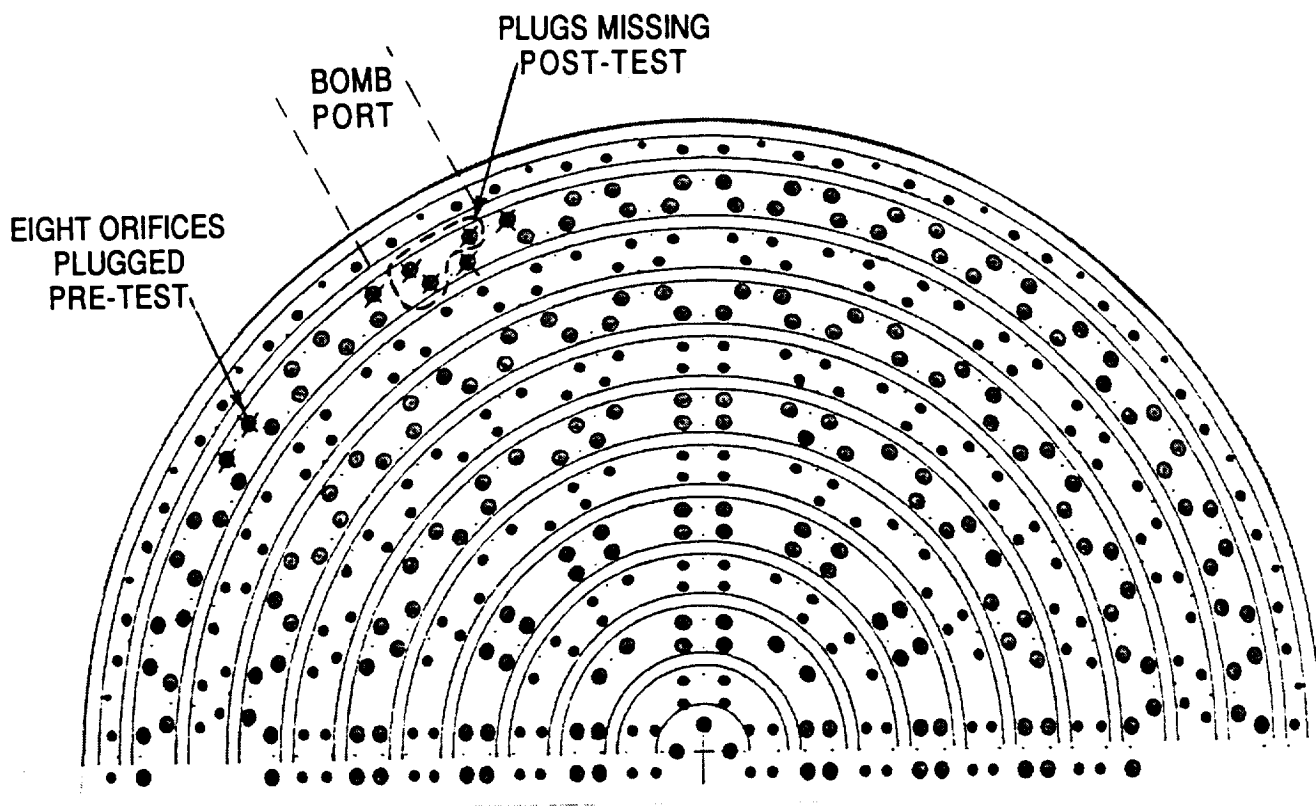


Figure 71. Injector Face Showing Eight Oxidizer Orifices Plugged Prior to Test 015-008 and Three Missing Plugs Post-Test

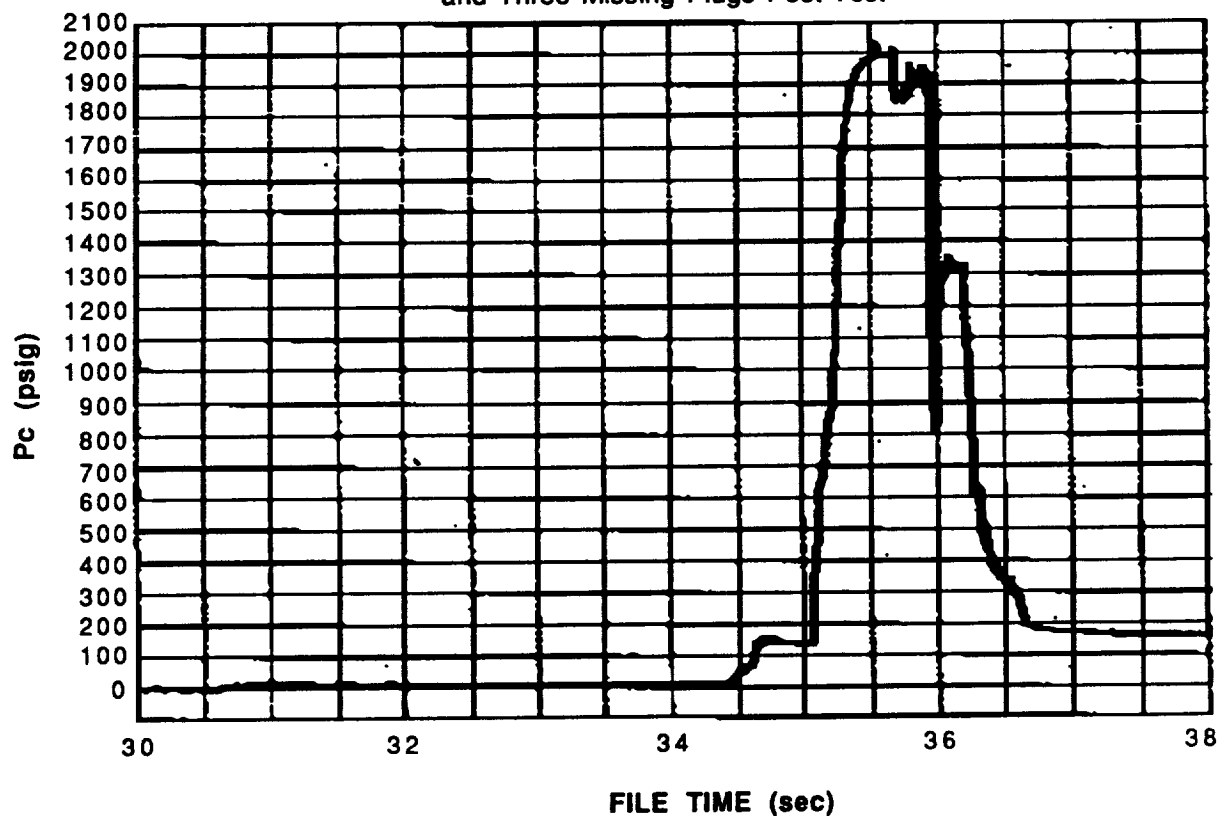


Figure 72. Static Chamber Pressure (Inj. End), Test 015-009, Canted-Fan Injector

6.5.1.6 Stability Data and Analysis

High-frequency data obtained in all the mainstage tests (including Test No. 4, which demonstrated only transition to mainstage) are summarized in Table 11.

A 400-Hz oscillation in the LOX manifold was present in all tests (including the preliminary LOX blowdowns and LOX/TEA/TEB ignition tests) during priming.* In the transition to mainstage, a characteristic 1125-Hz oscillation appeared in the combustor as well as in the LOX manifold. This is probably the first longitudinal mode of the chamber. Both 1125-Hz oscillations were damped out when mainstage pressure was attained. Another characteristic combustor oscillation was an 875-Hz chug during shutdown. The amplitude of this disturbance was decreased in the course of testing by modification of the LOX purge system to provide higher purge flowrates.

These three typical pressure and acceleration frequencies are shown in Figure 73 (LOX priming oscillation, 400 Hz), Figure 74 (LOX manifold oscillation, transition to mainstage, 1125 Hz) and Figure 75 (chug oscillation during shutdown, 825 Hz).

Expanded pressure traces from Test No. 7 (Figure 76) show no evidence of bomb detonation; traces from Test No. 9 (Figure 77) do show the detonation.

Test measurements showed that acoustic cavity gas temperatures were substantially higher than had been anticipated (by ~33%), which affected the cavity tuning. The quarter-wave slots originally designed were for the 1T mode (1.328-in. long, 8.6-percent open area) and the 2T mode (0.800-in. long, 6.4-percent open area). For Tests No. 1-6, the estimated 1T resonant frequency with the higher temperature, estimated to be about 3400° F, and including the effect of a small gap behind the 1T cavities, was 4000 Hz; for Tests No 7-9, the gap was filled with RTV sealant and the predicted resonant frequency then increased to 6000 Hz. For the 2T cavities, in all tests, the predicted resonant frequency was 10,400 Hz with the 3400° F gas temperature.

These results suggest that cavity detuning was the cause of the 4125-Hz oscillation in Test No. 7. To determine whether such detuning was feasible, n-tau stability analyses

* The LOX manifold high-frequency transducer malfunctioned in Test No. 6 and yielded no data.

Table 11. High-Frequency Test Data

Test No.	Parameter	Observed Frequency	Amplitude	Relative time of disturbance
4	CHAMBER PRESS	1100 HZ	138 PSI P-P	TRANSITION TO M/S
4	CHAMBER PRESS	875 HZ	330 PSI P-P	CHUG AT SHUTDOWN
4	LOX INJ PRESS	400 HZ	290 PSI P-P	EARLY PRIMING
4	LOX INJ PRESS	875 HZ	470 PSI P-P	CHUG AT SHUTDOWN
4	LOX INJ PRESS	1100 HZ	175 PSI P-P	TRANSITION TO M/S
4	FUEL INJ PRESS	6000 HZ	120 PSI P-P	M/S
4	FUEL INJ PRESS	3000 HZ	120 PSI P-P	M/S
4	AXIAL ACCEL	-	500 G P-P	M/S
4	RADIAL ACCEL	12000 HZ	550 G P-P	M/S
4	TANG ACCEL	-	200 G P-P	M/S
6	CHAMBER PRESS	1150 HZ	300 PSI P-P	TRANSITION TO M/S
6	FUEL INJ PRESS	3000 HZ	120 PSI P-P	M/S
6	FUEL INJ PRESS	6000 HZ	120 PSI P-P	M/S
6	RADIAL ACCEL	1150 HZ	200 G P-P	TRANSITION TO M/S
6	TANG ACCEL	1150 HZ	150 G P-P	TRANSITION TO M/S
6	AXIAL ACCEL	1150 HZ	300 G P-P	TRANSITION TO M/S
7	CHAMBER PRESS	1125 HZ	500 PSI P-P	TRANSITION TO M/S
7	CHAMBER PRESS	4125 HZ	625 PSI P-P	M/S
7	LOX INJ PRESS	400 HZ	250 PSI P-P	EARLY PRIMING
7	LOX INJ PRESS	1125 HZ	230 PSI P-P	TRANSITION TO M/S
7	LOX INJ PRESS	4125 HZ	200 PSI P-P	M/S
7	FUEL INJ PRESS	3000 HZ	280 PSI P-P	M/S
7	FUEL INJ PRESS	6000 HZ	280 PSI P-P	M/S
7	RADIAL ACCEL	4125 HZ	1550 G P-P	M/S
7	AXIAL ACCEL	4125 HZ	1100 G P-P	M/S
7	TANG ACCEL	4125 HZ	850 G P-P	M/S
8	CHAMBER PRESS	1150 HZ	504 PSI P-P	TRANSITION TO M/S
8	LOX INJ PRESS	400 HZ	300 PSI P-P	EARLY PRIMING
8	LOX INJ PRESS	1150 HZ	260 PSI P-P	TRANSITION TO M/S
8	FUEL INJ PRESS	3000 HZ	480 PSI P-P	M/S
8	FUEL INJ PRESS	6000 HZ	480 PSI P-P	M/S
8	RADIAL ACCEL	-	550 G P-P	M/S
8	AXIAL ACCEL	-	480 G P-P	M/S
8	TANG ACCEL	-	460 G P-P	M/S
9	CHAMBER PRESS	1125 HZ	490 PSI P-P	TRANSITION TO M/S
9	CHAMBER PRESS	9300 HZ	910 PSI P-P	M/S
9	CHAMBER PRESS	875 HZ	440 PSI P-P	CHUG AT SHUTDOWN
9	LOX INJ PRESS	400 HZ	380 PSI P-P	EARLY PRIMING
9	LOX INJ PRESS	1125 HZ	240 PSI P-P	TRANSITION TO M/S
9	LOX INJ PRESS	875 HZ	310 PSI P-P	CHUG AT SHUTDOWN
9	LOX INJ PRESS	9300 HZ	180 PSI P-P	M/S
9	BOMB PULSE	-	588 PSI M-P	M/S
9	RADIAL ACCEL	9300 HZ	1600 G P-P	M/S
9	AXIAL ACCEL	9300 HZ	1610 G P-P	M/S
9	TANG ACCEL	9300 HZ	1060 G P-P	M/S
9	FUEL INJ PRESS	3000 HZ	200 PSI P-P	M/S

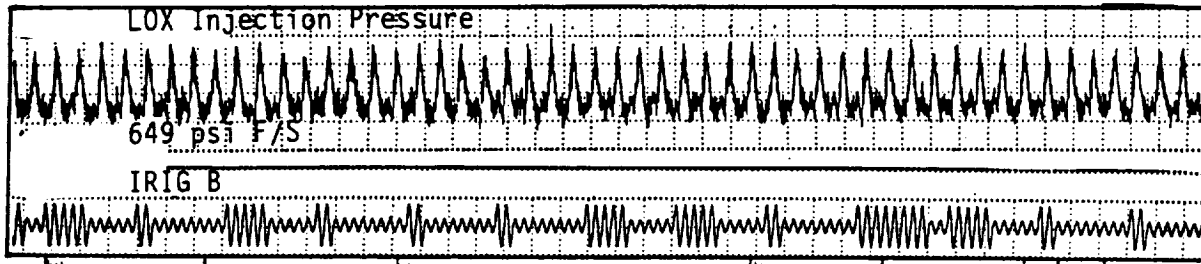


Figure 73. LOX Manifold Priming Oscillation, 400 Hz (Test No. 3)

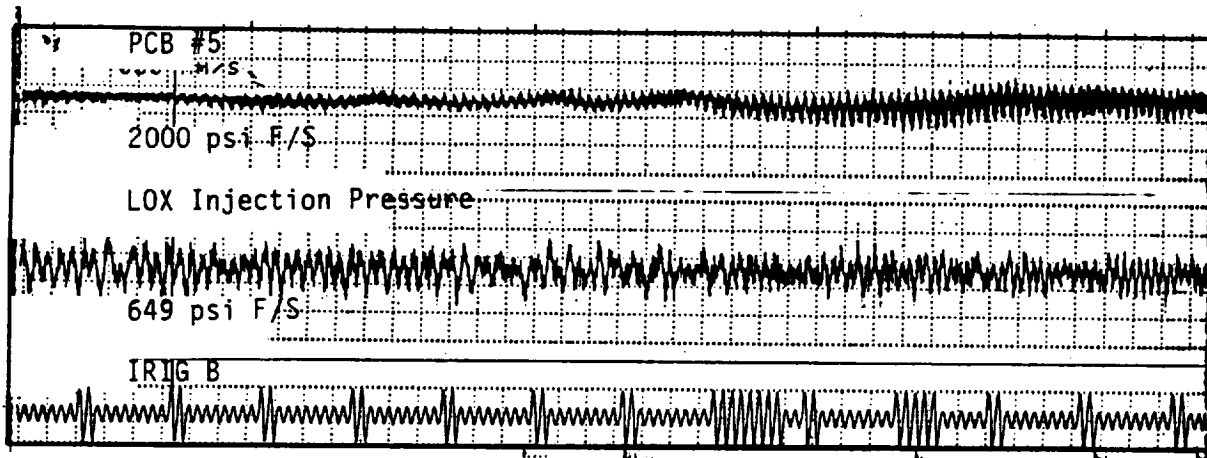


Figure 74. LOX Manifold Oscillation, Transition to Mainstage, 1125 Hz (Test No. 7)

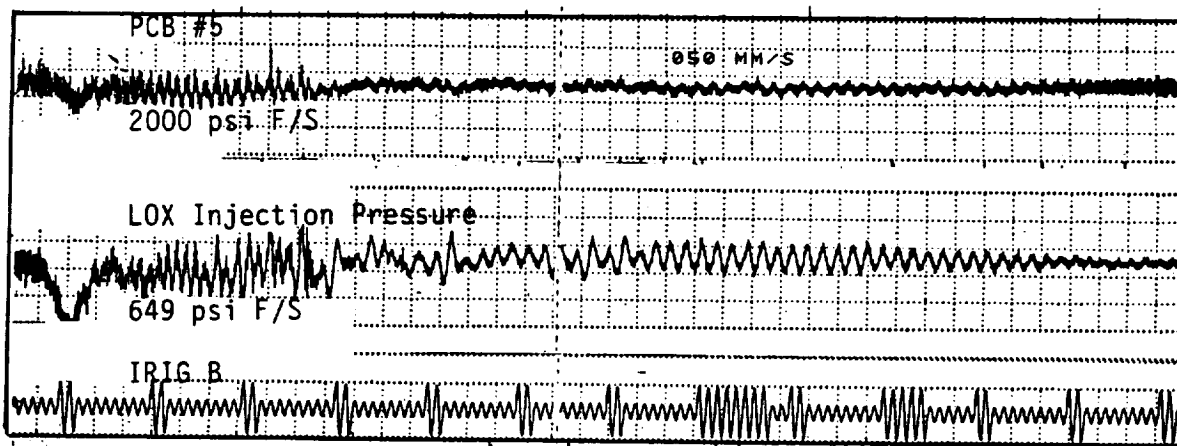


Figure 75. LOX Manifold Shutdown Chug, 825 Hz (Test No. 7)

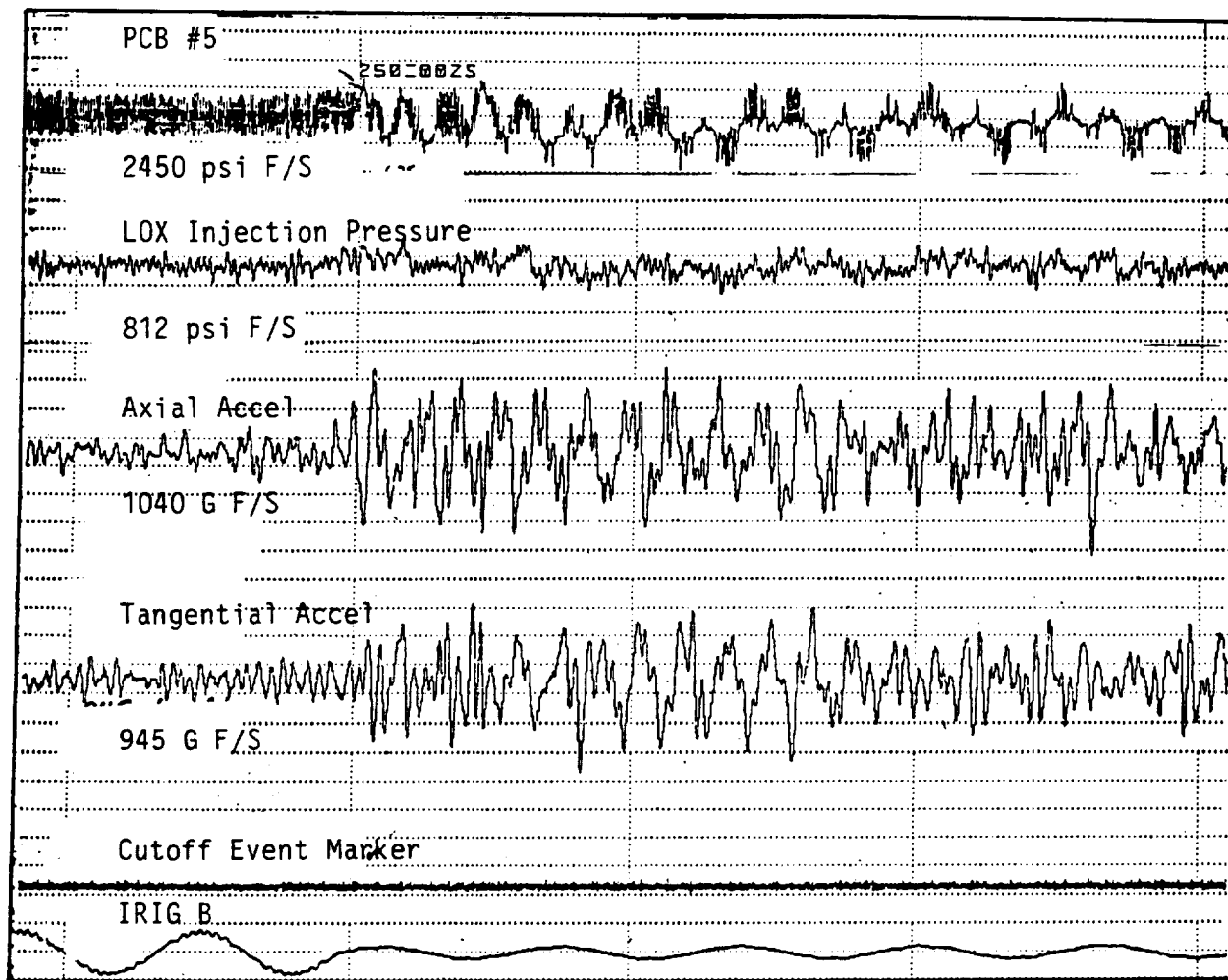


Figure 76. Test No. 7 High Frequency Data

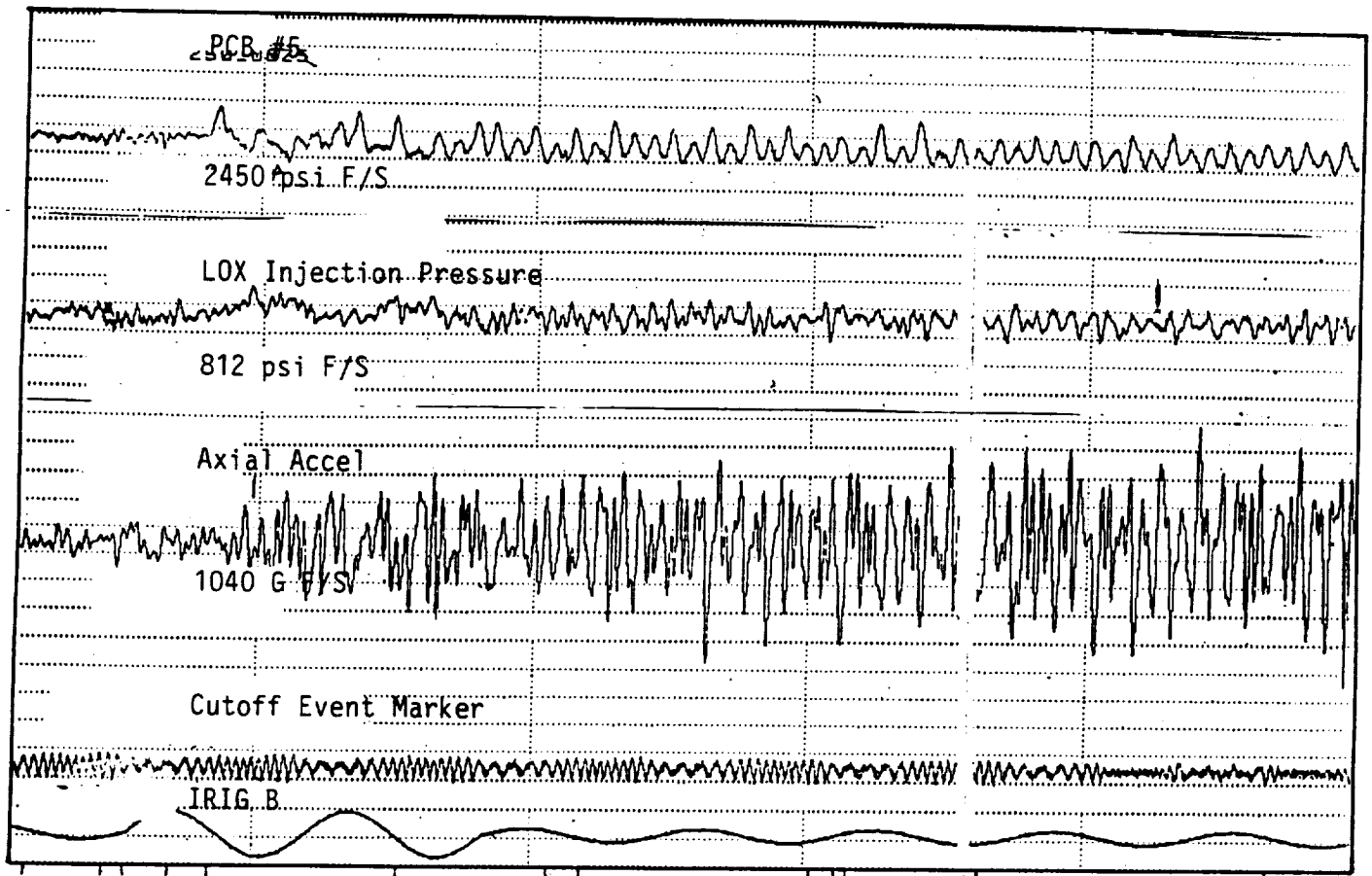


Figure 77. Test No. 9 High Frequency Data

were carried out. The resulting neutral stability curves (Figure 78) support the detuning hypothesis. Analyses were also made for unimodal acoustic cavities in which all of the cavity open area was either in the 1T or 2T mode (Figure 79). A 2.5-percent gain in stability margin is predicted by the increase in 1T open area from 8.6-percent to 15-percent.

The combustion response region, which is typically represented by a rectangular "box" in n -tau sensitive time lag plots, is deduced from the Reardon correlations (Ref. 4). A review of the experimental data underlying these correlations suggests that a particular combustor can respond over a wide band width. Thus, instead of a box, a single line should be used, across the entire range, at the appropriate value of the interaction index. The sensitive time lag curves of the first four tangential modes were calculated and are shown in Figure 80 with a line separating the stable and unstable regions. These results suggest that several modes may be driven in this combustor. On the basis of the sound velocity represented by the 1T frequency in Test No. 7, the high-amplitude 9300-Hz oscillation triggered by the bomb in Test No. 9 is indicated to be the 3T mode, which possibly had the least amount of damping available. It appears feasible to stabilize the combustor with a bimodal (or trimodal) acoustic cavity.

The stability data and recommendations are summarized as follows:

1. The 5.7-inch injector/combustor is spontaneously stable but dynamically unstable.
2. Both 1T and 3T modes were observed, in different tests.
3. Use of bimodal or trimodal acoustic cavity slots would very probably eliminate the instability.

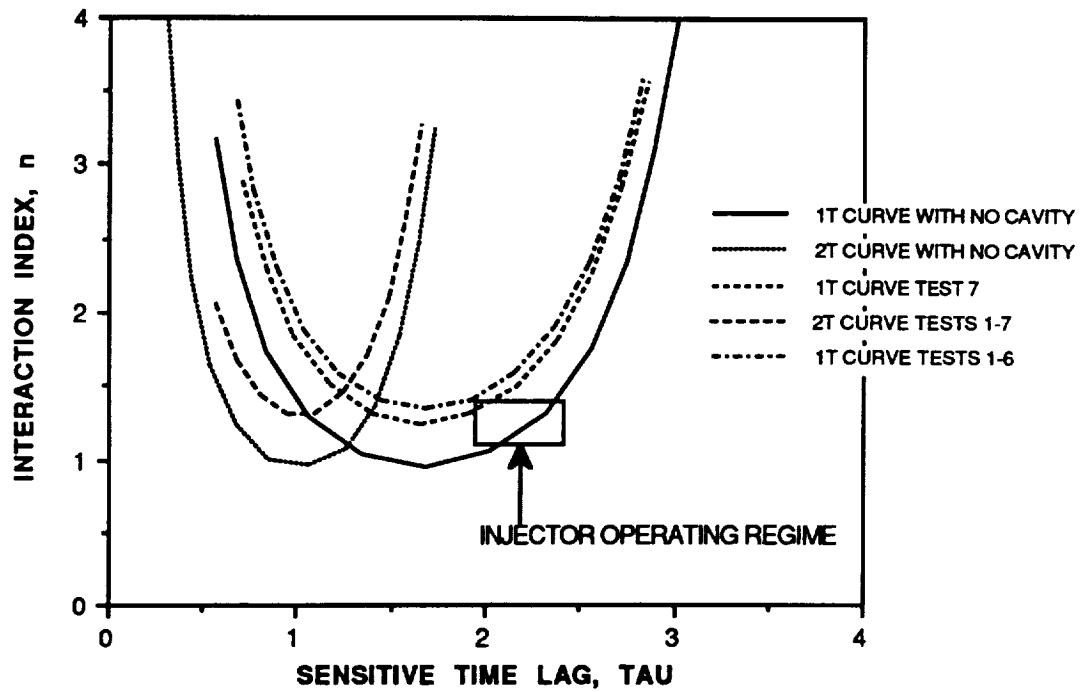


Figure 78. Neutral Stability Map of 5.7-inch Combustor, with and without Bimodal Acoustic Cavities

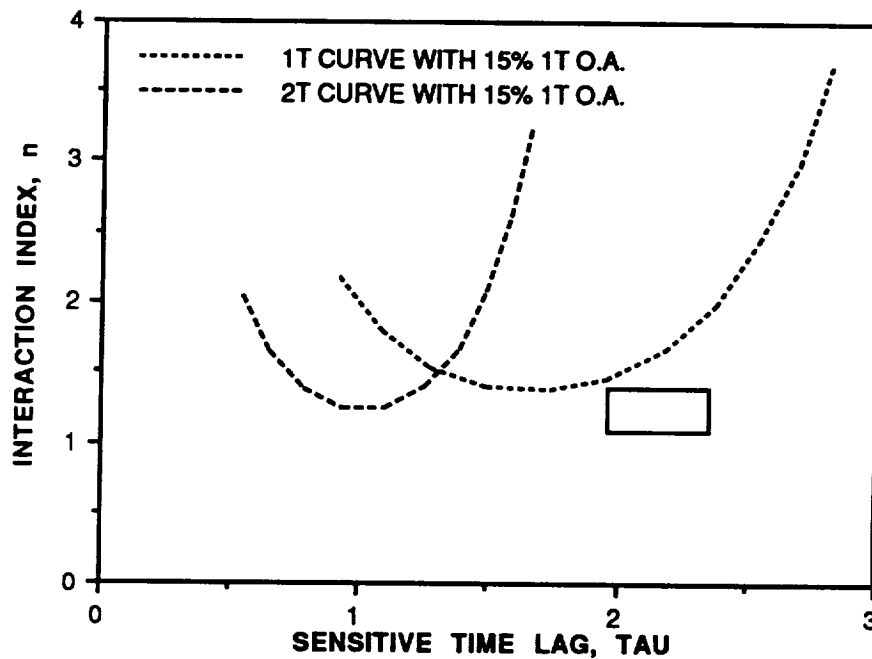


Figure 79. Neutral Stability Map of 5.7-inch Combustor, Unimodal Acoustic Cavities

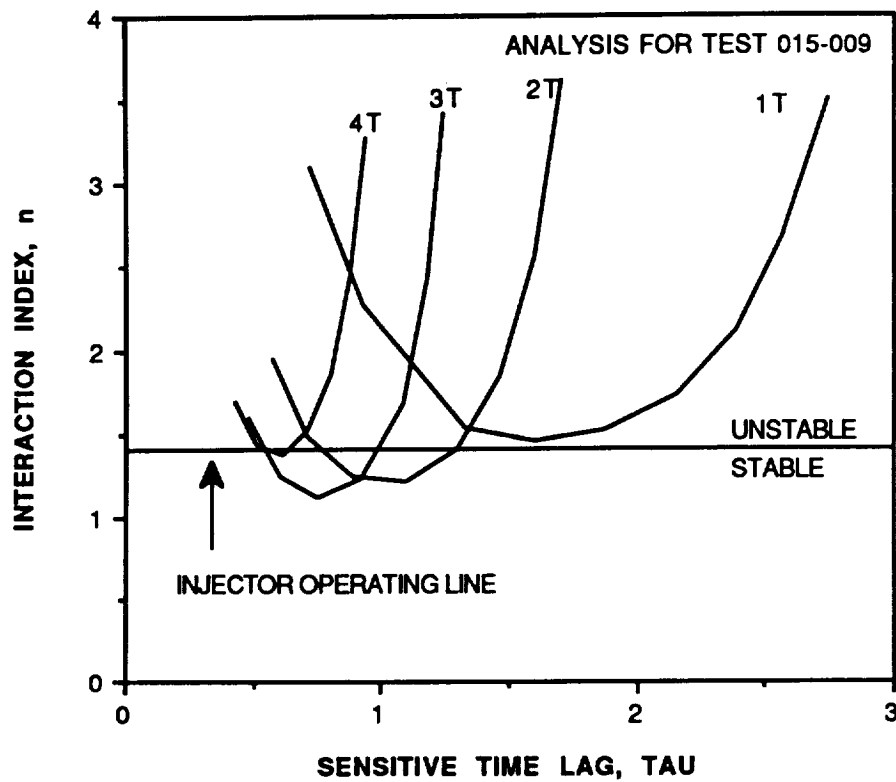


Figure 80. Neutral Stability Map of 5.7-Inch Combustor, Showing Tangential Modes with Expanded Injector Combustion Response

TASK II

7.0 TWO-DIMENSIONAL COMBUSTOR PRELIMINARY DESIGN

7.1 INTRODUCTION

Preparation of the preliminary design of a 2-D combustor constituted the final task of the first phase of the overall program. The original plan for the second phase of this program included detail design, fabrication and assembly of the combustor. This would have been the next step in the demonstration of the applicability of the Isolated Combustion Compartment (ICC) concept to a 750,000-lb-thrust, high pressure, LOX/RP-1 engine. However, as described in later sections of this report, Phase B was replanned to perform additional analysis and testing of the 3.5-inch injectors.

The present preliminary design task included two steps: (1) generation of the 2-D combustor component and assembly concepts, based on its anticipated test requirements and applicable thermal, acoustic, and structural analyses, and (2) preparation of layout drawings which show the configurations in sufficient detail to permit subsequent detailed designs.

7.2 REQUIREMENTS OF THE 2-D COMBUSTOR

The design requirements of the 2-D combustor included the following:

1. Thrust level on the order of 150,000 to 200,000 lb.
2. Inclusion of several separate combustion chambers, to simulate the ICC concept.
3. ICC's of the 2-D combustor to model an ICC of a full-size 3-D configuration.
4. Structural and thermal characteristics of the 2-D combustor which will allow about ten, two-second-duration, dynamic stability tests at 2000 psia chamber pressure.
5. Use of the injector pattern and acoustic cavity design previously demonstrated to give stable combustion, with acceptable c^*

efficiency and heat flux levels, in the 5.7-inch subscale combustor.

6. Emphasis on fabrication and operational simplicity.

7.3 DESIGN METHODOLOGY

Proper modeling of a circular 3-D combustor by a smaller, rectangular, 2-D version should include identification of acoustic mode frequency, injection element geometry and density, orifice sizes, mass flow density, chamber pressure, and contraction ratio. In the present application, the characteristics of a large 3-D combustor, which the 2-D would model, constituted the first design anchor. The second guide for the 2-D conceptual design was the subscale 5.7-inch combustor, which was presumed to have satisfactory performance, heat flux, and stability. (The 2-D design was completed before the start of the 5.7-inch combustor tests). This led to the following comparisons between the 5.7-inch, 2-D, and full-scale 3-D combustors with regard to the modeling parameters:

1. $P_c = 2000$ psia

This will be the same in all three combustors.

2. Contraction Ratio = 2.5

This parameter has a significant effect on chamber acoustics and hence on stability. It will be the same in all three combustors.

3. Acoustic Mode Frequency

The 1T frequency of the 5.7-inch combustor will be maintained in the ICC's of the 2-D and full-scale 3-D combustors.

4. Injection Element Geometry

The same canted-fan like-doublet element pattern will be used in all three injectors.

5. Injection Orifice Sizes

The same injection orifice sizes will be used in all three injectors.

6. Injection Element and Flowrate Densities

With linear-type elements in a round injector, the element spacing varies from the outer ring to the center, whereas, in a rectangular injector, the spacing is constant across the face. The geometry within each pair of interacting oxidizer and fuel doublets in the 2-D ICC injector is the same as that in the 5.7-inch design. To maintain identity of the other parameters, however, the spacing between adjacent columns of elements in the 2-D ICC is slightly larger than in the 5.7-inch injector. While this would not affect intra-element functioning, it might alter inter-element mixing. However, the average number of orifices per unit area of injector face is the same in all three injectors. Consequently, with the same injection pressure drops, the mass flowrate per unit area is also identical.

7. The injection pressure drops will be the same in all three designs.

8. The acoustic cavity open area, as a fraction of the total combustion chamber cross-section, will be the same in all three designs.

The values of these parameters in the 5.7-inch, 2-D ICC, and 3-D ICC designs are summarized in Table 12.

7.4 COMBUSTOR DESIGN AND ASSEMBLY

7.4.1 SIZING OF COMBUSTOR

The 2-D combustor design process began with the estimation of an appropriate combustion chamber size and configuration for a full-scale 3-D combustor which incorporates the ICC concept. The use of identical ICC's in a cylindrical chamber must leave substantial "wasted" injector face area, either throughout the face (with a circular

Table 12. Combustor Parameters

Parameter	5.7-inch Subscale	2-D ICC	3-D ICC
Chamber pressure, psia	2000	2000	2000
1T frequency, Hz	4940	4940	4940
Contraction ratio	2.5	2.5	2.5
Injector pattern	CF/LD*	CF/LD	CF/LD
No. of orifices, ox/fuel	372/376	324/324	300 to 400 ea.
Diameter of orifices, in., ox/fuel	.058/.037	.058/.037	.058/.037
Avg. \dot{w}/A , lb/sec/in ²	4.51	4.51	4.51
Injector DP, psi, ox/fuel	400/425	400/425	400/425
Injection orifice density, No./in ²	29.7	29.8	29.8
Acoustic cavity open area, %	15	15	15

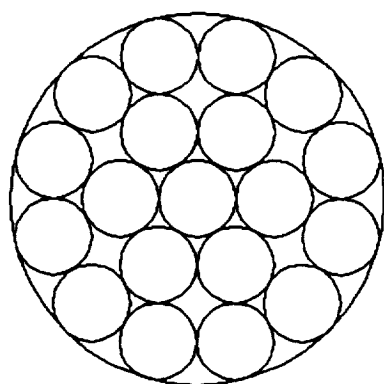
* Canted-fan like-doublet

ICC) or around the periphery (with a square or hexagonal ICC, Figure 81). Such unused area would be detrimental because of significant reduction of the effective contraction ratio, difficulty in cooling these regions, and altered acoustic characteristics. A segmental configuration, however, with keystone-shaped ICC's (Figure 81), not only uses all of the injector face area, but is similar to baffled patterns successfully employed in numerous earlier LOX/RP-1 engines.

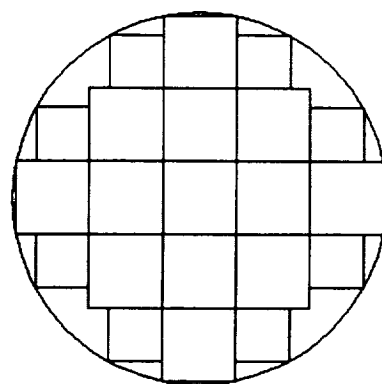
As illustrated in Figure 82, sizing of the 2-D combustor was based on both a hypothetical, full-scale, 3-D combustor and the tested 5.7-inch subscale combustor. The requirement that the ICC's of the 2-D and 3-D units have the same 1T frequency as the subscale combustor translates to making the 2-D chamber overall width equal to 85-percent of the full-scale 3-D cylindrical chamber diameter and also establishes the width of each 2-D ICC (4.83-in.). The height, which can be a convenient dimension less than 4.83-in., was set at 4.50-in., to accommodate the required number of injection elements and to simulate a (hypothetical) ICC in a full-scale 3-D combustor, both in size and in the proportion of peripheral to total injection elements.

The 2-D combustor incorporates five identical ICC's, 4.83-in. in width and 4.50-in. in height, separated by 0.5-in walls, to give an overall width of 26.15-in. By the 85-percent rule, the diameter of the full-scale 3-D chamber which this 2-D configuration models would be about 31-in. (also including four ICC wall thicknesses). A conceptual configuration of a 21-compartment injector for a 2000 psia, 750,000-lb engine, with approximate dimensions, is shown in Figure 83.

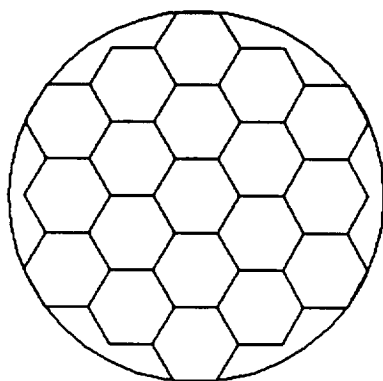
In sizing the 2-D combustor throat for the specified 2.5 contraction ratio, the question arises as to whether the cross-sectional areas of the four ICC walls should be considered part of the chamber area. For calculations of engine thrust, the contraction ratio is defined as the ratio of the chamber area at the start of nozzle convergence to the area of the throat. However, to maintain the flow dynamics in the ICC's (where the susceptibility to instability is greatest) similar to that in the 5.7-in. subscale combustor, the contraction ratio of the 2-D chamber should exclude the ICC wall areas.



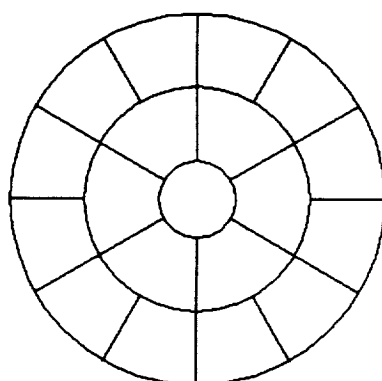
ROUND



SQUARE



HEXAGONAL

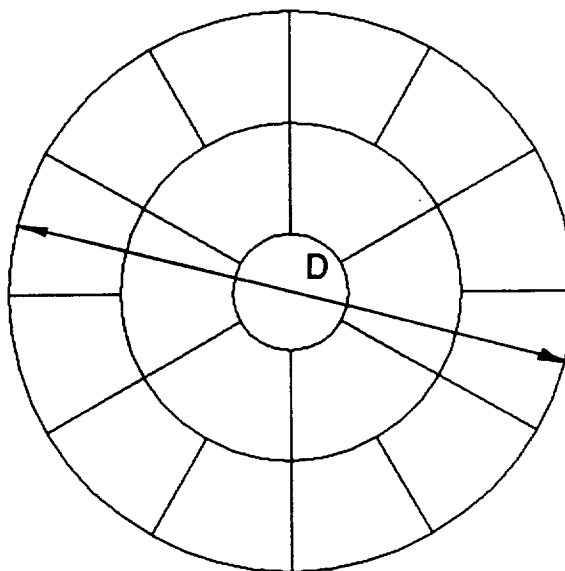
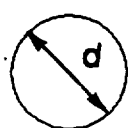


KEYSTONE

Figure 81. ICC Configurations in Full-Size 3-D Combustor

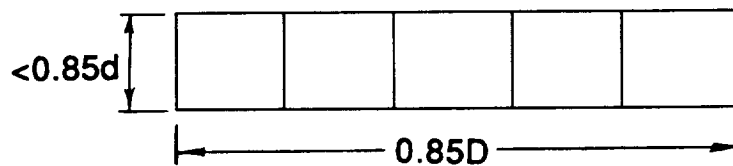
Subscale Combustor

$d = 5.66 \text{ in.}$
 $f_{1T} = 4940 \text{ Hz}$



3-D Combustor

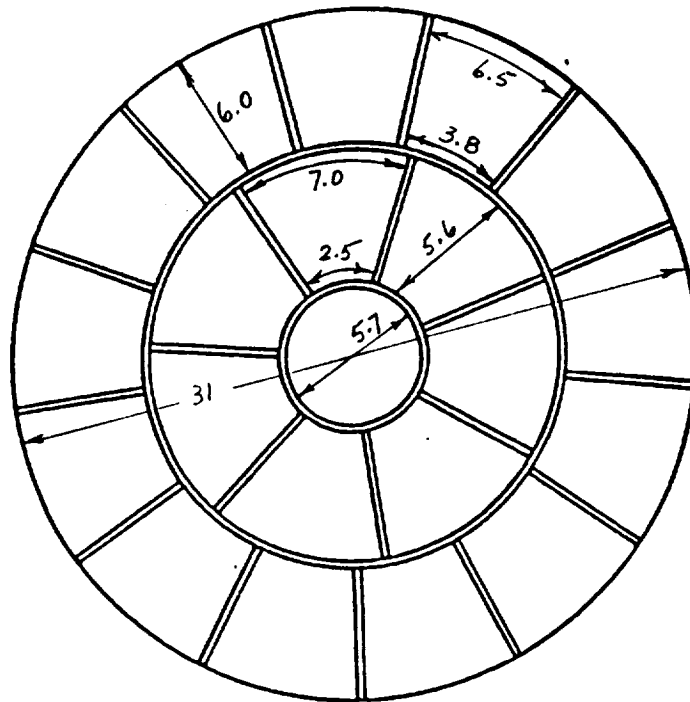
$D = 31 \text{ in.}$
 $f_{1T} = 4940 \text{ Hz}$



2-D Combustor

$f_{1T} = 4940 \text{ Hz}$
 $f_{1T} \text{ (overall)} = 916 \text{ Hz}$

Figure 82. Relationships of Subscale, 2-D and Full-Size 3-D Combustors



Dimensions are approximate for 2000 psia,
750k-lb thrust engine
Requires 3 ICC configurations

Figure 83. Full-Size, 3-D, Compartmental Injection Concept

Since the maintenance of similar flow dynamics is more consistent with the objectives of 2-D modeling and testing, the latter procedure was adopted. Pertinent 2-D size data are as follows:

$$\text{Area per ICC} = 4.83 \times 4.50 = 21.735 \text{ in}^2$$

$$\text{Area of five ICCs} = 21.735 \times 5 = 108.68 \text{ in}^2$$

$$\text{Area of four ICC walls} = 4.50 \times 0.5 \times 4 = 9.00 \text{ in}^2$$

$$\text{Area of chamber downstream of ICC walls} = 117.68 \text{ in}^2$$

$$\text{Contraction ratio} = 2.50$$

$$\text{Throat area based on total chamber area} = 47.07 \text{ in}^2$$

$$\text{Throat area based on total ICC area} = 43.47 \text{ in}^2$$

$$\text{Throat width based on total chamber area} = 10.46 \text{ in}$$

$$\text{Throat width based on total ICC area} = 9.66 \text{ in (design value)}$$

7.4.2 DESIGN OF COMBUSTOR

The 2-D combustor, designed as workhorse hardware to serve for a limited number of short-duration dynamic stability tests at 2000 psia, consists of injector and combustion chamber assemblies bolted to each other. It is designed to be fired with the long dimension in a horizontal orientation, for maximum operational efficiency.

7.4.3 CHAMBER ASSEMBLY

7.4.3.1 Description

The chamber assembly of the 2-D combustor (Drawing No. 7R030042, Figure 84) consists of a ZrO₂-coated OFHC copper liner, with a quartz-phenolic ablative throat, within a cast high-strength steel shell. The steps involved in fabrication and assembly of the chamber are as follows:

1. A sand casting of the shell will be made. The material will be Atlas Alloy 857, a chrome-molybdenum high-strength steel. The one-piece ribbed structure will have about the same cost as a bolted or welded assembly while providing at least equal strength.

2. A draw broach process will be used to obtain the finished internal dimensions of the shell. Conventional machining of the inner contour would be difficult and costly; broaching is a much better alternative. The outer surface of the casting will be painted, for corrosion prevention.
3. Machine four OFHC copper slabs to finish dimensions.
4. Furnace-braze the copper slabs into the steel shell (pressure bag process) in two braze steps, one for the narrow slabs and one for the broad slabs.
5. Machine the injector end of the assembly for sealing surface.
6. Mill retaining grooves for the ICC walls in the copper liners.
7. Machine ports for instrumentation, bombs, and igniter inlets.
8. Coat copper walls with zirconium oxide.
9. Machine ablative throat sections.
10. Install ablative sections, with high-temperature RTV at interfaces.
11. Install CRES end plate, with RTV at interfaces.

The outer shell structure includes lugs for slings as well as supports for mounting the combustor on rails. Rail mounting will allow convenient separation of the injector and chamber assemblies without time-consuming disconnect and reconnect of the propellant supply lines.

7.4.3.2 Thermal Analysis

The planned short duration (≤ 2 sec) of the 2-D combustor tests will permit use of uncooled copper heat-sink inner walls. In the high heat flux region, starting upstream of the throat at Mach number of about 0.5, replaceable quartz-phenolic ablative inserts will be used. The excellent structural and heat flux capabilities of this material are expected to permit multiple-test use of the inserts. They will be held in place by the exit plate (Figure 83), which is bolted to the steel jacket of the combustor. High-temperature RTV will be used as sealant for the throat inserts.

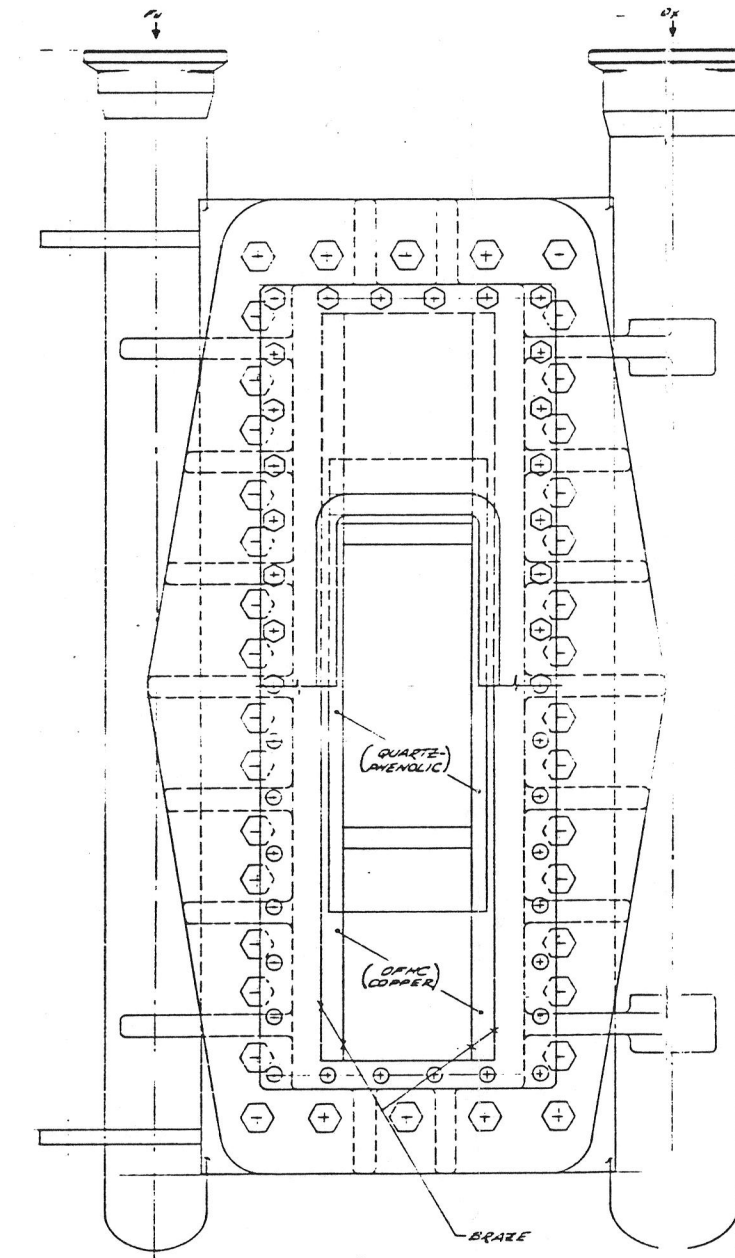
The Thermal Analysis Program (TAP) was used to estimate liner temperatures at the end of a two-second firing. The liner is OFHC copper, coated with zirconium oxide, with quartz-phenolic ablative inserts in the throat region. The thermal model was divided into 12 zones, corresponding to 12 hot gas boundary nodes and 12 film coefficients. Conservative hot gas temperatures and film coefficients were obtained from the test data of the high heat flux, 3.5-inch injectors. All boundaries except the hot gas wall surface were assumed to be adiabatic. The hot gas surface in the model was stepped (Figure 85), to maintain regular element geometry. The zirconium oxide layer was considered as a time- and temperature-invariant thermal resistance which was included in the overall heat transfer coefficient along with the hot gas film resistance. The model did not account for charring and ablation of the throat material.

At the end of two seconds, the maximum temperatures were 953° F for the copper liner (at the junction with the throat insert) and 87° F for the steel shell (at the upstream end). The time-temperature curve of the copper wall at the throat insert is shown in Figure 86. Temperatures throughout the liner after two seconds are indicated in Figure 87. The uncooled liner is therefore suitable for two second tests, with the provision that its temperature at test start is not greater than about 300° F (to keep the final maximum temperature less than about 1200° F).

7.4.3.3 Structural Analysis

Preliminary structural analyses were carried out on the 2-D combustor shell casting and the bolts joining the chamber and injector assemblies. The Atlas Alloy 857 casting material has 70,000 psi yield and 95,000 psi ultimate strengths. The criteria used for evaluation of the casting were a safety factor of 1.1 against yielding and 1.5 against ultimate (for pressure loads). In addition, a limit load factor of 1.2 was used on the 2000 psi operating pressure. The resulting safety factors for the chamber casting are 1.15 against yielding and 1.57 against ultimate.

Analysis of the 0.75-inch-diameter bolts (tensile strength = 125,000 psi) showed a safety factor of four.



INFORMATION ONLY

ORIGINAL PAGE IS
OF POOR QUALITY

[illegible]

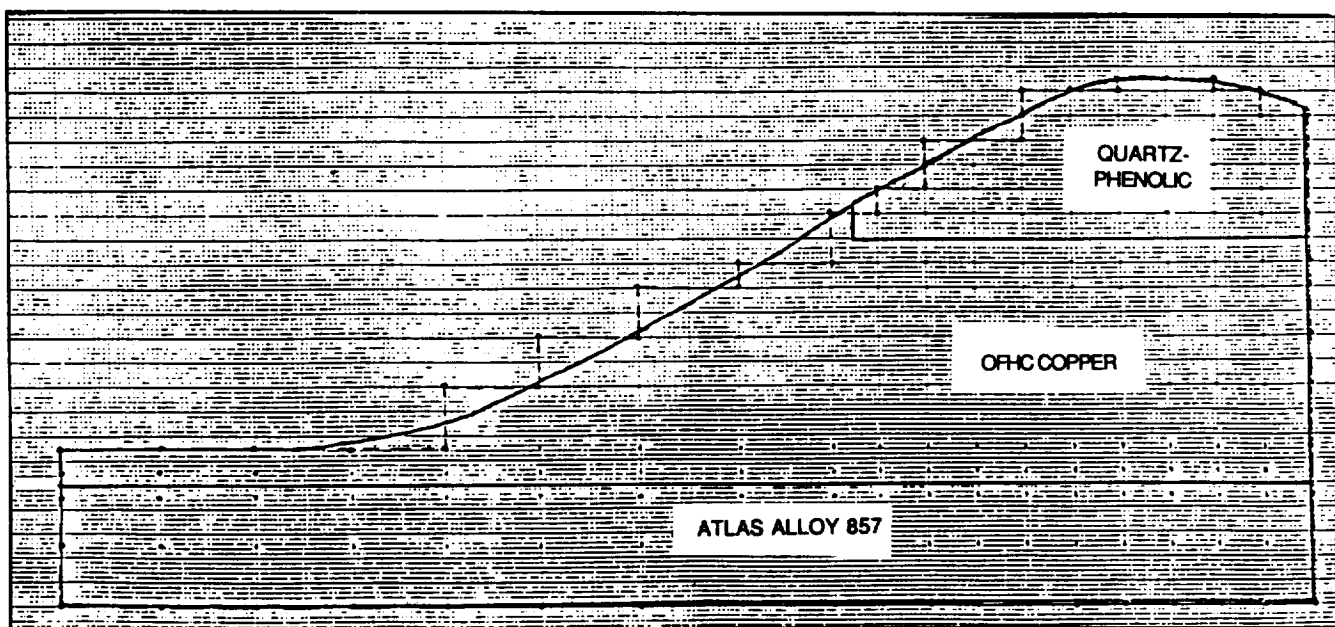


Figure 85. Nodal Network for Thermal Model of 2-D Combustor Wall

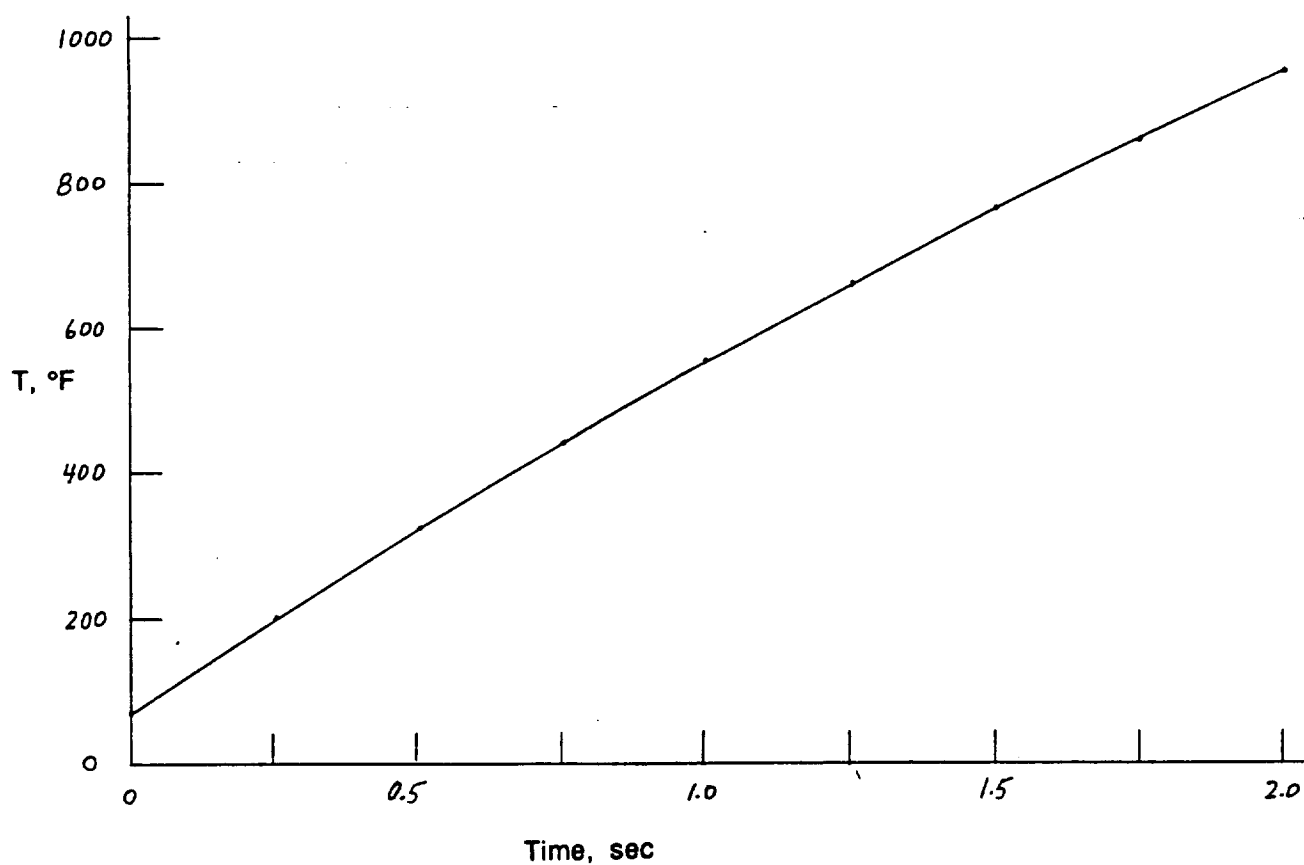


Figure 86. Temperature of Copper Wall at Junction with Ablative Throat Insert

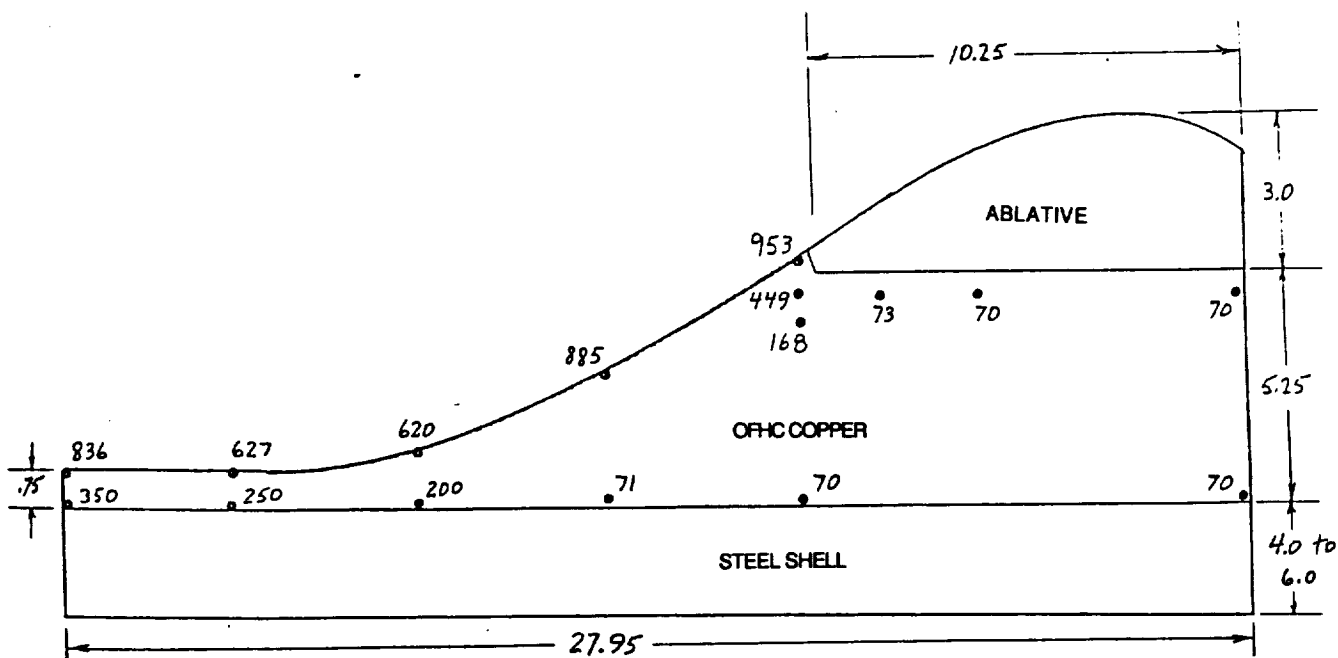


Figure 87. Estimated Temperature (°F) of Coated Copper Liner of 2-D Combustor at End of 2-sec Firing at 2000 psia P_c

7.4.4 INJECTOR ASSEMBLY

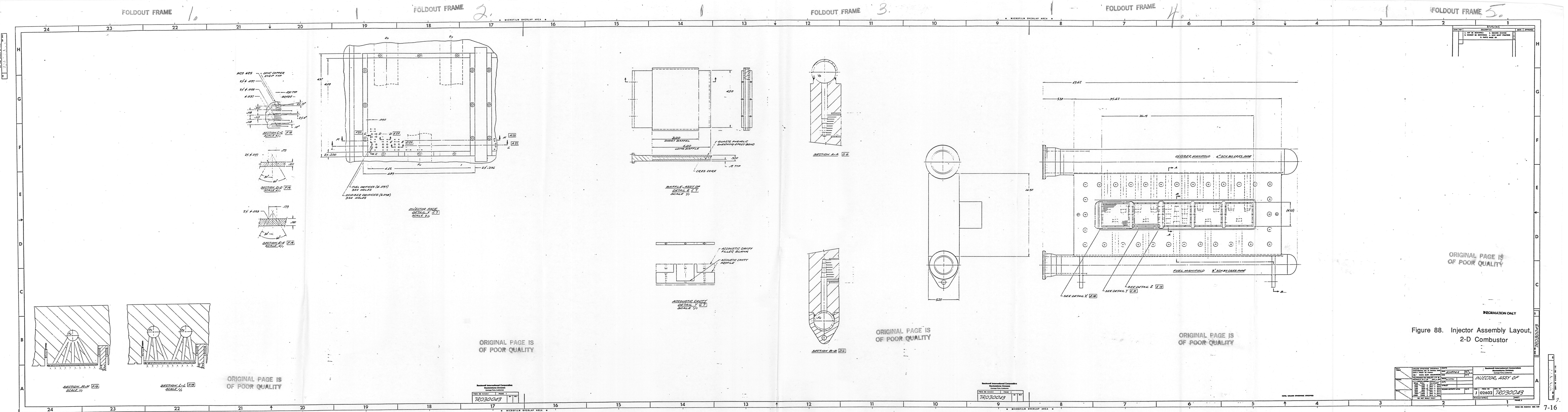
7.4.4.1 Description

The 2-D injector assembly (Drawing No. 7R030043, Figure 88) includes the propellant manifolds, the feeder passages and orifices of five identical injectors, and supports for the ICC walls (or baffles).

Following are the steps involved in fabrication of the injector assembly:

1. Starting with a rectangular block of Inconel-625, drill the bolt holes, machine the sealing surface, and machine the sides to accommodate the propellant manifolds. These manifolds are schedule-80 stainless steel pipes (3-in. for fuel and 4-in. for oxidizer) with Grayloc connectors at the inlets.
2. Mill the acoustic cavity and ICC wall support slots into the block; drill and tap bolt holes for the walls.
3. Machine the grooves for the injector orifice strips.
4. Step-drill the propellant cross-passages.
5. Drill the propellant down-comers.
6. Weld the propellant manifolds to the sides of the Inconel block.
7. EDM the orifices into the machined OFHC copper strips.
8. Braze the strips into the block
9. Attach the ICC walls to the injector assembly.

Structural analysis of the injector showed safety factors of 1.4 against yielding and 3.1 in ultimate.



7.4.4.2 Injector Pattern

The element type used in the 5.7-in subscale injector (like-doublers with 14-degree canted, edge-impinging fans) was retained in the 2-D injectors. The orifices will be drilled into alternating oxidizer and fuel strips, corresponding to the rings in the round injector. A quadrant of the orifice pattern in one of the 2-D ICC injectors is shown in Figure 89. There is a total of 324 each oxidizer and fuel orifices, arrayed in nine columns of doublers. The peripheral zones of the injectors are slightly more fuel rich than the interiors because, in the long dimension, the outer rows of doublers are fuel and, in the short dimension, each fuel doubler is displaced 0.050-in. towards the wall from its interacting oxidizer doubler.

The design parameters of the 5.7-inch and 2-D injectors were listed in Table 12. Except for the total number of orifices, all the parameters are identical in the two designs. To achieve this, the nominal total propellant flowrate in a 2-D ICC (98.02 lb/sec) will be somewhat lower than in the 5.7-in subscale combustor (113.50 lb/sec), but will be comparable to that in a full-scale 3-D ICC.

The geometries of the individual elements in the 5.7-inch and 2-D injectors are compared in Figure 90. They are identical, except for a slight increase in the distance between the fuel and oxidizer doublers in the latter design to accommodate the rectangular pattern.

7.4.4.3 Acoustic Cavity Analysis

Acoustic analyses were carried out to duplicate the 1T frequencies of the 5.7-in subscale injector in the 2-D ICC's and to design appropriate acoustic cavities for the latter.

As pointed out above, the 1T mode of the 5.7-in subscale combustor was duplicated by specification of the 4.83-in length of the 2-D ICC. The 1T frequency of the entire 2-D chamber is low (916 Hz) and should be suppressed by the baffles, which will have the longest practical lengths (4-in.). Within the 2-D rectangular ICC's, the first three characteristic frequencies of the 4.83 x 4.50 chambers are:

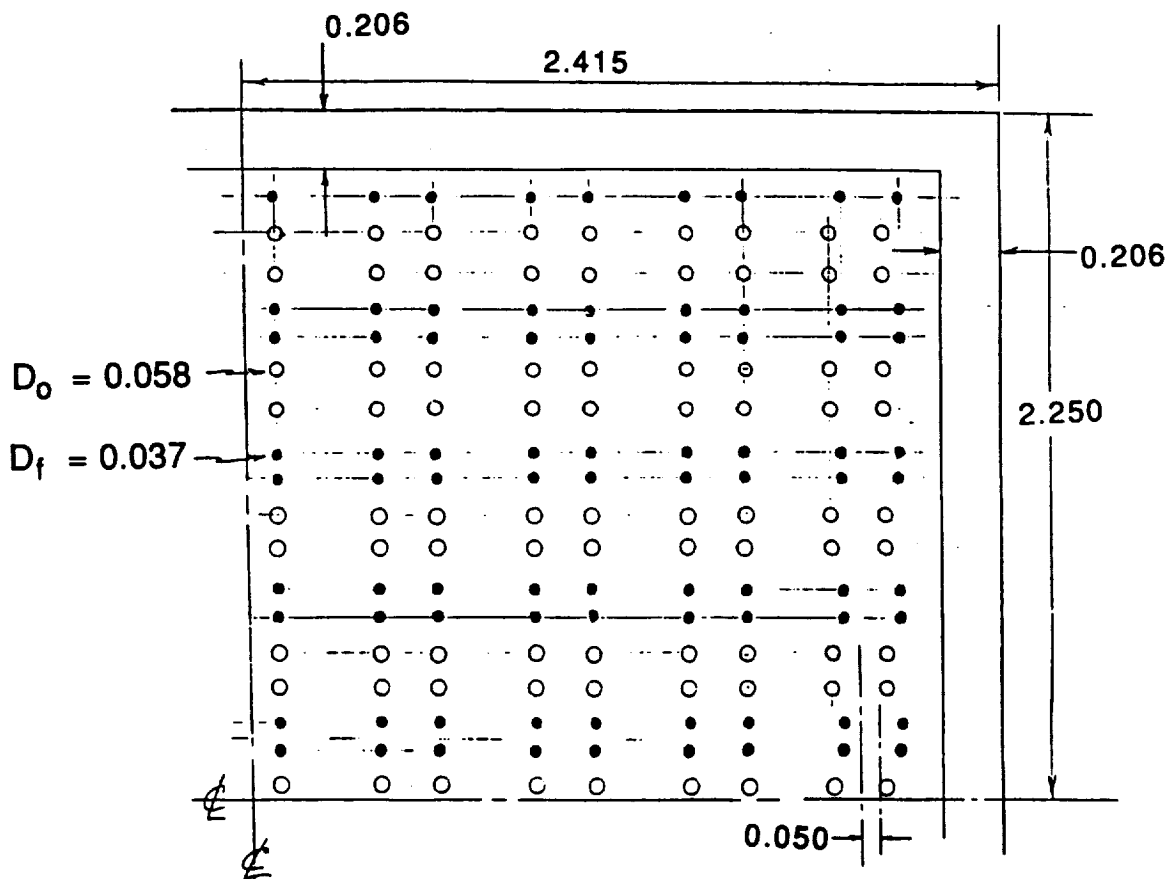
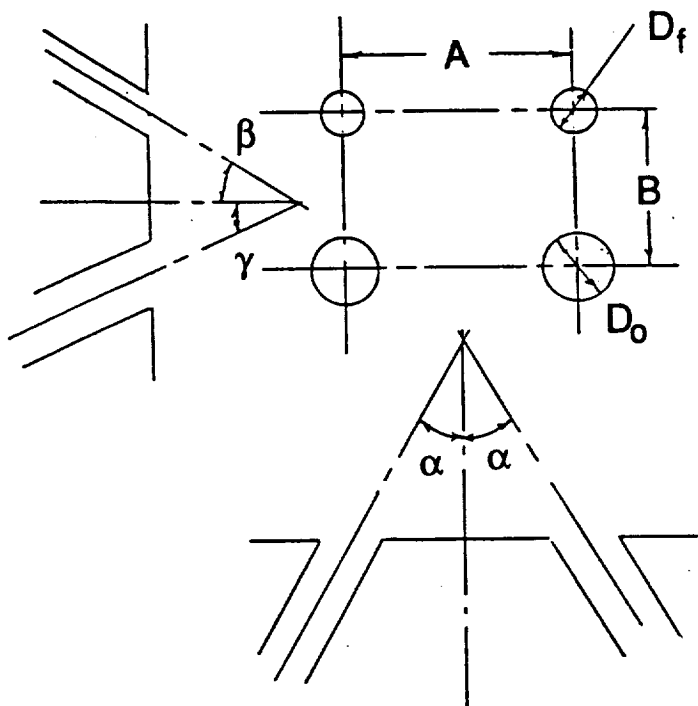


Figure 89. Quadrant of 2-D ICC Canted-Fan Like-Doublet Injection Pattern



	5.7-in Injector	2-D ICC Injector
D_o , in.	0.058	0.058
D_f , in.	0.037	0.037
A, in.	0.175	0.173
B, in.	0.092	0.11
α , °	30	30
β , °	10	10
γ , °	4	4

Figure 90. Comparison of Canted-Fan Like Doublet Elements in 5.7-inch and 2-D ICC Injectors

$$f_{10} = 4940 \text{ Hz}$$

$$f_{01} = 5323 \text{ Hz}$$

$$f_{11} = 7275 \text{ Hz}$$

For comparison, the first two tangential modes of the 5.7-in subscale combustor are:

$$f_{1T} = 4940 \text{ Hz}$$

$$f_{2T} = 8227 \text{ Hz}$$

Thus, the lowest transverse and the first combined mode of the rectangular compartment are close to the first two cylindrical transverse modes. The 5323-Hz rectangular compartment mode is uniquely different, however, and forces a requirement for three tuned quarter wave cavity depths to damp potential compartment instability modes.

Based on the acoustic cavity temperatures measured in the tests of the 3.5-inch circumferential-fan like-doublet injector (about 2250° F), the quarter-wave acoustic slot lengths and open areas listed in Table 13 were specified.

The f_{10} and f_{01} absorbers (two slots each) were centered along the ICC walls, where the antinodes for those modes are located. That is, the f_{10} absorbers were centered along the 4.50-in. walls and the f_{01} absorbers were centered along the 4.83-in. walls. The f_{11} absorbers were located at the corners, as sketched in Figure 91.

7.4.4.4 Baffle Design

The ICC walls, which are the chamber baffles, are 0.5-in. thick and consist of a 0.25-in. CRES core covered with 0.125-in. of quartz-phenolic ablative. They are mounted in the body of the injector assembly and fit into grooves machined into the chamber liner, to prevent baffle oscillation.

The baffles, which are replaceable, are 3 or 4 inches in length. This range was derived from an estimation of the vaporization efficiency of like-doublet RP-1 elements as a function of distance from the injector face, using the Rocketdyne SDER computer code. (Figure 92). Mixing losses were assumed to be negligible and LOX vaporization is extremely rapid, so RP-1 vaporization efficiency corresponded essentially to combustion

Table 13. Acoustic Cavity Slots for 2-D ICC

Acoustic Mode	Frequency, Hz	Slot Length, in.	Open Area, %
10	4940	1.52	4.5
01	5323	1.41	4.5
11	7275	1.03	6.0
			<hr/>
			15.0

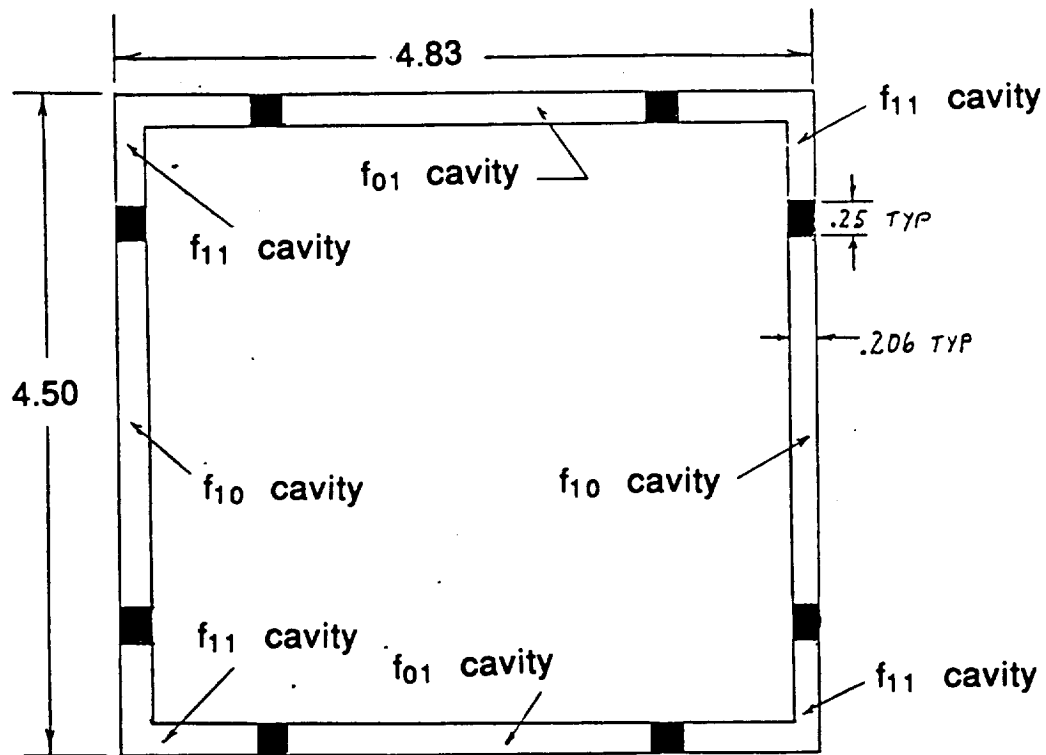


Figure 91. Acoustic Cavity Configuration, 2-D ICC

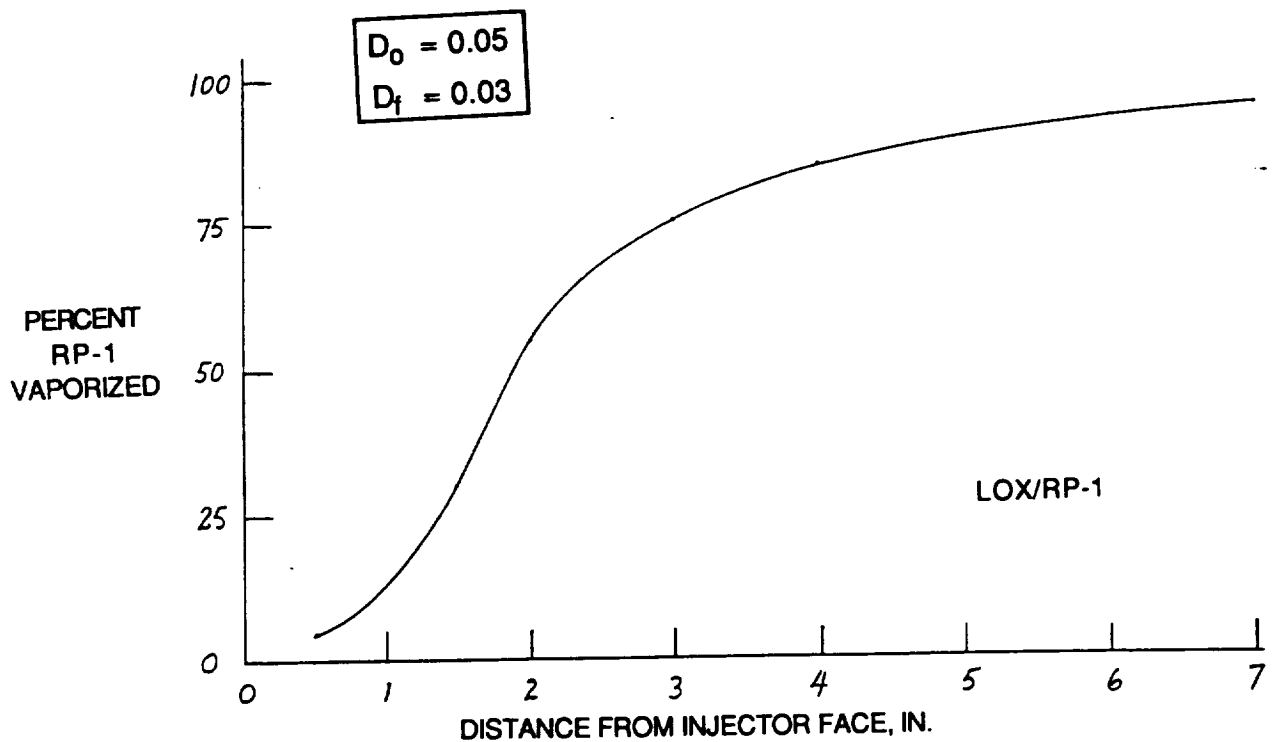


Figure 92. Vaporization Efficiency of RP-1 Like-Doublet Elements

efficiency. With the assumption that RP-1 vaporization is the controlling factor in the extent of LOX/RP-1 combustion, the estimated efficiency for 0.030-inch-diameter fuel orifices is about 78-percent at 3 inches from the injector face and 86-percent at 4 inches. By extending the baffle lengths to a distance at which combustion is mostly completed (and well beyond the point of maximum combustion rate), the baffles not only define the ICC boundaries but also function as chamber stabilization devices by preventing full chamber modes from occurring. It may be assumed that the turbulence and mixing in the region immediately downstream of the baffles will promote completion of the combustion process before the start of convergence.

7.4.4.5 Ignition

The 2-D combustor will employ the same TEA/TEB (15/85) ignition method as the subscale LOX/RP-1 combustors. The TEA/TEB will be injected through a port in the side wall of each ICC. The lines between the TEA/TEB main valve and each of the injection ports will have the same length, to produce simultaneous ignition in the five chambers.

7.4.5 INSTRUMENTATION AND BOMB LOCATIONS

Provisions will be made in the 2-D combustor detail design for the installation of low- and high-frequency pressure transducers required for combustion stability diagnostics. Ports will be provided within the ICC's and in the chamber downstream of the baffles. Feed system pressure measurements will be made in both propellant manifolds.

The high-frequency pressure transducers will be located near the corners of the two end ICC's, for detection of the first three modes at or near their pressure antinodes, and as close as possible to the injector face. In the other compartments, the transducers will be located at about two inches (one-half the baffle length) from the injector face, to identify longitudinal compartment modes. High-frequency pressure transducers will also be positioned about one-half-inch downstream of the baffles, midway along the short dimension of the chamber.

Bomb ports in three of the ICC compartments will be close to the injector face, near the corners of the compartments, to excite simultaneously the first three modes at their common antinode location. In the other two compartments, the bomb ports will be located

at the center of the 4.5-inch wall, to excite the lowest-frequency (and potentially least stable) compartment mode. In addition, two bomb ports will be provided immediately downstream of the baffles, also centered in the short dimension of the combustor.

The locations and numbers of ports for TEA/TEB injection, low- and high-frequency pressure transducers, thermocouples, and bombs are summarized in Table 14.

Table 14. Ignition, Instrumentation & Bomb Locations

Location	TEA/TEB Ignition Ports	Low-Freq. Pressure Ports	High-Freq. Pressure Ports	Thermo- couple Ports	Bomb Ports
Oxidizer Manifold		2	2	2	
Fuel Manifold		2	2	2	
ICC Chambers	5	5	10		5
Immediately Downstream of Baffles		3	3		2
Start of Convergence		3			
Acoustic Cavities				20	
Totals	5	15	17	24	7

8.0 PHASE B

Task III - Subscale Injector Stability Evaluation

TASK III

9.0 INTRODUCTION

Upon completion of the 5.7-inch Canted-Fan injector testing, a decision was made by NASA-MSFC and Rocketdyne personnel to modify the direction of the program. The original program logic called for the design, fabrication and delivery to MSFC of a two dimensional injector and combustor to simulate stability parameters of a full scale (750,000 lb thrust) combustor. The results of the 5.7-inch testing, however, convinced all parties involved that additional stability information was required in order to build large high performing LOX/RP-1 rocket engines. At the conclusion of the 5.7-inch testing, a decision was made to return to 3.5-inch hardware to gain the most stability information possible with the remaining contract funds and still pursue the Isolated Combustion Compartment, ICC, objective of the program.

The obvious advantages associated with returning to the 3.5-inch hardware to perform a stability investigation included the existence of five available injectors, seven calorimeter cooled combustor spools, two calorimeter cooled throat sections, three uncooled bomb spools, previous hot fire and cold flow test results and the required instrumentation and instrumentation ports to perform a proper stability investigation. During previous 3.5-inch testing, the H-1 Derivative was the only injector which was tested for dynamic (bomb test) stability. Furthermore, the dynamic stability tests which were performed with the H-1 Derivative injector included first tangential (8000 Hz) acoustic cavities. All of the 3.5-inch injectors (H-1 Derivative, Box-Doublet, Circumferential-Fan, LOX Showerhead and the O-F-O Triplet) were capable of facilitating acoustic cavities.

The replanned Task III involved in-depth stability and performance analysis and hot-fire testing of subscale injectors with two major objectives:

- 1) Characterize and develop a main injector element configuration, applicable to large booster engines, to be incorporated within a baffle compartment or Isolated Combustion Compartment (ICC) with appropriate acoustic damping.
- 2) Increase the generic technology base of the LOX/RP-1 propellant combination at high chamber pressures and, with additional test data, improve existing stability

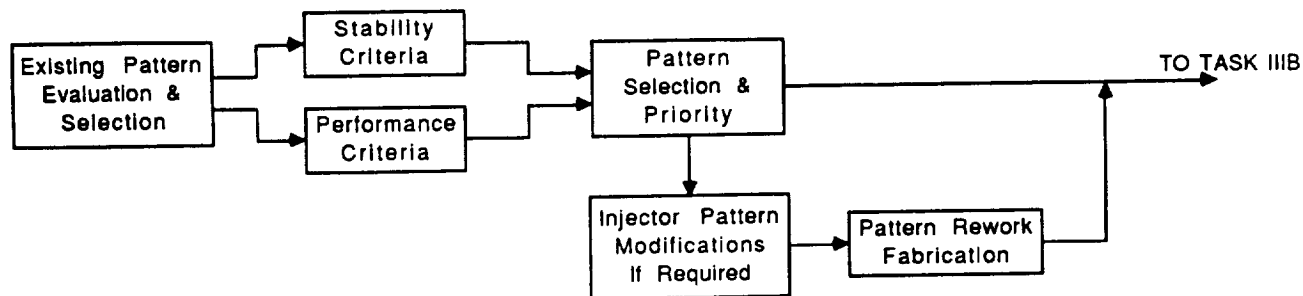
and performance design and analysis techniques, as well as improve acoustic cavity design methodology.

Two primary analytical computer programs were used to perform the in-depth investigation of the five 3.5-inch injectors. The Standardized Distributed Energy Release (SDER) computer program was used to predict the injection, atomization, vaporization, mixing, and overall combustion performance characteristics of each injector. The results are presented in the form of vaporization curves, near injector distribution plots (color plots and contours), near injector mass flux plots and the absolute values of the combustion performance predictions for each injector.

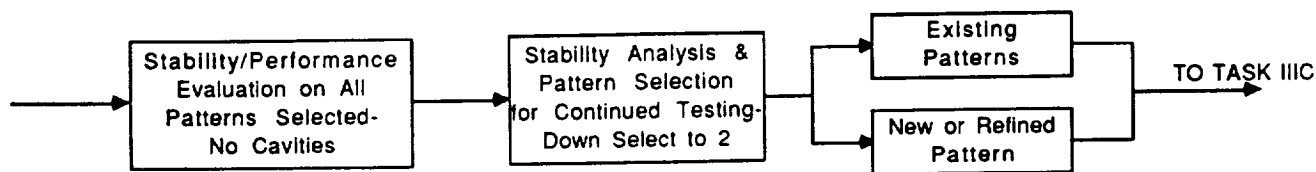
The Three-Dimensional Oscillatory Rocket Combustor (TDORC) computer program was used in the analysis of the injectors to predict the relative chamber response (damping). The computer program has, as an input, the vaporization profile of each injector, and can predict the relative acoustic stability margin difference between the candidate injectors. Furthermore, TDORC can predict the effects on acoustic stability of acoustic cavities and chamber geometry. This analysis, developed at Colorado State University, implements a classical time lag approach. One of the drawbacks of the time lag analysis is the empirical approach. Mechanistic modeling of the combustion process is not undertaken in the analysis, but correlative data is typically used to predict the driving capability of a given injector or combustion process. At the beginning of this task, a limited amount of data was available for predicting the combustion response of injectors utilizing LOX/RP-1 propellants. An increase in the overall stability data base would result from the proposed 3.5-inch injector testing.

The planning of the additional testing with the 3.5-inch hardware was based to some extent on the applicability of the hardware on hand. The hardware could be configured to investigate the following parameters: chamber length, acoustic cavity configurations, bomb tests and operating conditions such as chamber pressure and mixture ratio. Finally, the development of an additional 3.5-inch test program would benefit from the previous task of this program.

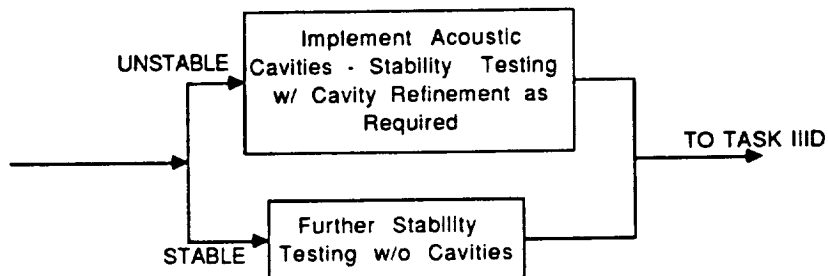
The program logic diagram for the revised Task III effort is shown in Figure 93.



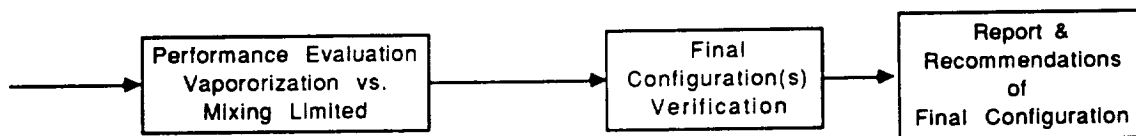
TASK IIIA - REVIEW & PLANNING



TASK IIIB - SCREENING TESTS



TASK IIIC - STABILITY EVALUATION



TASK IIID - PERFORMANCE EVALUATION

TASK IIIE - FINAL DOWN SELECT

Figure 93. Phase B Program Flow Diagram

TASK III

10.0 PRETEST ANALYSIS

10.1 INTRODUCTION

As stated earlier, detailed performance and stability analyses were performed for each of the five candidate injectors. The performance predictions were made with the Standardized Distributed Energy Release (SDER) computer program, and the stability predictions were made with the Three Dimensional Oscillatory Rocket Combustor (TDORC) computer program. The results of interest provided by the analyses include vaporization and reaction curves, mixing efficiencies, vaporization efficiencies, near injector mixing profiles, near injector mass flux and acoustic stability characteristics. It should be noted that all of the candidate injectors had been previously tested. All of the information gathered in the previous tests were incorporated in the analyses in order to anchor the codes and aid in the determination of the matrix. The most important result of the analyses was to determine the relative difference between the five candidate injectors to aid in the process of finding an ICC injector and an unstable injector to meet the program requirements.

10.2 PERFORMANCE ANALYSIS RESULTS

The performance analysis is composed of a detailed injector description for SDER input, execution of the SDER program and post execution reduction which includes contour plotting and color maps of the near injector normalized fuel fraction, contour plotting of the near injector mass flux and the steady-state vaporization curves for each injector which will be displayed later with the results of each of the candidate injectors for comparison.

10.2.1 H-1 DERIVATIVE MIXING EFFICIENCIES

The near injector mixing results for the H-1 Derivative injector are displayed in Figures 94 and 95. Figure 94 is a contour representation of the near injector mixing pattern described by the normalized fuel fraction. The normalized fuel fraction is defined by:

$$(ff)_n = (1+MR)_{\text{overall}} / (1+MR)_{\text{local}}$$

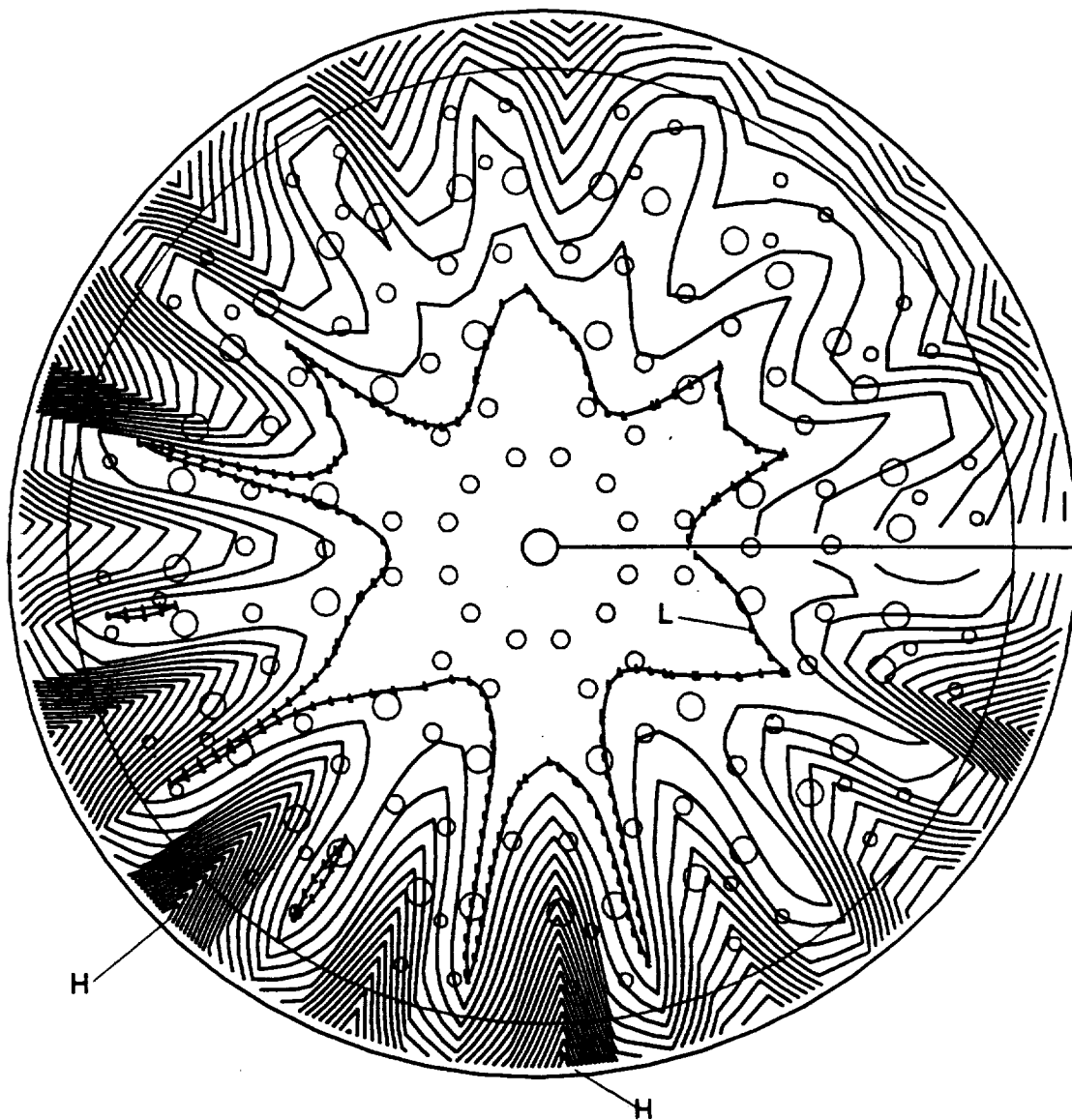


Figure 94. Normalized Fuel Fraction Contours of the H-1 Derivative Injector

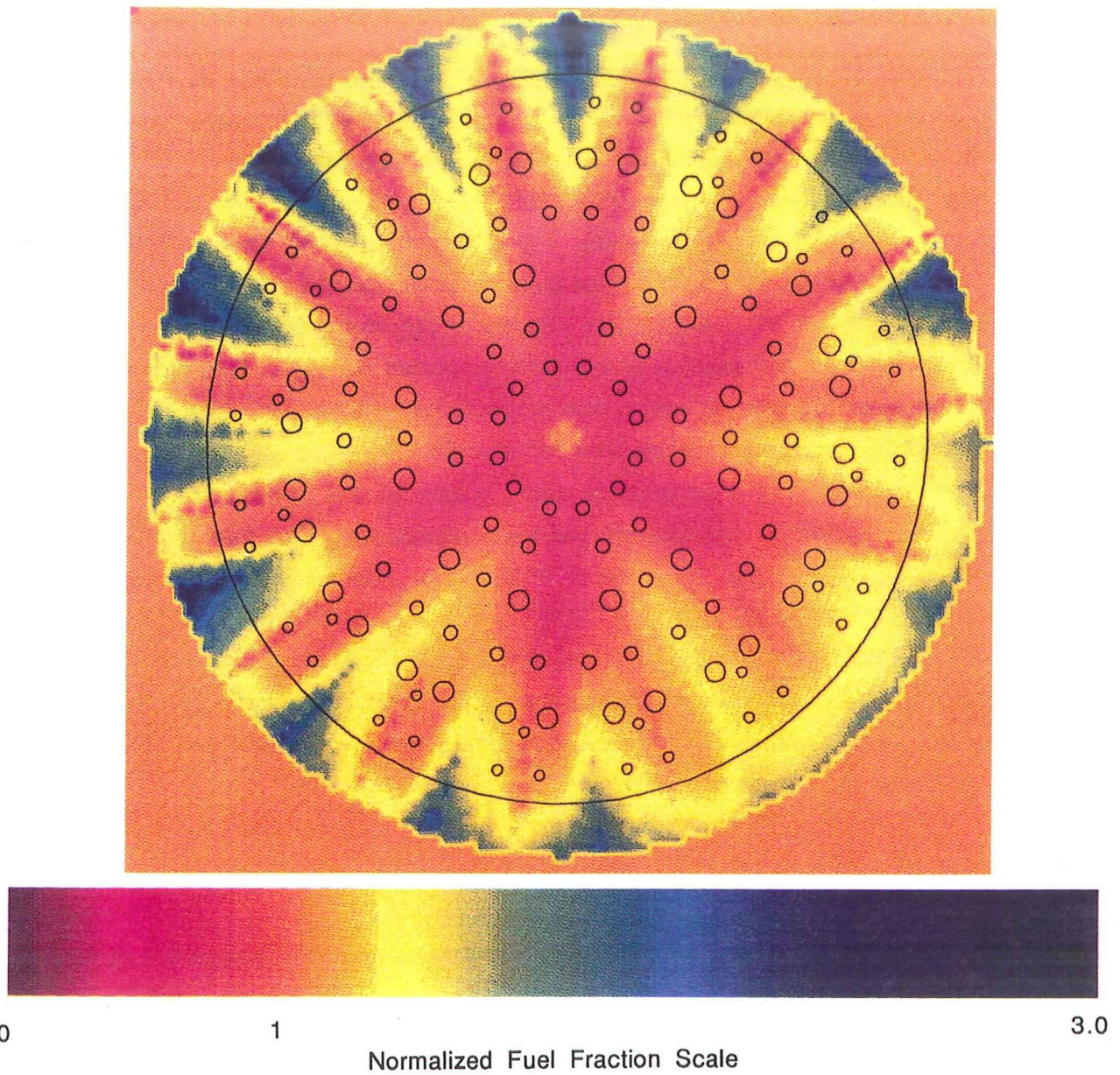


Figure 95. Normalized Fuel Fraction Plot of the H-1 Derivative Injector

The minimum $(ff)_n$ value is marked by an "L" on the contours, while the maximum is marked with an "h". An $(ff)_n$ value of 1 corresponds to a local fuel fraction that is equivalent to the overall fuel fraction of the injector. The minimum fuel fraction for the H-1 Derivative injector was predicted to be 0.71, while the maximum was predicted to be 3.00. The same results are plotted in Figure 95, but the results are shown in a color plot showing the mixing regions. In Figure 95 the color red represents a LOX rich region, while the color blue represents a fuel rich region. The near injector mass flux predictions for the H-1 Derivative injector are displayed in Figure 96. The low mass flux is denoted by an "L" and the high flux by an "H". The results suggest a high mass flux in the center of the injector, and a declining flux gradient in the radially outward direction. One reason for this trend is the inclusion of acoustic cavity area at the radial periphery in which no propellant flux occurs. The vaporization predictions for the H-1 Derivative injector are 100% for both oxidizer and fuel. The axial locations where vaporization is predicted to be complete are 3.5 and 16.7-inches for the oxidizer and fuel, respectively. The losses with the H-1 Derivative injector are predicted to be due to mixing. The predicted mixing efficiency of the H-1 Derivative injector is 96.2%. The "ZOM" variable in SDER, which represents the axial region in which spray mixing of the propellants occurs, can be adjusted to anchor the analysis to a given injector. The recommended "ZOM" value was incorporated for the H-1 Derivative injector, but with some of the five candidate injectors a value of the "ZOM" plane was determined from previous hot fire tests.

10.2.2 O-F-O TRIPLET MIXING EFFICIENCIES

The near injector mixing results for the O-F-O Triplet injector are displayed in Figures 97 and 98. The contour in Figure 97 shows a minimum normalized fuel fraction of 0.47, and a maximum $(ff)_n$ of 1.40. The color representation of the normalized fuel fraction is presented in Figure 98. The mass flux predictions for the O-F-O Triplet injector are presented in Figure 99. The results are similar to the H-1 Derivative injector, in that the high mass flux is in the center of the injector, but that the low mass flux region is radially inboard in comparison to the H-1 Derivative injector results. This result is a function of the injector design and the acoustic cavity orientation difference between the H-1 Derivative and the O-F-O Triplet injectors. The O-F-O Triplet injector was predicted to have 100% vaporization efficiency with respect to both propellants, and the axial location where vaporization is predicted to be complete is 1.0 and 13.6-inches for the LOX and RP-1, respectively. The O-F-O Triplet injector mixing efficiency was predicted to be 95.2%

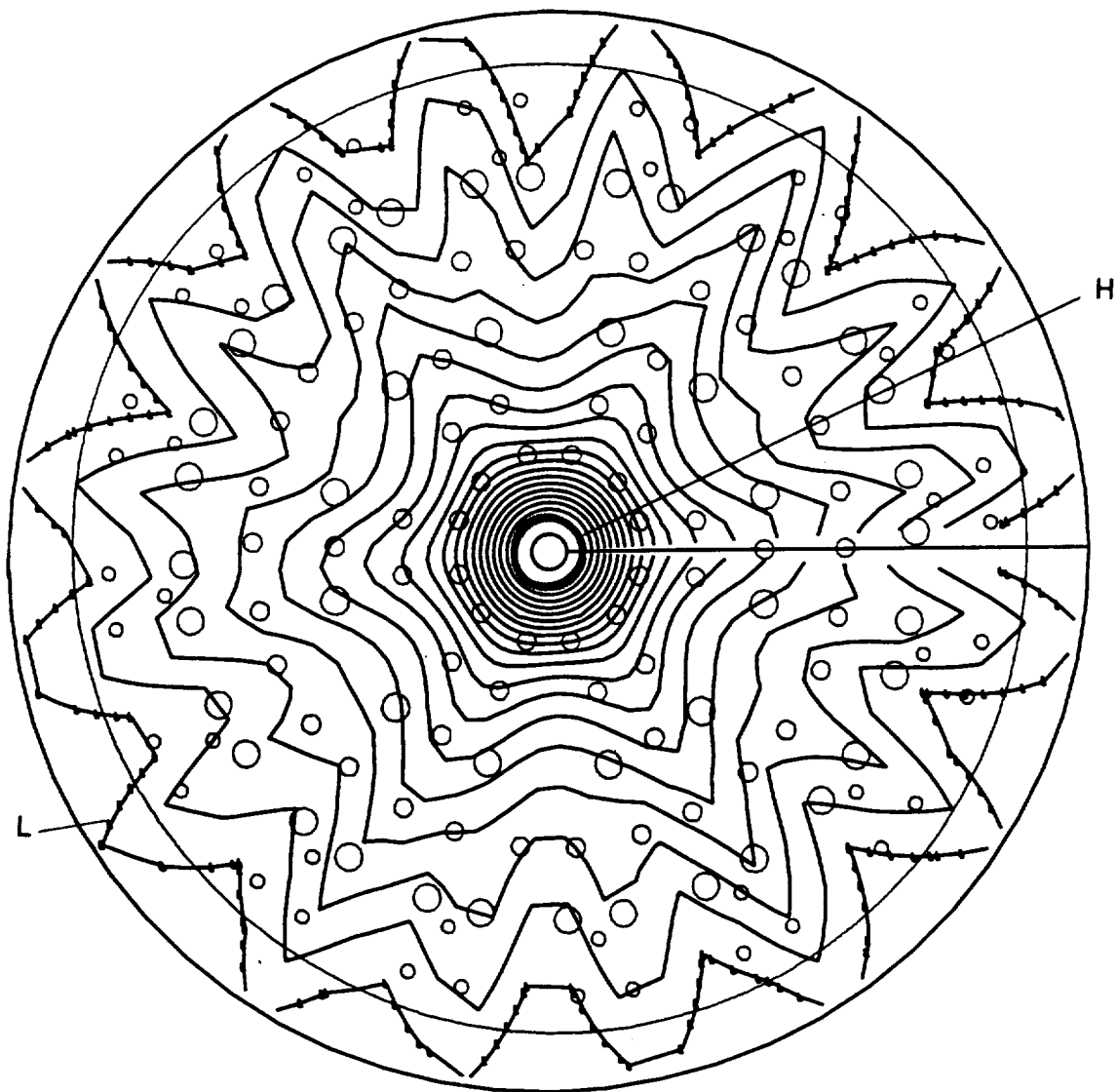


Figure 96. Mass Flux Contour of the H-1 Derivative Injector

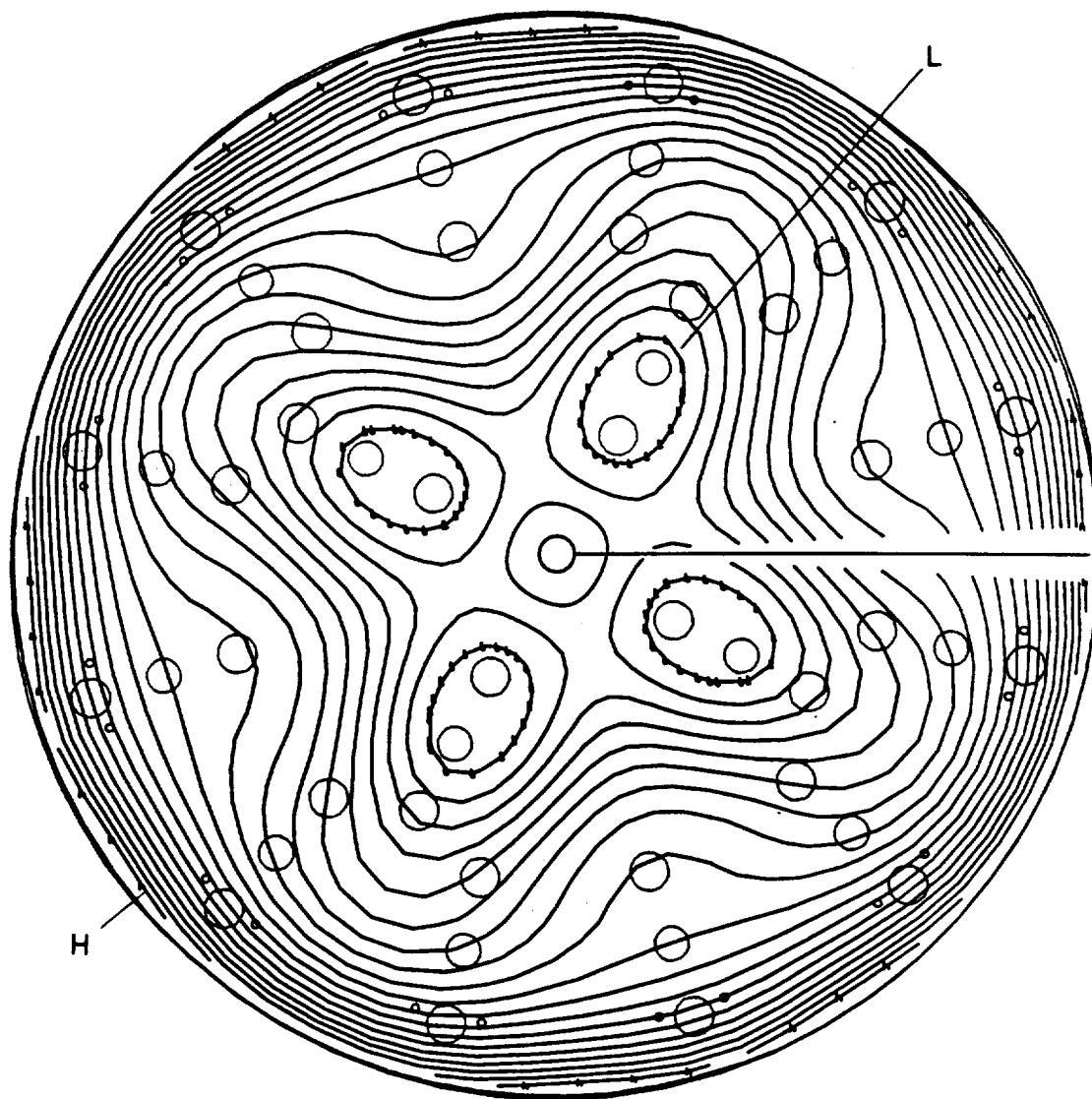


Figure 97. Normalized Fuel Fraction Contours of the O-F-O Triplet Injector

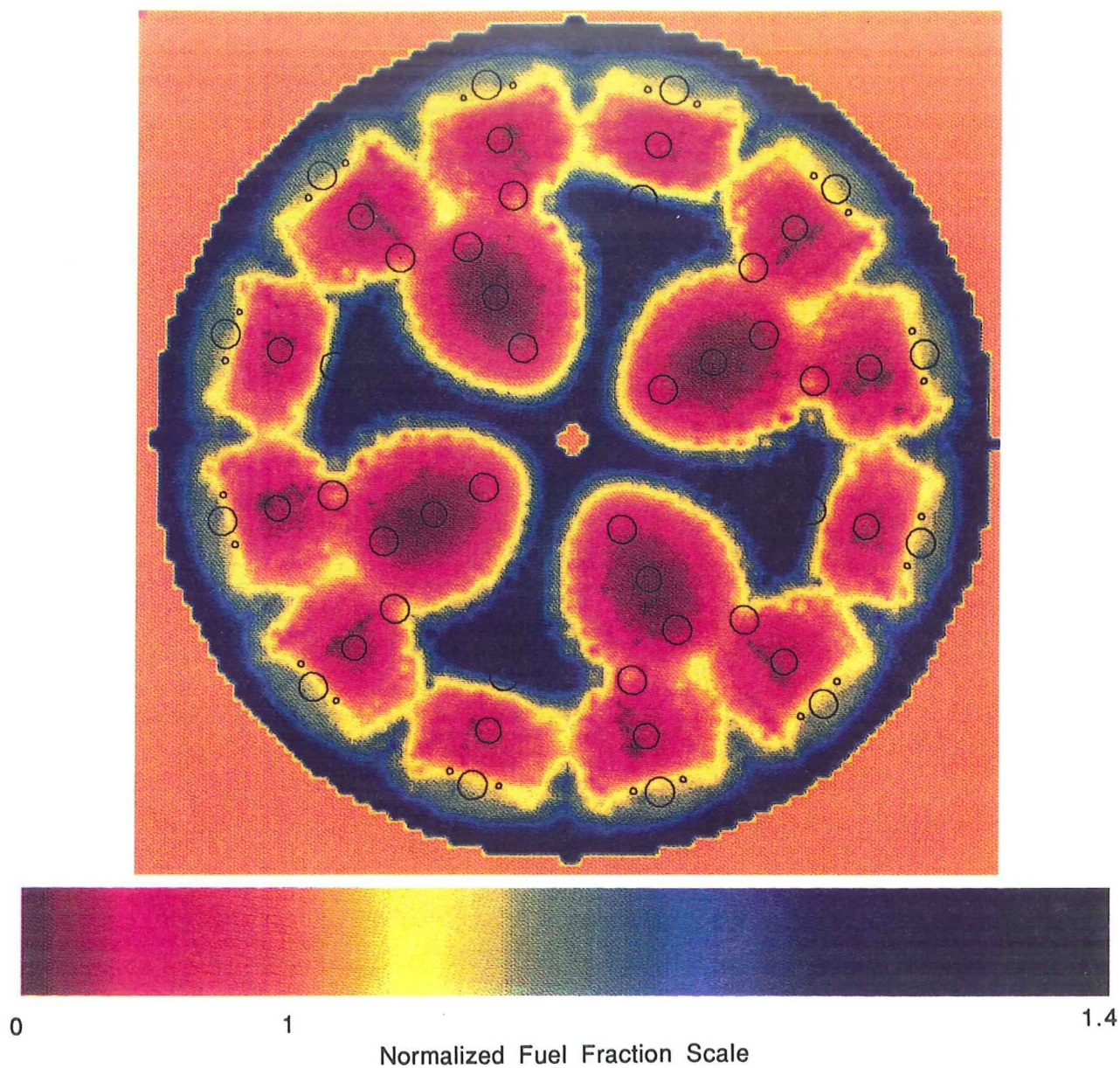


Figure 98. Normalized Fuel Fraction Plot of the
O-F-O Triplet Injector

ORIGINAL PAGE IS
OF POOR QUALITY

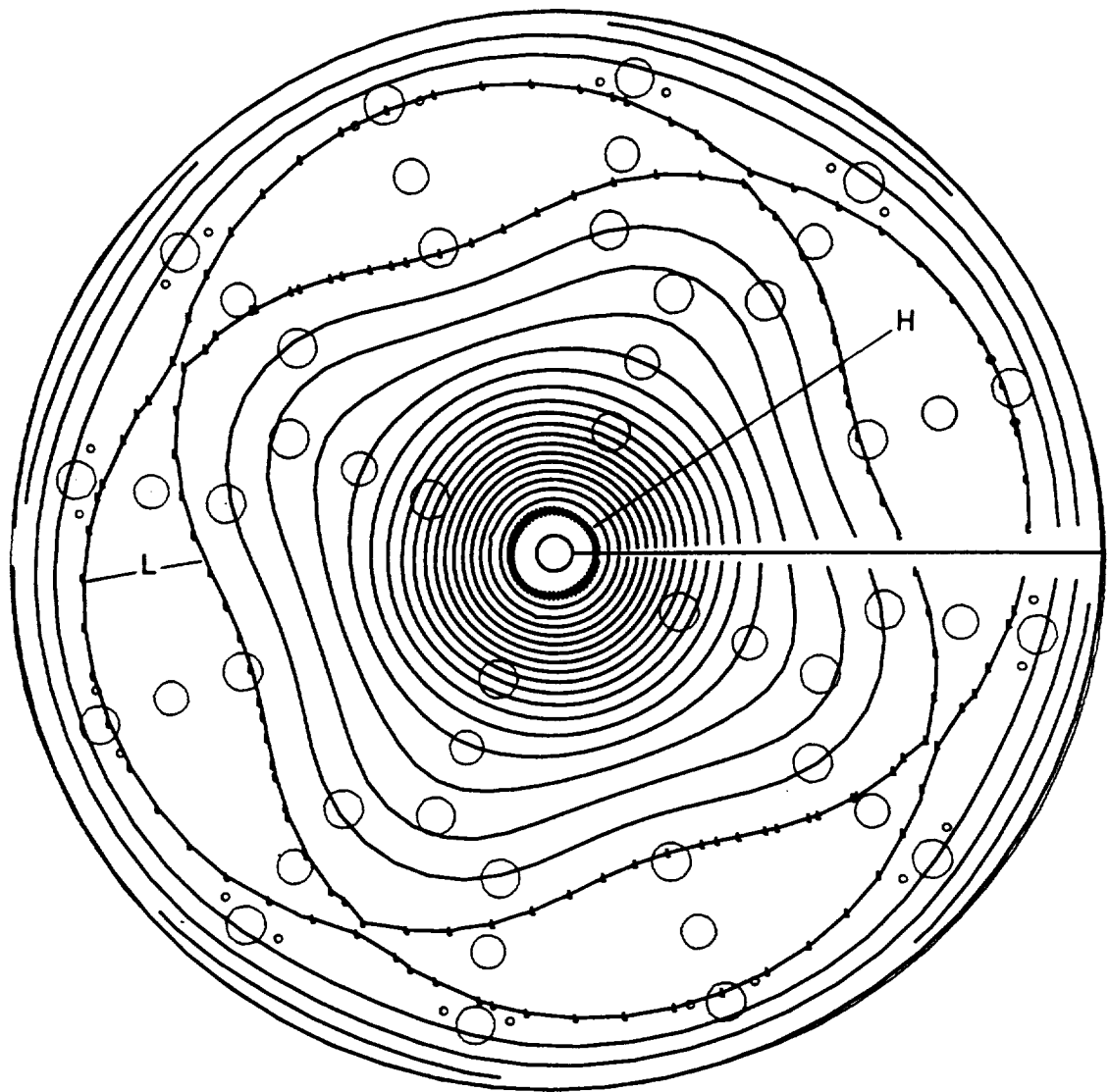


Figure 99. Mass Flux Contour of the O-F-O Triplet Injector

with the recommended value for the "ZOM" plane. This is contrary to early test results, but it was thought that a first longitudinal instability was causing low combustion efficiency in the preliminary 3.5 inch testing with the O-F-O Triplet injector. This hypothesis was later verified.

10.2.3 CIRCUMFERENTIAL-FAN MIXING EFFICIENCIES

The same SDER analysis was performed for the Circumferential-Fan injector. Two versions of the injector have been fabricated. The original Circumferential-Fan injector was destroyed in a test stand incident while being used on another program. Because of high chamber wall heat flux experienced with the original injector, a slight modification was made to the pattern in the replacement. The two fuel fraction contours for the original and modified Circumferential-Fan injectors are displayed in Figures 100 and 101, respectively. The difference between the two injectors was a radially outward translation of the outer fuel elements, and the removal of a radially outward cant to the outer oxidizer and fuel elements. The modification resulted in a 33% reduction in the heat load to the combustor wall. The results of the modification are visible in the fuel fraction contours. With the original Circumferential-Fan injector, the lowest (LOX rich) fuel fraction was predicted to be at the combustor wall and had a value of 0.82. The high fuel fraction was predicted to be radially inboard of the combustor wall and had a value of 6.10. With the new design, the high fuel fraction was moved to the combustor wall, and had a value of 1.44. The low fuel fraction was shifted radially inboard and was predicted to be 0.82. These results suggest that the wall heat flux should be reduced due to the modification, but that the combustion efficiency should remain relatively unchanged due to better mixing. This particular application of SDER is thought to be a significant design tool, with respect to chamber compatibility issues. This effect is further seen in the color plots shown in Figures 102 and 103 which are for the original and modified Circumferential-Fan injectors, respectively. The mass flux contours for the modified Circumferential-Fan injector are displayed in Figure 104. The predictions show that the highest mass flux with this injector is near the radial periphery of the combustor. The acoustics of the combustion chamber typically have the highest pressure amplitude at the radial periphery, and consequently having a large mass flux at this location is thought to be a destabilizing attribute. The vaporization efficiency of the modified Circumferential-Fan injector was predicted to be 100%. The mixing efficiency was predicted to be 95.2%.

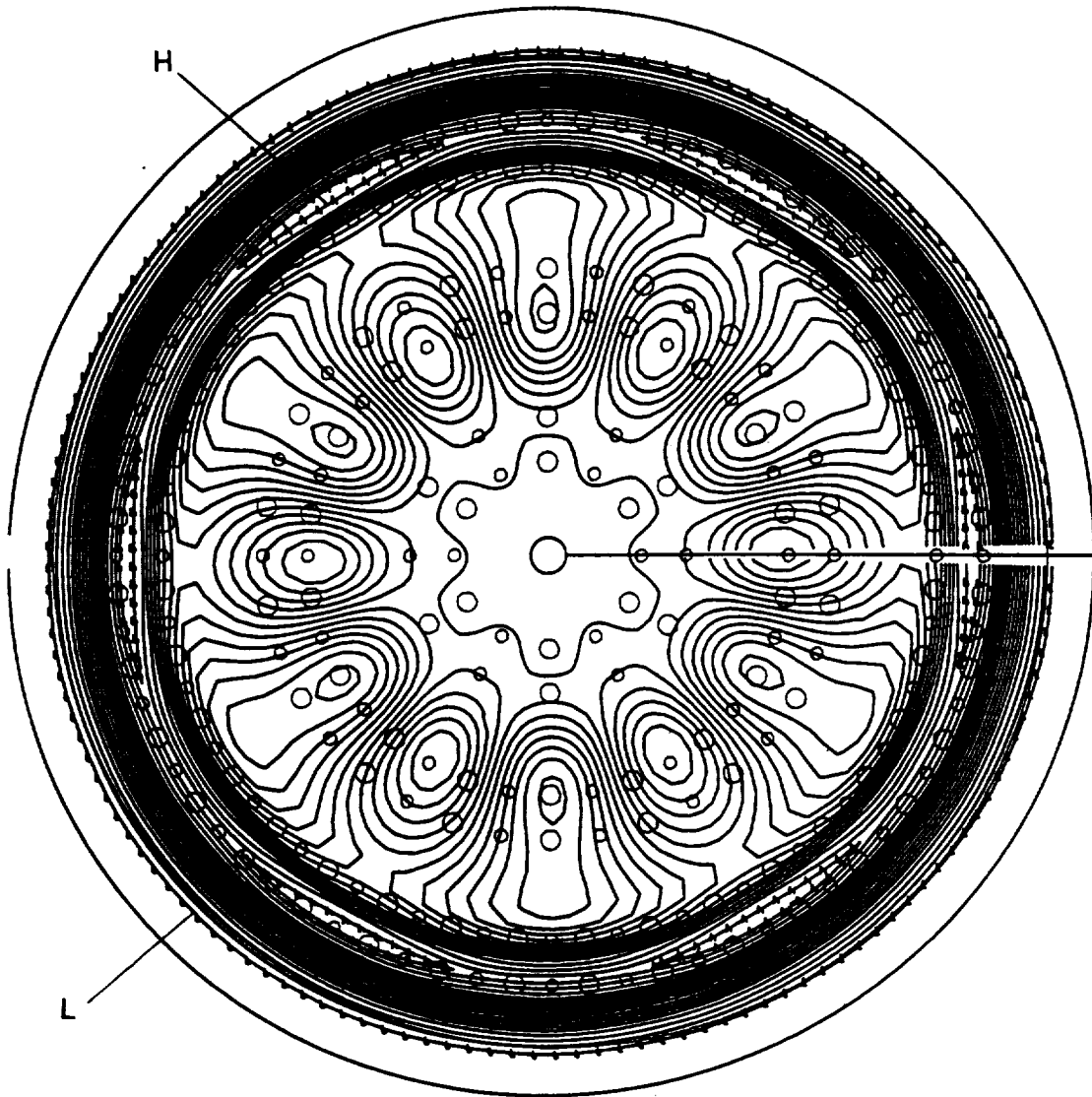


Figure 100. Normalized Fuel Fraction Contours of the Original Circumferential-Fan Injector

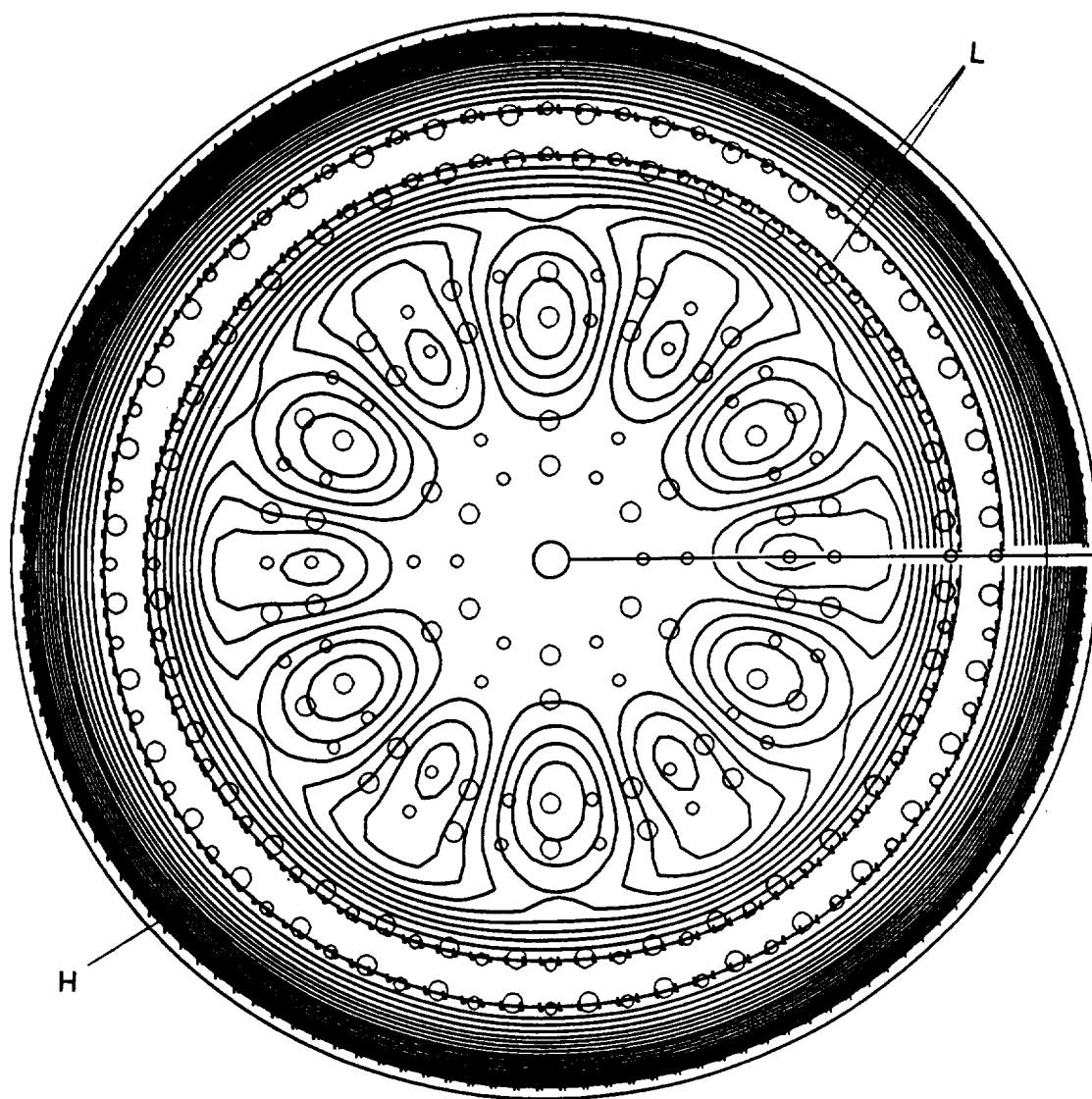


Figure 101. Normalized Fuel Fraction Contours of the Modified Circumferential-Fan Injector

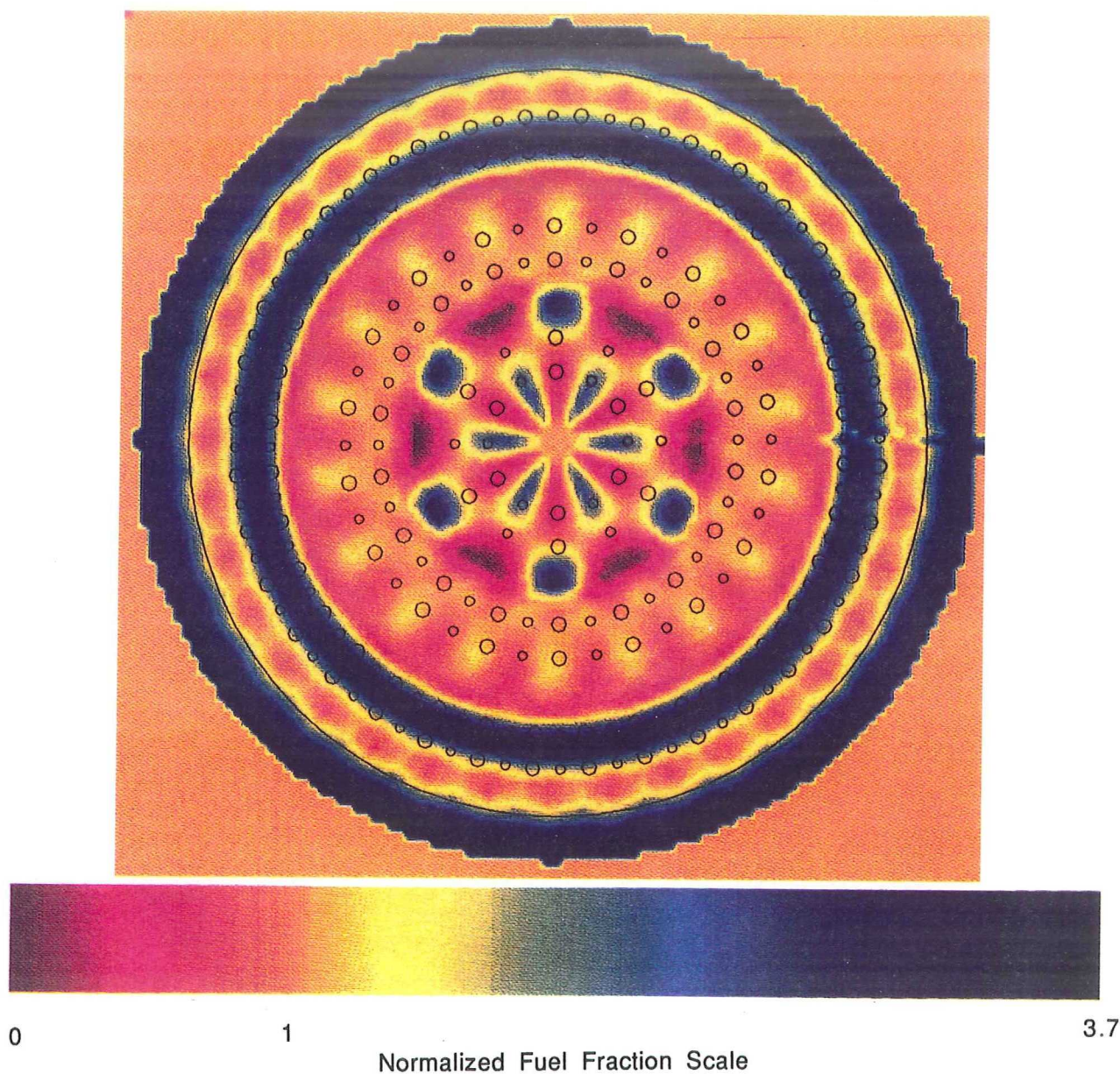


Figure 102. Normalized Fuel Fraction Plot of the Original Circumferential-Fan Injector

ORIGINAL PAGE IS
OF POOR QUALITY

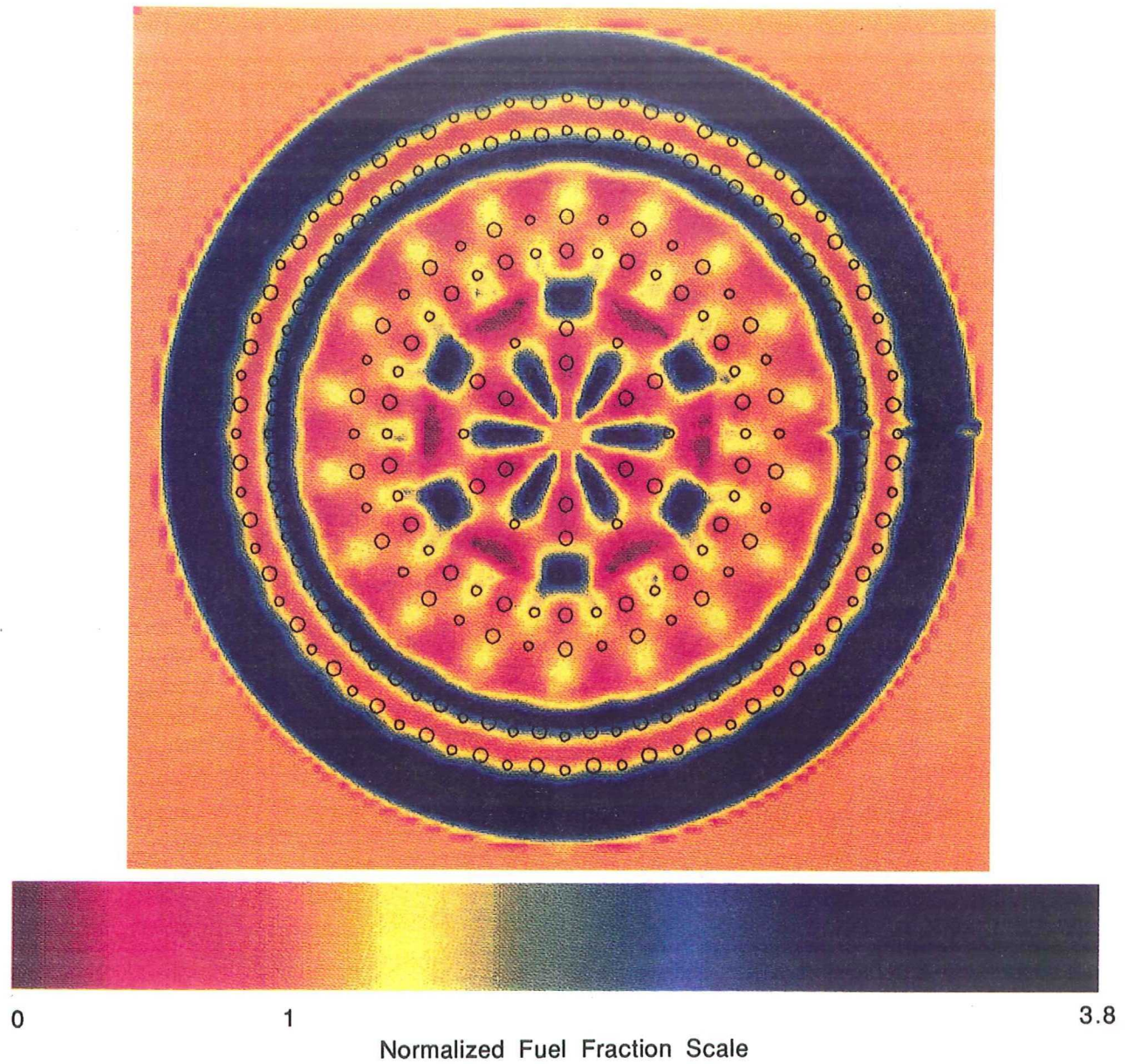


Figure 103. Normalized Fuel Fraction Plot of the Modified Circumferential-Fan Injector

ORIGINAL PAGE IS
OF POOR QUALITY

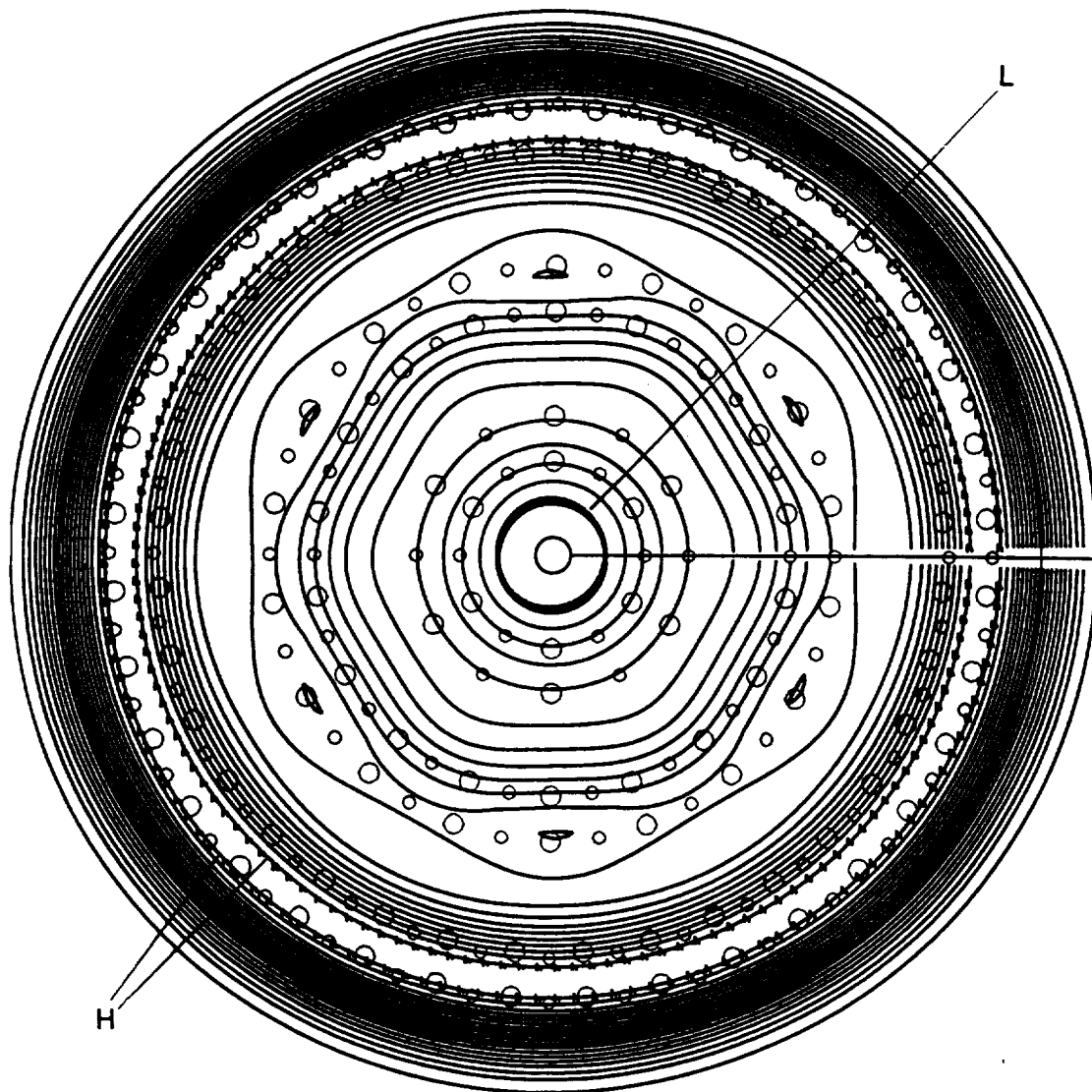


Figure 104. Mass Flux Contour of the Modified Circumferential-Fan Injector

10.2.4 BOX-DOUBLET MIXING EFFICIENCIES

The normalized fuel fraction for the Box-Douplet injector is displayed in Figure 105. With this particular injector the low fuel fraction, which has a value of 0.63, and the high fuel fraction, which has a value of 2.04, both exist at the radial periphery of the injector. This particular injector design may be prone to chamber streaking, and during the XLR-132 engine program, in which a similar injector design was incorporated, eight chamber streaks were discovered during the testing of this regen cooled hardware. The Heavy Hydrocarbon Main Injector Technology Program, however, implements combustor hardware which is circumferentially cooled with water and not as susceptible to chamber streaking as an axially cooled regen chamber. The color representation of the normalized fuel fraction is displayed in Figure 106. The mass flux contour is given in Figure 107. Unlike the Circumferential-Fan injectors, the Box-Douplet pattern is predicted to have a low mass flux at the radial periphery and the highest mass flux at the center of the injector. The vaporization efficiency of the Box-Douplet injector was predicted to be 100% for both the oxidizer and fuel side. The mixing efficiency of the injector was predicted to be 95.6%.

10.2.5 LOX SHOWERHEAD MIXING EFFICIENCIES

The final injector to be analyzed with SDER was the LOX Showerhead. Designed to be similar in nature to a coaxial type injector, the normalized fuel fraction contour for the LOX Showerhead injector is displayed in Figure 108. The minimum fuel fraction was 0.69 at the center of the elements, while the maximum fuel fraction was 3.69 which is at the radial periphery of each element. The color representation of the normalized fuel fraction is displayed in Figure 109. The attempt at simulating a coaxial type injector was successful, but the mixing efficiency predictions for this injector are low at 92.7%. The predictions, however, do indicate that the injector is mixing limited, such that 100% vaporization of each propellant should occur. The mass flux contour for the LOX Showerhead injector is displayed in Figure 110. Element isolation can again be seen in the mass flux profile. The high mass flux occurs at the center of each element and the low mass flux occurs at the extremes of each element.

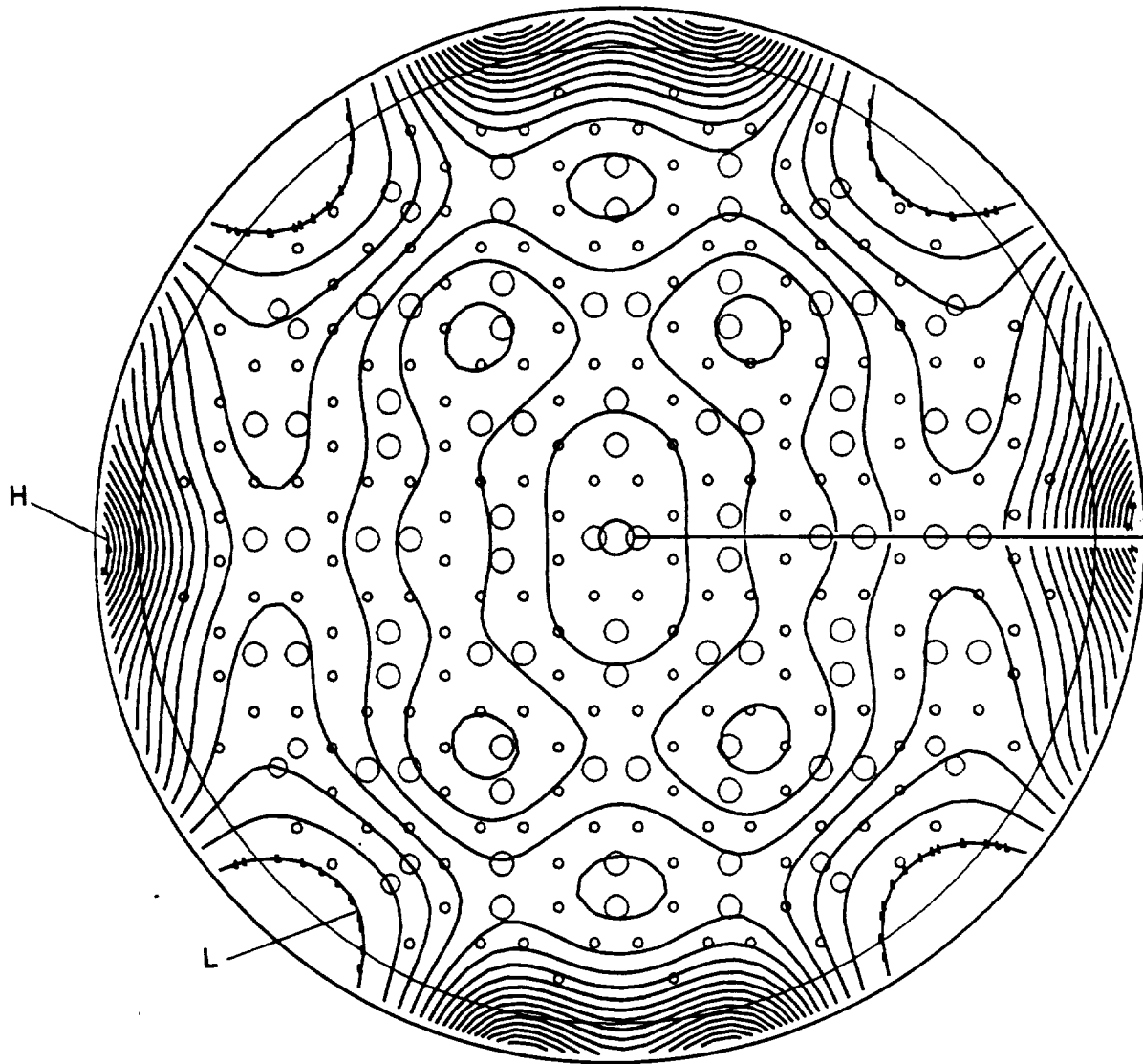


Figure 105. Normalized Fuel Fraction Contours of the Box-Doublet Injector

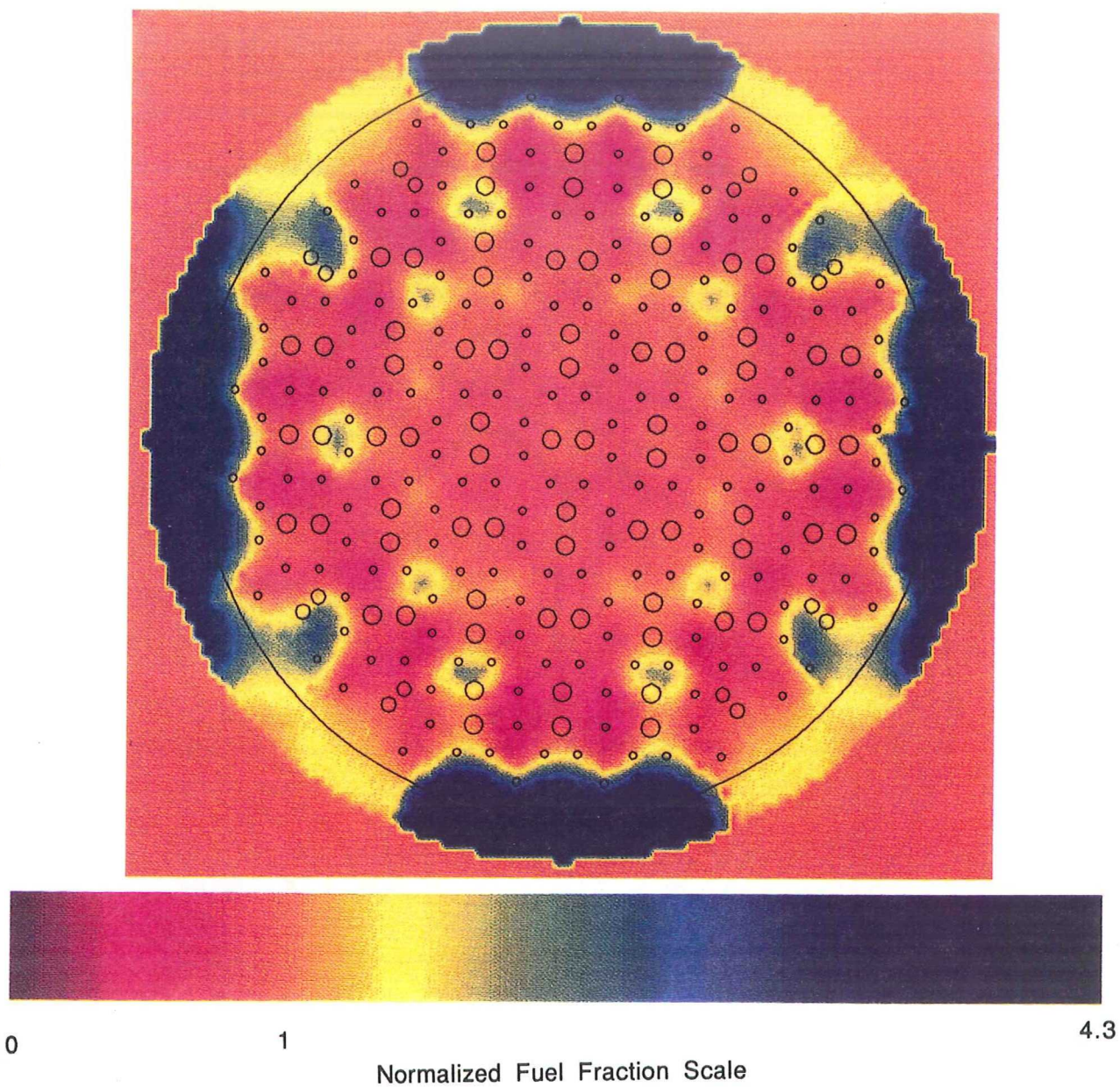


Figure 106. Normalized Fuel Fraction Plot of the Box-Doublet Injector

ORIGINAL PAGE IS
OF POOR QUALITY

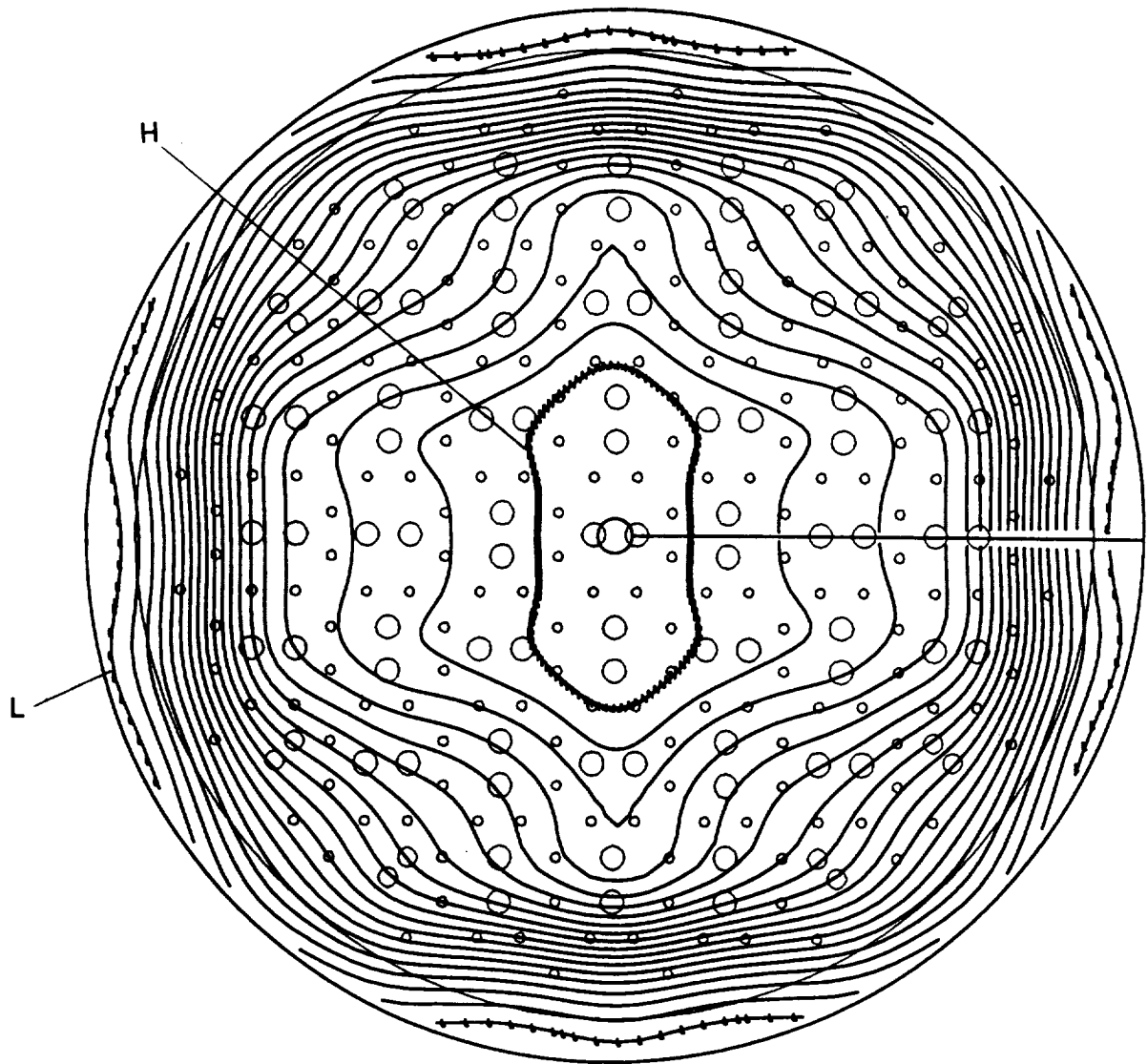


Figure 107. Mass Flux Contour of the Box-Doublet Injector

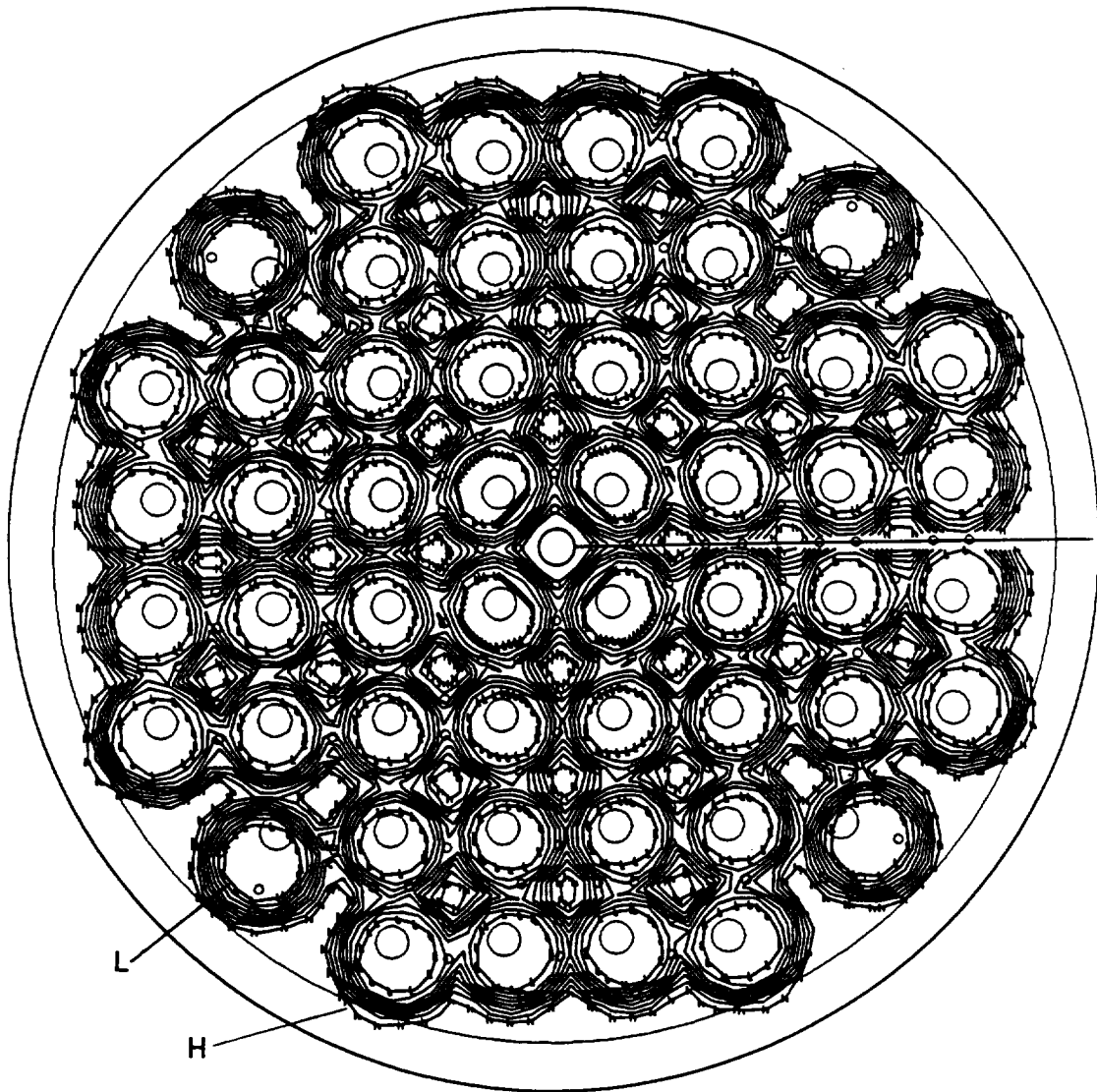


Figure 108. Normalized Fuel Fraction Contours of the LOX Showerhead Injector

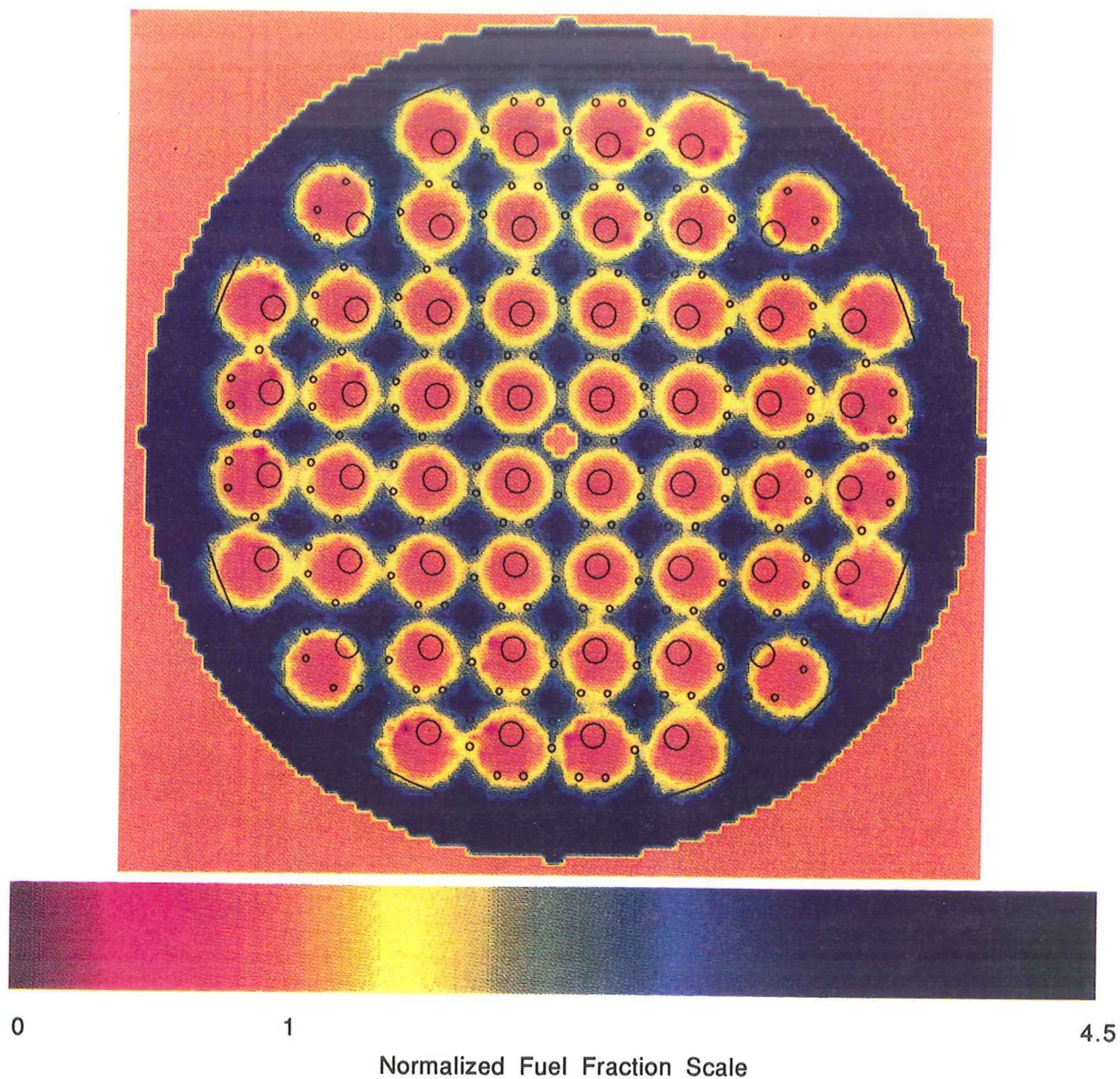


Figure 109. Normalized Fuel Fraction Plot of the
LOX Showerhead Injector

ORIGINAL PAGE IS
OF POOR QUALITY

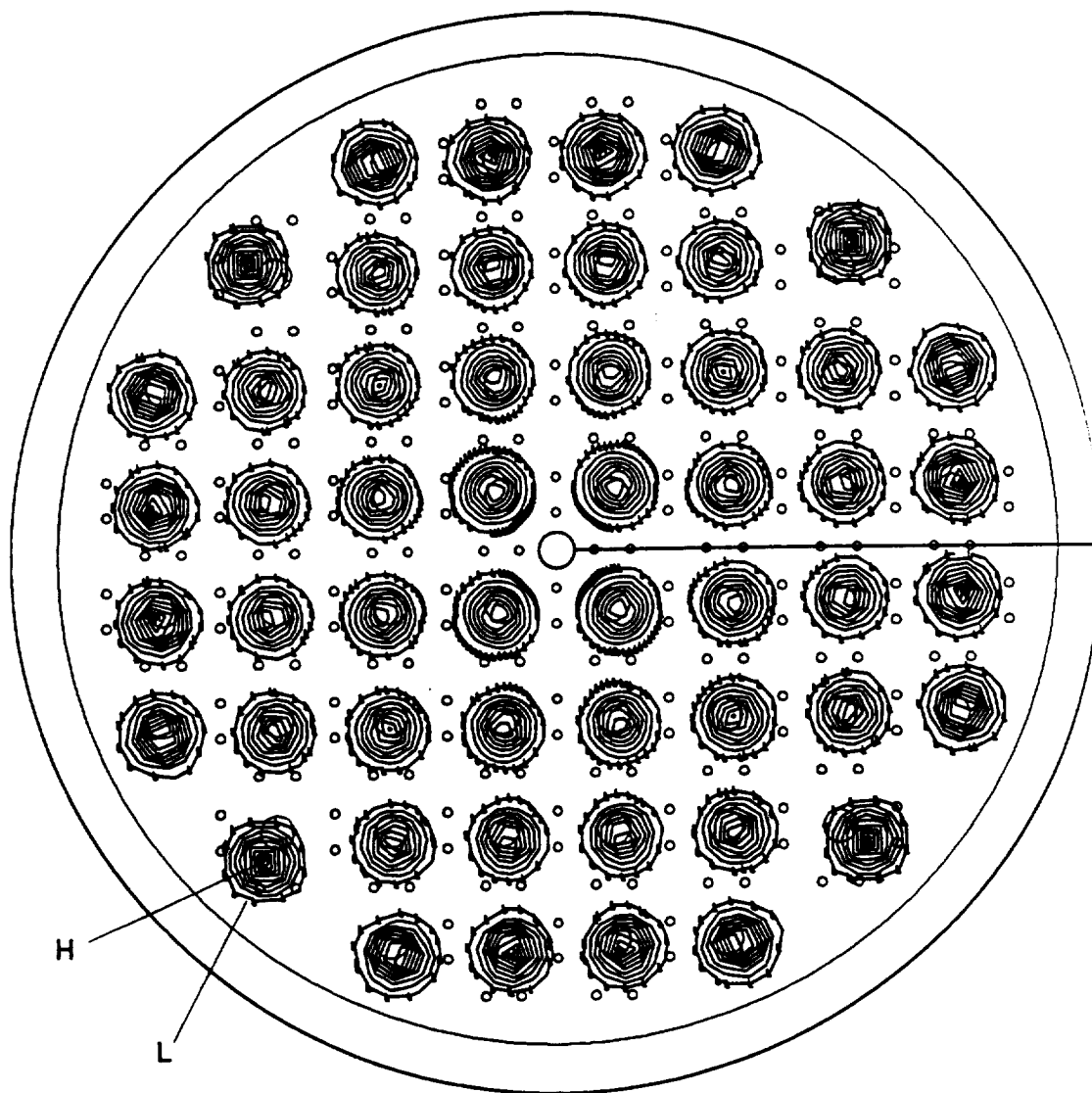


Figure 110. Mass Flux Contour of the LOX Showerhead Injector

10.2.6 INJECTOR REACTION CURVES

The reaction curves for all five candidate injectors are shown in Figure 111. The results predict that one injector, the O-F-O Triplet, has a very rapid rate of reaction, while three injectors, the Circumferential-Fan, Box-Doublet and H-1 Derivative, have moderate reaction profiles, and that the LOX Showerhead has a relatively slow rate of reaction due to the showerhead design of the LOX orifice. These results show the relative performance difference between the various injectors, and were incorporated in the stability analysis to determine the effect of the product gas generation profile on intrinsic acoustic instability.

10.3 STABILITY ANALYSIS RESULTS

The stability analyses were performed in order to evaluate the relative stability margin of each of the five candidate injectors. The predictions indicate that the combustion profile of each injector does have an effect on the chamber response. The classical non-dimensional chamber response variable, N , is defined in the following manner.

$$N = w'/p'' P_C/W_C$$

Where

- N is the chamber response
- w' is the product gas flowrate perturbation
- p' is the chamber pressure perturbation
- P_C is the steady state chamber pressure
- W_C is the steady state chamber flowrate

The value of N is typically expressed in terms of the interaction index, n , and the sensitive time lag, τ . The transformation is defined in the following manner.

$$N = n(1 - \exp(-i\omega\tau))$$

Where

- i is the square root of -1
- ω is the angular frequency

Based on n and τ values, the relative amount of chamber damping can be predicted. The combustion driving source, however, is not modeled in the technique and has classically been determined empirically.

The neutral stability map for the H-1 Derivative injector is displayed in Figure 112. This figure displays the relative damping of the chamber if a wave which neither grows nor decays were to exist in the chamber. The results are based on the time dependent solution of the linearized governing equation of motion. The time dependence is assumed to be harmonic.

$$p'(r, \theta, z, t) = p'(r, \theta, z) \exp(i\omega t)$$

Where r, θ , and z are cylindrical coordinates
 t is time

In this equation, ω is complex, which gives the following time dependence.

$$\omega = \omega \text{ (real)} + i \lambda$$

Where ω (real) is the real part of the angular frequency
 λ is the imaginary part of the angular frequency

Therefore, in these plots the value of λ is assumed to be zero. If λ is negative, the wave will predictively grow, and if λ is positive, the wave will decay with time. The results displayed in Figure 112 show the neutral stability curves for the H-1 Derivative injector for the 1L, 2L, 3L, 1T, 2T, 1R and 3T modes. The minimum interaction index values for these curves are tabulated in the table shown below (all injectors are included in this table).

Table 15. Stability Analysis Results

Mode	Minimum n values				
	H-1	O-F-O	CIRC-FAN	BOX	LOX S/H
1L	0.87	0.66	0.83	0.84	1.0
2L	1.1	0.86	1.0	1.0	2.3
3L	1.3	0.94	1.2	1.2	2.2
1T	0.77	0.85	0.81	0.79	0.84
2T	0.93	0.83	0.78	0.86	1.3
1R	1.5	0.88	1.0	0.89	1.3
3T	1.0	0.79	0.82	0.98	1.3

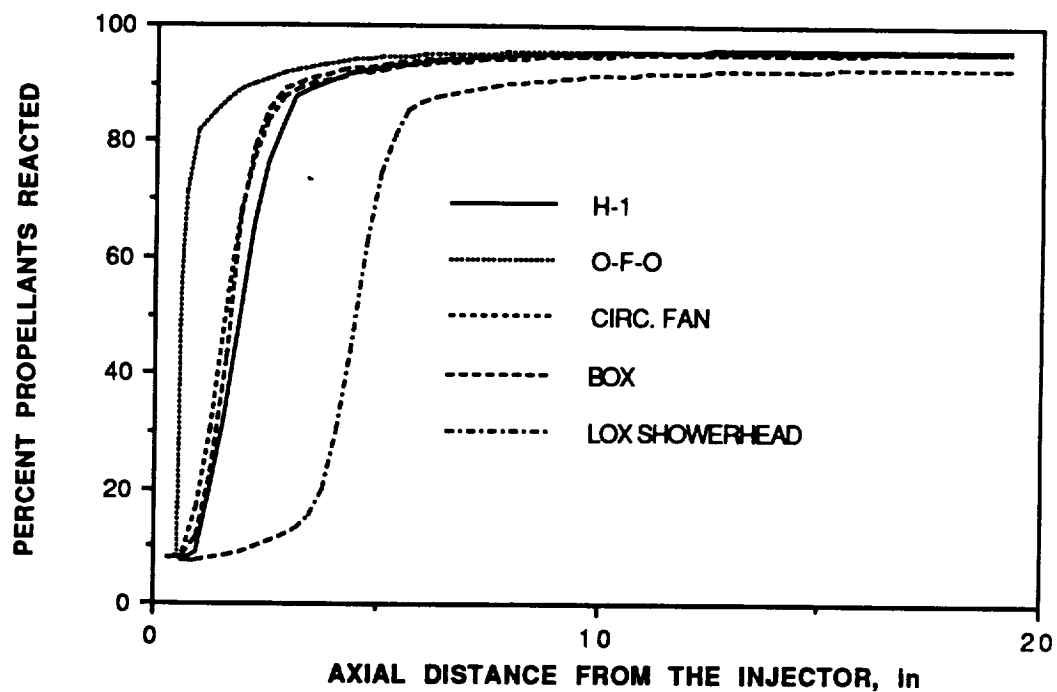


Figure 111. Propellant Reaction Profiles

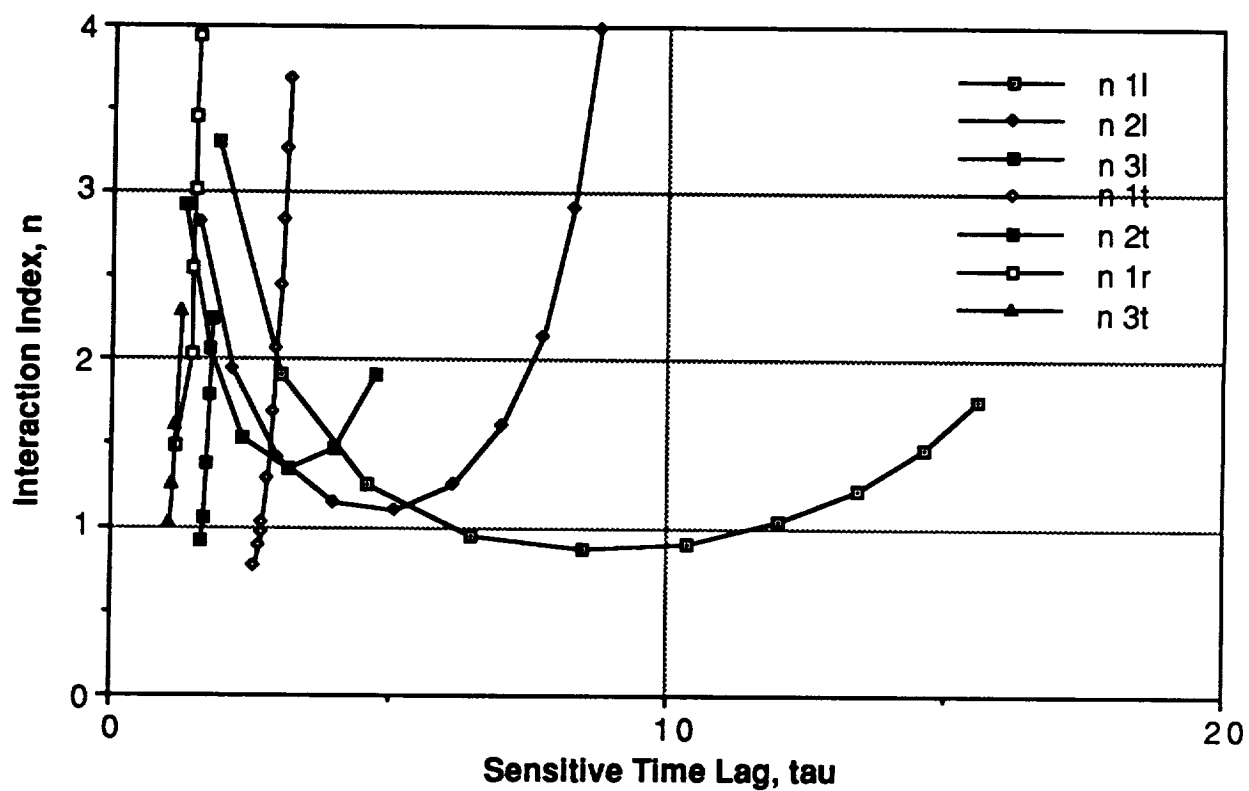


Figure 112. H-1 Derivative Injector Neutral Stability Map

Another option of the TDORC code is the ability to empirically determine the combustion response. This done by including test data in the form of ω (real) and λ as program input and calculating the n and τ values. This was done for the H-1 Derivative stability bomb tests; the n and τ values were calculated to be 0.46 and 0.37 ms, respectively. These results are plotted on the Reardon correlation, obtained from NASA SP-194, in Figures 113 and 114 for comparison. The time lag data which has been collected to date (Figure 113) shows that the original correlation of increasing time lag with decreasing orifice size for like elements to be incorrect. What the results now show is that the frequency bandwidth which can be driven with liquid-liquid, LOX/RP-1 propellants is quite large. The data in Figure 113 appears to be in two groups. Based on the data collected during this program, the group of data with larger time lag values (with respect to a given orifice diameter) appear to be longitudinal modes (H-1 Derivative stability bomb tests and O-F-O Triplet tests). The data with the lower time lag data (5.7-inch Canted-Fan tests) was the result of a transverse instability. A similar result was also presented in Figure 114. The O-F-O Triplet and H-1 Derivative interaction index values were plotted with Reardon's data. The unstable, O-F-O Triplet data seem to fall within the data scatter, while the stable, H-1 Derivative results do not.

The neutral stability maps for the O-F-O Triplet, Circumferential-Fan, Box-Doublet and the LOX Showerhead are shown in Figures 115, 116, 117 and 118. During previous tests, the O-F-O Triplet injector exhibited a first longitudinal mode of instability. The growth rate was calculated from the test data, and had a value of 174 sec^{-1} . The growth rate of the O-F-O Triplet injector was calculated from the data displayed in Figure 119. Future efforts with the O-F-O Triplet injector will have to incorporate a geometrical chamber design which is more compatible with respect to longitudinal stability.

Summarizing the stability results, the absolute values of n in Table 15 give the relative chamber response difference between the various injectors. A low minimum n value should be associated with decreasing stability margin. It should be noted, however, that part of the intrinsic acoustic stability problem is not included in the analysis. That part is the combustion response. Insufficient test data is available to predict the combustion response of the various injectors utilizing LOX/RP-1 propellants. This was evidenced during the 5.7-inch testing under this program, and one of the goals of the additional 3.5-inch testing was to generate more complete combustion response correlations with the test data.

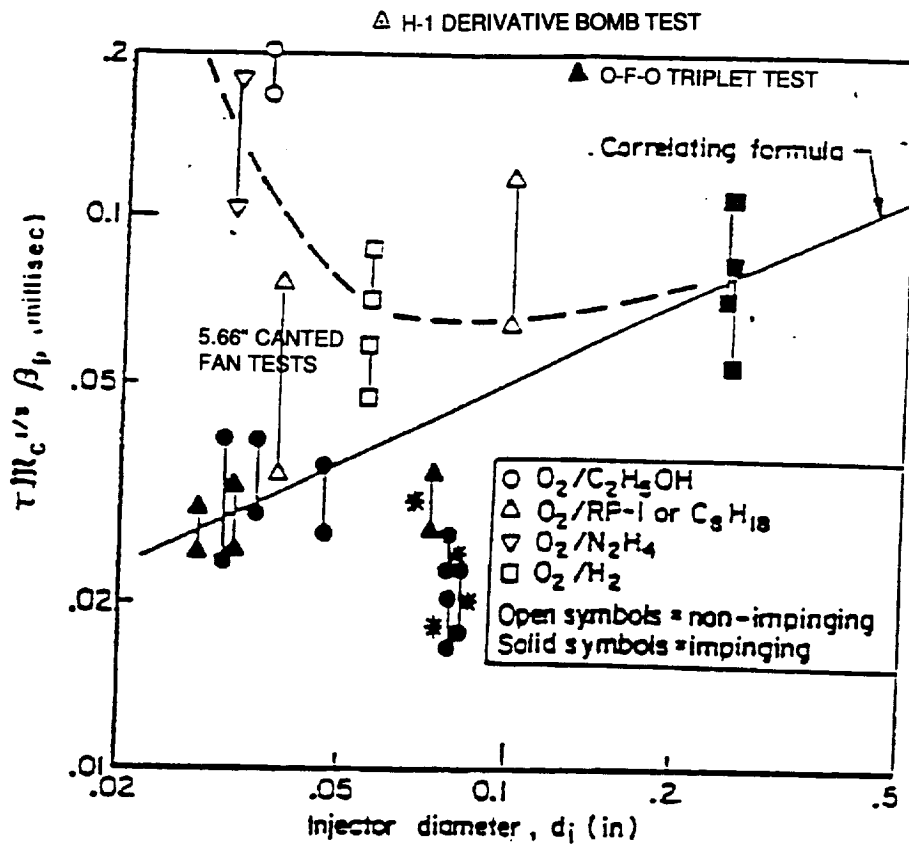


Figure 113. Sensitive Time Lag Correlation, Non-Coaxial Injectors, Non-Hypergolic Propellants

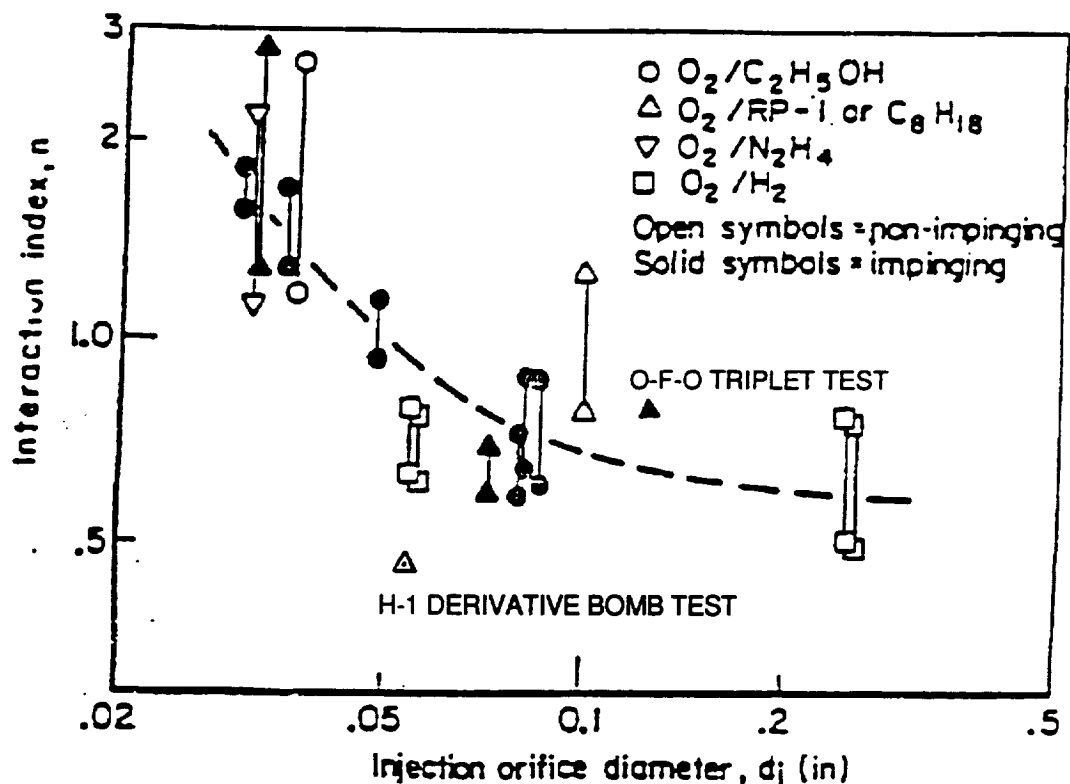


Figure 114. Pressure Interaction Index Correlation, Non-Coaxial Injectors, Non-Hypergolic Propellants

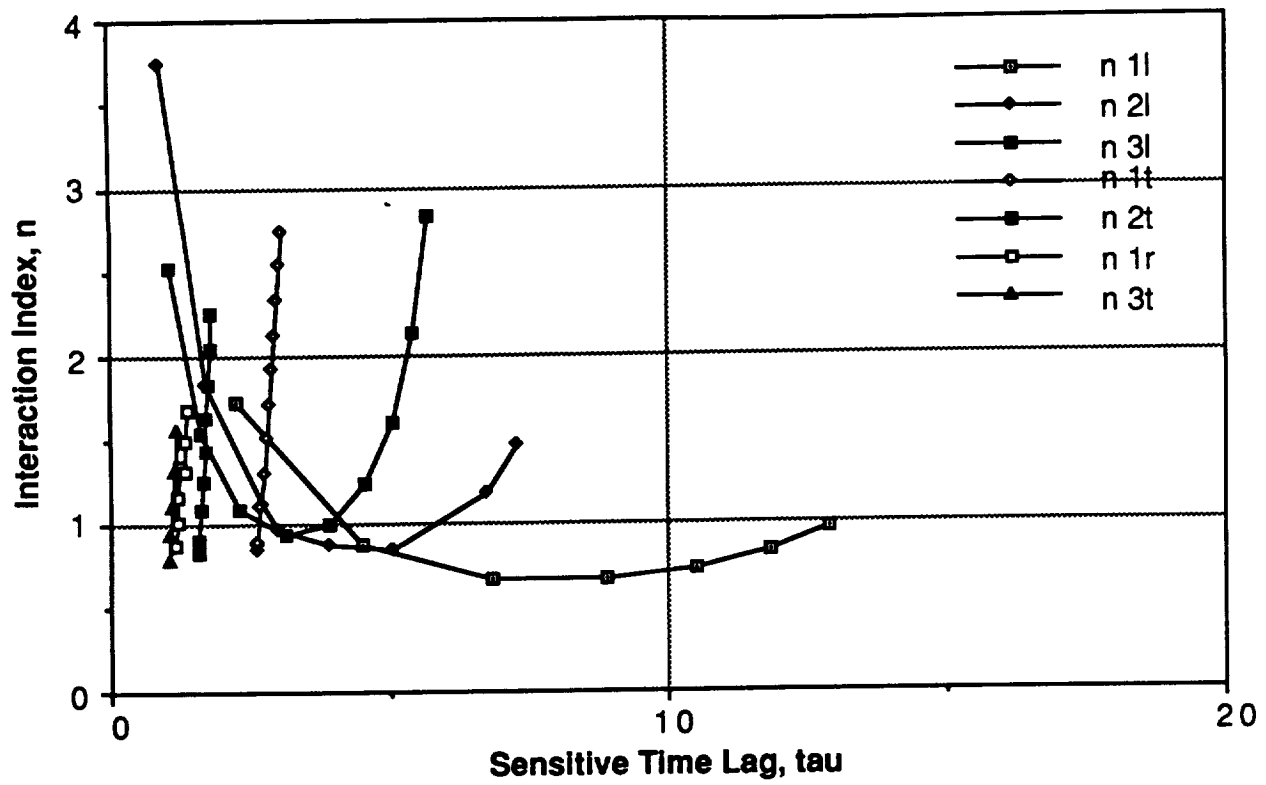


Figure 115. O-F-O Triplet Injector Neutral Stability Map

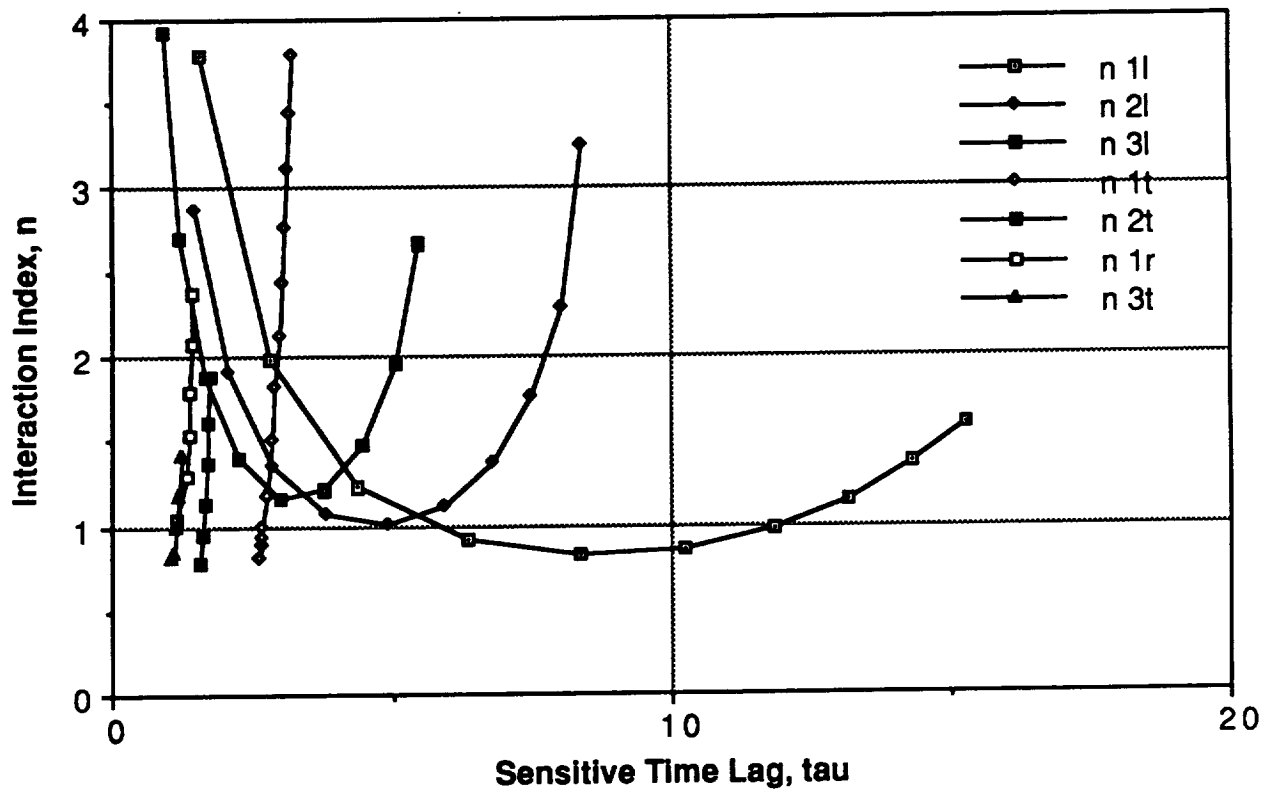


Figure 116. Circumferential-Fan Injector Neutral Stability Map

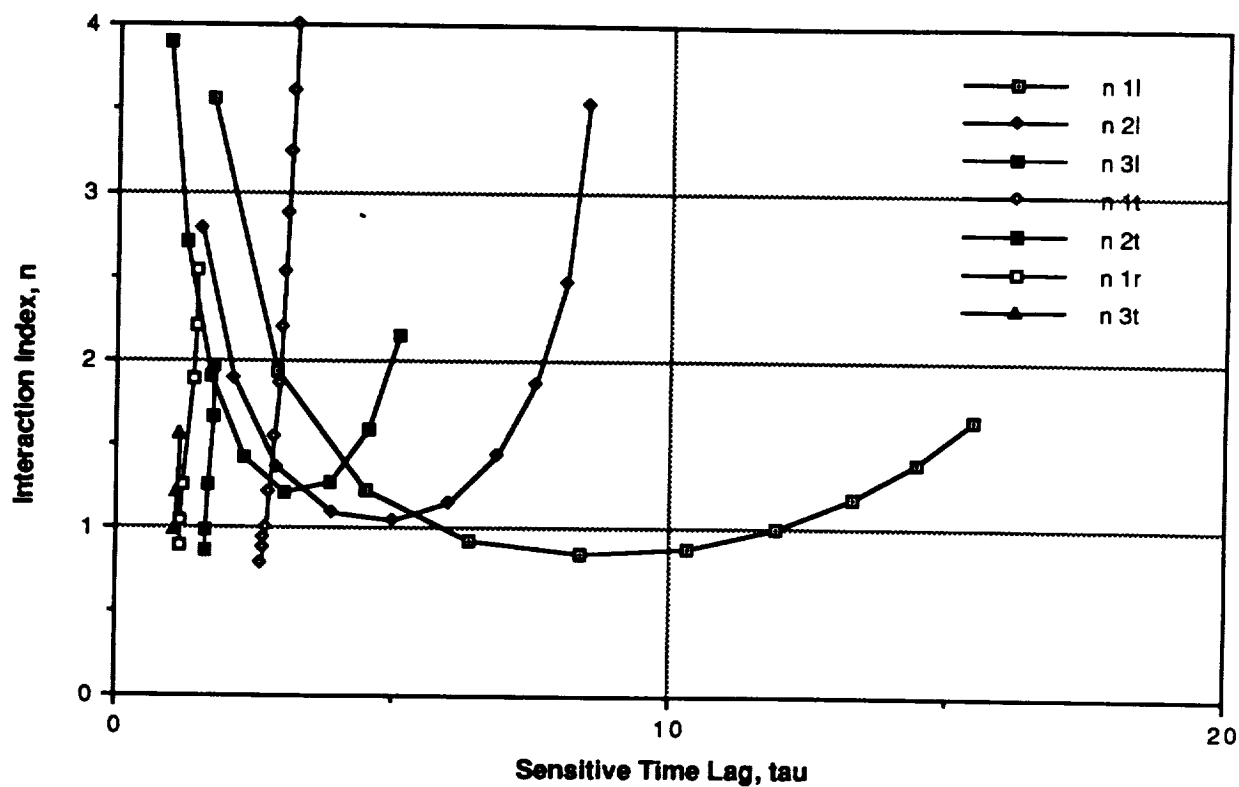


Figure 117. Box-Doublet Injector Neutral Stability Map

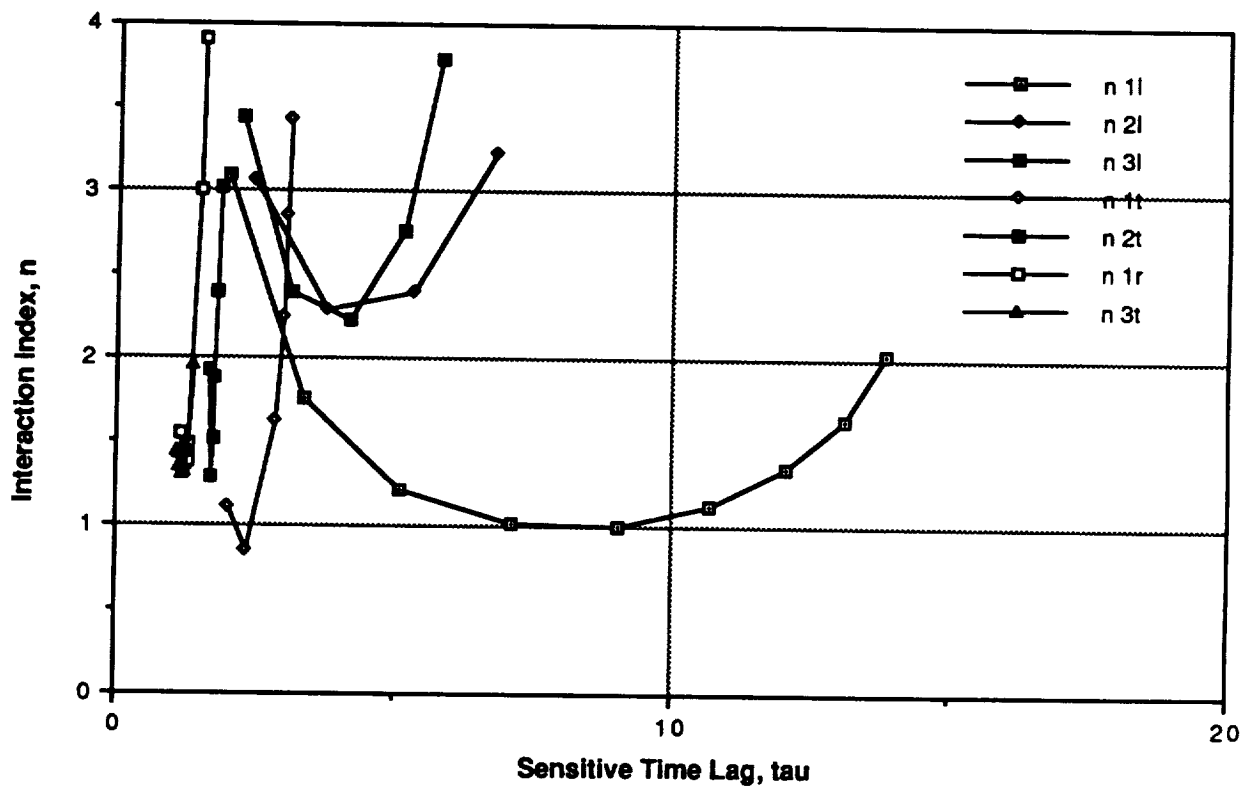


Figure 118. LOX Showerhead Injector Neutral Stability Map

An analysis was performed to determine if injector rework could be performed on the O-F-O Triplet injector to eliminate the first longitudinal mode of instability. An additional time lag analysis was performed in which the O-F-O Triplet injector was analyzed while being implemented in a 12.25-inch long combustor, and the results of the analysis are presented in Figure 120. Enumerated results of the figure are presented in the following table.

<u>Injector</u>	<u>Chamber Length</u>	<u>Minimum n Values</u>	
		<u>1L mode</u>	<u>1T mode</u>
O-F-O Triplet	19.35 inches	0.66	0.85
O-F-O Triplet	12.25 inches	0.80	0.59
H-1 Derivative	19.35 inches	0.87	0.77

Based on this chamber response analysis, the longitudinal stability margin is predicted to increase by 21% with a 7.1-inch shorter chamber. Consequently, the first tangential stability margin is predicted to decrease by 24% with the shorter chamber. The H-1 Derivative results are presented for referencing purposes since the injector has been shown to be dynamically stable without acoustic aids. Based on these results, it was recommended that the O-F-O Triplet injector be tested in a short (13.4-inch) combustion chamber during the screening tests, but with a 1T cavity included in the hardware. Furthermore, if the first longitudinal mode was eliminated by using the short chamber, screening tests without the 1T cavity were recommended.

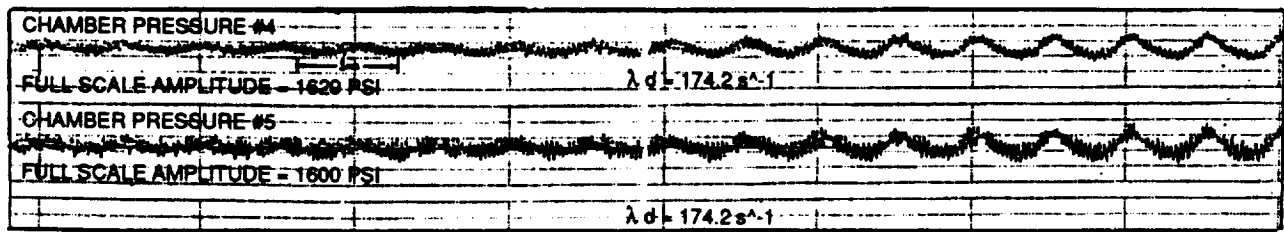


Figure 119. O-F-O Triplet Injector Test High Frequency Data

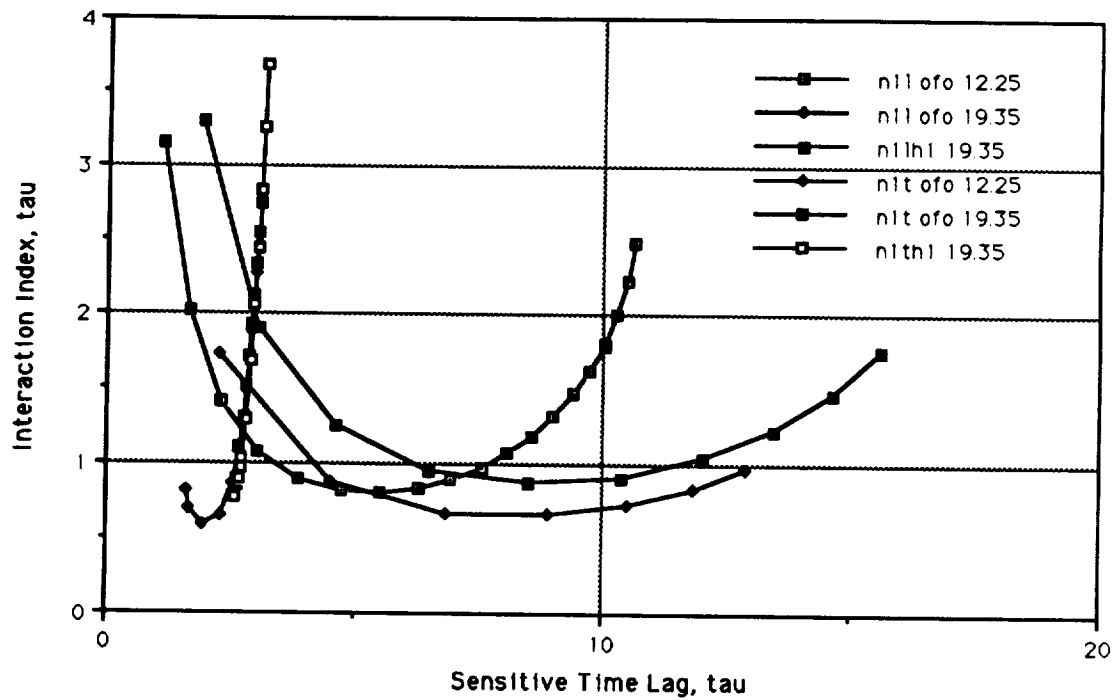


Figure 120. O-F-O Triplet Injector Longitudinal Stability Investigation Data

TASK III

11.0 TASK II TEST SUMMARY

11.1 INTRODUCTION

All of the candidate injectors that were considered for additional testing under this phase of the program had been previously tested under Task II of this contract. While the detailed results of those tests are included under previous sections of this report, a brief summary is included here for reference. Performance, heat flux and stability results are presented in Table 16. Injector orifice sizes and impingement lengths are tabulated in Table 17.

11.2 DATA SUMMARY

11.2.1 H-1 DERIVATIVE INJECTOR

The H-1 Derivative injector, shown in Figure 121, was the only 3.5-inch diameter injector that was stability bomb rated prior to this test series. It was demonstrated to be spontaneously and dynamically stable with the inclusion of 1T acoustic cavities. Its corrected c-star efficiency was 95.8%.

11.2.2 BOX-DOUBLET INJECTOR

The Box-Doublet injector, shown in Figure 122, was spontaneously stable with 1T acoustic cavities and demonstrated a corrected c-star efficiency of 94.6%.

11.2.3 CIRCUMFERENTIAL-FAN INJECTOR

The modified Circumferential-Fan injector (Figure 123) was spontaneously stable with 1T acoustic cavities, with a corrected c-star efficiency of 95.0%.

11.2.4 O-F-O TRIPLET INJECTOR

The O-F-O Triplet injector (Figure 124) spontaneously experienced a non-damaging first-longitudinal (1L) instability when tested with 1T acoustic cavities. Its corrected c-star efficiency was 93.4%.

11.2.5 LOX SHOWERHEAD INJECTOR

The LOX Showerhead injector (Figure 125), also spontaneously stable, had the lowest performance of all the 3.5-inch injectors at 90.1% corrected c-star efficiency.

Table 16. Summary of Task II 3.5-Inch Injector Tests

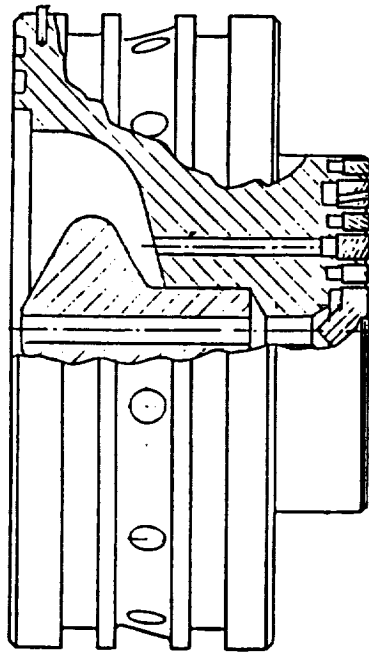
Pc = 2000 psia, MR = 2.8

Injector Pattern	C* Eff	Peak Heat Flux Btu/in ² -s	Stability (1)
H-1 Derivative	96%	64	Spontaneously stable Dynamically stable
LOX Showerhead	90%	37	Spontaneously stable
O-F-O Triplet	93%	52	Spontaneously unstable (1L instability)
Circumferential-Fan	95%	62	Spontaneously stable
Box Like-Doublet	95%	48	Spontaneously stable

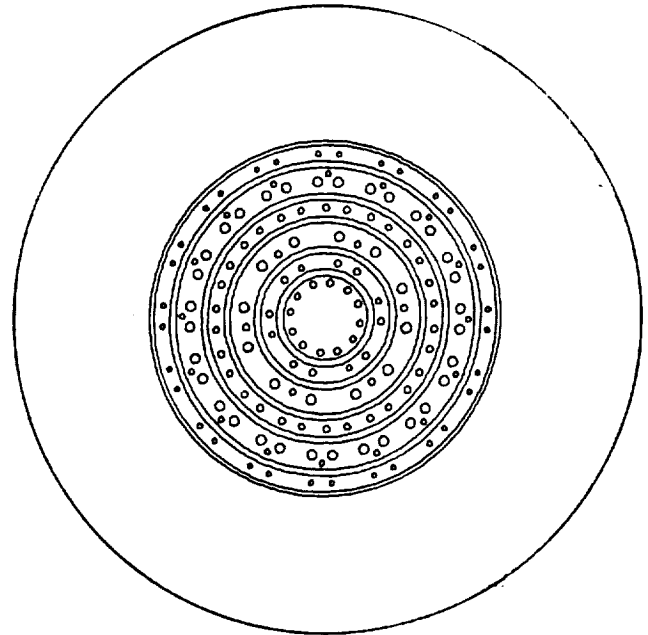
(1) All tests were performed with 1T (8000 Hz) acoustic cavities

Table 17. 3.5-Inch Injector Configurations

Injec No.	Pattern	LOX Orifices		RP-1 Orifices		Impingement Length, In	Fuel In Periphery
		No.	Diam., In	No.	Diam., In		
1	H-1 Derivative	16 18 32 12	.046 .060 .088 .090	32 42	.046 .060	0.200 to 0.480	Fuel in outer ring
2	LOX Showerhead/ RP-1 Doublets	32 20	.096 .106	208 16 8	.030 .040 .025	0.100	Yes (2%)
3	O-F-O Triplet	32	.125	16 24	.111 .026	0.350	Yes (8%)
4	Like Doublets, Circumferential Fans	120	.064	120	.042	0.125	No
5	Like Doublets, Box Pattern	74 16	.079 .064	200	.033	0.125	Yes (8%)

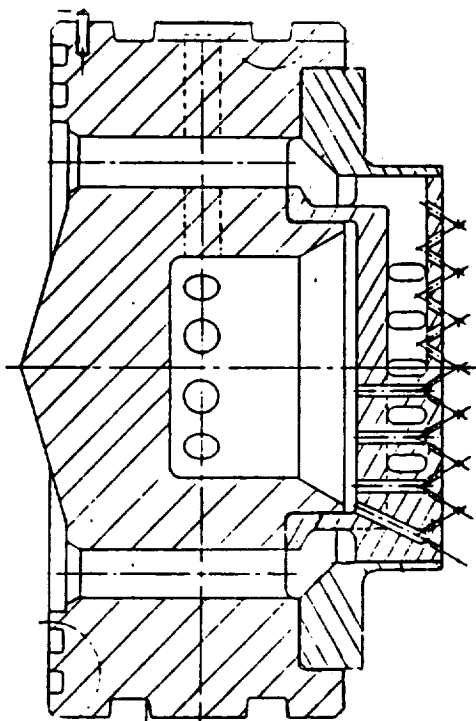


CROSS-SECTION

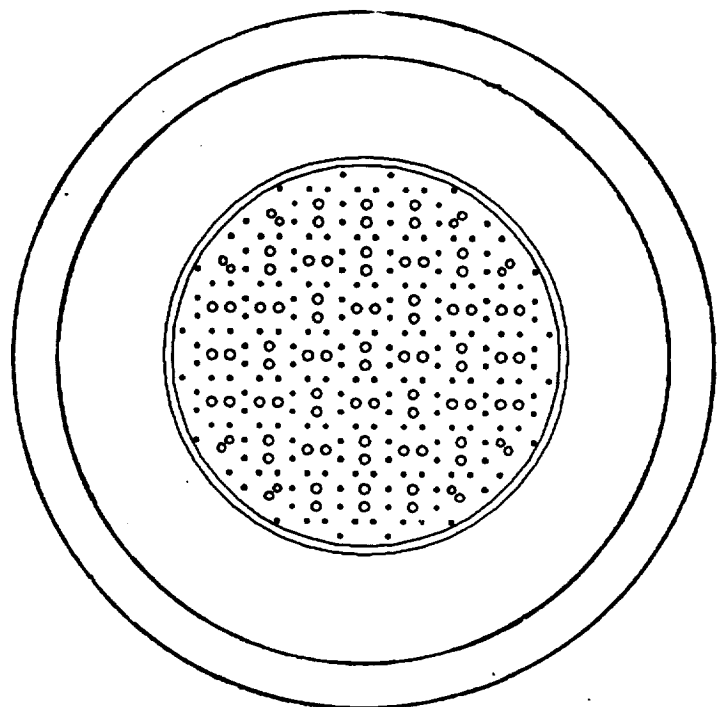


INJECTOR FACE

Figure 121. H-1 Derivative Injector Pattern and Cross-Section

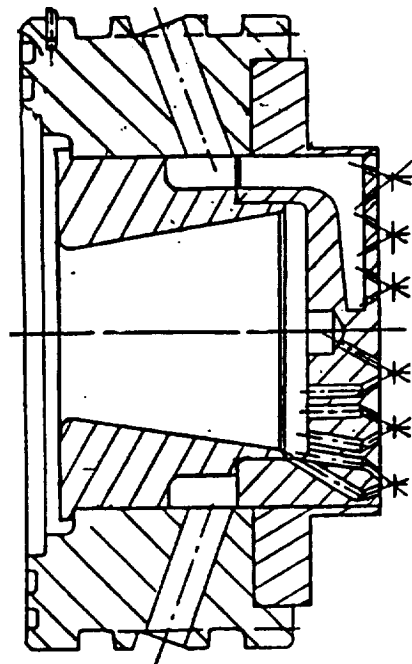


CROSS-SECTION

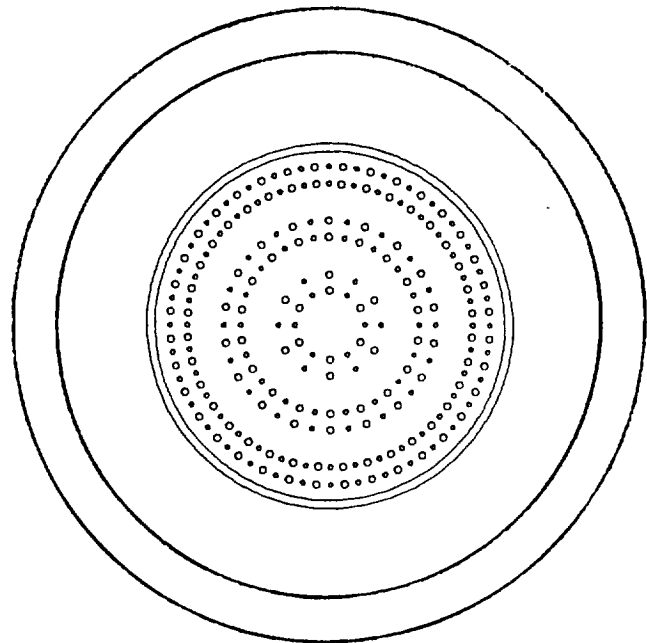


INJECTOR FACE

Figure 122. Box-Doulet Injector Pattern and Cross-Section

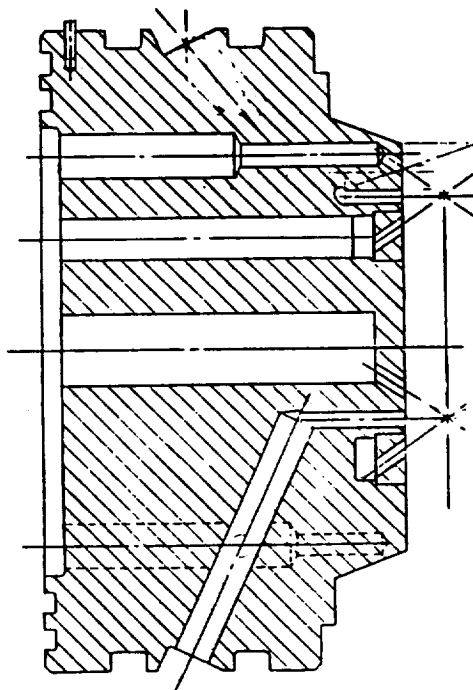


CROSS-SECTION

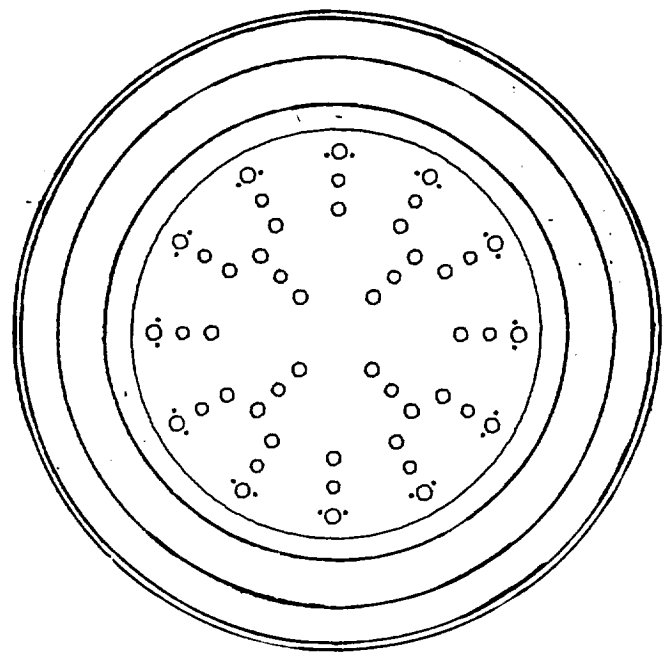


INJECTOR FACE

Figure 123. Circumferential-Fan Injector Pattern & Cross-Section

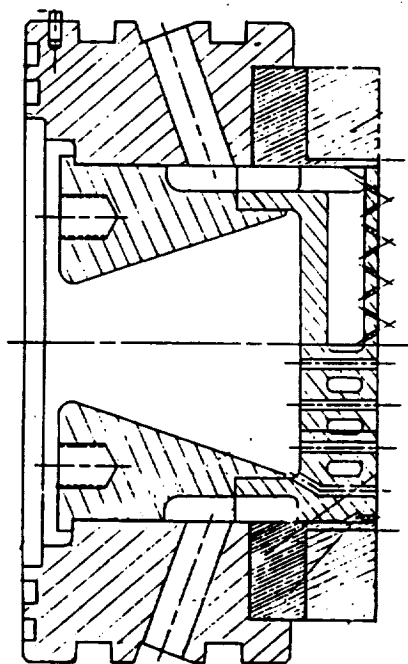


CROSS-SECTION

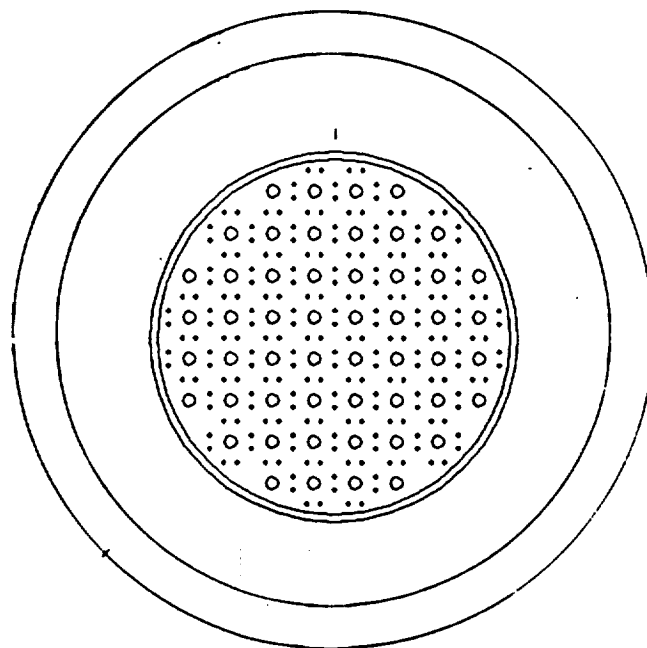


INJECTOR FACE

Figure 124. O-F-O Triplet Injector Pattern and Cross-Section



CROSS-SECTION



INJECTOR FACE

Figure 125. LOX Showerhead Injector Pattern and Cross-Section

TASK III

12.0 HOT-FIRE TEST PLANS

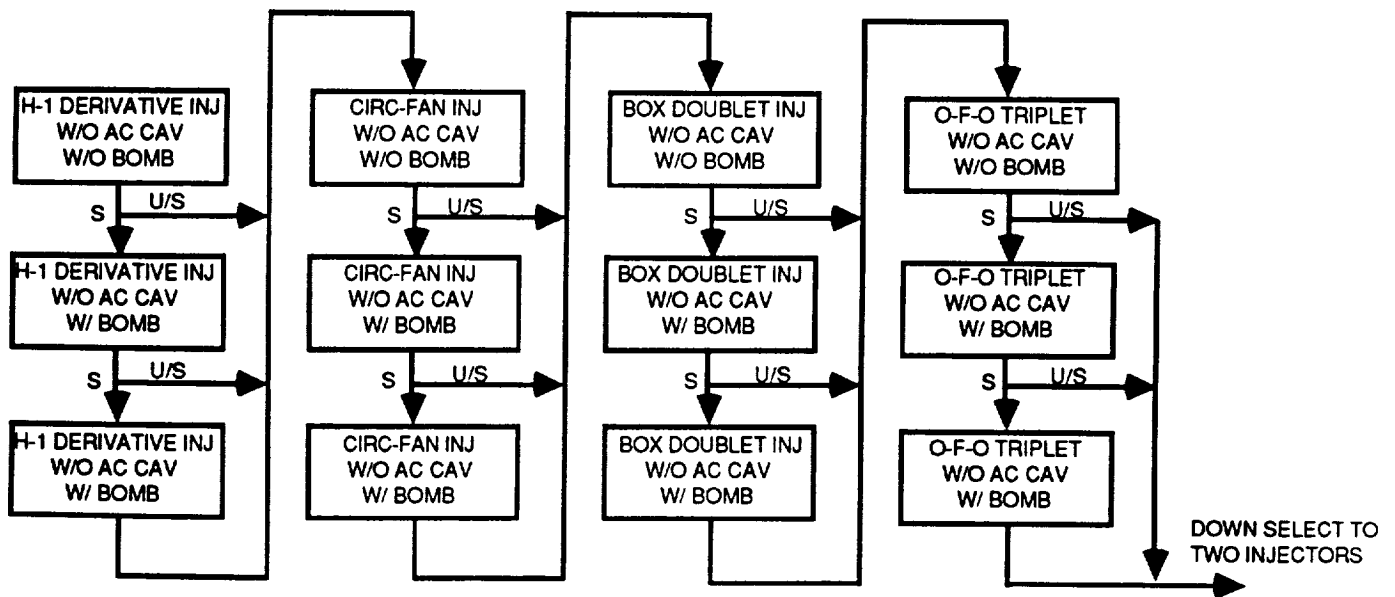
12.1 TEST HARDWARE AND FACILITY

The hot-fire testing performed in support of this phase of the program was carried out at the 3.5-inch scale. The advantage of testing at this scale was the availability of existing injectors and chamber hardware. All of the components required to perform the series of tests described in this section were previously fabricated and tested under Task II of this contract. A description of the injectors and combustor hardware is included in Section 5.0 of this report. However, several modifications were necessary. The existing bomb ring was modified for the inclusion of a third high-frequency pressure transducer in compliance with CPIA-247. In addition, during Task II testing, each of the five injectors required its own water cooled acoustic cavity ring configuration during Task II testing. This arrangement was very inflexible for making changes. Modifications to the cavities (open area changes, retuning, etc.) would have been time consuming and costly with this system. Therefore, one of the existing blank cavity rings was modified to be compatible with all of the 3.5-inch diameter injector configurations, and to accept OFHC copper inserts which made up the actual cavities. The inserts were fabricated inexpensively with a short lead time. This configuration allowed acoustic cavities to be replaced quickly and easily.

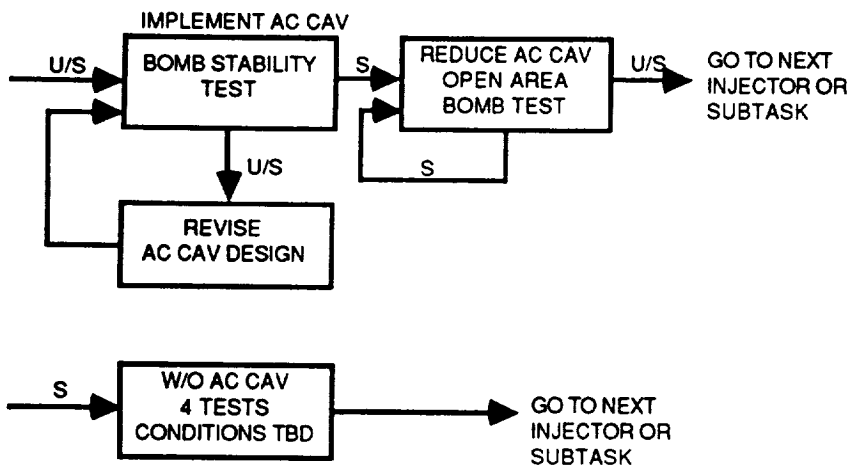
Testing was conducted at the same facility as the previous hot-fire testing performed under this contract, described in Section 5.0 of this report. No modifications to the test stand were necessary.

12.2 TEST LOGIC

The initial test logic under which this phase of the testing effort was begun is shown in Figure 126. The testing was broken down into four separate series. The first of these, the Screening Test series (Task IIIB), involved the testing of four different injector patterns; H-1 Derivative, Box-Doublet, Circumferential-Fan and O-F-O Triplet. The only 3.5-inch diameter injector that was excluded from additional testing under Task III was the LOX Showerhead. With its low c-star performance of 90%, it was not considered to be a good candidate for performance or stability investigations. Under the Screening Test series, each of the four candidate injectors could have been included in a maximum number of three hot-



TASK IIIB - SCREENING TESTS



TASK IIIC STABILITY EVALUATION

REDUCE CHAMBER LENGTH

INJECTOR 1
5 SEC PERF TEST
3 TESTS

INJECTOR 2
5 SEC PERF TEST
3 TESTS

GO TO TASK IIIE

TASK IIID - PERFORMANCE EVALUATION (OPTIONAL)

DOWN SELECT TO FINAL
INJECTOR CONFIGURATION

CONDITIONS TBD
10 TESTS

TASK IIIE - FINAL DOWN SELECT

Figure 126. Task III Test Logic

fire tests, all at 2000 mainstage chamber pressure and 2.8 mixture ratio. No acoustic aids were to have been utilized. The objective of the first test with each injector was to evaluate the spontaneous stability characteristics of that pattern, and to verify the performance. If this test was spontaneously stable, i.e. a combustion instability did not self-induce, then a test would be conducted with the inclusion of a stability rating bomb in order to evaluate the dynamic stability characteristics of the injector. If the combustion process recovered from the bomb induced overpressure, then a repeat bomb stability test would have been conducted at identical conditions for redundancy. If, at any time during this test series, an instability should occur, the plan was to discontinue testing with that injector and progress to the next pattern.

A down-selection of injectors was planned after completion of the Screening Test series. It was anticipated that two injectors might be chosen for additional testing. The first injector, stable with high performance, would be a candidate for the Isolated Combustion Compartment (ICC) concept in accordance with the original program objectives. Secondly, it was hoped that at least one unstable configuration would be identified that could be utilized for continued stability testing. This would meet the revised program objectives of increasing the generic technology base with LOX/RP-1 and improve predictive analytical techniques.

The second series of tests shown in the test logic were identified as the Stability Evaluation tests, Task IIIC. Under this subtask, it was envisioned that the unstable injector configuration would be tested with various acoustic cavity open areas in an attempt to determine the stability limits of that injector, and with subsequent correlations, improve on the existing acoustic cavity design methodology. The stable ICC candidate injector would also be tested during this series to better verify its stability characteristics.

The third test series, Performance Evaluation (Task IIID), was included to determine the effects of chamber length on performance. The 3.5-inch diameter hardware configuration used in all testing up to this point consisted of individual components bolted together to make up an injector-to-chamber length of 19.4-inches. By removing one of the chamber components, it was possible to test with a 6-inch shorter chamber and evaluate the change in performance. This information would then be compared with analytically derived predictions of vaporization vs. chamber length. Anchoring of performance computer codes could be performed, as necessary.

Finally, based on the results of Subtasks IIIB, IIIC and IIID, a final down-selection of injector patterns, including appropriate testing, was planned.

It should be noted here that the wording in the contract Statement of Work was such that the actual test plans were flexible and deliberately vague. Depending on the results of preceding tests, various courses of action could, with MSFC approval, be followed. What is presented here as the original test logic is based on anticipated test results. In fact, as will be discussed in the following sections of this report, several modifications to this plan were made.

TASK III

13.0 3.5-INCH INJECTOR SCREENING TEST SERIES

13.1 INTRODUCTION

Of the five candidate 3.5-inch diameter injectors, the only injector that had previously been stability bomb tested (with 1T acoustic cavities) was the H-1 Derivative. In these tests, the bomb induced overpressure damped out at a decay rate of 447 sec^{-1} in the first longitudinal mode (1226 Hz). CPIA-247 requires that a disturbance of this size damp within $1250/f^{0.5}$ (f =frequency) milliseconds for dynamic stability to be claimed. This corresponds to a minimum decay rate of 19.4 sec^{-1} at 1226 Hz. The 447 sec^{-1} observed during the bomb test is considerably better than this. The high-frequency chamber pressure response is presented in Figure 127. Based on this data, and the high measured c-star performance (96%), the H-1 Derivative injector was considered to be the most desirable injector with which to begin the screening test series.

13.2 H-1 DERIVATIVE INJECTOR

13.2.1 TEST 015-010

Three tests were planned for the H-1 Derivative injector, per the test matrix, Figure 126, without acoustic cavities. The first test (015-010) was performed without a stability bomb in order to evaluate the spontaneous stability characteristics of this injector without acoustic aids. The sequenced duration was obtained (approximately 1.2 seconds of mainstage combustion) at a nozzle stagnation pressure of 2021 psia and 2.8 mixture ratio. A plot of the injector end chamber pressure is presented in Figure 128. The c-star efficiency, corrected for heat loss to the chamber walls, was 96.7%. The time span over which performance was averaged is indicated in Figure 128. No high amplitude oscillations were observed from the high frequency pressure transducer data. A bomb mock-up had been installed in the uncooled bomb spool downstream of the injector face in order to plug the opening where a stability bomb is normally installed. A post-test hardware inspection revealed that significant erosion had occurred in the bomb spool and the copper blank acoustic cavity immediately upstream of the bomb mock-up (which was still intact). The hardware damage was not so severe as to preclude further testing, and it was felt that the probability of additional erosion was low due to the fact that the next test would be of shorter

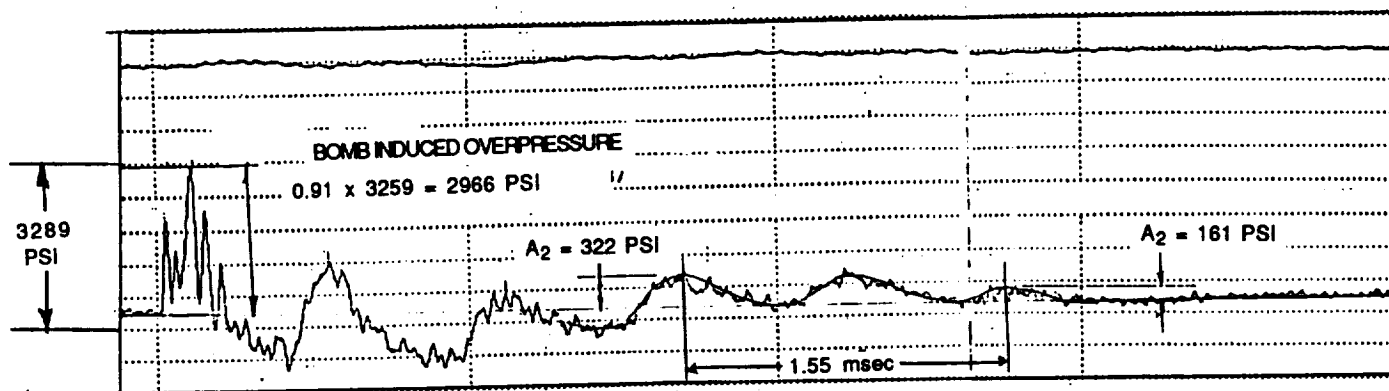
duration and would not have a similar protrusion into the combustion chamber throughout the entire test.

13.2.2 TEST 015-011

Therefore, a second test, Test 015-011, was conducted. The duration was approximately 0.8 second of mainstage combustion (2001 psia nozzle stagnation pressure) and a 2-grain bomb was detonated to evaluate the dynamic stability of the H-1 Derivative injector without acoustic aids. The high frequency data indicated that the bomb detonated prematurely during the start transient at about 1420 psia and that the overpressure (~500 psi) damped out in 5 to 6 msec. A plot of the injector end chamber pressure is shown in Figure 129. Corrected c-star efficiency was 96.7%. The high frequency chamber pressure trace is presented in Figure 130. The decay rate of the bomb overpressure damping was calculated to be 482 sec^{-1} , which agrees closely with the bomb test overpressure decay rate of 447 sec^{-1} calculated from the previous testing of this injector.

All tests up to this point indicate that the H-1 Derivative injector is spontaneously and dynamically stable without the benefit of acoustic aids. It should be noted, however, that no dynamic stability test has been conducted with this injector and without acoustic cavities at mainstage P_c (2000 psia). Per the current test logic plan, additional bomb testing with this injector would have normally been conducted. However, it was believed that sufficient data existed to characterize the H-1 Derivative injector and further testing with this injector was not performed during the screening test series. Instead, screening tests were performed on the remainder of the 3.5-inch diameter injectors as laid out in the test logic, starting with the Circumferential-Fan injector.

The bomb spool hot gas wall erosion incurred during the tests was repaired by OFHC copper welding and hand blending.



In the classical linearized theory, a harmonic time dependence of $e^{i\omega\tau}$ is assumed. In this equation, ω is complex and can be written in the following form:

$$\omega = \omega_r + \lambda i$$

The time dependence then becomes

$$P(x,y,z,t) = P(x,y,z) \frac{e^{i\omega_r\tau}}{e^{\lambda\tau}}$$

Writing this in terms of the test data,

$$\frac{A_1}{A_2} = \frac{e^{\lambda\tau_2}}{e^{\lambda\tau_1}} \quad \text{or} \quad \lambda = \frac{\ln \left(\frac{A_1}{A_2} \right)}{(\tau_2 - \tau_1)}$$

$$\lambda = \frac{\ln \left(\frac{322}{161} \right)}{1.55 \times 10^{-3} \text{ sec}} = 447 \text{ sec}^{-1}$$

Figure 127. H-1 Derivative Injector Bomb Test Data

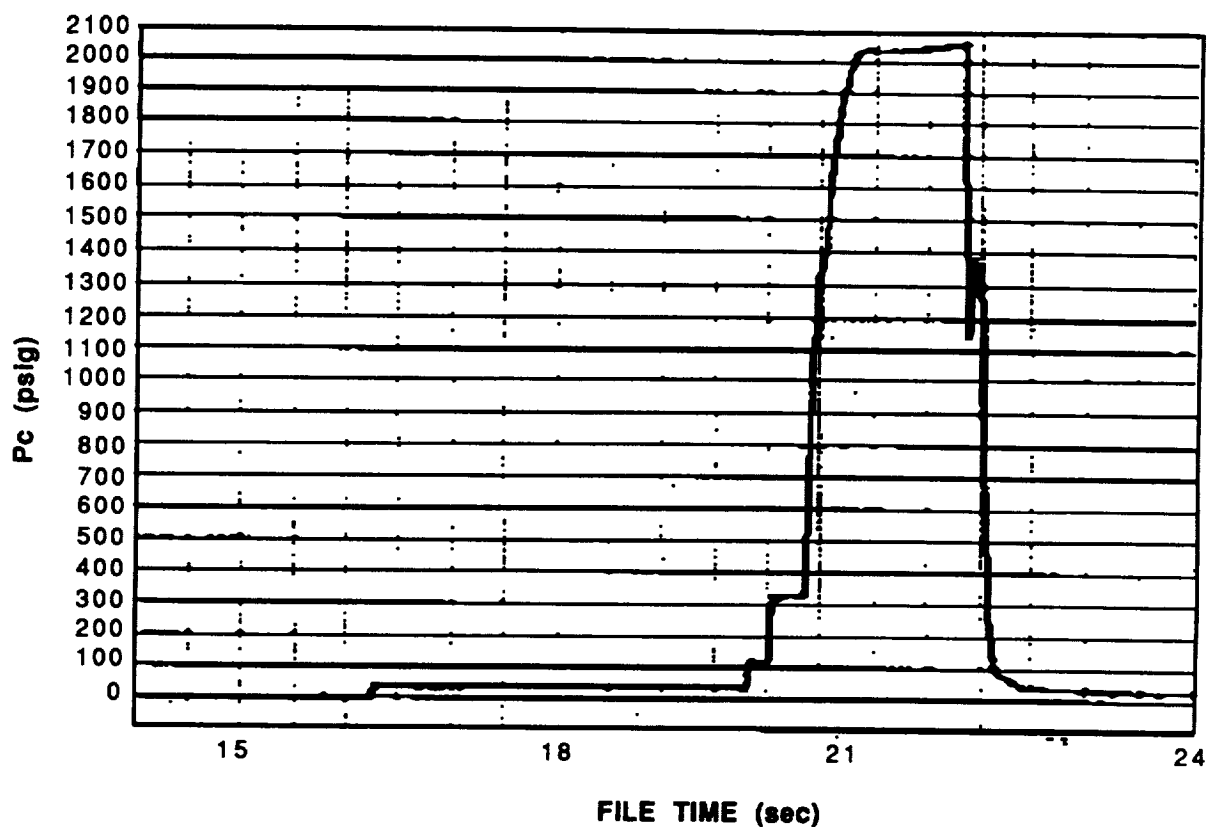


Figure 128. Static Chamber Pressure (Inj. End), Test 015-010, H-1 Derivative Injector

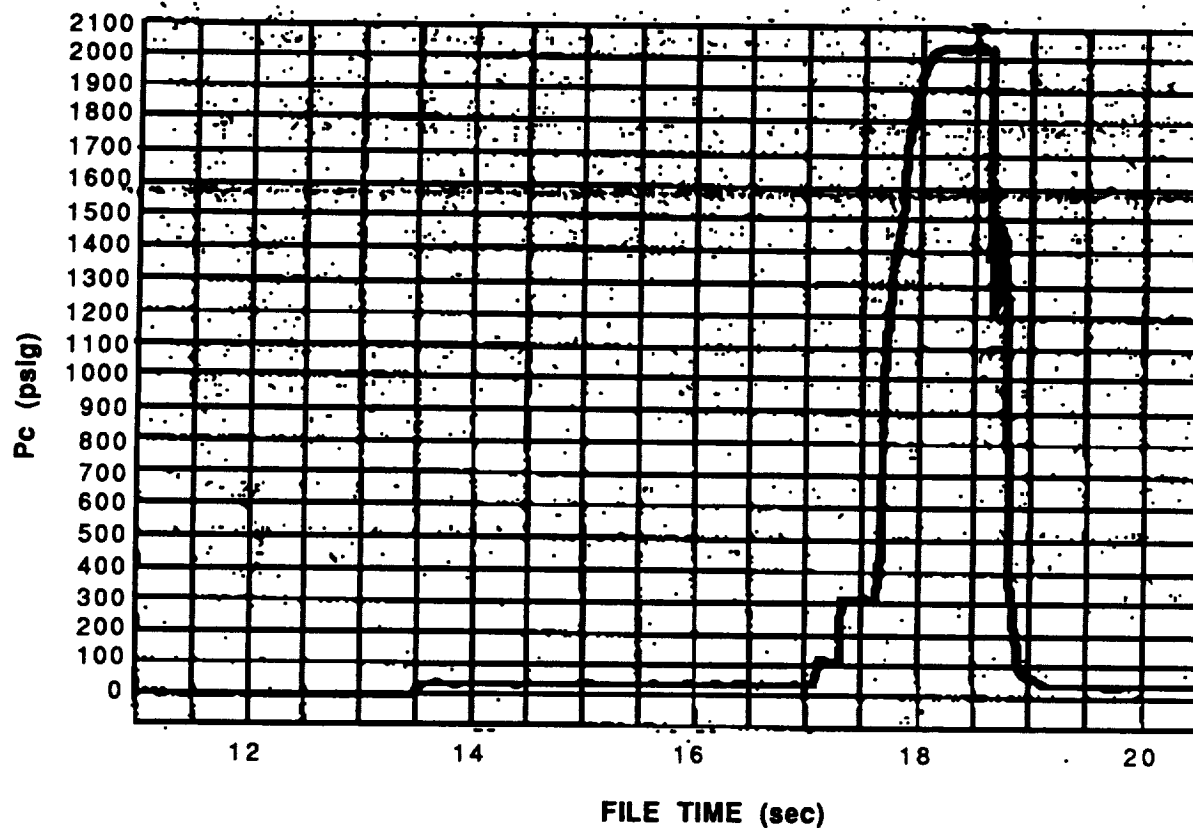


Figure 129. Static Chamber Pressure (Inj. End), Test 015-011, H-1 Derivative Injector

13.3 CIRCUMFERENTIAL-FAN INJECTOR

13.3.1 TEST 015-012

The first test which was conducted with the Circumferential-Fan injector, Test 015-012, was without acoustic cavities at a nominal chamber pressure of 1966 psia (nozzle stagnation) and a 2.77 mixture ratio. The injector end chamber pressure is shown in Figure 131. The corrected c-star efficiency was 94.0%. The purpose of this test was to determine the spontaneous stability characteristics of the Circumferential-Fan injector pattern without acoustic aids. The sequenced duration was obtained (approximately 0.5-sec. of mainstage combustion). No high amplitude organized pressure disturbances were measured during the test and the hardware showed no signs of erosion or other damage. High frequency data from this test is presented in Figure 132 in the form of two chamber pressure traces, a LOX manifold pressure trace, a fuel manifold pressure trace and three accelerometer traces. The full scale sensitivity is shown on the results. With the exception of a few anomalous spikes in the axial accelerometer and a 60 Hz electrical disturbance in the tangential accelerometer, the results show that the instrumentation was in working order and that the test was stable. It should be noted that for this injector, nominal acceleration levels are on the order of 80-100 g's and nominal peak-to-peak pressure fluctuations in the combustor are approximately 115 psi. The 5% white noise level of the chamber pressure is fairly common with all of the 3.5 inch LOX/RP-1 injectors. The pressure fluctuations in the oxidizer manifold are quite large and organized. These oscillations are due to the manifold design and the location of the high frequency pressure transducers. At cut-off, an oscillation is visible in the LOX manifold, chamber pressure and accelerometers. The disturbance is thought to be a chug due to the hydraulic resonance within the LOX dome. The frequency of the oscillation is approximately 1250 Hz. The 1250 Hz oscillation during cut-off is characteristic of all of the LOX/RP-1 injectors tested to date with varying duration and amplitude.

13.3.2 TEST 015-013

The next test performed, Test 015-013, included the detonation of a 2-grain stability bomb in order to evaluate the dynamic stability characteristics of this injector without acoustic aids. The target test conditions and duration were the same as Test 015-012. The mainstage nominal operating conditions of this test included a chamber pressure of 2017 psia and a mixture ratio of 2.77. During the test, the bomb center, composed of an epoxy mixture,

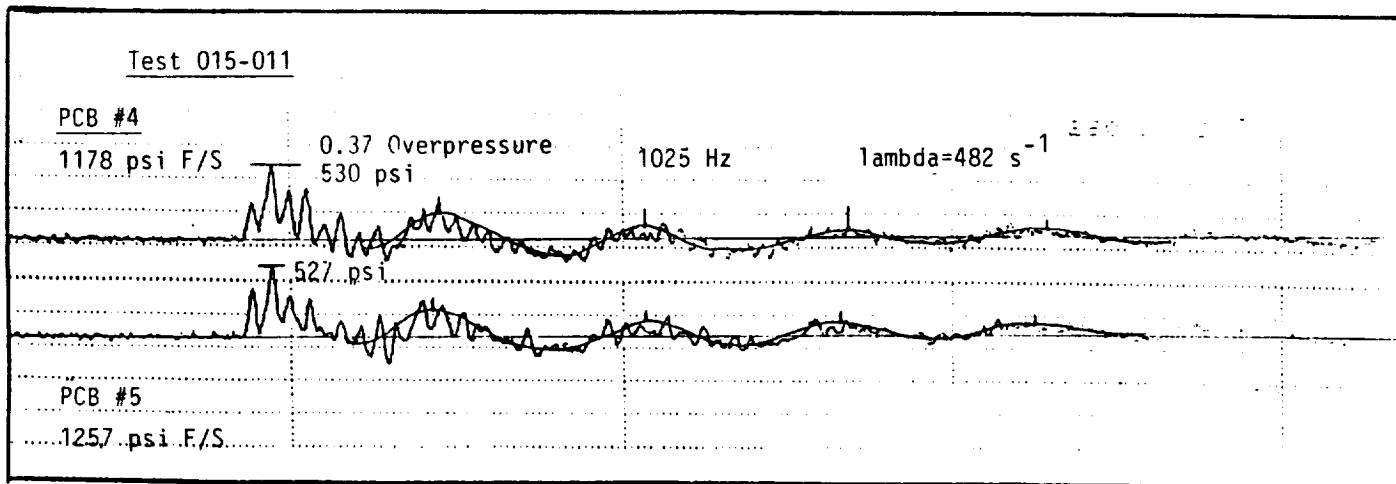


Figure 130. Test 015-011 High Frequency Data

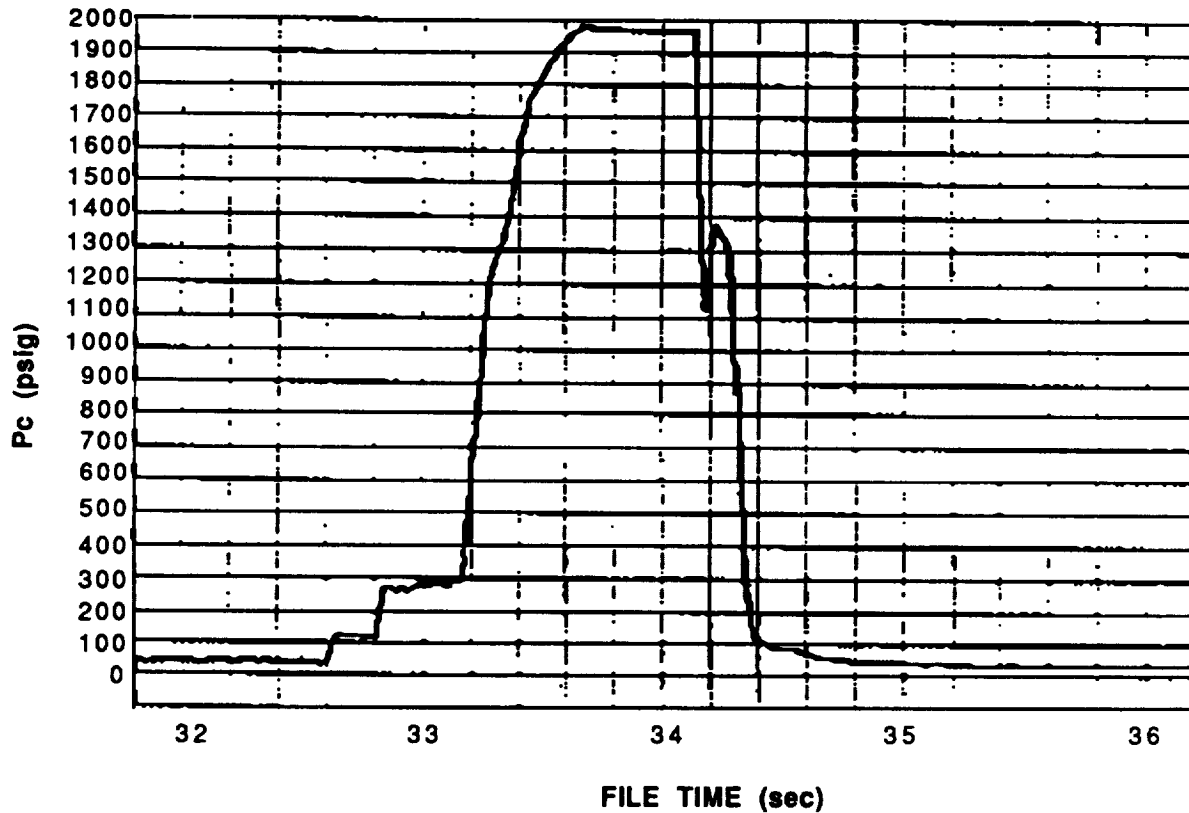


Figure 131. Static Chamber Pressure (Inj. End), Test 015-012, Circumferential-Fan Injector

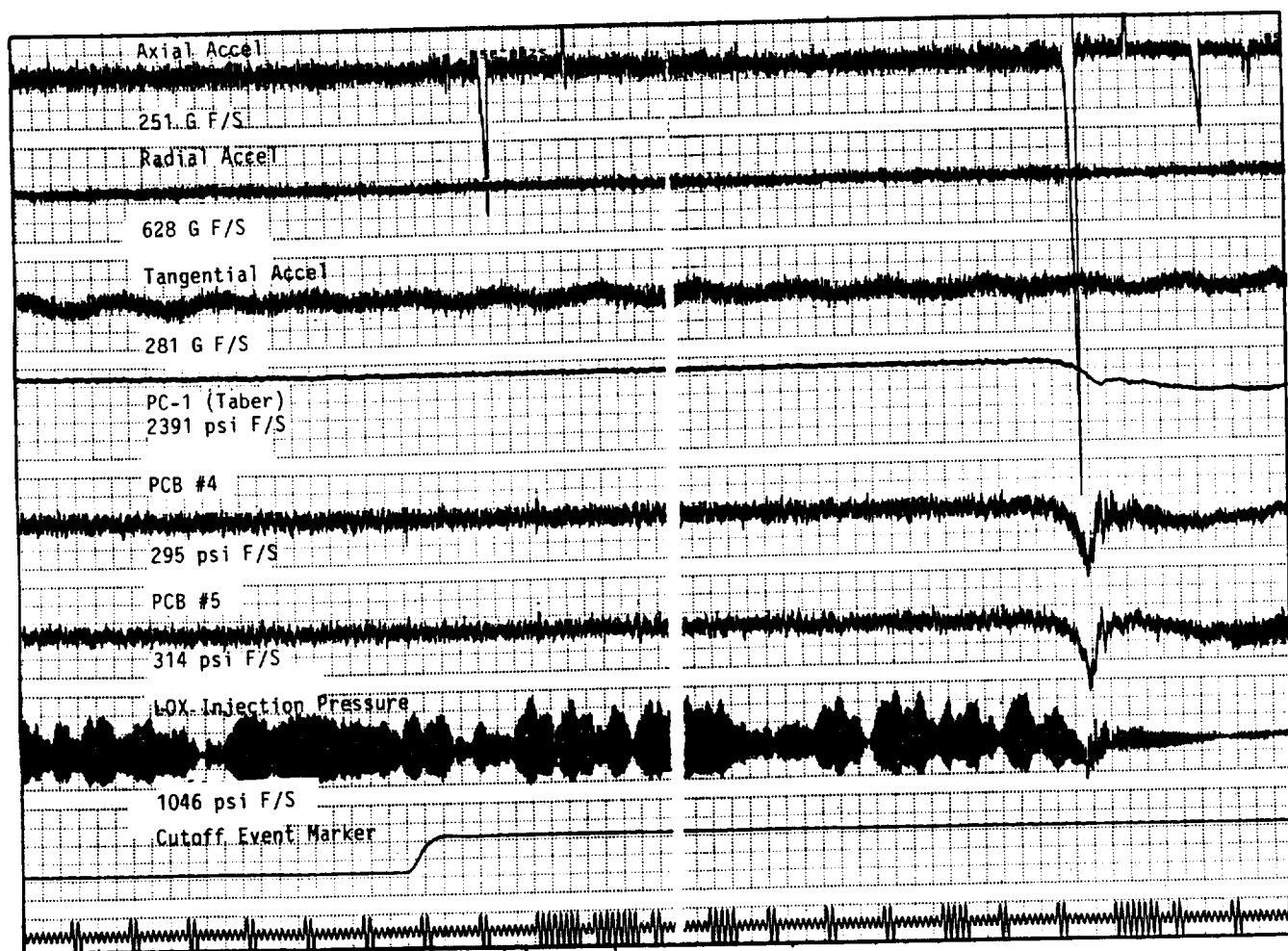


Figure 132. Test 015-012 High Frequency Data

burned through to atmosphere, resulting in a hot gas leak 1-inch downstream of the injector face. At about the same time, high pressure disturbances on the order of 400 to 1000 psi peak-to-peak developed in the chamber at a frequency of 7500 Hz. Later in the test, the amplitude of the chamber pressure oscillations increased to about 9300 psi peak-to-peak. Based on the fact that a substantial hot gas leak was present, however, it was inconclusive from this test whether this injector configuration was dynamically stable or unstable. A plot of the injector end chamber pressure is shown in Figure 133. Corrected c-star efficiency was 97.0%. This is considerably higher than that measured in previous tests. It is theorized that this increase is due to the presence of a transverse instability. The high frequency data of this test is shown in Figures 134, 135 and 136. Figure 134 displays two chamber pressure traces, three accelerometer traces and the LOX manifold pressure traces at the onset of wave motion. The activity during the sustained wave motion is displayed in Figure 135 which contains the same parameters as Figure 134.

Substantial erosion was sustained in the bomb spool around the bomb port, the hot gas wall at the first water channel in the first calorimeter chamber section burned through locally in line with the bomb port and the injector face showed some minor erosion. Several actions were taken to resolve the damaged hardware. The bomb spool was repaired by reaming out an oversized hole at the bomb port location and welding a copper insert with the proper inside diameter. The calorimeter section was replaced with an identical spare chamber. The injector was cold flowed with water and it was determined that the flow pattern had not been disrupted by the erosion. A zirconium-oxide coating was applied to the center of the injector (where the erosion occurred) to act as a thermal barrier.

13.3.3 TEST 015-016

Two more tests utilizing the Circumferential-Fan injector were conducted and were dynamic stability rating tests, incorporating the use of 2 grain bombs. In Test 015-016, it appeared that the bomb either prematurely detonated or burned at relatively low chamber pressure. The high frequency data from test 015-016 is presented in Figure 137. Two large spikes in the traces, which can be seen in all high frequency chamber transducer measurements and in the tangential accelerometer measurement, approximately coincide with the time of the perturbation noted in the high speed film. These spikes occurred at a nominal chamber pressure of approximately 1200 psig, as noted in the steady-state

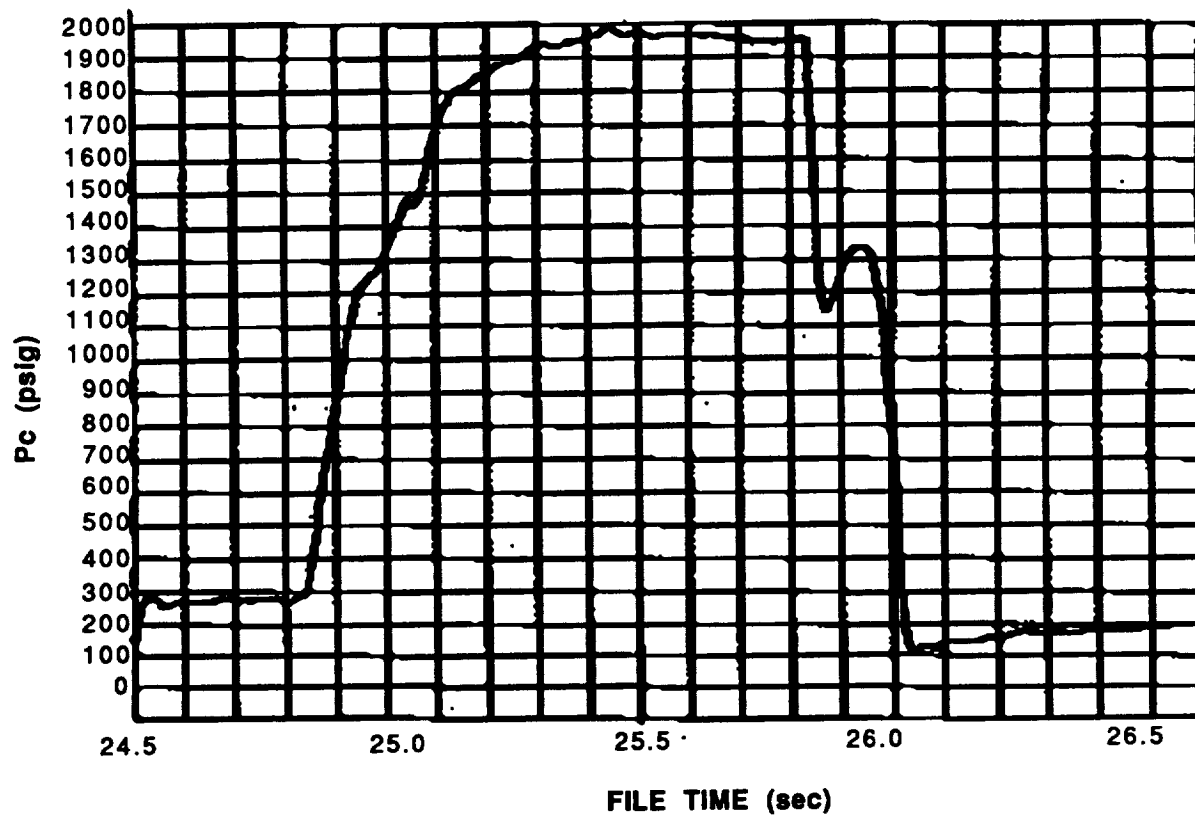


Figure 133. Static Chamber Pressure (Inj. End), Test 015-013, Circumferential-Fan Injector

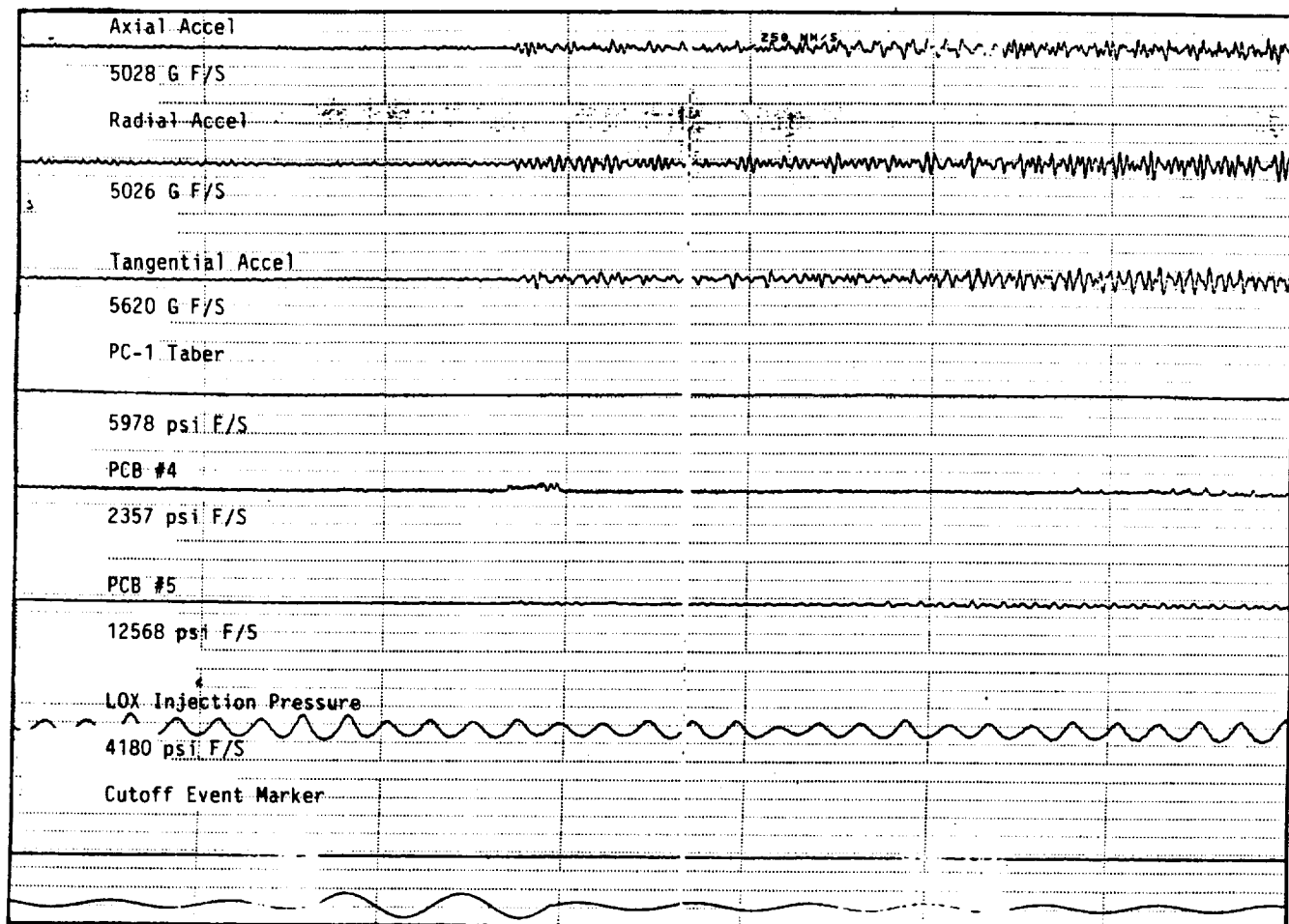


Figure 134. Test 015-013 High Frequency Data - Initial Wave Motion

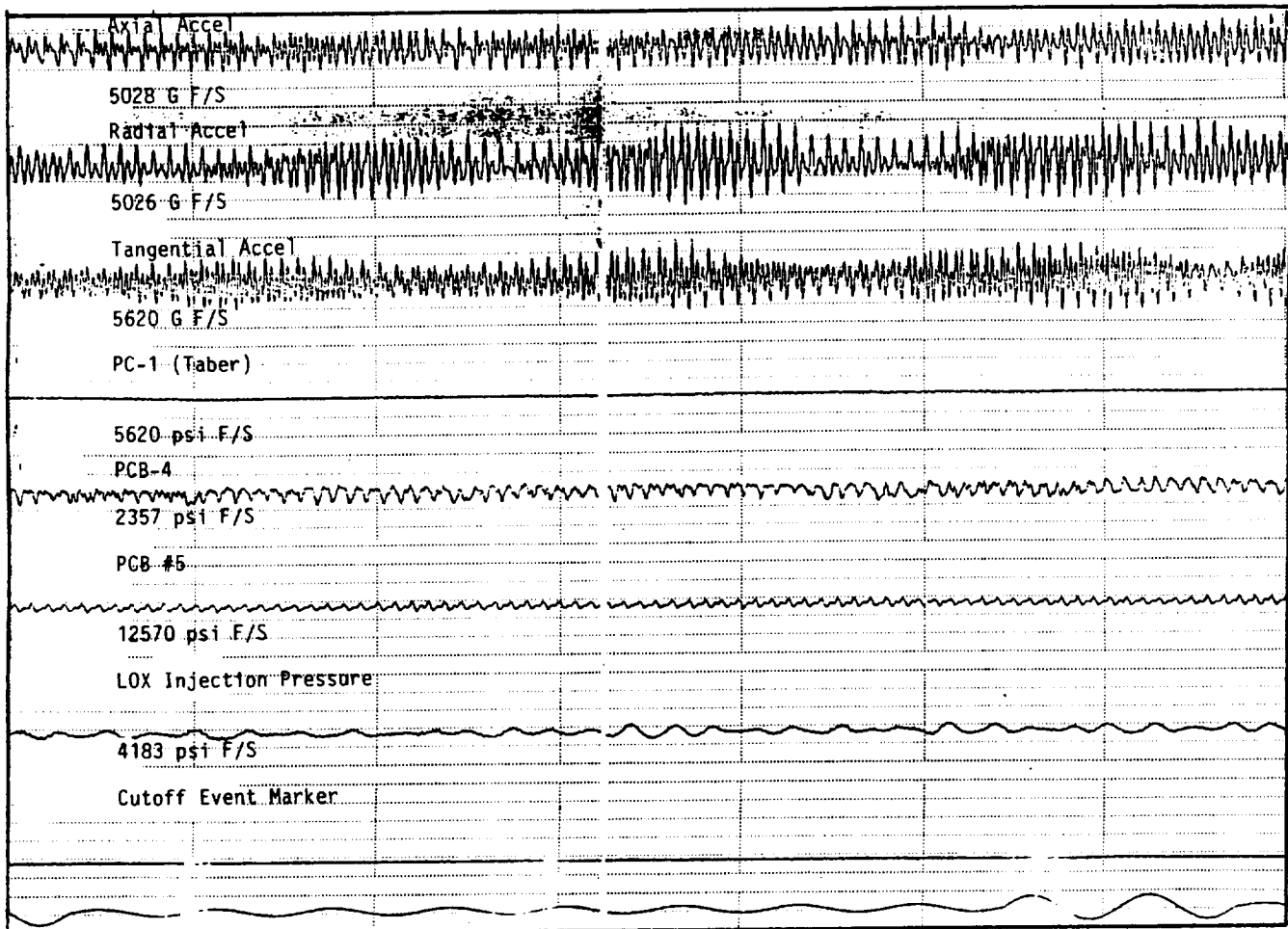


Figure 135. Test 015-013 High Frequency Data - Sustained Wave Motion

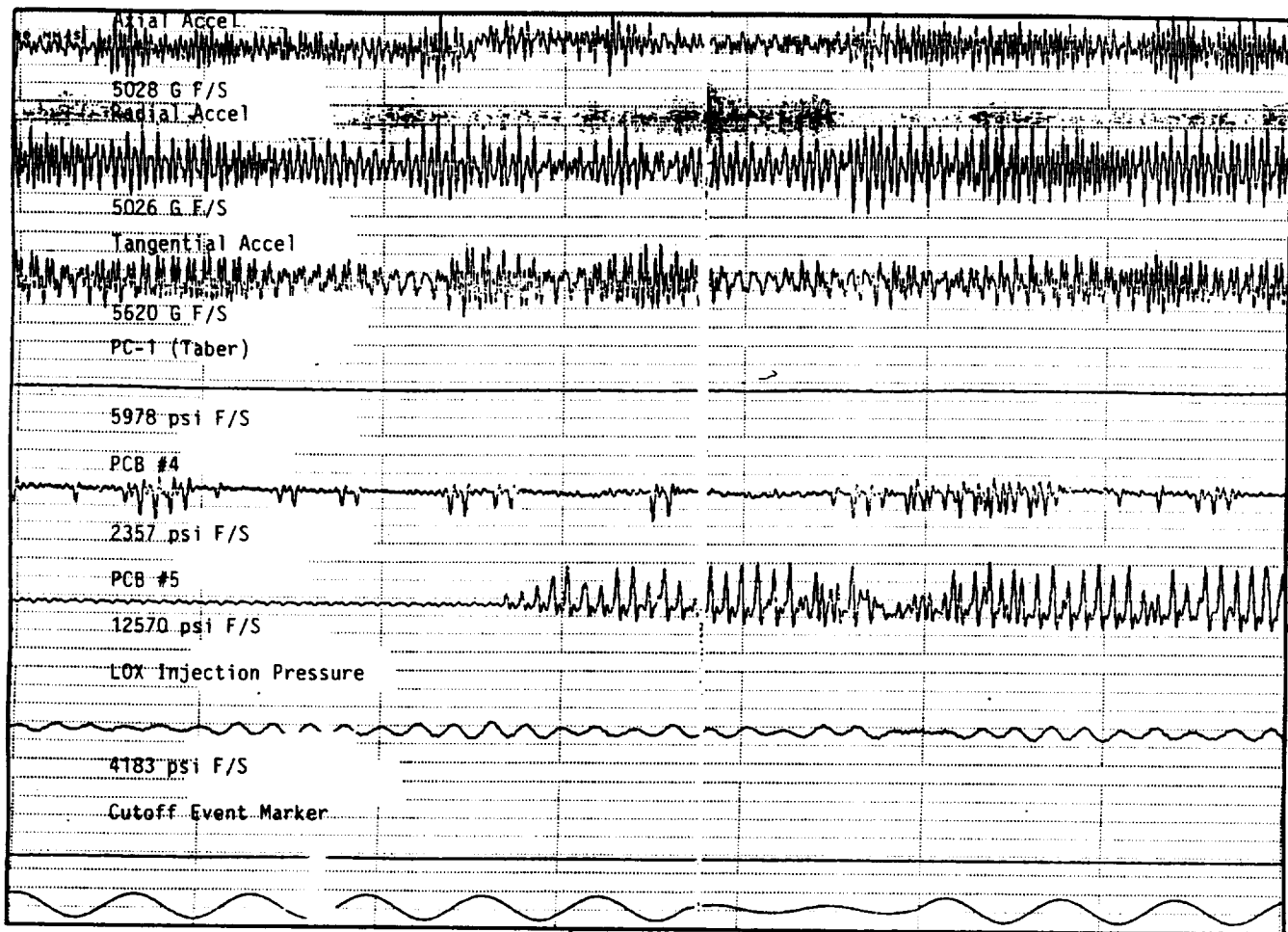


Figure 136. Test 015-013 High Frequency Data - Large Amplitude Pressure Disturbance

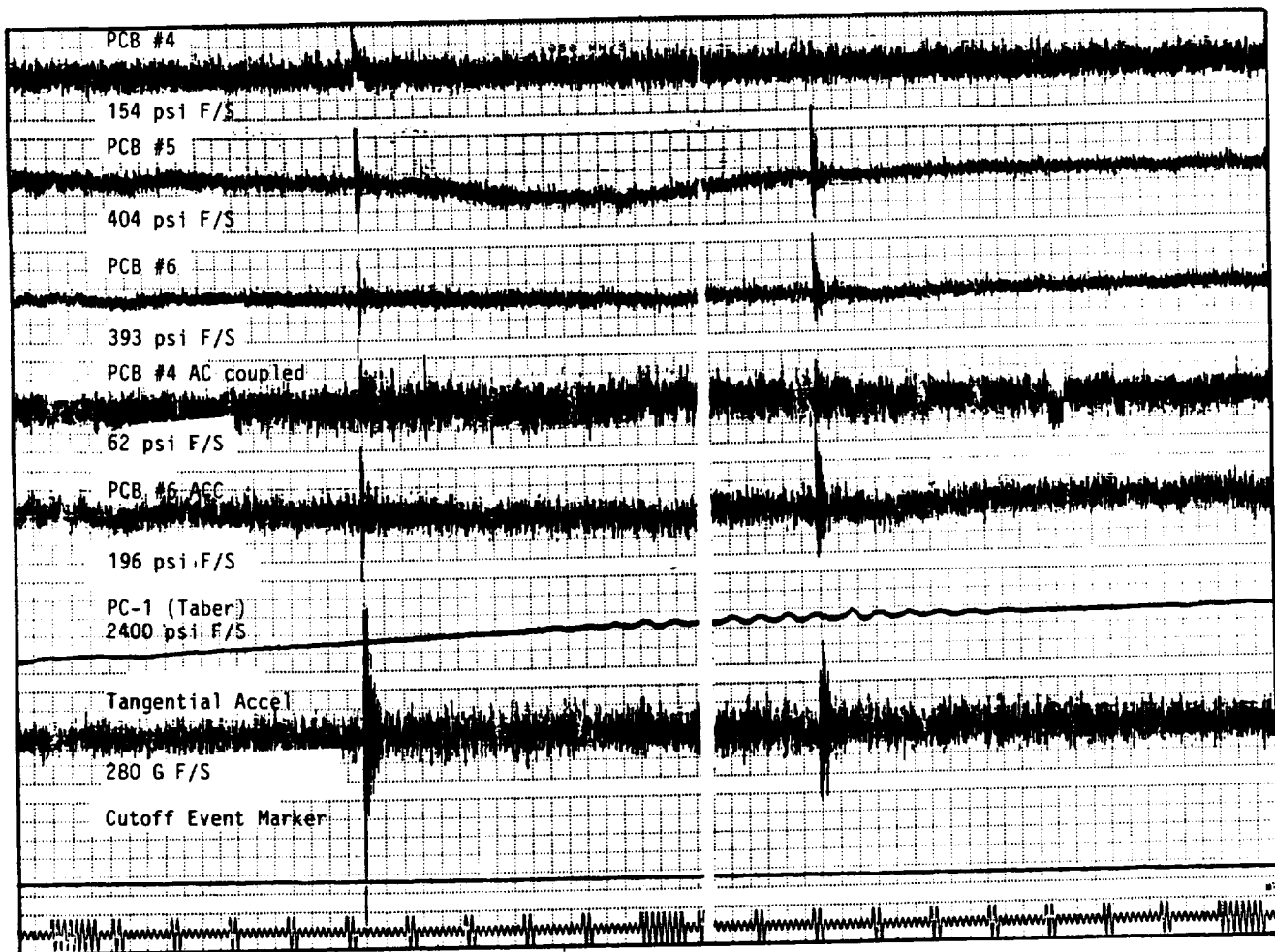


Figure 137. Test 015-016 High Frequency Data - Early Perturbation

chamber pressure trace shown in Figure 138. The corrected c-star efficiency was 94.7%. The ring down frequency of the spikes is approximately 10,000 Hz, and the peak-to-peak amplitude was measured at 400 psi on Pc-5. After the chamber pressure recovered from the two spikes, stable operation occurred during the remainder of the test. Nominal mainstage operating conditions for this test include a chamber pressure of 1988 psia (nozzle stagnation) and a mixture ratio of 2.79.

13.3.4 TEST 015-017

The next test (015-017) was performed to obtain better dynamic stability characteristics of the Circumferential-Fan injector. Again, a perturbation was noted in the high speed film during the start transient and is noted on the chamber pressure CRT, Figure 139. The corrected c-star efficiency was 97.2%. As stated earlier, it is not uncommon to experience improved performance during transverse instabilities. The high frequency data from test 015-017 is displayed in Figures 140, 141, 142 and 143. In these figures, it is evident that a relatively steep fronted perturbation was evidenced before the oscillatory wave motion began. The pressure spike, which coincided with the timing of the perturbation observed in the film, occurred before the scheduled bomb detonation signal and may be due to premature detonation of the bomb. The instability displayed in the data is at a frequency of 8000 Hz (1T mode) and an amplitude of approximately 1000 psi peak-to-peak overpressure. The maximum acceleration levels were 1510 g's, 2110 g's and 2140 g's for the axial, radial and tangential accelerometers, respectively. Due to a high attrition rate of high frequency pressure transducers in an unstable combustion environment, Pc-5 and Pc-6 transducers appeared to have failed during this test. This was substantiated with post test pulse checks of the transducers and by the measured acceleration levels.

During Test 015-017, a hot gas leak occurred when the water cooled Pc-4 adapter structurally failed, resulting in a leak path through the water coolant channel. The pressure trace at the time when the failure is believed to have occurred is displayed in Figure 144. Based on Test 015-017 results, it appears that the Circumferential-Fan injector is spontaneously stable and dynamically unstable without acoustic cavities.

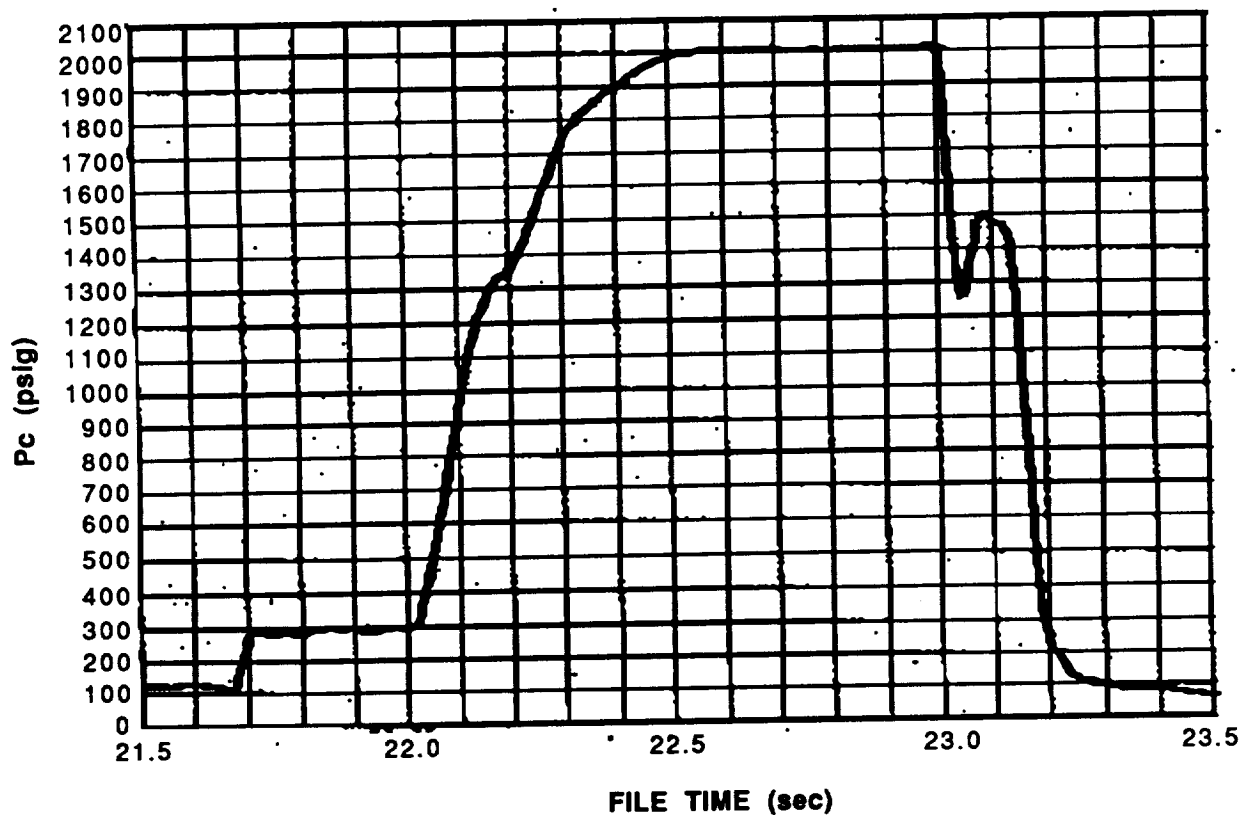


Figure 138. Static Chamber Pressure (Inj. End), Test 015-016, Circumferential-Fan Injector

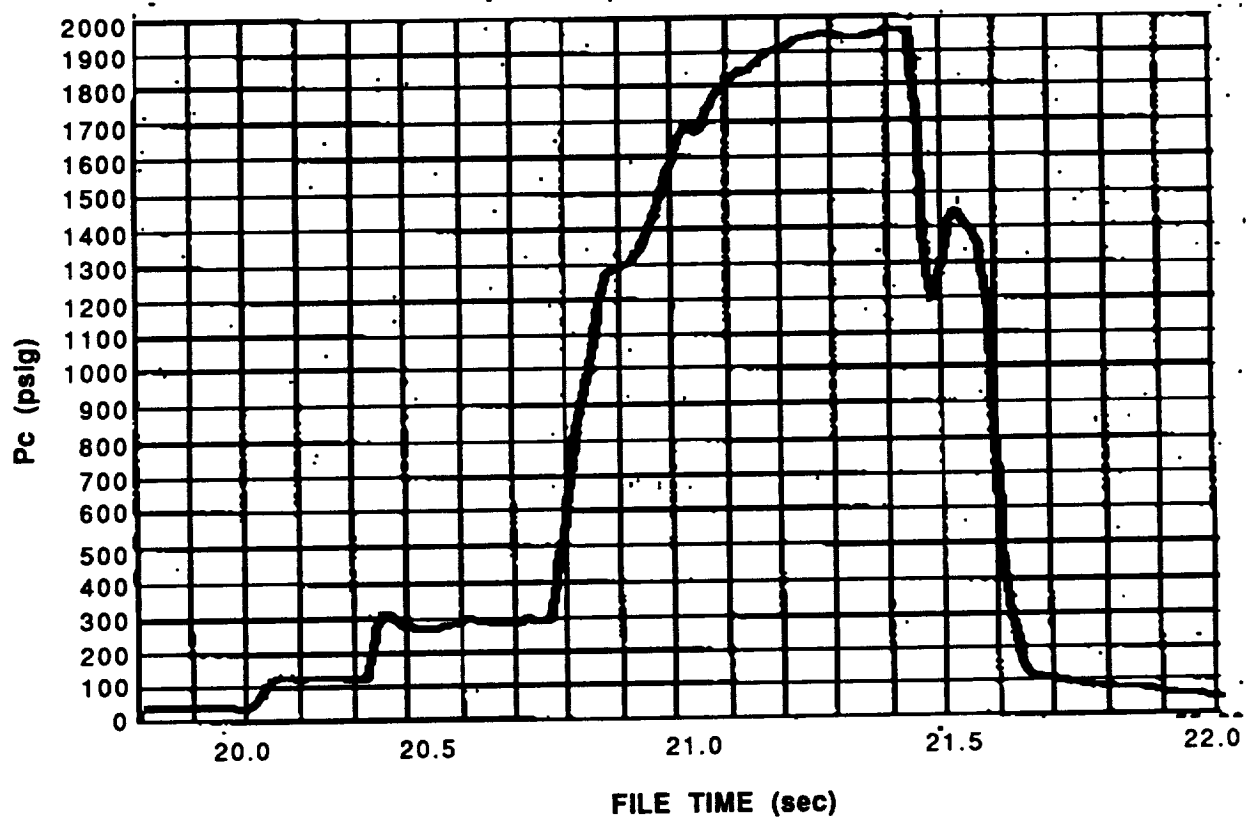


Figure 139. Static Chamber Pressure (Inj. End), Test 015-017, Circumferential-Fan Injector

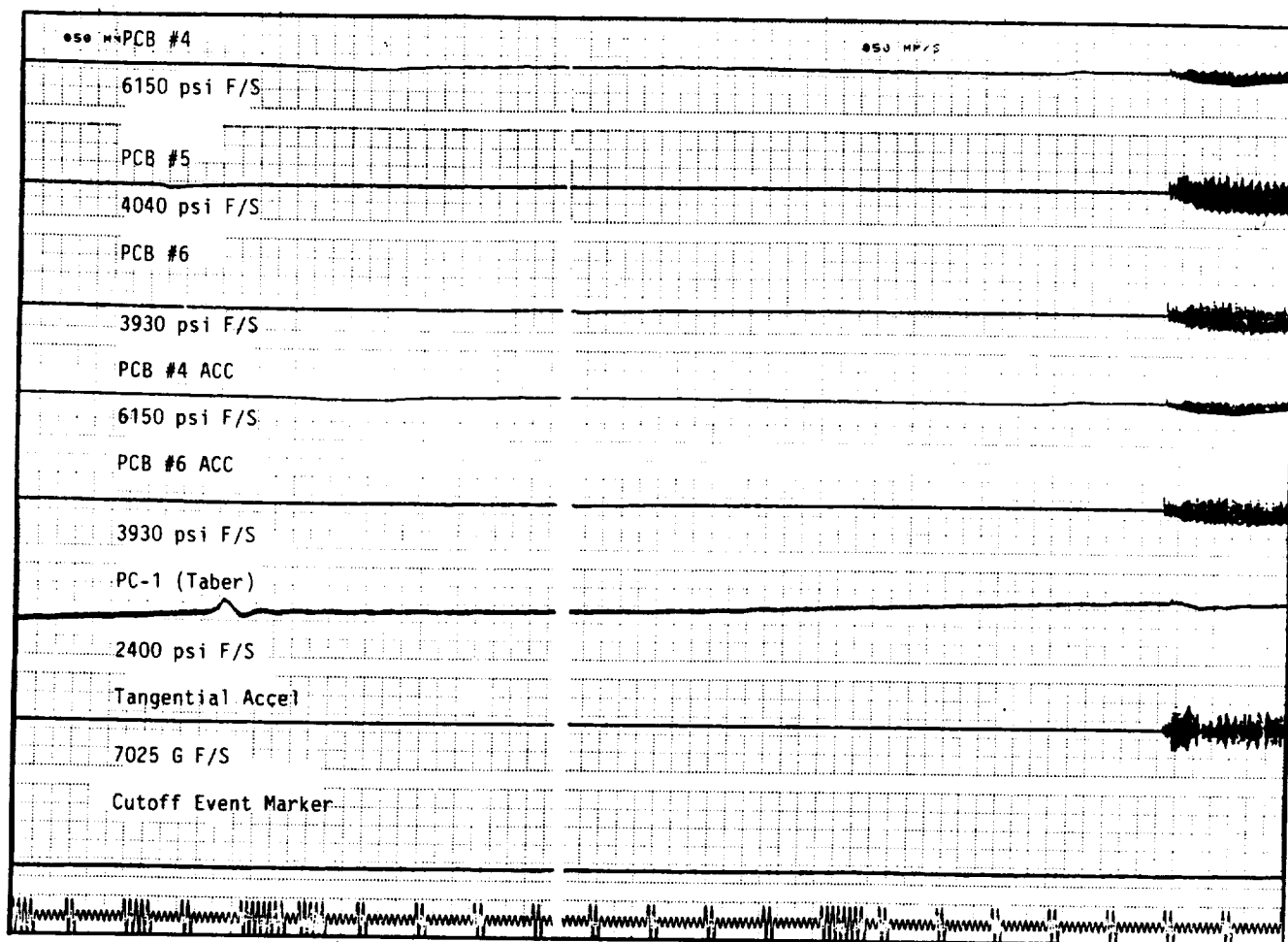


Figure 140. Test 015-017 High Frequency Data - Initial Wave Motion

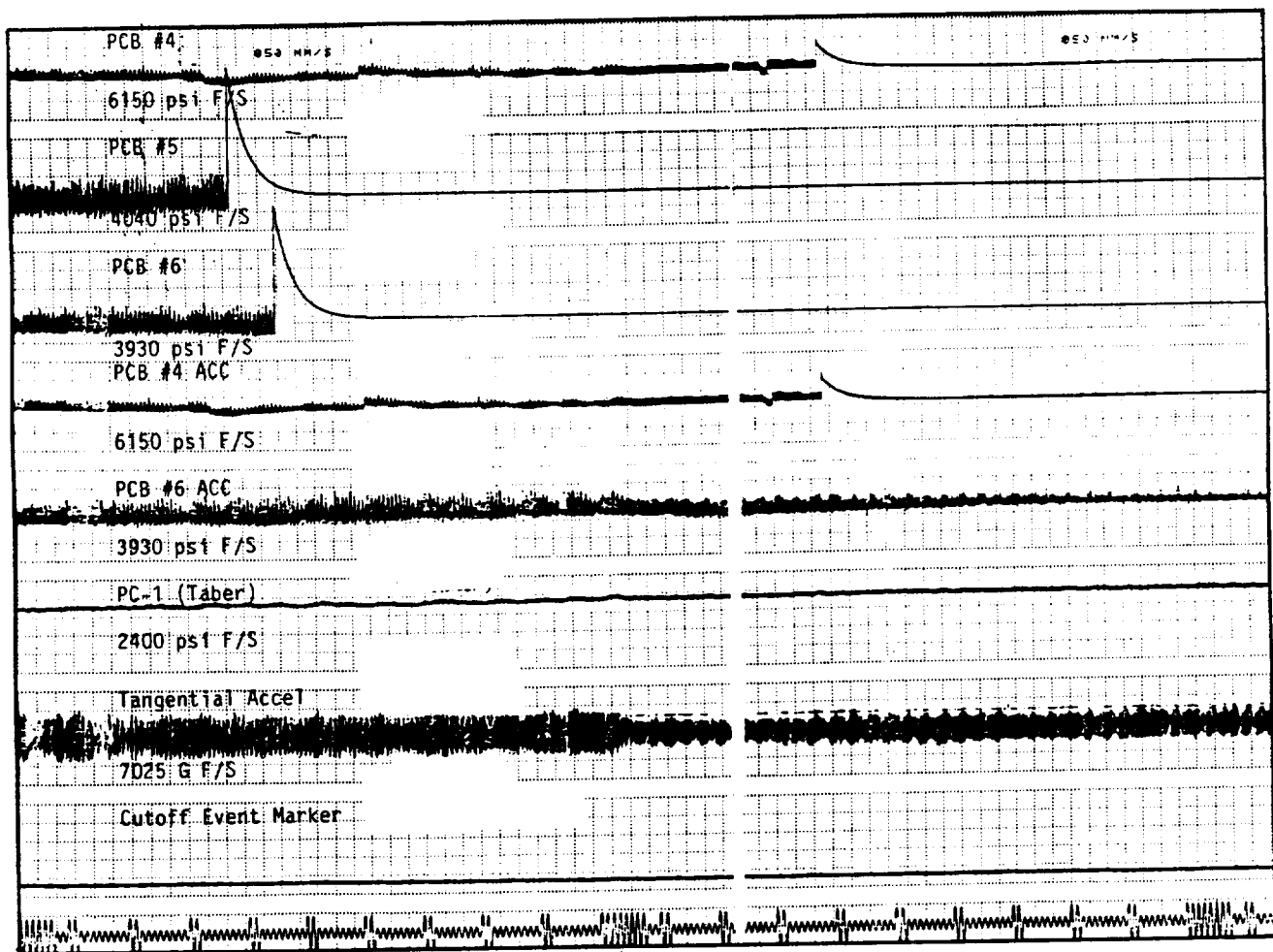


Figure 141. Test 015-017 High Frequency Data - PCB Malfunction

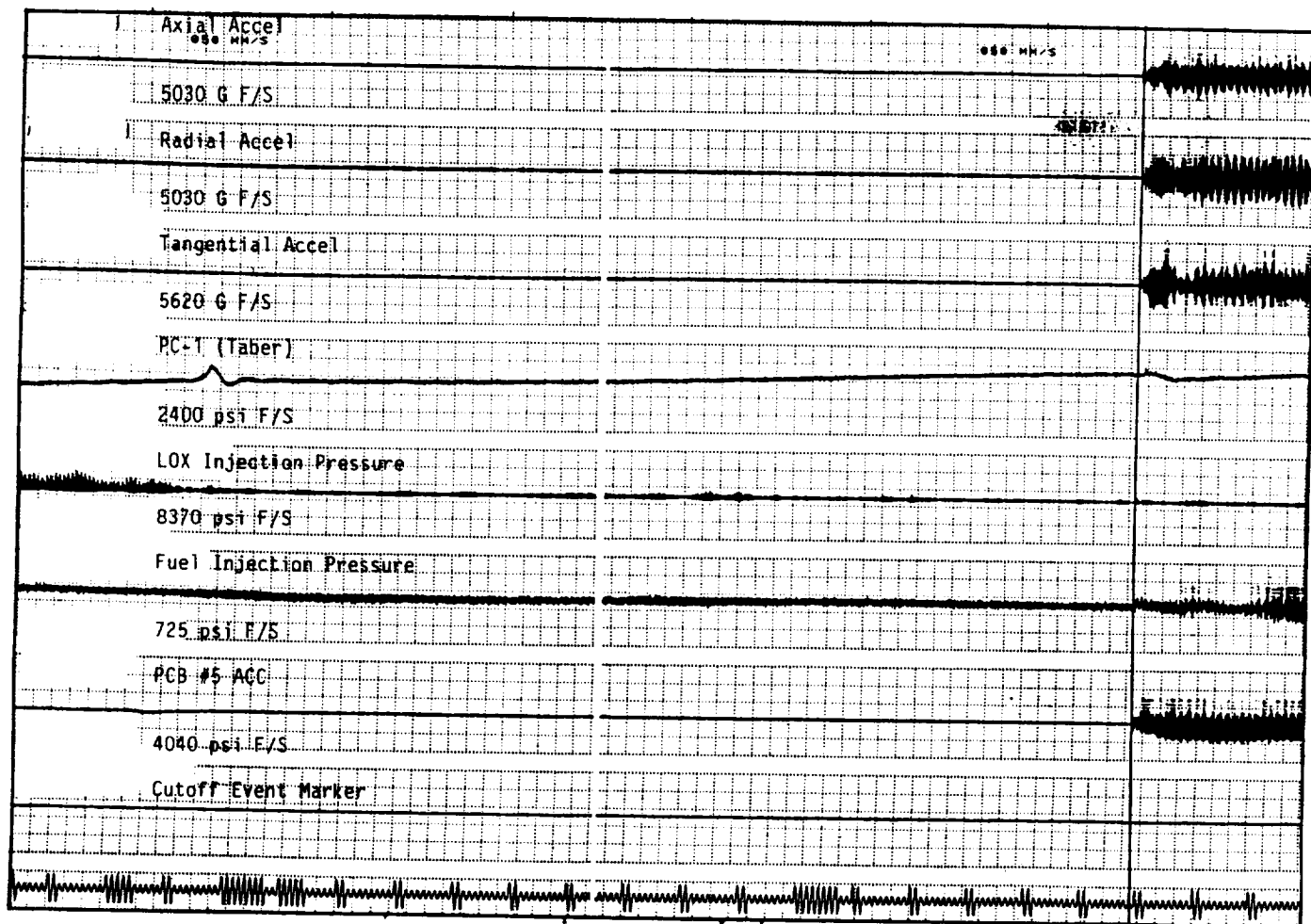


Figure 142. Test 015-017 High Frequency Data - Initial Wave Motion

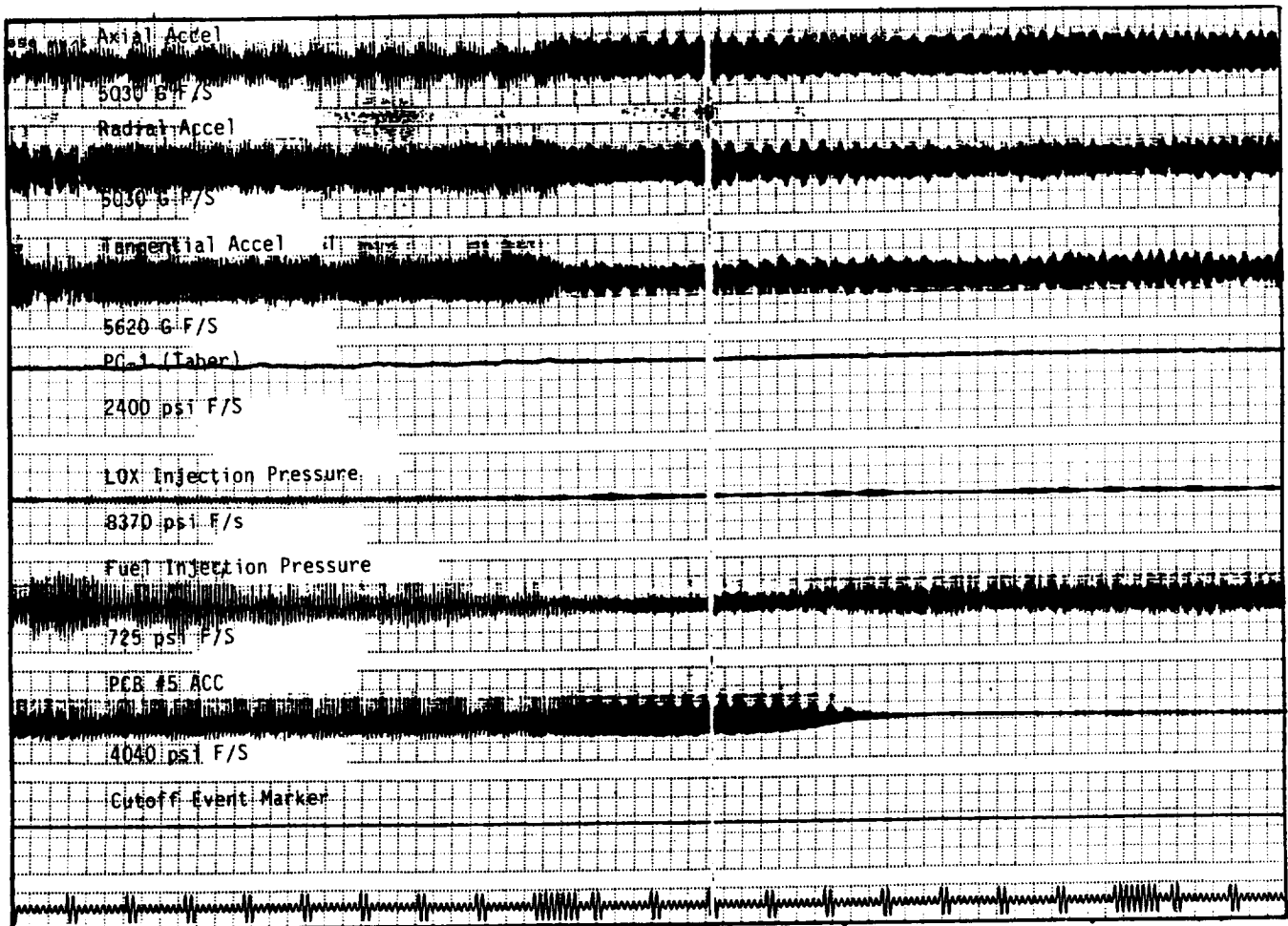


Figure 143. Test 015-017 High Frequency Data - Sustained Wave Motion

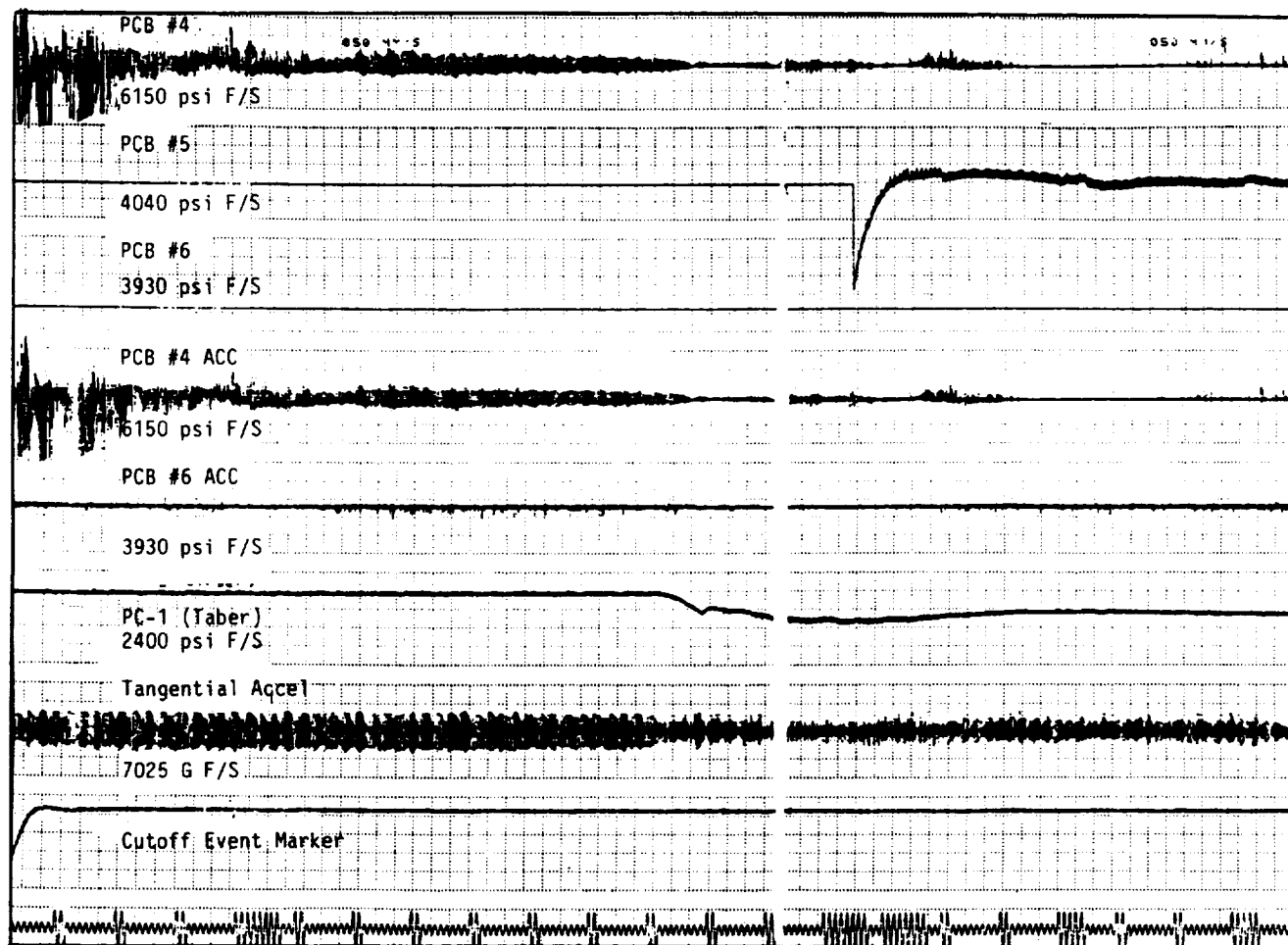


Figure 144. Test 015-017 High Frequency Data - PCB Structural Failure

13.4 BOX-DOUBLET INJECTOR

13.4.1 TEST 015-014

In accordance with the test matrix, two tests were conducted with the Box-Doublet injector. The first test, Test 015-014, was performed in order to demonstrate the spontaneous stability characteristics of the injector without acoustic cavities. Nominal mainstage operating conditions include a chamber pressure of 1966 psia (nozzle stagnation) and a mixture ratio of 2.77. The injector end chamber pressure plot is presented in Figure 145. The corrected c-star efficiency was 94.6%, with the time span indicated on the chamber pressure plot. The high frequency data obtained during this test is displayed in Figure 146. As evidenced by the data, no instability was encountered during this test, which progressed to a sequenced duration cut off. The 1250 Hz oscillation which occurred at the end of the test as the chamber pressure ramped down is larger in amplitude than had previously been seen with the other injectors. The oscillation peak-to-peak amplitudes were measured to be 440 psi, 430 psi and 360 psi by PCB transducers Pc-4, Pc-5 and Pc-6, respectively. During this test, the axial accelerometer failed.

13.4.2 TEST 015-015

In the next test (015-015), the dynamic stability characteristics of the Box-Doublet injector were demonstrated. Nominal mainstage operating conditions included a chamber pressure of 1999 psia (nozzle stagnation) and a mixture ratio of 2.77. Figure 147 contains an injector end pressure trace of the test. The corrected c-star efficiency was 95.3%. The initiation of the instability which occurred during the test is displayed in Figure 148 in the form of high frequency data. The overpressure due to the bomb was approximately 800 psi mean-to-peak during Test 015-015, and the maximum overpressure of the instability was 1540 psi, 1420 psi and 1650 psi measured on Pc-4, Pc-5 and Pc-6, respectively. Like the Circumferential-Fan injector, the frequency of the instability was approximately 8000 Hz (1T). During Test 015-015, the bomb detonated as sequenced. The major conclusion from review of Test 015-015 data is that the Box-Doublet pattern is dynamically unstable without acoustic cavities.

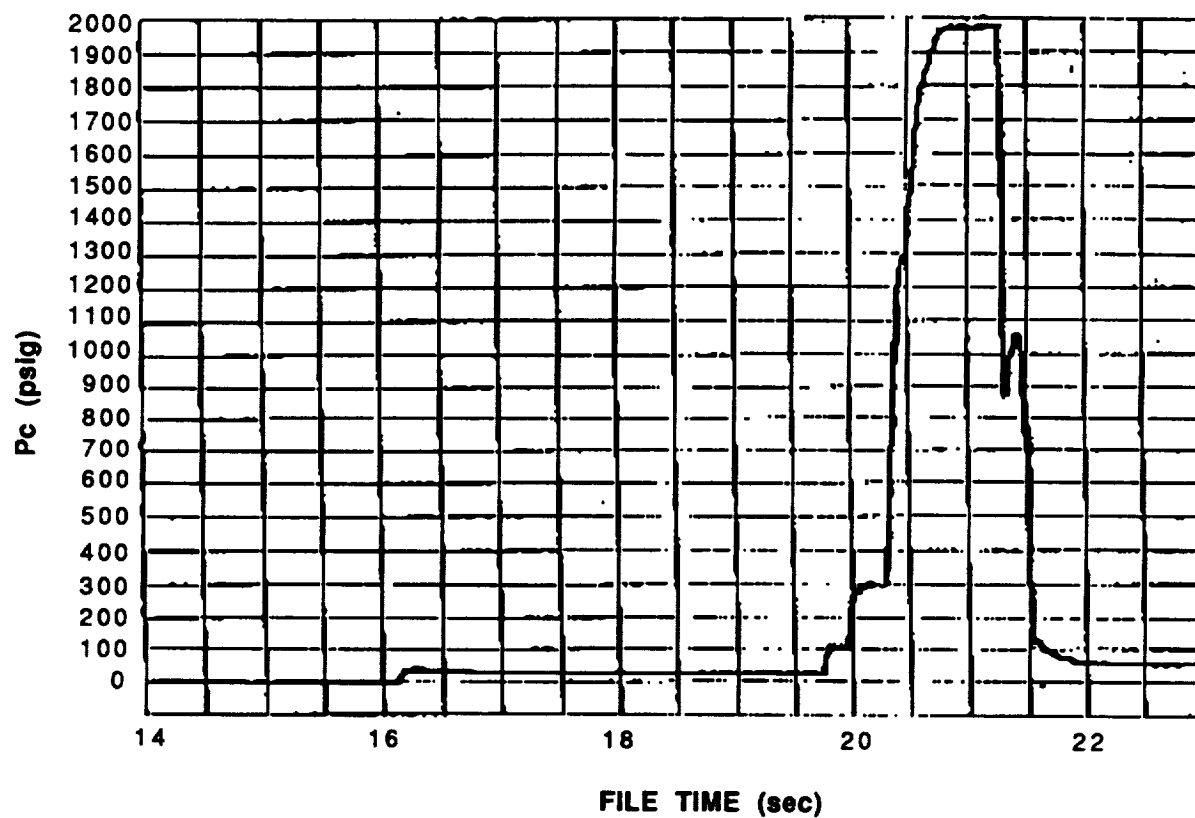


Figure 145. Static Chamber Pressure (Inj. End), Test 015-014, Box-Doublet Injector

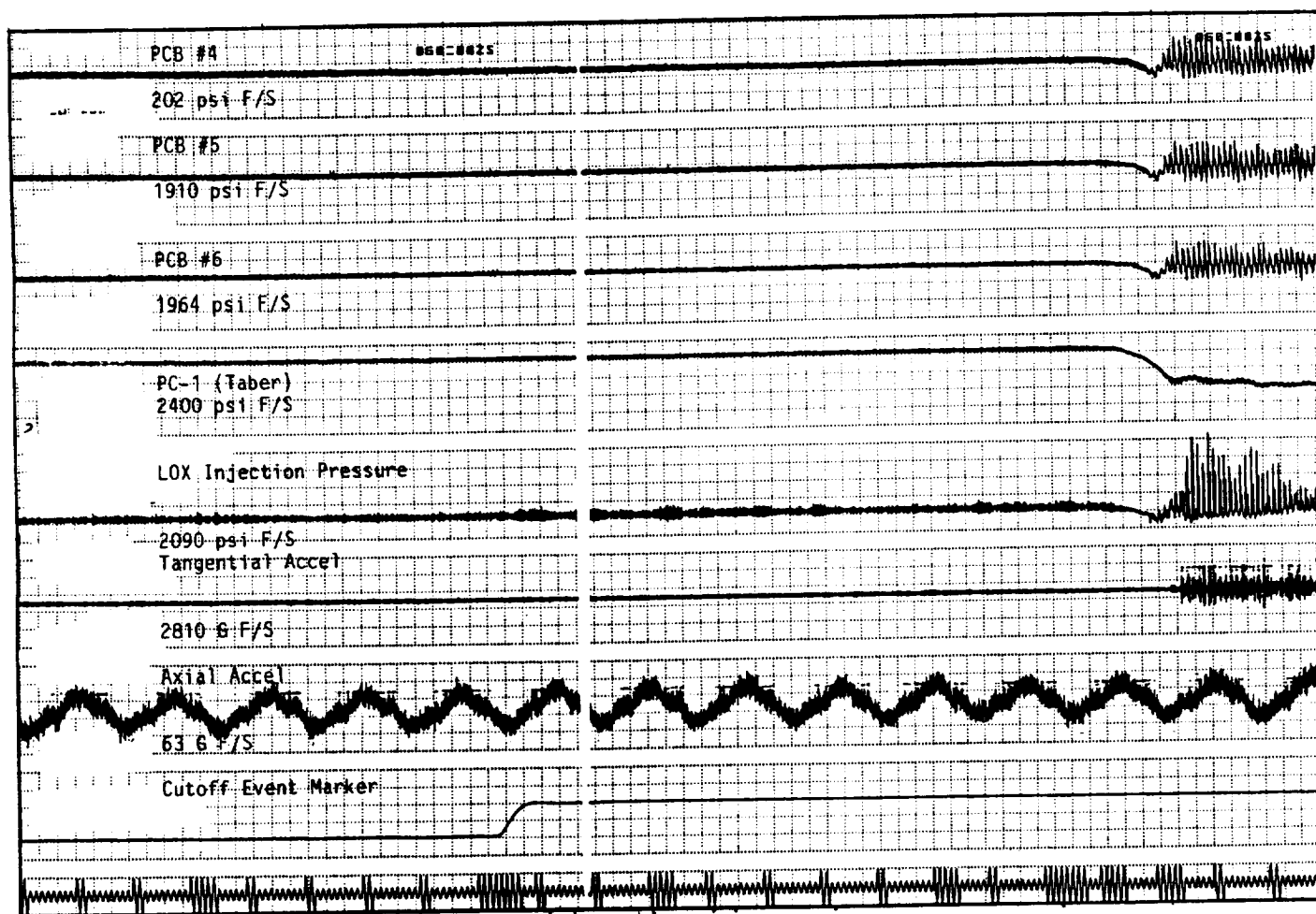


Figure 146. Test 015-014 High Frequency Data at Test Cut-Off

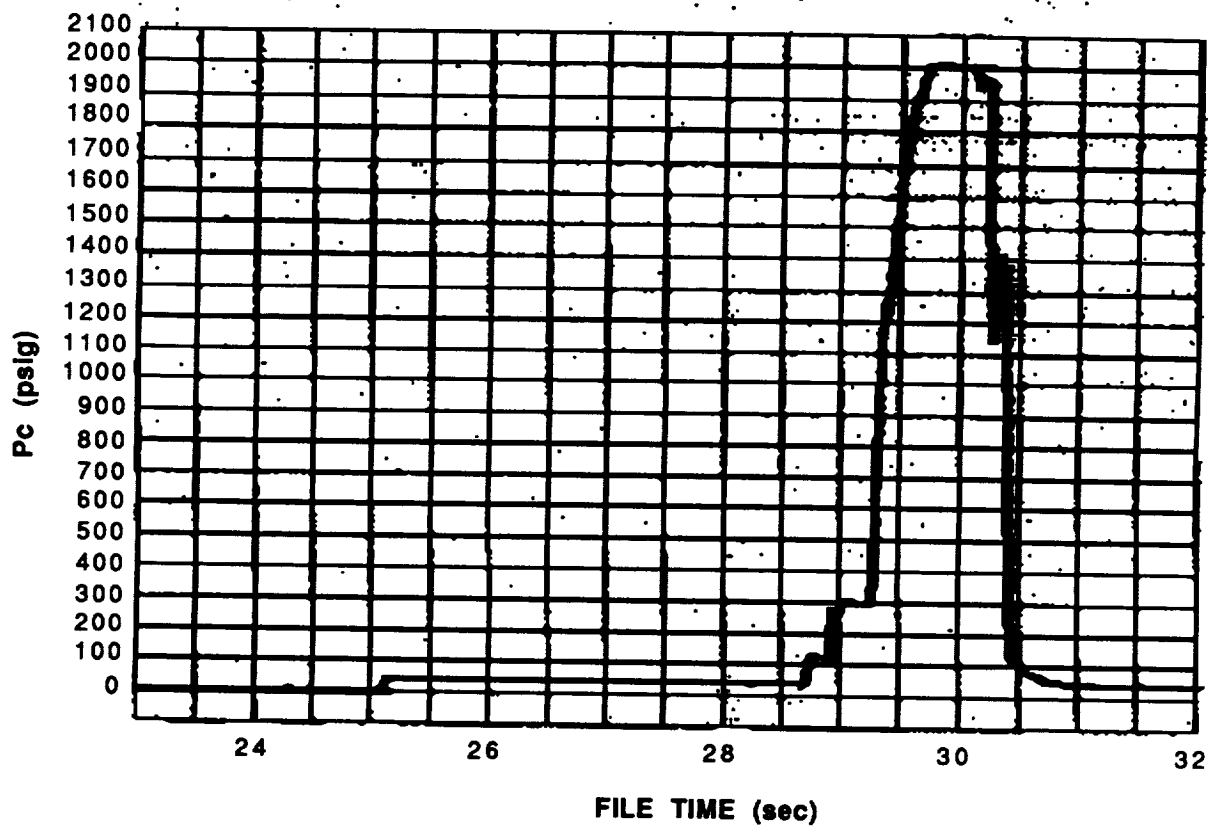


Figure 147. Static Chamber Pressure (Inj. End), Test 015-015, Box-Doublet Injector

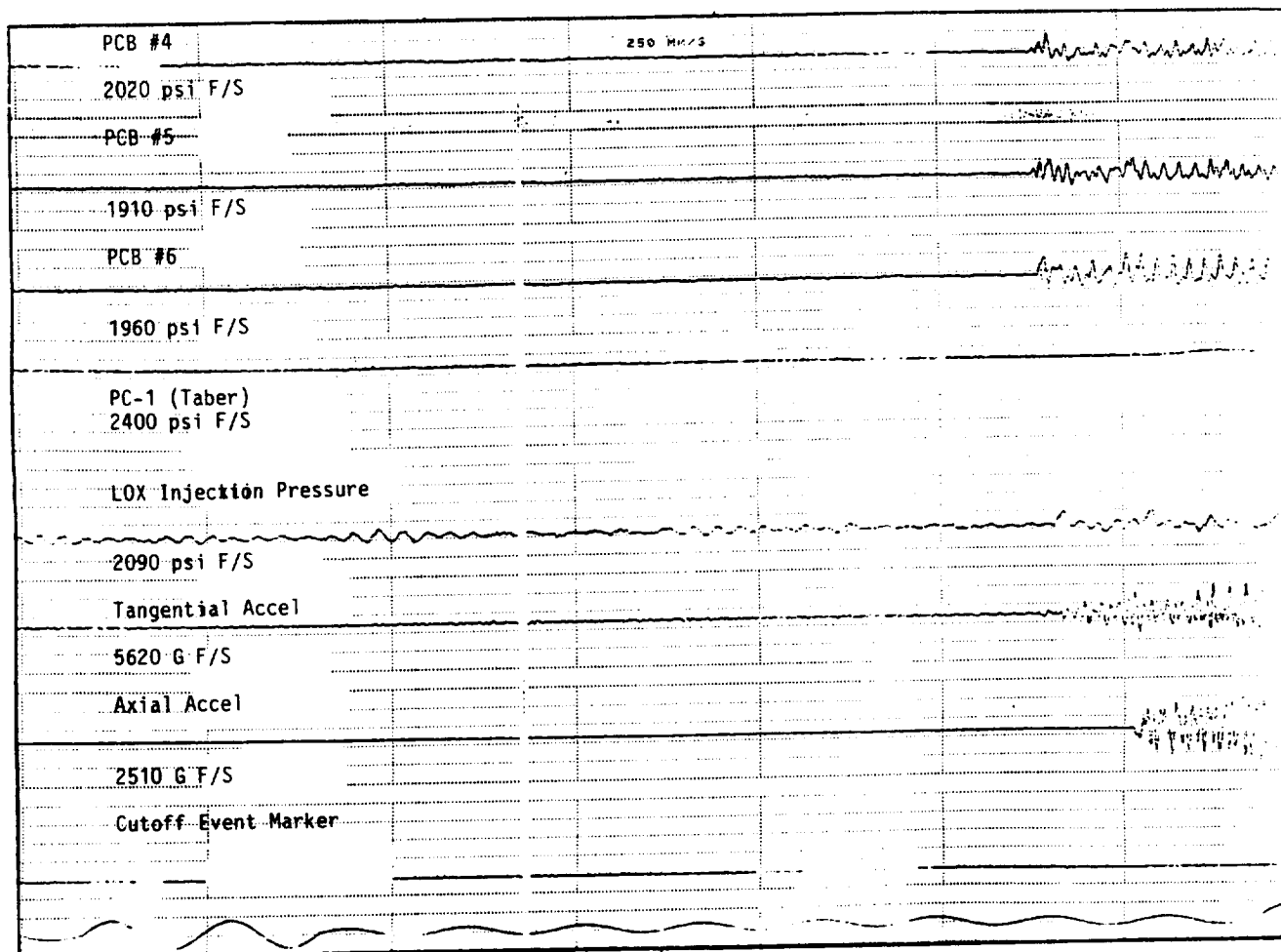


Figure 148. Test 015-015 High Frequency Data - Bomb Detonation & Instability

13.5 O-F-O TRIPLET INJECTOR

Previous tests with the O-F-O Triplet injector were performed under Task II of this program. During these tests, a first longitudinal instability was encountered along with relatively low performance (c-star efficiency ~93%). The combustion chamber utilized in the Task II testing was 19.4 inches in length, and a first tangential acoustic cavity was incorporated in the hardware. Results of the O-F-O Triplet stability analysis suggested that the amplitude of the first longitudinal (1L) instability would be reduced as the chamber length is decreased. Additionally, it was speculated that the longitudinal instability may have been the cause of the low performance obtained with this injector. This analysis is described in detail in later in this report.

In an attempt to reduce the amplitude of the longitudinal oscillations and to improve performance, two tests were performed with the O-F-O Triplet using a 6-inch shorter chamber (injector to throat length = 13.4-inch). Although the original test logic indicated that the screening tests would not implement acoustic aids, both tests included the use of acoustic cavities tuned to the first tangential mode (8000 Hz), in order to change only one variable at a time.

13.5.1 TEST 015-018

The first test which was performed, Test 015-018, was a non-bomb test. A plot of the injector end chamber pressure is shown in Figure 149. The high-frequency data obtained during this test is presented in Figure 150. The results of this test indicate that a 1L instability still exists in the combustor, but at a maximum amplitude of 182 psi peak-to-peak. The growth rate for this test was calculated to be 86.4 s^{-1} . A trend observed in the data is that the longitudinal instability trends appear and then disappear. This may be due to changing operating conditions which do not appear in the steady state data. It is still apparent that the stability margin of the O-F-O Triplet injector was increased by 50% by making the combustion chamber six inches shorter in length. The corrected c-star efficiency which was calculated for this non-bomb test was 98.1%. Also, during this test, some erosion was visible in the uncooled bomb spool. The damage appeared minor and a decision was made to perform a bomb test.

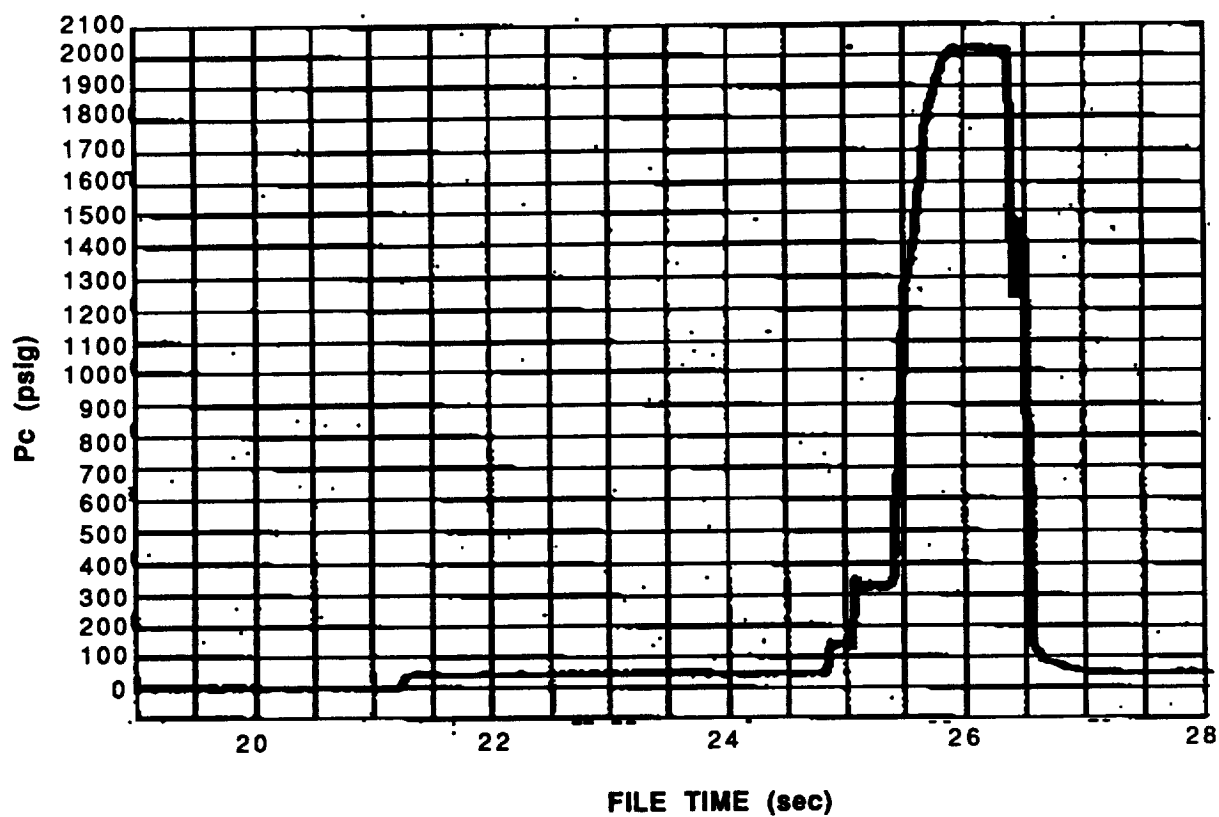


Figure 149. Static Chamber Pressure (Inj. End), Test 015-018, O-F-O Triplet Injector

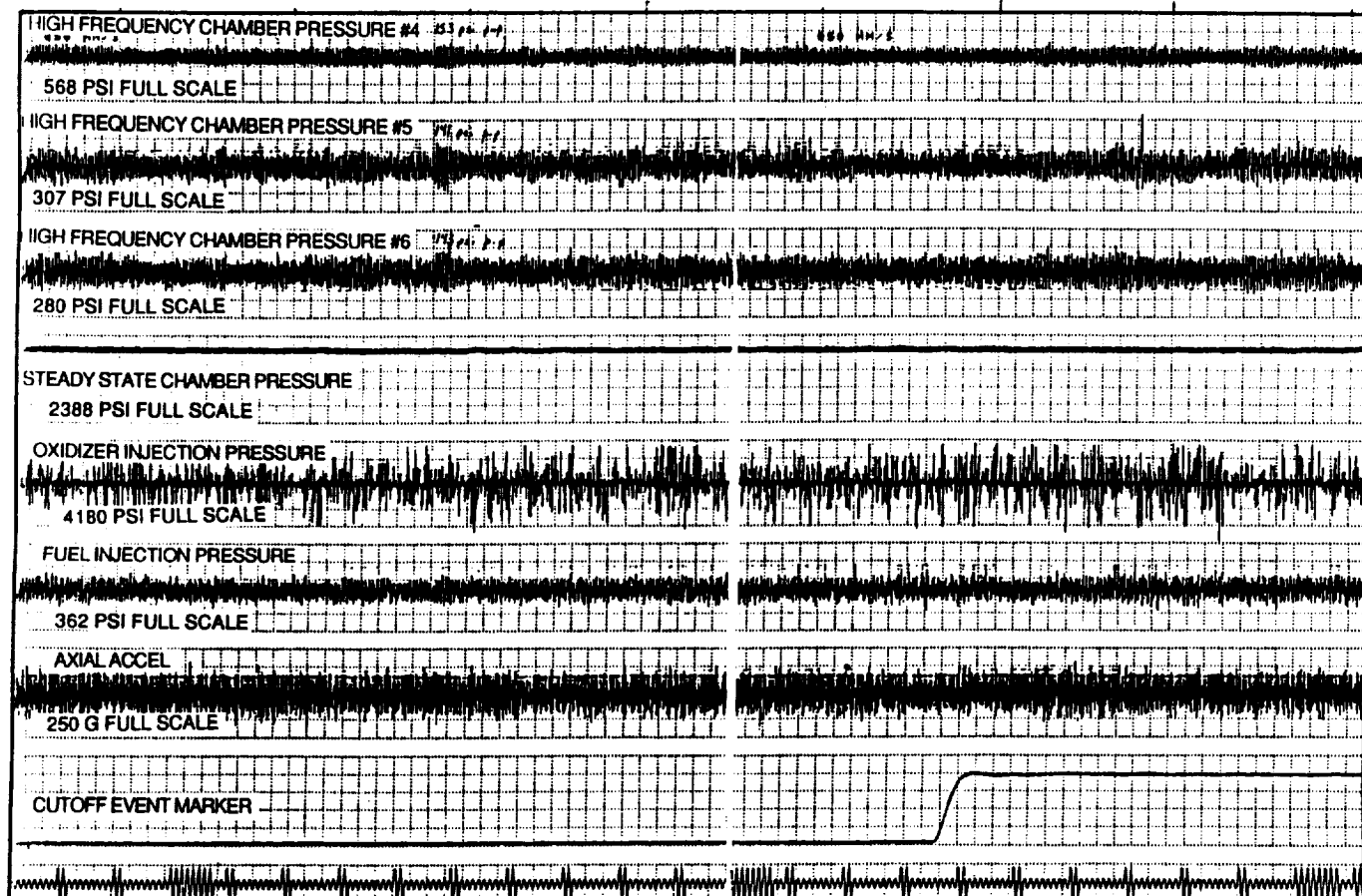


Figure 150. O-F-O Triplet High Frequency Test Data -
(Chamber Length = 13.4-In.)

13.5.2 TEST 015-019

In the following test, a bomb was detonated in the combustor during mainstage operation. The injector end pressure of Test 015-019 is presented in Figure 151. The high frequency data for this test is presented in Figure 152. As observed in the data, a maximum mean-to-peak overpressure of 369 psi occurred. The 1L mode was present in the pressure traces when the bomb was detonated and as the bomb overpressure decayed the chamber pressure recovered to the 1L mode. Higher frequencies may have occurred during the bomb ring down, but damped out within 6 milliseconds of the bomb detonation. The accelerometers used to detect hardware vibrations and consequently unstable combustion did not respond to the first longitudinal wave motion. The accelerometers did respond to the bomb detonation as can be seen in Figure 152. The corrected c^* efficiency which was calculated for this bomb test was 99.0%. After this bomb test, major erosion was visible in the bomb spool. At that time it appeared that better boundary layer cooling would be required for further testing of the O-F-O Triplet injector. The O-F-O Triplet injector was not damaged during either of the tests.

The analytical predictions which were made before testing were then compared to the actual data. The chamber response model predicted a 22% increase in the stability margin (relative to the first longitudinal mode of instability) of the O-F-O Triplet injector by making the combustor six inches shorter in length. Test results indicate that a 50% increase in stability margin was obtained with the O-F-O Triplet injector by decreasing the chamber length. Another trend which is suggested by the recent test data is the increase in performance. It would appear realistic that the low performance measured with the O-F-O Triplet injector during the higher amplitude 1L instability was due to the instability. The results of the recent O-F-O Triplet injector tests were compared to the performance results with SDER predictions. The SDER predictions (95.5% c^* efficiency) suggested that the O-F-O Triplet injector was mixing limited and that complete vaporization would occur. The test results indicate that the mixing efficiency is probably higher than that predicted by SDER, but that complete vaporization does occur with the 13.4 inch long combustor. This is in agreement with the SDER results.

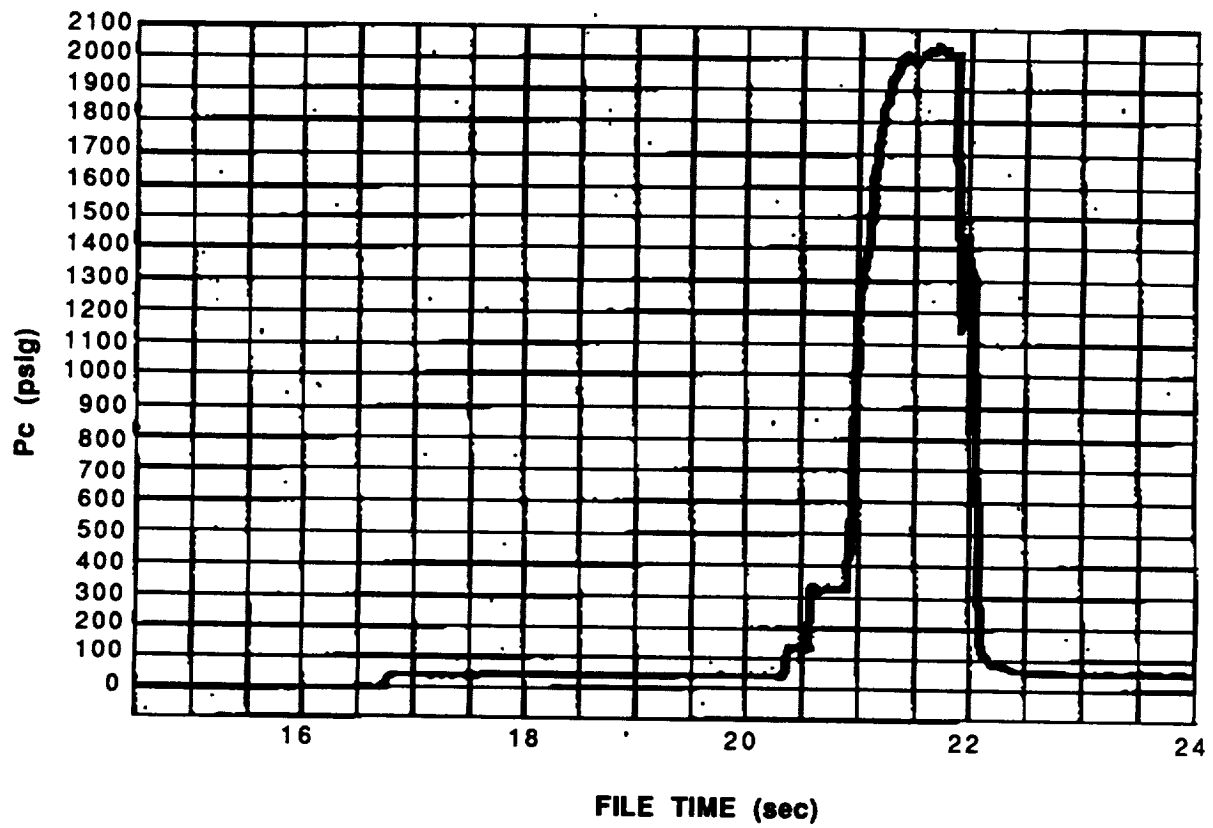


Figure 151. Static Chamber Pressure (Inj. End), Test 015-019, O-F-O Triplet Injector

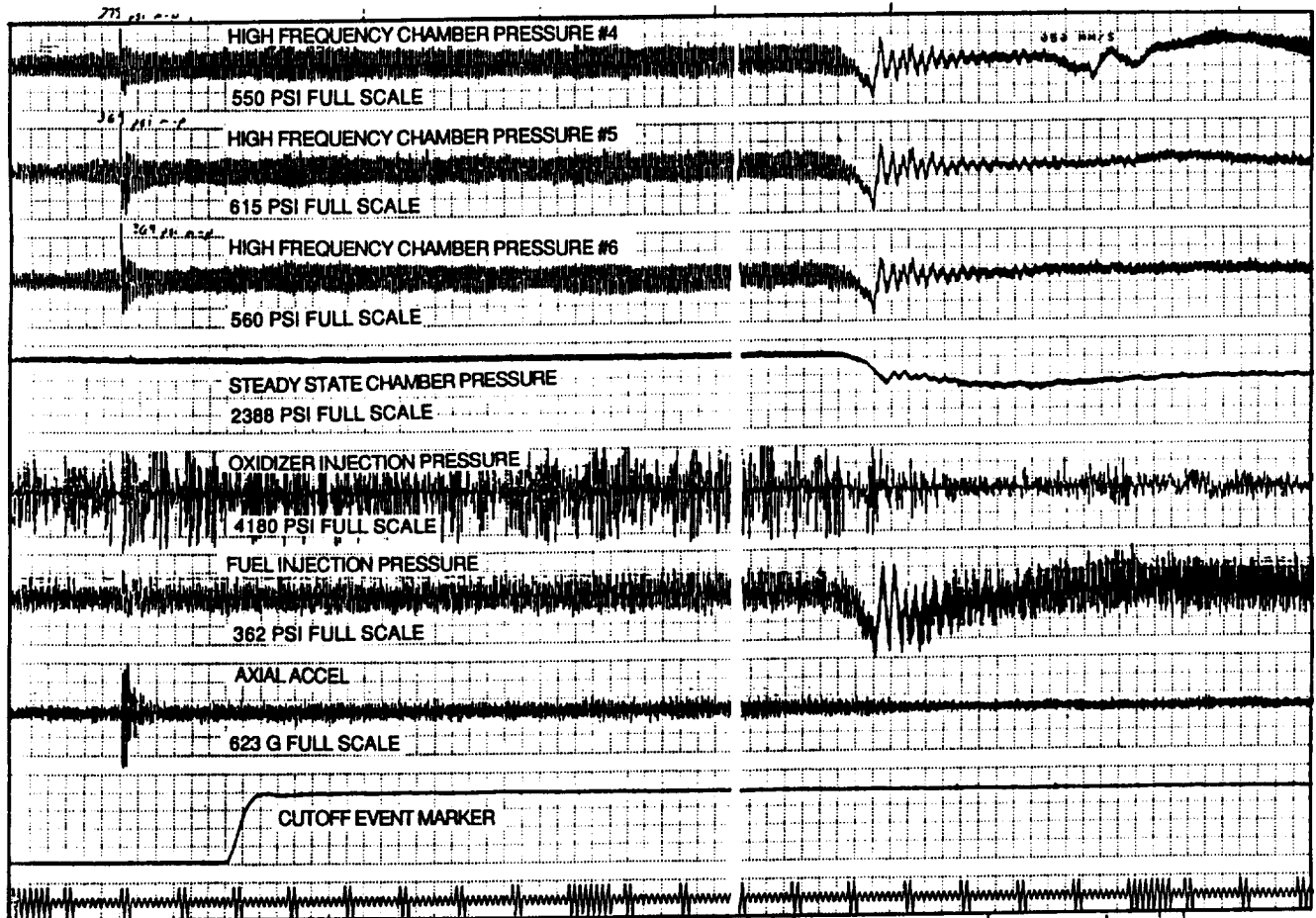


Figure 152. O-F-O Triplet High Frequency Test Data -
(Chamber Length = 13.4-In.)

13.6 BOMB REDESIGN

In an effort to determine the cause of the bomb failure in Test 015-013 and to evaluate possible design modifications, a number of proof pressure tests were conducted with used bombs of a similar design to that which was used in this test. Additionally, test samples were made up with the potting epoxy at various mixture ratios, both with and without imbedded wires similar to the lead wires from the charge assembly. These samples were then proof pressure tested. Table 18 contains a synopsis of these specimens and the test results. In summary, all specimens with the previously used epoxy mixture, TETA/Epon 826, leaked at very low pressures (~100 psig), while the specimens with a more flexible epoxy combination, Versamid/Epon 826, could withstand very high pressures (~5000 psig) without any visible leaks. Based on these test results, it was decided that there remained a possibility of another hot gas leak using the existing bomb design and that new bombs would be assembled for all future dynamic stability tests incorporating the following changes. The major change implemented was that the insulation on the stranded lead wires from the charge assembly was locally stripped and the bare wires were soldered to solid lead wires to eliminate a possible leak path through the wire. The wires were then potted into the stainless steel holder with Versamid/Epon 826 epoxy. Figure 153 shows a sketch of the bomb design.

Table 18. Stability Bomb Test Specimen Summary

Test Specimen	Epoxy	Results
Thermocoupled Bomb (used in Test 015-010)	TETA/ Epon 826	Leaked @ 100 psig around lead wires.
Used bomb from previous 3.5-inch testing	TETA/ Epon 826	Leaked @ 100 psig around lead wires.
Spliced stranded to solid lead wire, cast with epoxy, fitted w/ shrink tube	TETA/ Epon 826	No leak initially @ 100 psig. Pressure increased to 1200 psig, dropped to 0, increased to 100 psig. Heavy leakage around wires.
Stripped section of stranded wire & solder filled. Fitted w/ shrink tube.	TETA/ Epon 826	Leaked @ 100 psig around lead wires.
Stripped section of stranded wire & epoxy filled. Fitted w/ shrink tube.	TETA/ Epon 826	No leak initially @ 100 psig. Pressure increased to 1200 psig, dropped to 0, increased to 100 psig. Heavy leakage around wires.
Cast holder. No lead wires.	TETA/ Epon 826	Leaked @ 100 psig.
Solder spliced solid to stranded wire w/ 3 to 4 hr. ambient cure followed by heated cure (Qty 2).	TETA/ Epon 826	Leaked @ 100 psig.
Cast holder - no lead wires; extended ambient cure.	TETA/ Epon 826	Leaked through plug @ 100 psig.
Cast holder - no lead wires; full heated cure.	TETA/ Epon 826	Leaked around plug @ 100 psig.
Spliced solder joint w/ extended ambient cure.	TETA/ Epon 826	Leaked around plug @ 100 psig.
Used bombs from XLR-132 program (Qty 2).	TETA/ Epon 826	Leaked around plug @ 100 psig.
Cast holders w/ no lead wires (Qty 3).	Versamid/ Epon 826	No leaks @ 2000 psig.
Conax fitting w/ solid insulated wires.	N/A	No leaks @ 1200 psig.
Cast holder w/o lead wires. Epoxy MR 5:3.	Versamid/ Epon 826	No leaks up to 4500 psig - then small leak developed.
Cast holder w/o lead wires. Epoxy MR 2:1.	Versamid/ Epon 826	No leak @ 5000 psig.
Solid insulated wires in epoxy @ MR 5:3.	Versamid/ Epon 826	No leak up to 4700 psig - then small leak developed @ edge of casting.
Solid 24 gauge insulated wire. Epoxy MR 2:1 (Qty 2).	Versamid/ Epon 826	One specimen did not leak @ 5000 psig; 2nd specimen developed leak @ 4000 psig.
Solid 18 gauge varnished wire. Epoxy MR 2:1 (Qty 2).	Versamid/ Epon 826	No leaks @ 5000 psig.

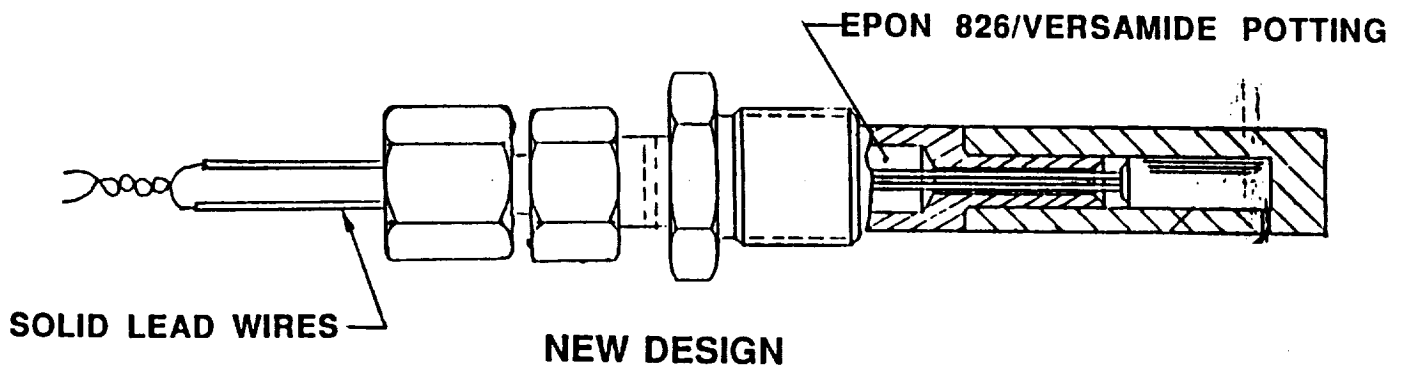
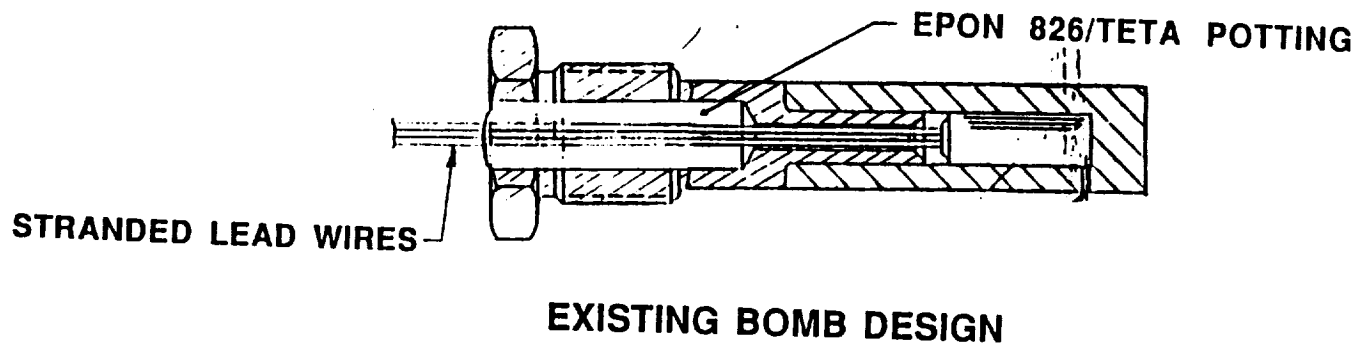


Figure 153. Stability Rating Bomb Redesign

TASK III

14.0 INJECTOR DOWN-SELECTION

14.1 INJECTOR SELECTION

With the conclusion of the screening tests of the H-1 Derivative, Circumferential-Fan, Box-Douplet and the O-F-O Triplet injectors, a review of the data was made and a down selection was recommended. During the down selection process, acoustic cavity issues were resolved, and the longitudinal instability of the O-F-O Triplet was addressed.

During the initial stages of the down selection process, the program goals were reviewed. The goals of the program include increasing the stability and performance data base of combustors at high chamber pressures ($P_c > 2000$ psia) with LOX/RP-1 propellants and developing the Isolated Combustion Compartment (ICC) concept which would be utilized in the design and development of full scale boosters. Another factor which was also considered in the down selection process, is the robustness of a given injector.

The review of the hot fire data revealed the following general characteristics of each injector. The H-1 Derivative injector exhibited 96 to 97 percent c-star efficiency for performance, and was both spontaneously and dynamically stable at nominal operating conditions ($P_c = 2000$ psia, $MR = 2.8$) without acoustic aids. Dynamic stability is rated on a combustor's ability to recover from an artificially induced, high amplitude pressure disturbance, which in this program is generated by the detonation of stability bombs. Following the screening tests, the H-1 Derivative injector was undamaged and had exhibited the performance and stability characteristics required to meet the ICC criteria.

The Circumferential-Fan injector exhibited 94 to 95 percent c-star efficiency at nominal operating conditions. This injector was shown to be spontaneously stable and dynamically unstable without acoustic aids. During heat flux testing performed under an AFAL contract with this injector (total mainstage test time ~30 to 35 seconds), no incidence of a transverse mode instability was observed, but first tangential acoustic cavities were incorporated during all of the heat flux tests. The Circumferential-Fan injector was damaged during the first and third bomb tests of the screening process both of which resulted in a first tangential instability. Rework of the injector would have been necessary before additional hot-fire testing could have been performed. Furthermore, two of the six

inch calorimeter spools were also damaged during the unstable combustion. In both cases, the calorimeter spool which was installed closest to the injector was damaged.

The Box-Doublet injector also exhibited 94 to 95 percent c-star efficiency. This injector was found to be spontaneously stable and dynamically unstable. Upon completion of the screening tests, the Box-Doublet injector was undamaged, and no hardware damage has occurred during the testing of this injector. During the screening tests, some problems had occurred during previous tests with respect to the bombs. Early detonation of the bombs and hot gas leaks through the bomb occurred during the testing of the H-1 Derivative and Circumferential-Fan injectors. There were no bomb anomalies during the screening tests with the box doublet injector.

The final injector tested during the screening phase of the program was the O-F-O Triplet injector. This injector is the only injector tested which has an unlike injector pattern. In the past, unlike injector patterns have been characterized by unstable combustion and an extreme thermal environment in the near injector region of the combustor. During the screening tests, the length of the combustion chamber used with the O-F-O Triplet injector was reduced six inches (from 19.4 to 13.4 inches) in an attempt to eliminate the first longitudinal (1L) mode of instability. This injector exhibited 98 to 99 percent c-star efficiency during these tests. A first tangential acoustic cavity was incorporated during these tests to reduce the risk of hardware damage. The longitudinal instability, however, was not eliminated during the screening tests, but a 50 percent reduction in amplitude was observed with the shorter combustion chamber. The increase in performance with this injector (from 93 to 98 percent c-star efficiency) was attributed to the attenuation of the 1L mode. The O-F-O Triplet injector was undamaged during the screening tests, but the uncooled bomb spool was eroded near the injector face. A modification of the injector's boundary layer coolant flow would be required before additional tests could be performed.

In order to aid in the down selection process, a summary was compiled which listed various parameters and concerns of the four injectors screened. The summary follows.

Stability and Performance Test Variables

Four injectors: H-1 Derivative, Box-Doublet, Circumferential Fan and O-F-O Triplet

Test Parameters

Pc: 1700 to 2300 psi

MR: 2.5 to 3.1

Chamber length: 19 to 7 inch configurations possible

Acoustic cavity configuration:

1T cavities

High frequency cavities

Multi-modal cavities

Acoustic cavity open area:

6 to 30 %

Injector pattern modifications

Concerns

Injector durability

Chamber compatibility

The basic parameters of interest include the specific injector, chamber pressure, mixture ratio and the use of stability aids, in the form of acoustic cavities. Two parameters of interest specific to an acoustic cavity include cavity design and cavity open area. The open area of a cavity was defined as the ratio of cavity area at the cavity-chamber interface to the injector face area and is typically expressed as a percentage. Axially oriented acoustic cavities are typically considered as a component of the injector, while radially oriented cavities are not. Two basic concerns were noted with respect to the down-selection process and include the injector durability and the combustion chamber compatibility with the specific injectors.

The down-selection criteria were prioritized in the following order: transverse stability technology, longitudinal stability technology, performance technology and other factors. The other factors include: injector condition, effect of the injector on the rest of the hardware, operating conditions, hardware damage specific to bomb tests.

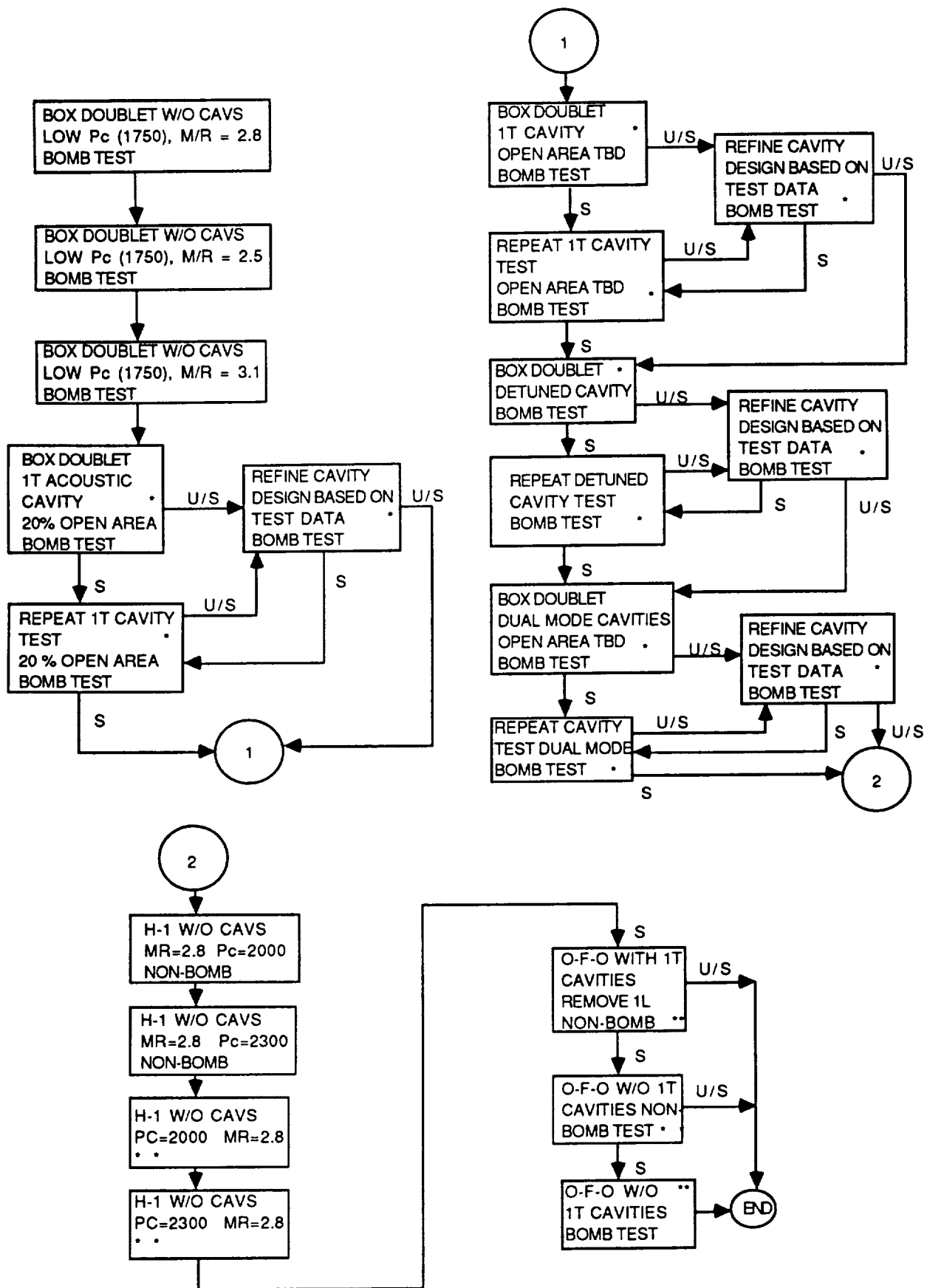
The down-selection recommendation included using the Box-Doublet injector to enhance the existing transverse dynamic instability data base. Tests to be performed with the Box-Doublet injector included: dynamic stability tests at low chamber pressure (~1750 psi)

and three mixture ratio values (2.5, 2.8 and 3.1), acoustic cavity configuration tests and acoustic cavity open area tests. The matrix included four different cavity configurations which include an optimized cavity geometry, a detuned cavity geometry, a tuned cavity which does not include optimized open area and a multi-tuned acoustic cavity. The test matrix is displayed in Figure 154.

In order to investigate the ICC concept, the H-1 Derivative injector was selected for additional testing. The H-1 Derivative injector was the only injector that met the criteria applicable to the ICC concept, which included high performance and stable combustion. The recommended tests with the H-1 Derivative injector include studies on the vaporization limits of the injector (short chamber) and the dynamic stability effects of operating the injector at high chamber pressures.

Finally, the recommended down-selection included testing of the O-F-O Triplet injector to investigate longitudinal mode instabilities. Several factors still needed to be investigated with respect to longitudinal instability which include injector resistance, the effects on operating conditions, and the effects on combustion efficiency. It should be noted, that the c-star efficiency of the O-F-O Triplet injector was increased by five to six percent by making the combustion chamber length six inches shorter. This dramatic effect on the combustion process would be well worth investigating both analytically and experimentally. The O-F-O Triplet injector required modifications for chamber compatibility and longitudinal stability reasons.

The detailed test plan for the down-selected injectors is presented in Figure 154. The test plan was approved by MSFC personnel. Designed to be flexible in nature, the test plan shows that the Box-Doublet injector was to be tested first without acoustic cavities. After the initial operating condition tests were completed, the Box-Doublet injector was to be utilized for an acoustic cavity study. The useful data to be obtained from these tests would include the cavity effectiveness in damping instabilities, the thermal environment inside the cavity (temperature measurements) and the compatibility of the various cavity designs. The H-1 Derivative and O-F-O Triplet tests were scheduled to follow the acoustic cavity tests if time and budget permitted.



* Pc = 2000 psi, M/R = 2.8 ** CHAMBER LENGTH = 13.4 INCHES

Figure 154. Task III Revised Test Matrix

14.2 TEST RESULTS

14.2.1 BOX-DOUBLET, LOW CHAMBER PRESSURE TESTS

The first three tests performed after the down-selection was approved were the low P_c (1750 psia), bomb tests at three mixture ratio values (2.5, 2.8 and 3.1) utilizing the Box-Doublet injector without acoustic cavities. The tests were performed to evaluate the dynamic stability of this injector at off-nominal mixture ratios. The low chamber pressure operating condition was suggested in order to reduce the risk of hardware damage and to further expand the stability data base. Analyses were performed prior to testing with SDER and the results indicated that unstable combustion would occur at each mixture ratio value.

14.2.1.1 Test 015-032

As predicted, all three tests were dynamically unstable. The first of the low P_c tests, Test 015-032, was targeted for 1750 psia chamber pressure and 2.8 mixture ratio. Actual mainstage operating conditions included a chamber pressure of 1762 psia (nozzle stagnation) and a mixture ratio of 2.78. The chamber pressure CRT is presented in Figure 155. The high frequency data obtained during this test is displayed in Figure 156. The data indicates that the bomb detonated as sequenced, approximately 30 milliseconds prior to duration cut-off. The three high frequency pressure transducers registered 380, 520 and 520 psi overpressures, respectively, due to bomb detonation. An instability in the first tangential mode was initiated at 7500 Hz. The oscillation peak-to-peak amplitudes were measured to be 580, 700 and 690 psi by the three PCB transducers, respectively. The test hardware was undamaged by the instability. It is interesting to note that the static chamber pressure trace drops when the instability occurs. This phenomena has been observed in other tests with instabilities in transverse modes and can best be explained by increased combustion occurring between the injector face and the pressure tap location (2 inches downstream of the injector face). This results in increased pressure at the injector, due to the increased combustion, while the static (measured) pressure 2 inches downstream of the injector is decreased due to higher gas velocities as well as higher Rayleigh line losses. The increase in percent reacted close to the injector face during unstable combustion is hypothesized to be caused by increased droplet vaporization and breakup due to the high amplitude tangential wave velocity.

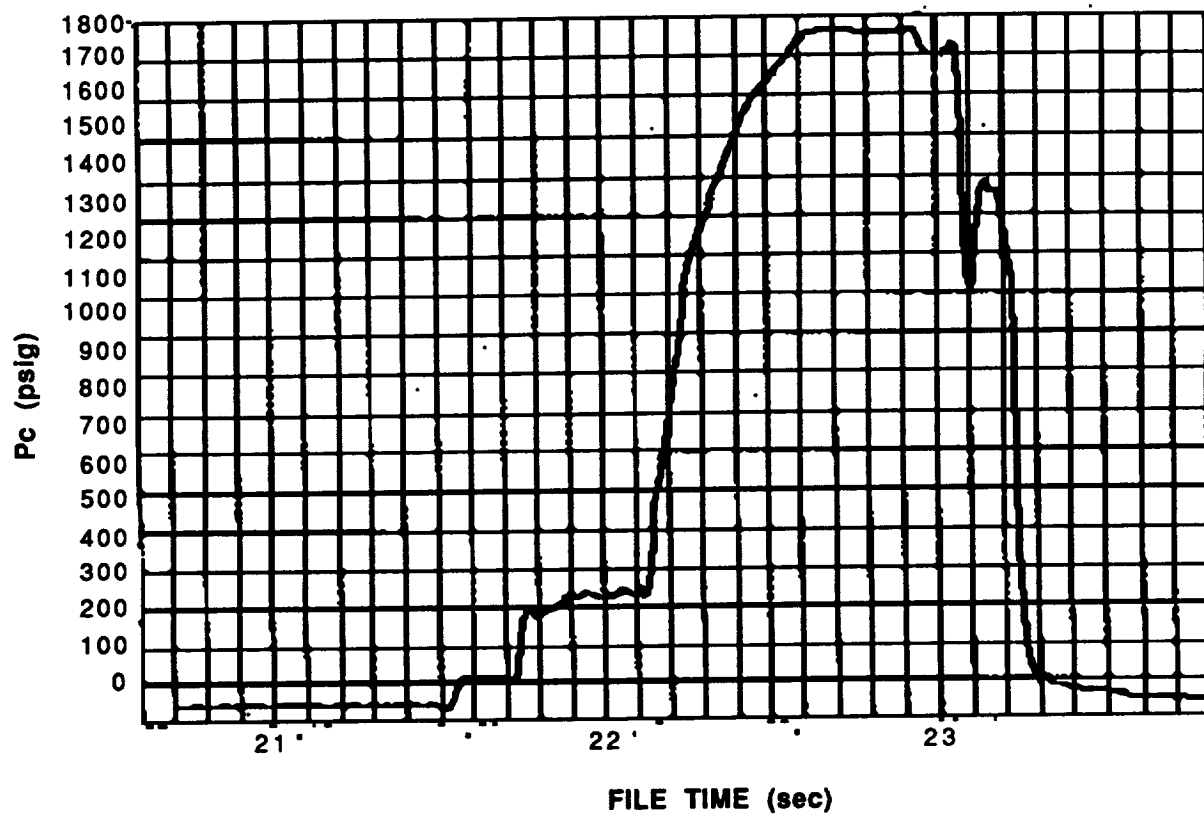


Figure 155. Static Chamber Pressure (Inj. End), Test 015-032, Box-Doublet Injector

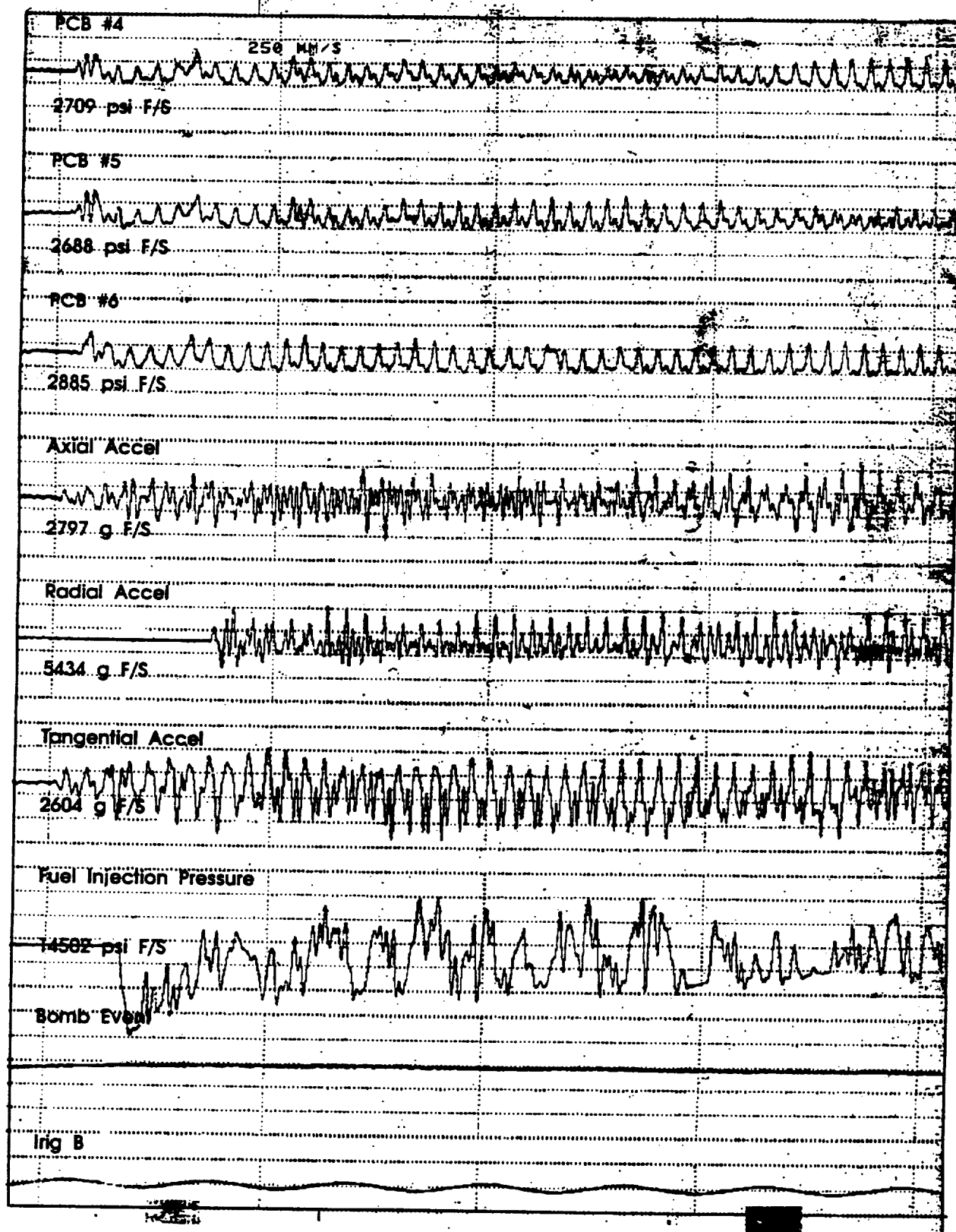


Figure 156. Test 015-032 High Frequency Data

14.2.1.2 Test 015-033

In the next test (015-033), the dynamic stability characteristics of the Box-Doublet injector were demonstrated at 1718 psia chamber pressure and 2.46 mixture ratio. Figure 157 contains a pressure trace of the test. As in the previous test, the bomb detonated as sequenced and triggered an instability in the 1T mode. The amplitudes of the bomb overpressure and subsequent oscillations were similar to those observed in Test 015-032. The test hardware was not damaged after this test.

14.2.1.3 Test 015-034

During the third test of this series (015-034), the data indicates that the stability bomb detonated prematurely during the start transient at about 1300 psia chamber pressure. The chamber pressure trace is shown in Figure 158. An instability was triggered in the 1T mode which lasted for approximately 300 milliseconds before cutoff. The cut signal was triggered by the TASCOS (Turbine Acceleration Safety Cut Off System) as soon as it was armed. Because of this event, past test high frequency data was reviewed to determine if the TASCOS could be armed earlier in the sequence without significant risk of an erroneous cut due to spurious signals during the start transient. It was decided to arm TASCOS 350 milliseconds earlier in future tests. At about 200 milliseconds after the premature bomb firing, the water cooled adapter for the chamber PCB-6 burned through resulting in a hot gas leak. Fifty milliseconds later, PCB-5 also burned through and 120 milliseconds after that the remaining PCB (-4) burned through. The relative timing of these events can be seen in the high frequency data, presented in Figures 159 and 160. Substantial erosion was sustained in the bomb spool which housed the three PCB adapters. In addition, the first calorimeter chamber section downstream of the bomb spool showed erosion to the water channels in two sections, and the throat section developed a water leak in the convergent section. It was decided to repair the damaged bomb spool and throat section while continuing to hot-fire test with existing back-up hardware.

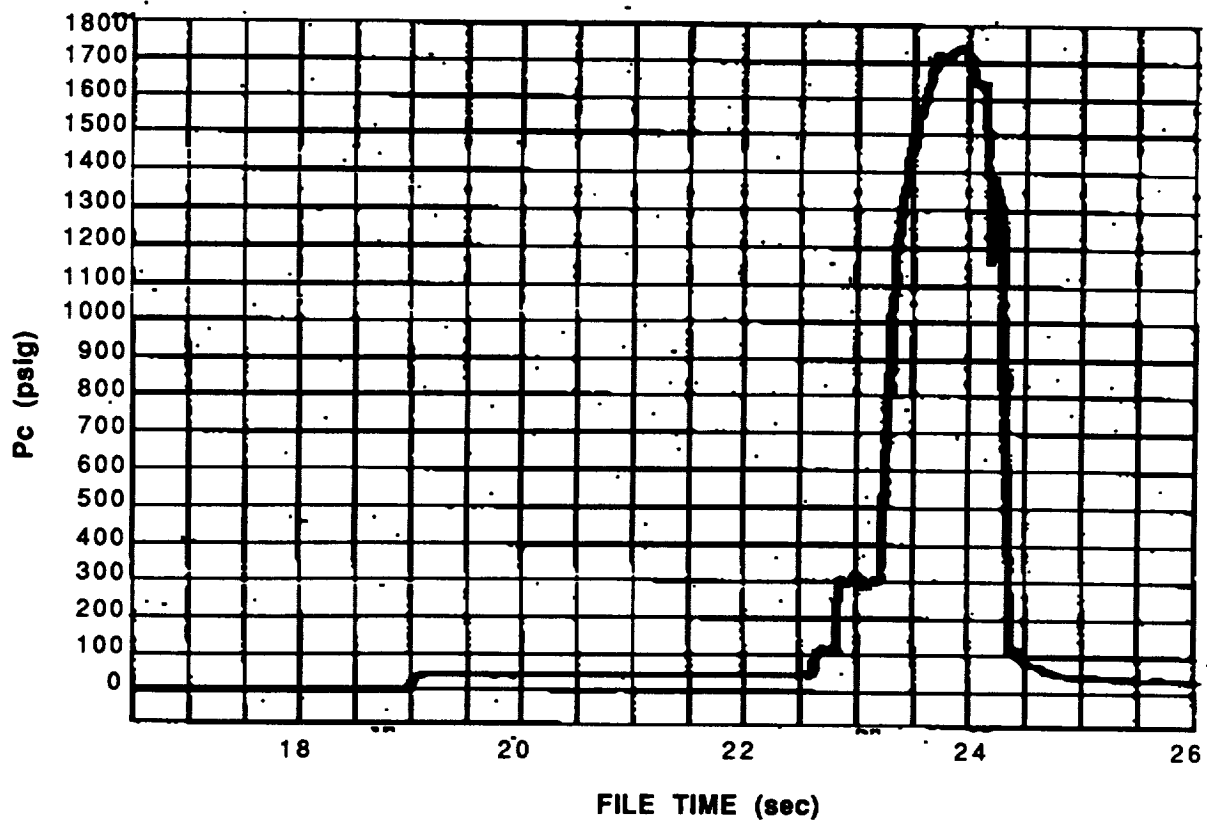


Figure 157. Static Chamber Pressure (Inj. End), Test 015-033, Box-Doublet Injector

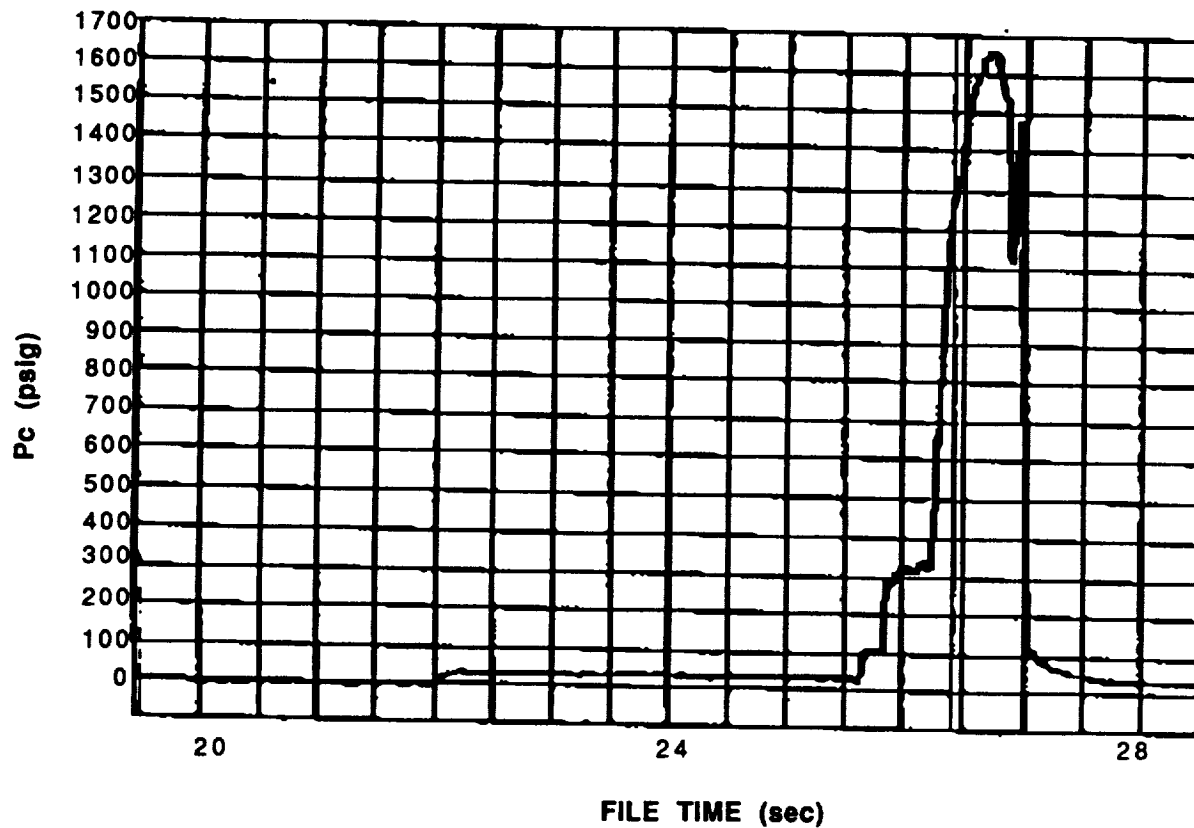


Figure 158. Static Chamber Pressure (Inj. End), Test 015-034, Box-Doublet Injector

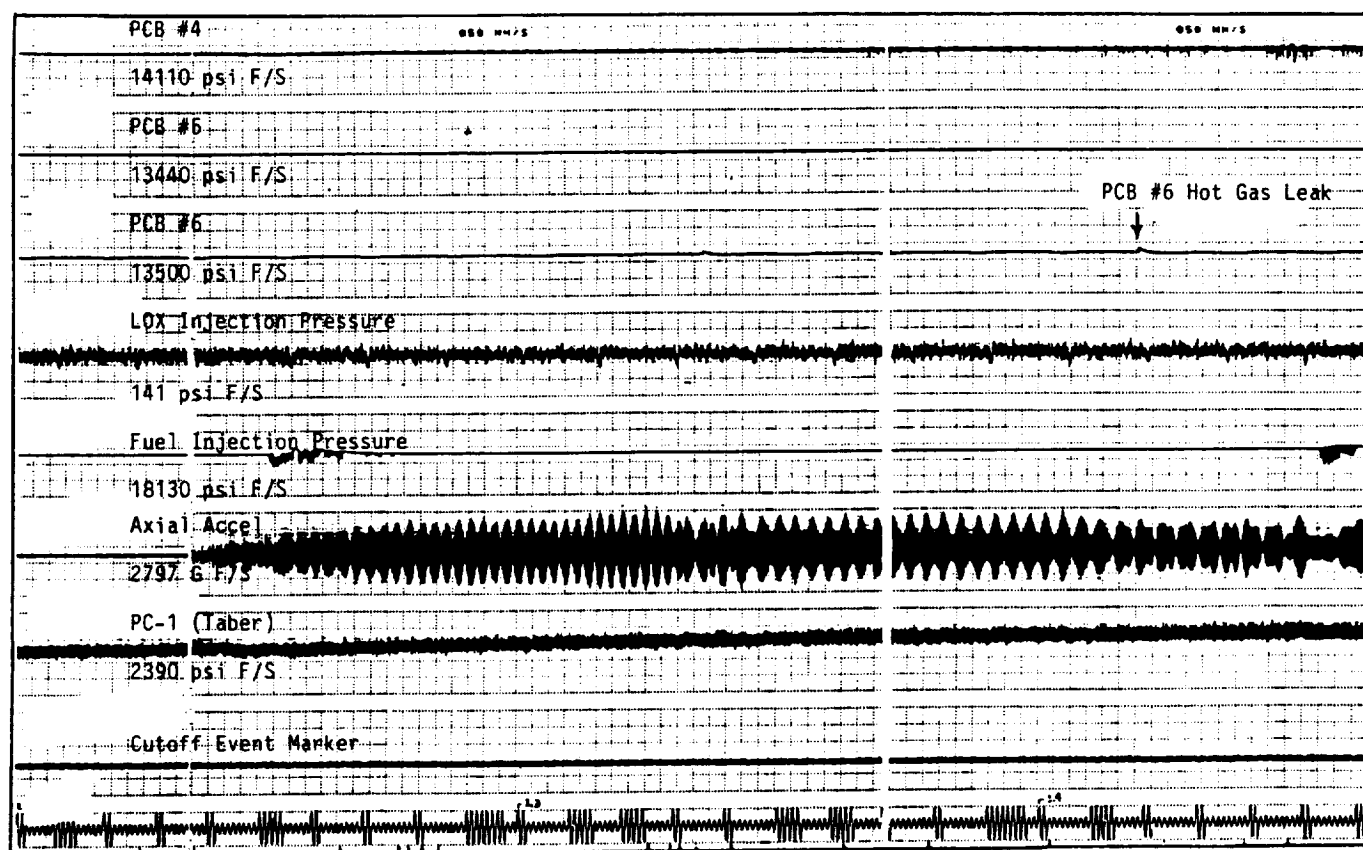


Figure 159. Test 015-034 High Frequency Data

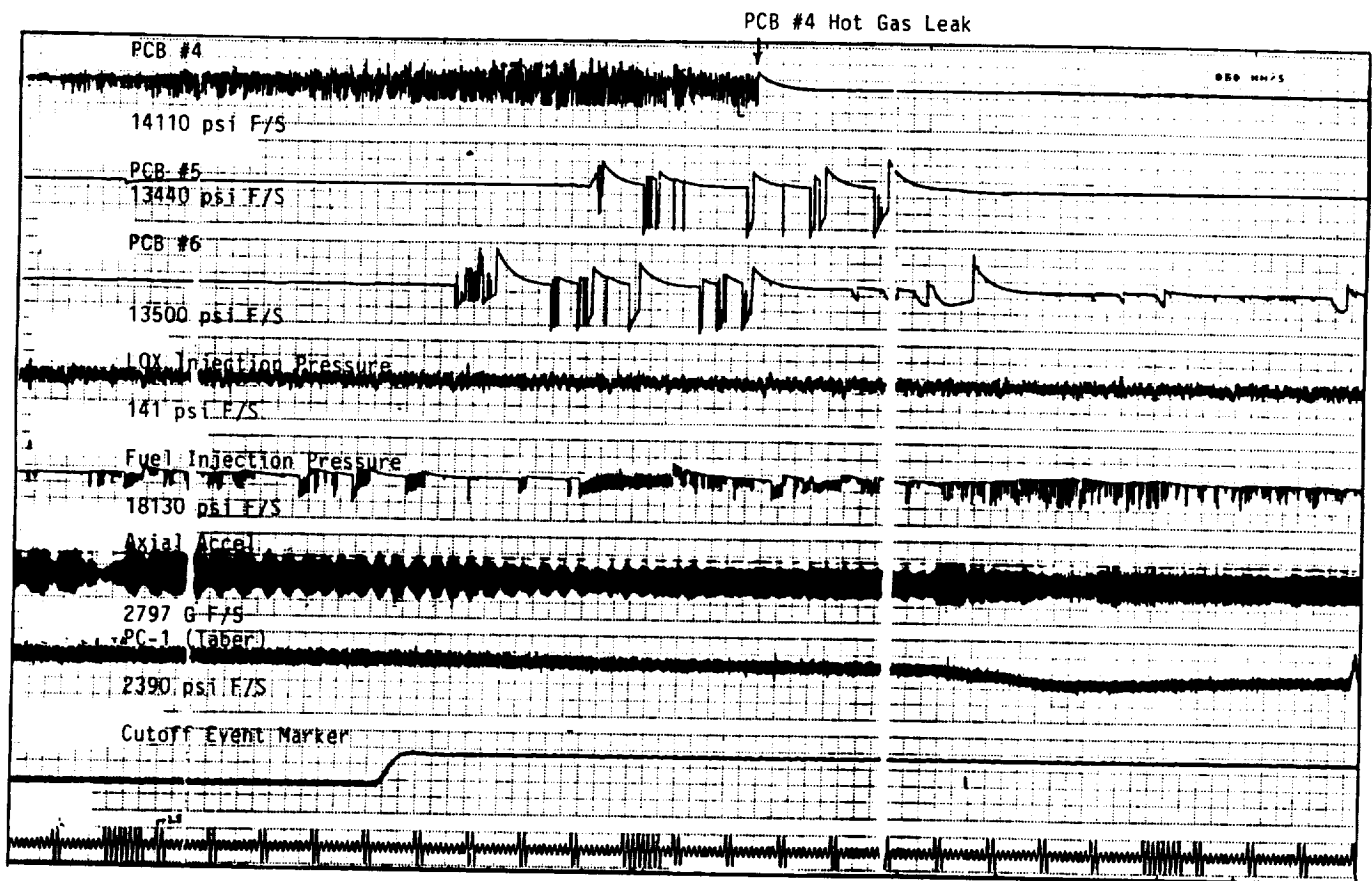


Figure 160. Test 015-034 High Frequency Data

14.2.2 PCB ADAPTER REDESIGN

The PCB water cooled adapters had a high attrition rate since the commencement of testing under Task III. Hot gas leaks had occurred in two previous tests through the adapters, and erosion of other adapters has been observed after hot fire tests. Detail drawings of the adapter were obtained from the vendor and the resultant examination of the part and the drawing suggested that the adapter was structurally inadequate for this application. As a result, Rocketdyne designed a more rugged adapter that utilizes a helium bleed for coolant of the transducer instead of low pressure water. The two designs are shown in Figure 161.

14.2.3 BOX-DOUBLET ACOUSTIC CAVITY TESTS

The purpose of the next tests were to determine the dynamic stability characteristics of the the Box-Doublet injector with the inclusion of a first tangential mode acoustic cavity. The acoustic cavity was sized to damp pressure disturbances in the 8000 Hz frequency range.

14.2.3.1 Test 015-035

During the first test (015-035), an unusual instability was observed. Previous dynamic stability tests indicated that bomb detonation with the Box-Doublet injector would result in an 8000 Hz first tangential instability. An 8000 Hz, 20% open area acoustic cavity had been incorporated with the Box-Doublet injector. During this test, the bomb detonated prematurely, just after reaching mainstage, resulting in an instability with a frequency of 5700 Hz. The injector-end chamber pressure is presented in Figure 162. The maximum amplitude of the pressure oscillations was 500 psi peak-to-peak, which is approximately one third of that measured during Test 015-015, which exhibited a pure 8000 Hz 1T instability. The data for this test is displayed in Figures 163, 164, 165 and 166. The pressure measurements for Test 015-035 are particularly interesting with respect to the measured frequency. The pressures measured with PCB-4 and PCB-5 are not as similar to each other as they were in test 015-015, and do not indicate the same modal dependence throughout the test. Based on the pressure measurements, the bomb detonation was followed by a first longitudinal mode decreasing in pressure amplitude. A high frequency signal (~18,000 Hz) is transposed on the initial pressure signal. At a distinct time, PCB-5 began to measure the 5700 Hz disturbance while PCB-4 still displayed a dominant 1L mode. As the test progressed both transducers displayed the 5700 Hz disturbance. This particular instability is not well understood and some hypotheses are presented later in this report.

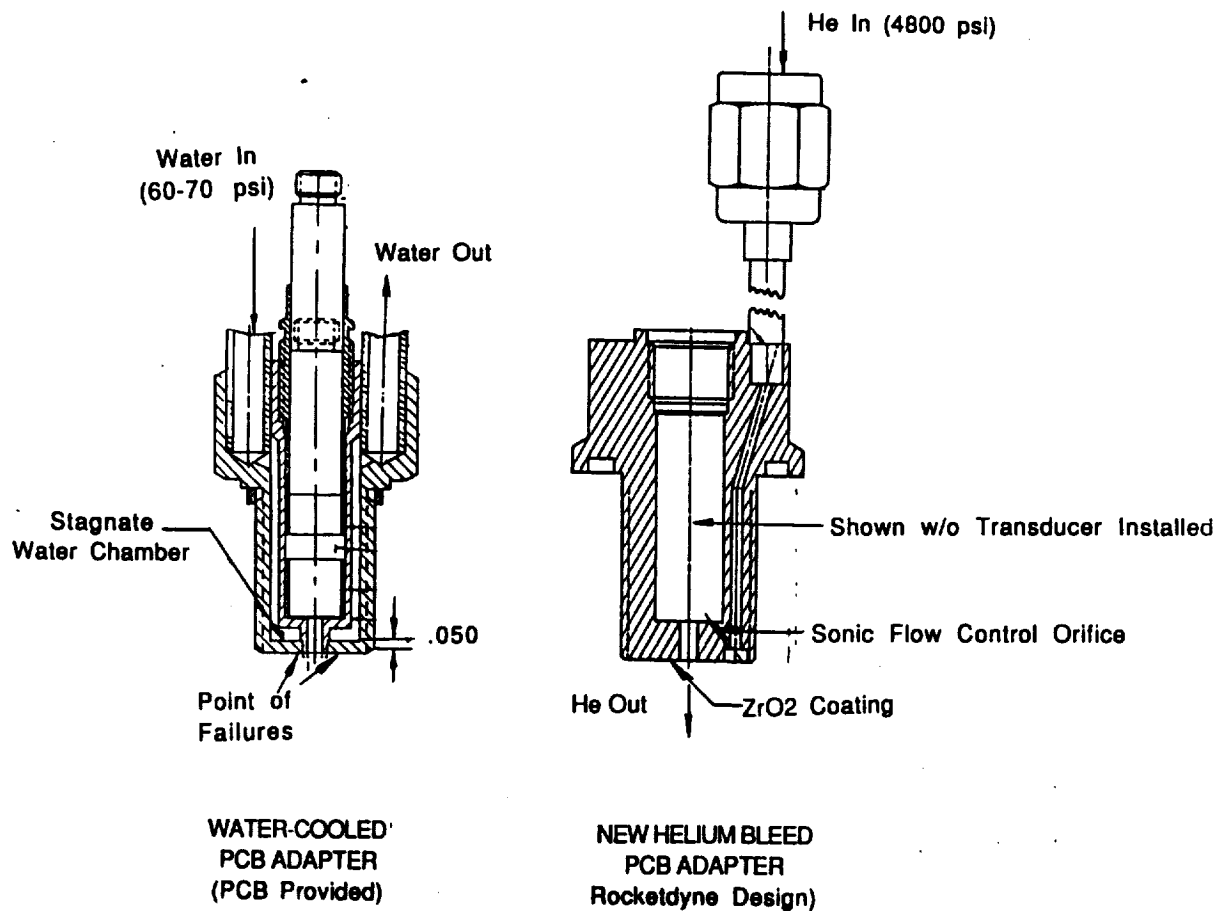


Figure 161. PCB Adapter Design

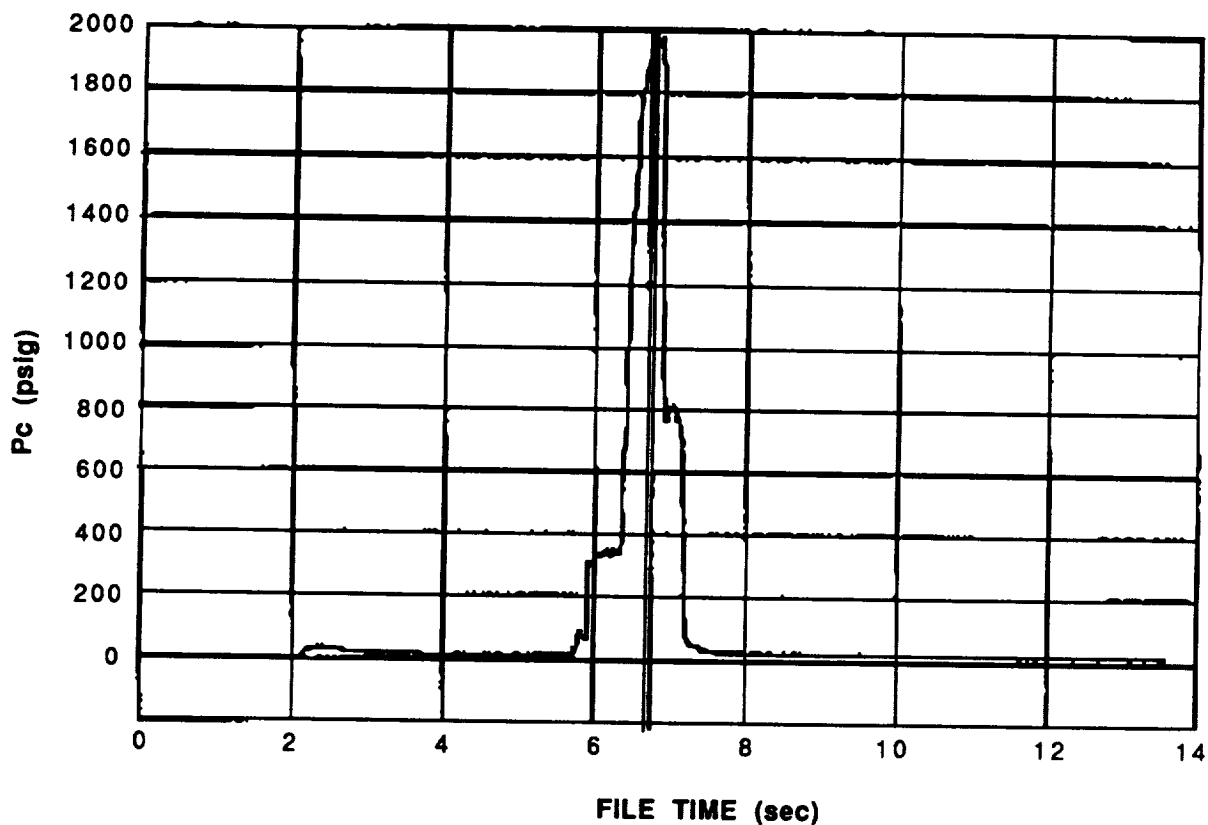


Figure 162. Static Chamber Pressure (Inj. End), Test 015-035, Box-Doublet Injector

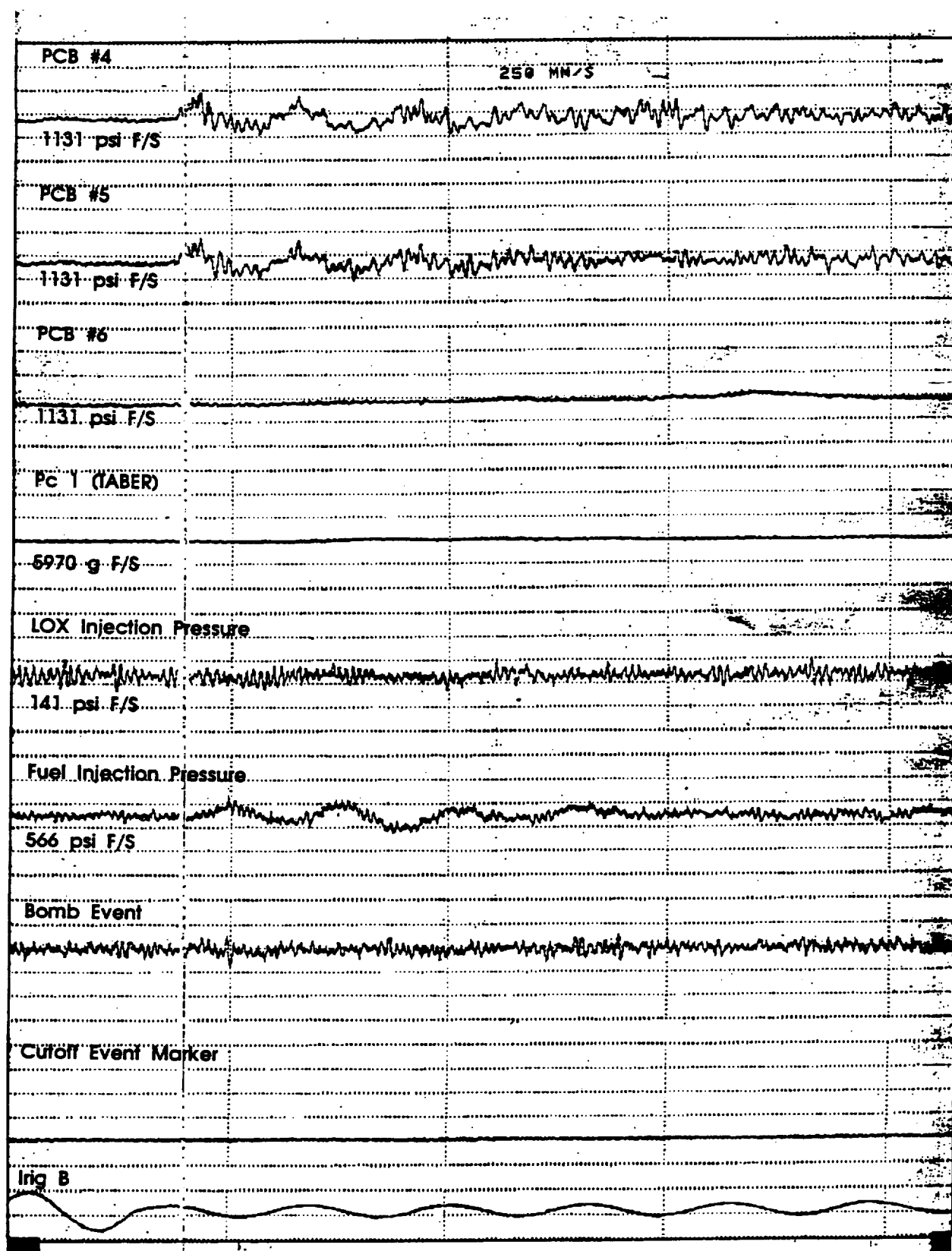


Figure 163. Test 015-035 High Frequency Data

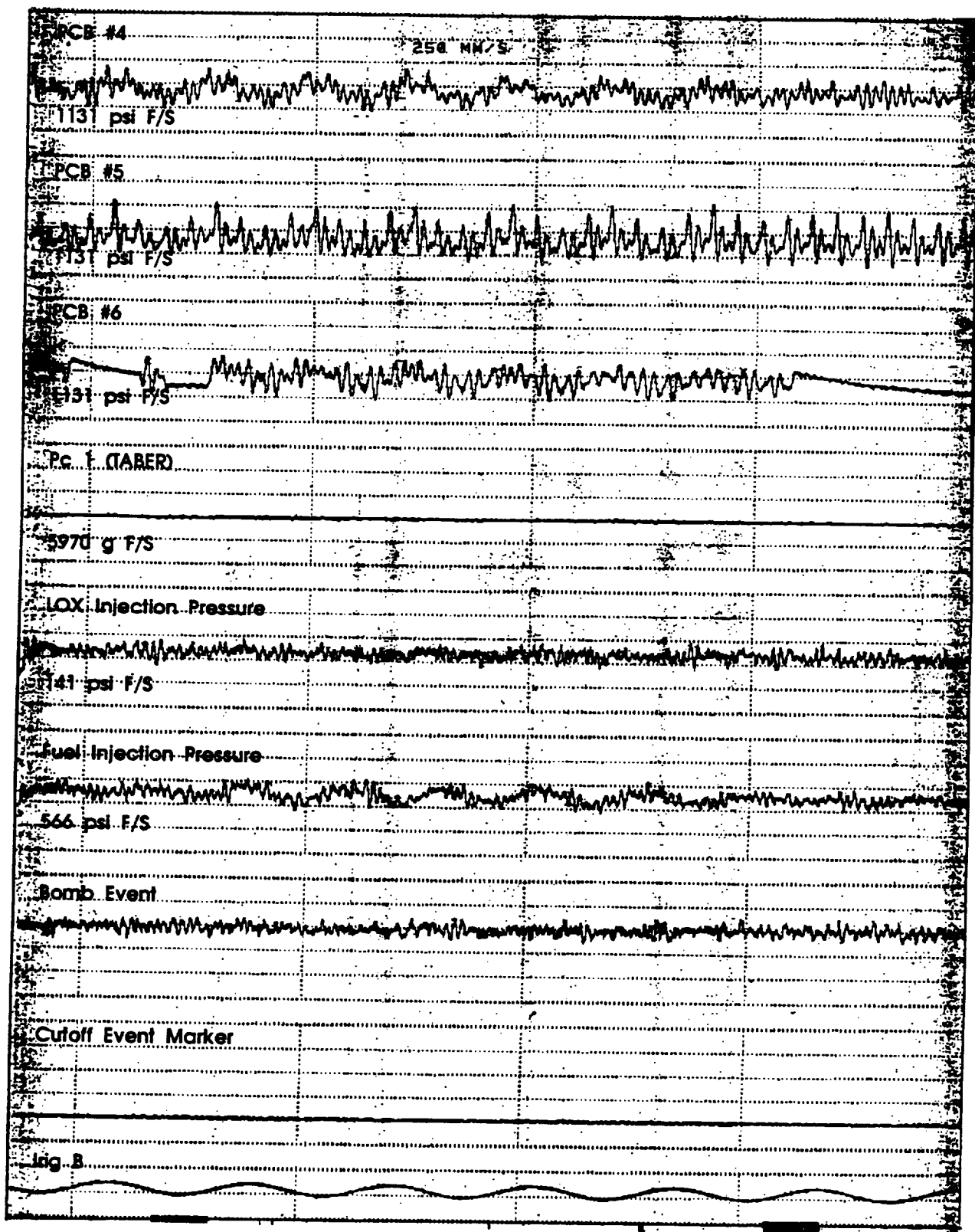


Figure 164. Test 015-035 High Frequency Data

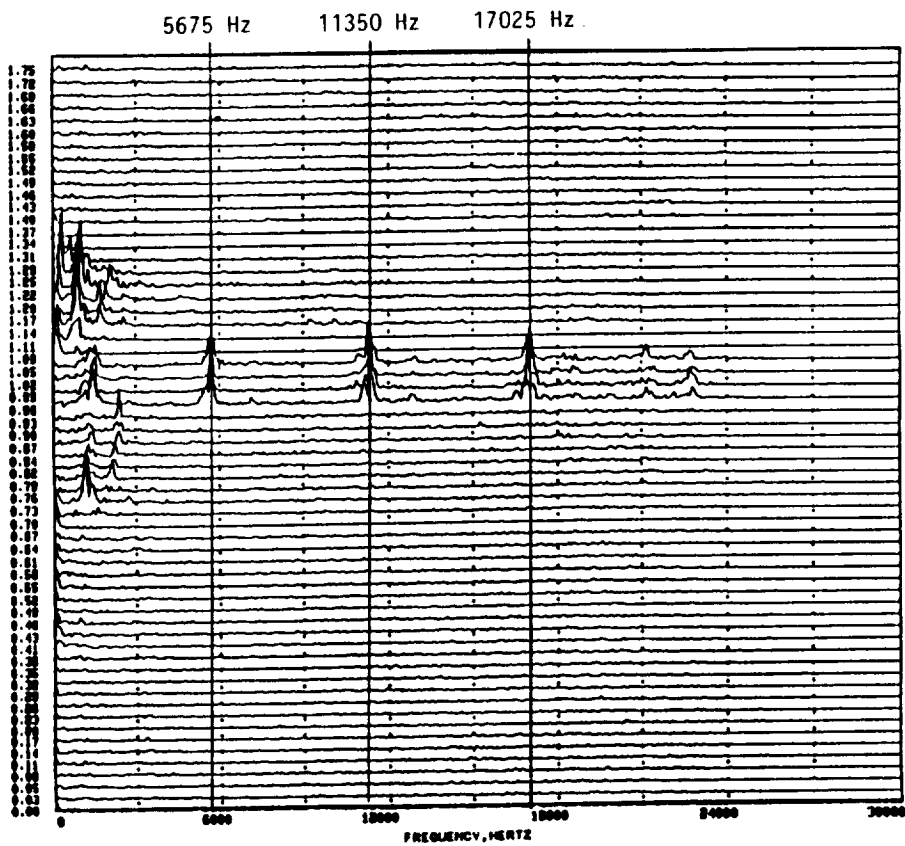


Figure 165. Test 015-035 PCB #4 Isoplot

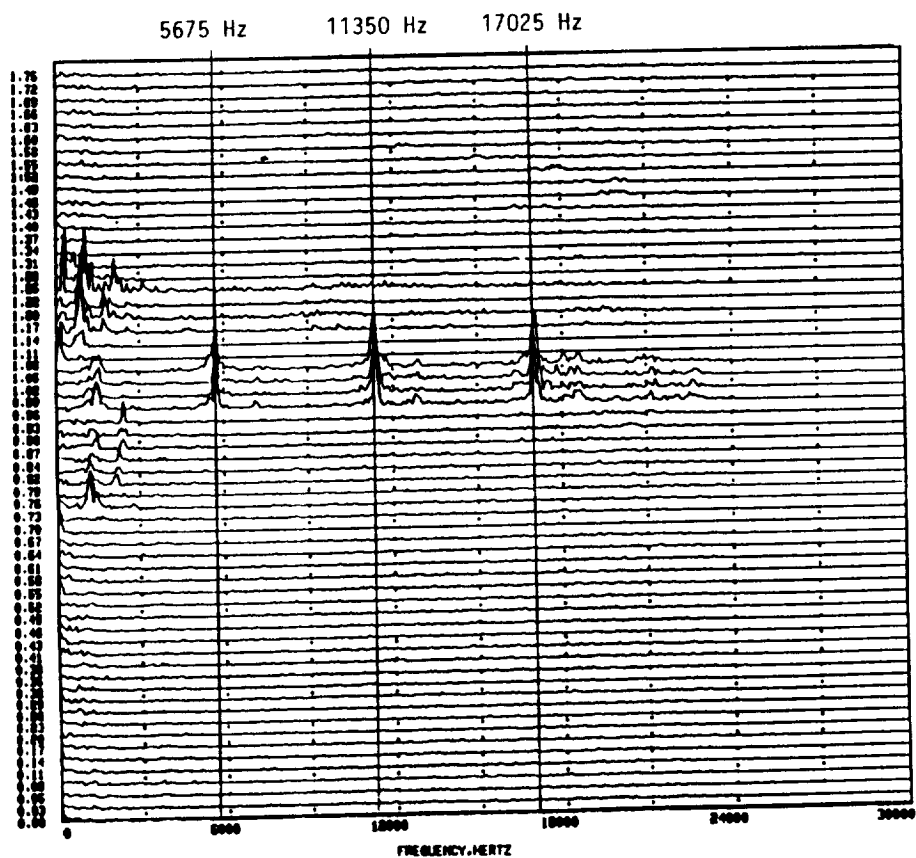


Figure 166. Test 015-035 PCB #5 Isoplot

The predicted bandwidth of the acoustic cavity used in Test 015-035 is displayed in Figure 167. The center curve represents the best prediction of the cavity bandwidth. A line has been drawn at the 5700 Hz frequency to show that this instability occurred at a location which is considered to be outside of the cavity bandwidth, which indicates a possible cause of the instability, but does not isolate the specific mechanism.

The acoustic cavity temperature values were also measured during Test 015-035 and are presented in Figure 168. The general location of the thermocouples is also displayed in the figure. This data indicates a temperature profile exists in the cavity backing volume such that the gas temperature linearly decreases with radial distance from the chamber hot gas wall. One of the key issues regarding acoustic cavity design is the approximation which is usually made regarding the thermal and acoustical environment existing in the cavity. The data presented in Figure 168 may be useful in future modeling efforts.

The results which were obtained during Test 015-035 indicate that the driving mechanisms (injection, atomization, vaporization and mixing) associated with instabilities while utilizing LOX/RP-1 propellants have a wide bandwidth. The 5700 Hz instability is not easily explained. Some hypotheses are as follows:

- 1) The vaporization process is slightly coupled with the chamber 1T acoustics (outside of the cavity bandwidth) and is able to drive the 5700 Hz wave motion.
- 2) The combustion process is coupling with the injection process which is characterized by the propellant flight time from injection to impingement.
- 3) The instability may simply be a 1T instability the frequency of which has been suppressed due to the inclusion of the 1T acoustic cavity.

Due to the unexpected results of Test 015-035, continuation of testing in accordance with the original test matrix, was no longer appropriate. Due to the flexibility of the test matrix, a modification was made and approved by MSFC personnel, and is displayed in Figure 169. The plans were to conduct the next series of tests with bi-tuned acoustic cavities (5% open area tuned to 5700 Hz and 8% open area tuned to 8000 Hz) in an effort to eliminate the 5700 Hz instability. If these tests demonstrate stable characteristics, testing would have continued with reduced open area cavities, as previously planned.

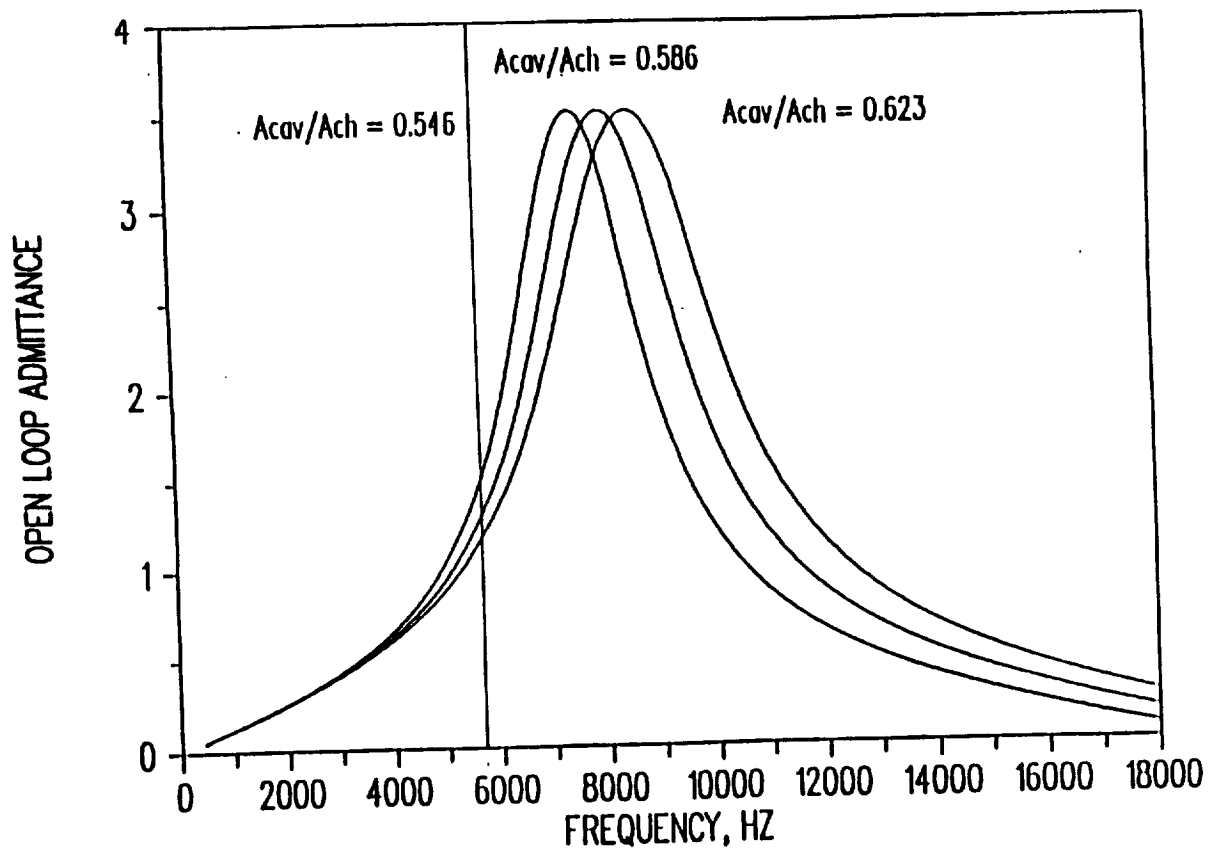


Figure 167. Predicted Cavity for Test 015-035

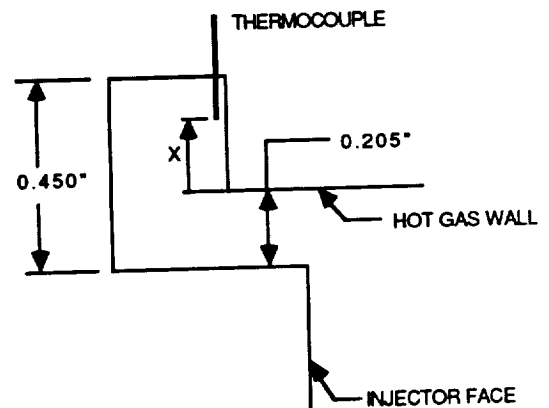
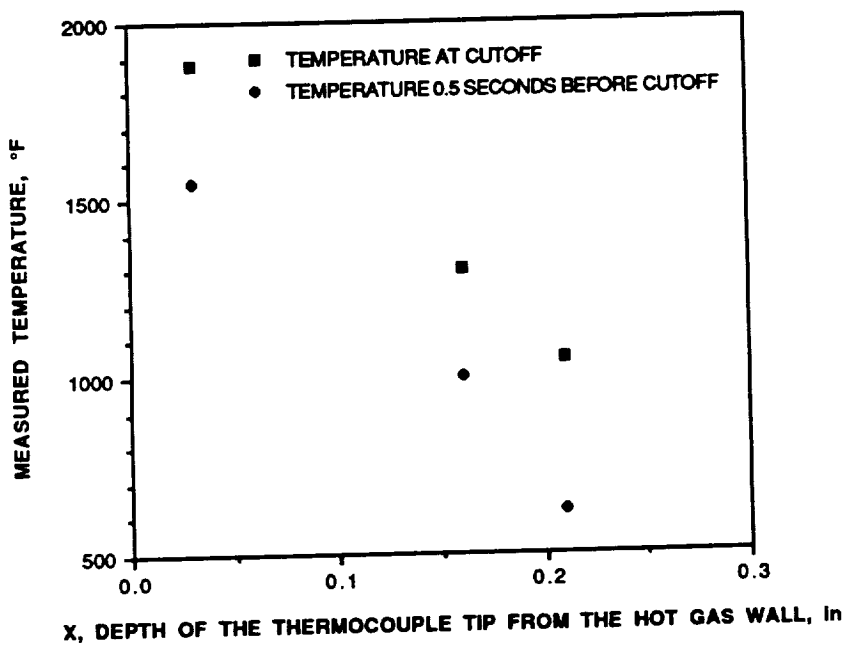
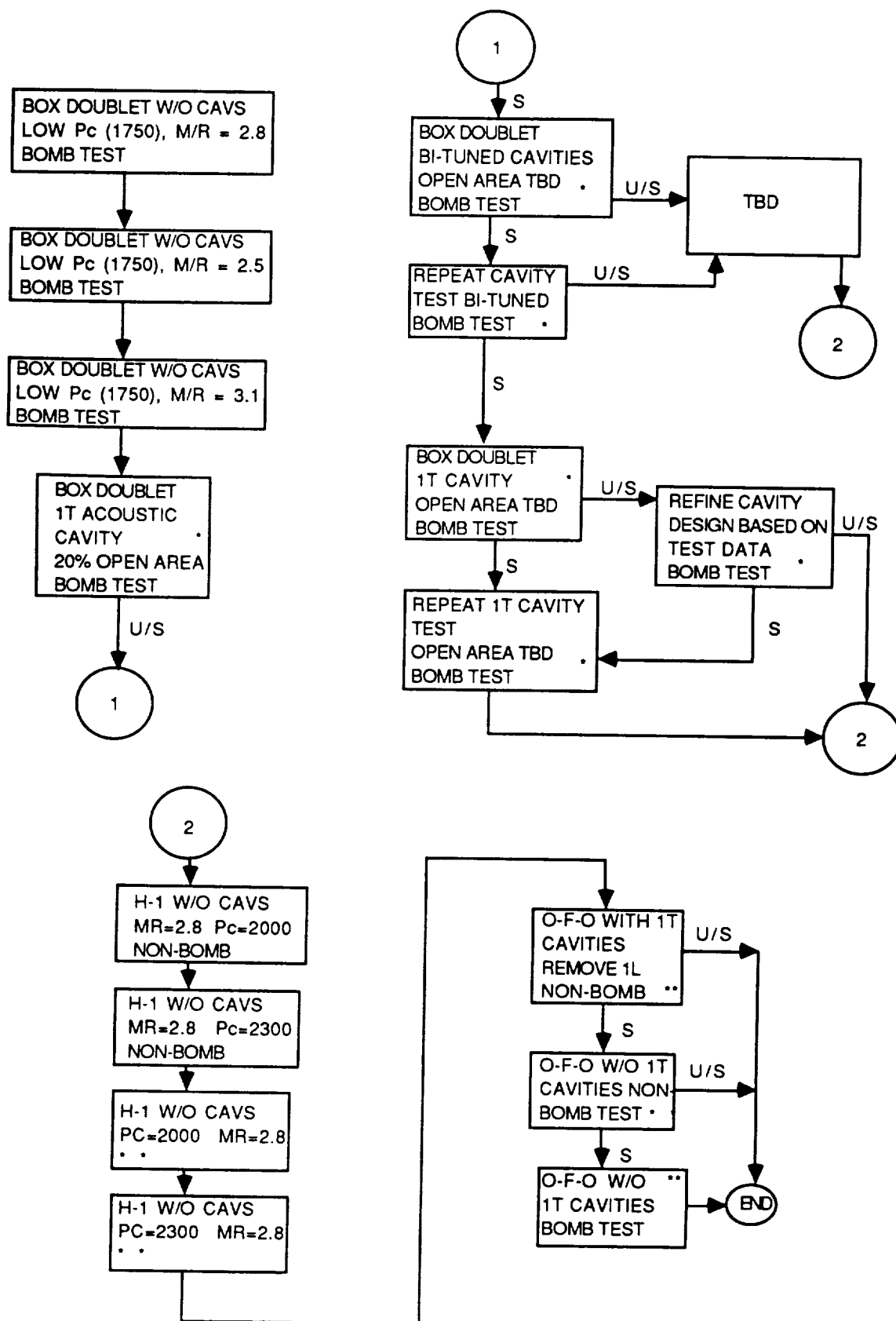


Figure 168. Test 015-035 Acoustic Cavity Temperature



* Pc = 2000 psi, M/R = 2.8 ** CHAMBER LENGTH = 13.4 INCHES

Figure 169. Modified Task III Test Matrix

14.2.3.2 Test 015-036

Test 015-036 was a dynamic stability test which included the Box-Doublet injector with the bi-tuned acoustic cavity. The injector end pressure trace of this test is presented in Figure 170. The time dependent high frequency data for Test 015-036 is shown contiguously in Figures 171 and 172. The frequency dependent data is shown for pressure transducers 4 and 5 in Figures 173 and 174, respectively. During this test, the cavities were effective in damping the transverse modes and the dominant mode of oscillation was a 1300 Hz first longitudinal mode. At the end of the test, the 5700 Hz disturbance was observed which is believed to be due to erosion of the acoustic cavity ring and retuning of the cavities to an 8000 Hz configuration. Nominal operating conditions for this test included a chamber pressure of 2021 psia (nozzle stagnation) and a corrected c-star efficiency of 95.9%.

During the design of the acoustic cavity ring, the cavity was designed for a minimum frequency of 8000 Hz with 20% open area. In order to design the cavity for 5700 Hz, a compromise had to be made by reducing the total cavity open area. The design of the 5700 Hz cavity involved reducing the total cavity open area. The design of the 5700 Hz cavity involved reducing the aperture width of the cavity and maintaining the same cavity backing volume. This effectively reduced the resonant frequency of the acoustic cavity. In the final configuration, there was 8% cavity open area tuned to 8000 Hz and 5% cavity open area tuned to 5700 Hz. These results were generated with a 2-D cavity acoustic model, which is required for the aforementioned design iteration. Based on the test results, it would appear that the acoustic cavity model gives predictive design dimensions.

14.2.4 H-1 DERIVATIVE PERFORMANCE TESTS

Since the H-1 Derivative injector met the ICC requirements, further testing was performed to investigate the vaporization limits of the injector with respect to chamber pressure and combustor length.

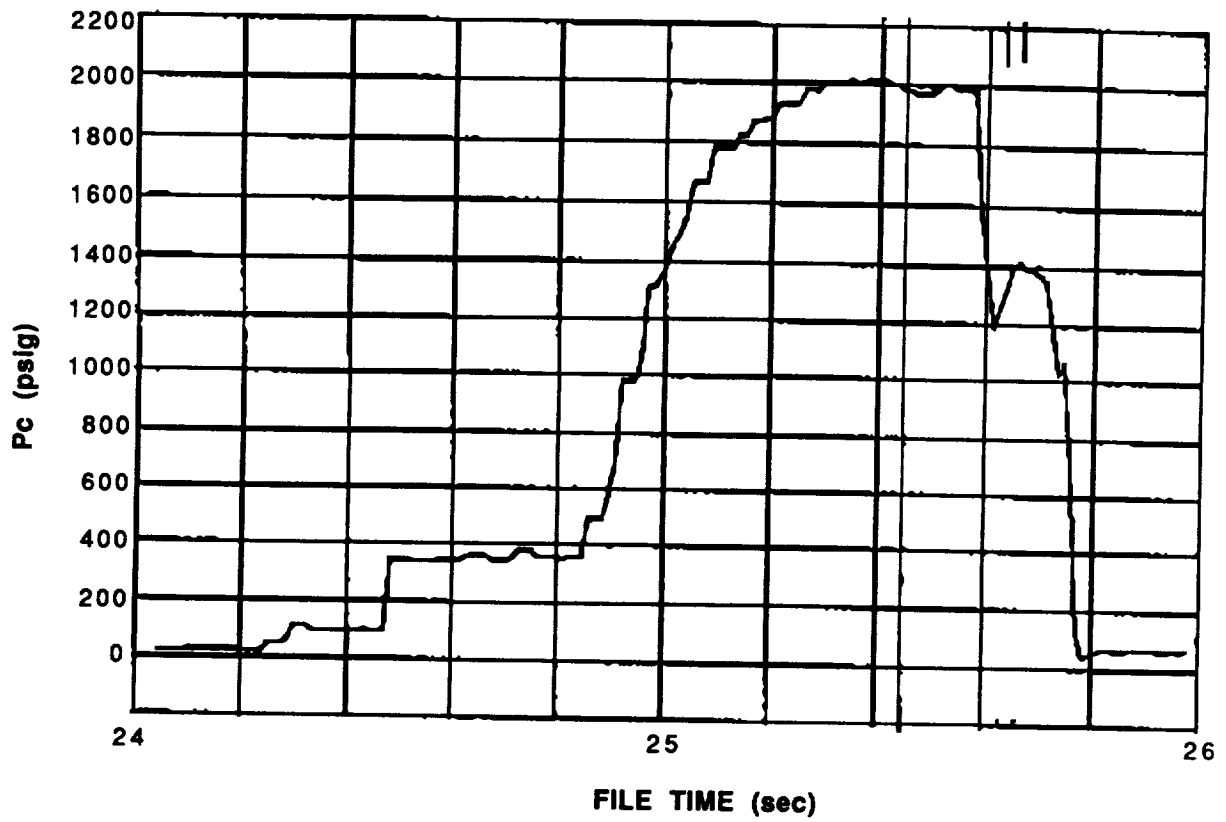


Figure 170. Static Chamber Pressure (Inj. End), Test 015-036, Box-Doublet Injector

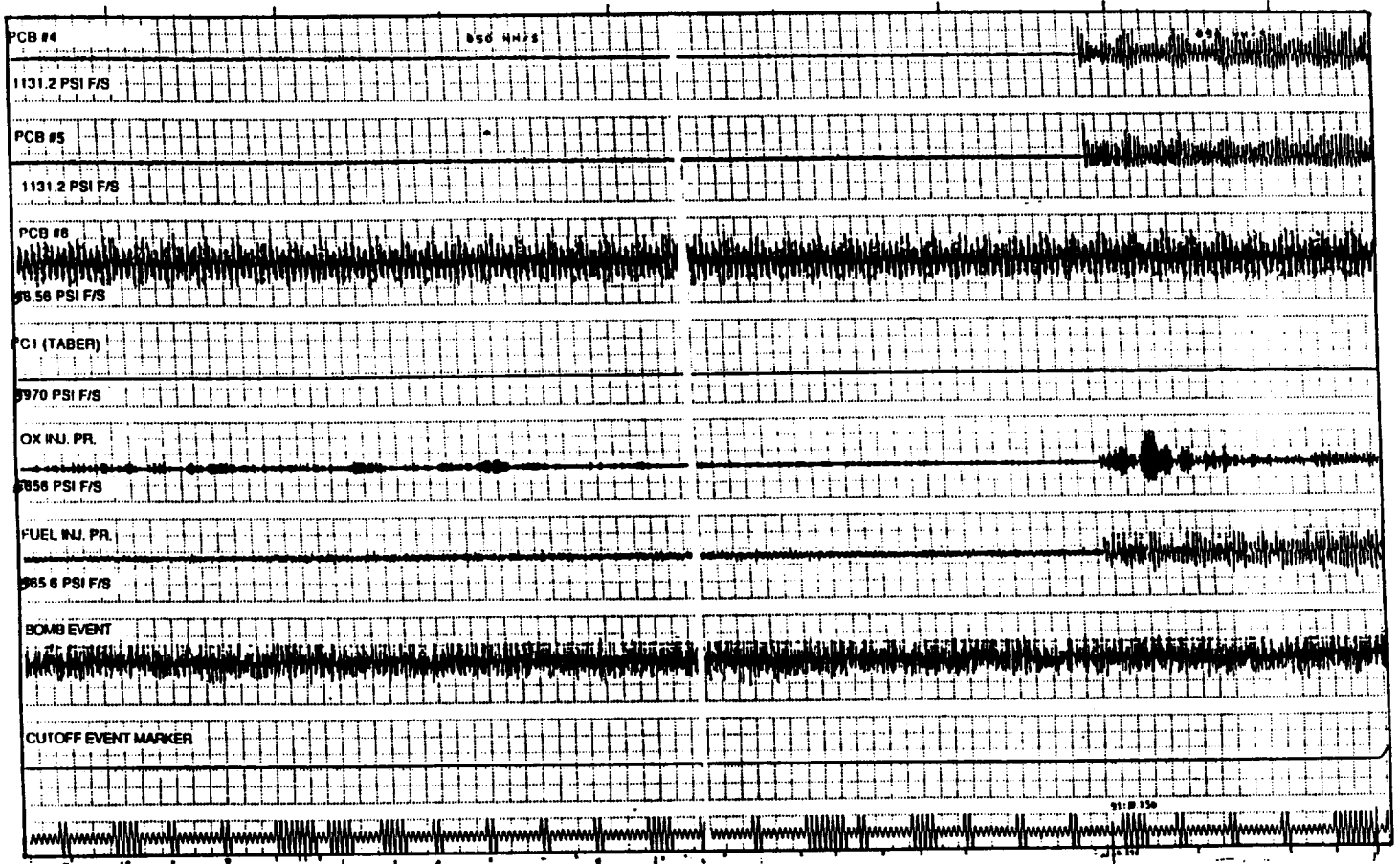


Figure 171. Test 015-036 High Frequency Data

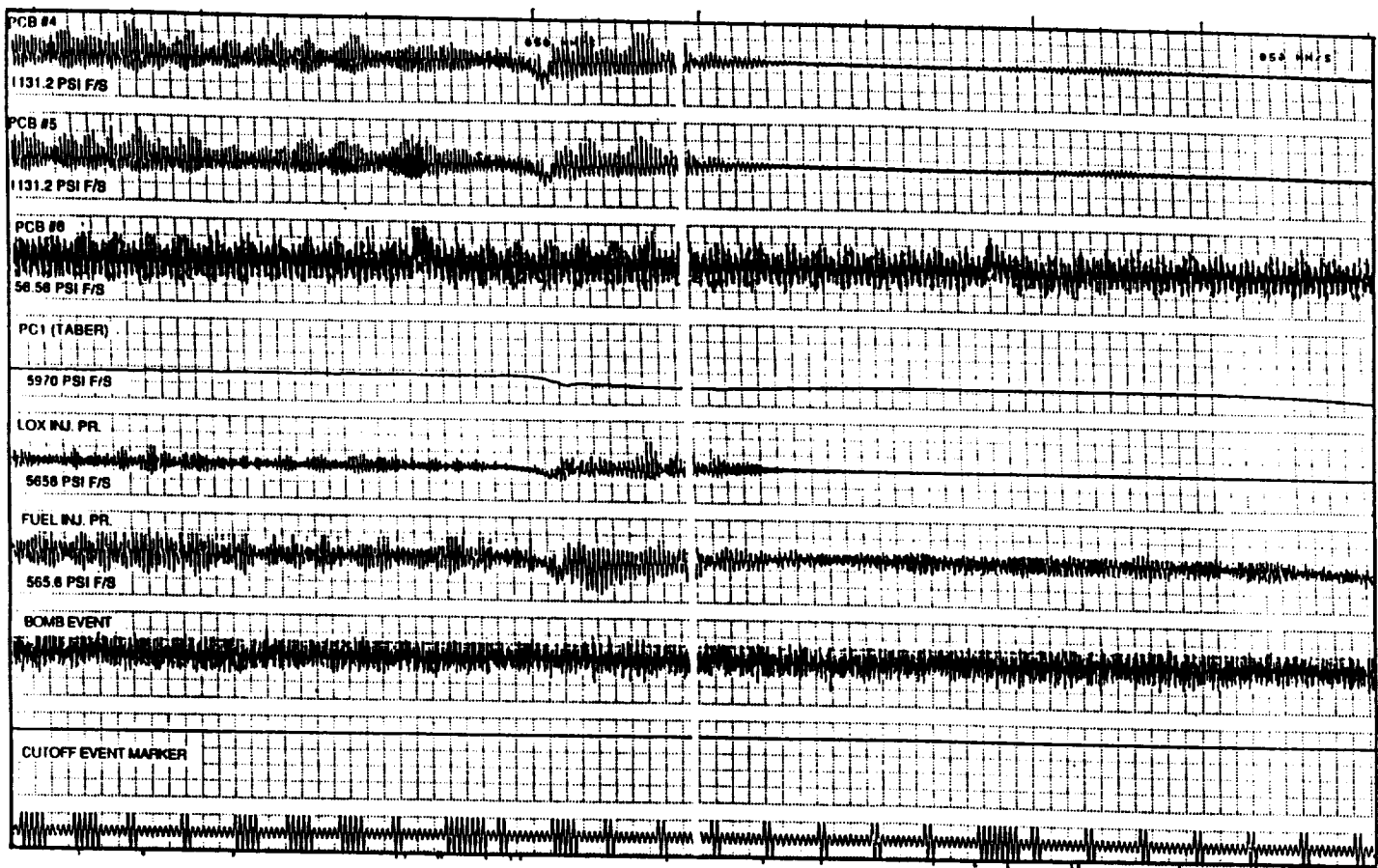


Figure 172. Test 015-036 High Frequency Data

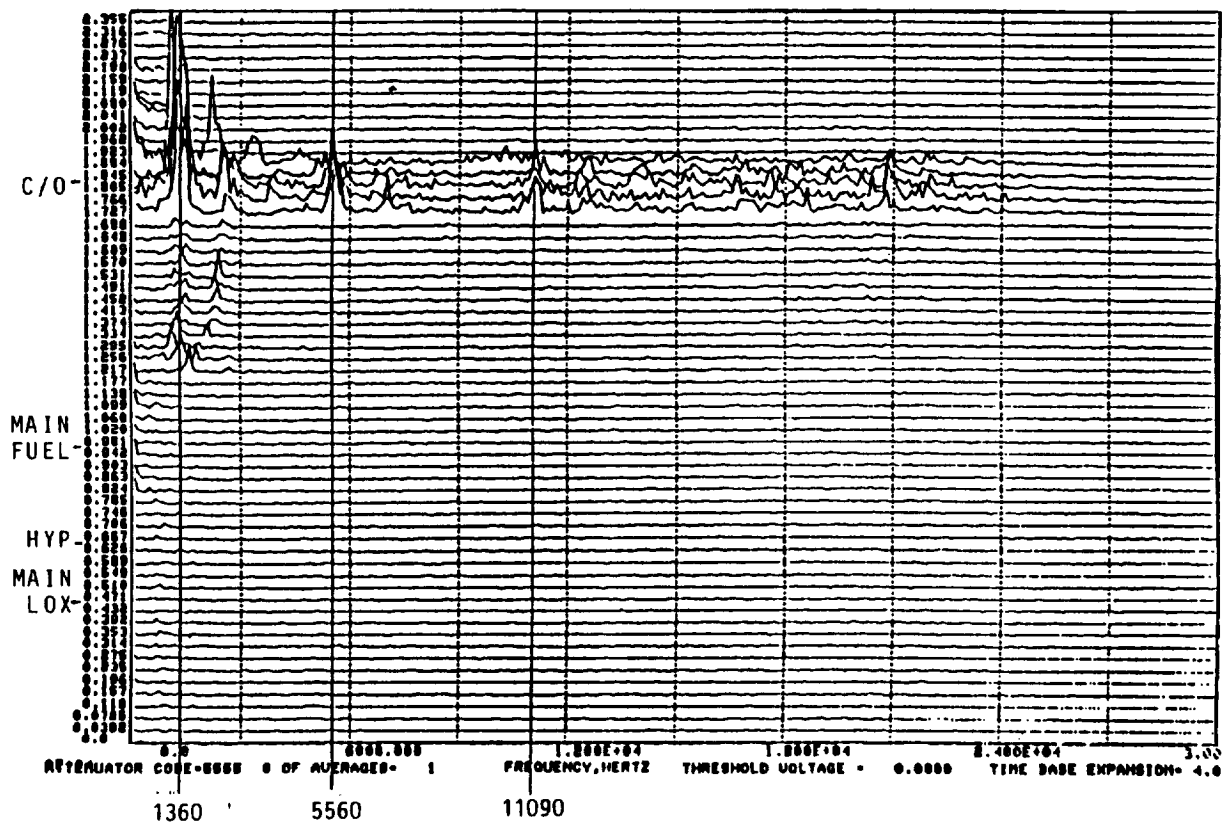


Figure 173. Test 015-036 PCB #4 Isoplot

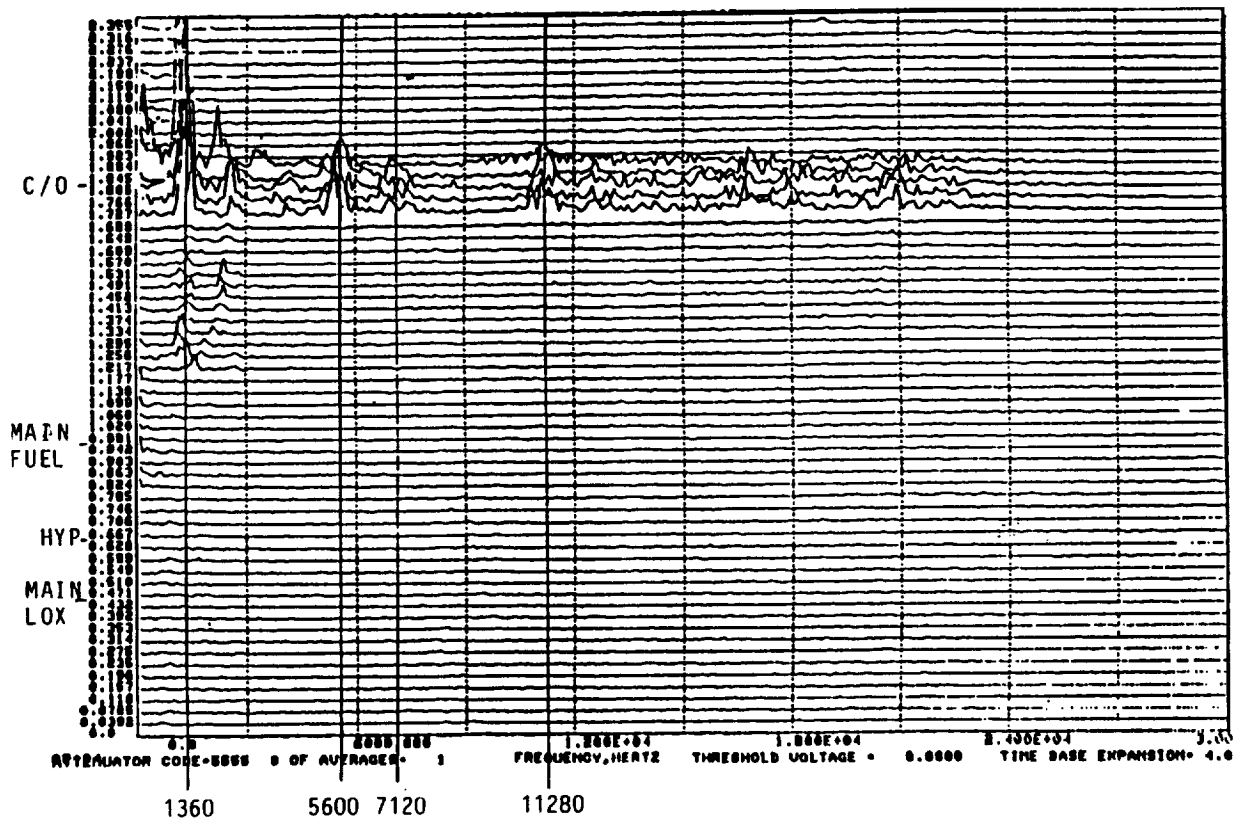


Figure 174. Test 015-036 PCB #5 Isoplot

14.2.4.1 Test 015-038

Test 015-038 was performed to further establish the baseline operating conditions while utilizing the H-1 Derivative injector at 2000 psia chamber pressure and a 2.8 mixture ratio. The results of Test 015-038 include a chamber pressure of 1998 psia (nozzle stagnation) and a corrected c-star efficiency of 97.7%. The injector-end chamber pressure CRT is shown in Figure 175.

14.2.4.2 Test 015-039

Test 015-039 was also an H-1 Derivative injector performance test, but the targeted chamber pressure was 2300 psia (nozzle stagnation). The results of test 015-039 include a chamber pressure of 2291 psia (nozzle stagnation) and a corrected c-star efficiency of 98.3%. The injector-end chamber pressure CRT is shown in Figure 176. As evidenced by the test data, the H-1 Derivative injector displayed slightly higher performance at the higher chamber pressure, which is within the range of data "scatter" that has been observed with this injector. All of the data collected up to this time with the H-1 Derivative injector had been with a 19.4 inch long combustor. Testing with a shorter chamber (13.4") was planned next to increase the current vaporization data base.

14.2.4.3 Test 015-041

Test 015-041 was performed as a continuation of the performance test series with the H-1 Derivative injector. Test 015-041 was conducted with a 13.4 inch chamber length in order to establish the vaporization limits of this injector pattern. The injector had previously been modeled on the SDER computer code and results indicated a 1.5% decrease in performance in reducing the chamber length from 19.4 to 13.4 inches. The injector-end pressure trace of Test 015-041 is shown in Figure 177. The corrected c-star efficiency was 97.1% at 2000 psia chamber pressure and 2.8 mixture ratio. The performance values from these tests were within the range of data "scatter" that has been measured with this injector. Since no significant change in performance was observed with the shorter chamber length, further testing in this series was considered unnecessary. The next test series was performed at off nominal operating conditions with the Box-Doublet injector, with and without acoustic cavities, in an attempt to isolate the mechanism of the unstable combustion.

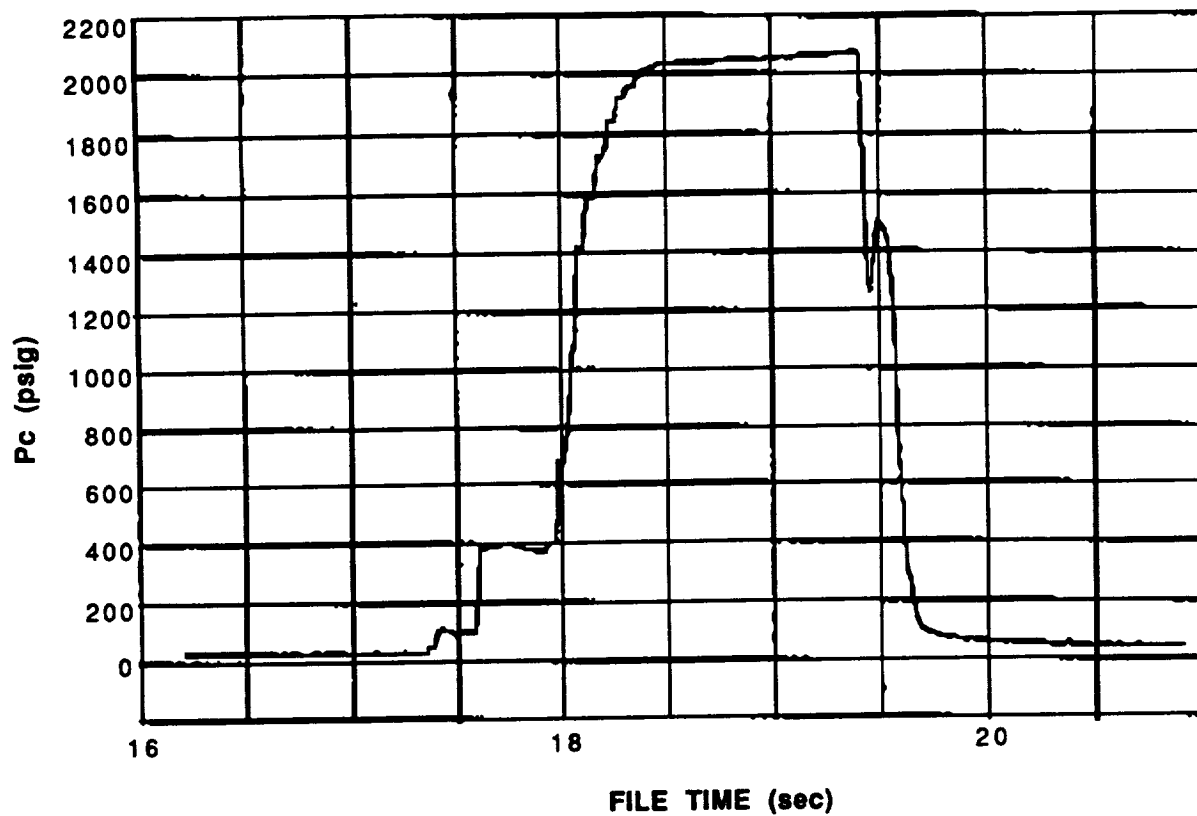


Figure 175. Static Chamber Pressure (Inj. End), Test 015-038, H-1 Derivative Injector

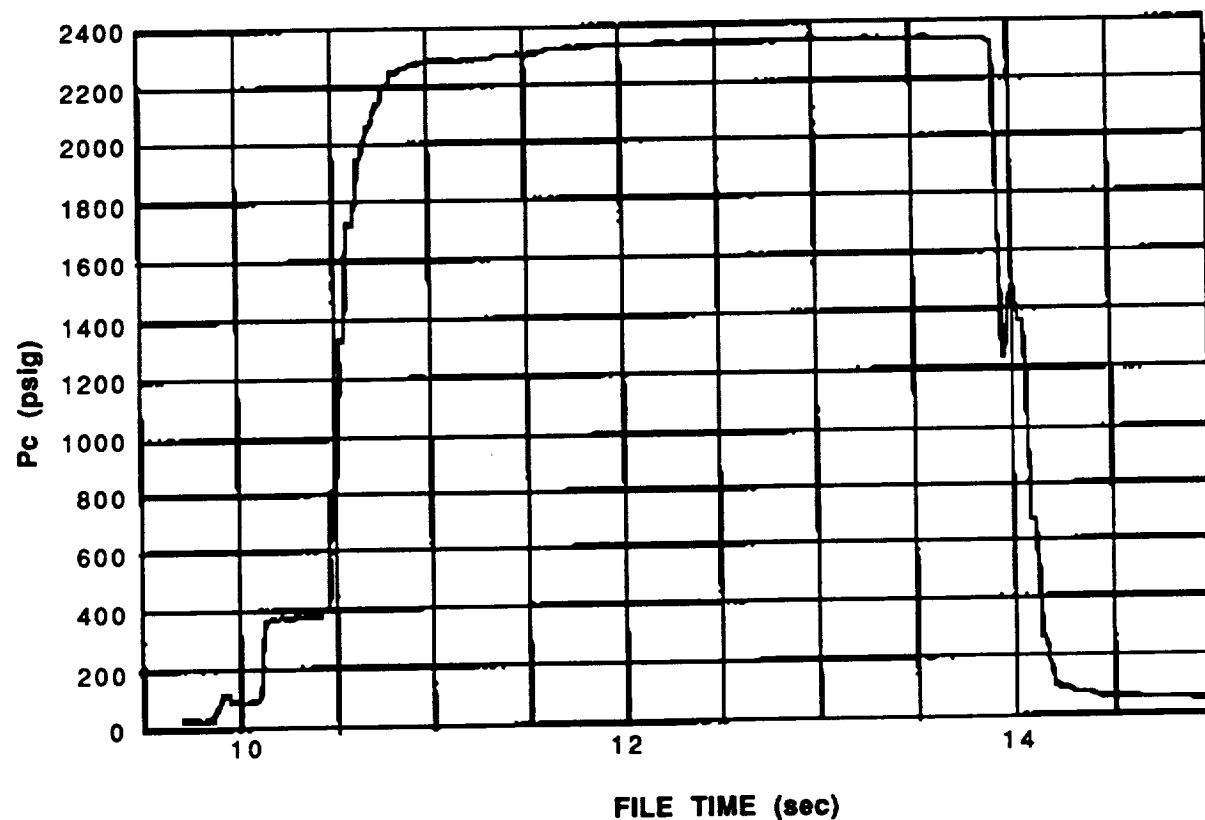


Figure 176. Static Chamber Pressure (Inj. End), Test 015-039, H-1 Derivative Injector

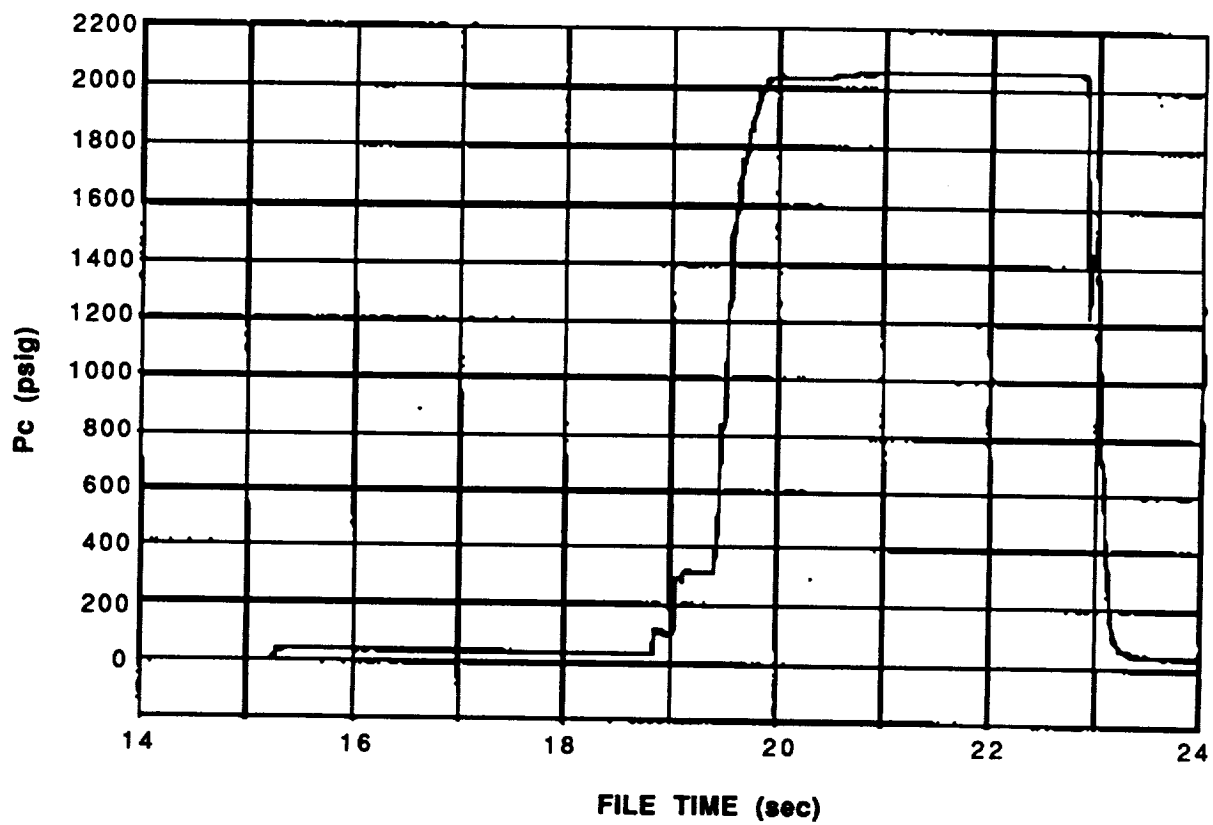


Figure 177. Static Chamber Pressure (Inj. End), Test 015-041, H-1 Derivative Injector

14.2.5 BOX-DOUBLET, INSTABILITY MECHANISM INVESTIGATION

After the initial screening tests were performed in Task III of this program, an analytical investigation was conducted to determine the mechanistic stability differences between the H-1 Derivative injector, which was dynamically stable, and the Box-Douplet and Circumferential-Fan injectors, which were dynamically unstable. At this point, the program was focused on continuing analysis and testing of both a stable injector and an unstable injector. The stable injector was the H-1 Derivative and the unstable candidates were the Box-Douplet and the Circumferential-Fan injectors. The Circumferential-Fan injector could not be tested without considerable rework due to hardware damage and erosion incurred during previous testing. Therefore, the Box-Douplet injector was down-selected for further study. An analysis was performed on the H-1 Derivative and Box-Douplet injectors which focused on the initial drop size and relative velocities (drops and combustion gas) of the two injectors.

Figure 178 shows the SDER predicted drop size values of the H-1 Derivative and Box-Douplet injectors at various axial locations and chamber pressures at 2.8 mixture ratio. The predictions indicate that the average nominal H-1 Derivative injector fuel drop size at 2000 psia P_c is 280 microns at 0.5-inch downstream of the injector. The predicted average nominal Box-Douplet injector drop size at 2000 psia P_c is 180 microns at the same axial location. The Box-Douplet injector is predicted to have fuel drop sizes of 190 and 210 microns at 1500 and 1000 psia chamber pressures, respectively. The drop size variation of the Box-Douplet injector at the lower chamber pressures is credited to the reduced kinetic energy of the impinging jets, which is due to the decrease in injection velocity. Another trend which is predicted in Figure 178 is the increase in drop size with respect to axial location. This phenomena is predicted due to the increase in the droplet bulk temperature with respect to axial location. It should be noted that decreasing the droplet size at the injection plain is typically thought to be a destabilizing effect. Smaller drops are thought to be more responsive to the high amplitude, steep-fronted pressure waves which are generated by bomb detonation during dynamic stability tests. The general dynamic stability trend with respect to drop size is thought to be a decreasing stability margin with decreasing drop size. This has been shown to some extent with the testing to date.

Another operating condition investigated during the analytical study, was the relative velocity difference between the fuel drops and the combustion gas in combustors implementing the H-1 Derivative and Box-Douplet injectors. The results of this study are

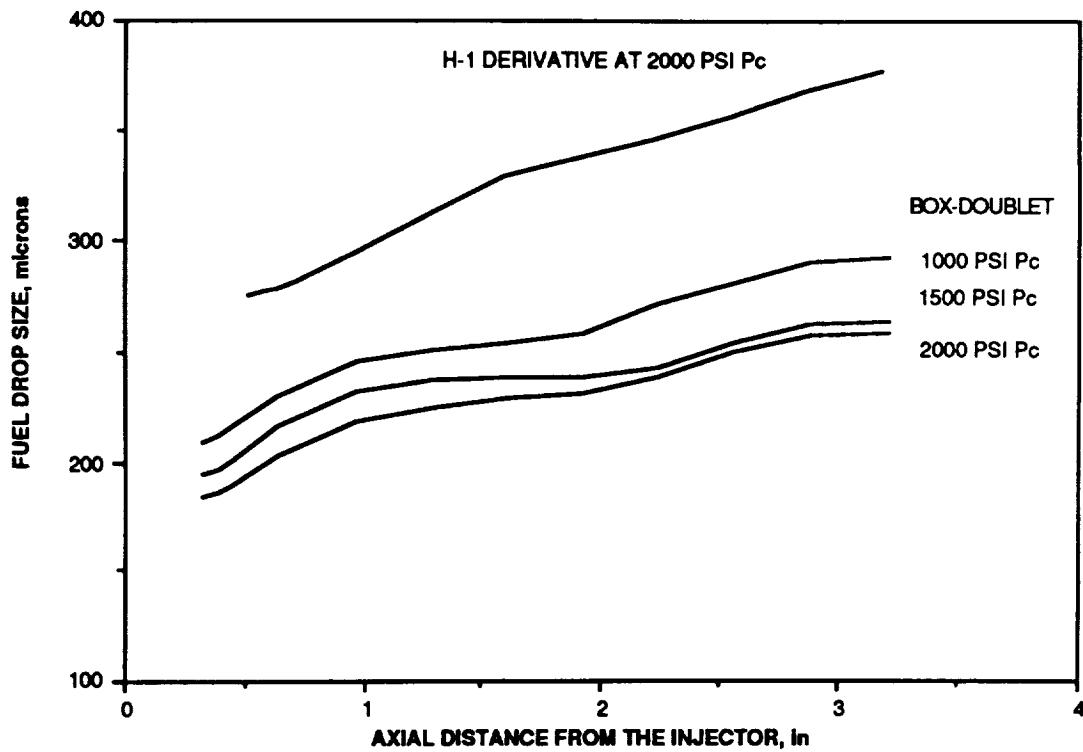


Figure 178. Injector Droplet Size Comparison

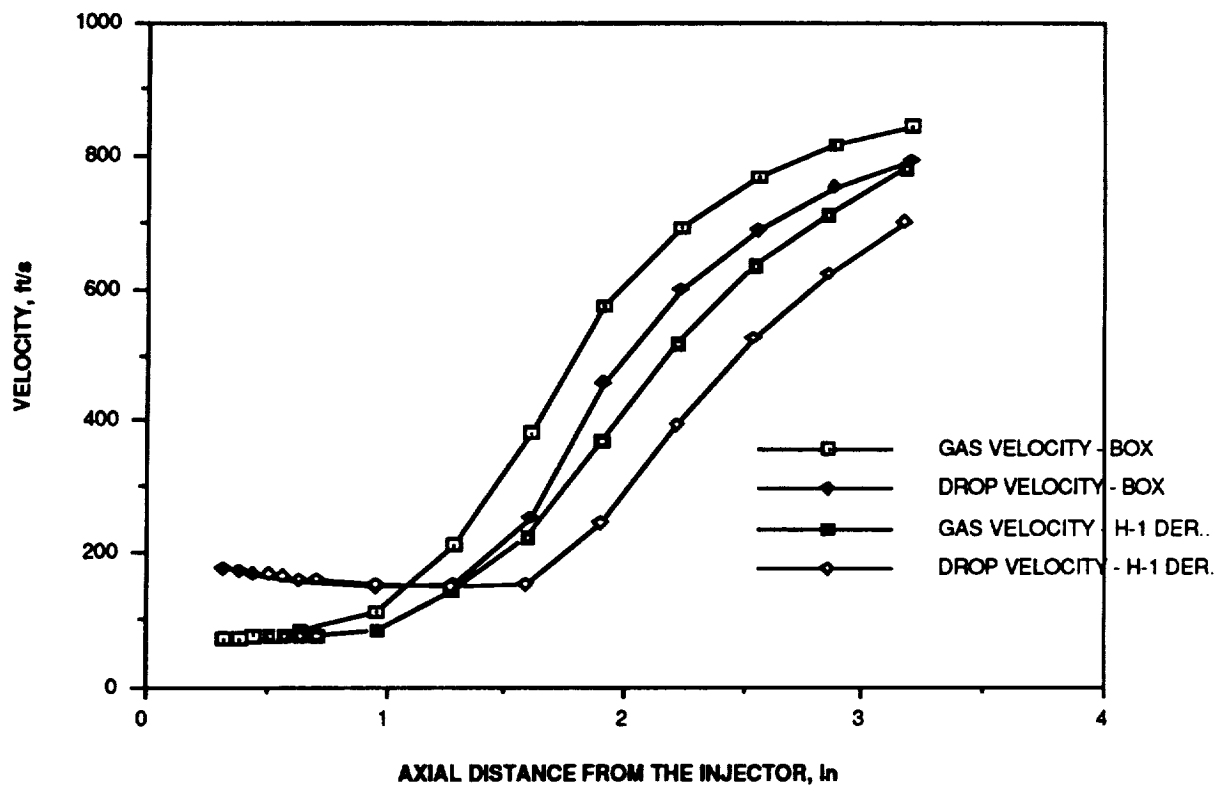


Figure 179. Injector Velocity Comparison

presented in Figure 179. The specific results indicate that the relative velocity differences are 66 and 88 ft/s for the Box-Doublet and H-1 Derivative injectors, respectively. At the time of the analysis, the relative velocity operating parameter was not thought to be as strong of an influence with respect to dynamic instability as the drop size parameter.

Based on the results of the analytical study, two tests with the Box-Doublet injector were scheduled in the Task III test matrix to determine the validity the drop size hypothesis. The two tests (015-042 and -043) were conducted at lower than nominal chamber pressures, and the results are presented below.

14.2.5.1 Test 015-042

Test 015-042 was the first low chamber pressure test conducted with the Box-Doublet injector without acoustic cavities. The targeted operating conditions were 1500 psia chamber pressure, a LOX flowrate of 24.7 lb/s, a fuel flowrate of 8.8 lb/s, 2.8 mixture ratio and a mainstage duration of 0.5 seconds. Actual test conditions were 1424 psia chamber pressure, a LOX flowrate of 24.2 lb/s, a fuel flow of 9.0 lb/s, 2.68 mixture ratio and a mainstage duration of 0.5 seconds. A plot of chamber pressure vs. time is shown in Figure 180. The high frequency data indicated that the bomb detonated as sequenced and that the perturbation induced a first tangential instability which had a frequency of 7725 Hz. The initial bomb perturbation had a 518 psi mean-to-peak overpressure which corresponds to 36% of the chamber pressure. The maximum amplitude of the instability was 555 psi peak-to-peak overpressure which corresponds to 39% of the chamber pressure. During this test, the first harmonic of the instability (frequency equal to 15,450 Hz) was evident in the high frequency pressure traces presented in Figure 181. An isoplot, which shows frequency content in the chamber pressure as a function of time, has been included in Figure 182.

14.2.5.2 Test 015-043

Test 015-043 was the second low chamber pressure test conducted with the Box-Doublet injector without acoustic cavities. The targeted operating conditions were 1000 psia chamber pressure, a LOX flowrate of 16.5 lb/s, a fuel flowrate of 5.9 lb/s, 2.8 mixture ratio and a mainstage duration of 0.5 seconds. Actual test conditions were 947 psia chamber pressure, a LOX flowrate of 17.4 lb/s, a fuel flow of 6.3 lb/s, 2.77 mixture ratio and a mainstage duration of 0.5 seconds. A chamber pressure trace is presented in Figure 183.

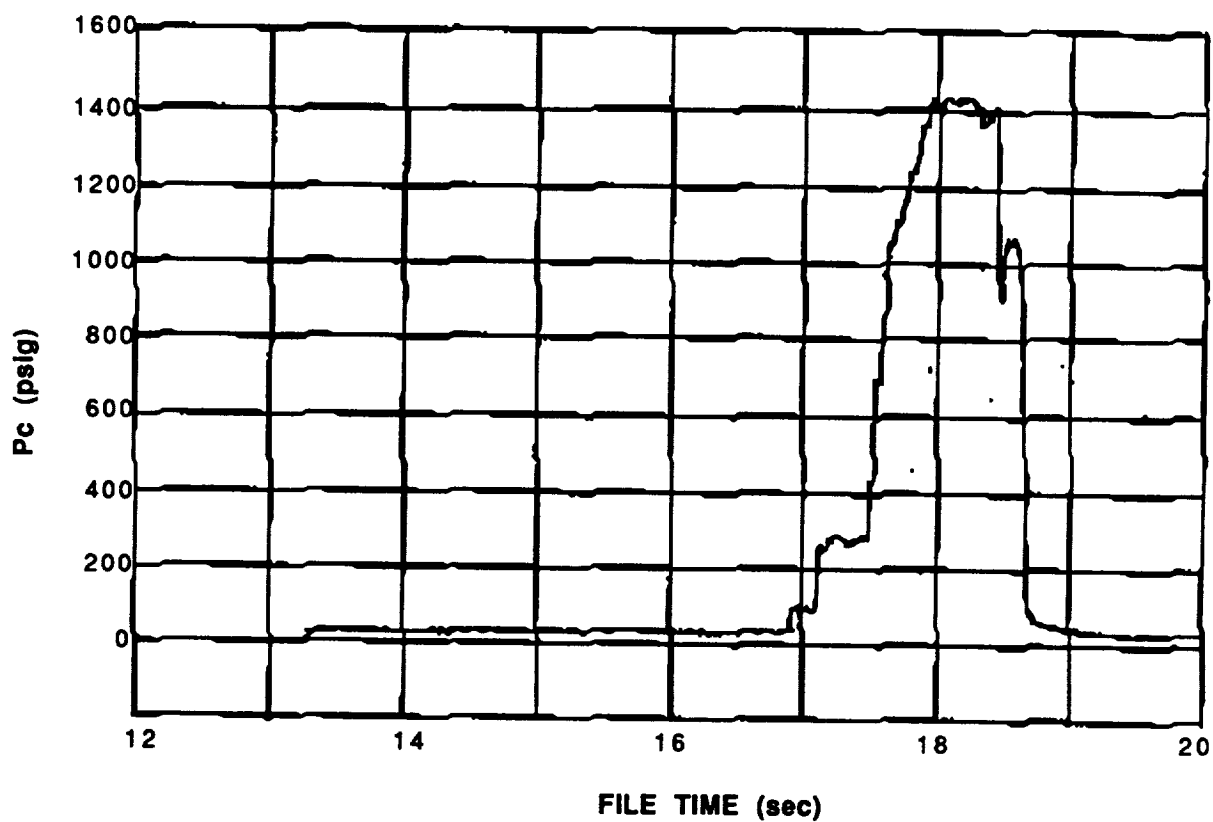


Figure 180. Static Chamber Pressure (Inj. End), Test 015-042, Box-Doublet Injector

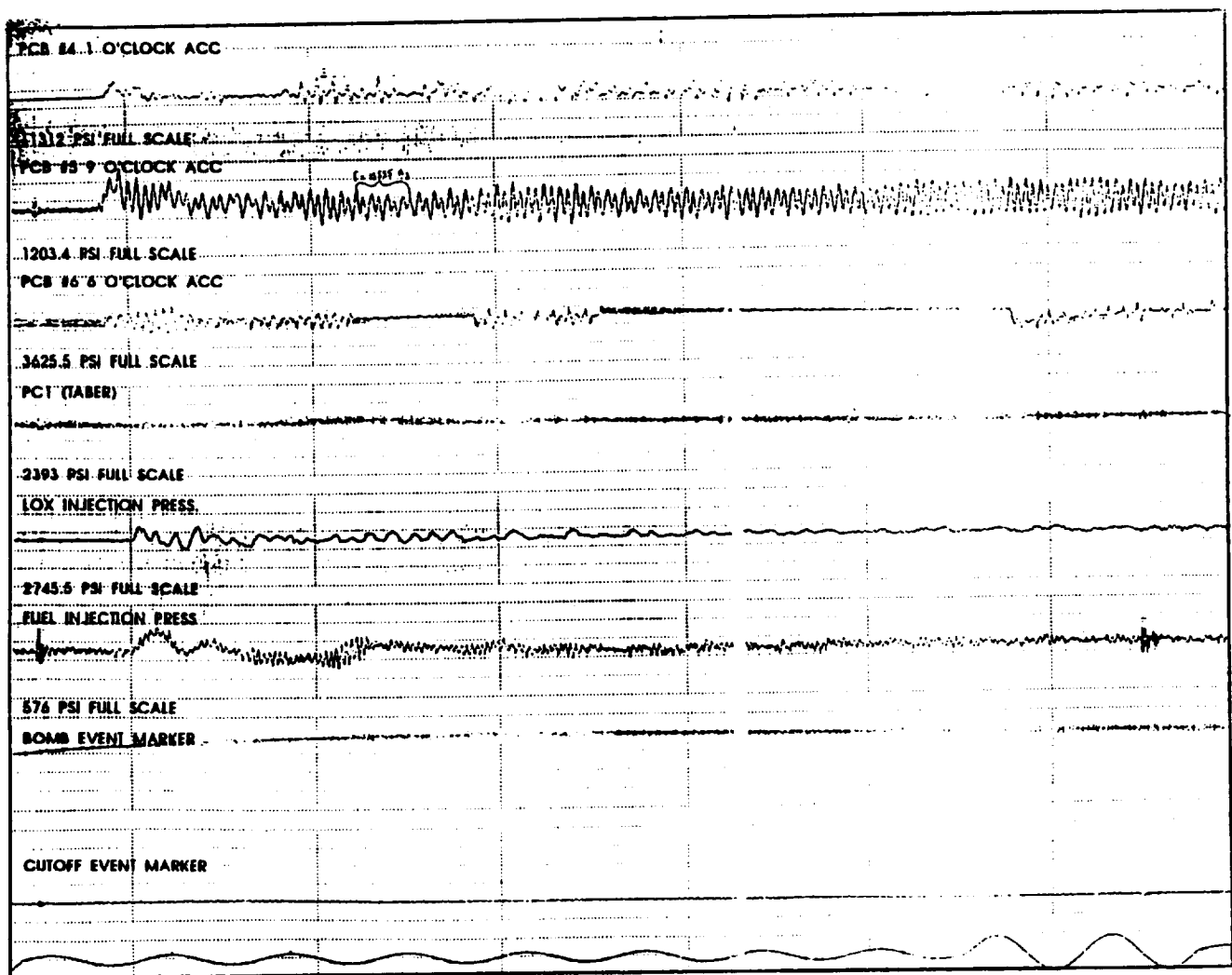


Figure 181. Test 015-042 High Frequency Data

ORIGINAL PAGE IS
OF POOR QUALITY

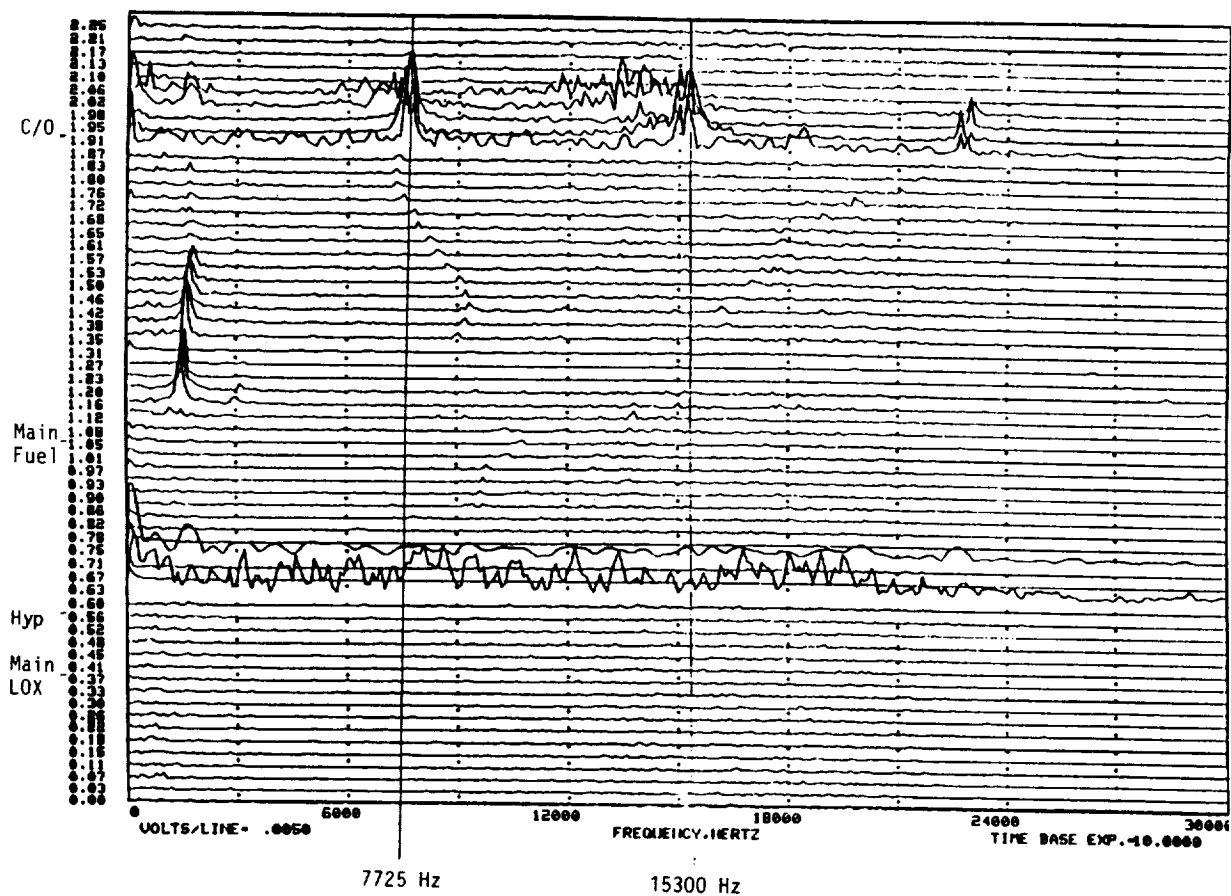


Figure 182. Test 015-042, PCB #5 Isoplot

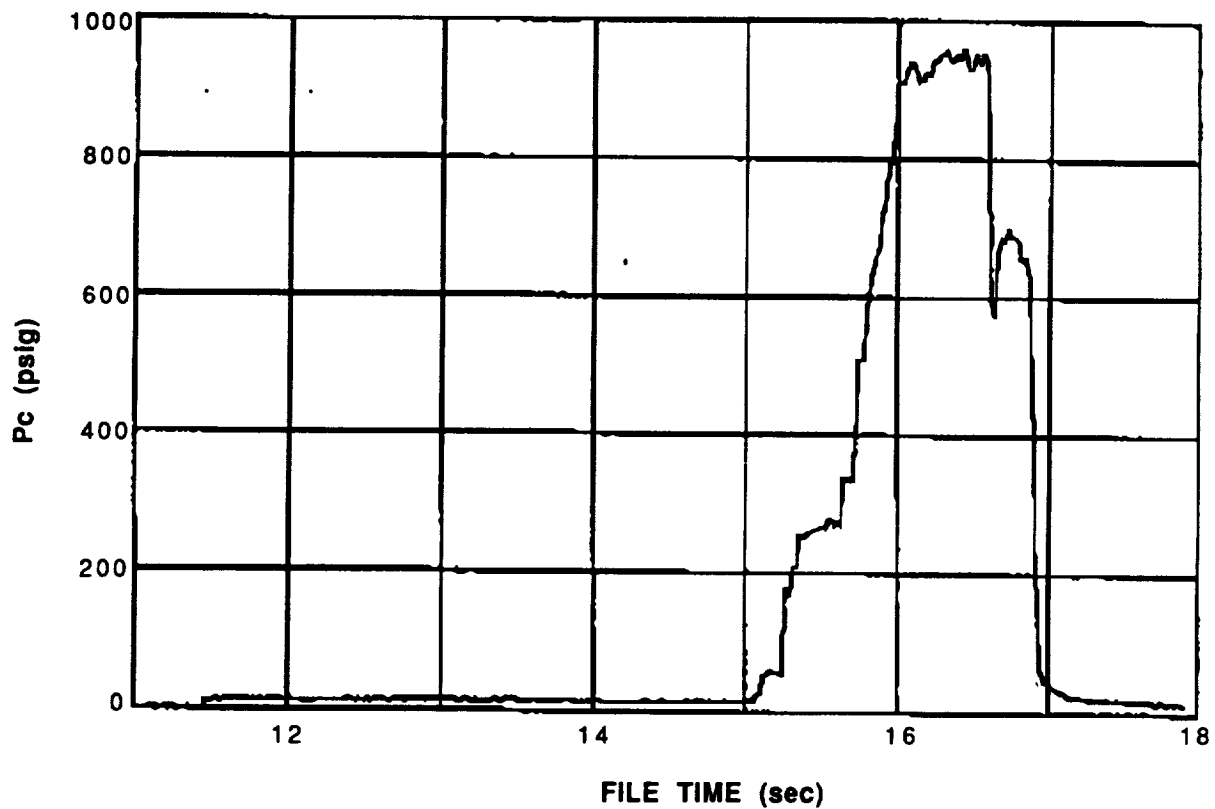


Figure 183. Static Chamber Pressure (Inj. End), Test 015-043, Box-Doublet Injector

The high frequency data indicated that the bomb detonated as sequenced and that the perturbation induced a first tangential instability which had a frequency of 7390 Hz. The initial bomb perturbation had a 370 psi mean-to-peak overpressure which corresponds to 39% of the chamber pressure. The maximum amplitude of the instability was 463 psi peak-to-peak overpressure which corresponds to 49% of the chamber pressure. During this test, the first harmonic of the instability (frequency equal to 14,780 Hz) was again evident in the high frequency pressure traces presented in Figure 184. An isoplot is included in Figure 185.

In conclusion, the two low pressure tests conducted with the Box-Doublet injector displayed first tangential instabilities which had similar acoustic characteristics as the instabilities that were induced at nominal (2000 psia) chamber pressures. The drop size hypothesis has not been completely disproved, but based on the analysis, the Box-Doublet injector still produces significantly smaller drops at 1000 psia chamber pressure than the H-1 Derivative injector at 2000 psia chamber pressure.

14.2.5.3 Tests 015-045 & 015-046

The last tests performed under this contract, included the Box-Doublet injector with 8000 Hz, 1T acoustic cavities operating at off nominal (chamber pressure of 1000 to 1750 psia) conditions. The purpose of these tests was to isolate the mechanism(s) associated with the 5700 Hz instability which occurred in Test 015-035. Specifically, the tests were oriented at significantly changing the injection velocity to see if the 5700 Hz oscillation was coupled to jet oscillations.

During Test 015-045, a bomb test was scheduled at targeted operating conditions of 1500 psia chamber pressure, a mixture ratio of 2.8, and the inclusion of 8000 Hz acoustic cavities. The results of the test indicated that a high amplitude pressure disturbance was not generated during the test, and that a repeat of the test was required.

Test 015-046 had the same targeted test conditions as Test 015-045. During this test, a high amplitude pressure disturbance was generated during the test and useful high frequency data was collected. The purpose of this test was to change the injection velocity and determine the injection velocity effect on the 5700 Hz oscillation. The isoplot for this test is displayed in Figure 186. As seen in the data, the frequency of the instability was 5280 Hz which is a 7% decrease. In the event that the injection velocity was coupled with the

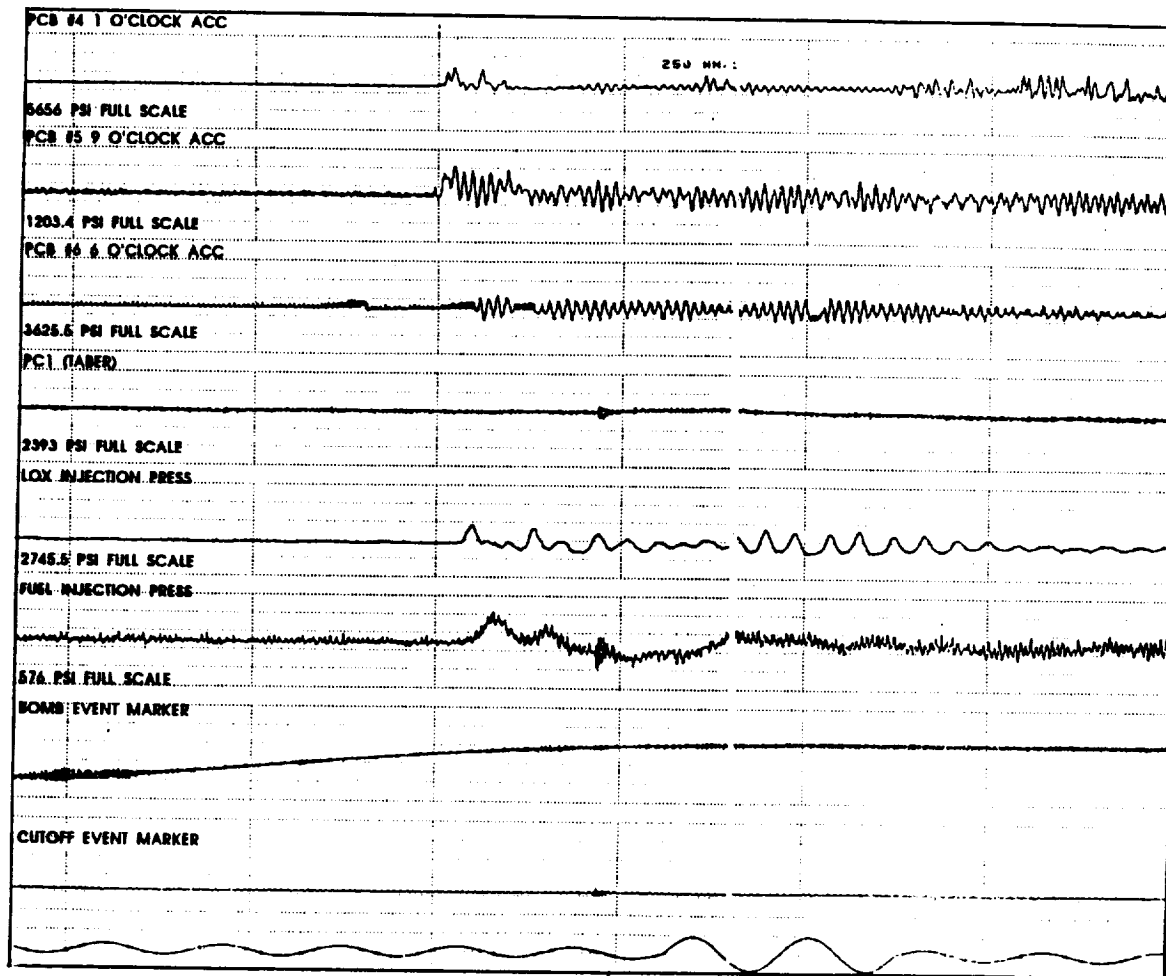


Figure 184. Test 015-043 High Frequency Data

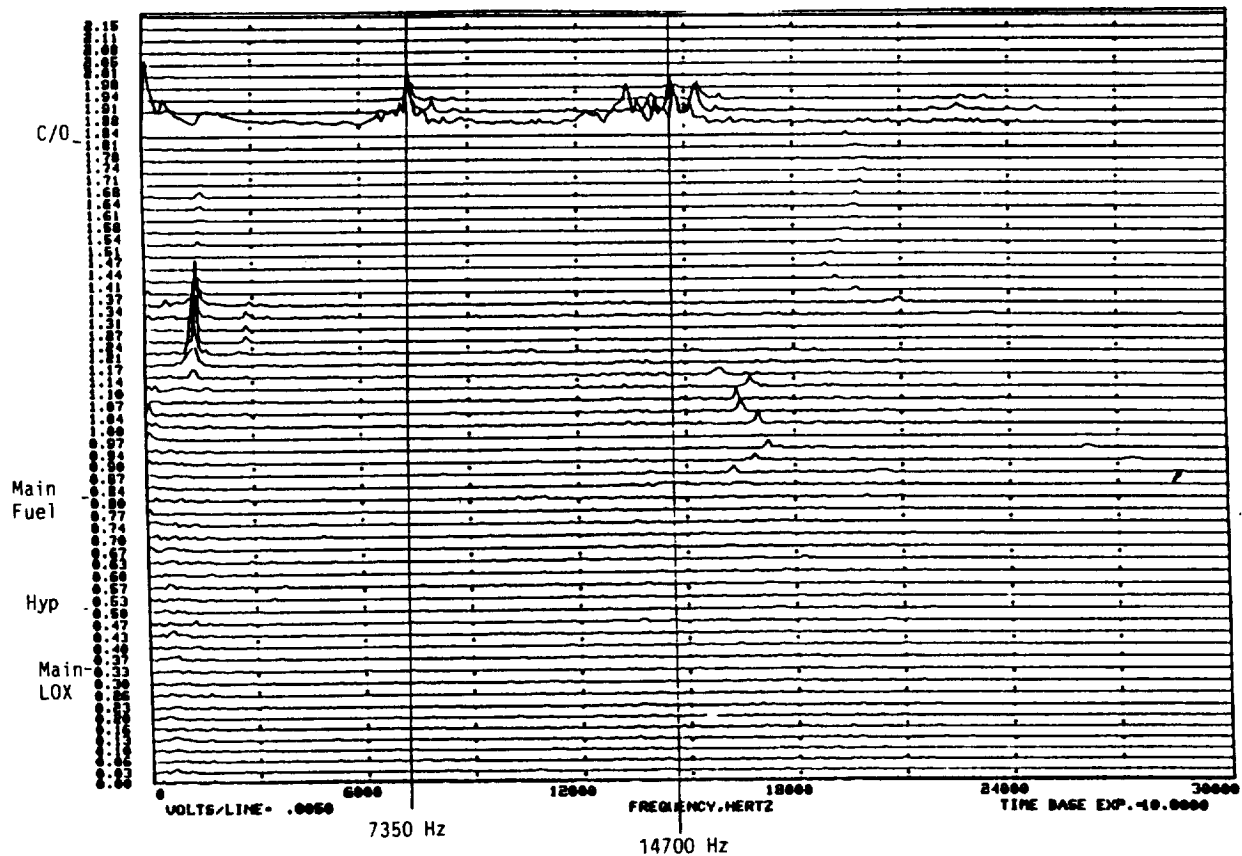


Figure 185. Test 015-043 PCB #5 Isoplot

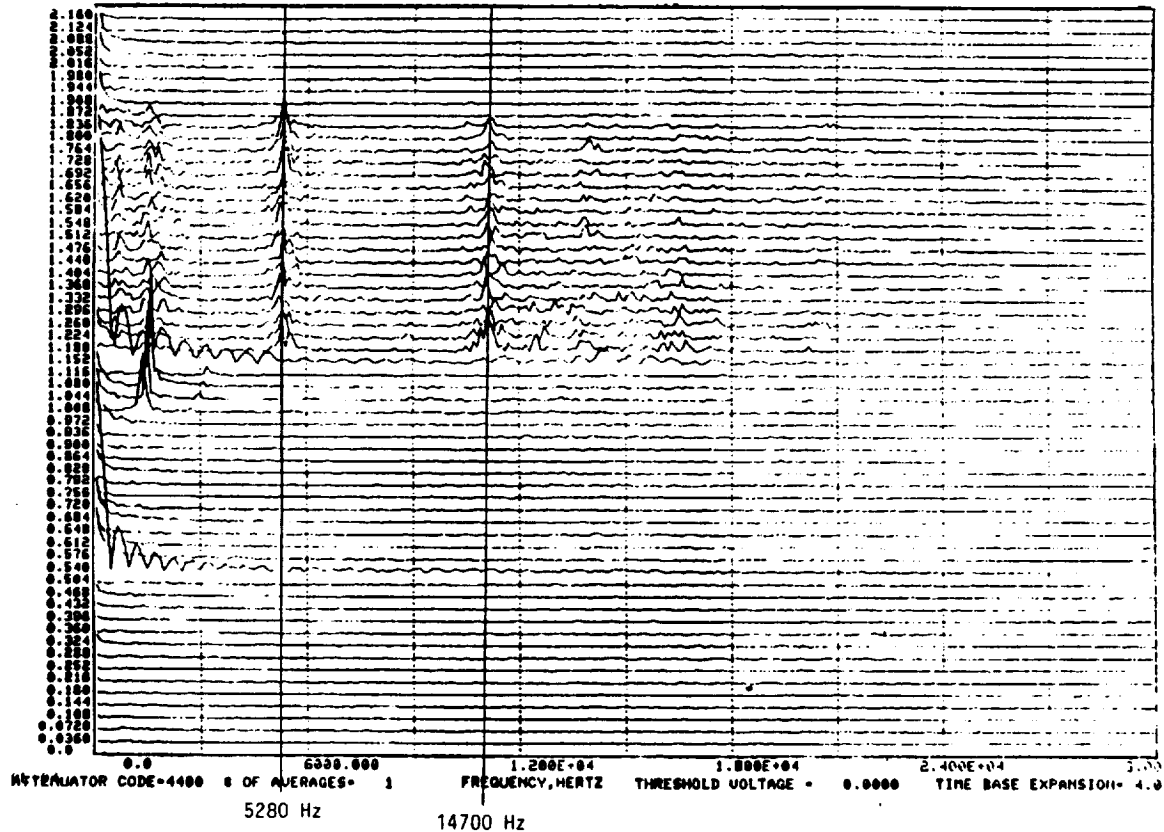


Figure 186. Test 015-046 PCB #4 Isoplot

oscillation, a 25% decrease in frequency would be expected. Another concept which has recently been examined is feed system coupling on the oxidizer side. A decrease in the oxidizer acoustic velocity by 7% is a realistic quantity between 2000 and 1500 psi conditions. At -207 degrees F, the sound speed suppression is exactly 7% with LOX at 2000 and 1500 psi. The LOX at these two conditions is much more compressible than RP-1. The LOX density decreases by 2.6% between 2000 and 1500 psi chamber pressures, while the RP-1 density only decreases by 0.3%. Once again, further work is required to isolate the specific mechanism of instability, but the results presented above suggest that the oxidizer feed system does play a part in the 5700 Hz instability. A feed system and chamber analysis would be required to substantiate this hypothesis, and the occurrence of the longitudinal mode which occurred with the bi-tuned cavities would aid in the analysis. Acoustic cavities are typically thought to be frequency and not mode dependent devices. The effectiveness of the cavities in damping the 5700 Hz oscillation is substantiated with these tests.

The time lag data which was collected during Phase B testing has been included in Figure 187. All of the data represents injectors which utilize LOX/RP-1 propellants at various chamber pressure and mixture ratio values. The plot displays the product of the time lag and mean chamber Mach number raised to the one-third power as a function of mean fuel orifice diameter. The amount of damping is not indicated by these results, but observed frequencies can be deduced from the data and show a wide bandwidth for a given fuel orifice diameter. The original LOX/RP-1 database consisted of 6 points. It was increased to 15 points (an increase of 150%) due to Phase B testing under this program.

15.0 REFERENCES

1. Rupe, J. H., "The Liquid-Phase Mixing of a Pair of Impinging Streams", Progress Report 20-195, Jet Propulsion Laboratory, Pasadena, CA, 6 August 1953
2. Muss, J. A., and Pieper, J. L., "Performance and Stability Characterization of LOX/Hydrocarbon Injectors", AIAA-88-3133, AIAA/ASME/SAE/ASEE 24th Joint Propulsion Conference, Boston, 11 July 1988
3. Crocco, L., "The Sensitive Time Lag Theory", in Liquid Propellant Rocket Combustion Instability, D. T. Harrje, Editor, NASA SP-194, 1972, pp. 170-194.
4. Mitchell, C. E. , and Eckert, K., "A Simplified Computer Program for the Prediction of the Linear Stability Behavior of Liquid Propellant Combustors", NASA CR-3169, August 1979. (A 1986 update of the code by Mitchell was used).
5. Crocco and Chang, "Theory of Combustion Instability in Liquid Propellant Rocket Motors", Butterworth Scientific Publications 1956
6. Reardon, F. H., "High Frequency: Sensitive Time Lag Model", in Liquid Propellant Rocket Combustion Instability, D. T. Harrje, Editor, NASA SP-194, 1972, p. 283.
7. Webber, W. T., "Estimating Stability and Performance for a Big Booster", Rocketdyne Internal Letter CDR-85-252, 20 November 1985
8. "LOX/Hydrocarbon Thrust Chamber Technology", AFAL Contract No. F04611-86-C-0088 (Ongoing program at Rocketdyne)
9. Tuegel, L. M., "LOX/RP-1 Injector Evaluation" , Final Report, Task No. 61253, Rocketdyne IR&D Report No. ITR 88-047, October 1988.
10. Pavli, A. J., "Design and Evaluation of High Performance Rocket Engine Injectors for Use with Hydrocarbon Fuels", NASA TM-79319, September 1979
11. Swallom, D. W., et al., "High Power Magnetohydrodynamic System", AFAPL-TR-78-51, Vol. I-II, July 1978

APPENDIX A

INJECTOR TECHNOLOGY REVIEW AND TECHNICAL PROGRAM PLAN

INTRODUCTION

This appendix, consisting of the report prepared in Task I of the Program, is made up of two parts. The first is a review of the status of the technology supporting the design of injectors suitable for large (750,000-lb-thrust), high-pressure (2000-3000 psia), high performance (minimum 97-percent c^* efficiency), LOX/RP-1 engines. The second part outlines a program plan to remedy the technical deficiencies identified in the literature review and indicates possible time phasing of the tasks involved.

The propellant injection process, which is controlled by the injector design, is critically important in determining the three basic combustor characteristics: performance, stability, and heat flux. Injector technology is primarily concerned with establishing criteria and techniques for conflicting design requirements. Consequently, both the injector technology status summary and the technical program plan are discussed in terms of combustor performance efficiency, combustion stability, and chamber/throat heat flux and compatibility.

HYDROCARBON SELECTION

Although the original plan for the present program included evaluations of heavy hydrocarbon fuels other than RP-1 (such as the JP series or various gasoline blends), it quickly became apparent that there is no basis, at present, for consideration of alternate hydrocarbons. They offer no overall advantages in physical or chemical properties, availability, handling and safety, or cost. Most important, the extensive background of LOX/RP-1 rocket engine experience, particularly in the form of large-engine analytical, experimental, and production data bases, makes RP-1 the only currently feasible heavy hydrocarbon fuel. Hence, LOX/RP-1 was the only propellant combination considered in this review and in the remainder of the program.

INJECTOR TECHNOLOGY REVIEW

Although a number of analytical and theoretical studies have been made on high-pressure LOX/RP-1 injectors, test data in the 2000-3000 psia chamber pressure range are very limited. Consequently, major portions of this review discuss injector technology status based on data at lower pressures. Reasonable extensions to higher levels are indicated, as appropriate.

The discussions are separately focussed on the effects of LOX/RP-1 injector design on combustor performance, stability, and heat flux. In practical applications, however, these effects overlap and may even conflict. For example, high performance efficiency is encouraged by effective mixing and combustion of the propellants near the injector face, but this also decreases stability. Injector design requirements must therefore be examined in the light of their combined effects on all three combustor characteristics.

PERFORMANCE

Early LOX/RP-1 Performance Technology

Production Engine Injectors. Current LOX/RP-1 injector technology has its foundation in the experience obtained in the design, development, and operation of the injectors for the early (pre-1970) LOX/RP-1 engines. Salient characteristics of these engines are summarized in Table A-1 (Ref. A-10). All these injectors used like-impinging (doublet or triplet) elements, in concentric ring patterns, with radially oriented spray fans. However, chamber pressures were much lower than the presently targeted range (2000-3000 psia). The comparatively low performance of these injectors was an acceptable trade-off for their greater stability, compared to unlike-impinging injection elements, because it was then generally agreed that, for LOX/RP-1 injectors, high performance and a high degree of combustion stability were mutually exclusive.

Early High-Pressure Injectors. In 1959, a series of LOX/RP-1 tests was carried out at Rocketdyne at chamber pressures of 1500-2000 psia. Experimental, tubular, cooled and uncooled chambers were used, primarily for heat transfer information, with like-impinging injection elements. Performance levels were in the range of 90-94 percent c^* efficiency, comparable to that in the 1100-psia F-1 engine.

TABLE A-1 PRODUCTION ENGINE LOX/RP-1 INJECTORS

VEHICLE, ENGINE	INJEC. DIAM. in	CHAMBER LENGTH, in	L*, in	INJECTION ELEMENTS						P _c , psia	THRUST, K-lb _f	SHIFTING η _{c*} , percent	STABILITY AIDS
				TYPE		NUMBER		ORIFICE DIAM., in					
				O	F	O	F	O	F				
JUPITER, S-3	20.9	28	39	LD	LD	361	361	.113	.089	530	150	93	NONE
THOR, MB-3	20.9	28	39	LT	LD	355	582	.113	.064	588	170	94	BAFFLES
ATLAS BOOSTER, MA-5	20.9	28	39	LT	LD	335	582	.113	.064	577	165	94	BAFFLES
ATLAS SUSTAINER, MA-5	12.4	28	43	LT	LD	144	175	.120	.094	706	57	95	NONE
TITAN I, BOOSTER	21.6	-	-	LD	LD	560	610	.119	-	637	180	96	NONE
TITAN I, STAGE 2	14.2	-	-	LD	LD	328	392	.085	.057	682	80	97	NONE
DELTA, H-1	20.9	28	39	LT	LD	365	612	.120	.082	705	205	96	BAFFLES
SATURN 1-C, F-1	39.2	40	48	LD	LD	714	702	.242	.281	1100	1522	92	BAFFLES

* LD = LIKE DOUBLET

LT = LIKE TRIPLET

Subsequently, a three-test series of high-pressure LOX/RP-1 firings was conducted at Rocketdyne in 1961. Chamber pressures were 2000 to 2800 psia, with an injection density of about 8 lb/sec/in² (compared to 4.8 lb/sec/in² in the F-1 engine). To obtain the high injection density, the 3.50-inch-diameter injector had 61 coaxial elements, with LOX injected through the central tubes and RP-1 through the surrounding annuli. A long ($L^* = 62$ in.), low contraction ratio (2.14) heat sink chamber was used, with no expansion section ($\epsilon = 1.00$). Performance was difficult to measure because of the very short test durations (0.3 to 1.3 sec) and absence of a nozzle, but these tests demonstrated that very high injection density levels could be achieved.

In a 1964 experimental study of LOX/RP-1 injectors (Ref. A-1), the performance and stability characteristics of coaxial, micro-orifice, and like-doublet injectors were determined at a nominal chamber pressure of 1000 psia. Propellant mixture ratios were 0.5 to 3.0. An uncooled copper combustion chamber was used, with a water-cooled throat and uncooled nozzle extension; $D_c = 3.73$ in., $\epsilon_c = 4.5$, $L^* = 34$ and 47.5 in., and $\epsilon = 16$. For the conventional concentric tube injector (fuel surrounding oxidizer), performance was fairly high (c^* efficiency = 93-95%) at mixture ratios above 1.5 but dropped (c^* efficiency = 88-90%) at lower mixture ratios. The reverse concentric tube (oxidizer surrounding fuel) gave moderate performance (c^* efficiency = 92%) at 2.35 mixture ratio. The micro-orifice injector, which consisted of alternating fuel and oxidizer rings in a welded 0.010-inch-thick face of porous nickel alloy with a 3-percent open area consisting of 0.005-inch-diameter holes, showed low performance (c^* efficiency = 86-90%) in three tests at 1.5 to 2.1 mixture ratio. The like-impinging jet injector also yielded low performance (c^* efficiency = 85-90%), based on two tests at mixture ratios of 1.9 and 3.3.

A LOX/kerosene engine under development in Germany from 1957 to 1967 used a LOX-cooled thrust chamber and had operating goals of 98-percent combustion efficiency at 1233 psi chamber pressure and 2.7 mixture ratio (Ref. A-7). Information as to whether these goals were actually achieved is not available, nor are details of the injector design.

The LOX/kerosene propellant combination has reportedly been used in Russian high-pressure rocket engines for many years. Unfortunately, reliable design and performance information is difficult to obtain.

Recent LOX/RP-1 Performance Technology

A comparatively small amount of design and test effort at moderate and high pressures has been expended on LOX/RP-1 combustors since 1970. Results of work at lower pressures will therefore be included in this review, for completeness.

Pavli (NASA-Lewis). Results of an experimental program to determine the performance of combustors using LOX with three heavy hydrocarbon fuels were reported in 1979 (Ref. A-15). The fuels were RP-1, JP-10, and liquified natural gas; only the RP-1 data will be reviewed here. The primary program objectives were measurement of the combustion efficiency and stability of four injector types over ranges of chamber length and mixture ratio, all at 600 psia chamber pressure, and assessment of the adequacy of the Priem-Heidmann vaporization model (Ref. A-17) in predicting performance of heavy hydrocarbon fuels. Chamber and throat diameters were 5.39-in. and 2.60-in., respectively, ($\epsilon_c = 4.3$) in all tests. Typical test data are summarized in Table A-2.

The injector design process in this investigation sought first to produce high vaporization efficiency, as the key to high performance with low-volatility fuels. Analyses of various injector configurations with the Priem-Heidmann model led to selection of an O-F-O triplet as the element of choice. The first injector had 37 triplet elements located on a square grid on the injector face, in a mutually perpendicular orientation. A second 37-element injector used a "reverse" triplet, F-O-O-F, with two central oxidizer showerheads, to minimize orifice size disparity. The same square grid, mutually perpendicular, element orientation was used as in the first injector. The third injector was the same as the second, except that 97 elements were used, with smaller orifices. The fourth injector was a conventional, 37-element, like-doublet configuration arranged in a circular pattern with circumferential (non-intersecting) spray fans.

Chamber length (injector to throat) was varied from 10-in. to 22-in. by use of spool pieces; mixture ratio ranged from 2.4 to 3.4. A 16-chamber acoustic cavity ring was included for some of the tests. A heat sink combustor was used, with a water-cooled throat. Test durations were short (0.8 sec), but steady state combustion appeared to have been achieved. Performance data were summarized as follows:

1. Performance levels of LOX/RP-1 at mixture ratio 2.7 were high for the triplet and split triplet configurations (c^* efficiency = 99-100%) but significantly

Table A-2

LOX/RP-1 Test Data (Pavli, NASA Lewis, 1979)

Pc = 600 psiaM.R. = 2.7Duration = 1.0 sec

Injector Type	No. of Elements	D _o , in	D _f , in	Chamber		η_{c^*} , %	Acoustic Cavities	Spontaneous Instability	f, Hz	P-P Amplitude, % of P _c
				L, in	D, in					
O-F-O Triplet	37	.061	.055	16	5.4	100	Yes	Yes	1440	8
		.067	.062	14		100	No	No	--	--
		.073	.067	10		99	No	No	--	--
F-O-O-F Split Triplet	37	.060	.040	14	5.4	100	No	No	--	--
		.067	.043	14		--	No	Yes	5120	100
		.073	.047	14		100	No	No	--	--
F-O-O-F Split Triplet	97	.037	.024	14	5.4	--	No	Yes	5440	93
		.047	.028	10		98	Yes	No	--	--
Like Doublets (in Alternating Rings)	37	.062	.040	22	5.4	94	Yes	No	--	--
		.068	.044	22		96	Yes	No	--	--
		.073	.047	14		94	No	Yes	1440	8

lower for the like-doublet (c^* efficiency = 94-96%). Efficiency was slightly improved by increasing chamber length.

2. Experimental data for the triplet and split triplet injectors agreed with the vaporization model predictions; like-doublet injector data did not. Performance of the doublet configuration seemed to be dominated by mixing losses. The triplet design had inter-element mixing of dissimilar droplets (oxidizer-rich and oxidizer-lean) due to the mutually perpendicular element orientation, whereas the doublet design, with parallel spray orientation, minimized inter-element mixing. The only mixing mechanism available in the doublet injector was diffusion of the concentric zones of vaporized propellants.

Huebner (Rocketdyne). The fuel used in this study of a gas generator for a 30 MW magnetohydrodynamic system (Ref. A-23) was JP-4. The results obtained are included in this review because JP-4 is chemically and physically very similar to RP-1. A rectangular injector (7.75-in. X 6.12-in.) was employed, with a pattern of like-doublet, edge-impinging elements ($D_o = .052$ -in., $D_f = .035$ -in.), in a combustor with 1.85 contraction ratio. At a chamber pressure of 440 psia, measured c^* efficiency was 98-99 percent at mixture ratios of 2.8 to 3.34 (stoichiometric).

LaBotz, et al. (Aerojet). Two different injector types were designed and fabricated for tests to determine the combustion and heat transfer characteristics of LOX/RP-1 at chamber pressures up to 2000 psia (Ref. A-9). The injector patterns were a transverse like-on-like (TLOL) and a pre-atomized triplet (PAT). One of each of these configurations was designed for 1200 psia and 2000 psia pressure, differing only in orifice diameters. The injector bodies were fabricated from 304L CRES and had central igniter ports. The injector faces were made by diffusion bonding a stack of thin nickel platelets which had been photoetched to provide the holes for propellant flow.

The TLOL like-impinging-doublet element was included in this study on the basis of its record in early LOX/RP-1 production engines. (The "transverse" designation refers to the flow passages which supplied the injection orifices; these passages were parallel to the injector face, i.e., transverse to the chamber axis.) Both oxidizer and fuel fans were radially oriented, with planar spray impingement. The injection pattern consisted of 132 elements arranged in seven rings.

The design goal for the PAT element was higher performance potential than the TLOL pattern, even at the risk of decreased combustion stability. To achieve the higher performance, only unlike-impinging elements were considered: conventional F-O-F triplets, splash plate unlike doublets, and a pre-atomized triplet, which consisted of two splash plate-generated fuel sprays impinging on one central doublet-generated oxidizer spray (Fig. A-1).

The fuel splash plate elements form fans of droplets at acute angles (30-45°) to the injector axis; the oxidizer doublet elements form axially directed fans. This injector contained 120 PAT elements arranged in concentric rings. The PAT element was selected because it was considered to have the highest probability of achieving the high performance level of EDM-drilled triplets without unacceptable sacrifice of stability.

Three, 4.80-inch-diameter, combustion chambers were used in the test program: an uncooled, graphite-lined, steel-shell, short-duration, workhorse chamber; an axially slotted, copper-lined, EFNi-jacketed, water-cooled chamber with 2.93 contraction ratio; and a circumferentially slotted, copper-lined, EFNi-jacketed, water-cooled, calorimeter chamber with 2.63 contraction ratio. Chamber lengths (injector to throat) were 11.0 and 15.0 in. A 12-chamber acoustic cavity ring, which could be tuned by placing block inserts in the cavities, was located between the injector and the combustion chamber.

A preliminary test series with both injectors eliminated the TLOL pattern because of spontaneous instabilities. Two multi-point tests were then conducted at 1980 psia with the PAT injector, using heated (200F) fuel (to simulate regeneratively cooled chamber conditions). Performance data of both injector types at 2.8 mixture ratio were as follows:

<u>INJECTOR</u>	<u>CHAMBER LENGTH, IN.</u>	<u>FUEL TEMP. °F</u>	<u>ERE, %</u>
TLOL	11	75	96
TLOL	15	100	97
PAT	11	49	94
PAT	11	238	96
PAT	15	70	96
PAT	15	236	97

The major portion of the performance loss in both injectors was ascribed to non-uniform mixing rather than to incomplete vaporization, so that performance increases were to be sought

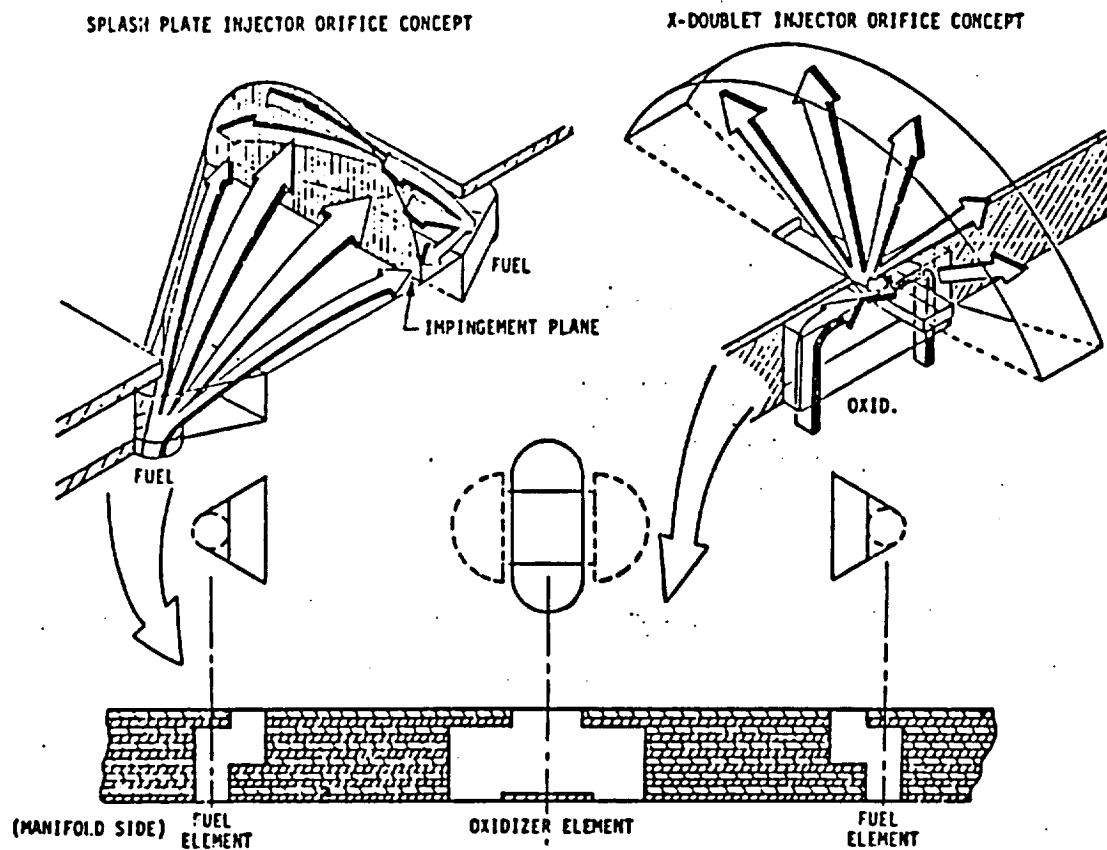


Figure A-1. Schematic of Pre-atomized Triplet Injector Element (Ref. A-9)

in injector mixing efficiency improvements. Although fuel heating raised performance by reducing its viscosity (and thus improving its levels of atomization and vaporization), the increase was less than theoretically predicted. It was concluded that the PAT injector was superior to the TLOL from the standpoint of fuel vaporization rate, high-frequency combustion stability, and injector face and chamber wall thermal compatibility; performance of the PAT was lower, however, because of less efficient mixing.

Schoenman & Gross (Aerojet). Following the tests discussed in the preceding section, a design and fabrication program was conducted to provide a stable, high-performing, compatible injector for testing with LOX/RP-1 (Ref. A-21). The injector design requirements were as follows:

Chamber pressure:	2000 to 3000 psia
Mixture ratio:	2.8
Characteristic velocity efficiency	>97%
Chamber pressure oscillations:	< $\pm 5\%$ of P_c
Chamber diameter:	5.66 in.
Throat diameter:	3.31 in.
Chamber length (injector to throat):	13.97 in.

The injector design was based on that used in the previous tests (Ref. A-9). It had a core pattern of 72 pre-atomized triplet (PAT) elements, consisting of two fuel fans impinging on a central oxidizer fan (Fig. A-1), which injected 80-percent of the flow. The remaining 20-percent was injected through 96 tangential fan, pre-atomized doublet (XDT), barrier compatibility elements in the two outer rows. Two changes were made in the earlier design: increase in the fuel total included impingement angle from 60 degrees to 90 degrees, to improve intra-element mixing, and addition of outer barrier elements, to lower heat transfer rates at the throat. As before, a central tube was provided within the injector body for the TEA/TEB ignition fluid.

Bailey (NASA-MSFC). The injector described in the preceding paragraph was tested with an uncooled resonator body and a calorimeter chamber (Ref. A-3). Three firings were conducted, at chamber pressures of 1726 to 2263 psia and mixture ratios of 2.0 to 2.8. Predicted c^* efficiencies were about 98-percent for the PAT core elements and about 95-percent for the outer doublet barrier elements, for an overall efficiency of approximately 97-percent. However, the measured overall c^* efficiencies ranged from 91-percent to 94-percent,

implying that the performance of both the core and barrier elements was significantly lower than predicted.

Price and Masters (NASA-Lewis). The primary objective of this investigation (Ref. A-16) was to study the behavior of LOX as chamber coolant. Separate sources of LOX were used for the injector and for coolant so that reported performance data are for LOX/RP-1. The injectors used at 1200 and 2000 psia chamber pressure had 37 O-F-O triplet elements plus 24 showerhead elements in the outer ring (fuel orifices adjacent to the wall and inner oxygen orifices). The thrust chamber liners were OFHC copper, with 100 axial milled slots closed out with electroformed nickel. Chamber diameter was 4.8-in., with a 2.6-in. throat diameter ($\epsilon_c = 1.85$) and injector-to-throat length of 11.5-in. A 16-cavity quarter-wave resonator was included in the thruster.

At 2.8 mixture ratio, c^* efficiency was reported as 95-96 percent; however, the efficiencies based on throat stagnation pressures were recalculated to be 93-95 percent. The low performance was ascribed to the peripheral showerhead elements, which were added to reduce wall temperatures. In tests without the showerheads, at 600 psia, c^* efficiency was about 3-percent higher.

Muss and Pieper (Aerojet). Results of a series of high-pressure LOX/RP-1 tests have recently been reported (Ref. A-12-A). Two injectors were used: an O-F-O triplet pattern (39 elements, $D_o = D_f = 0.125$ -in.) and a like-doublet pattern (105 elements, $D_o = 0.089$ -in., $D_f = 0.058$ -in.). Chamber length (13-in. and 20-in.), chamber pressure (1700 to 2000 psia), and mixture ratio (2.1 to 3.6) were varied. The combustion chamber had an ablative liner and throat; test durations were on the order of one second. The O-F-O triplet injector was the higher performing (c^* efficiency = 96 to 102 percent), with lower performance in the shorter chamber. The like-doublet injector had moderate performance (c^* efficiency = 93-98 percent) with both chamber lengths. However, the use of an ablating throat, combined with very short test durations, may be compromising factors in these data.

STABILITY

Introduction

Combustion instability has been a major problem in the design and development of nearly all liquid rocket engines, and a tremendous amount of effort has been devoted to advancing its understanding and eventual solution. The earlier results of this work have been presented in extensive, detailed monographs on rocket engine combustion stability (Ref. A-11) and on combustion stabilization devices (Ref. A-12) published by NASA in 1972 and 1974, respectively.

In general, combustion instability results from a coupling of the combustion process and the fluid dynamics and acoustics of the engine system. Consequently, such instability may be minimized by reducing the coupling of the pressure and velocity oscillations in the combustion chamber with the driving combustion process and/or by increasing the damping characteristics of the system. Stabilization "aids" are mechanical devices which reduce coupling (such as injector face baffles) or increase damping (such as acoustic absorbers). Stability may also be achieved by modification of the combustion process, primarily by changing injector characteristics which control such critical factors as propellant injection velocities and degree of mixing, flame front location, and mass and mixture ratio distributions.

This review will emphasize the influence of injector design on combustion stability, as applied to high-pressure, high-performance, LOX/RP-1 combustors, rather than on use of stabilization aids. Nevertheless, since such aids are still essential for maintaining stable combustion in this type of combustor, some discussion of their application will be presented.

The focus will be on high-frequency acoustic instability rather than low-frequency instability because the latter is generally feed-system related and is the easier to solve, both analytically and experimentally.

Early LOX/RP-1 Combustors

Pre-1970 LOX/RP-1 engines (Table A-1) had numerous occurrences of both spontaneous and induced (dynamic) instabilities. This experience, together with results of many analytical and technology studies (Ref. A-11), led to some general conclusions, summarized as follows:

1. Factors which tend toward increasing combustion efficiency also tend to decreasing combustion stability. Such factors include:
 - Smaller drop sizes (i.e., smaller orifice diameters)
 - Combustion closer to injector face (i.e., small jet impingement distances)
 - Increasing mass and mixture ratio uniformity
2. Factors which "extend" the combustion zone tend to favor stable combustion. Such factors include:
 - Use of like-impinging rather than unlike-impinging injection elements
 - Larger drop sizes
 - Higher mass flowrates near the center of the chamber, away from the walls
3. Increase in chamber pressure tends to decrease combustion stability.
4. When baffles are used as stability aids, the smaller the characteristic dimension of the baffle compartment (i.e., the higher the compartment acoustic frequency), the greater the stabilizing effect.

During the development of the F-1 engine, a large number of injector types were tested in full-scale and in two-dimensional combustors to ascertain their stability characteristics. None was ever suggested as a possible replacement for the baffled, like-impinging, F-1 injector. Following are some of the configurations tested in full-scale injectors (Ref. A-19), all of which were spontaneously or dynamically unstable:

1. Triplet (O-F-O); unbaffled; spontaneous, undamped instability on reaching mainstage
2. Splash ring (fuel showerheads strike splash rings, self-impinging oxidizer triplets): unbaffled; undamped, bomb-induced instability; no spontaneous instability
3. Shielded stream (standard, like-impinging pattern, with tube extensions on the orifices to protect the streams prior to impingement); unbaffled; undamped, bomb-induced instability
4. Spray nozzle (small, separate, spray nozzles for fuel and oxidizer in alternating rings); baffled; spontaneous, undamped, instability during start.
5. Coaxial with swirl (coaxial elements, oxidizer in center, variable injection plane, tangential swirler design); baffled; unbombed tests; damped and undamped spontaneous instabilities.

Several injector types were studied in the 1964 experimental investigation of LOX/RP-1 combustors previously discussed (Ref. A-1). These tests were conducted at nominal 1000 psia chamber pressure, with no stability aids. The conventional concentric tube element (fuel surrounding oxidizer) gave consistently unstable combustion at mixture ratios greater than 1.5; at lower mixture ratios, combustion was stable. The reverse concentric element (oxidizer surrounding fuel) was unstable and also had low performance and severe injector face overheating. Limited tests of a micro-orifice injector showed stable combustion but structural limitations of the micro-orifice material precluded its use. The like-impinging jet injector gave stable combustion and low performance, in agreement with similar injectors in the large LOX/RP-1 production engines.

Nearly all of the LOX/RP-1 production engines used baffles as stability aids (Table A-1). A study of the use of acoustic chamber liners as stability aids in LOX/RP-1 combustors was reported in 1967 (Ref. A-2). The perforated combustion chamber liner within an outer shell formed a parallel array of Helmholtz resonators. The thrust chamber used in these tests had a diameter of 3.7-in., a characteristic length (L^*) of 47.5-in. and a contraction ratio of 4.5. A 152-element, stainless steel, concentric tube injector (oxidizer in center tube) was used, with copper chamber sections and nozzle. The throat section was water cooled; both uncooled (zirconia-coated stainless steel) and water cooled (welded stainless steel tubes, with holes drilled between the tubes) acoustic liners were employed. At the nominal chamber pressure of 1000 psia, self-induced combustion instability and bomb-induced disturbances were

consistently damped by both the cooled and uncooled acoustic liners. A half-length cooled liner at the injector end of the chamber was as effective as the full-length liner.

Recent LOX/RP-1 Combustors

Pavli (NASA-LEWIS). In this test series at 600 psia (Ref. A-15), spontaneous instability occurred in some of the LOX/RP-1 tests with several types of injectors (O-F-O and F-O-F triplets and like doublets). With the triplet configurations, instability was observed with and without the presence of acoustic cavities; with the like doublet, instability occurred only in the absence of the resonator ring.

Huebner (Rocketdyne). The rectangular injector used in the 30 MW gas generator tests with LOX/JP-4 (Ref. A-23) had trimodal acoustic cavity slots around its periphery, with a total open area of about 15-percent of the chamber cross-section. This combustor was stable, with less than 3-percent peak-to-peak pressure oscillations at 440 psia chamber pressure. No dynamic stability tests were carried out.

LaBotz, et al. (Aerojet). Two injector types (transverse like-on-like, TLOL, and pre-atomized triplet, PAT) were tested in this program. In preliminary tests at 1700-1900 psia with a "tuned" acoustic cavity absorber (Ref. A-9), the TLOL injector was spontaneously unstable in the I-T mode and was not tested further. Contrary to pretest analyses, which predicted the PAT injector to be less stable than the TLOL, the opposite was found to be the case. In two multi-point tests (12- and 20-sec. durations), the PAT configuration was stable. No bomb testing for dynamic stability was conducted.

Schoenman & Gross (Aerojet). Stability analyses were carried out as part of the design of the pre-atomized triplet injector (Ref. A-21), with the following results:

- Chug mode: Stable at 2000-3000 psia; chugging at 420 Hz predicted at chamber pressures below 1790 psia
- Longitudinal mode: Predicted unstable in 1-L mode (1400 Hz) at 2000 psia but stable at 3000 psia
- High-frequency modes: Bituned, 12-cavity, acoustic ring designed, with nine cavities at 1-T mode (4700 Hz) and three cavities at 2-T mode (7800 Hz)

In limited testing of this injector (Ref. A-3), no stability results were reported, although the tests were carried out at 2000 psia, where 1-L mode oscillations were predicted.

Muss and Pieper (Aerojet). In this recent work (Ref. A-12-A), the statistical and dynamic combustion stabilities of O-F-O triplet and like-doublet injectors were evaluated with various baffle and acoustic cavity arrangements. Both injectors were dynamically stable with either a bimodal quarter-wave acoustic resonator or a 3-bladed baffle configuration. However, with no stability aids, both injectors were unstable in the first tangential mode; the O-F-O triplet had a spontaneous instability while the like-doublet was perturbed to instability by a bomb. When damping was provided for only the 1-T mode, the triplet injector was stable in all tests, while the like-doublet was perturbed to a 2-T instability by a combustion bomb.

HEAT TRANSFER

Introduction

Injector-influenced heat transfer considerations are those related to injector face cooling and those related to the combustion chamber wall. Both will be discussed in this review, with major emphasis on the latter.

Injector Face Cooling

Although injectors for high-pressure, high-performance LOX/RP-1 combustors will be subject to fairly high injector face heat flux levels, analytical procedures for design of appropriate cooling methods are well-developed and have been experimentally demonstrated. In the simplest cooling technique, high thermal conductivity material (copper or nickel) is used for the injector face, with cooling provided by the flowing propellants through back side convection and orifice passage regenerative-conduction cooling. The injector thermal analysis must, of course, include proper temperature limits for avoidance of RP-1 coking. No requirements for specific technology advances to provide adequate face cooling of high-pressure LOX/RP-1 injectors are presently indicated.

Combustion Chamber Cooling

Early LOX/RP-1 chamber cooling technology is exemplified by that used in the H-1 and F-1 engines. In both cases, the injectors employed like-impinging elements in alternating ring configurations, with large diameter orifices (Table A-1). They used auxiliary RP-1 film cooling and exhibited low throat heat transfer rates (4 to 8 Btu/in²-sec). Under these conditions, RP-1 regenerative cooling through brazed tubular chamber walls was satisfactory, particularly since carbon deposition on the walls provided a thermal barrier with favorable heat transfer effects.

At high chamber pressures and combustion efficiencies, however, the carbon thermal barrier will not be significant and estimated throat heat flux will be about an order of magnitude greater than in the pre-1970 engines. Manifestly, corresponding advanced chamber cooling techniques will be needed, which will impact injector design. High-pressure engine experience and extensive analytical studies indicate that regenerative cooling in a chamber consisting of a slotted liner with electroformed channel closeout is the best, basic, state-of-the-art approach.

Possible coolants are RP-1 or oxygen, for which some high-pressure experimental data are available, or hydrogen (in a tripropellant engine configuration), for which only analytical projections have been made.

RP-1 Cooling. Two major drawbacks to the use of RP-1 as regenerative coolant in the wall channels of high-pressure LOX/RP-1 combustors are the comparatively low temperature (550F, Ref. A-18) at which it begins to decompose and form carbonaceous deposits ("coking") and its erosive effect on copper and copper alloys (Ref. A-8), which are, at present, the only viable chamber liner materials. Analytical studies (Ref. A-6, A-14, and A-22) indicate that RP-1 cooling, with its coking temperature limitation and its high turbopump discharge pressure requirements, effectively limits LOX/RP-1 engine chamber pressure to about 2000 psia. Moreover, available test data, discussed below, indicate that the actual heat flux, as measured in high-pressure, high-performance, LOX/RP-1 combustors, may be substantially higher than the analytical estimates.

A recent analytical study of RP-1 regenerative cooling of high-pressure LOX/RP-1 combustion chambers (Ref. A-4) indicated that attainable chamber pressures might be increased by addition of a thin ceramic (ZrO_2) coating to the chamber wall and/or by use of "short" chambers to decrease the cooling requirements. Use of short chambers, in turn, requires development of highly efficient injectors to maintain a high performance level.

Oxygen Cooling. The use of oxygen as regenerative coolant in a LOX/RP-1 engine is an obvious alternative to the use of RP-1. However, there has been a general aversion to using oxygen for regenerative cooling, for two basic reasons: (1) if leakage through a wall crack allowed oxygen into the chamber, it might react with the fuel-rich combustion gases and overheat the wall, and (2) possible difficulties in injector functioning with hot gaseous oxygen.

Enough experimental work has now been reported to indicate that high-pressure regenerative cooling with oxygen may be feasible. Early work (1957-1967) in Germany (Ref. A-7) developed a LOX/kerosene engine that had a milled channel, OFHC copper, thrust chamber, with electroplated copper or nickel closeout. The combustor diameter was 7.09-in., with a contraction ratio of 2.57. Hot oxygen from a preburner was fed to the combustion chamber as an annular stream along the wall, which prevented the deposition of soot. Nevertheless, in spite of the resulting high heat transfer rates, regenerative cooling by oxygen was satisfactory over the tested ranges of chamber pressure (290 to 1230 psi) and mixture ratio (2.2 to 4.5).

In more recent work at NASA-Lewis (Ref. A-16), an experimental LOX/RP-1 study was conducted with supercritical LOX as regenerative coolant. The objectives of this program were to evaluate the cooling characteristics of LOX, the buildup of soot on the hot-gas-side chamber wall, and the effect of a LOX leak through the wall on the structural integrity of the combustor. A series of tests was carried out in which soot deposit thickness on the wall was measured at chamber pressures of 600 (M.R. = 2.2 to 2.9), 1200 (M.R. = 1.9 to 3.0) and 2000 (M.R. = 1.8 to 2.7) psia. To determine the effect of an oxygen leak, a cyclic hot-fire test series was conducted (at 600 psia) until a crack developed in the hot gas wall.

The O-F-O triplet element injectors and the milled channel chambers used in these tests were described above, in the discussion of injector performance.

Results of this test series were summarized as follows:

1. Successful cooling with LOX was demonstrated.
2. Oxygen passing through wall cracks formed by cyclic firings did not react with the carbon layer on the wall nor with the copper wall itself.
3. At 2.8 mixture ratio, soot thickness varied inversely with chamber pressure at the throat and remained constant in the cylindrical portion of the thruster. Soot deposition was least in the throat region. At a given location, soot thickness decreased as mixture ratio increased from two to three.
4. Performance levels of the triplet injectors were 99-percent c^* efficiency at 600 psia, 95-percent c^* efficiency at 1200 psia, and 96-percent c^* efficiency at 2000 psia. (The 600-psia unit did not include the outer zone showerhead elements that were in the larger injectors.)

Analytical evaluations of LOX cooling indicate that this technique would permit chamber pressures up to about 3000 psia, a substantial increase over RP-1 cooling (Ref. A-5).

Hydrogen Cooling. The excellent cooling capability of hydrogen has been thoroughly studied and demonstrated in a number of functioning LOX/H₂ engines (J-2, ASE, RS-44, RL-10, SSME). However, its use in a LOX/RP-1 engine, in which it would constitute a third propellant, has not yet been tested even in experimental thrust chambers. Analytical estimates indicate that use of LH₂ as regenerative coolant would permit LOX/RP-1 engine chamber pressures up to 5000 psi (Ref. A-5). It would also eliminate the coolant passage coking and

erosion problems of RP-1 and might permit gas-augmented atomization of the RP-1, which would improve performance and/or shorten chamber length.

Recent LOX/RP-1 Heat Transfer Technology

Results of post-1970 experimental work on high-pressure LOX/RP-1 injector heat transfer technology are summarized in this section.

LaBotz. et al. (Aerojet). Two injector types were tested in this program: a transverse like-on-like (TLOL) and a pre-atomized triplet (PAT), as described above. However, hot-fire tests in water-cooled thrust chambers were carried out only with the PAT injector, at approximately 2000 psia chamber pressure, mixture ratio range of 2.0 to 4.4, and chamber lengths of 11-in. and 15-in. (Ref. A-9). Results were summarized as follows:

1. Chamber throat heat flux is a strong, direct, linear function of mixture ratio.
2. The difference in total heat load between the 11-in and 15-in chambers was significantly greater than had been analytically predicted.
3. Most important, measured heat flux in the cylindrical combustion chamber was only one-third the predicted level, but rose sharply in the convergent section, reaching values at the throat (on the order of 70 Btu/in²-sec at 2.8 mixture ratio and 1980 psia) which were about 70-percent greater than forecast analytically. No conclusive evidence was found for any of the possible explanations which were suggested for this wide difference.
4. The thermal data and post-test hardware examinations gave no evidence of significant carbon deposition on the chamber wall.

Schoenman & Gross (Aerojet). Heat transfer analyses were conducted as part of an injector design (Ref. A-21). This injector was a modification of the original PAT pattern which had the very high nozzle throat heating rates discussed above. Design changes involved modifications of the elements to improve mixing and addition of outer barrier doublet elements to decrease heat flux in the throat region.

Bailey (NASA-MSFC). The injector fabricated in Ref. A-21 was combined with an uncooled resonator ring and a calorimeter chamber in a three-test series. Chamber pressures were 1726 to 2263 psia, at mixture ratios of 2.0 to 2.8. The primary program goal was to determine whether the injector changes had reduced the nozzle throat heating rates. Test data

showed that the barrier elements had effected a dramatic reduction in throat heat flux. At mixture ratio 2.8, the earlier injector exhibited throat heat flux of 70 Btu/in²-sec, whereas the modified injector had throat heat flux of about 41 Btu/in²-sec. As pointed out above, this heat rate decrease was accompanied by a substantial decrease in performance.

ANALYTICAL STUDIES

High-Pressure LOX/Hydrocarbon Engine Studies

A number of configurations of advanced, high-pressure, LOX/Hydrocarbon rocket engines were analyzed in several recent studies. Although no technology advances are made in such analyses, they do indicate current and projected technical status. Consequently, conclusions as to the characteristics of high-pressure LOX/RP-1 engines reported in these studies, even though they may disagree, are of interest in this review and are briefly discussed in this section.

Rocketdyne Studies. Three gas-generator-cycle LOX/RP-1 engines, cooled, respectively, with RP-1, LOX, or LH₂, were analyzed in this study (Ref. A-20). Analytical conclusions were summarized as follows:

1. The RP-1-cooled configuration cannot be used at chamber pressures higher than about 2000 psia. Maximum chamber pressure is increased to about 3500 psia with LOX cooling and to about 5000 psia with LH₂ cooling.
2. Use of a tripropellant concept (RP-1 and H₂ as fuels) makes this configuration competitive with other LOX/Hydrocarbon engines at equivalent chamber pressure.
3. All high-pressure LOX/RP-1 engines with high performance requirements have potentially major stability problems.

Trade studies were conducted to select main injectors and combustion chambers for each engine configuration. The approach used was to select a primary injector/chamber system and then to vary key parameters (orifice sizes, chamber length, number of baffles, acoustic cavities, etc.), thus defining several potential systems. For each system, estimates of performance, weight, pressure drops, cost, and current technology level were made and the optimum combinations were selected. For the main injectors, a like-doublet box pattern was chosen for liquid/liquid injection and a coaxial element for gas/liquid injection. A copper alloy chamber liner with slotted axial coolant channels and a typical contraction ratio of 2.7 was also selected.

Pratt & Whitney Studies. In this study (Ref. A-22), both gas generator and staged combustion cycle LOX/RP-1 engines were analyzed, with RP-1, LOX, or LH₂ cooling. Estimated upper chamber pressure limits were 2500 psia for RP-1 cooling, 2020 psia for LOX cooling, and 5100 psia for LH₂ cooling. Although the LOX/RP-1 propellant combination was not analyzed in great detail, some of the relevant conclusions were as follows:

1. A fairly low near-term c^* efficiency goal (94-percent) can be met; the far-term goal (97-percent) is less predictable.
2. Acoustic liners that will "ensure" stable combustion can be designed for all the engine configurations.
3. Hydrogen is the best coolant; oxygen is the worst coolant; RP-1, while a better coolant than oxygen, is limited to low operating pressures because of its coking limit bulk temperature (300F).

Aerojet Studies. Results of analytical studies of high pressure LOX/Hydrocarbon engines are reported in Ref. A-13 and A-14. For LOX/RP-1 engines, cooling with RP-1 limits chamber pressure to about 1200 psia, cooling with LOX limits pressure to about 3000 psia, and cooling with LH₂ limits pressure to about 5800 psia. Relevant study conclusions were:

1. Tripropellant engines (LOX/RP-1/LH₂) offer the most potential when factors such as performance, materials compatibility, coking, and growth margin are considered.
2. LOX-cooled, gas generator cycle engines are competitive with RP-1-cooled engines.
3. A multiple-tuned, acoustic cavity resonator may be required to damp high-frequency instability modes.

Chamber Cooling Studies

Methods of adequately cooling the combustors of high-pressure LOX/RP-1 engines have been studied analytically because of the special problems associated with the use of RP-1 as regenerative coolant. In one recent study (Ref. A-4), maximum chamber pressure limits were determined for LOX/RP-1 with and without a carbon layer on the chamber wall or with several other thermal barriers (ceramic coating, graphite liner, film cooling, transpiration cooling, zoned combustion, or combinations of these).

Without thermal barrier enhancement, the maximum attainable chamber pressure with RP-1 cooling was on the order of 2000 psi, due to the low coolant wall temperature required to avoid coking and to the comparatively long chamber required to meet performance criteria. The best enhancement is obtained with a carbon layer on the wall (which may not form) combined with a ceramic coating (ZrO_2). Another enhancement technique is the use of film cooling along the wall; transpiration cooling through porous wall material is probably not feasible with RP-1 because of potential coking problems.

INJECTOR TECHNOLOGY STATUS SUMMARY

Results of the very limited experimental work that has been carried out with LOX/RP-1 injectors at high chamber pressure (2000 psi and over) confirm the inherent difficulty of achieving high performance (97-percent minimum c^* efficiency) in combination with stable combustion and acceptable heat flux levels. While each of these goals can be separately attained, at the expense of one or both of the other two, no tests have yet demonstrated unequivocally that all three can be simultaneously achieved, even in small-scale, low-thrust hardware.

Performance

Although the injection densities required for LOX/RP-1 chamber pressures in the 2000-3000 psia range are greater than those associated with existing production engines, there is no reason to believe that the classical requirements for high performance do not remain applicable. High degrees of mixing uniformity and liquid atomization, which are the essential requirements, can be obtained with several demonstrated injection patterns. However, the injection process substantially affects combustion stability and chamber heat flux as well as combustion efficiency, so the selection of a pattern and the distribution of the elements across the injector face must take all three characteristics into account. Consequently, injection element parameters which give good mixing and atomization and therefore high performance (such as unlike impingement, very small orifice diameters, high element density, and efficient intra- and inter-element mixing), may have to be compromised or not used at all because of their adverse effects on stability and heat flux.

The only LOX/RP-1 injection element which has demonstrated c^* efficiency as high as 96 percent at the 2000-psia chamber pressure level is a pre-atomized triplet, when it was distributed uniformly across the injector face (including the peripheral region). However, the

throat heat flux measured in this case was 70-percent higher than predicted. Reduction of the heat flux to acceptable levels by inclusion of barrier elements in the outer region of the injector lowered the c^* efficiency to 91-94 percent. Reported c^* efficiencies of 96-102 percent with O-F-O triplet injectors were obtained in short duration tests with ablating throats; these results are therefore open to question.

Performance technology for high-pressure LOX/RP-1 injectors at the start of the present program can be easily summarized:

1. High performance *per se* has been demonstrated, but high performance combined with acceptable heat flux and dynamic stability has not.
2. Injector configurations which are amenable to significant heat flux control with minimum adverse effect on performance and stability are yet to be developed.

Stability

Experience indicates that the stability characteristics of a large, high-performance, LOX/RP-1 injector must be a critical concern in its design. Theoretically, of course, this should not be the case, because any injector of this type will not be used without stability aids (baffles, acoustic cavities, acoustic liners). If the technology of stability aids were sufficiently advanced, they could be designed so that any incipient instability would be instantly damped or absorbed without affecting the combustion process. Therefore, the effect of the injector in initiating a disturbance would be of little consequence and would not compromise its design. Unfortunately, stability aid technology is still far from this point. Available analytical methods are not able to predict reliably the damping capability of stability aids, particularly in regimes for which there are no anchoring test data. Neither can the tendency toward instability initiation of a given injection element be reliably predicted at untested operating conditions.

It follows that the likelihood of any injector type initiating and sustaining combustion instability must be predicted as well as possible from experience and analysis and that stability aids must be designed on the same basis. The effects of the combination of injector and stability aids can be determined only by testing.

The current status of high-pressure LOX/RP-1 injector stability technology rests only on a small number of tests in the 2000 psia chamber pressure range with acoustic cavities or baffles as stability aids. A like-doublet injector was spontaneously unstable; a pre-atomized triplet and

an O-F-O triplet were stable. The experimental evidence indicates that any practical injection element can be stabilized with properly developed stability aids.

Heat Flux

Chamber heat flux considerations can affect the design of a high-pressure LOX/RP-1 injector in several ways. Analyses and background experience indicate that only a regeneratively cooled, copper alloy, combustion chamber would be appropriate in this type of engine. Given that requirement, there are a number of factors and options which further influence the heat transfer aspects of injector design:

1. Use of RP-1 as regenerative coolant, without enhancement, limits chamber pressure to the 2000 psia range. If RP-1 must be used at higher pressures, enhancement by such techniques as the installation of a thin ceramic chamber liner, use of fins in the coolant channels, film cooling, or modification of the combustion chamber (short lengths, sharp radius of curvature at the throat) will be necessary. Such enhancement techniques cannot be considered part of injector development technology.
2. Special considerations involved in the use of RP-1 as coolant relate to coking and erosion. Again, these are important problems to be solved but are not included as part of injector technology.
3. If RP-1 is used as coolant, it will enter the injector manifold at elevated temperatures which will be further raised as it flows through the injector face. This affects injector design because hot RP-1 increases the possibility of progressive coking and blocking of orifices, particularly if the orifices are small.
4. Cooling with LOX is an alternative to cooling with RP-1. Limited experimental data indicate that such cooling is feasible. It would also raise the maximum attainable chamber pressure compared to that with RP-1 cooling, although conflicting estimates have been reported in this regard. The important effect on injector design of using LOX as coolant would be the conversion to gas/liquid injection from liquid/liquid injection, which involves a different technology. Fortunately, a solid experience base for high-pressure gas/liquid injectors is available from the extensive development efforts carried out for the Space Shuttle Main Engine.
5. A third method of chamber cooling is by use of LH₂, which converts the LOX/RP-1 engine to a tripropellant system and permits chamber pressures as high as 5000

psia. The effect on the main injector of using LH₂ cooling will depend on the particular engine system. In one gas generator cycle, all the hydrogen is burned in the gas generator; the product gas powers the turbines and is then injected into the engine nozzle. This retains the main injector for LOX/RP-1. In another cycle, with a greater proportion of hydrogen, some of the hydrogen is directed to the main injector after the cooling circuit. This requires a tripropellant injector, which offers many possible design variants and would require technological development.

6. The options of using substantial film cooling or mixture ratio bias as a means of reducing chamber wall and throat heat flux are probably not viable, because the resulting loss of combustion efficiency would not be acceptable.

At the start of the present program, high-pressure LOX/RP-1 injector heat transfer technology status consisted of the demonstration at 2000 psia chamber pressure that provision of cooling barrier elements around the injector periphery lowers excessively high throat heat flux but simultaneously lowers c* efficiency to an unacceptable level.

INJECTOR TECHNICAL PLAN

INTRODUCTION

The preceding review has shown that substantial technology advances are required before a large, high-pressure, LOX/RP-1 injector can be designed and demonstrated which will meet the goals of high performance, stable combustion (with suitable stability aids), and chamber compatibility. The technical problem is to achieve these goals simultaneously, without unacceptable sacrifice of any one of them. A plan to develop the requisite technology is outlined in this section. As before, high-pressure injector performance, stability, and heat flux characteristics and requirements will be discussed separately, for convenience, with the recognition that they are actually very interdependent.

COOLING METHOD SELECTION

As the first task of the present program on LOX/Heavy Hydrocarbon Main Injector Technology, this review concentrated on the liquid/liquid injection of LOX and RP-1. However, because of the difficulties associated with the use of RP-1 as regenerative coolant in a high-pressure thruster, it is possible that the cooling method will be modified and the injection process will involve fluids other than liquid LOX and liquid RP-1, even though the engine remains a LOX/RP-1 system. Depending on the choice of engine cycle and coolant, the main injector may alternatively be a gas/liquid type (GOX/RP-1) or a tripropellant type (LOX/RP-1/GH₂), each depending on a technology base substantially different from that of a liquid/liquid injector. Manifestly, the first task of an injector technology plan is to choose an appropriate cooling technique for the selected LOX/RP-1 engine.

The injection type selection process is indicated in Fig. A-2. The choice of cycle for the LOX/RP-1 engine, the chamber pressure to be used, and the injection mode will be based on four factors:

- Mission Requirements
- Cycle Analyses Results
- LOX/RP-1 Engine Experience
- Available Cooling Methods

Effort in some of these areas has already been substantially completed and may only need refining; in others, significant technology tasks are still required.

Mission Requirements Analyses

The need for a new, high-pressure, LOX/Hydrocarbon engine for a variety of missions has been identified in a number of studies. In the present program, the hydrocarbon fuel is assumed to be RP-1.

Engine Cycle Analyses

Following the mission requirement studies, extensive engine cycle analyses were made, in which each of three hydrocarbons (methane, propane, and RP-1), LOX, and LH₂ were examined as fuel and/or coolant in various high-pressure engine cycles (Ref. A-14, A-20, and A-22). None of the candidate fuels, coolants, or cycles has yet been selected for development and the engine analyses and LOX/Hydrocarbon test programs are being continued.

Cooling Method Selection

Before the best method of cooling a high-pressure LOX/RP-1 chamber can be chosen, several technology areas must be investigated to augment, complete, or verify existing experimental data and analyses.

RP-1/Copper Compatibility. The incompatibility of RP-1 with copper, manifested in corrosion of copper alloy coolant channels and deposition of carbonaceous solids on the hot

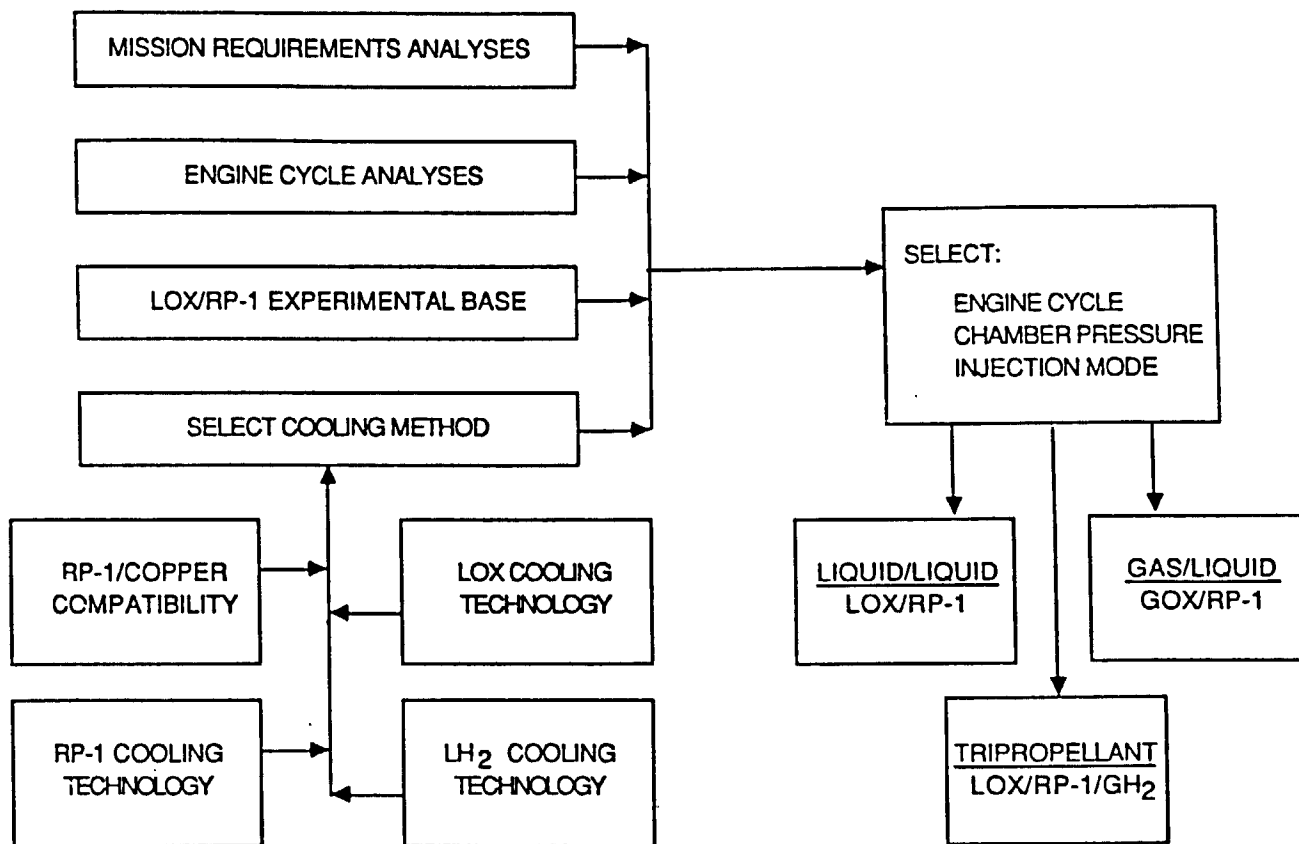


Figure A-2. Selection of Engine Cycle, Cooling Method, and Injection Mode

metal surface, has been studied extensively and is a critical factor in the selection of a suitable coolant for LOX/RP-1 engines (Ref., A-6, A-8, A-14 and A-18).

The reaction of hydrocarbons with copper depends on the wall temperature, fluid velocity, impurities in the fuel, and the presence of coke-type deposits. Little information is available on the absolute rate and level of attack as functions of fuel composition and wall conditions. The corrosion may possibly be prevented by plating the copper with electroless nickel. To evaluate the feasibility of RP-1 as regenerative coolant, further experimental work is required to determine the mechanism of the reaction and to develop a "fix". This would include: (1) determination of the role of direct-resistance heating on the observed corrosion (by test firing a high-pressure, hydrocarbon-cooled combustor); (2) determination of the effects on corrosion rates of flow parameters (temperature, pressure, flowrate) and of impurities in the fuel (particularly sulfur); (3) determination of corrosion mechanisms; and (4) development and evaluation of protective measures (e.g., metal coating or alloying; use of fuel additives).

RP-1 Cooling Technology The substantial data base on RP-1 regenerative cooling available from the classic LOX/RP-1 engines is only partially relevant to the problems presented in high-pressure, high heat flux applications. For successful RP-1 cooling at high pressures, the use of fluid or solid thermal barriers would very probably be necessary. Three types of fluid thermal barriers may be considered: film cooling, throat region transpiration cooling, and outer zone mixture ratio biasing.

Film cooling has been successfully used in many liquid propellant engines, particularly with LOX/RP-1 propellants. This cooling enhancement technique results in increased cycle life and raises allowable chamber pressures. The penalty, however, is a significant decrease in performance (0.5 to 3 percent, depending on the proportion of fuel used for film cooling). Another drawback of film cooling, in which the coolant is injected around the periphery of the injector face, is that it is most effective at the upstream end of the chamber, where it is least needed, and least effective at the throat, where it is needed most. Analytical methods for film cooling design are fairly well developed. Technically, the effectiveness of film cooling for a given injector design can be measured by tests with and without such cooling, and could be traded against the measured effects on performance.

Throat region transpiration cooling consists of passing the coolant through a porous wall in the throat section. Although this is the most efficient use of the coolant, it would be more

suitable with light hydrocarbons, oxygen, or hydrogen than with RP-1, which has a comparatively low specific heat and presents the real possibility of coking.

Mixture ratio bias, or zoned combustion, reduces wall heat flux by incorporating peripheral elements which operate at a mixture ratio below nominal (if the nominal mixture ratio is lower than stoichiometric), while the core elements operate at slightly above nominal mixture ratio. This provides a reduced-temperature combustion gas along the wall without changing the overall mixture ratio or flowrate. The limiting case of zoned combustion is film cooling, in which the outer zone mixture ratio is zero. This approach is most useful for injector designs which yield abnormally high heat flux.

Solid thermal barriers on the chamber wall can be effective means of heat flux reduction. Such barriers include carbon deposited by the combustion gas, high-temperature liners (such as graphite, silicon carbide, hafnium carbide, rhenium, tungsten, or iridium) or refractory ceramic oxide coatings (such as ZrO_2). Critical requirements for a successful liner include: non-oxidizability (or oxidizable to a thin protective scale), high melting point, thermal conductivity compatible with fabricability as a thin shell, and thermal fatigue resistance. Carbon deposited on the chamber wall in a high-pressure LOX/RP-1 combustor cannot be relied upon as a thermal barrier because limited experimental data indicate that such deposition may not occur or may be too thin to be significant. The mechanical liners hold promise of significant benefit in decreasing heat flow to the regenerative coolant, but all require substantial development. Technologies to be studied include: candidate material screening, oxidation rate data acquisition, thermo-mechanical analyses and tests, and fabrication studies and demonstrations.

In this regard, technological advances to improve the chamber wall copper alloy now considered to be the best chamber material for a high-performance, high-pressure, LOX/RP-1 combustor are important. Studies are being made to improve this alloy (NARloy-Z) and to develop microcomposite materials such as a Cu-Nb composite.

LOX Cooling Technology. The favorable thermodynamic and transport properties of oxygen make it a potentially attractive regenerative coolant which would not have the erosion/corrosion and coking problems of RP-1. Limited experimental data confirm the potential of oxygen as chamber coolant. The major concern in this application is the potential hazard of an oxygen leak from a coolant passage into the combustion chamber in a high-pressure system. A decision as to the viability of oxygen as coolant in a high-

pressure, high-performance, LOX/RP-1 engine will require technology advances, particularly relating to the consequences of a coolant leak in a critical combustor region (such as immediately upstream of the throat).

Another potentially useful application of oxygen cooling is as a throat region transpiration coolant, which would also require experimental demonstration. A major favorable result of using oxygen as regenerative coolant would be the change of the main injector to a gas/liquid type, which is inherently higher performing than a liquid/liquid configuration.

LH₂ Cooling Technology. Although the use of LH₂ as a regenerative coolant in a high-pressure engine is a relatively mature technology, the introduction of a third propellant to the LOX/RP-1 system would add substantial complexity. If hydrogen cooling were adopted, its effect on injector design would depend on the engine cycle selected. In one gas generator cycle, no hydrogen would be introduced through the main injector, which would remain liquid/liquid LOX/RP-1; in another, a tripropellant injector would be required (with the hydrogen gas possibly injected through a porous injector face or through an element which augments RP-1 atomization). Both cases would emphasize injector designs for high performance and stability potential because regenerative hydrogen cooling could accommodate even high heat flux levels. Technology advances in tripropellant injection methods would be required if this system were selected. Use of a staged combustion engine cycle would also require gas/liquid injection technology.

Recent experimental evidence of high-pressure LOX/Hydrocarbon combustor throat heat flux levels 50- to 70-percent greater than analytical predictions favors the use of hydrogen as coolant, particularly if the performance decreases inherent in the use of substantial film cooling or mixture ratio bias are unacceptable.

INJECTOR MODE SELECTION

The technology advances in the various LOX/RP-1 cooling methods would be used as they become available to carry out analytical and systems studies upon which the choices of a particular cooling technique and engine cycle would be based. These choices, in turn, will establish the type of injector which would be needed and the injector development process could then begin.

The general scheme for designing, testing, and demonstrating an injector suitable for the selected LOX/RP-1 engine (Fig. A-3) is the same for any injector type. Concepts for candidate injection elements are generated on the basis of existing experience and analyses and then subjected to cold-flow tests to determine their mixing and atomization characteristics. The cold-flow data are compared with similar data from known injectors for an indication of hot-fire behavior and are also used as inputs to various performance and stability computer models. Results of the model calculations assist in choosing the candidates for hot-fire testing. Since the stability and heating rate behavior of an injector are greatly dependent on non-injection characteristics of the thruster (such as the use of stability aids and cooling enhancement), the latter must be considered in the injector designs to the extent that the then current technology permits. Small-scale hot-fire tests of promising injection concepts are conducted to identify the most favorable one(s) for subsequent testing in larger scale hardware. The design which completes this process, in conjunction with improvements which would be made in the injector, stability aids, and cooling enhancement methods during the hot-fire testing, is then the best available at the existing technology level.

TECHNOLOGY DEVELOPMENT SCHEDULE

A rough time table for advancement of the technologies required for design and demonstration of a main injector suitable for a high-pressure, high-performance, LOX/RP-1 engine is shown in Fig. A-4. The major technology studies relate to provision of adequate engine cooling. Although combustion stability is equally essential for engine functioning, existing techniques for design of stability aids will probably not be significantly improved in the near future. They must be considered adequate, with the absolute requirement of demonstration in hot-fire testing.

Cooling Technology

Cooling technology advances for RP-1 or LOX regenerative cooling are required for design of the respective types of LOX/RP-1 engines, because either propellant may have characteristics which would eliminate it from consideration or impose unacceptable restrictions on engine design, cost, or function.

RP-1 Cooling. Before RP-1 can be considered as a regenerative coolant at high pressures, improvements in three technologies will be needed:

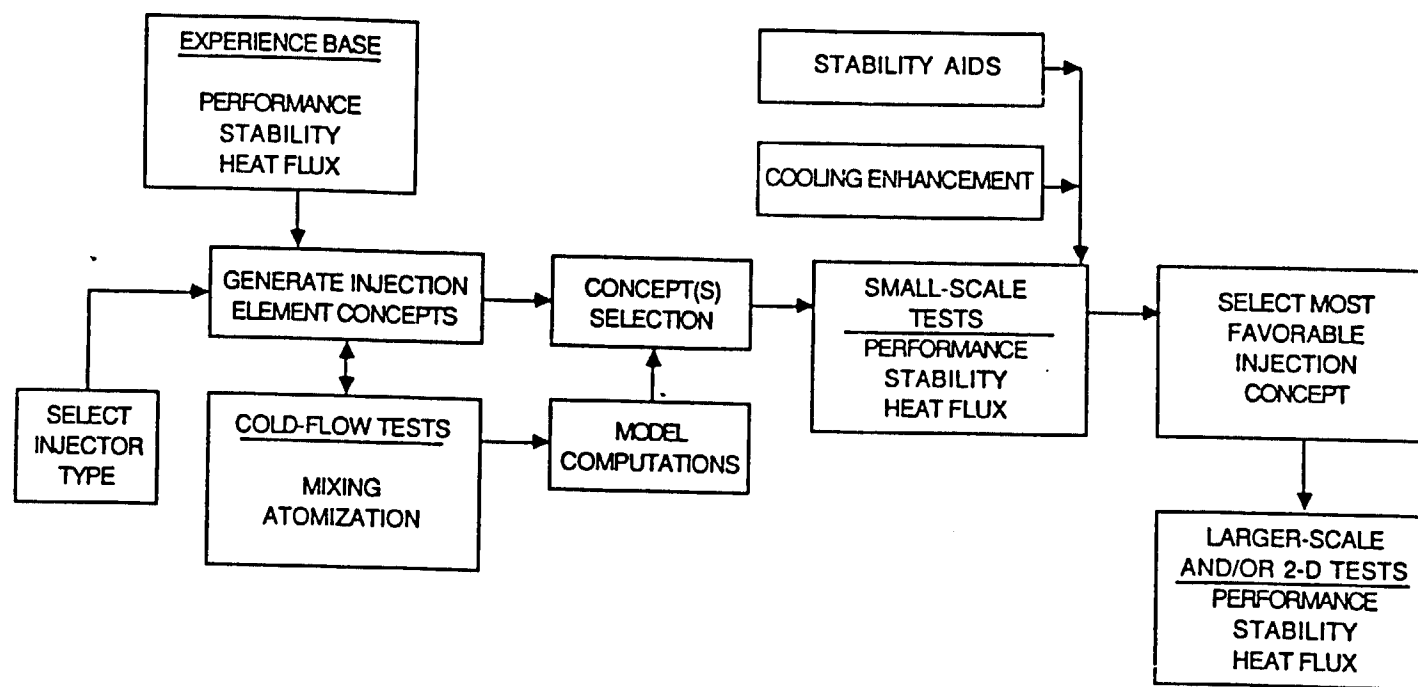


Figure A-3. Selection and Demonstration of Injection Concept

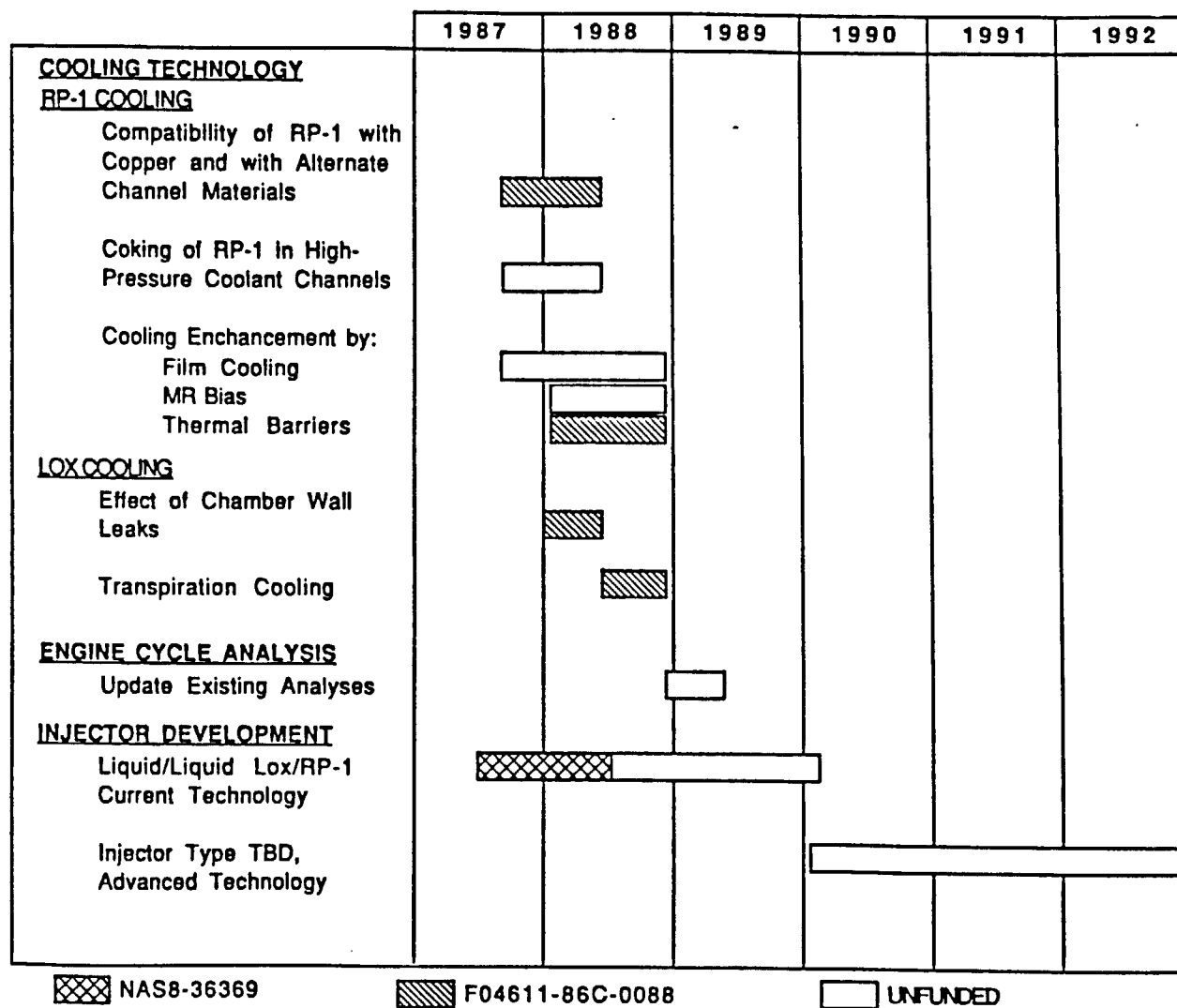


Figure A-4. Technology Development Schedule

1. **Compatibility.** The erosion/corrosion of copper and copper alloys by RP-1 must be eliminated or drastically reduced. Studies of the action of RP-1 on modified copper alloys and on other materials suitable for coolant channels are required. Such studies are planned in the current Air Force "LOX/Hydrocarbon Thrust Chamber Technology Program" (Contract No. F04611-86-C-0088).
2. **Coking.** The tendency of hydrocarbons to dissociate, crack, and carbonize increases with temperature and pressure. RP-1 in chamber cooling channels may be subject to pressures of 5000 psi or higher and temperatures up to 500 F. Its behavior in this environment requires investigation.
3. **Cooling enhancement.** Various methods of cooling enhancement have been proposed to permit the use of RP-1 as regenerative coolant at high pressure. Film cooling has been studied in a limited manner and should be further investigated by determining its effect on the heat flux and performance of various LOX/RP-1 injector configurations. Mixture ratio bias is a less drastic approach than film cooling and should also be investigated. Use of physical thermal barriers to reduce heat flow to the coolant liquid requires more extensive studies, first to develop application methods for suitable coatings and then to determine their effectiveness and durability.

LOX Cooling. The conceivable catastrophic consequences of a leak of LOX coolant into a high-pressure combustor require more investigation than the limited work reported to date. Such determinations, as well as a study of the potential of LOX as a throat region transpiration coolant, should be planned .

Engine Cycle Analysis

The knowledge of advanced cooling technologies which will be available, together with the experimental measurements of heat flux which are being made in on-going high-pressure LOX/RP-1 programs, will permit updates to be made in existing engine cycle analyses. These will define the cycle which holds the most promise for development and will thereby determine the type of main injector needed.

Injector Development

Either a liquid/liquid or gas/liquid main injector will be required by a LOX/RP-1 engine, depending on the selected engine cycle and coolant:

LIQUID/LIQUID	
ENGINE CYCLE	COOLANT
GAS GENERATOR GAS GENERATOR (ALL H ₂ GOES TO GG)	RP-1 LH ₂

GAS/LIQUID	
ENGINE CYCLE	COOLANT
GAS GENERATOR GAS GENERATOR (SOME H ₂ GOES TO MAIN INJECTOR)	LOX LH ₂
STAGED COMBUSTION	ANY

Although the characteristics of liquid/liquid and gas/liquid injectors are very different, the development process for both would follow the path indicated in Fig. A-3. The present program started the process for liquid/liquid injectors, using advanced injection concepts combined with current cooling and stability aid technologies. A similar program would be required for a gas/liquid injector.

REFERENCES

- A-1. Bailey, C. R., "Performance and Stability of Rocket Engine Injectors Using LOX/RP-1 Propellants", NASA TM X-53126, September 1964
- A-2. Bailey, C. R., "An Investigation of the Use of Acoustic Energy Absorbers to Damp LOX/RP-1 Combustion Oscillations", NASA TN D-4210, November 1967
- A-3. Bailey, C. R., "RP-1 and Methane Combustion and Cooling Experiments", in Advanced Earth-to-Orbit Propulsion Technology 1986, Vol. II, Edited by R. J. Richmond and S. T. Wu, NASA Conference Publication 2436, May 1986
- A-4. Cook, R. T., "Advanced Cooling Techniques for High-Pressure Hydrocarbon-Fueled Engines", NASA CR-159790, October 1979
- A-5. Cook, R. T. and Kirby, F. M., "Lox/Hydrocarbon Combustion and Cooling Survey", in Advanced Earth-to-Orbit Propulsion Technology 1986, Vol. II, Edited by R. J. Richmond and S. T. Wu, NASA Conference Publication 2436, May 1986
- A-6. Cook, R. T. and Bissell, W. R., "Oxygen/Hydrocarbon Booster Rocket Engine Study", NASA Contract NAS8-36357, Report No. RI/RD 86-280, Rocketdyne Division, Rockwell International Corp., Canoga Park, CA, November 1986
- A-7. Dederra, H. and Kirner, E., "High Pressure Rocket Engine Liquid Oxygen Technology", International Astronautical Federation, 26th Congress, Paper No. IAF-76-174, October 1976
- A-8. Giovanetti, A. J., Spadacinni, L. H. , and Szetela, E. J., "Deposit Formation and Heat Transfer in Hydrocarbon Rocket Fuels", NASA CR-168277, October 1983

- A-9. LaBotz, R.J., Rousar, D. C., and Valler, H. W., "High-Density Fuel Combustion and Cooling Investigation", NASA CR-165177, Contract NAS 3-21030, August 1980
- A-10. "Liquid Rocket Engine Injectors", NASA Space Vehicle Design Criteria. NASA SP-8089, March 1976
- A-11. "Liquid Propellant Rocket Combustion Instability", D. T. Harrje, Editor, NASA SP-194, 1972
- A-12. "Liquid Rocket Engine Combustion Stabilization Devices" NASA Space Vehicle Design Criteria, NASA SP-8113, November 1974
- A-12A. Muss, J. A. and Pieper, J. L., "Performance and Stability Characterization of LOX/Hydrocarbon Injectors", AIAA-88-3133, AIAA/ASME/SAE/ASEE 24th Joint Propulsion Conference, Boston, July 11, 1988
- A-13. O'Brien, C. J. and Ewen, R. L., "Advanced Oxygen-Hydrocarbon Rocket Engine Study", NASA Contract No. NAS8-33452, Report No. 33452F, April 1981
- A-14. O'Brien, C. J., Chen, F. F., and Vice, D. D., "Hydrocarbon Engine Study", NASA Contract NAS8-36359, Report No. 36359F, Aerojet Tech Systems Co., Sacramento, CA, September 1986
- A-15. Pavli, A. J., "Design and Evaluation of High Performance Rocket Engine Injectors for Use with Hydrocarbon Fuels", NASA TM-79319, September 1979
- A-16. Price, H. G. and Masters, P.A., "Liquid Oxygen Cooling of High Pressure LOX/Hydrocarbon Rocket Thrust Chambers", NASA TM-88805, August 1986
- A-17. Priem, R. J. and Heidmann, M. F., "Propellant Vaporization as a Design Criterion for Rocket-Engine Combustion Chambers", NASA TR R-67, 1960

- A-18. Roback, R., Szetela, E. J., and Spadacinni, L. J., "Deposit Formation in Hydrocarbon Rocket Fuels", NASA CR-165405, August 1981
- A-19. History of Project First. F-1 Combustion Stability Program, Prepared by Rocketdyne Engineering, Report No. R-5615-16, NASA Contract No. NASA-6, February 1967
- A-20. "Final Study Report for the Space Transportation Booster Engine Phase A Study", NASA Contract No. NAS8-36856, Prepared by Rocketdyne Division, Rockwell International Corp., Canoga Park, CA 91303, March 1987
- A-21. Schoenman, L. and Gross, R. S., "Design, Fabrication, Test, and Delivery of a High-Pressure Oxygen/RP-1 Injector", Contract NAS8-33651, NASA Report 33651F, September 1981
- A-22. Visek, W. A., Jr., "Hydrocarbon Rocket Engine Study", NASA Contract NAS8-36355, Report No., FR-19481-2, Pratt & Whitney Division, United Technologies Corp., West Palm Beach, FL, October 1986
- A-23. Swallom, D. W., et al., "High Power Magnetohydrodynamic System", AFAPL-TR-78-51, Vol I-II, July 1978

APPENDIX B

INJECTOR DETAIL DRAWINGS

This appendix presents the detail design drawings of the injectors used in the hot-fire evaluation tests.

<u>Figure</u>	<u>Injector</u>	<u>Diameter, in.</u>
B - 1 - A B - 1 - B	H-1 Derivative	3.5
B - 2 - A B - 2 - B	LOX Showerhead	3.5
B - 3 - A B - 3 - B	O-F-O Triplet	3.5
B - 4 - A B - 4 - B	Like-Doublet, Circumferential Fans	3.5
B - 5 - A B - 5 - B	Like-Doublet, Box Pattern	3.5
B - 6 - A B - 6 - B	Like-Doublet, Canted Fans	5.7

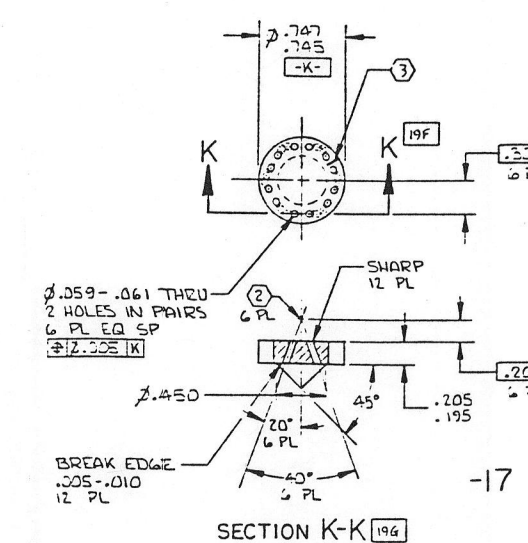
FOLDOUT FRAME

FOLDOUT FRAME 2

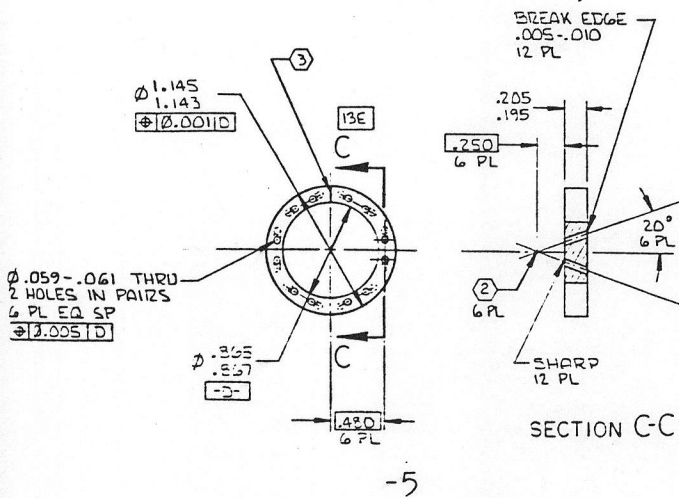
FOLDOUT FRAME 3

FOLDOUT FRAME 4

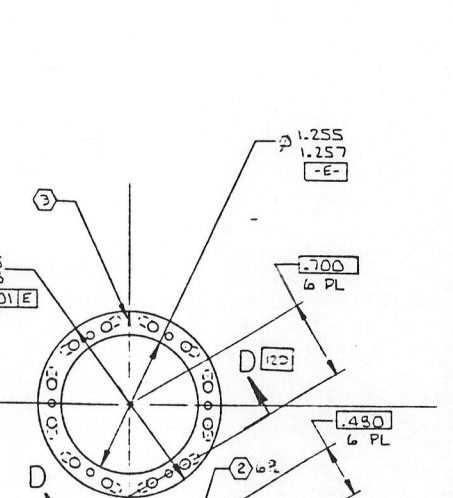
FOLDOUT FRAME 5



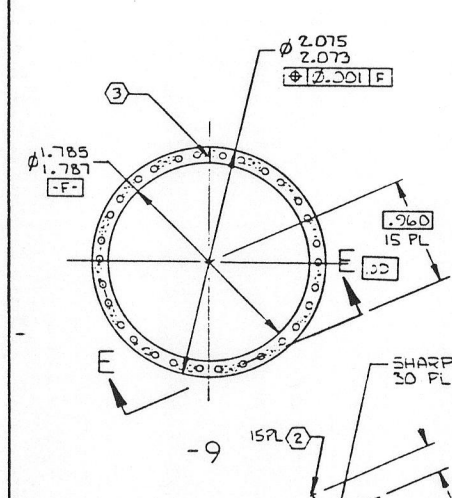
SECTION K-K [18]



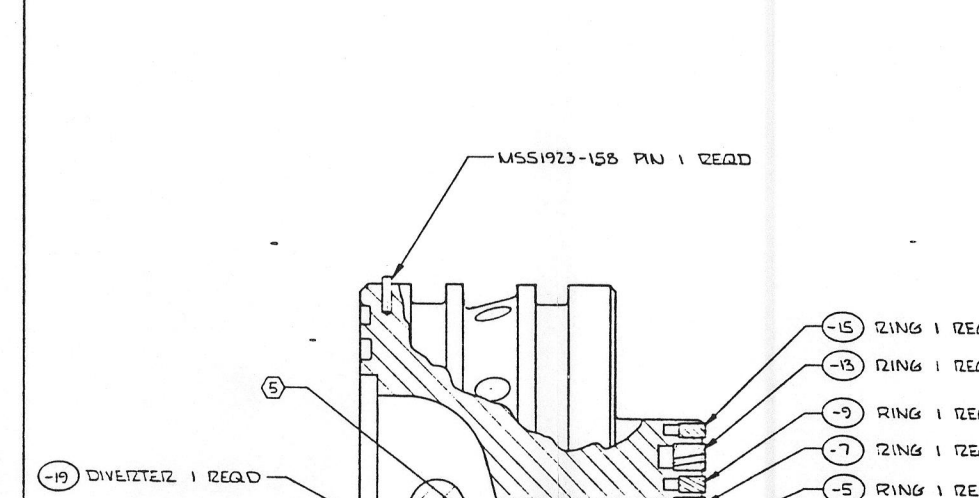
SECTION C-C [46]



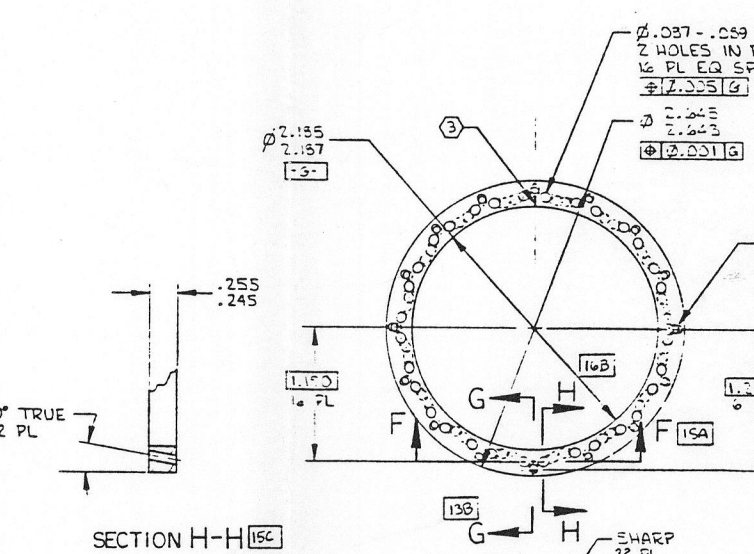
SECTION D-D [12]



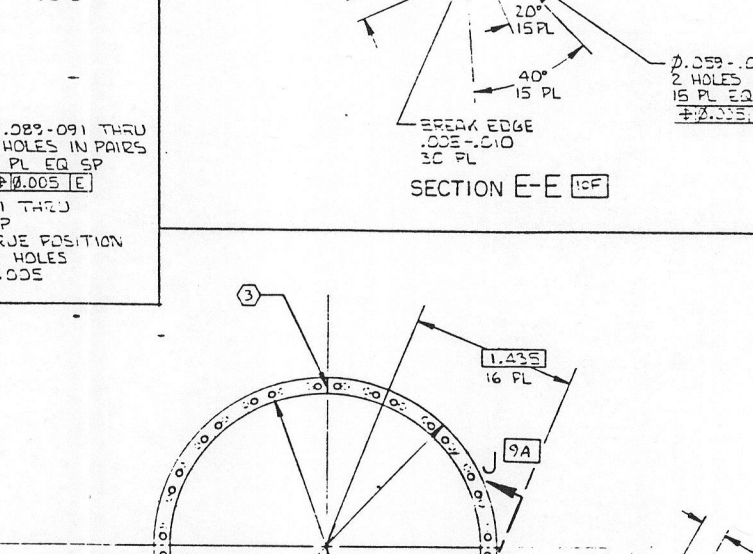
SECTION E-E [16]



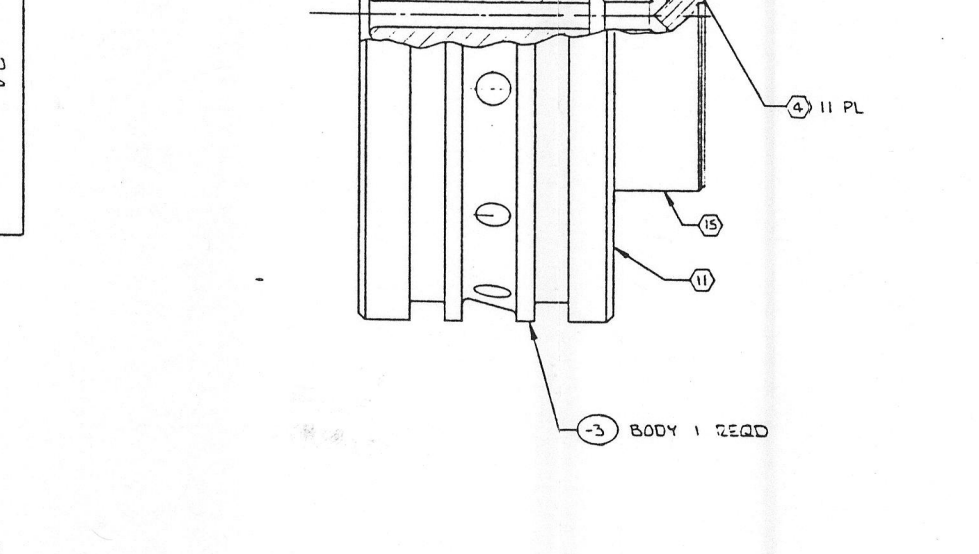
SECTION F-F [14]



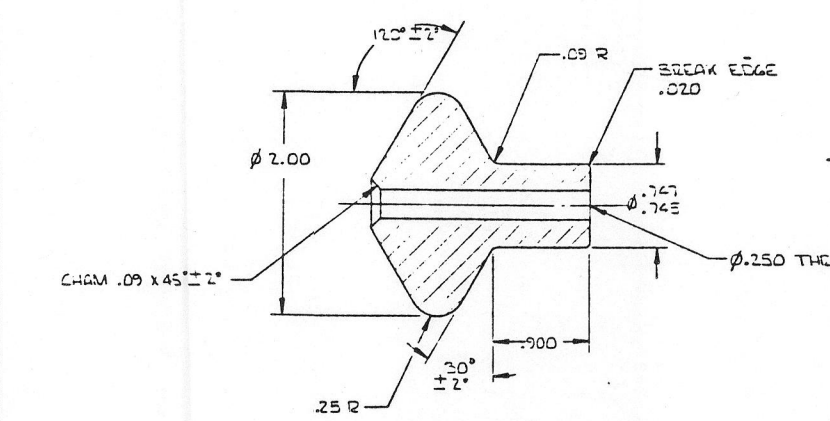
SECTION G-G [18]



SECTION H-H [12]



SECTION J-J [10]



SECTION I-I [16]

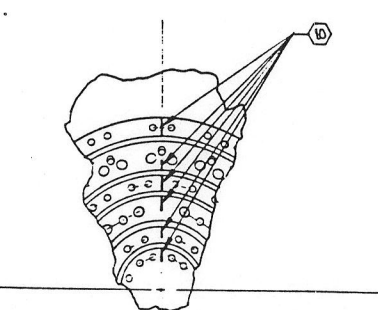
ORIGINAL PAGE IS
OF POOR QUALITY

Figure B-1-A. H-1 Derivative Injector, 3.5-inch Diameter, Sheet 1

1. VERIFY OFHC BY TESTING PER QSO10-047
2. NICKEL PLATE .002-.004 THICK, INDICATED SURFACE ONLY, PER QAW09-005
3. SEALING SURFACE REQUIREMENTS PER QF0004-027
4. ALLOWABLE ALTERNATES: 316, 316L OR 304 CRES PER QJ05-163
5. ALLOWABLE ALTERNATE: COPPER PER ASTM F48 (4)
6. DEEP ELECTROCHEMICAL ETCH IDENTIFY ASSY PER QF0004-044 TYPE II
7. DURING BRAZE, ALIGN SCRIBE MARKS WITHIN .010 TOTAL TRUE POSITION
8. CLEAN ASSY PER RADIO-004
9. CLEAN COPPER DETAILS PER RADIO-046
10. CLEAN CRES DETAILS PER RADIO-018
11. DRAWING INTERPRETATION PER QF0004-018
12. BRIZE PER RADIO-010 USING QSO10-064 (WELD) BRIZE ALLOY OR (4)
13. BRIZE PER RADIO-010 USING QSO10-065
14. UNWELD BRIZE ALLOY
15. SCRIBE 1/2 LONG LINE & APPROX .002 DEEP ON SURFACE INDICATED. LOCATE TRUE POSITION TO ADJACENT HOLES WITHIN .010 TOTAL. DO NOT SCRIBE HOLE EDGES
16. THEORETICAL CENTERLINES SHALL INTERSECT WITHIN .0005 TRUE POSITION
17. MACHINE PER RADIO-016

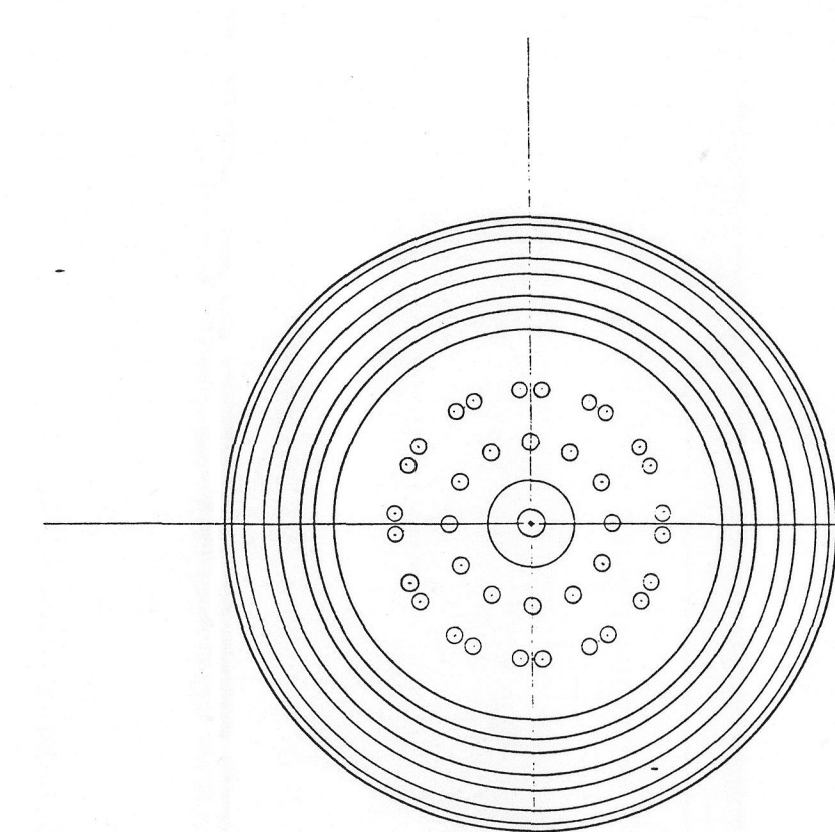
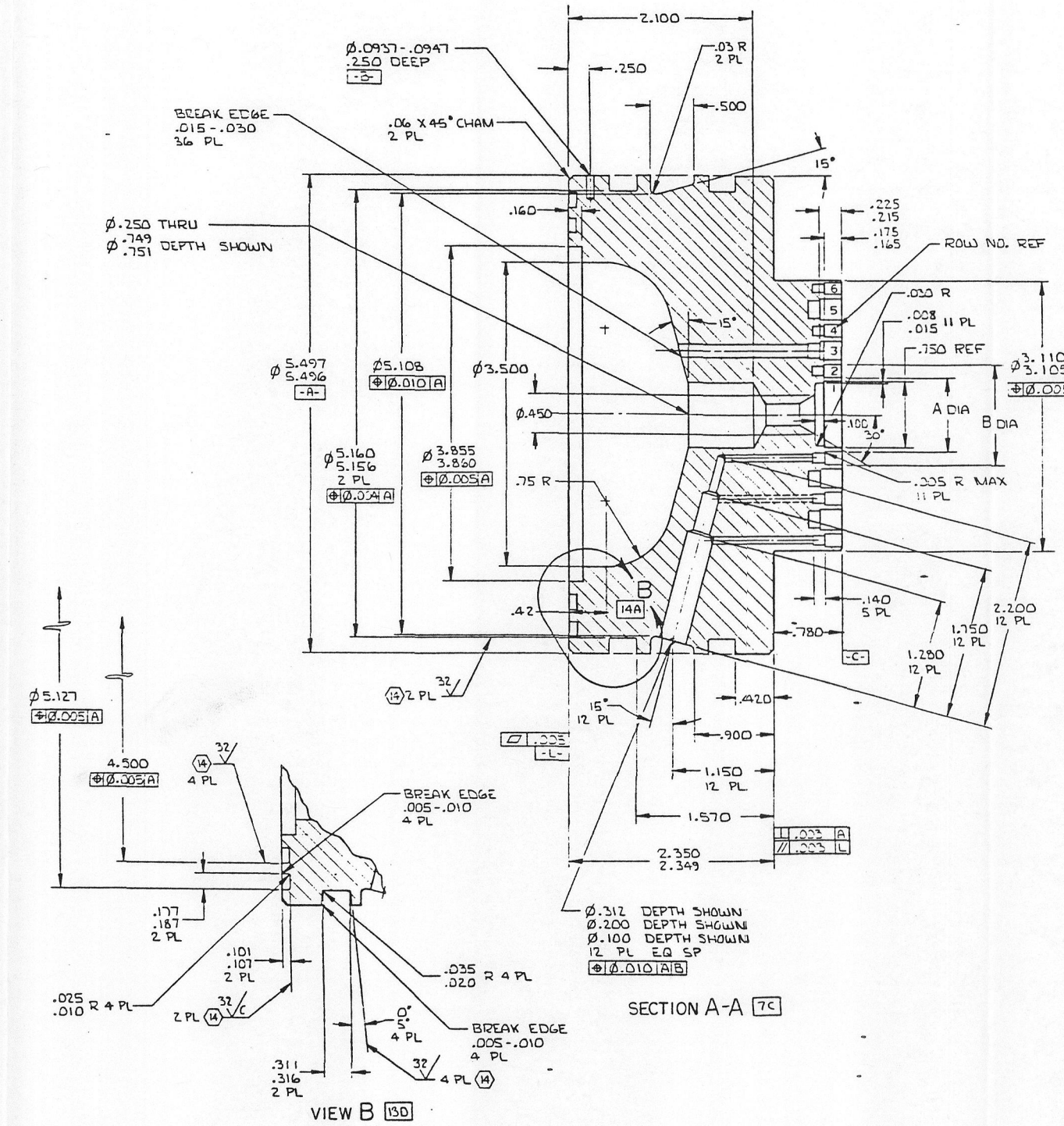
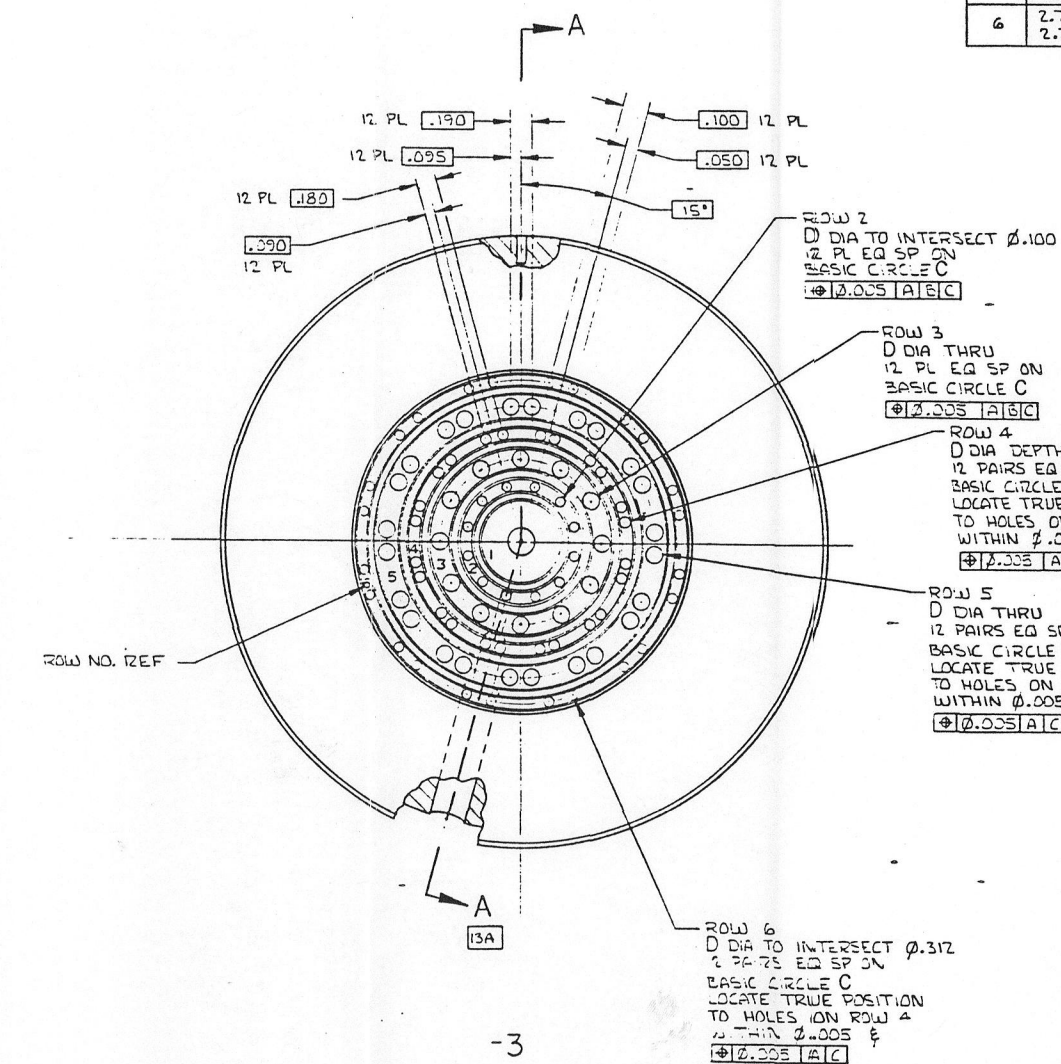
RELEASED
DOCUMENT

REV	DATE	DESCRIPTION	BY	CHKD
1	10/1/68	ISSUED FOR PRODUCTION	J. J. J.	J. J. J.
2	10/1/68	REVISIONS	J. J. J.	J. J. J.
3	10/1/68	REVISIONS	J. J. J.	J. J. J.
4	10/1/68	REVISIONS	J. J. J.	J. J. J.
5	10/1/68	REVISIONS	J. J. J.	J. J. J.
6	10/1/68	REVISIONS	J. J. J.	J. J. J.
7	10/1/68	REVISIONS	J. J. J.	J. J. J.
8	10/1/68	REVISIONS	J. J. J.	J. J. J.
9	10/1/68	REVISIONS	J. J. J.	J. J. J.
10	10/1/68	REVISIONS	J. J. J.	J. J. J.

B-2

REV	DATE	DESCRIPTION	BY	CHKD
1	10/1/68	ISSUED FOR PRODUCTION	J. J. J.	J. J. J.
2	10/1/68	REVISIONS	J. J. J.	J. J. J.
3	10/1/68	REVISIONS	J. J. J.	J. J. J.
4	10/1/68	REVISIONS	J. J. J.	J. J. J.
5	10/1/68	REVISIONS	J. J. J.	J. J. J.
6	10/1/68	REVISIONS	J. J. J.	J. J. J.
7	10/1/68	REVISIONS	J. J. J.	J. J. J.
8	10/1/68	REVISIONS	J. J. J.	J. J. J.
9	10/1/68	REVISIONS	J. J. J.	J. J. J.
10	10/1/68	REVISIONS	J. J. J.	J. J. J.

INJECTOR, 3.50 INCH,
LOX/H2, ASSY OF
J 02602 7R033441

ORIGINAL PAGE IS
OF POOR QUALITYORIGINAL PAGE IS
OF POOR QUALITYORIGINAL PAGE IS
OF POOR QUALITY

TABULATION BLOCK				
ROW NO	A DIA	B DIA	C DIA	REF NO. HOLES
1	NONE	.751	NONE	NONE
2	.861	1.151	1.005	12
3	1.251	1.681	1.466	12
4	1.781	2.081	1.930	12
5	2.181	2.651	2.415	12
6	2.751	3.041	2.895	12

Figure B-1-B. H-1 Derivative Injector, 3.5-inch Diameter, Sheet 2

RELEASED
DOCUMENT

SEE SHEET 1

B-3

7R033441	2
7R033441	2

FOLDOUT FRAME

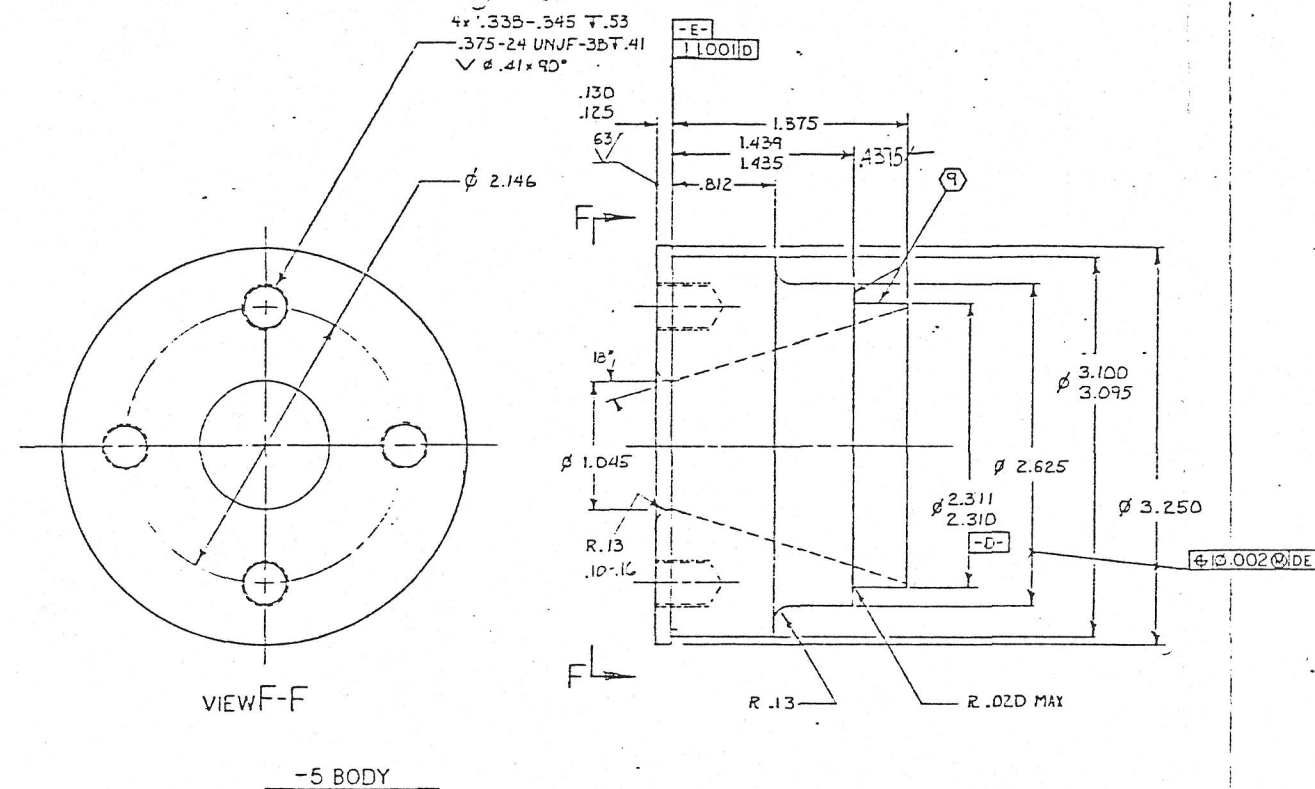
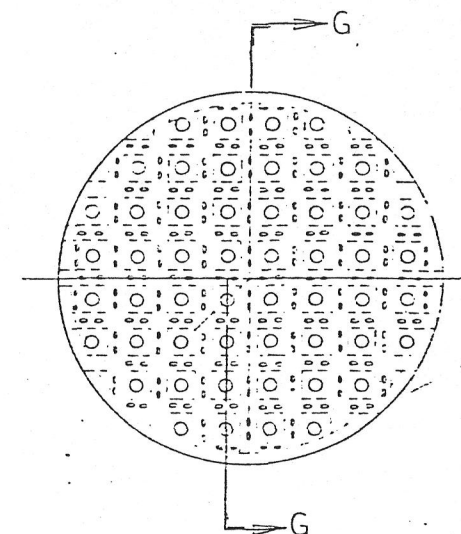
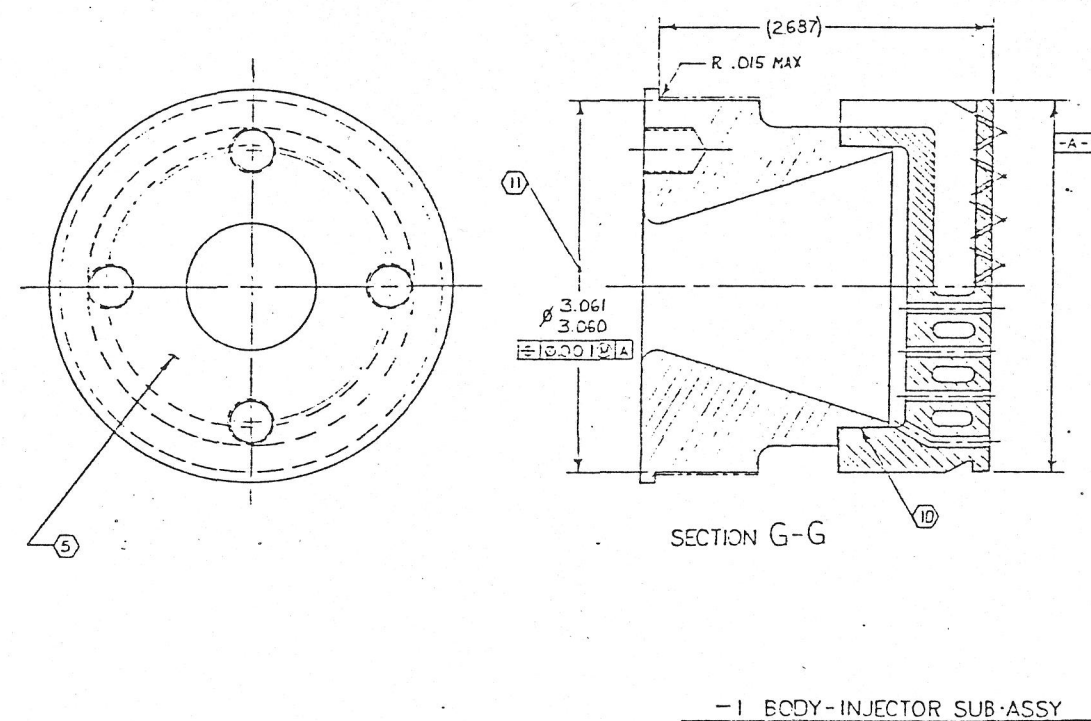


Figure B-2-B. LOX Showerhead Injector, 3.5-inch Diameter, Sheet 2



ORIGINAL PAGE IS
OF POOR QUALITY

B-5

RELEASED
DOCUMENT

ORIGINAL PAGE IS
OF POOR QUALITY

ORIGINAL PAGE IS
OF POOR QUALITY

FOLDOUT FRAME

ORIGINAL PAGE IS
OF POOR QUALITY

RELEASED
DOCUMENT

SECTION A-A 30

SECTION B-B 35
SCALE: $\frac{4}{1}$

NOTE CONT.

7. SEAL SURFACE REQUIREMENTS PER RFD004-021.
10. AFTER BRAZING, BEFORE EDM MACHINING, VERIFY JOINT INTEGRITY AS FOLLOWS, USE DRAINING TRO35413-1:
 - A. HYDROSTATIC PROOF TEST WITH WATER AT AMBIENT TEMPERATURE AT 1045-1095 PSIG (BOTH SIDES, SEPARATELY) MAINTAIN PRESSURE FOR 30 SECONDS MINIMUM, REDUCE PRESSURE TO ZERO, REPEAT FOR A TOTAL OF 5 CYCLES, BURST PRESSURE CALCULATED: 1570 PSI
 - B. LEAK CHECK WITH HELIUM AT AMBIENT TEMPERATURE AT 70-80 PSIG FOR 5 MINUTES MINIMUM.
11. DRIFTE AXIS MUST INTERSECT WITHIN A .005 SPHERE CENTERED ON A THEORETICAL IMPINGEMENT POINT.
12. UPON COMPLETION OF FABRICATION, WATER FLOW CALIBRATE THE INJECTOR ASSEMBLY TO CHARACTERIZE FUEL AND OXIDE FLOW RESISTANCE.
13. DIMENSION APPLY AFTER BRAZING.

NOTE: UNLESS OTHERWISE SPECIFIED

1. DRAWING INTERPRETATIONS PER RF0004-01B.
2. MACHINE PER RA0103-01G.
3. MACHINE PER RA0103-01G, EDM ONLY.
4. CLEAN PER RA0110-04G.
5. IDENTIFY PER RF0004-04G, TYPE II, DEEP ELECTROCHEMICAL ETCH.
6. ALTERNATE MATERIAL OFHC COPPER PER ASTM-AF68, MATERIAL VERIFY PER NOTE 7 BEFORE MACHINING.
7. FOR MATERIAL PURCHASED TO ASTM-AF68, 1 SPECIMEN CUT FROM THE MATERIAL SHALL BE TESTED PER RB0170-04G.
8. FURNACE BRAZE PER RA0107-C1D, USING RB0170-06S (NICORO).

Figure B-3-A. O-F-O Triplet Injector, 3.5-inch Diameter, Sheet 1

1	3	MS51923-153		PIN				1	20
1	2	-5		RING	DFHC COPPER	R20170-047	(6X7)	2	20
1	1	-3		BODY	DFHC COPPER	R20170-047	(6X7)	2	20
-1		7R035320		INJECTOR ASSY					
QTY REQD	FIND NO.	PART OR IDENTIFY NO.	FCSM	NOTE: ILLUSTRATION OR DESCRIPTION	MATERIAL	SPECIFICATION NOTES, SUPPLIER		3M	ZONE

PARTS LIST

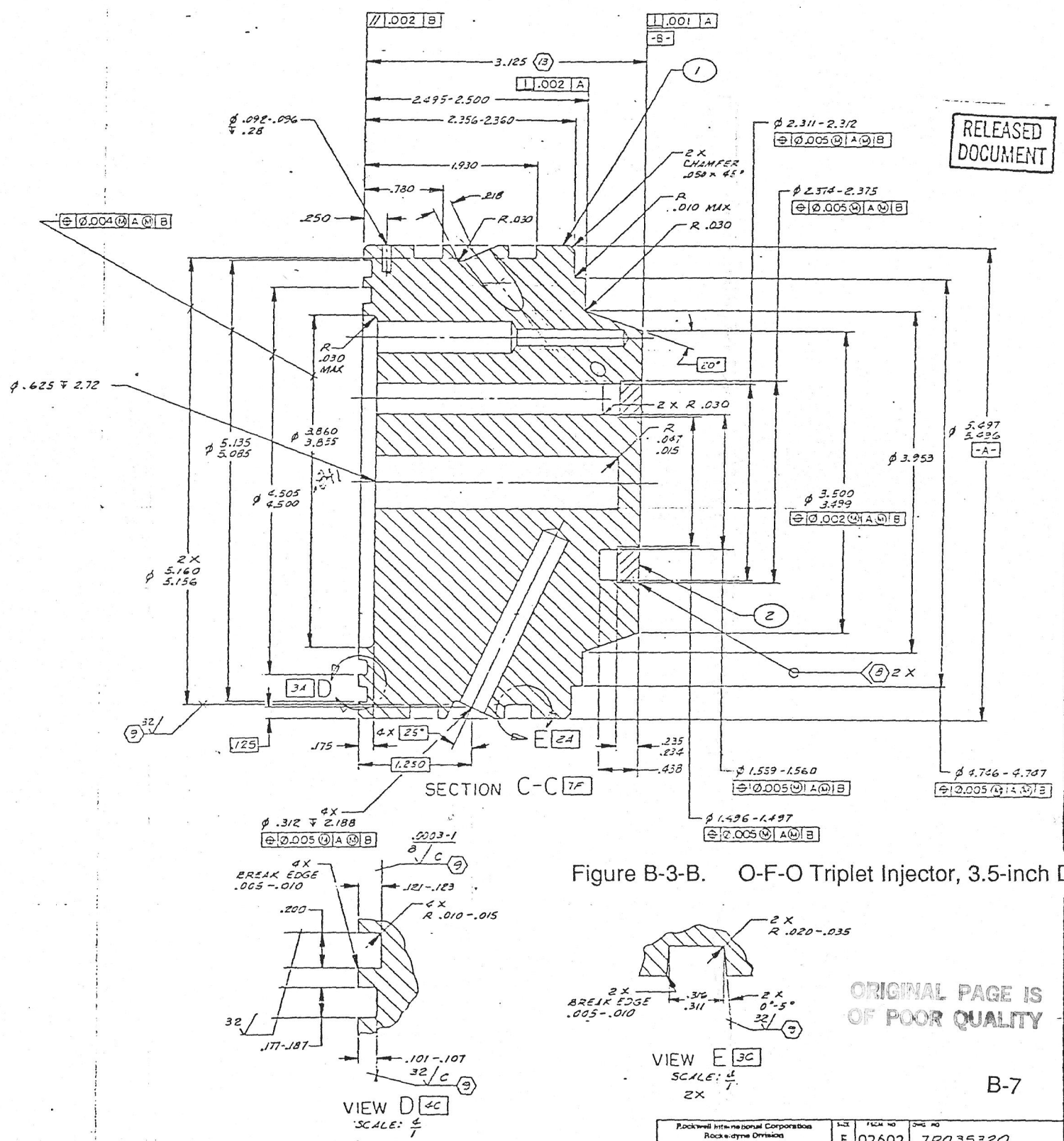
HEAT TREAT		UNLESS OTHERWISE SPECIFIED DIMENSIONS ARE IN INCHES AND APPLY FROM 10 POUNDS ESI / MACH. BLOW ROUGHNESS TOLERANCES ON ANGLES ± 1° IF NOT SPECIFIED DIMENSIONS AS ± .01 .005 ± .010 OVER THRU .005 ± .010 .010 ± .015 .015 ± .020 .020 ± .025 .025 ± .030 .030 ± .035 .035 ± .040 .040 ± .045 .045 ± .050 .050 ± .055 .055 ± .060 .060 ± .065 .065 ± .070 .070 ± .075 .075 ± .080 .080 ± .085 .085 ± .090 .090 ± .095 .095 ± .100 .100 ± .105 .105 ± .110 .110 ± .115 .115 ± .120 .120 ± .125 .125 ± .130 .130 ± .135 .135 ± .140 .140 ± .145 .145 ± .150 .150 ± .155 .155 ± .160 .160 ± .165 .165 ± .170 .170 ± .175 .175 ± .180 .180 ± .185 .185 ± .190 .190 ± .195 .195 ± .200 .200 ± .205 .205 ± .210 .210 ± .215 .215 ± .220 .220 ± .225 .225 ± .230 .230 ± .235 .235 ± .240 .240 ± .245 .245 ± .250 .250 ± .255 .255 ± .260 .260 ± .265 .265 ± .270 .270 ± .275 .275 ± .280 .280 ± .285 .285 ± .290 .290 ± .295 .295 ± .300 .300 ± .305 .305 ± .310 .310 ± .315 .315 ± .320 .320 ± .325 .325 ± .330 .330 ± .335 .335 ± .340 .340 ± .345 .345 ± .350 .350 ± .355 .355 ± .360 .360 ± .365 .365 ± .370 .370 ± .375 .375 ± .380 .380 ± .385 .385 ± .390 .390 ± .395 .395 ± .400 .400 ± .405 .405 ± .410 .410 ± .415 .415 ± .420 .420 ± .425 .425 ± .430 .430 ± .435 .435 ± .440 .440 ± .445 .445 ± .450 .450 ± .455 .455 ± .460 .460 ± .465 .465 ± .470 .470 ± .475 .475 ± .480 .480 ± .485 .485 ± .490 .490 ± .495 .495 ± .500 .500 ± .505 .505 ± .510 .510 ± .515 .515 ± .520 .520 ± .525 .525 ± .530 .530 ± .535 .535 ± .540 .540 ± .545 .545 ± .550 .550 ± .555 .555 ± .560 .560 ± .565 .565 ± .570 .570 ± .575 .575 ± .580 .580 ± .585 .585 ± .590 .590 ± .595 .595 ± .600 .600 ± .605 .605 ± .610 .610 ± .615 .615 ± .620 .620 ± .625 .625 ± .630 .630 ± .635 .635 ± .640 .640 ± .645 .645 ± .650 .650 ± .655 .655 ± .660 .660 ± .665 .665 ± .670 .670 ± .675 .675 ± .680 .680 ± .685 .685 ± .690 .690 ± .695 .695 ± .700 .700 ± .705 .705 ± .710 .710 ± .715 .715 ± .720 .720 ± .725 .725 ± .730 .730 ± .735 .735 ± .740 .740 ± .745 .745 ± .750 .750 ± .755 .755 ± .760 .760 ± .765 .765 ± .770 .770 ± .775 .775 ± .780 .780 ± .785 .785 ± .790 .790 ± .795 .795 ± .800 .800 ± .805 .805 ± .810 .810 ± .815 .815 ± .820 .820 ± .825 .825 ± .830 .830 ± .835 .835 ± .840 .840 ± .845 .845 ± .850 .850 ± .855 .855 ± .860 .860 ± .865 .865 ± .870 .870 ± .875 .875 ± .880 .880 ± .885 .885 ± .890 .890 ± .895 .895 ± .900 .900 ± .905 .905 ± .910 .910 ± .915 .915 ± .920 .920 ± .925 .925 ± .930 .930 ± .935 .935 ± .940 .940 ± .945 .945 ± .950 .950 ± .955 .955 ± .960 .960 ± .965 .965 ± .970 .970 ± .975 .975 ± .980 .980 ± .985 .985 ± .990 .990 ± .995 .995 ± 1.000 1.000 ± 1.005 1.005 ± 1.010 1.010 ± 1.015 1.015 ± 1.020 1.020 ± 1.025 1.025 ± 1.030 1.030 ± 1.035 1.035 ± 1.040 1.040 ± 1.045 1.045 ± 1.050 1.050 ± 1.055 1.055 ± 1.060 1.060 ± 1.065 1.065 ± 1.070 1.070 ± 1.075 1.075 ± 1.080 1.080 ± 1.085 1.085 ± 1.090 1.090 ± 1.095 1.095 ± 1.100 1.100 ± 1.105 1.105 ± 1.110 1.110 ± 1.115 1.115 ± 1.120 1.120 ± 1.125 1.125 ± 1.130 1.130 ± 1.135 1.135 ± 1.140 1.140 ± 1.145 1.145 ± 1.150 1.150 ± 1.155 1.155 ± 1.160 1.160 ± 1.165 1.165 ± 1.170 1.170 ± 1.175 1.175 ± 1.180 1.180 ± 1.185 1.185 ± 1.190 1.190 ± 1.195 1.195 ± 1.200 1.200 ± 1.205 1.205 ± 1.210 1.210 ± 1.215 1.215 ± 1.220 1.220 ± 1.225 1.225 ± 1.230 1.230 ± 1.235 1.235 ± 1.240 1.240 ± 1.245 1.245 ± 1.250		7		COMMENTS 1.1552-36369 QTRN D.RODIN DATE 04-21-81 DR. J. MARTINS QTRN D.RODIN S.FISHER DATE 04-21-81 MATERIAL F.N. NAGER STRENGTH 4340 DESIGN ACTIVITY APPRO D.A. MOSES DATE 3/24/81		Rockwell International Corporation Rock steady Division Camarillo Park, California	
FINISH		NONE		TRIPLET INJECTOR- ASSEMBLY OF 3.5 HEAVY HYDROCARBON MAIN INJECTOR					
MATERIAL		NOTED		E 02602 7R035320					
		DO NOT SCALE PRINT		SCALE 2/1 FINISHED SHEET 1 OF 2					

SECTION F F 6F

ORIGINAL PAGE IS
OF POOR QUALITY

VIEW E 3C
SCALE: $\frac{d}{1}$
2X

Rockwell International Corporation Rockwell Division Concord, California	INVT	ITEM NO	QTY NO
E	02602	7R035320	
QTY 2	DATE 09-03-73	WAL. DIS. NO. 53	WAL. # 022
2		1	AP TU-7



FOLDOUT FRAME

FOLDOUT FRAME

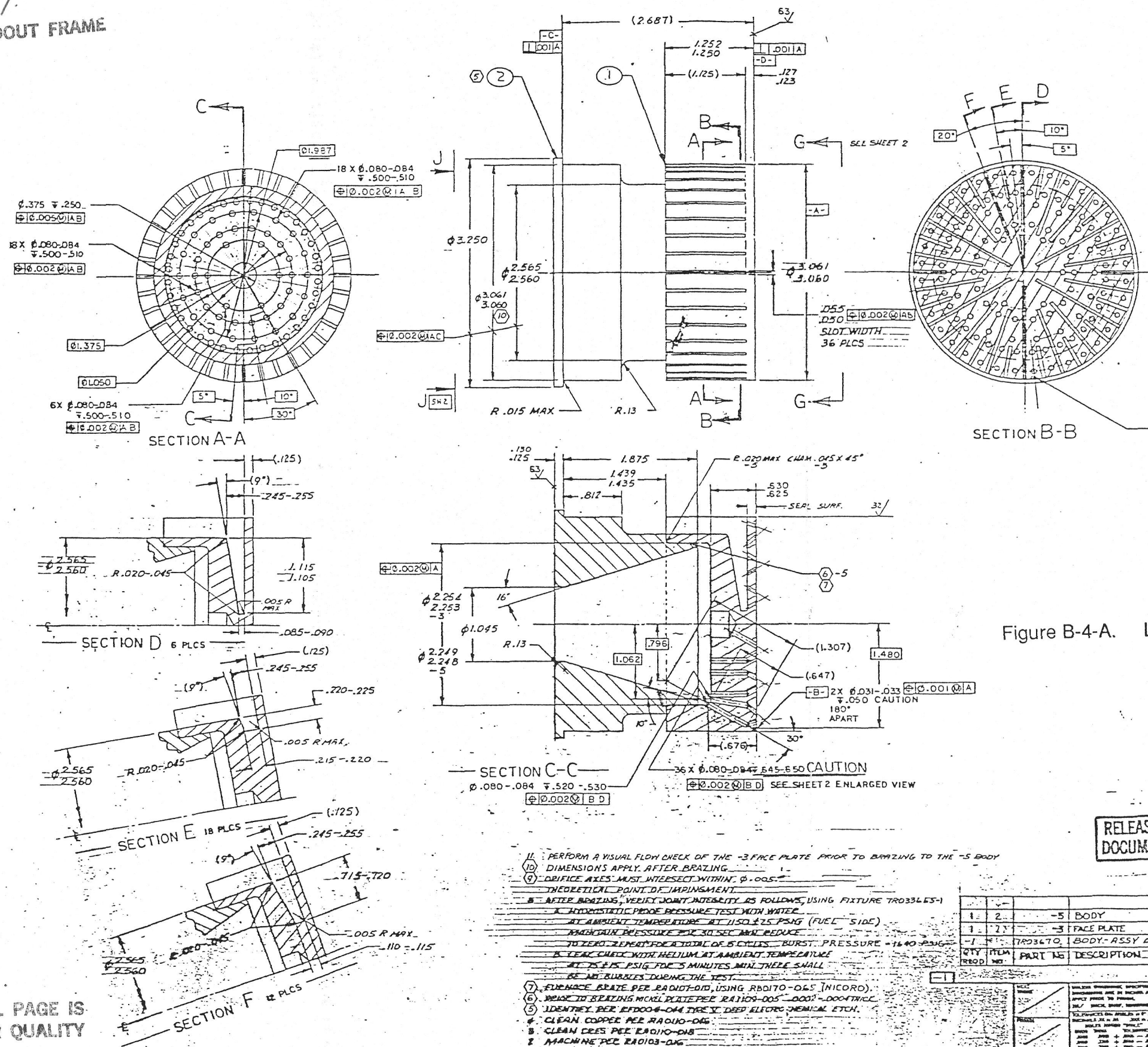


Figure B-4-A. Like-Doublet, Circumferential Fan Injector, 3.5-inch Diameter, Sheet 1

RELEASED DOCUMENT

QTY	ITEM	PART NO	DESCRIPTION	MATERIAL	SIZE	SPECIFICATION
1	2	-5	BODY	367 CRES BAR	#6012516	QQ-S-763, CLASS 347 COND A
1	2	-3	FACE PLATE	OFHC COPPER	#34 x 3016	RBO170-047 COND A
1	4	TRO33670	BODY- ASSY OF			

BODY- INJECTOR, ASSY OF

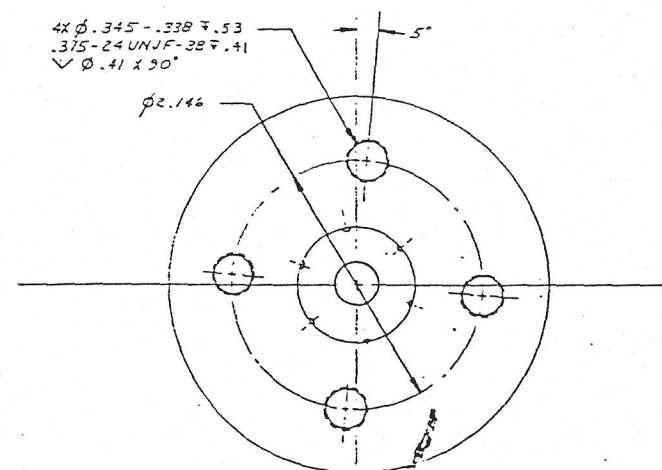
E 02662 7R033670

ORIGINAL PAGE IS OF POOR QUALITY

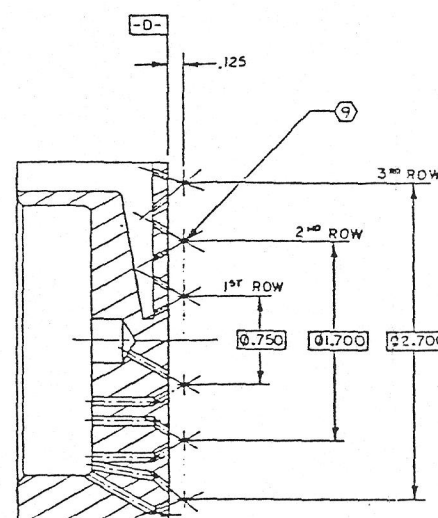
B-8

FOLDOUT FRAME 2.

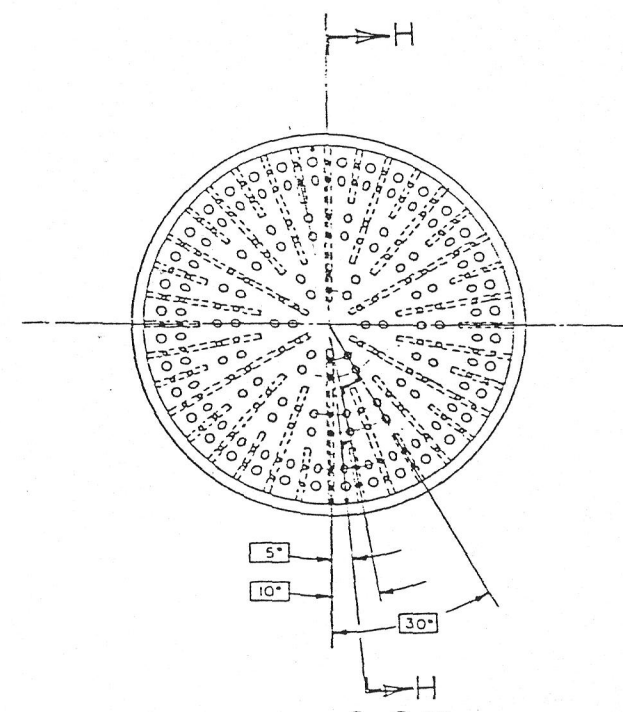
DATE/TIME		DESCRIPTION	DATE	INITIALS
		1. NAME BE RECORDED		
		2. RECORD CHANGE		
		3. CHECK BE RECORDED		
		4. RUN SHOP PRACTICE		
		5. PARTS MADE OK		
A		SEE SHEET 1		
				USE FOR LTP (m)
				AFEBB7 LXNAPP/6




VIEW J-J SHI
-S REF

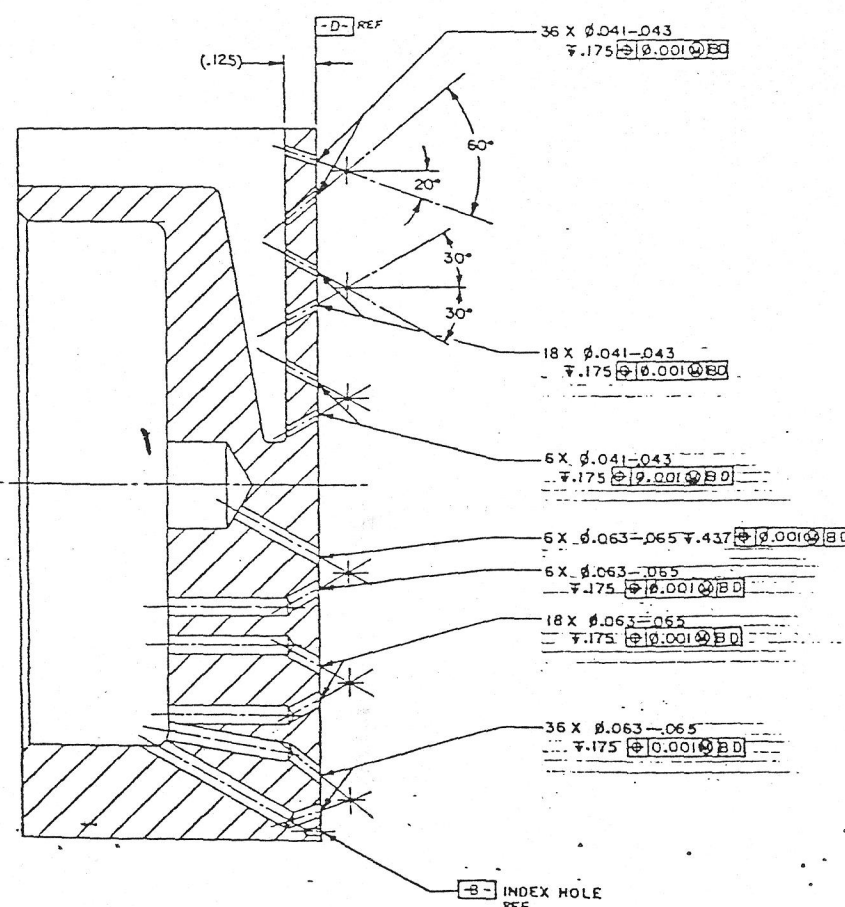


— SECTION H-H —



— VIEW G-G  SHEET 1 —

INJECTOR PATTERN		SPACING
1 ST ROW	6 FUEL & OX DOUBLETS	50°
2 ND ROW	18 FUEL & OX DOUBLETS	20°
3 RD ROW	36 FUEL & OX DOUBLETS	10°



→ ENLARGED VIEW
SCALE $\frac{4}{1}$

ORIGINAL PAGE IS
OF POOR QUALITY

Figure B-4-B. Like-Doublet, Circumferential Fan Injector, 3.5-inch Diameter, Sheet 2

RELEASED
DOCUMENT

ORIGINAL PAGE IS
OF POOR QUALITY

Registered International Correspondence Correspondence Division Chicago Post, California	NAME E	TICKET NO 02502	DMC NO 7R033670
--	-----------	--------------------	--------------------

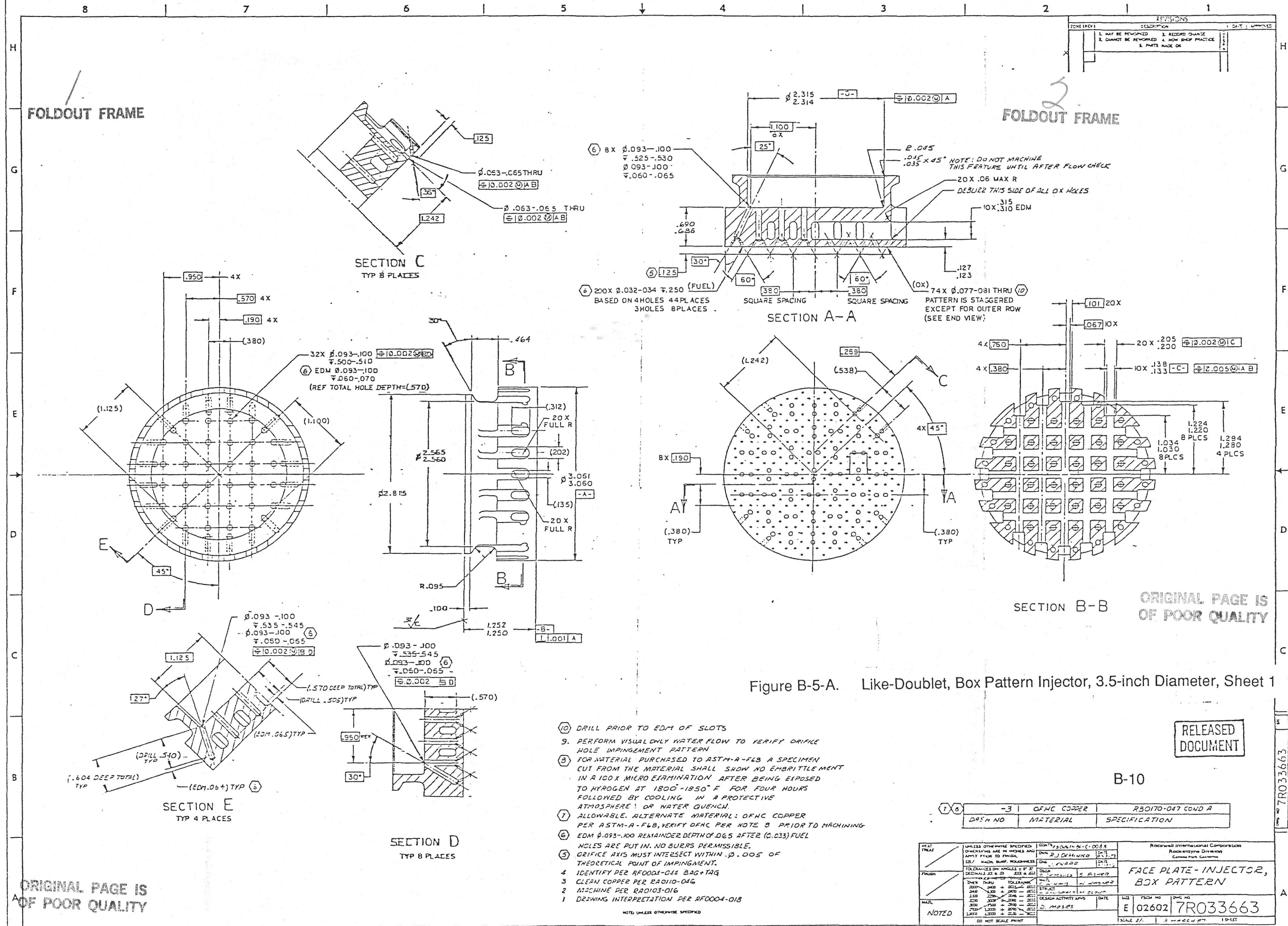


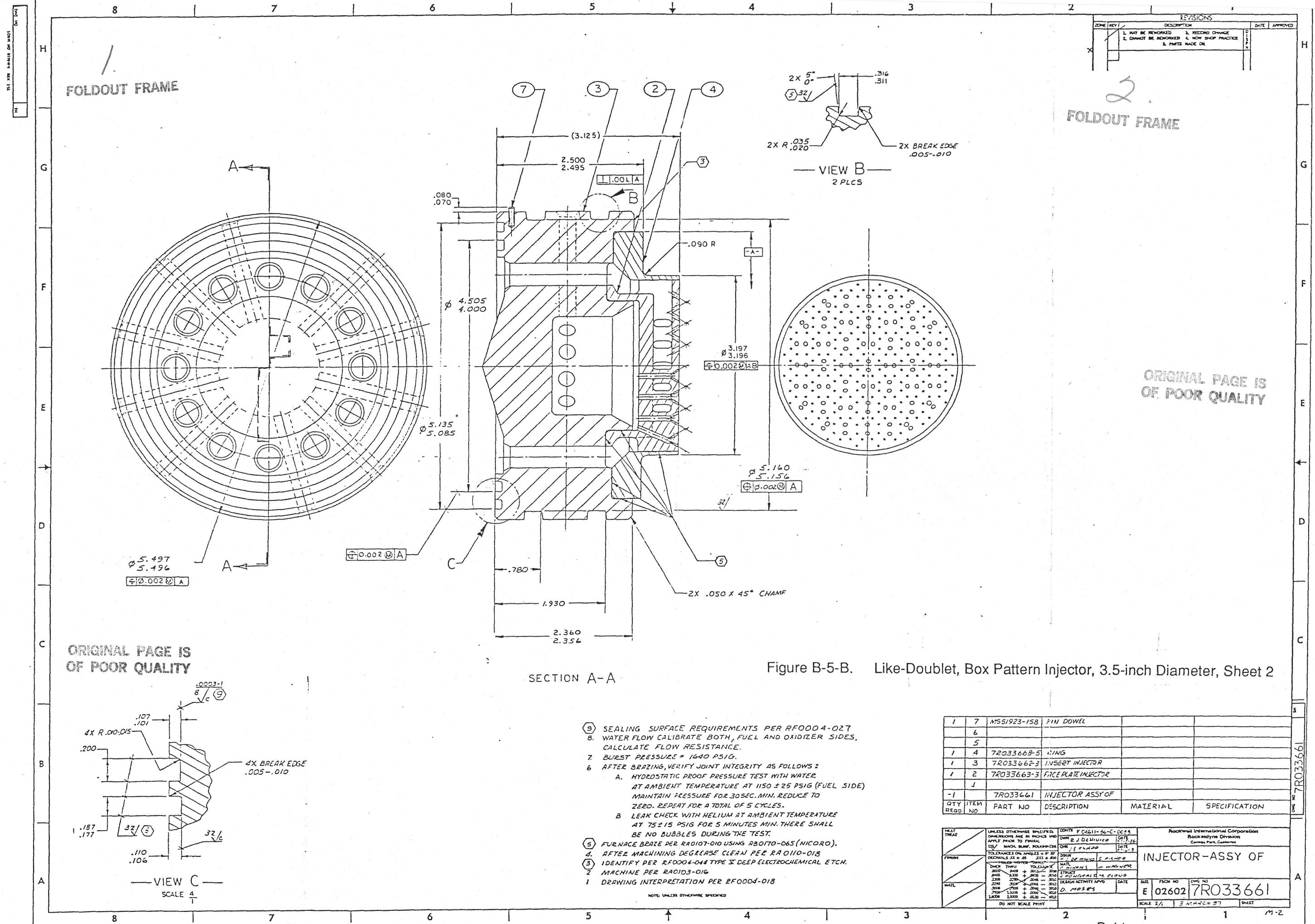
Figure B-5-A. Like-Doublet, Box Pattern Injector, 3.5-inch Diameter, Sheet 1

RELEASED
DOCUMENT

B-10

1	8	-3	OFHC COPPER	R50170-047 COND A
		DASH NO	MATERIAL	SPECIFICATION

<p>PREL DETAIL</p> <p>UNLESS OTHERWISE SPECIFIED DIMENSIONS ARE IN INCHES AND ANGLES PRIOR TO FINISH</p> <p>12% MATCH MARK REQUIREMENT</p> <p>TOLERANCES ON FINISHES OF 5 DECIMALS IN. & 30 SECS. & 30</p> <p>OTHER TYPICAL TOLERANCES</p> <p>±.005 ±.010 ±.015 ±.020 ±.025 ±.030 ±.035 ±.040 ±.045 ±.050 ±.055 ±.060 ±.065 ±.070 ±.075 ±.080 ±.085 ±.090 ±.095 ±.100 ±.105 ±.110 ±.115 ±.120 ±.125 ±.130 ±.135 ±.140 ±.145 ±.150 ±.155 ±.160 ±.165 ±.170 ±.175 ±.180 ±.185 ±.190 ±.195 ±.200 ±.205 ±.210 ±.215 ±.220 ±.225 ±.230 ±.235 ±.240 ±.245 ±.250 ±.255 ±.260 ±.265 ±.270 ±.275 ±.280 ±.285 ±.290 ±.295 ±.300 ±.305 ±.310 ±.315 ±.320 ±.325 ±.330 ±.335 ±.340 ±.345 ±.350 ±.355 ±.360 ±.365 ±.370 ±.375 ±.380 ±.385 ±.390 ±.395 ±.400 ±.405 ±.410 ±.415 ±.420 ±.425 ±.430 ±.435 ±.440 ±.445 ±.450 ±.455 ±.460 ±.465 ±.470 ±.475 ±.480 ±.485 ±.490 ±.495 ±.500 ±.505 ±.510 ±.515 ±.520 ±.525 ±.530 ±.535 ±.540 ±.545 ±.550 ±.555 ±.560 ±.565 ±.570 ±.575 ±.580 ±.585 ±.590 ±.595 ±.600 ±.605 ±.610 ±.615 ±.620 ±.625 ±.630 ±.635 ±.640 ±.645 ±.650 ±.655 ±.660 ±.665 ±.670 ±.675 ±.680 ±.685 ±.690 ±.695 ±.700 ±.705 ±.710 ±.715 ±.720 ±.725 ±.730 ±.735 ±.740 ±.745 ±.750 ±.755 ±.760 ±.765 ±.770 ±.775 ±.780 ±.785 ±.790 ±.795 ±.800 ±.805 ±.810 ±.815 ±.820 ±.825 ±.830 ±.835 ±.840 ±.845 ±.850 ±.855 ±.860 ±.865 ±.870 ±.875 ±.880 ±.885 ±.890 ±.895 ±.900 ±.905 ±.910 ±.915 ±.920 ±.925 ±.930 ±.935 ±.940 ±.945 ±.950 ±.955 ±.960 ±.965 ±.970 ±.975 ±.980 ±.985 ±.990 ±.995 ±.1000 ±.1005 ±.1010 ±.1015 ±.1020 ±.1025 ±.1030 ±.1035 ±.1040 ±.1045 ±.1050 ±.1055 ±.1060 ±.1065 ±.1070 ±.1075 ±.1080 ±.1085 ±.1090 ±.1095 ±.1100 ±.1105 ±.1110 ±.1115 ±.1120 ±.1125 ±.1130 ±.1135 ±.1140 ±.1145 ±.1150 ±.1155 ±.1160 ±.1165 ±.1170 ±.1175 ±.1180 ±.1185 ±.1190 ±.1195 ±.1200 ±.1205 ±.1210 ±.1215 ±.1220 ±.1225 ±.1230 ±.1235 ±.1240 ±.1245 ±.1250 ±.1255 ±.1260 ±.1265 ±.1270 ±.1275 ±.1280 ±.1285 ±.1290 ±.1295 ±.1300 ±.1305 ±.1310 ±.1315 ±.1320 ±.1325 ±.1330 ±.1335 ±.1340 ±.1345 ±.1350 ±.1355 ±.1360 ±.1365 ±.1370 ±.1375 ±.1380 ±.1385 ±.1390 ±.1395 ±.1400 ±.1405 ±.1410 ±.1415 ±.1420 ±.1425 ±.1430 ±.1435 ±.1440 ±.1445 ±.1450 ±.1455 ±.1460 ±.1465 ±.1470 ±.1475 ±.1480 ±.1485 ±.1490 ±.1495 ±.1500 ±.1505 ±.1510 ±.1515 ±.1520 ±.1525 ±.1530 ±.1535 ±.1540 ±.1545 ±.1550 ±.1555 ±.1560 ±.1565 ±.1570 ±.1575 ±.1580 ±.1585 ±.1590 ±.1595 ±.1600 ±.1605 ±.1610 ±.1615 ±.1620 ±.1625 ±.1630 ±.1635 ±.1640 ±.1645 ±.1650 ±.1655 ±.1660 ±.1665 ±.1670 ±.1675 ±.1680 ±.1685 ±.1690 ±.1695 ±.1700 ±.1705 ±.1710 ±.1715 ±.1720 ±.1725 ±.1730 ±.1735 ±.1740 ±.1745 ±.1750 ±.1755 ±.1760 ±.1765 ±.1770 ±.1775 ±.1780 ±.1785 ±.1790 ±.1795 ±.1800 ±.1805 ±.1810 ±.1815 ±.1820 ±.1825 ±.1830 ±.1835 ±.1840 ±.1845 ±.1850 ±.1855 ±.1860 ±.1865 ±.1870 ±.1875 ±.1880 ±.1885 ±.1890 ±.1895 ±.1900 ±.1905 ±.1910 ±.1915 ±.1920 ±.1925 ±.1930 ±.1935 ±.1940 ±.1945 ±.1950 ±.1955 ±.1960 ±.1965 ±.1970 ±.1975 ±.1980 ±.1985 ±.1990 ±.1995 ±.2000 ±.2005 ±.2010 ±.2015 ±.2020 ±.2025 ±.2030 ±.2035 ±.2040 ±.2045 ±.2050 ±.2055 ±.2060 ±.2065 ±.2070 ±.2075 ±.2080 ±.2085 ±.2090 ±.2095 ±.2100 ±.2105 ±.2110 ±.2115 ±.2120 ±.2125 ±.2130 ±.2135 ±.2140 ±.2145 ±.2150 ±.2155 ±.2160 ±.2165 ±.2170 ±.2175 ±.2180 ±.2185 ±.2190 ±.2195 ±.2200 ±.2205 ±.2210 ±.2215 ±.2220 ±.2225 ±.2230 ±.2235 ±.2240 ±.2245 ±.2250 ±.2255 ±.2260 ±.2265 ±.2270 ±.2275 ±.2280 ±.2285 ±.2290 ±.2295 ±.2300 ±.2305 ±.2310 ±.2315 ±.2320 ±.2325 ±.2330 ±.2335 ±.2340 ±.2345 ±.2350 ±.2355 ±.2360 ±.2365 ±.2370 ±.2375 ±.2380 ±.2385 ±.2390 ±.2395 ±.2400 ±.2405 ±.2410 ±.2415 ±.2420 ±.2425 ±.2430 ±.2435 ±.2440 ±.2445 ±.2450 ±.2455 ±.2460 ±.2465 ±.2470 ±.2475 ±.2480 ±.2485 ±.2490 ±.2495 ±.2500 ±.2505 ±.2510 ±.2515 ±.2520 ±.2525 ±.2530 ±.2535 ±.2540 ±.2545 ±.2550 ±.2555 ±.2560 ±.2565 ±.2570 ±.2575 ±.2580 ±.2585 ±.2590 ±.2595 ±.2600 ±.2605 ±.2610 ±.2615 ±.2620 ±.2625 ±.2630 ±.2635 ±.2640 ±.2645 ±.2650 ±.2655 ±.2660 ±.2665 ±.2670 ±.2675 ±.2680 ±.2685 ±.2690 ±.2695 ±.2700 ±.2705 ±.2710 ±.2715 ±.2720 ±.2725 ±.2730 ±.2735 ±.2740 ±.2745 ±.2750 ±.2755 ±.2760 ±.2765 ±.2770 ±.2775 ±.2780 ±.2785 ±.2790 ±.2795 ±.2800 ±.2805 ±.2810 ±.2815 ±.2820 ±.2825 ±.2830 ±.2835 ±.2840 ±.2845 ±.2850 ±.2855 ±.2860 ±.2865 ±.2870 ±.2875 ±.2880 ±.2885 ±.2890 ±.2895 ±.2900 ±.2905 ±.2910 ±.2915 ±.2920 ±.2925 ±.2930 ±.2935 ±.2940 ±.2945 ±.2950 ±.2955 ±.2960 ±.2965 ±.2970 ±.2975 ±.2980 ±.2985 ±.2990 ±.2995 ±.3000 ±.3005 ±.3010 ±.3015 ±.3020 ±.3025 ±.3030 ±.3035 ±.3040 ±.3045 ±.3050 ±.3055 ±.3060 ±.3065 ±.3070 ±.3075 ±.3080 ±.3085 ±.3090 ±.3095 ±.3100 ±.3105 ±.3110 ±.3115 ±.3120 ±.3125 ±.3130 ±.3135 ±.3140 ±.3145 ±.3150 ±.3155 ±.3160 ±.3165 ±.3170 ±.3175 ±.3180 ±.3185 ±.3190 ±.3195 ±.3200 ±.3205 ±.3210 ±.3215 ±.3220 ±.3225 ±.3230 ±.3235 ±.3240 ±.3245 ±.3250 ±.3255 ±.3260 ±.3265 ±.3270 ±.3275 ±.3280 ±.3285 ±.3290 ±.3295 ±.330</p>



REVISIONS		DATE	APPROVED
1	MAY BE REMOVED		
2	CANNOT BE REMOVED		
3	NOT SHOWN PRACTICE		
4	NOT SHOWN PRACTICE		

QTY	ITEM	PART NO	DESCRIPTION	MATERIAL	SPECIFICATION
1	7	MSS1923-158	PIN DOWEL		
1	4	72033668-5	RING		
1	3	72033662-3	INSERT INJECTOR		
1	2	72033663-3	FACE PLATE INJECTOR		
1	1	72033661	INJECTOR ASSY OF		

- ⑤ SEALING SURFACE REQUIREMENTS PER RF0004-027
⑥ WATER FLOW CALIBRATE BOTH, FUEL AND OXIDIZER SIDES. CALCULATE FLOW RESISTANCE.
⑦ BURST PRESSURE = 1640 PSIG.
⑧ AFTER BRAZING, VERIFY JOINT INTEGRITY AS FOLLOWS:
A. HYDROSTATIC PROOF PRESSURE TEST WITH WATER AT AMBIENT TEMPERATURE AT 1150 ± 25 PSIG (FUEL SIDE) MAINTAIN PRESSURE FOR 30 SEC. MIN. REDUCE TO ZERO. REPEAT FOR A TOTAL OF 5 CYCLES.
B. LEAK CHECK WITH HELIUM AT AMBIENT TEMPERATURE AT 75 ± 15 PSIG FOR 5 MINUTES MIN. THERE SHALL BE NO BUBBLES DURING THE TEST.
⑨ FURNACE BRAZE PER RAD107-010 USING RBO110-065 (NICORO).
⑩ AFTER MACHINING DEGREASE CLEAN PER RA0110-018
⑪ IDENTIFY PER RF0004-044 TYPE X DEEP ELECTROCHEMICAL ETCH.
⑫ MACHINE PER RAD103-016
⑬ DRAWING INTERPRETATION PER RF0004-018

HEAT TREAT	UNLESS OTHERWISE SPECIFIED, DIMENSIONS ARE IN INCHES AND APPLY PRIOR TO FINISH.	CONTR # <u>FCG11-46-C-004</u>	Rockwell International Corporation Rocke Estate Division Carmel, Pa. 15401	
		DR # <u>2</u>	DATE <u>3-16-97</u>	
FINISH	TOL: MAXIMUM ALLOW. DIMENSIONS TO FOLLOW ON ANGLES IS 0.007 INSTEAD OF 0.005 IN ALL OTHER DIMENSIONS.	DATE <u>3-16-97</u>	DATE	
		DESIGN <u>FCG11-46-C-004</u>	DATE	
HAZ.	DRAWN <u>W. MOSE</u>	INJECTOR-ASSY OF		
		MATERIAL <u>304 STAINLESS STEEL</u>		
	DATE <u>3-16-97</u>	HAZ. <u>HAZARDOUS TO HEALTH</u>		
	DATE <u>3-16-97</u>	HAZ. <u>HAZARDOUS TO HEALTH</u>		
	DATE <u>3-16-97</u>	HAZ. <u>HAZARDOUS TO HEALTH</u>		
	DATE <u>3-16-97</u>	HAZ. <u>HAZARDOUS TO HEALTH</u>		
	DATE <u>3-16-97</u>	HAZ. <u>HAZARDOUS TO HEALTH</u>		
	DATE <u>3-16-97</u>	HAZ. <u>HAZARDOUS TO HEALTH</u>		
	DATE <u>3-16-97</u>	HAZ. <u>HAZARDOUS TO HEALTH</u>		
	DATE <u>3-16-97</u>	HAZ. <u>HAZARDOUS TO HEALTH</u>		
	DATE <u>3-16-97</u>	HAZ. <u>HAZARDOUS TO HEALTH</u>		
	DATE <u>3-16-97</u>	HAZ. <u>HAZARDOUS TO HEALTH</u>		
	DATE <u>3-16-97</u>	HAZ. <u>HAZARDOUS TO HEALTH</u>		
	DATE <u>3-16-97</u>	HAZ. <u>HAZARDOUS TO HEALTH</u>		
	DATE <u>3-16-97</u>	HAZ. <u>HAZARDOUS TO HEALTH</u>		
	DATE <u>3-16-97</u>	HAZ. <u>HAZARDOUS TO HEALTH</u>		
	DATE <u>3-16-97</u>	HAZ. <u>HAZARDOUS TO HEALTH</u>		
	DATE <u>3-16-97</u>	HAZ. <u>HAZARDOUS TO HEALTH</u>		
	DATE <u>3-16-97</u>	HAZ. <u>HAZARDOUS TO HEALTH</u>		
	DATE <u>3-16-97</u>	HAZ. <u>HAZARDOUS TO HEALTH</u>		
	DATE <u>3-16-97</u>	HAZ. <u>HAZARDOUS TO HEALTH</u>		
	DATE <u>3-16-97</u>	HAZ. <u>HAZARDOUS TO HEALTH</u>		
	DATE <u>3-16-97</u>	HAZ. <u>HAZARDOUS TO HEALTH</u>		
	DATE <u>3-16-97</u>	HAZ. <u>HAZARDOUS TO HEALTH</u>		
	DATE <u>3-16-97</u>	HAZ. <u>HAZARDOUS TO HEALTH</u>		
	DATE <u>3-16-97</u>	HAZ. <u>HAZARDOUS TO HEALTH</u>		
	DATE <u>3-16-97</u>	HAZ. <u>HAZARDOUS TO HEALTH</u>		
	DATE <u>3-16-97</u>	HAZ. <u>HAZARDOUS TO HEALTH</u>		
	DATE <u>3-16-97</u>	HAZ. <u>HAZARDOUS TO HEALTH</u>		
	DATE <u>3-16-97</u>	HAZ. <u>HAZARDOUS TO HEALTH</u>		
	DATE <u>3-16-97</u>	HAZ. <u>HAZARDOUS TO HEALTH</u>		
	DATE <u>3-16-97</u>	HAZ. <u>HAZARDOUS TO HEALTH</u>		
	DATE <u>3-16-97</u>	HAZ. <u>HAZARDOUS TO HEALTH</u>		
	DATE <u>3-16-97</u>	HAZ. <u>HAZARDOUS TO HEALTH</u>		
	DATE <u>3-16-97</u>	HAZ. <u>HAZARDOUS TO HEALTH</u>		
	DATE <u>3-16-97</u>	HAZ. <u>HAZARDOUS TO HEALTH</u>		
	DATE <u>3-16-97</u>	HAZ. <u>HAZARDOUS TO HEALTH</u>		
	DATE <u>3-16-97</u>	HAZ. <u>HAZARDOUS TO HEALTH</u>		
	DATE <u>3-16-97</u>	HAZ. <u>HAZARDOUS TO HEALTH</u>		
	DATE <u>3-16-97</u>	HAZ. <u>HAZARDOUS TO HEALTH</u>		
	DATE <u>3-16-97</u>	HAZ. <u>HAZARDOUS TO HEALTH</u>		
	DATE <u>3-16-97</u>	HAZ. <u>HAZARDOUS TO HEALTH</u>		
	DATE <u>3-16-97</u>	HAZ. <u>HAZARDOUS TO HEALTH</u>		
	DATE <u>3-16-97</u>	HAZ. <u>HAZARDOUS TO HEALTH</u>		
	DATE <u>3-16-97</u>	HAZ. <u>HAZARDOUS TO HEALTH</u>		
	DATE <u>3-16-97</u>	HAZ. <u>HAZARDOUS TO HEALTH</u>		
	DATE <u>3-16-97</u>	HAZ. <u>HAZARDOUS TO HEALTH</u>		
	DATE <u>3-16-97</u>	HAZ. <u>HAZARDOUS TO HEALTH</u>		
	DATE <u>3-16-97</u>	HAZ. <u>HAZARDOUS TO HEALTH</u>		
	DATE <u>3-16-97</u>	HAZ. <u>HAZARDOUS TO HEALTH</u>		
	DATE <u>3-16-97</u>	HAZ. <u>HAZARDOUS TO HEALTH</u>		
	DATE <u>3-16-97</u>	HAZ. <u>HAZARDOUS TO HEALTH</u>		
	DATE <u>3-16-97</u>	HAZ. <u>HAZARDOUS TO HEALTH</u>		
	DATE <u>3-16-97</u>	HAZ. <u>HAZARDOUS TO HEALTH</u>		
	DATE <u>3-16-97</u>	HAZ. <u>HAZARDOUS TO HEALTH</u>		
	DATE <u>3-16-97</u>	HAZ. <u>HAZARDOUS TO HEALTH</u>		
	DATE <u>3-16-97</u>	HAZ. <u>HAZARDOUS TO HEALTH</u>		
	DATE <u>3-16-97</u>	HAZ. <u>HAZARDOUS TO HEALTH</u>		
	DATE <u>3-16-97</u>	HAZ. <u>HAZARDOUS TO HEALTH</u>		
	DATE <u>3-16-97</u>	HAZ. <u>HAZARDOUS TO HEALTH</u>		
	DATE <u>3-16-97</u>	HAZ. <u>HAZARDOUS TO HEALTH</u>		
	DATE <u>3-16-97</u>	HAZ. <u>HAZARDOUS TO HEALTH</u>		
	DATE <u>3-16-97</u>	HAZ. <u>HAZARDOUS TO HEALTH</u>		
	DATE <u>3-16-97</u>	HAZ. <u>HAZARDOUS TO HEALTH</u>		
	DATE <u>3-16-97</u>	HAZ. <u>HAZARDOUS TO HEALTH</u>		
	DATE <u>3-16-97</u>	HAZ. <u>HAZARDOUS TO HEALTH</u>		
	DATE <u>3-16-97</u>	HAZ. <u>HAZARDOUS TO HEALTH</u>		
	DATE <u>3-16-97</u>	HAZ. <u>HAZARDOUS TO HEALTH</u>		
	DATE <u>3-16-97</u>	HAZ. <u>HAZARDOUS TO HEALTH</u>		
	DATE <u>3-16-97</u>	HAZ. <u>HAZARDOUS TO HEALTH</u>		
	DATE <u>3-16-97</u>	HAZ. <u>HAZARDOUS TO HEALTH</u>		
	DATE <u>3-16-97</u>	HAZ. <u>HAZARDOUS TO HEALTH</u>		
	DATE <u>3-16-97</u>	HAZ. <u>HAZARDOUS TO HEALTH</u>		
	DATE <u>3-16-97</u>	HAZ. <u>HAZARDOUS TO HEALTH</u>		
	DATE <u>3-16-97</u>	HAZ. <u>HAZARDOUS TO HEALTH</u>		
	DATE <u>3-16-97</u>	HAZ. <u>HAZARDOUS TO HEALTH</u>		
	DATE <u>3-16-97</u>	HAZ. <u>HAZARDOUS TO HEALTH</u>		
	DATE <u>3-16-97</u>	HAZ. <u>HAZARDOUS TO HEALTH</u>		
	DATE <u>3-16-97</u>	HAZ. <u>HAZARDOUS TO HEALTH</u>		
	DATE <u>3-16-97</u>	HAZ. <u>HAZARDOUS TO HEALTH</u>		
	DATE <u>3-16-97</u>	HAZ. <u>HAZARDOUS TO HEALTH</u>		
	DATE <u>3-16-97</u>	HAZ. <u>HAZARDOUS TO HEALTH</u>		
	DATE <u>3-16-97</u>	HAZ. <u>HAZARDOUS TO HEALTH</u>		
	DATE <u>3-16-97</u>	HAZ. <u>HAZARDOUS TO HEALTH</u>		
	DATE <u>3-16-97</u>	HAZ. <u>HAZARDOUS TO HEALTH</u>		
	DATE <u>3-16-97</u>	HAZ. <u>HAZARDOUS TO HEALTH</u>		
	DATE <u>3-16-97</u>	HAZ. <u>HAZARDOUS TO HEALTH</u>		
	DATE <u>3-16-97</u>	HAZ. <u>HAZARDOUS TO HEALTH</u>		
	DATE <u>3-16-97</u>	HAZ. <u>HAZARDOUS TO HEALTH</u>		
	DATE <u>3-16-97</u>	HAZ. <u>HAZARDOUS TO HEALTH</u>		
	DATE <u>3-16-97</u>	HAZ. <u>HAZARDOUS TO HEALTH</u>		
	DATE <u>3-16-97</u>	HAZ. <u>HAZARDOUS TO HEALTH</u>		
	DATE <u>3-16-97</u>	HAZ. <u>HAZARDOUS TO HEALTH</u>		
	DATE <u>3-16-97</u>	HAZ. <u>HAZARDOUS TO HEALTH</u>		
	DATE <u>3-16-97</u>	HAZ. <u>HAZARDOUS TO HEALTH</u>		
	DATE <u>3-16-97</u>	HAZ. <u>HAZARDOUS TO HEALTH</u>		
	DATE <u>3-16-97</u>	HAZ. <u>HAZARDOUS TO HEALTH</u>		
	DATE <u>3-16-97</u>	HAZ. <u>HAZARDOUS TO HEALTH</u>		
	DATE <u>3-16-97</u>	HAZ. <u>HAZARDOUS TO HEALTH</u>		
	DATE <u>3-16-97</u>	HAZ. <u>HAZARDOUS TO HEALTH</u>		
	DATE <u>3-16-97</u>	HAZ. <u>HAZARDOUS TO HEALTH</u>		
	DATE <u>3-16-97</u>	HAZ. <u>HAZARDOUS TO HEALTH</u>		
	DATE <u>3-16-97</u>	HAZ. <u>HAZARDOUS TO HEALTH</u>		
	DATE <u>3-16-97</u>	HAZ. <u>HAZARDOUS TO HEALTH</u>		
	DATE <u>3-16-97</u>	HAZ. <u>HAZARDOUS TO HEALTH</u>		
	DATE <u>3-16-97</u>	HAZ. <u>HAZARDOUS TO HEALTH</u>		
	DATE <u>3-16-97</u>	HAZ. <u>HAZARDOUS TO HEALTH</u>		
	DATE <u>3-16-97</u>	HAZ. <u>HAZARDOUS TO HEALTH</u>		
	DATE <u>3-16-97</u>	HAZ. <u>HAZARDOUS TO HEALTH</u>		
	DATE <u>3-16-97</u>	HAZ. <u>HAZARDOUS TO HEALTH</u>		
	DATE <u>3-16-97</u>	HAZ. <u>HAZARDOUS TO HEALTH</u>		
	DATE <u>3-16-97</u>	HAZ. <u>HAZARDOUS TO HEALTH</u>		
	DATE <u>3-16-97</u>	HAZ. <u>HAZARDOUS TO HEALTH</u>		
	DATE <u>3-16-97</u>	HAZ. <u>HAZARDOUS TO HEALTH</u>		
	DATE <u>3-16-97</u>	HAZ. <u>HAZARDOUS TO HEALTH</u>		
	DATE <u>3-16-97</u>	HAZ. <u>HAZARDOUS TO HEALTH</u>		
	DATE <u>3-16-97</u>	HAZ. <u>HAZARDOUS TO HEALTH</u>		
	DATE <u>3-16-97</u>	HAZ. <u>HAZARDOUS TO HEALTH</u>		
	DATE <u>3-16-97</u>	HAZ. <u>HAZARDOUS TO HEALTH</u>		

FOLDOUT FRAME

FOLDOUT FRAME

ORIGINAL PAGE IS
OF POOR QUALITY

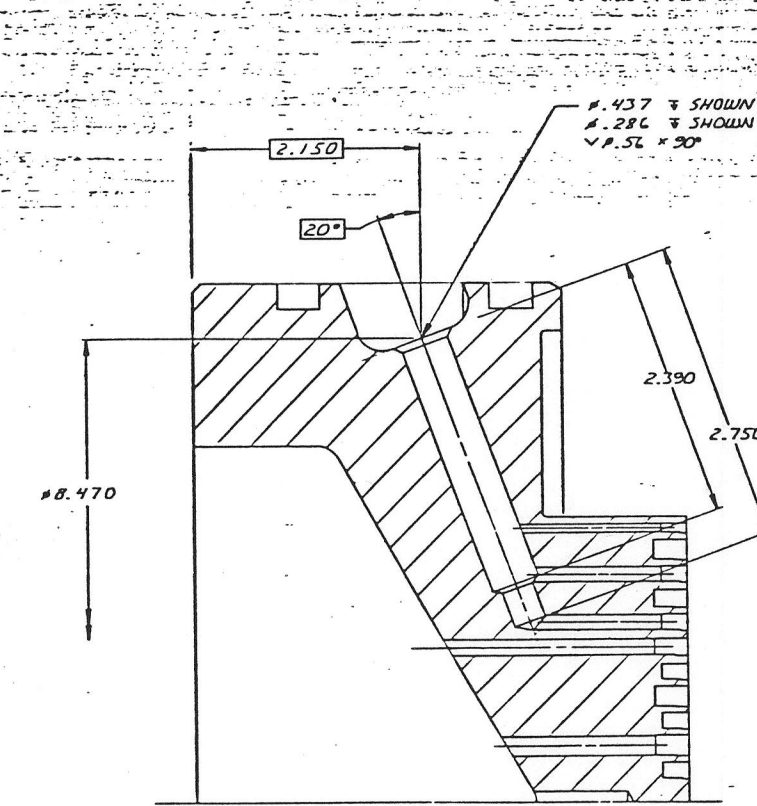
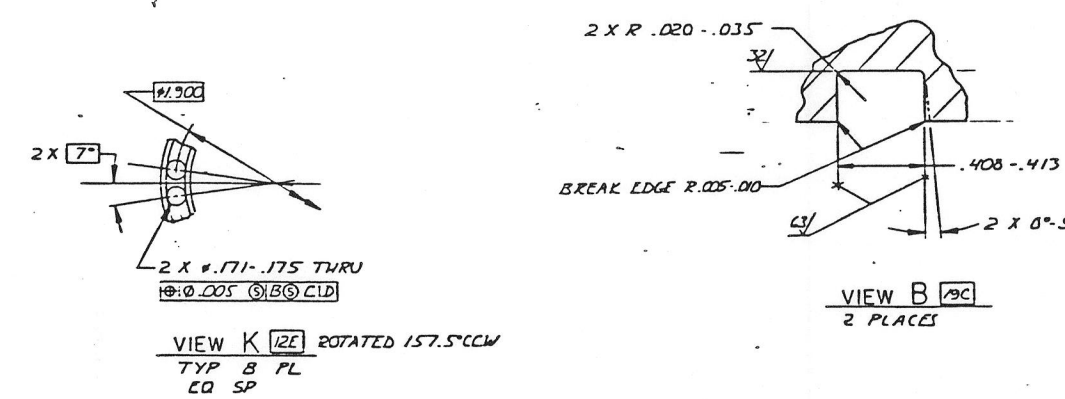
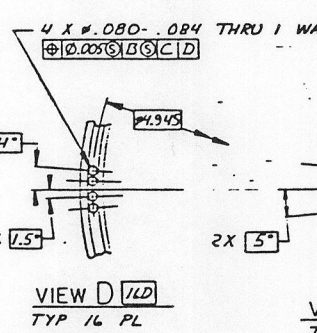
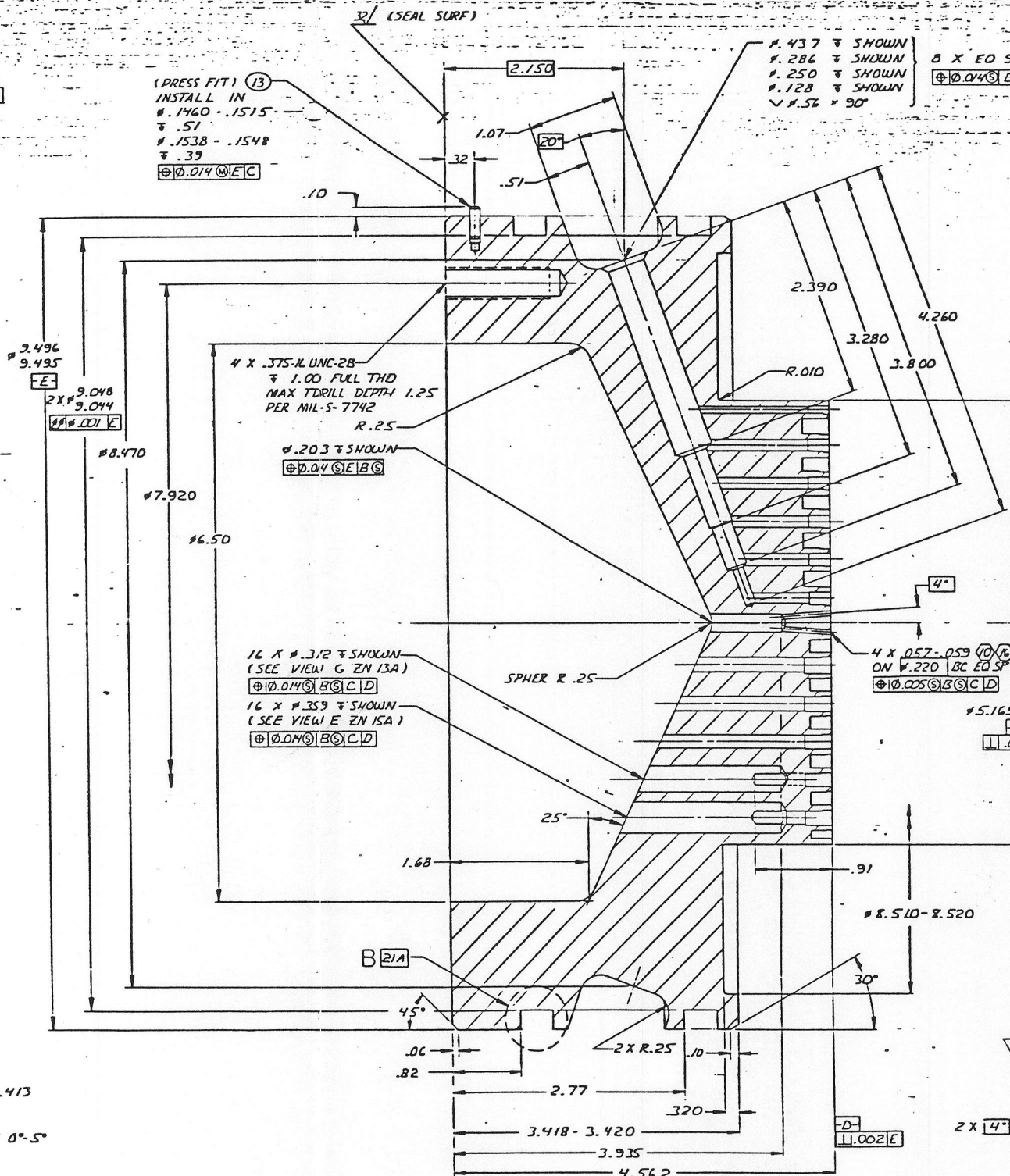
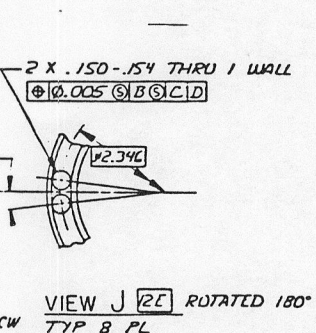
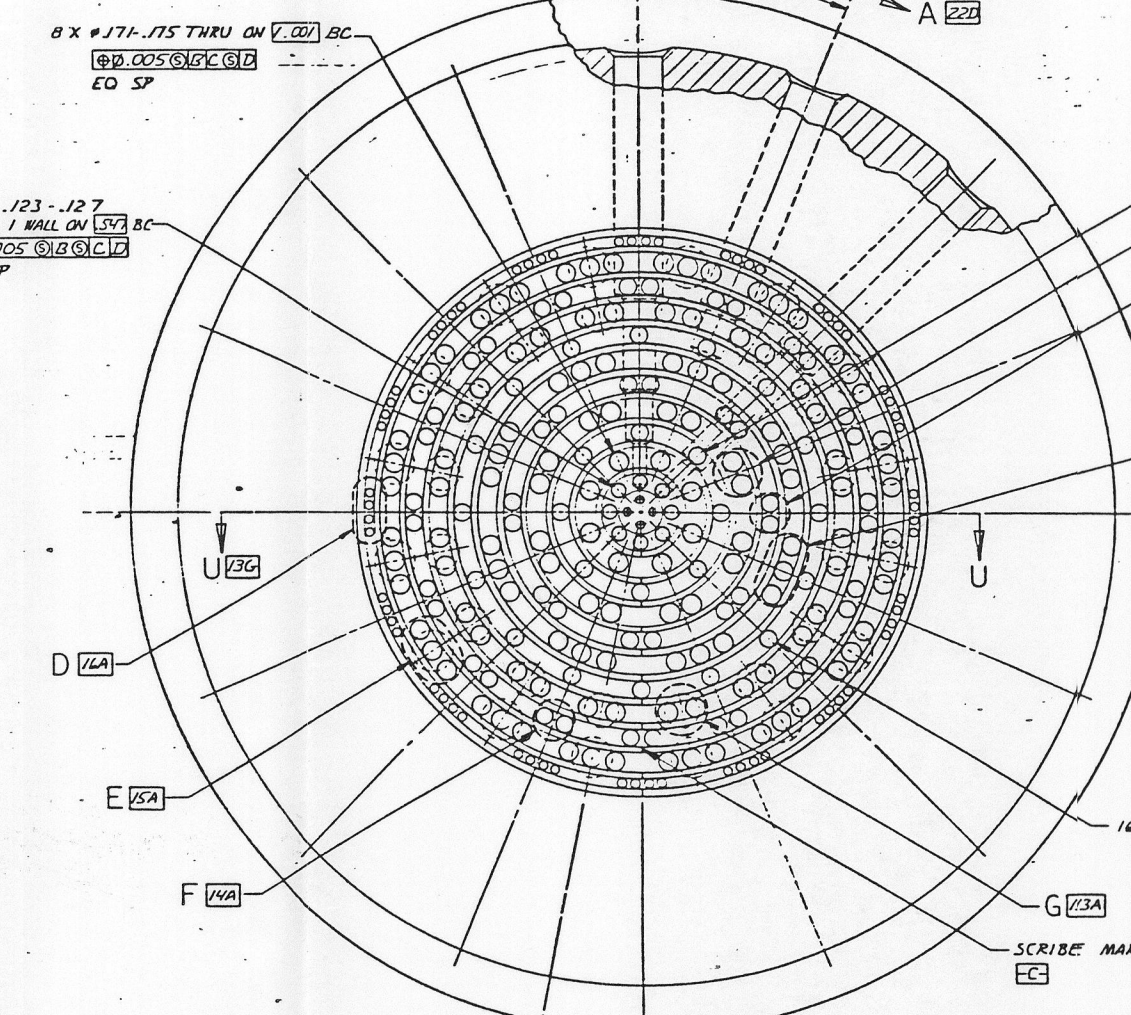
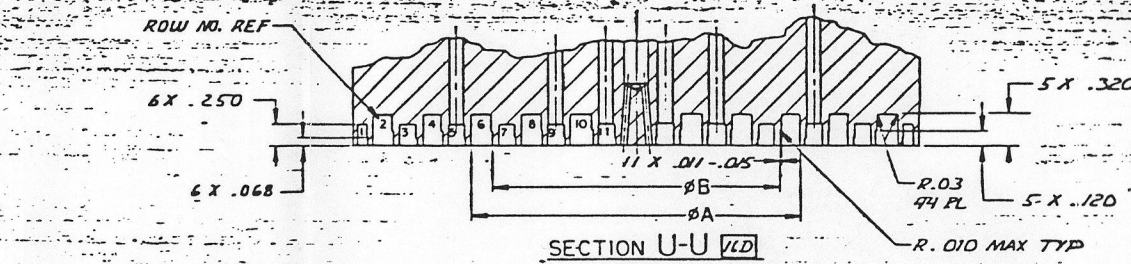
FOLDOUT FRAME

ORIGINAL PAGE IS
OF POOR QUALITY

FOLDOUT FRAME

ORIGINAL PAGE IS
OF POOR QUALITY

FOLDOUT FRAME

ORIGINAL PAGE IS
OF POOR QUALITYORIGINAL PAGE IS
OF POOR QUALITYVIEW B (26)
2 PLACESVIEW E (15) ROTATED 117.5° CCW
TYP K PLVIEW F (16) ROTATED 78.75° CCW
TYP K PLVIEW G (17) ROTATED 102.5° CCW
TYP K PLVIEW H (18) ROTATED 157.5° CCW
TYP B PLVIEW J (22) ROTATED 180°
TYP B PL

SECTION L-L (14)

ROW NO.	BA (2027)	BB (2027)
1	5.041	4.849
2	4.753	4.378
3	4.282	3.950
4	3.854	3.493
5	3.397	3.067
6	2.971	2.606
7	2.510	2.162
8	2.086	1.714
9	1.618	1.291
10	1.195	.806
11	.710	.344

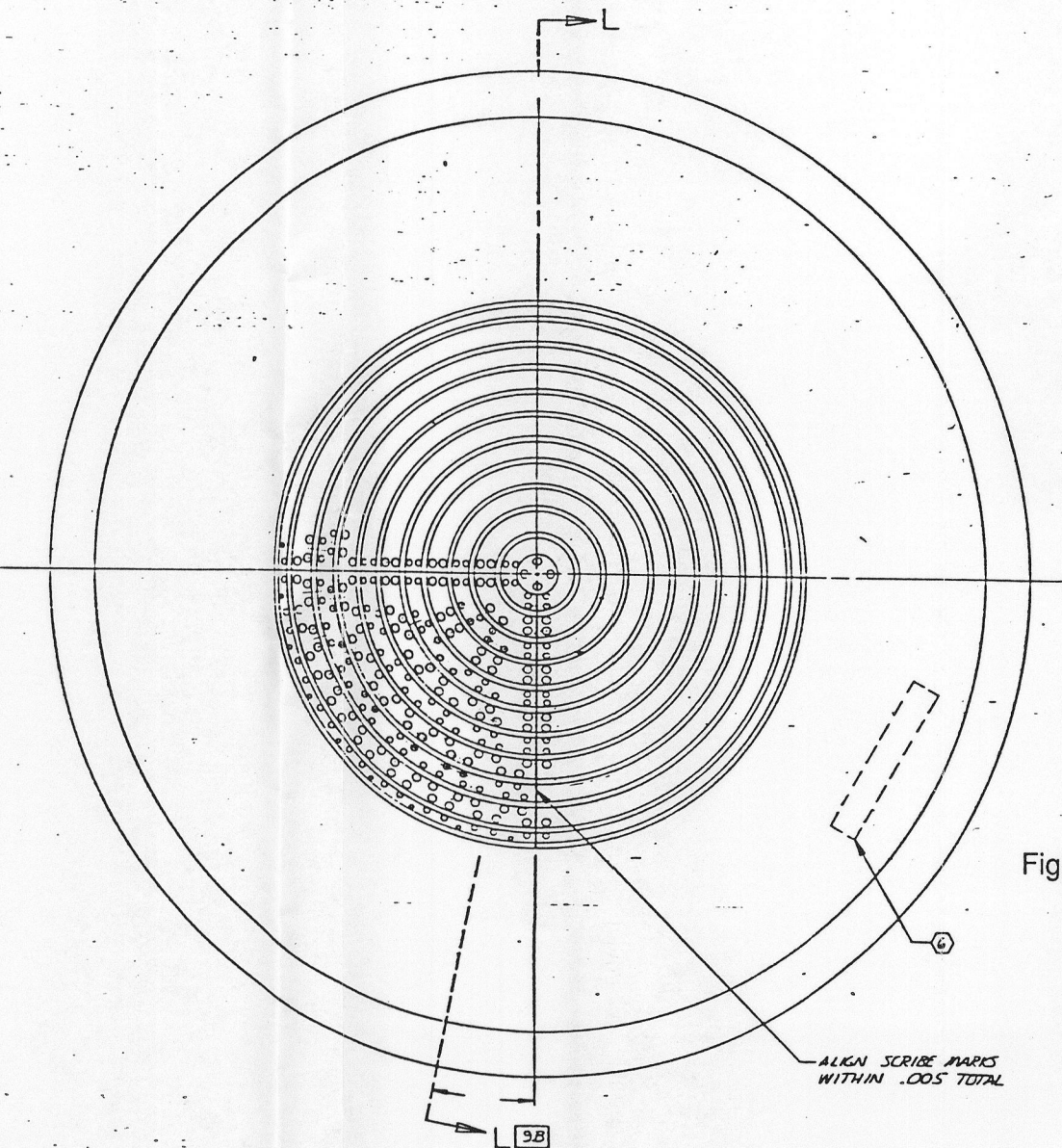
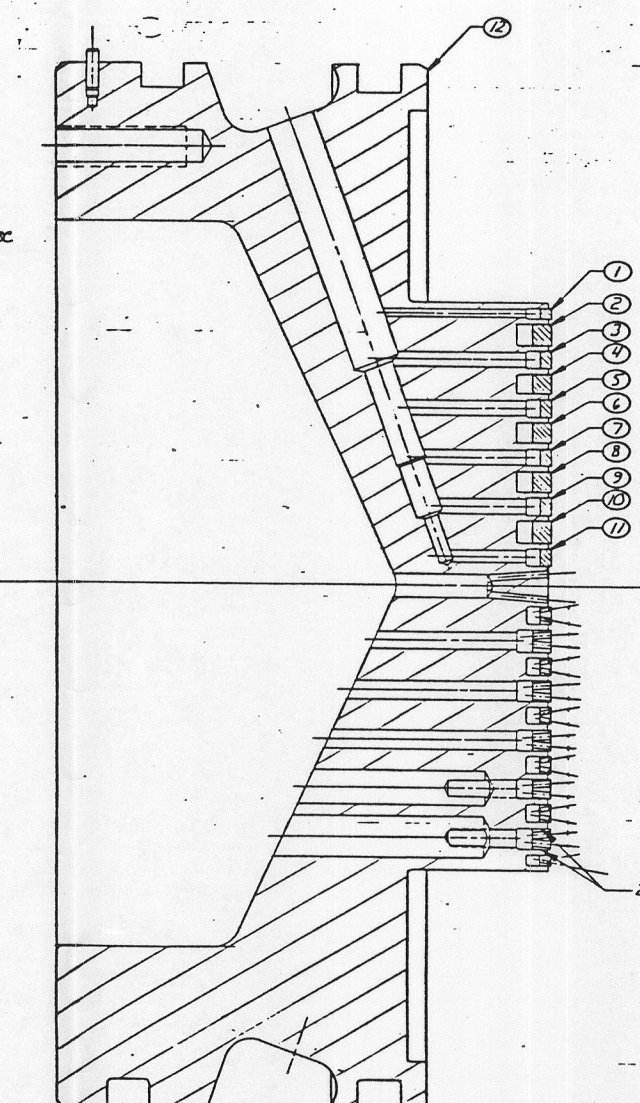


Figure B-6-A. Like-Doublet, Canted Fan Injector, 5.7-inch Diameter, Sheet 1

B-12

(CANTED FAN LIKE IMPINGING DOUBLET
INJECTOR)

REVISION	DATE	BY	CHKD
1			
2			
3			
4			
5			
6			
7			
8			
9			
10			
11			
12			
13			
14			
15			
16			
17			
18			
19			
20			
21			
22			
23			
24			

1. MACHINE PER RADIO-OL
2. THEORETICAL CENTERLINES SHALL INTERSECT WITHIN SPHERICAL K.O.S TRUE POSITION
3. SCRIBE MARK .003 WIDE MAX
4. BRAZE PER RADIO-OL USING RADIO-OL (NICKEL) BRAZE ALLOY
5. VERIFY OFHC BY TESTING PER RADIO-OL
6. ELECTROCHEMICAL ETCH IMPRESSION STAMP OR HYDROGEN PART NUMBER. CHARACTERS .12 HIGH
7. NICKEL PLATE ALL SURFACES TO BE BRAZED .0002-.0004 THICK PER RA 1109-005
8. DIMENSIONS APPLY AFTER PLATING
9. CLEAN COPPER DETAILS PER RADIO-OL. CLEAN CRES DETAILS PER RADIO-OL. LOK CLEAN ASSY PER RADIO-OL
10. EDM PERMITTED
11. ALLOWABLE ALTERNATE: RBO/70-077 CONA
12. DIMENSIONS GIVEN ARE FOR REFERENCE ONLY. MATCH MACHINE TO PROVIDE .003-.005 DIAMETRAL CLEARANCE ON F.C. AND F.F. OF ITEMS 1 THRU 11 RINGS.
13. PRIOR TO MACHINING, ANNEAL OFHC MATERIAL AT 1900-1925°F, 10-30 MINUTES IN ARID OR HYDROGEN ATM.
14. WIRE EDM PERMISSIBLE. WIRE SIZE .006 MAX. RETAIN WASTE STOCK (FOR BEZEL SAMPLES)
15. PROOF PRESSURE TEST WITH WATER AT AMBIENT TEMPERATURE AT 105-109.5 PSIG. MAINTAIN PRESSURE FOR 30 SECONDS MIN. AND REPEAT FOR A TOTAL OF 5 CYCLES. CALCULATED BUOY PRESSURE 670 PSI. BOTH CIRCUITS TO BE SEPARATELY TESTED. TESTS MAY BE PERFORMED PRIOR TO DRILLING DRIFTE HOLES.

REV	DATE	DESCRIPTION	MATERIAL	SPEC	SH 1294
1	13	RD/22-3003-0906	PIN	CRES	1
2	12	BODY	347 CRES	00-5-763	1
3	11	RING(S)	OFHC COPPER ASTM F436	2	30
4	10				50
5	9				50
6	8				20
7	7				100
8	6				120
9	5				140
10	4				170
11	3				190
12	2				192
13	1				220
14	1	7R035427	ASSY		1
15	1	7R035427	VSCM		1

PARTS LIST	DESCRIPTION	MATERIAL	SPEC	SH 1294
1	INJECTOR ASSY OF			
2	INJECTOR ASSY OF			
3	INJECTOR ASSY OF			
4	INJECTOR ASSY OF			
5	INJECTOR ASSY OF			
6	INJECTOR ASSY OF			
7	INJECTOR ASSY OF			
8	INJECTOR ASSY OF			
9	INJECTOR ASSY OF			
10	INJECTOR ASSY OF			
11	INJECTOR ASSY OF			
12	INJECTOR ASSY OF			
13	INJECTOR ASSY OF			
14	INJECTOR ASSY OF			
15	INJECTOR ASSY OF			
16	INJECTOR ASSY OF			
17	INJECTOR ASSY OF			
18	INJECTOR ASSY OF			
19	INJECTOR ASSY OF			
20	INJECTOR ASSY OF			
21	INJECTOR ASSY OF			
22	INJECTOR ASSY OF			
23	INJECTOR ASSY OF			
24	INJECTOR ASSY OF			

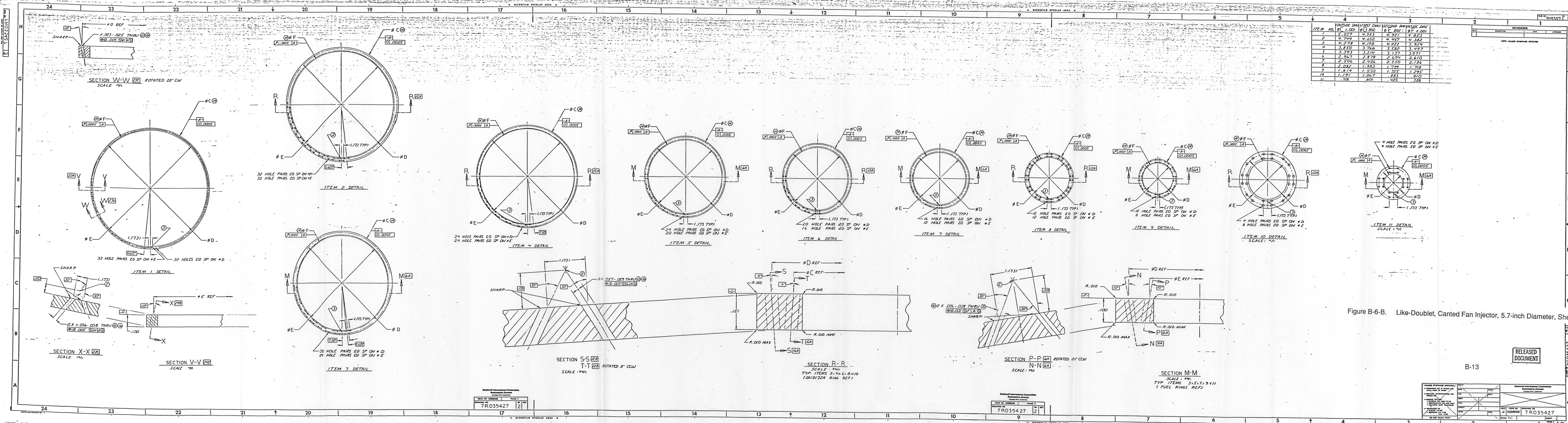


Figure B-6-B. Like-Doublet, Canted Fan Injector, 5.7-inch Diameter, Sheet 2

B-13

RELEASED DOCUMENT

PREPARED BY 7R035427		CHECKED BY 7R035427	
DESIGNED BY 7R035427		DRAWN BY 7R035427	
APPROVED BY 7R035427		REVIEWED BY 7R035427	

APPENDIX C

DATA REDUCTION METHODS

The purpose of the hot-fire tests was to obtain experimental data on high-pressure c^* efficiency, heat flux, and combustion stability, to characterize the test injectors. The test data reduction methods are described in this appendix.

DETERMINATION OF c^*

Characteristic velocity efficiency is defined by the following equation:

$$\eta_{c^*} = \frac{(P_c)_o (A_t)_{\text{eff}} g_c}{(\dot{w}_T) (c^*)_{\text{theo}}}$$

where

$(P_c)_o$	=	stagnation pressure at the throat, psia
$(A_t)_{\text{eff}}$	=	effective sonic throat area, in ²
g_c	=	conversion factor (32.174 lbf-ft/lbf-sec ²)
\dot{w}_T	=	total propellant flowrate, lbf/sec
$(c^*)_{\text{theo}}$	=	theoretical characteristic velocity based on one-dimensional shifting equilibrium, ft/sec.

To use c^* efficiency as a measure of the extent to which the injector/chamber combination releases the total chemical energy of the combustion reactions, and to have a common basis for comparison of different injector/chamber combinations, that portion of the released energy which does not appear as measured chamber pressure must be included in the efficiency calculation. This is approximated by application of the following factors to the measured test parameters.

<u>CORRECTION</u>	<u>FUNCTION</u>
• Stagnation pressure	Corrects measured chamber pressure to throat stagnation pressure
• Heat loss	Corrects measured chamber pressure for heat loss to chamber walls

- Wall friction Corrects measured chamber pressure for losses due to wall friction
- Throat area change Corrects geometric throat area for changes during firing
- Throat C_d Corrects throat area for non-unity discharge coefficient
- Injection momentum Corrects measured chamber pressure for effects of propellant injection momentum

Throat Stagnation Pressure

Chamber pressure was measured near the injector, $(P_c)_{inj}$, and at the start of the nozzle convergence, $(P_c)_{ni}$; the former is assumed to be the pressure at zero gas velocity and the latter is the static pressure at the nozzle inlet. By assuming that combustion is completed prior to convergence, a uniform ideal gas in the chamber, and isentropic flow in the convergent section, both measured chamber pressures can be converted to throat stagnation pressure.

For a contraction ratio of 2.53 and a typical gamma value of 1.134, the Mach number at the start of contraction is 2.43 and

$$(P_t)_o = 0.969 (P_c)_{inj}$$

$$(P_t)_o = 1.034 (P_c)_{ni}$$

Throat stagnation pressures were calculated from measured nozzle inlet pressures; agreement between the values calculated from $(P_c)_{inj}$ and $(P_c)_{ni}$ was generally within one percent.

Heat Loss Correction

Measured chamber pressure must be corrected for heat lost to the coolant between the injector and the throat. This has frequently been done by reducing the combustion gas temperature by an amount equivalent to the measured heat flux to the coolant water and correcting the theoretical c^* for the lowered gas temperature. However, this involves judgements as to whether the heat lost from the combustion gas is from the bulk flow or only from the flow near the wall and the selection of an appropriate value of the gas specific heat.

A more direct estimation of the effect of chamber heat loss, and the one used in this program, is made by subtracting the measured heat flux equivalent from the enthalpy of the injected propellants and using this corrected enthalpy to calculate the theoretical value of c^* on which c^* efficiency is based. Such calculations were made for a chamber pressure of 2000 psia over ranges of mixture ratio (2.2 to 3.6) and heat flux (zero to 800 Btu/lb of RP-1). The corrected theoretical c^* curves are shown in Fig. C-1 and C-2.

Results obtained by both correction methods are listed in Table 6 in the body of this report. The enthalpy reduction method is the preferred procedure. Estimated error limits of the tabulated c^* efficiencies are on the order of ± 1 -percent.

Wall Friction

Theoretically, corrections should be made for energy losses due to drag forces resulting from the viscous action of the combustion gases on the chamber walls upstream of the throat. However, for contraction ratios greater than two, the gas velocities in the cylindrical chamber and the converging portion of the nozzle are low enough to make viscous drag losses negligibly small. This applies to the combustors used in the present program.

Throat Area Change

Temperature gradients produced in an uncooled nozzle during firing result in thermal stresses which may affect the throat radius. Hence the geometric throat diameter at ambient temperatures may need to be corrected for this change to obtain the actual throat diameter during firing. In the water cooled nozzle used in this testing, estimated thermally induced changes in throat diameter are less than the probable error (on the order of ± 0.001 -inch) in measurement of the ambient temperature diameter. Any throat area change correction

factor would therefore be negligible. In addition, the throat diameter was measured after each hot-fire test; no erosion was detected during the 3.5-inch and 5.7-inch injector test series.

Throat Discharge Coefficient

The geometric throat area is corrected to an effective aerodynamic area by use of a discharge coefficient (C_d), which is defined as the ratio of the actual mass flowrate through the throat to the theoretical maximum based on the geometric area and ideal, uniform, one-dimensional flow with no boundary layer. One widely used empirical correlation (Ref. C-1) applied to the test combustor geometries gives a $(C_d)_t$ of 0.998. This value was used to correct the geometric throat areas.

Injection Momentum

This factor corrects for the momentum-aspiration effects of the inflowing propellants and is particularly applicable to chamber pressure measurements made through a port in the injector face. For measurements made through the chamber wall near the injector face, as in the present test hardware, this effect is obscured by recirculation of the gases in this region and by the location of the flame front. The excellent agreement between values of throat stagnation pressures calculated from $(P_c)_{inj}$ and $(P_c)_{ni}$ indicate that any correction for injection momentum was negligible.

Other minor correction factors (injector face heat loss, propellant impurities, etc.) were considered to be negligible.

Propellant Flowrates

LOX and RP-1 flowrates were controlled and measured by cavitating venturis, in which the throat pressure is equal to the vapor pressure of the liquid at its inlet temperature, as long as both the inlet and outlet pressures are greater than the vapor pressure and the outlet

pressure is less than 85% of the inlet pressure. The mass flowrate of the liquid is given by:

$$\dot{w} = \frac{C_D A}{12} (2g \rho \Delta P)^{1/2}$$

where

$C_D A$ = Effective throat area of venturi (calibrated), in²

ρ = Liquid density at venturi inlet, lb/ft³

ΔP = ($P_{inlet} - P_{vapor}$), lb/in²

g = 32.174 lbf-ft/lbf-sec²

The cavitating venturies were calibrated with water against NBS-traceable turbine flowmeters. For RP-1, the $C_D A$ values were the same as for water; for LOX, the $C_D A$ values were corrected for usage at cryogenic temperatures.

HEAT FLUX DETERMINATION

Chamber and throat heat flux levels were determined by measurements of flowrates in the water circuits (with a calibrated critical orifice at the outlet of each water line), the corresponding temperature increases, and the chamber inner wall areas encompassed by each circuit:

$$(Q/A)_i = (\dot{w}_{H_2O} \Delta T / A)_i$$

where

$(Q/A)_i$ = Heat flux at i^{th} circuit, Btu/in²-sec

\dot{w}_{H_2O} = Water flowrate in i^{th} circuit, lb/sec

ΔT = Temperature increase in i^{th} circuit, °F

A = Inner wall area covered by i^{th} circuit, in²

STABILITY CHARACTERIZATION

Data from the PCB transducers and the accelerometers were recorded on high-frequency tapes which were processed to give Statos and PSD graphs. From these, the amplitudes and frequencies of the oscillations were determined, to establish the level of combustion stability. In the bombed tests, dynamic stability was determined by measurement of combustor recovery time from the bomb detonation.

REFERENCE

C-1. Arbit, H. A., and Clapp, S. D., "Fluorine-Hydrogen Performance Evaluation, Phase I, Part I", NASA CR-54978, July 1966, page 140.

LOX/RP1 THEORETICAL C-STAR /2000 PC/
WITH HEAT LOSS TO FUEL

08-10-1988

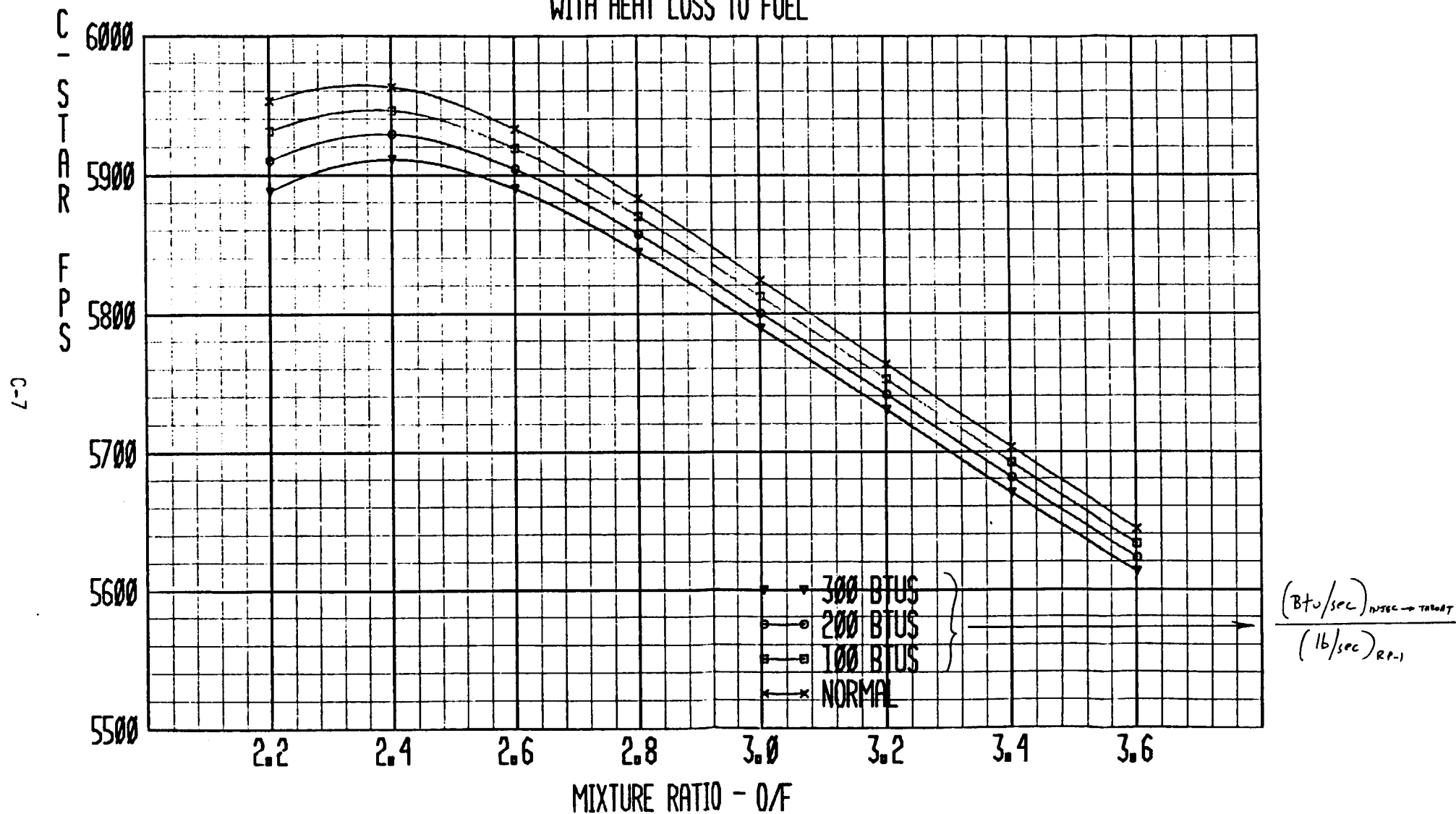


Figure C-1

LOX/RP1 THEORETICAL C-STAR /2000 PC/
WITH HEAT LOSS TO FUEL

08-10-1988

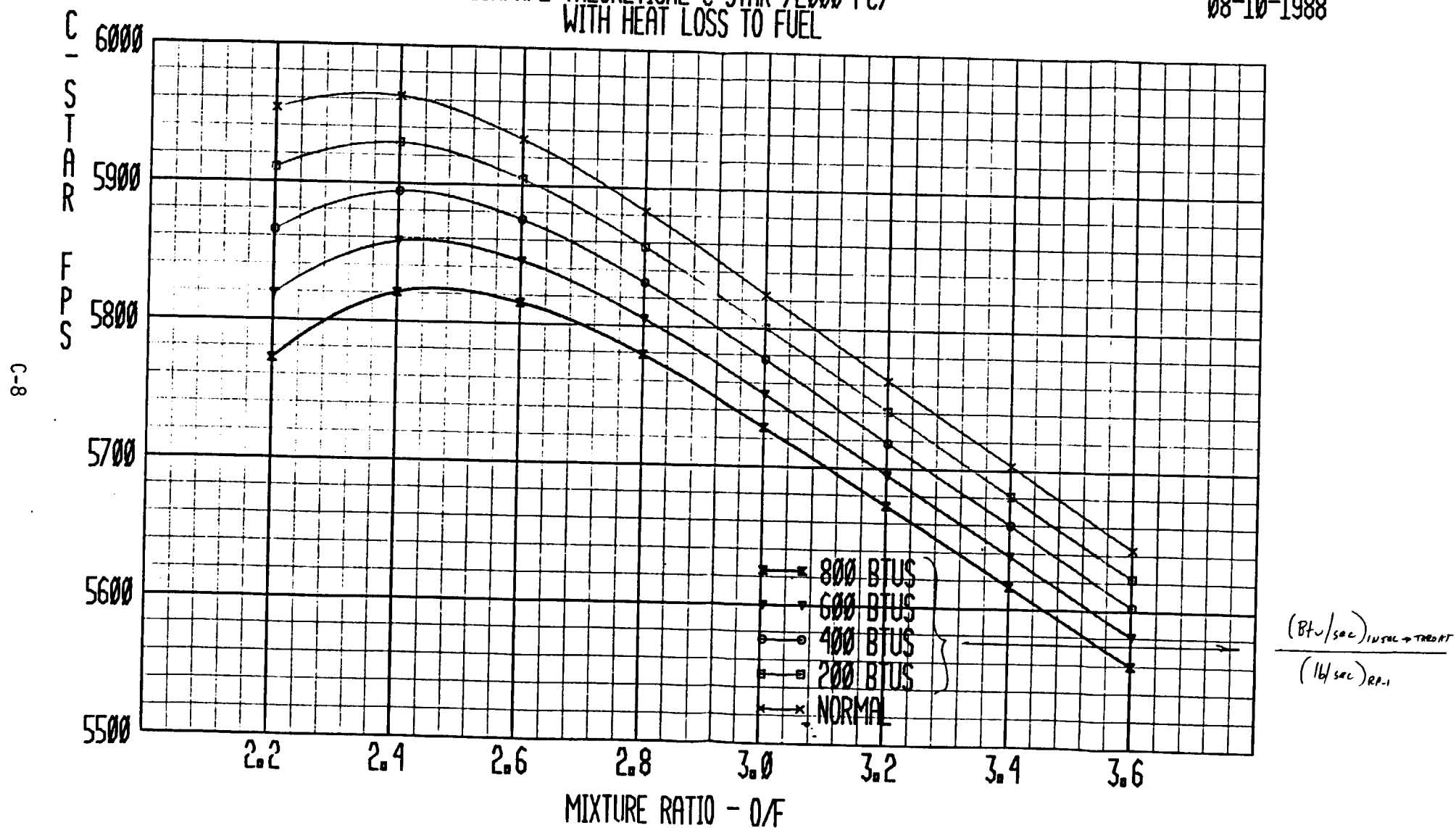


Figure C-2

Report Documentation Page

1. Report No.		2. Government Accession No.		3. Recipient's Catalog No.	
4. Title and Subtitle Heavy Hydrocarbon Main Injector Technology Program Final Report				5. Report Date April 1991	
				6. Performing Organization Code	
7. Author(s) H.A. Arbit, L.M. Tuegel, F.E. Dodd				8. Performing Organization Report No. RI/RD 91-118	
				10. Work Unit No.	
9. Performing Organization Name and Address Rockwell International Rocketdyne Division 6633 Canoga Avenue Canoga Park, CA 91303				11. Contract or Grant No. NAS8-36369	
				13. Type of Report and Period Covered Contractor Report Final	
12. Sponsoring Agency Name and Address National Aeronautics and Space Administration Marshall Space Flight Center Huntsville, AL 35812				14. Sponsoring Agency Code	
15. Supplementary Notes Project Managers, C.R. Bailey, J. Hutt, and M. Rocker.					
16. Abstract <p>The Heavy Hydrocarbon Main Injector Technology Program was an analytical, design and test program to demonstrate an injection concept applicable to an Isolated Combustion Compartment (ICC) of a full scale, high-pressure, LOX/RP-1 engine.</p> <p>In Phase A, of the two-phase program, several injector patterns were tested in a 3.5-inch combustor. Based on these test results, features of the most promising injector design were incorporated into a 5.7-inch injector which was then hot-fire tested. In turn, a preliminary design of a 5-compartment 2-D combustor was based on this pattern.</p> <p>During Phase B, it was felt that additional subscale work was required and technology could be advanced by substituting additional subscale testing for the original program plan to design and fabricate a 2-D combustor to be tested by MSFC. The additional subscale injector testing and analysis was performed with an emphasis on improving analytical techniques and acoustic cavity design methodology. Several of the existing 3.5-inch diameter injectors were hot-fire tested with and without acoustic cavities for spontaneous and dynamic stability characteristics.</p> <p>Results of the program indicated a performance range from 88 to 99% c-star efficiency with the five 3.5 inch and one 5.7 inch injectors. An H-1 derivative 3.5 inch injector showed the most promise as an applicable full scale injector pattern. The performance of this injector ranged from 96 to 98% c-star efficiency, and the injector was spontaneously and dynamically stable.</p>					
17. Key Words (Suggested by Author(s)) Hydrocarbon, RP-1, Stability, Performance, Acoustic, Combustion, Injector, Rocket			18. Distribution Statement Unclassified - Unlimited		
19. Security Classif. (of this report) Unclassified		20. Security Classif. (of this page) Unclassified		21. No of pages 320	
				22. Price*	